Carbonyl-Sulfur Bond Activation for Cross-Coupling Chemistry

Dissertation

der Mathematisch-Naturwissenschaftlichen Fakultät

der Eberhard Karls Universität Tübingen

zur Erlangung des Grades eines

Doktors der Naturwissenschaften

(Dr. rer. nat.)

vorgelegt von

Valentin Jacob Geiger

aus Freudenstadt

Tübingen

2022

Gedruckt mit der Genehmigung der Mathematisch-Naturwissenschaftlichen Fakultät der Eberhard Karls Universität Tübingen.

Tag der mündlichen Qualifikation:	08.12.2022
Dekan:	Prof. Dr. Thilo Stehle
1. Berichterstatter:	Prof. Dr. Ivana Fleischer
2. Berichterstatter:	Prof. Dr. Thomas Ziegler
3. Berichterstatter:	Prof. Dr. Olga Garcia Mancheño

TABLE OF CONTENTS

1. INTRODUCTION

1.1 General Introduction

This thesis covers the topic of carbonyl-sulfur (C(O)-S) bond scission under transition metal-catalysis for cross-coupling methodology. To introduce the topics touched upon, the current chapter summarizes central aspects: cross-coupling reactions in chemistry, classification and comparison of iron-, cobalt- and nickel-catalyzed cross-coupling reactions and characteristics of transmetalation reagents utilized in cross-coupling chemistry.

1.1.1 Cross-Coupling Reactions in Chemistry

The term "cross-coupling" is usually referring to the chemical reaction joining two organic fragments under transition metal-catalytic conditions. This type of transformation allows a valuable C-C bond formation between an aryl (or alkyl) halide and different types of organometallic or organometalloid compounds. Historically, earliest advances on the topic can be deduced from works of Ullmann in 1901[1], Job in 1924[2] and Kharasch in 1942[3].[4] Decades later, research enabled the development of methods with high synthetic utility due to transition metal-catalyzed cross-coupling reactions allowing novel transformations. This led to a rapid increase in research interest in the following decades.[4b] For their crucial work in establishing this area of chemistry, Negishi, Heck and Suzuki were awarded the Nobel prize in 2010.[5] Reactions now associated with their names, line up in a basic toolbox of methodologies, which mainly differ in the nature of the carbon-fragment that is coupled to the organohalide, e.g. Kumada-Corriu-coupling – Grignard reagents[6], Negishi-coupling – organozinc reagents[7], Suzuki-Miyaura-coupling – organoboronic acids[8], Stille-coupling – organotin reagents[9], Mizoroki-Heck-reaction – alkenes[10], Cassar-Heck-Sonogashira coupling – alkynes[11]. Most of these reactions employed Pd-catalysts to achieve the designated transformations. Since then, the research on this topic progressed: Transformations such as Pd-catalyzed C-heteroatom bond formation, e.g. C-N (Buchwald-Hartwig)[12] or C-S (Migita)[13] cross-coupling, have been ensuingly developed. Similarly, reactions like Fukuyama-[14], Liebeskind-Srogl-[15] and Chan-Lam cross-coupling[16] further established the potential of using other building blocks than organohalides, such as thioesters. However, examples with similar conversions of thioesters were known previously.[9a, 17] Approaches such as cross-nucleophile-coupling[18], dehydrogenative cross-coupling[19] or cross-electrophile-coupling[20] are all areas of modern chemical research, which potentially lead to more efficient or more valuable synthetic transformations. Also, electrochemically[21] or photochemically[22] steered cross-coupling methodologies have gained a rising interest. Nonetheless, "classic" cross-coupling reactions continue to bear a central role in process chemistry, especially Suzuki-Miyaura coupling which is a major reaction in pharmaceutical production.[23] Hence, the key role of palladium in cross-coupling still persists.[23b, 24] Mainly, high prices of the noble transition metal promote efforts to search for a suitable replacement as

catalyst. Then again, the chemical industry's utilization of palladium is only a minor use in comparison to other industries and prices are fluctuating due to connected markets.[25] Still, replacing the noble metal with the less noble counterpart nickel is a feasible approach towards more cost-efficient and environmentally friendly process chemistry.[26] Therefore, due to similar characteristics to their fifth-row homologues, iron-, cobalt- and nickel-based catalysts have received an increased interest in recent years, in the context of developing more sustainable catalytic methodologies.

1.1.2 Classification and Comparison of Fe-, Co- and Ni-Catalyzed Cross-Coupling Reactions

Capturing increasing interest of chemical research, not only for cross-coupling reactions, iron-, cobalt- or nickel-catalyses are incentivized by low prices of the raw materials. Especially, iron is unrivaled in terms of cost efficiency in comparison to all other transition metals (Figure 1.1).

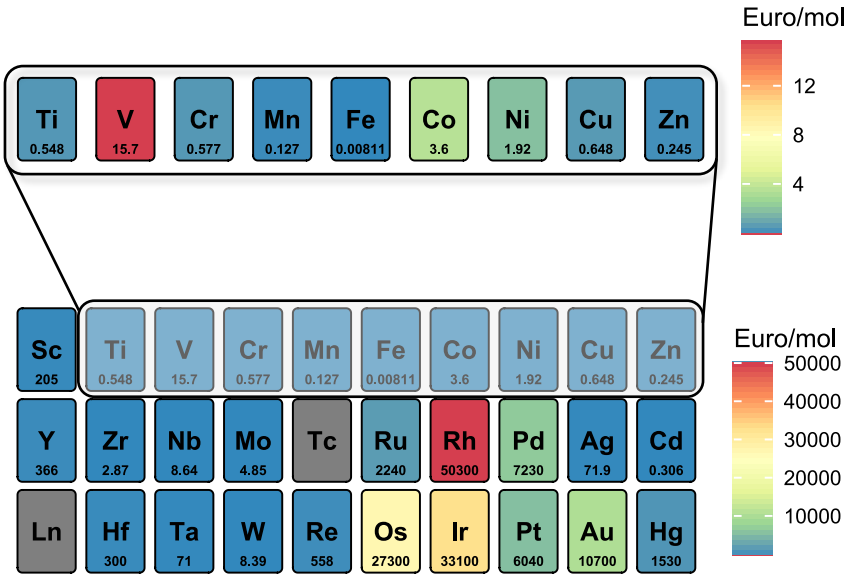

Figure 1.1. Raw metal market prices of transition metals in €/mol. For visualization purposes, selected first-row transition metals are displayed twice. The prices are assessed on market metal prizes and reflect a monthly average.[27]

Comparably high prices for cobalt and nickel in first-row transition metals are reflective of their utilization in material applications, i.e. use of cobalt and nickel in batteries as cathode material (lithium cobalt oxide or lithium nickel cobalt aluminum oxide), use of cobalt as substitute of platinum in proton-exchange membrane fuel cells or nickel in resistant materials such as Hastelloy.[28] With predicted rising demands, cobalt has been classified to possess a moderate and nickel a very low supply risk of critical raw material infrastructure. Then again, reduced use of cobalt in battery materials is a major goal in research.[29] However, while prices of raw materials do change over time as demand fluctuates, the assessment of a transition metal does not only consist of its availability and price but implements factors such as environmental impact. A study from 2014 assessed cradle-to-gate (leaving out recycling) global warming potential, cumulative energy demand, terrestrial acidification and freshwater eutrophication, as refinery and purification of raw materials vary in environmental impact.[30] Not surprisingly, the carbon footprint of first-row transition metals is comparably low due to their higher abundance – with exception of scandium – with iron, cobalt and nickel possessing comparably low carbon foot prints (1.5, 8.3 and 6.5 kg(CO_2-equiv.) kg^{-1} respectively). Nonetheless, as catalysts for cross-coupling reactions and thereby synthesis of pharmaceutical compounds, another crucial property is the toxicity of the metal. Due to this, governmental guidelines recognize and reflect high toxicities of cobalt and nickel as well as the low danger of iron impurities (Figure 1.2).[31]

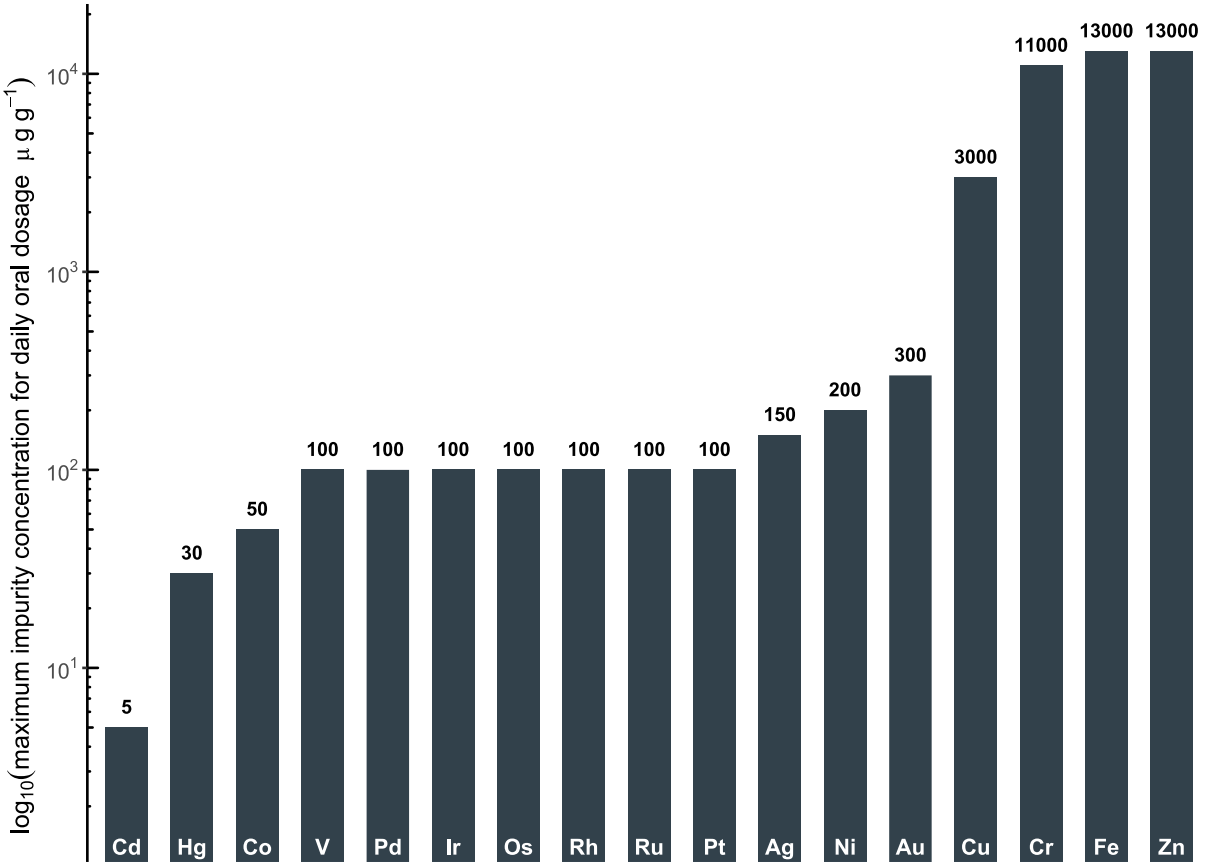

Figure 1.2. Maximum elemental impurities allowed for drugs administered orally from the ICH guideline Q3D (R1) from 2018[31a] – non-transition metals are omitted. The values for iron and zinc are based on EMEA guidelines.[32] Bars are plotted on a logarithmic scale for visualizing purposes (non-logarithmic numbers are displayed).

Heuristically, palladium is still favored to iron-, cobalt- or nickel-catalysts due to i) the well-studied mechanisms with prevalent two-electron pathways, ii) highly optimized methodologies with high turn-over numbers at low temperatures and low catalyst loadings, and iii) a privileged pool of ligands allowing for challenging conversions, e.g. difficult enantioselective reactions.[23b, 24] Nevertheless, examples of applications of non-precious metals are known to literature, e.g. Ni-catalyzed Corriu-Kumada coupling[33] for the synthesis of **3** an intermediate in the synthesis of potential HIV-1 protease inhibitors or Fe-catalyzed cross-coupling in synthesis of **6**, which is an intermediate in the synthesis of the calcimimetic cinacalcet (Scheme 1.1.).[34] Usually, due to considerable side reactions, the first-row transition metals can exhibit problematic functional group tolerances. In terms of Ni-catalysis, common side reactions can be protodehalogenation or protodeborylation.[35] While this is not only decreasing product yield, it also necessitates higher catalyst loadings and therefore more expensive purifications. Nevertheless, the accumulating research resulted in application of Ni-catalysis in instances such as Suzuki-Miyaura-coupling[36], Buchwald-Hartwig amination[37], Fukuyama cross-coupling[38] and challenging enantioselective cross-couplings[39]. For this, an advantage of the 3d metal is its ability to activate less reactive electrophiles.[40]

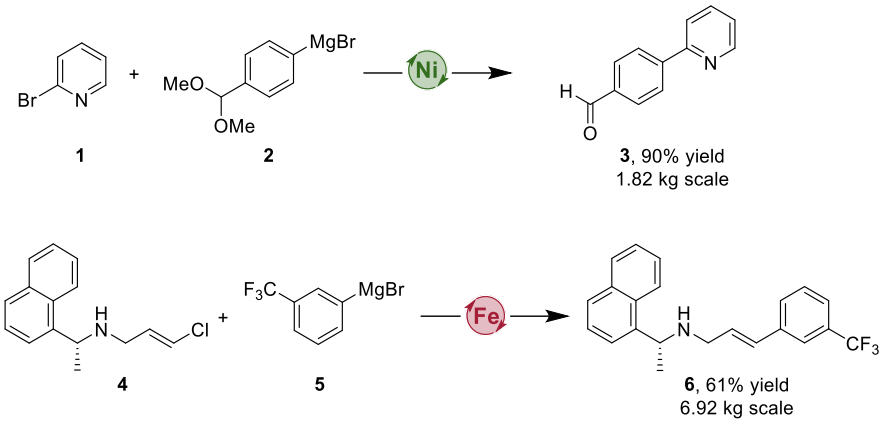

Scheme 1.1. Large scale cross-coupling reactions utilizing Ni- or Fe-catalyzed cross-coupling reactions with Grignard reagents.[33-34]

Additionally, a rich-redox chemistry allows for readily accessible 1-electron pathways.[40b] Usually this relies on the use of Ni(0)-precursors, which are prone towards decomposition. To circumvent this, the development of air-stable Ni(0)-precursors is a topic of modern chemical research.[41] In comparison, iron and cobalt are considered well suited for the coupling of challenging C(sp^3)-organic fragments. This is due to an inhibited β-hydrogen elimination, using iron or cobalt catalysis which allows for an ease in coupling.[42] Most notably, the two metals are able to perform these couplings in absence of ligands further incentivizing their use.[43] However, these conversions often need excess amounts of polar co-solvents, e.g. *N*-methyl pyrrolidone (NMP), which possess major drawbacks such as reprotoxic properties.[44]

1.1.3 Transmetalation Reagents

As a central step of a cross-coupling reaction, transmetalation represents the transfer of the second organic fragment to the catalyst.[45] This step can make use of a spectrum of coupling partners possessing a carbon-metal or a carbon-metalloid bond and even heteroatoms such as nitrogen or sulfur can be coupled. Generally, organometallic transmetalation reagents act as nucleophile, reductant or base (Scheme 1.2).

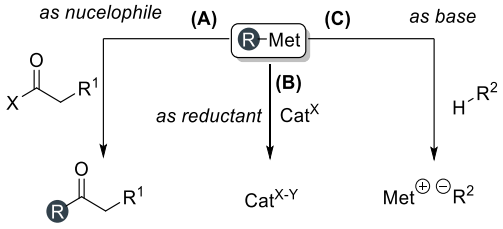

Scheme 1.2. General reactivities of organometallic reagents (R-Met), e.g. nucleophilic acyl substitution **(A)**, reduction of a catalyst (Cat) **(B)** or deprotonation **(C)**.[46]

As these reactivities influence not only the success of the cross-coupling reaction but also the tolerance of functional groups and importantly the activation of the catalyst, the choice of reagent can be considered of major importance. In literature, a plethora of transmetalation reagents have been implemented with transition metal-catalysis, e.g. organolithium[47], -sodium[48], -magnesium[6a], -calcium[49], -titanium[50], -zirconium[51], -manganese[52], -copper[53], -zinc[7], -mercury[54], -boron[55], -aluminum[56], -silicon[57], -indium[58], -germanium[59], -tin[9a], -lead[60] and -bismuth[61] (Scheme 1.3). These reagents vary not only due to their metallic/metalloid centers. The subsequent inherently different properties such as lower C-metal bond polarization or the availability of low-lying empty p-orbitals[62] dictate their respective reactivities. Concomitant lower basicity and/or lower reductive strength play a pivotal role increasing in functional group tolerance while potentially requiring activating reagents, e.g. stochiometric amount of bases often necessary in Suzuki-Miyaura-coupling or fluorides activating silanes. Likewise, ligands or substituents needed for stabilization have to be taken into account.[61] Especially, propensities for α- or β-elimination are a central restriction of alkyl-bearing transmetalation reagents. In addition to that, practical aspects from safety concerns to ease in purification are judicious aspects to consider. To this end, a recent example of replacement of pinacol boronates by 1,1,2,2-tetraethylethylene glycol esters, which are more persistent during silica gel chromatography, exemplifies that feasible optimizations in synthesis of more practical building blocks for Suzuki Miyaura-coupling are still sought after.[63]

Additionally, factors apart from the reagents themselves contribute to the overall aptitude of transmetalation reagents. Counterion[50] and salt effects[64] have been shown to be key in the patchwork of reactivities. For example, equilibria influenced by polar co-solvents such as NMP were identified to favor the formation of more reactive species in $C(sp^3)$-$C(sp^3)$ Negishi coupling.[65] To a similar extend,

salt influences were discovered to have an impact on C(sp^2)-C(sp^2) Negishi coupling[66], a reaction often used in process chemistry.[67]

Thus, with rising demands in terms of green chemistry, mainly regarding atom-economy and metal availability, the development and understanding of the spectrum of transmetalation reagents as stochiometric components of cross-coupling reactions is a key aspect.

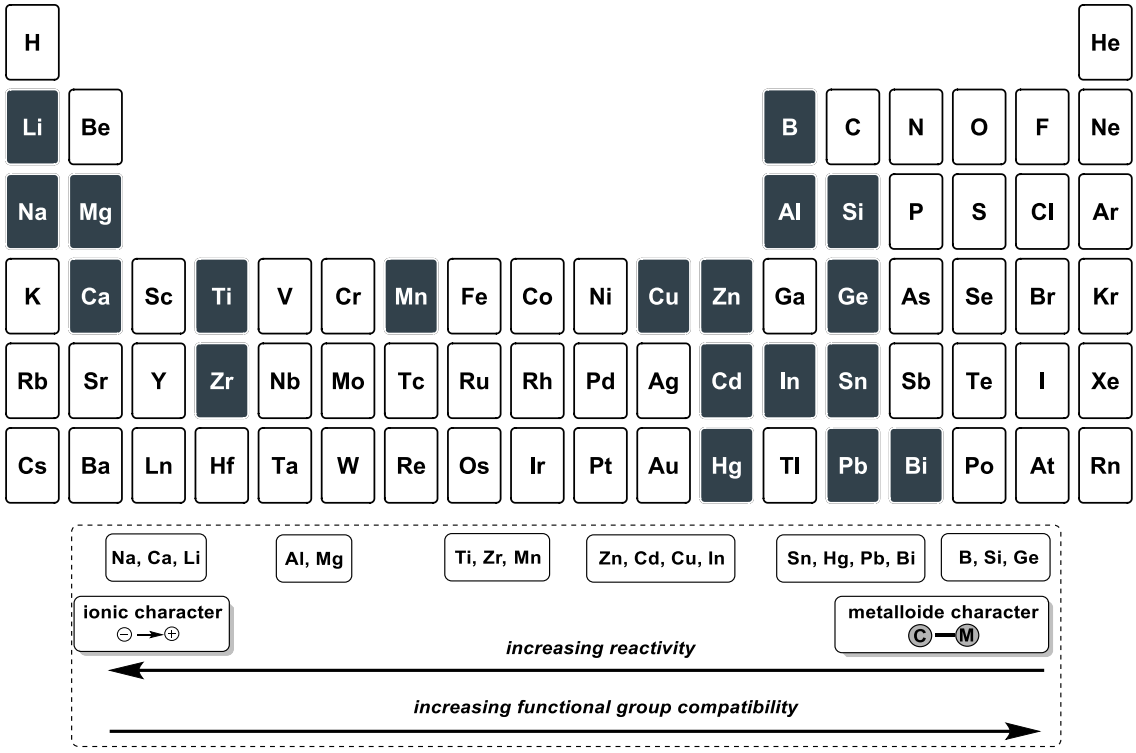

Scheme 1.3. Periodic system highlighting the elements which were reportedly employed in transition metal-catalyzed reactions as transmetalation reagent listed above. Classes of organometallic compounds (bottom) were adapted from cited reference by Knochel and co-workers.[68] (Omitted are organometallic reagents without literature precedence of transition metal-catalyzed cross-couplingreaction)

1.2 References

[1] F. Ullmann, J. Bielecki, *Ber. Dtsch. Chem. Ges.* **1901**, *34*, 2174–2185.

[2] R. R. A. Job, *Cr. Hebd. Acad. Sci.* **1924**, *179*, 330–332.

[3] M. S. Kharasch, E. K. Fields, *J. Am. Chem. Soc.* **1941**, *63*, 2316–2320.

[4] a) C. C. C. Johansson Seechurn, M. O. Kitching, T. J. Colacot, V. Snieckus, *Angew. Chem. Int. Ed.* **2012**, *51*, 5062–5085; b) C. C. C. Johansson Seechurn, A. DeAngelis, T. J. Colacot, in *New Trends in Cross-Coupling: Theory and Applications*, The Royal Society of Chemistry, **2015**, pp. 1–19.

[5] *The Nobel Prize in Chemistry 2010*, NobelPrize.org, https://www.nobelprize.org/prizes/chemistry/2010/summary/, (accessed 11.07.2022).

[6] a) K. Tamao, K. Sumitani, M. Kumada, *J. Am. Chem. Soc.* **1972**, *94*, 4374–4376; b) R. J. P. Corriu, J. P. Masse, *J. Chem. Soc., Chem. Commun.* **1972**, 144a–144a.

[7] E. Negishi, A. O. King, N. Okukado, *J. Org. Chem.* **1977**, *42*, 1821–1823.

[8] N. Miyaura, K. Yamada, A. Suzuki, *Tetrahedron Lett.* **1979**, *20*, 3437–3440.

[9] a) D. Milstein, J. K. Stille, *J. Am. Chem. Soc.* **1978**, *100*, 3636–3638; b) J. K. Stille, *Angew. Chem. Int. Ed.* **1986**, *25*, 508–524.

[10] a) R. F. Heck, J. P. Nolley, *J. Org. Chem.* **1972**, *37*, 2320–2322; b) M. Tsutomu, M. Kunio, O. Atsumu, *Bull. Chem Soc. Jpn.* **1971**, *44*, 581.

[11] a) K. Sonogashira, Y. Tohda, N. Hagihara, *Tetrahedron Lett.* **1975**, *16*, 4467–4470; b) L. Cassar, *J. Organomet. Chem.* **1975**, *93*, 253–257; c) H. A. Dieck, R. F. Heck, *J. Organomet. Chem.* **1975**, *93*, 259–263.

[12] a) J. Louie, J. F. Hartwig, *Tetrahedron Lett.* **1995**, *36*, 3609–3612; b) A. S. Guram, R. A. Rennels, S. L. Buchwald, *Angew. Chem. Int. Ed.* **1995**, *34*, 1348–1350.

[13] T. Migita, T. Shimizu, Y. Asami, J.-i. Shiobara, Y. Kato, M. Kosugi, *Bull. Chem Soc. Jpn.* **1980**, *53*, 1385–1389.

[14] H. Tokuyama, S. Yokoshima, T. Yamashita, L. Shao-Cheng, L. Leping, T. Fukuyama, *J. Braz. Chem. Soc.* **1998**, *9*, 381–387.

[15] L. S. Liebeskind, J. Srogl, *J. Am. Chem. Soc.* **2000**, *122*, 11260–11261.

[16] a) D. M. T. Chan, K. L. Monaco, R.-P. Wang, M. P. Winters, *Tetrahedron Lett.* **1998**, *39*, 2933–2936; b) P. Y. S. Lam, C. G. Clark, S. Saubern, J. Adams, M. P. Winters, D. M. T. Chan, A. Combs, *Tetrahedron Lett.* **1998**, *39*, 2941–2944.

[17] a) C. Sik Cho, K. Itotani, S. Uemura, *J. Organomet. Chem.* **1993**, *443*, 253–259; b) C. Cardellicchio, V. Fiandanese, G. Marchese, L. Ronzini, *Tetrahedron Lett.* **1985**, *26*, 3595–3598.

[18] a) W. Shi, C. Liu, A. Lei, *Chem. Soc. Rev.* **2011**, *40*, 2761–2776; b) C. Liu, H. Zhang, W. Shi, A. Lei, *Chem. Rev.* **2011**, *111*, 1780–1824.

[19] C.-J. Li, *Acc. Chem. Res.* **2009**, *42*, 335–344.

[20] a) D. J. Weix, *Acc. Chem. Res.* **2015**, *48*, 1767-1775; b) S. Kim, M. J. Goldfogel, M. M. Gilbert, D. J. Weix, *J. Am. Chem. Soc.* **2020**, *142*, 9902–9907.

[21] C. Ma, P. Fang, D. Liu, K.-J. Jiao, P.-S. Gao, H. Qiu, T.-S. Mei, *Chem. Sci.* **2021**, *12*, 12866–12873.

[22] A. Y. Chan, I. B. Perry, N. B. Bissonnette, B. F. Buksh, G. A. Edwards, L. I. Frye, O. L. Garry, M. N. Lavagnino, B. X. Li, Y. Liang, et al., *Chem. Rev.* **2022**, *122*, 1485–1542.

[23] a) D. G. Brown, J. Boström, *J. Med. Chem.* **2016**, *59*, 4443–4458; b) J. Magano, J. R. Dunetz, *Chem. Rev.* **2011**, *111*, 2177–2250.

[24] J. D. Hayler, D. K. Leahy, E. M. Simmons, *Organometallics* **2019**, *38*, 36–46.

[25] a) Nornickel, *Annual Report - Enabling the transition to a greener world*, **2020**, https://ar2020.nornickel.com/download/full-reports/ar_en_annual-report_pages_nornickel_2020.pdf; b) N. Willing, *Palladium price forecast: Will the market rebound in 2022?*, capital.com, **2022**, https://capital.com/palladium-price-forecast-and-market-outlook, (accessed 11.07.2022).

[26] M. C. Bryan, P. J. Dunn, D. Entwistle, F. Gallou, S. G. Koenig, J. D. Hayler, M. R. Hickey, S. Hughes, M. E. Kopach, G. Moine, et al., *Green Chem.* **2018**, *20*, 5082–5103.

[27] a) *Shanghai Metals Market (SMM) Spot prices*, https://www.metal.com/, (accessed 14.06.2022); b) *ARGUS Metals platform*, https://www.argusmedia.com/metals-platform/price/assessment/PA00177360000, (accessed 14.07.2022); c) *TM2 - Technology*

Metals Market, https://tm2.com/market/technology-metals-pipeline/osmium/, (accessed 14.07.2022); d) *Scrap Monster*, https://www.scrapmonster.com/metal-prices/minor-metals/mercury/749, (accessed 14.06.2022); e) Prices were calculated with a USD/Euro = 0.9574.

[28] European Commission, *Critical materials for strategic technologies and sectors in the EU - a foresight study*, **2020**.

[29] Editorial, *Nat. Energy* **2020**, *5*, 825–825.

[30] P. Nuss, M. J. Eckelman, *PLOS ONE* **2014**, *9*, e101298.

[31] a) ICH, *Guideline for elemental impurities Q3D(R1)*, https://www.ema.europa.eu/en/documents/scientific-guideline/international-conference-harmonisation-technical-requirements-registration-pharmaceuticals-human-use_en-32.pdf (accessed 13.07.2022); b) K. S. Egorova, V. P. Ananikov, *Angew. Chem. Int. Ed.* **2016**, *55*, 12150–12162.

[32] EMEA, *Guideline on the specification limits for residues of metal catalysts or metal reagents.*, https://www.ema.europa.eu/en/documents/scientific-guideline/guideline-specification-limits-residues-metal-catalysts-metal-reagents_en.pdf (accessed 13.07.2022).

[33] G. Bold, A. Fässler, H.-G. Capraro, R. Cozens, T. Klimkait, J. Lazdins, J. Mestan, B. Poncioni, J. Rösel, D. Stover, et al., *J. Med. Chem.* **1998**, *41*, 3387–3401.

[34] N. Tewari, N. Maheshwari, R. Medhane, H. Nizar, M. Prasad, *Org. Process Res. Dev.* **2012**, *16*, 1566–1568.

[35] M. J. Goldfogel, X. Guo, J. L. Meléndez Matos, J. A. Gurak, M. V. Joannou, W. B. Moffat, E. M. Simmons, S. R. Wisniewski, *Org. Process Res. Dev.* **2022**, *26*, 785–794.

[36] a) P.-A. Payard, L. A. Perego, I. Ciofini, L. Grimaud, *ACS Catal.* **2018**, *8*, 4812–4823; b) K. Wu, A. G. Doyle, *Nat. Chem.* **2017**, *9*, 779–784.

[37] J. P. Wolfe, S. L. Buchwald, *J. Am. Chem. Soc.* **1997**, *119*, 6054–6058.

[38] P. H. Gehrtz, P. Kathe, I. Fleischer, *Chem. Eur. J.* **2018**, *24*, 8774–8778.

[39] a) A. J. Oelke, J. Sun, G. C. Fu, *J. Am. Chem. Soc.* **2012**, *134*, 2966–2969; b) Z. Zhang, J. Zhang, Q. Gao, Y. Zhou, M. Yang, H. Cao, T. Sun, G. Luo, Z.-C. Cao, *Nat. Comm.* **2022**, *13*, 2953.

[40] a) V. P. Ananikov, *ACS Catal.* **2015**, *5*, 1964–1971; b) S. Z. Tasker, E. A. Standley, T. F. Jamison, *Nature* **2014**, *509*, 299–309.

[41] a) J. D. Shields, E. E. Gray, A. G. Doyle, *Org. Lett.* **2015**, *17*, 2166–2169; b) N. Hazari, P. R. Melvin, M. M. Beromi, *Nat. Rev. Chem.* **2017**, *1*, 0025.

[42] a) G. Manolikakes, in *Comprehensive Organic Synthesis II (Second Edition)* (Ed.: P. Knochel), Elsevier, Amsterdam, **2014**, pp. 392–464; b) G. Cahiez, A. Moyeux, *Chem. Rev.* **2010**, *110*, 1435–1462.

[43] a) G. Cahiez, H. Avedissian, *Tetrahedron Lett.* **1998**, *39*, 6159–6162; b) G. Cahiez, H. Avedissian, *Synthesis* **1998**, *1998*, 1199–1205.

[44] E. Bisz, M. Koston, M. Szostak, *Green Chem.* **2021**, *23*, 7515–7521.

[45] S. C. Rasmussen, *ChemTexts* **2020**, *7*, 1.

[46] S. Asako, I. Takahashi, H. Nakajima, L. Ilies, K. Takai, *Commun. Chem.* **2021**, *4*, 76.

[47] M. Yamamura, I. Moritani, S.-I. Murahashi, *J. Organomet. Chem.* **1975**, *91*, C39–C42.

[48] H. Kuniyasu, K. Takekawa, F. Yamashita, K. Miyafuji, S. Asano, Y. Takai, A. Ohtaka, A. Tanaka, K. Sugoh, H. Kurosawa, et al., *Organometallics* **2008**, *27*, 4788–4802.

[49] J. Langer, M. Köhler, H. Görls, M. Westerhausen, *J. Organomet. Chem.* **2014**, *751*, 563–567.

[50] A. Varenikov, M. Gandelman, *J. Am. Chem. Soc.* **2019**, *141*, 10994–10999.

[51] S. L. Wiskur, A. Korte, G. C. Fu, *J. Am. Chem. Soc.* **2004**, *126*, 82–83.

[52] M. S. Hofmayer, J. M. Hammann, G. Cahiez, P. Knochel, *Synlett* **2018**, *29*, 65–70.

[53] D. Castagnolo, M. Botta, *Eur. J. Org. Chem.* **2010**, *2010*, 3224–3228.

[54] N. A. Bumagin, P. G. More, I. P. Beletskaya, *J. Organomet. Chem.* **1989**, *364*, 231–234.

[55] N. Miyaura, A. Suzuki, *J. Chem. Soc., Chem. Commun.* **1979**, 866–867.

[56] H. Ogawa, Z.-K. Yang, H. Minami, K. Kojima, T. Saito, C. Wang, M. Uchiyama, *ACS Catal.* **2017**, *7*, 3988–3994.

[57] Y. Hatanaka, T. Hiyama, *J. Org. Chem.* **1988**, *53*, 918–920.

[58] Y.-H. Chen, P. Knochel, *Angew. Chem. Int. Ed.* **2008**, *47*, 7648–7651.

[59] T. Enokido, K. Fugami, M. Endo, M. Kameyama, M. Kosugi, *Adv. Synth. Catal.* **2004**, *346*, 1685–1688.

[60] S.-K. Kang, *Chem. Commun.* **1998**, 1317–1318.

[61] O. Yamazaki, T. Tanaka, S. Shimada, Y. Suzuki, M. Tanaka, *Synlett* **2004**, *2004*, 1921–1924.
[62] P. Knochel, R. D. Singer, *Chem. Rev.* **1993**, *93*, 2117–2188.
[63] N. Oka, T. Yamada, H. Sajiki, S. Akai, T. Ikawa, *Org. Lett.* **2022**, *24*, 3510–3514.
[64] P. Eckert, S. Sharif, M. G. Organ, *Angew. Chem. Int. Ed.* **2021**, *60*, 12224–12241.
[65] L. C. McCann, H. N. Hunter, J. A. C. Clyburne, M. G. Organ, *Angew. Chem. Int. Ed.* **2012**, *51*, 7024–7027.
[66] L. C. McCann, M. G. Organ, *Angew. Chem. Int. Ed.* **2014**, *53*, 4386–4389.
[67] P. W. Manley, M. Acemoglu, W. Marterer, W. Pachinger, *Org. Process Res. Dev.* **2003**, *7*, 436–445.
[68] B. Haag, M. Mosrin, H. Ila, V. Malakhov, P. Knochel, *Angew. Chem. Int. Ed.* **2011**, *50*, 9794–9824.

2. Aims of This Work

The synthetic employment of first-row transition metals is coveted due to their higher abundance, lower carbon-footprint and often lower prices compared to noble metals as well as due the advantage of applications without the necessity of ligands. In this thesis, first-row transition metals (especially iron, cobalt and nickel) will be studied for the conversion of carbonyl-sulfur (C(O)-S) motifs as a central focus, since only few reports on the reactivities and challenges of sulfurous building blocks as starting materials are known.

In the first part of this thesis, the development of a mild and efficient conversion of alkyl transmetalation reagents with thioesters was designated (Scheme 2.1). Thioesters constitute a suited substance class of organic building blocks since they possess a high reactivity under transition metal-catalysis combined with easy synthesis and storage. Since similar transformations in literature were mainly limited to the utilization of aryl organometallic reagents, the study of organomanganese reagents will be targeted, as this reagent class possesses a reportedly high functional group tolerance compared to organomagnesium reagents with the additional higher reactivity compared to the corresponding organozinc reagents. Therefore, the potential application in synthesizing highly functionalized ketones with aliphatic organomanganese reagents would demonstrate the advantages of this methodology. Additionally, investigations on the synthesis and reactivities of organomanganese reagents might further incentivize their use in cross-coupling reactions.

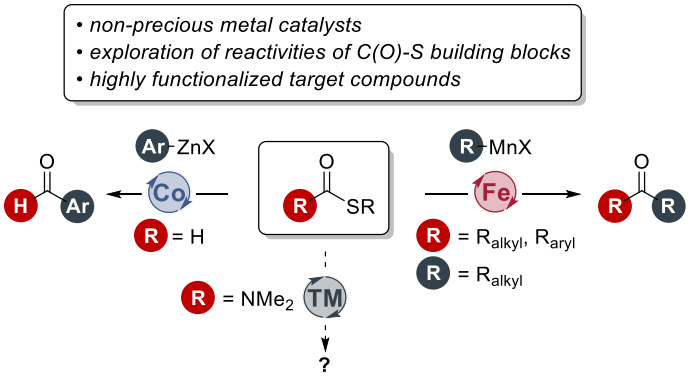

Scheme 2.1. Overview of target transformations of this thesis: acylation of organomanganese reagents (right), formylation of organozinc reagents (left) and studies towards potential application of thiocarbamates (bottom).

As a second part, the employment of thioformates as formyl-donors for cross-coupling reactions will be studied to enable such a transformation by first-row transition metal-catalysis. The reaction would allow for the transformation of highly functionalized organometallic compounds which can be obtained *via* metalation chemistry. Therefore, target compounds would be especially substrates difficult to obtain by carbonylation or alternative redox-intensive steps. In addition to that, the conditions of the studied methodologies should be applied to different carbonyl-sulfur building blocks to gain further insight into potential activations or applications of such transformations.

3. IRON-CATALYZED CROSS-COUPLING OF THIOESTERS WITH ORGANOMANGANESE REAGENTS

Parts of this chapter are reprinted with permission from V. J. Geiger, G. Lefèvre, I. Fleischer, *Chemistry – A European Journal*, DOI: 10.1002/chem.202202212. Copyright 2022 Wiley VCH; schemes, tables, figures and text may differ from this publication and additional results are included.

Author contribution:

The author of this thesis conducted the studies of organomanganese reagents, optimized reaction conditions, performed synthesis of starting materials and substate screening as well as data collection and analysis of NMR, IR, GC-MS results. The author compiled the results and drafted the article manuscript. Dr. G. Lefèvre provided experimental results for the paramagnetic ^{1}H NMR studies of the iron complexes and interpretation thereof. The HRMS analyses were performed by the MS department of the University of Tübingen. The EPR measurements were acquired with the aid of the NMR department of the University of Tübingen.

3.1 Introduction

3.1.1 Organomanganese Reagents

3.1.1.1 Historical Overview

Considering the important role of C-C cross-coupling reactions in synthetic chemistry, the plethora of studies about the associated transmetalation reagents led to a broad spectrum of coupling reagents discussed in earlier chapters (chapter **1.1.3**, p. 6). In previous literature, one of the many reagents studied are organomanganese compounds, for which their chemistry has been summarized in recent reviews.[1] Historically, these reagents were first mentioned in 1937 in works by Gilman and Bailie who employed phenyl manganese iodide synthesized from manganese(II) iodide and phenyl lithium (Scheme 3.1).[2] Within a comparative study of organometallic reagents, the conversion of azobenzene (**7**) was observed with phenyl manganese iodide (**8**).

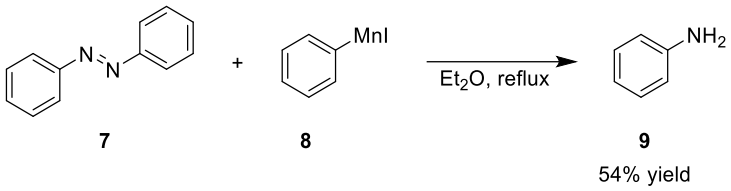

Scheme 3.1. Reaction by Gilman and Bailie being first to mention the utilization of organomanganese reagents.[2]

Subsequently, Gilman reported not only the use of phenyl manganese iodide but also allegedly a mixture with diphenyl manganese (Figure 3.1).[3] However, later observations indicate that the described mixture resembled oxidation products and likely did not contain diphenyl manganese.[4] Two decades after Gilman's work the synthesis of dimethyl manganese (**12**) from methyl lithium (**11**) was reported (Scheme 3.2). Therein, dimethyl manganese was described to be explosive to shock, highly pyrophoric but thermally stable at temperatures up to 80 °C.[4b] It was observed that the formation of trimethyl manganate (**13**) by addition of an extra equivalent of lithium reagent **11** furnished a thermally more stable and less reactive compound.

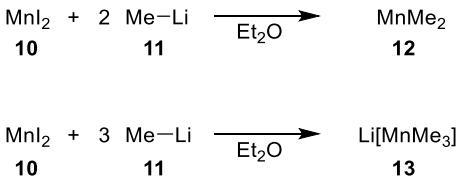

Scheme 3.2. Synthesis of dimethyl manganese and trimethyl manganate from methyl lithium.[4b]

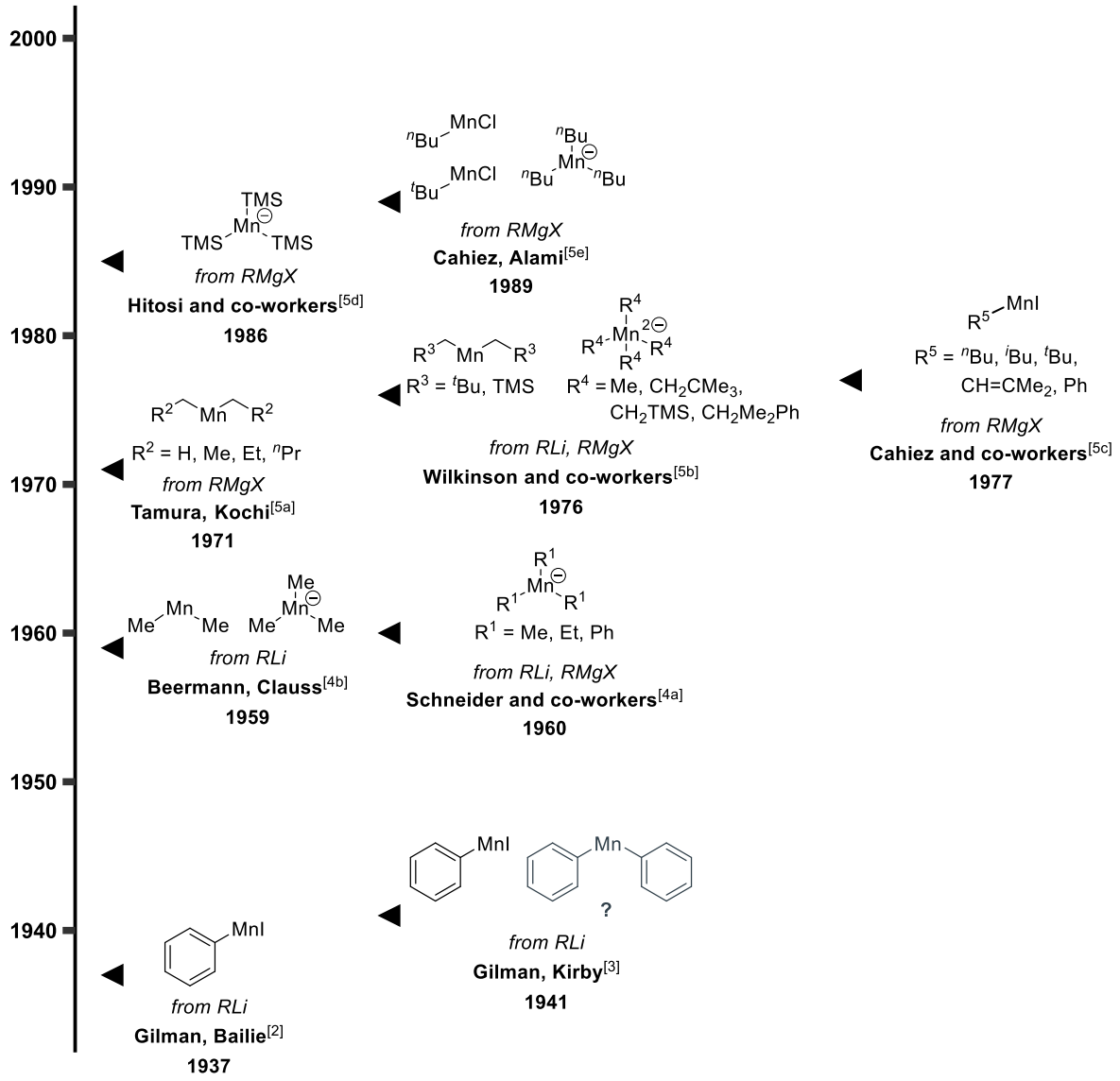

Figure 3.1. Historically important syntheses of organomanganese reagents from either organolithium or organomagnesium reagents with respective year of publication.[2–5] Counterions of manganates are omitted.

One year later, syntheses of different types of alkyl and aryl manganese compounds but also more specifically the formation of triorganyl manganates have been reported.[4a] Albeit, the only moieties included which contained available β-hydrogen atoms were synthesized as respective homoleptic manganates and not as organomanganese halides. This literature instance was likely first to demonstrate the synthesis of organomanganese compounds starting from Grignard instead of organolithium reagents. Then again, most of their syntheses were achieved using lithium reagents as they reported side product formation using Grignard reagents. For clarity, the postulated trialkyl manganates were solely based on chemometric experiments and not on structural characterization. Until today, no isolated homoleptic structure of a trialkyl- or triaryl manganese compound without a ligand is known in literature.

In a following study, reactions of aryl or vinyl halides were reported, which performed well in the coupling with **13** and less well with manganate **16** (Scheme 3.3).[6] Even so, the limitation to methylation of C(sp^2)-halides, **14** or **16**, was impeding synthetic application.

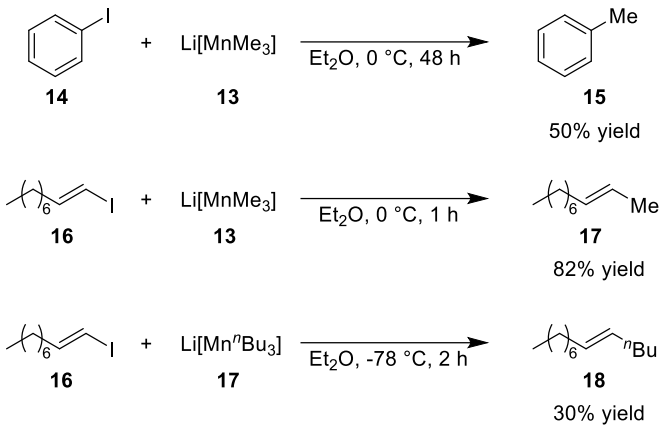

Scheme 3.3. Corey and co-workers' study of the reactivity of manganates with alkenyl or aryl iodides.[6]

After this, the decomposition behavior of β-hydrogen containing dialkyl manganese compounds was examined by Kochi and co-workers.[5a] They observed that while decomposition occurs with all moieties carrying β-hydrogen atoms, transition metals such as iron, cobalt and nickel led to more rapid decomposition. In addition to these findings, exchange reactions with alkyl halides and oxidation of manganese reagents by molecular oxygen are described in this work. Five years later, a variety of di- and tetra-substituted mangnanese reagents were characterized.[5b] Utilizing non-β-hydrogen containing moieties, i.e. neopentyl, neosilyl, neophenyl, structures of organomanganese compounds were studied *via* X-ray and electron paramagnetic resonance (EPR) spectroscopy pioneering the structural elucidation of organomanganates. This study provided examples of some organomanganates that can persist sublimation conditions at elevated temperatures.

The first work in the field of synthetic utilization of organomanganese reagents was reported in 1977 by Cahiez and Normant (Scheme 3.4).[5c, 7] In two separate examples, it was demonstrated that starting from **10**, alkyl manganese iodides **19** can be obtained, which was employed in reactions such as 1,2-addition to aldehydes furnishing secondary alcohols, e.g. **21**.

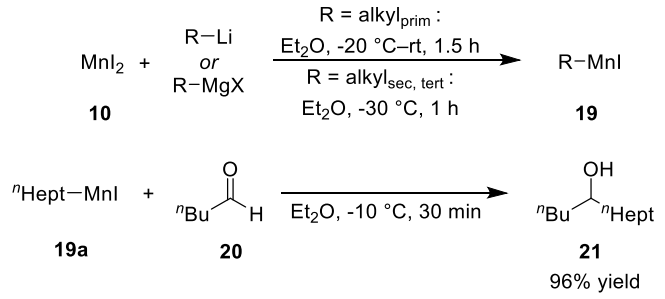

Scheme 3.4. Pioneering work by Cahiez and co-workers in utilization of alkyl manganese iodides by 1,2-addition to aldehydes.[5c]

3.1.1.2 Synthesis of Organomanganese Reagents

Undoubtedly, Cahiez's work promoted the organomanganese chemistry to a feasible synthetic option. Importantly, this was achieved by omitting the necessity of soluble manganese iodide or bromide for the transmetalation (Scheme 3.5, **(A)**). Generally, simple manganese chloride only leads to feasible yields under specific conditions with organolithium reagents **(B)**. Therefore, the procedure was adapted enhancing solubility through the stochiometric addition of lithium chloride to manganese chloride. The preformed lithium chloride manganese chloride ate complex is soluble in ethereal solvents such as THF and provides good yields in transmetalation reactions **(C)**.[5e]

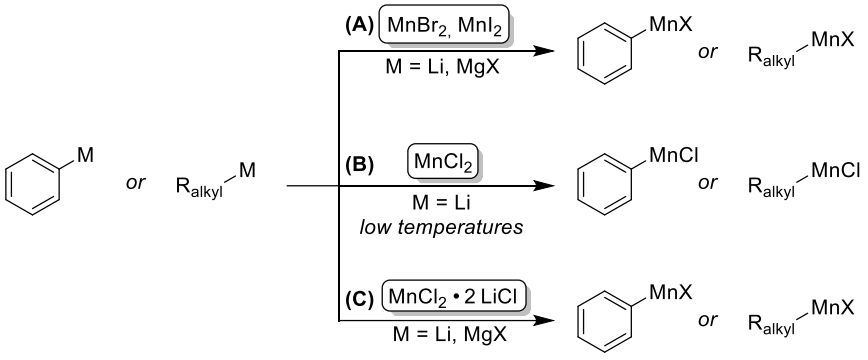

Scheme 3.5. Different syntheses of aryl (or alkyl) manganese halides from manganese(II) precursors.[5c, 5e, 8]

Generally, the synthesis of manganese reagents is mainly enabled through a salt metathesis performing these reactions with either organolithium or -magnesium reagents. However in recent years, the toolbox of syntheses has been equipped with more possibilities: Circumventing the use of magnesium, the utilization of non-passivated highly reactive (Rieke) metal colloids enables the synthesis of aryl manganese halides (Scheme 3.6).[9] Similarly, activation of manganese surface with salt additives can be used to synthesize aryl manganese reagents.[10]

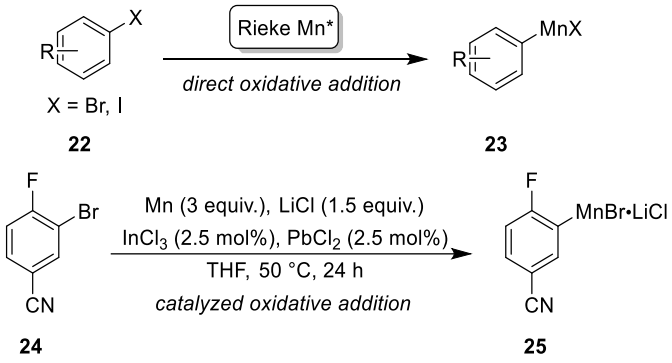

Scheme 3.6. Synthesis of organomanganese reagents from manganese metal.[9–10]

Even one-pot synthesis of Grignard reagents and subsequent transmetalation has been shown to be able to furnish benzylic manganese reagents.[11] Another feasible approach is the metalation of functionalized arenes with strong organometallic amides.[12] Especially this metalation reaction allows

for the synthesis of functionalized manganese reagents. Nevertheless, the described methodologies are mostly limited to aryl compounds.

3.1.1.3 Reactions of Organomanganese Reagents

With the synthesized manganous reagents at hand, the utility for non-catalytic reactions was studied in depth by Cahiez analogously to Grignard reagents, e.g. their addition to aldehydes or ketones to furnish alcohols[7, 13], reactions with acid anhydrides[14], acid chlorides[5c, 15] or acyl silanes yielding ketones[16] as well as *ortho*-aryl halide substitution of phenones[17] and 1,4-addition[5e] (Scheme 3.7).

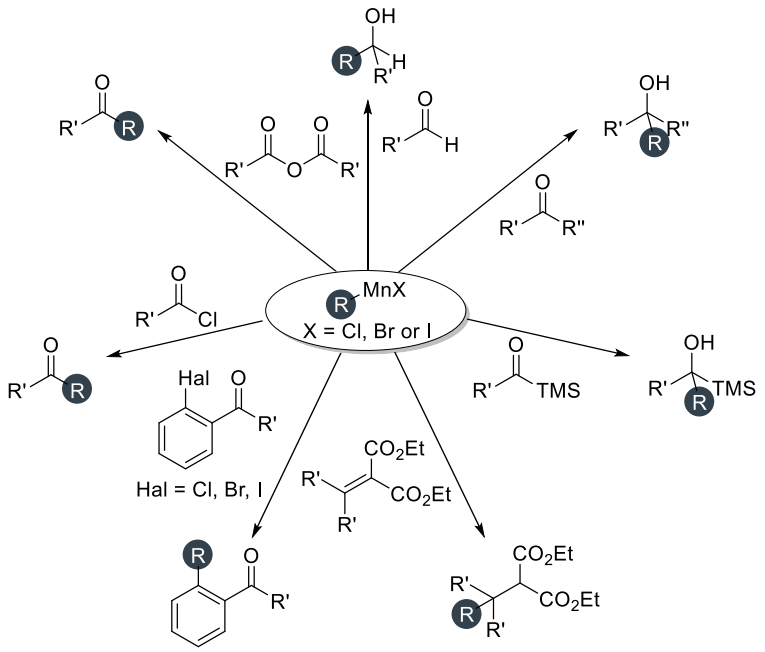

Scheme 3.7. Overview of non-transition metal-catalyzed transformations: reactions with carbonyls,[5c, 7, 13-16] aromatic substitution[17] or 1,4-addition.[5e]

During these studies, the reactivity and stability of organomanganese compounds has been approximated (Figure 3.2).[1a] Usually, manganates are considered most thermally stable and least reactive. Although, these compounds possess reactivities such as manganation which were reported, e.g. silylmanganation of alkynes using trisilylmanganates.[18] This exemplifies a reactivity rarely explored in literature. Other reported instances include 1,2-addition to carbonyls[19] or cyclizations of alkenyl substituted aryl iodides[20] which is a reactivity most similar to Pd-catalyzed reactions. Recently, it was demonstrated that metal-halogen exchange reaction can be observed with tetraorganyl manganates.[8]

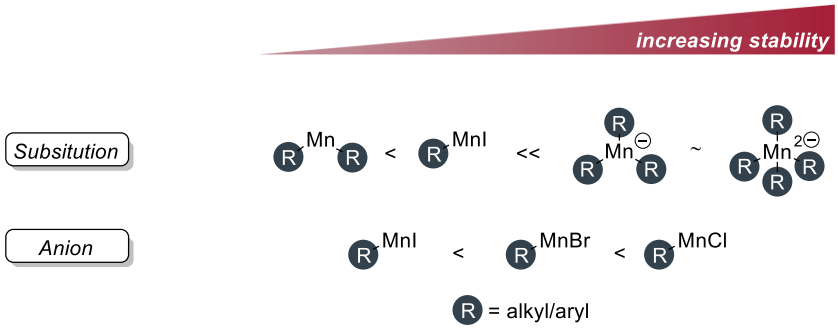

Figure 3.2. Approximation of the stabilities and anion influence on organomanganese compounds. Counterions for manganates are omitted.[1a]

3.1.1.4 Transition Metal-Catalyzed Reactions with Organomanganese Reagents

Moreover, organomanganese compounds were explored in transition metal-catalyzed reactions. In early works, mainly Cu-catalyzed 1,4-addition to vinylogous building blocks were reported. Interestingly, most of these early advances utilized aliphatic manganese reagents. In one report, Cu-, Ni-, and Fe-catalyzed transformations were screened with alkyl manganese reagents in Kumada-type couplings (Scheme 3.8).[21] The reaction was reliant on the use of NMP as polar co-solvent, except for reactions with phenyl manganese chloride, and worked with alkyl iodides and bromides but not chlorides.

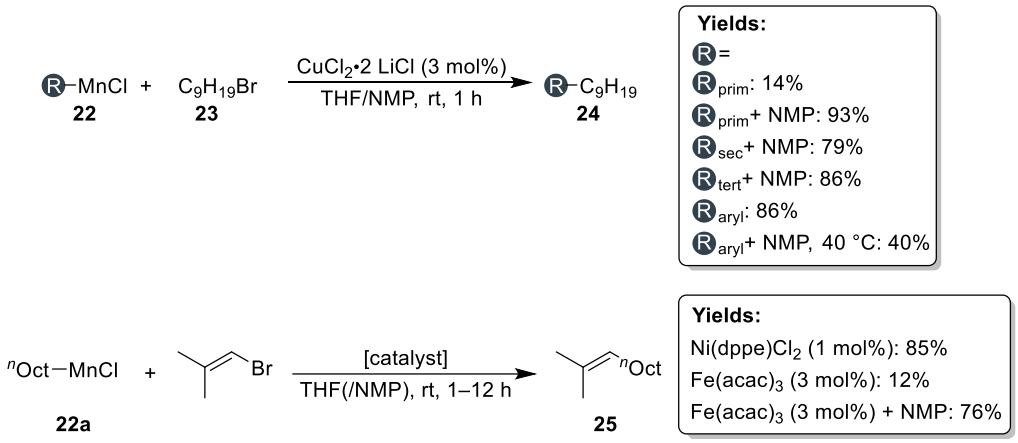

Scheme 3.8. Cahiez and co-workers' screenings on different transition-metal catalyzed C-C cross-coupling reactions employing alkyl manganese reagents.[21]

After these early publications, mainly non-β-hydrogen containing moieties (e.g. aryl and/or benzyl) were subsequently examined. Focus of this research can be summarized as such: firstly, the employment of organomanganese reagents enabling selective substitutions of challenging secondary C(sp^3)-electrophiles catalytically. This has been achieved for Fe- and Co-mediated reactions using bisaryl manganese reagents **26** (Scheme 3.9).[22]

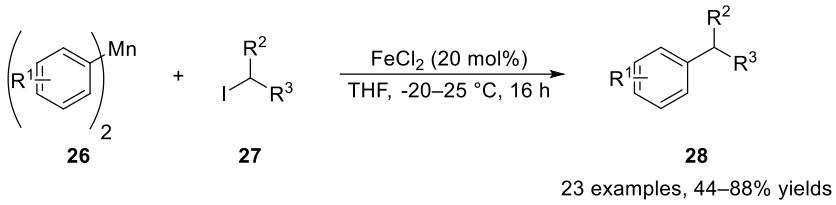

Scheme 3.9. Iron-mediated cross-coupling of secondary alkyl iodides with organomanganese reagents reported by Knochel and co-workers.[22a]

Secondly, catalytic conversions of aryl- or vinyl-halides have been more extensively studied with either benzylic or aryl manganese reagents and first-row transition metals as catalysts (Table 3.1). Ni-catalyzed coupling of aryl- and benzyl manganese reagents with aryl iodides or heteroaryl chlorides has been reported (Scheme 3.10). [23] This reaction necessitates the employment of 4-fluorostyrene as an additive to provide feasible yields. 4-Fluorostyrene is known in Ni-catalysis to facilitate reductive elimination step which is generally challenging for similar Ni-catalyzed reactions.[24]

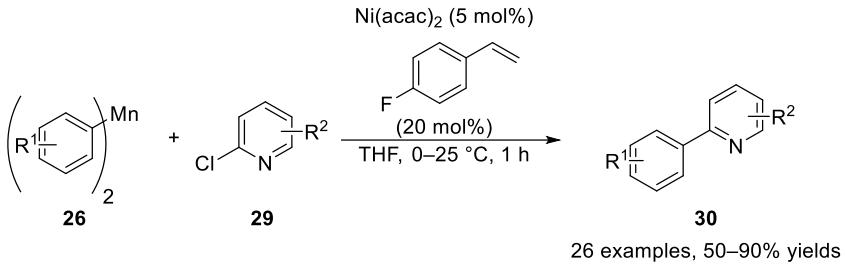

Scheme 3.10. Ni-catalyzed cross-coupling of bisaryl manganese reagents with heteroaryl chlorides reported by Knochel and co-workers.[23]

However, a frontrunner in the last decade of research for catalytic methodologies employing organomanganese reagents is iron. Comparing studies, the advantages of iron-catalyzed methodologies are ubiquitously demonstrated: While high catalyst loadings are sometimes necessary, the reactions usually do not rely on any ligand and can be performed with cheap and available precatalysts (Scheme 3.11).[25] It is important to add that the reactions employing vinyl(pseudo)halides also proceed without catalyst. Nevertheless, the *E/Z* selectivity is enhanced and yields increased, which is similar to previous reports.[6].

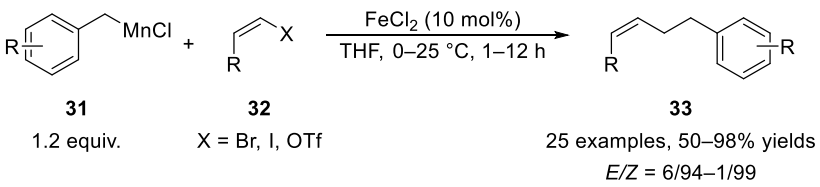

Scheme 3.11. Iron-catalyzed cross-coupling of vinyl(pseudo)halides with benzyl manganese halides reported by Knochel and co-workers.[25a]

Table 3.1. Overview of transition metal-catalyzed methodologies employing organomanganese compounds.

Entry	Group	Year	RMnX	Reactant	Catalyst (Loading)	Additive/Ligand	conditions	time
1	Lefevre[25b]	2020	Ar_2Mn	sp^2_{vinyl}-Br/I	$Fe(acac)_3$ (10 mol%)		0–rt	1 h
2	Knochel[25a]	2019	benzylMnCl	sp^2_{vinyl}-Br/I	$FeCl_2$ (10 mol%)		0–rt	1(–12) h
3	Knochel[22a]	2018	Ar_2Mn	sp^3-Br, sp^3-I	$FeCl_2$ (20 mol%)		-20–rt	16 h
4	Knochel[23]	2017	Ar_2Mn, benzylMnCl	sp^2_{aryl}-I, $sp^2_{heteroaryl}$-Cl	$Ni(acac)_2$ (5 mol%)	4-Fluorostyrene	0 °C	0.5 h
5	Knochel[22b]	2016	Ar_2Mn	sp^3-I	$CoCl_2$•LiCl (20 mol%)		-20–rt	8 h
6	Knochel[26]	2016	benzylMnCl	$sp^2_{(hetero)aryl}$-Br, sp^2_{aryl}-I	$FeCl_2$ (10 mol%)		0–rt	2–24 h
7	Knochel[10]	2011	ArMnBr	sp^2_{aryl}-I	Pd-PEPPSI (5 mol%)		0–25 °C	12 h
8	Schneider[27]	2006	ArMnCl	sp^2_{aryl}-Br	$Ni(acac)_2$ (5 mol%)	IPr•HCl	0–25 °C	0.25–24 h
9	Rieke[28]	2005	ArMnCl	sp^2_{aryl}-I, sp^2_{vinyl}-Br	$Pd(PPh_3)_4$ (3 mol%)		0 °C	20 min
10	Cahiez[29]	1999	ArMnBr	crotyl aldehyde	CuI (3 mol%)		-10 °C	2 h
11	Cahiez[30]	1997	ArMnCl	sp^2_{aryl}-Br/I/OTf	$PdCl_2(PPh_3)_2$ (1 mol%)	DME	rt	30 min
12	Cahiez[21]	1996	alkylMnCl	sp^2_{vinyl}-Cl/Br/I	$CuCl_2$ (3 mol%), $NiCl_2$(dppe) (1 mol%), $Fe(acac)_3$ (3 mol%)	NMP (for Fe)	rt	1–12 h
13	Cahiez[31]	1996	alkylMnCl	sp^2_{vinyl}-Cl/Br/I	$Fe(acac)_3$ (3 mol%)	NMP	rt	1 h
14	Cahiez[32]	1992	$(3\text{-furyl})_4MnLi_2$	acid chloride	$Fe(acac)_3$ (3 mol%)		-70 °C	30 min
15	Cahiez[33]	1990	alkylMnCl, ArMnCl	acrylic esters	CuCl (3 mol%)	TMS-Cl	0–rt	0.5–1.5 h
16	Cahiez[34]	1989	^{t}BuMnCl	acid chloride	CuCl (1 mol%)		-50 °C	0.5–1.5 h
17	Cahiez[35]	1989	alkylMnCl	vinyl-ketones	CuCl (5 mol%)		0 °C	2–4 h
18	Cahiez[36]	1989	alkylMnCl	vinyl-aldehydes	CuCl (5 mol%)		-30 °C	30 min

3.1.1.5 Comparison Organomagnesium, -manganese and -zinc halides

Organomanganese reagents are sometimes referred to as "soft" Grignard reagents.[1a] However, due to the position of manganese in the periodic table of elements (group 7) in between magnesium (group 2) and zinc (group 12), reactivities of organomanganese reagents can be compared to both, organomagnesium and organozinc reagents. So far, reactions typical for organozinc reagents, such as Reformatski-type reactions[37], have been explored with manganese, thereby indicating similar reactivities.[38] Hitherto, the employment of manganese can be considered comparably low in cost but not as low in toxicity (Table 3.2). The difference in Pauling electronegativity (EN) can be used to tentatively approximate the reactivity of the respective organometallic reagent. Especially this property highlights the intermediary reactivity of the organomanganese reagents: Due to lower difference in EN of the carbon-metal bond compared to magnesium, organomanganese halides are considered less reactive than Grignard reagents. Analogously, zinc possesses an even lower difference in carbon-metal EN and is considered even less polarized, therefore, less reactive.

Table 3.2. Comparison of organomagnesium, -zinc and -manganese compounds as well as properties of the respective metal.

Properties of the metal	Mg	Mn	Zn
Cost of metal [€/mol][39]	0.084	0.126	0.244
LD_{50}(oral) of MCl_2(• H_2O)	>5 g/kg[40]	236 mg/kg[41]	1.1 g/kg[42]
EN after Pauling[43]	1.31	1.55	1.65
Ox. states	1, 2	0–7	1, 2
Properties of the reagent	R–Mg	R–Mn	R–Zn
Synthesis from metal	✓	✓[9]	✓[44]
Transmetalation	From $MgCl_2$[45]	From MnI_2[5c] or ate complex[5e]	From $ZnCl_2$[44]
Metal halogen exchange	✓[46]	✓[8]	✓[47]
Substitution (R_xM, x =),	1–4[48]	1–4[1a]	1–4[49]
Stability of Ar-M at rt	✓	✓	✓
Stability of *n*-butyl-M at rt	✓	✗	✓
Tolerance of functional groups	Low-medium	Medium	Medium-high
Influence of NMP	Coordination of Mg^{2+}	unknown	Influence of equilibria[50]

However in view of the available redox states, manganese differs from its counterparts as it can adopt many more redox states. Nevertheless, no application of organomanganese halide reagents specifically using redox chemistry for synthetic purposes is known. In synthesis, manganese can be problematic as its chloride salt is low in solubility and the synthetic routes have been discussed in this chapter. To this end, available synthesis starting from i) the metal, e.g. Rieke metal or by surface activation or ii) metalation with reactive amide bases are known for all three metals.[51]

All of the compared reagents are capable of forming different homoleptic organyls (cationic $[RM]^+$, neutral $[R_2M]$, mono- $[R_3M]^-$ or dianionic $[R_4M]^{2-}$) compounds which are reported for the metal(+II) oxidation states. Other examples can be found in literature, such as hexaalkynyl mangantes(+III).[52] Nevertheless, the synthesis of anionic homoleptic manganese reagents is potentially to easiest synthetic avail, as equilibria or harsher reductants are often necessary in cases of magnesium.[48a] Albeit zincates can be obtained, generally these undergo complex equilibria with the present counterions.[53] Even so, equilibria of organomanganates are not reliably characterized, which makes their synthetic availability potentially questionable.

One drawback of manganese reagents is their lower stability under ambient or elevated temperatures. This generally applies more to the β-hydrogen containing molecules which therefore have to be synthesized at lower temperatures. Even so in certain instances in published literature, alkyl manganese reagents could be employed at ambient temperatures in presence of polar co-solvent NMP.[21] This co-solvent is also known in chemistry of organomagnesium and -zinc reagents: In studies on iron-catalyzed cross-coupling of Grignard reagents, NMP is a key stabilizer coordinating to magnesium cation allowing to form the reactive iron species. In turn, organozincate equilibria are known to play a crucial role for Negishi-type couplings.[54] These equilibria are salt dependent and inherently influenced by polar co-solvents such as NMP.[53-55] Hence, while NMP likely has an effect on all compared organometallic reagents, its influence potentially varies.

In view of the functional group tolerance, organomanganese reagents despite their reactivities tolerate similar functional groups compared to their zinc analogues with few exceptions. This might be key to enable new cross-coupling methodologies for organic synthetic purposes, especially with their similarity to Grignard reagents. Therefore, of interest when employing organomanganese reagents are iron-catalyzed cross-couplings lacking functional group tolerance due to inherent use of Grignard reagents. As this comparison demonstrates, the chemistry of organomanganese reagents is similar to the respective orgomagnesium or -zinc reagents in distinct properties. However, inherent practical drawbacks or higher toxicity might limit their usability.

3.1.2 Iron-Catalysis and Grignard Reagents

3.1.2.1 Early Developments

Iron-catalyzed cross-coupling reactions utilizing Grignard reagents have been intensively researched in recent decades and extensively reviewed.[56] The study of these reactions was pioneered by reports of Kochi on the role of iron in Kharasch-type reactions.[56l] In this work, catalytic amounts of iron were first observed to couple alkenyl bromides **35** with aliphatic Grignard reagents **34** (Scheme 3.12).[57]

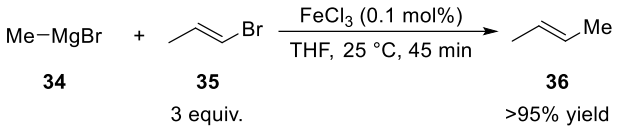

Scheme 3.12. Pioneering example of a cross-coupling of Grignard reagent and alkenyl bromides studied by Kochi and co-workers.[57]

In a subsequent report, a mechanism for this reaction was postulated by Kochi. Namely, an Fe^{+I}/Fe^{+III} catalytic cycle was hypothesized with the central steps based upon 2-electron processes: oxidative addition of the vinyl bromide **(A)**, transmetalation **(B)** and reductive elimination **(C)** of product **36** (Scheme 3.13).[58]

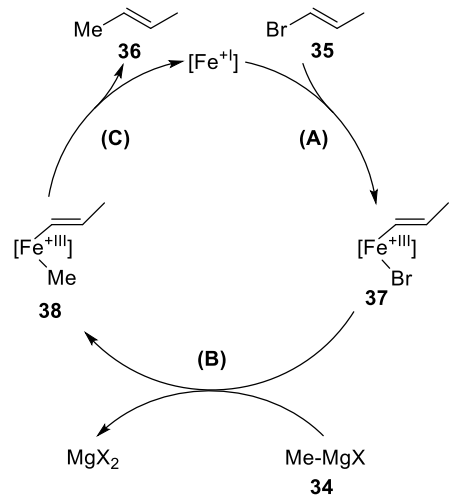

Scheme 3.13. Kochi and co-workers' postulated Fe^{+I}/Fe^{+III} reaction mechanism for the iron-catalyzed vinylation of Grignard reagents.[58]

While these observations reflect a germane example of an iron-catalyzed cross-coupling, the required excess of halide and limitations in terms of Grignard reagents were striking shortcomings of the method. Thereafter, 1,2-dimethoxyethane (DME) was identified as suitable solvent increasing the reaction yields while enabling to lower the amount of necessary vinyl halide.[59] Decades after Kochi, Cahiez and co-workers demonstrated in a key study that by utilization of polar co-solvent NMP, the excess of vinyl bromide **39** was circumvented, rendering this reaction more broadly applicable (Scheme 3.14).[60]

Notably, while NMP performed best, a spectrum of polar co-solvents, such as DMF or DMA, furnished high yields as well. Additionally, it was demonstrated that the iron precatalyst had almost no influence on the reaction outcome and that vinyl chlorides and iodides were converted under the same conditions. Futhermore, it was observed that even at short reaction times, catalyst loadings as low as 0.01 mol% still catalyzed the reaction with slightly decreased yields. With these results, the field of Fe-catalyzed cross-couplings gained increasing momentum.

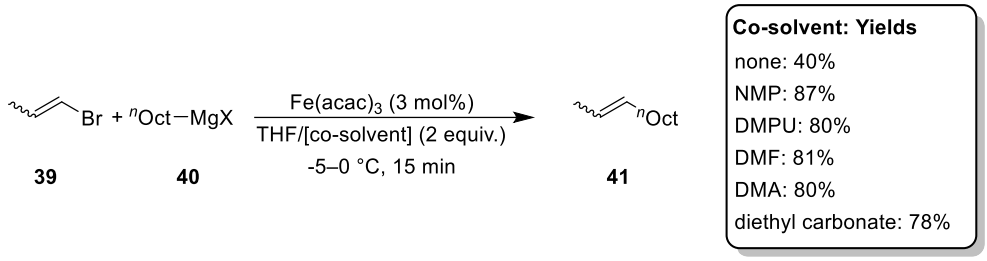

Scheme 3.14. Cahiez and co-workers' observations of the influence of polar co-solvents on iron-catalyzed cross-coupling of Grignard reagents.[60]

3.1.2.2 Different Iron-Catalyzed Cross-Coupling Reactions

Expanding on the methodologies from Cahiez, Fürstner and co-workers explored the reaction further by converting aryl halides **42**, e.g. aryl chlorides, tosylates and triflates, in excellent yields (Scheme 3.15).[61] However, in their study, iodides and bromides performed comparably poorly. This is distinctly different from trends in palladium-catalyzed C(sp^3)-C(sp^2) cross-couplings as chlorides or tosylates are considered more challenging.[59, 62] The main competition reaction in this case was observed to be a dehalogenation of aryl bromides and iodides leading to lower yields. As a characteristic property, the reaction proceeds under mild temperatures without any ligand. However, this advantage is usually limited to the coupling of alkyl magnesium halides with available β-hydrogen atoms.

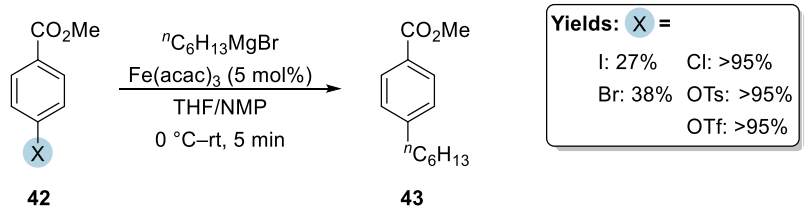

Scheme 3.15. Fürstner and co-workers' C(sp^3)-C(sp^2)-coupling of aryl halides with Grignard reagents under iron-catalysis.[61]

Hence, the cross-coupling of aryl Grignard reagents has been a topic of interest, especially for coupling of secondary alkyl halides, e.g. **44**. These electrophiles are generally more difficult for cross-coupling reactions due to their stronger C-halogen bond, increased steric bulk and intermediates prone to β-hydrogen elimination. This reaction has been achieved using Fe^{+III}-salen complexes[63], a low-valent Fe^{-II} complex[64], $Fe(acac)_3$ (though, necessitating diethyl ether as solvent and 2 equivalents of organometallic reagent)[65] and an Fe^{+III} chloride-tmeda system[66]. In quest for practicality, optimization was achieved by developing a simple to prepare and storable tmeda-ligated iron-precatalyst (Scheme 3.16).[67]

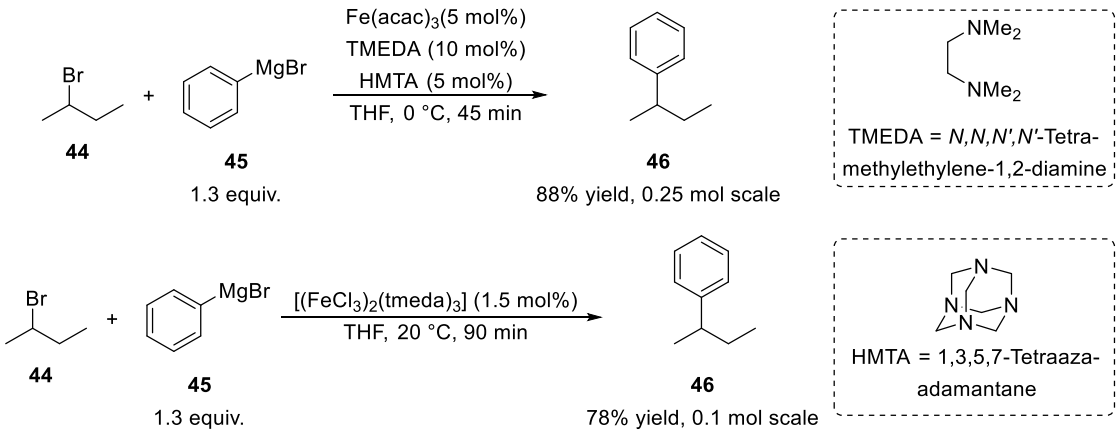

Scheme 3.16. Comparison of larger-scale reactions employing Cahiez and co-workers' iron-precatalyst for C(sp^2)-C(sp^3) cross-coupling.[67]

Advantageously, it also decreased the catalyst loading necessary for the conversion. In a separate report, this system was implemented in a one-pot reaction was by mixing aryl halide, alkyl halide, magnesium, TMEDA and iron salt.[68]

In contrast to alkyl halides, the cross-coupling of aryl halides is associated with major challenges as homo-coupling of both, nucleophile and electrophile, thwarts high yields – also in case of benzylic substrates.[56j] A key achievement of iron catalyzed C(sp^2)-C(sp^2)-cross-coupling has been that fluoride anion can facilitate the reaction (Scheme 3.17).[69] It was proposed that the suppression of the formation of unproductive organoferrate side products would be inhibited by strong coordination of the fluoride to the transition metal. Additionally, the employment of a N-heterocyclic carbene (NHC) ligand such as **L1** was mandatory as it suppressed the competing homo-coupling. Against this background, iron alkoxides were demonstrated to possess similar reactivity to fluorides in combination with NHCs, due to their strong bonding to the metal center.[70]

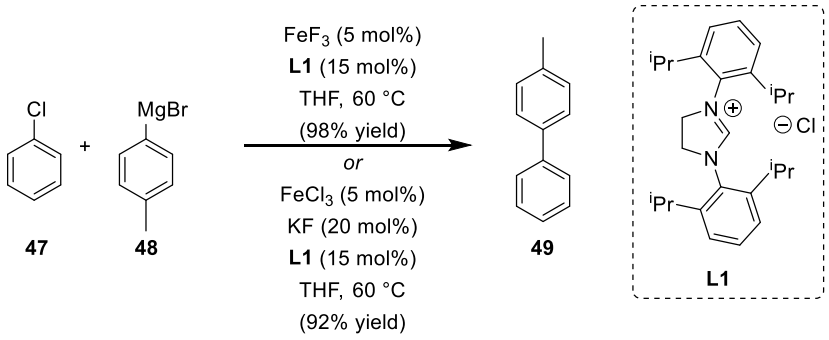

Scheme 3.17. An iron-catalyzed C(sp^2)-C(sp^2) cross-coupling of phenyl chloride with an aryl Grignard reagent by Nakamura and co-workers.[69]

As one of the main challenges, the role of a suitable ligand for iron has been affecting the optimization of cross-couplings. Next to NHCs other competent ligands were reported, such as TMEDA[67], Salen[63], β-aminoketonates[71], ionic liquids[72], amine bisphenolates[73], Pincer-type ligands[74], monodentate phosphites/arsines[75] and bidentate phosphines/arsines[75].[76] Especially well reported for C(sp^2)-C(sp^3) cross-coupling is the utilization of 1,2-bis(diphenylphosohino)benzene (Dppbz, **L2**)-based ligands. Although initially only superior in terms of decreasing the metal-ligand ratio - from 1:2 to 1:1[77] - the Dppbz-derived 1,2-bis[bis(3,5-di(*tert*-butyl)phenyl)phosphino]benzene (SciOPP, **L3**) ligands have been established as a proficient promotor in similar transformations. In contrast to the smaller bite angle of Dppbz-type ligands (Figure 3.3), the bidentate phosphine (9,9-Dimethyl-9*H*-xanthene-4,5-diyl)bis(diphenylphosphane) (Xantphos, **L4**) has been reported to enable challenging C(sp^3)-C(sp^3) cross-couplings.[78]

Generally, the employed ligands are regarded as necessary to circumvent the formation of aryl ferrate complexes, which are considered too unreactive and lead mostly to homo-coupling. Nevertheless in one report, a chiral Dppbz-type ligand has been leveraged to promote an enantioselective coupling of secondary alkyl chlorides with aryl Grignard reagents.[79]

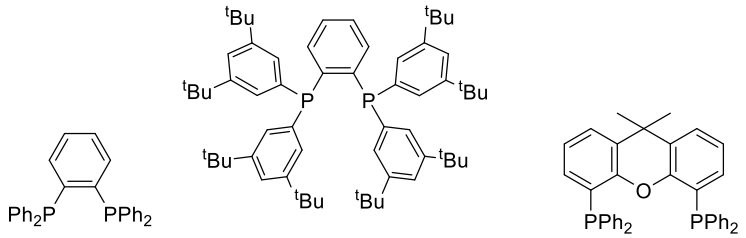

Figure 3.3. Comparison of bidentate phosphine bite-angles for iron-catalyzed cross-coupling reactions.[80]

Against this background, the spectrum of cross-couplings has been examined further by e.g. Sonogashira-type reactions[81], flow chemistry[82] or visible-light-promotion.[83] Especially, the high reactivity for activation of non-halide electrophiles is a potentially useful approach for synthesis. To this end, iron-catalyzed cross-coupling with Grignard reagents have been repeatedly validated (Table 3.3). Next to these versatile range of possible activations, the propensity for homo-coupling of iron for aryl Grignard reagents has been leveraged in biaryl synthesis.[84] As the merits of some of the mentioned reactions depend on the employment of NMP, substitution of this reprotoxic co-solvent is also a major goal. Greener alternatives such as *N,N′*-dimethylpropyleneurea (DMPU) or *N*-butyl pyrrolidone (NBP) have been reported to perform similarly.[85] When compared, NBP is preferred as DMPU possesses reprotoxic properties. Another potential approach in substituting NMP was exemplified in works of Cahiez, which utilized *in situ* formed iron thiolates in $C(sp^3)$-$C(sp^2)$ cross-coupling.[86]

While the discussed literature precedence mainly focused on Grignard reagents, methodologies have been explored using other organometallic or -metalloid compounds, e.g. organoboronic esters[87], organozinc[88], -aluminium[78b], -manganese[31–32, 60] and even -lithium[89] reagents.

Table 3.3. Overview of electrophiles coupled using Fe-catalyzed cross-coupling reactions with Grignard reagents extended upon from cited references.[56c, 56k, 90] The table does not represent current state of research in full and reports utilizing catalytic or stochiometric copper additives are omitted. (**highlighted**: The character of the electrophile.)

Grignard reagent	Alkyl (sp^3) 	Aryl (sp^2) 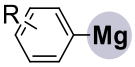	Alkynyl (sp) 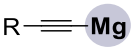
Electrophile:			
Alkyl (sp^3) 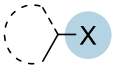	**$sp^3_{(prim.)}$**-Br[78c]/I[91]	**$sp^3_{(prim.)}$**-F[92]/Cl[64, 77]/Br[63-64, 67, 71-75, 93]/I[64, 66, 73-74]	**sp^3**-Cl[94]/ Br[94]/I[94]
		$sp^3_{(sec.)}$-Cl[66, 71–72, 75, 79, 93]/ Br[63–67, 71–75, 93]/I[66, 71–75]	**$sp^3_{(sec.)}$**-Br[95]/ I[95]
Alkenyl, aryl (sp^2) 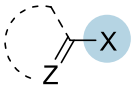	**$sp^2_{(vinyl)}$**-Cl[60, 82, 86]/Br[60, 86]/ I[60, 86] OTf[96]/OAc[97]/ OPiv[98]/carbamate[99]/SAr[100]	**$sp^2_{(vinyl)}$**- OTf[96]/OR[90]/OAc[97]/ OTs[101]/SAr[100]	**$sp^2_{(vinyl)}$**-Br[81]/ OTf[81]
	$sp^2_{(hetero-, aryl)}$-Cl[61, 85a, 102]/ OTf[61, 102]/phosphate[103]/ sulfamates[104]/carbamates[105]/ OTs[104, 106]	**$sp^2_{(hetero-, aryl)}$**-Cl[69–70]/ OTf[96]/OTs[101, 106]/ phosphate[103, 107] /sulfamates[101]	**$sp^2_{(hetero-, aryl)}$**-I[108]
	$sp^2_{(acyl)}$-Cl[96]/SR	**$sp^2_{(acyl)}$**-Cl[96]/CN[109]/SR[110]	
Alkynyl (sp) 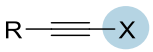	**$sp_{(alkynyl)}$**-Cl[82]		

3.1.2.3 Organoferrates

Existing research recognizes the central role of anionic iron (ate) complexes for cross-coupling reactions.[56a] While π-alkene organoferrates have been associated with species in C(sp^2)-C(sp^2)-cross-couplings[111], σ-organoferrates are heavily involved as catalytic intermediates. Indeed, the absence of ligands for a lot of iron-catalyzed cross-couplings, points towards σ-organoferrates as important species. With regards to chemical implications, it has to be pointed out that the nature of *in situ* synthesized ferrates is highly susceptible to a variety of influences. As a representative example, the investigations into Kochi's methylation of vinyl bromides (Scheme 3.12) underline the complexity of iron-catalyzed cross-coupling reactions. Methyl lithium with iron-precursor at low temperatures **(A)** was reported to

form a stabilized tetramethylferrate(+II) (**50**) with tetrahedral coordination which was characterized *via* crystallization and X-ray spectroscopy (Scheme 3.18).[112]

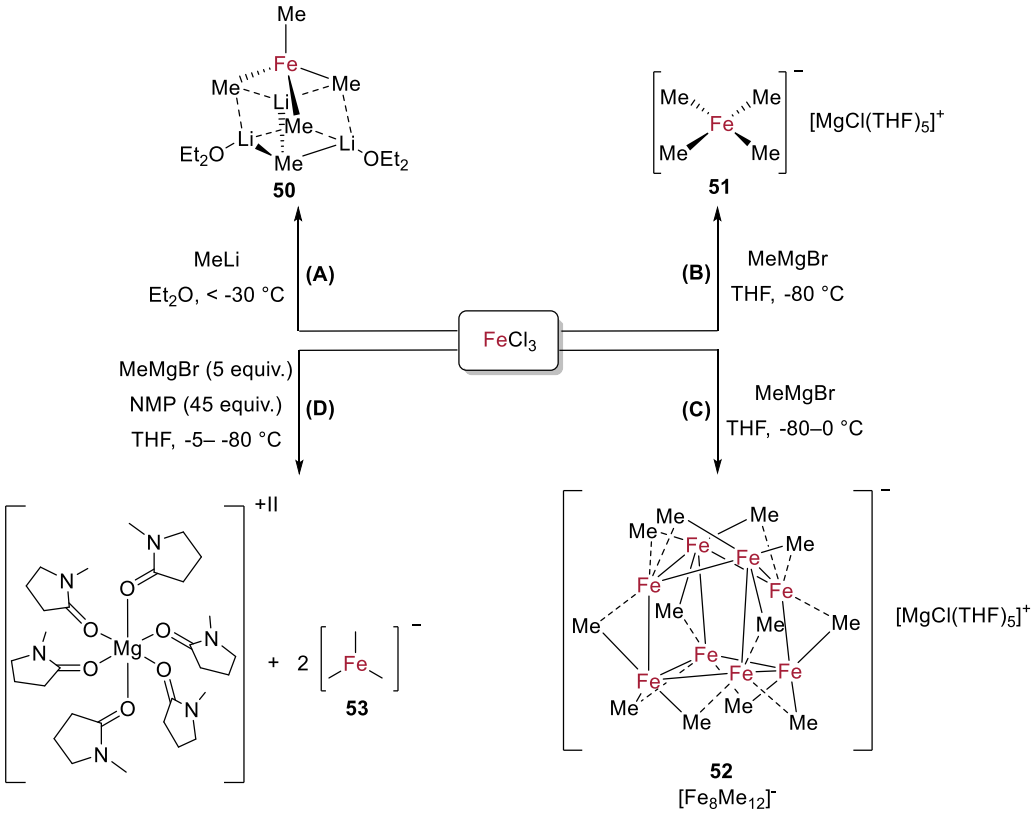

Scheme 3.18. Methylation of iron trichloride with different reagents leading to different species observed. Adapted from cited reference.[56l]

In contrast, the reaction with respective methyl magnesium bromideled to a different outcome **(B)**: the formation of homoleptic tetramethylferrate(+III) (**51**).[113] This ferrate appears to be prone to decomposition. With increased temperatures, it forms a cluster with the composition $[Fe_8Me_{12}]^-$ (**52**), possessing an average oxidation state of 1.4 **(C)**. Also, this compound has been characterized by crystallography and EPR and crucially corresponds to Kochi's observed intermediary species with $S = 1/2$.[114] Even so, NMP was reported to be capable of effecting this speciation. Therefore, in presence of the polar co-solvent a homoleptic trimethylferrate(+II) (**53**) was observed **(D)**.[115] In conceptual terms, not the structures themselves but the reactivities of the displayed complexes reflect the crucial importance of this speciation. For instance, the *ipso*-coordinated tetramethylferrate(+II) (**50**) is incompetent in converting aryl chlorides, yet, can convert aryl triflates or acyl halides.[116] DFT studies for the substitution of acyl halides have supported evidence that all four methyl groups can be transferred.[117] This reflects an alteration of reactivity known in case of the respective iron salt-Grignard reagent system. The cluster **52** formed in the absence of NMP could perform $C(sp^3)$-$C(sp^2)$ coupling, but only with additional Grignard reagent present.[114] Furthermore while the cluster is consumed in presence of electrophile, only traces of coupling have been observed. In comparison, the furnished iron-species **53** in presence of NMP was demonstrated to solely and quantitatively perform methylation of the same $C(sp^2)$-electrophile.[115] In view of this, the number of substituents but also the redox state is

affected by counter ions (Li^+ vs. Mg^{2+}), employed Lewis-basic stabilizers (NMP) and thermal conditions.

For clarity, these influences do furnish different iron species which can undergo cross-coupling-type chemistry or not. Respectively, not only methyl ferrate but also $[FeEt_3]^-$ (**55**) was observed spectroscopically to form in presence of NMP (Scheme 3.19).[118] Similarly, this homoleptic iron compound was found to be able to perform cross-coupling reactions without any additional reagent necessary. In absence of NMP, a cluster was characterized *via* X-ray spectroscopy with the formula $[Fe_8Et_{12}]^{2-}$ (**54**) with the only deviation of possessing an average redox state of 1.6 rather than 1.4 to the analogous methyl species **52**. This cluster was also unable to perform methylation on its own.

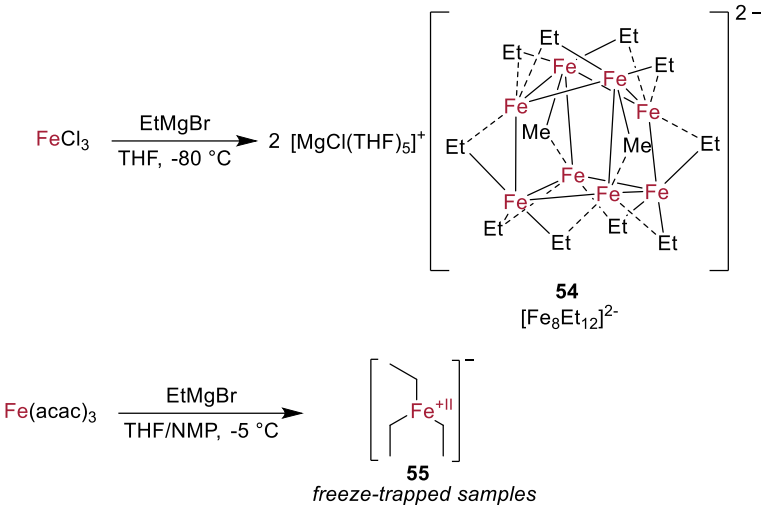

Scheme 3.19. Synthesized ethyl ferrate cluster or monomeric triethylferrate(+II) by Neidig and co-workers.[118]

As another example, benzylic ferrates also led to the formation of a similar type trisbenzylferrate(+II). For these tantamount organometallic species, slow oxidation was observed to furnish tetraalkylferrate(+III).[119] To this end, ESI-MS studies have supported the formation of the mentioned aliphatic alkylferrates(+III) when iron salt is exposed to Grignard reagent.[120] Although the method is blindsided by the neglection of non-charged species, $[FeR_4]^-$ compositions have been observed with *n*-hexyl-, *n*-octyl-, and *n*-decyl-magnesium bromide – with a prolonged lifetime for longer alkyl chains. Importantly, in these ESI studies the formation of $[Fe^{+III}R_4]^-$ was observed even quantitatively regardless if Fe^{+II} precursor was exposed to Grignard reagent which usually leads to reduction rather than oxidation. Nonetheless, the patchwork of ferrates was not strongly influenced by the presence of stochiometric amounts of TMEDA. Rather, the additive was reported to slow decomposition processes.

Regarding aryl ferrates, these also have been discerned to be readily influenced by bulk and molecular properties. Yet, even more competitive reactions in comparison to alkyl substituents complicate the overall reactivity: Dimeric structures, steric bulk of the aryls, the nucleophilic character of the transmetalation reagent, *ipso*-coordination can shift the equilibrium *in situ* of triarylorganoferrates(+II) to tetraarylorganoferrates(+III) and *vice versa*.[56f] For instance, reports exemplify this reactivity in

synthesis of homoleptic ate complexes such as $Fe(Mes)_3^-$ (**56**) which is readily formed from either $FeCl_2$ or $FeCl_3$ and mesityl magnesium bromide (Scheme 3.20) - in the latter case an extra equivalent of Grignard is necessary to reduce the metal.[119]

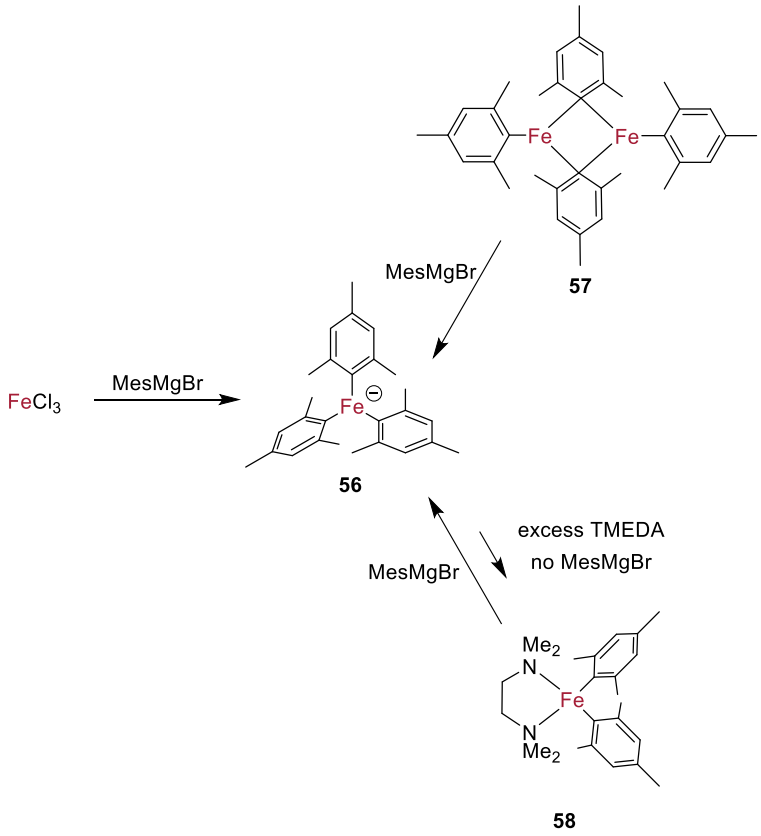

Scheme 3.20. Synthesis and equilibria of the stable trismesityliron(+II) complex.[119]

This iron-complex was shown to successfully react with octyl bromide. Upon treatment with excess TMEDA a complexation was observed but found to be partially reversible. The aptitude of organoferrates has been demonstrated in ESI studies where in case of phenyl a mixture of mainly $[FePh_3]^-$, $[FePh_4]^-$ and $[Fe_4Ph_7]^-$ was observed.[120] For this speciation, an influence of the oxidation state of the precursor was mentioned, which led to less cluster formation but also heterobimetallic complexes (e.g. $[Ph_5MgFe^{+III}Cl]^-$) when Fe^{+II} was employed. Formation of the higher aggregates was reported to be circumvented in the presence of TMEDA.

Regarding these literature reports, the closely related research to organyl ferrates is enabling insights into potential mechanistic pathways for iron-catalyzed cross-couplings.

3.1.2.4 Mechanistic Hypotheses

In view of the discussed reactivities of iron with Grignard reagents, a multitude of mechanistic proposals have been reported. Historically first, Kochi's postulated catalytic cycle was an initial attempt for a concise mechanism, an Fe^{+I}/Fe^{+III}-catalytic cycle (Scheme 3.12).[58]

Another prominent proposition for a reaction mechanism has been postulated by Fürstner. Namely, the formation of low-valent ("super-ate") iron species promoted by the reduction with alkyl Grignard reagent.[112] Particularly, low-valent ferrate(-II)-species, e.g. **59**, have been proposed to form and activate C-halogen bonds **(A)** (Scheme 3.21).

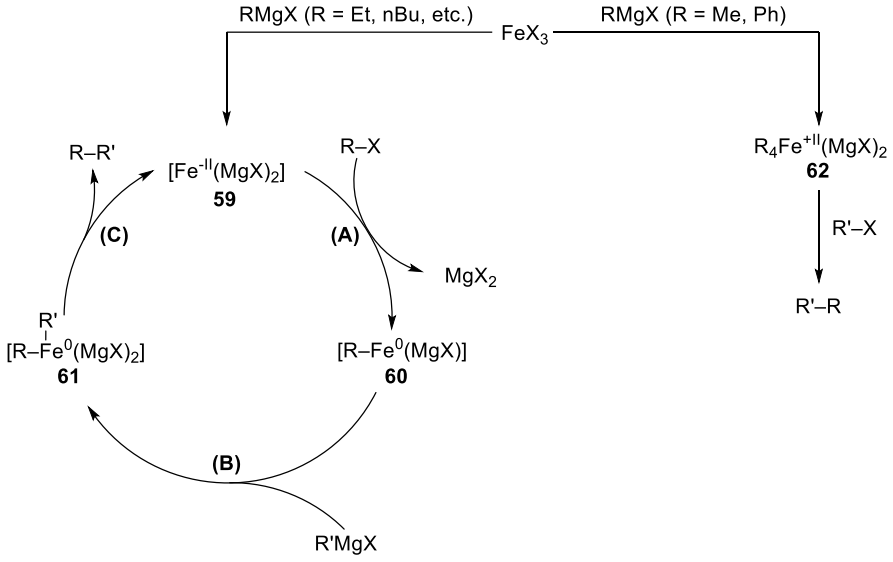

Scheme 3.21. Super-ate complex-based mechanism for the iron-catalyzed cross-coupling of Grignard reagents.[112]

Further mechanistic steps follow a general cross-coupling mechanism: transmetalation **(B)** and reductive elimination **(C)**. This postulated mechanism was based upon previous insights into the formation of inorganic Grignard reagents (IGR).[56c] These heterobimetallics with a general formula of MMgX - in which M is a different metal than magnesium – have been associated with iron-catalyzed synthesis of Grignard reagents.[121] Therein, the access of such low-valent iron species **59** was attributed to the access of a β-hydrogen elimination pathway.[112] Besides this, the active species for non-β-hydrogen containing Grignard reagents was proposed to be an organoferrate-type compound **62**.[112] This mechanism has been scrutinized and in view of further research, where it was even stated that iron(-II) intermediates are no longer considered relevant intermediates.[56j, 56k] However, the organoferrate manifold crucially still holds relevance.

Moreover, in recent literature the deeper understanding of ferrate chemistry led to the formulation of mechanisms without low redox states. The plethora of postulated mechanisms are ranging from $Fe^{+I}/Fe^{+II}/Fe^{+III}$[122], $Fe^{0}/Fe^{+I}/Fe^{+II}$[67], Fe^{+I}/Fe^{+III}[83], Fe^{+II}/Fe^{+II}[123], Fe^{+II}/Fe^{+III}[124] to Fe^{0}/Fe^{+II}[111] redox couples.[56l] At this point however, it is pertinent to consider the discussed differences in formation of

species when employing alkyl or aryl transmetalation reagents. Therefore, speciation differs when employing alkyl instead of aryl organometallic reagents. Also, the utilization of ligands and additives such as SciOPP, TMEDA or NMP arguably influences the reactions on- or off-cycle.

Most prominently in elucidation of the catalytic mechanism, the activation of the electrophile is a central aspect next to the formed molecular species. The bandwidth of considered activation processes consists of: single-electron-transfer (SET), atom-transfer (AT), oxidative addition (OA), S_N2-type, or σ-bond metathesis.[125] Not uncommonly, mechanistic proposals that include Fe^{+I} do consider radical pathways (Scheme 3.22, **(A)**) as an alternative to oxidative addition **(B)** to furnish the Fe^{+III} species **65**. In terms of activation from **64** to furnish **65**, radical clock experiments indicate single-electron processes **(A)**.[78a] Other instances elaborate on this, postulating a favored atom-transfer-initiated radical pathway from the alkyl halide, depending on the solvation of active catalyst.[125–126] Additionally, gas-phase fragmentation studies have supported the feasibility of a reductive elimination pathway from Fe^{+III} for $C(sp^2)$-$C(sp^3)$[127] and $C(sp^2)$-$C(sp^2)$[128] cross-coupling.

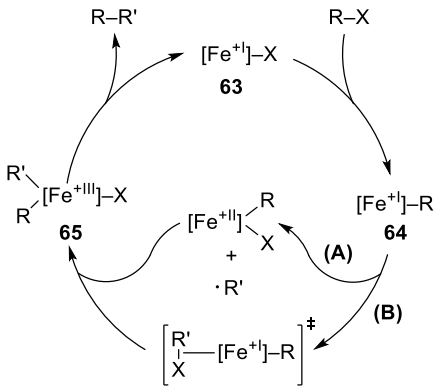

Scheme 3.22. A general mechanism including Fe^{+I} intermediates with either two-step radical addition or oxidative addition.[56j, 56k, 78a]

Recent investigations on the influence of TMEDA have demonstrated an elaborate role of Fe^{+II} intermediates. These were isolated and their structures characterized as well as observed in ^{57}Fe Mössbauer spectroscopy. For this, a similar mechanism was postulated, however, transmetalation occurred from Fe^{+II} intermediates **66**. Therefore, the crucial slow addition of Grignard reagent was connected to the suppression of off-cycle species **70** (Scheme 3.23). These results were studied in depth especially for $C(sp^2)$-$C(sp^3)$ cross-couplings, but ^{57}Fe Mössbauer spectroscopy results also indicated similar mechanisms for $C(sp^3)$-$C(sp^2)$ couplings. Even so, the latter reaction is usually performed in absence of TMEDA and might therefore follow a different pathway. These results on the role of TMEDA contrast reports in which the ligand was postulated to only act as a stabilizer for off-cycle reaction species, thereby, inhibiting catalyst decomposition.[129] Investigations into iron-catalyzed hydromagnesiation additionally indicated that TMEDA can help in assisting the reduction process of iron species.[130]

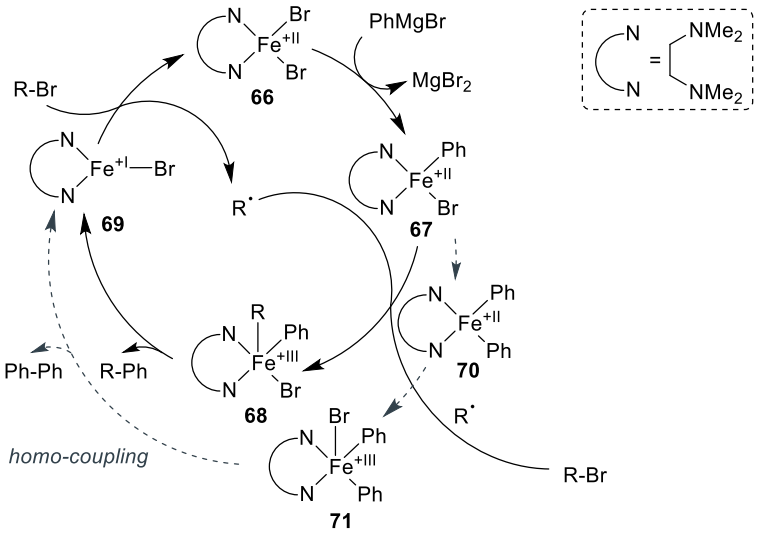

Scheme 3.23. Postulated $Fe^{+I}/Fe^{+II}/Fe^{+III}$ mechanism of tmeda-ligated iron.[122]

Other mechanistic proposals consider non-reductive elimination pathways as alternative (Scheme 3.24). This reaction proceeds with an organyl radical abstraction and therefore exclude reactive Fe^{+I} intermediates. Similarly to the aforementioned central role of **66**, it was deduced that mainly non-charged intermediates react with facile ligand exchange.[126b] Therefore, transmetalations proceed if the organometallic reagent can affect the Fe^{+II} intermediate. Additionally, a connection between the homo-coupling and the nature of nucleophile was postulated. Other related mechanistic proposals additionally include bimolecular activation processes, thereby, also excluding Fe^{+I} intermediates.[56k]

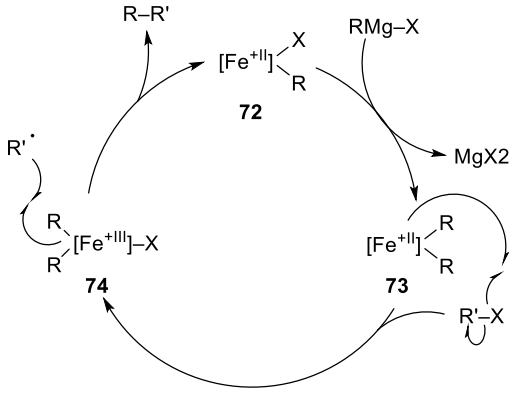

Scheme 3.24. Postulated mechanism for a Fe^{+II}/Fe^{+III} catalytic cycle.[94, 126b]

By contrast, the studies of $C(sp^2)$-$C(sp^2)$ cross-coupling in absence of ligand or additive were reported to be majorly influenced by the electronic properties of the coupling partners. Interestingly for a potential Fe^0/Fe^{+II} redox couple, stabilization was reported to be achieved by coordination with Mg^{2+}-counterions.[131] To this end, it was observed that the competing Grignard homo-coupling is enabled by the metalation of the electrophile **76** (Scheme 3.25).[111] This inherently leads to a competition of homo- *vs.* cross-coupling products which renders these reaction difficult in terms of selective product formation.

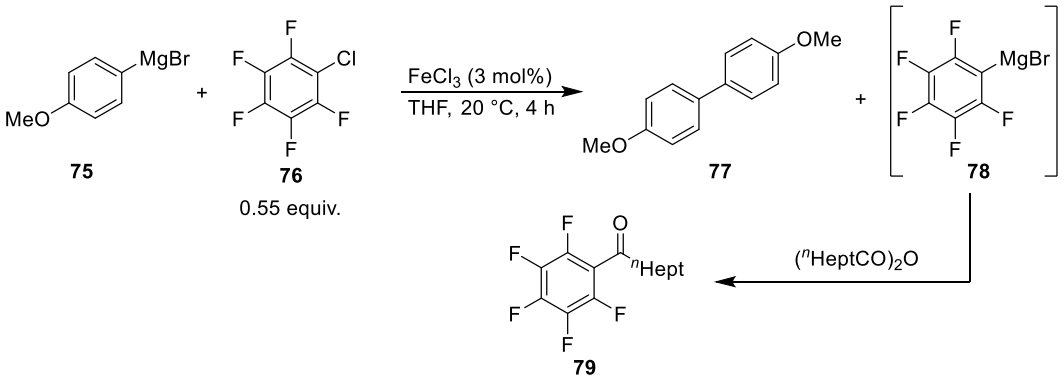

Scheme 3.25. Studies on cross-coupling of aryl Grignard reagents with aryl halides demonstrating the metalation of the electrophile.[111]

In view of these reports, the understanding of iron-catalyzed cross-couplings has increased tremendously in the last decades, but still requires further research. While different mechanistic proposals are reported, a lot of clear indications have been identified in case of ligand-promoted cross-couplings. Nevertheless, no wholistic understanding of the mechanisms has been achieved in absence of ligands or additives.

3.1.3 Approaches in Acylation Chemistry

Ketones are an ubiquitous compound class in organic synthesis. Reactions to obtain ketones include a wide range from non-catalytic to catalytic methodologies. One of the possibilities to synthesize ketones is the reaction of carboxylic acid derivatives with organometallic reagents. Generally, for such a reaction, the broadly available acyl halides are unsuited as carboxylic acid derivatives in non-catalytic synthesis of ketones when utilizing Grignard reagents.[132] For this, significant side product formation is reported in literature. This is due to a problematic subsequent addition of organometallic reagent even at low temperatures leading to high amounts of tertiary alcohol and other side products, diminishing reaction yields.[132–133] To this end, the use of certain carboxylic acid derivatives as acyl donors is a common approach, allowing very specific transformations suitable for late-stage functionalization and preventing overaddition. Examples of acyl donors that react without a transition metal-catalyst include prominently Weinreb-amides[134] **80**, Staab-Joost imidazolides[135] **81**, acyl hydrazides[136] **82**, certain Boc-protected amides **83**[137] or *S*-(2-pyridyl thioesters) **84**[138] (Scheme 3.26). Generally, these acyl building blocks stabilize the primary tetrahedral addition product **85** due to a chelation of the magnesium center with a donor moiety (D).

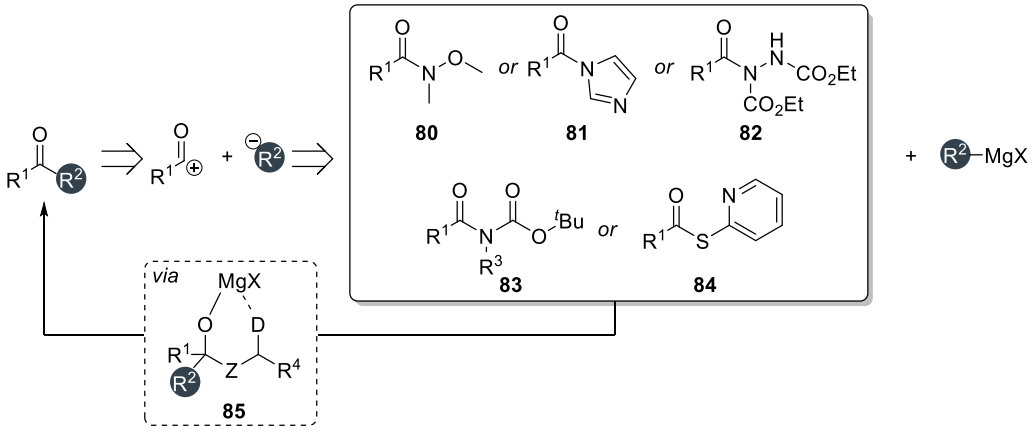

Scheme 3.26. Starting materials and intermediate for non-catalytic synthesis of ketones by reaction with Grignard reagents.[134-138]

Related methods have been disclosed in literature such as ligation of Grignard reagent with an additional ligand[132], 1,4-addition of released thiolate thereby creating a chelating donor *in situ* [139], flow-chemistry steered reactions[140] or less reactive organometallic compounds.[5c, 141] Similar to the ligation, employment of Grignard amide adducts **88** have been demonstrated to convert carboxylates directly into phenones **89** (Scheme 3.27).[142]

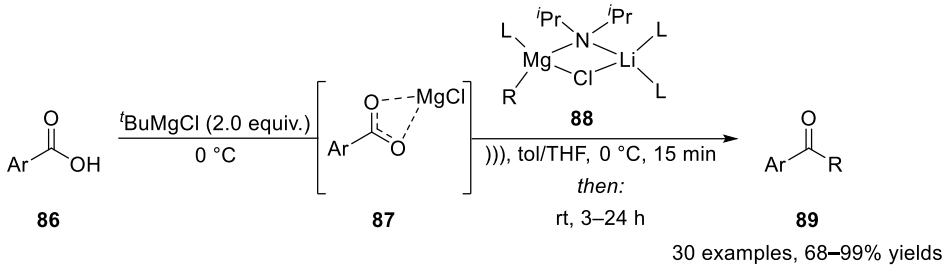

Scheme 3.27. Activation of carboxylic acids *via* Grignard reagents and reaction with Grignard amide.[142]

Albeit, circumvention of catalytic methodology might be an attractive choice, higher selectivity and higher yields can incentivize the utilization of transition metal-catalysis. Equally to non-catalytic methods, a multitude of acylation building blocks have been explored for cross-coupling purposes, e.g. reactive acyl chlorides **90**[88a, 96, 143], acyl fluorides **91**[144], (*in situ* formed) anhydrides **92**[145], thioesters **93**[146], 2-pyridyl esters **94**[147], phenyl esters **95**[148], specific amides **96**[149] or acyl imidates **97**[150] (Figure 3.4).

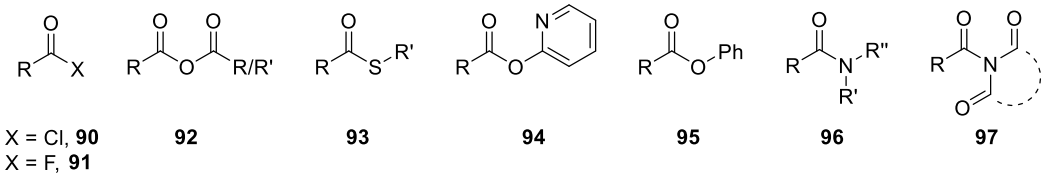

Figure 3.4. Overview of acylation reagents utilized in transition metal-catalyzed cross-coupling.[88a, 96, 143–150]

Amongst these reagents, acyl chlorides possess the highest reactivity which has been leveraged in a variety of ketone syntheses utilizing a plethora of organometallic reagents.[151] Conveniently, the acylation of Grignard reagents was also achieved using iron-catalysis (Scheme 3.28).[96] Although low temperatures are mandatory for the reaction, the conversion of **90** occurs more rapidly than the competing 1,2-addition. Therefore, the methodology enables the synthesis of ketones **99** with a tolerance of functional groups such as esters, aryl chlorides/bromides or olefins.

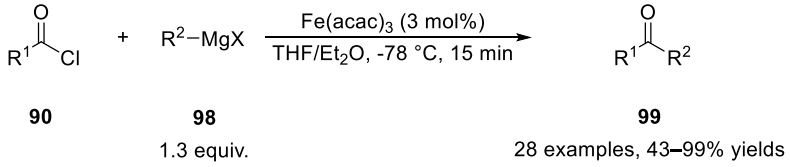

Scheme 3.28. Acylation of Grignard reagents utilizing iron-catalysis.[96]

As a related methodology, the coupling of benzylic and aryl zinc reagents was reported under iron catalysis (Scheme 3.29).[88a] While the method lacked high yields for alkyl acid chlorides, the utilization of zinc reagents diminished side reactions leading to high yields. However, it has to be mentioned that the reaction proceeds without catalyst in yields up to 74%.

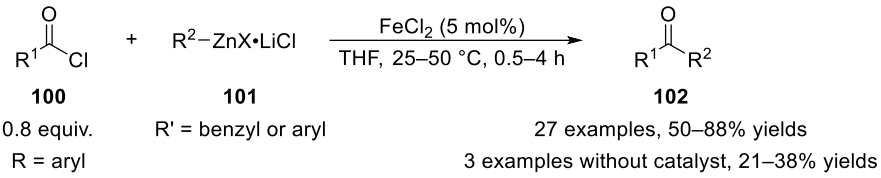

Scheme 3.29. Cross-coupling of acyl halides with benzyl- or aryl zinc reagents furnishing ketones.[88a]

Although less reactive than acyl halides, thioesters constitute a noteworthy compound class as their acylating reactivity is a key reaction in biochemistry, e.g. acetyl CoA (formation of citrate during tricarboxylic acid cycle)[152], long chain aliphatic acyl CoA (carrier during β-oxidation)[153] or acetoacetyl CoA (intermediate in the mevalonate pathway)[154]. Also, thioesters bear several advantages in chemical synthesis: Firstly, they are accessible *via* thiolytic cleavage of carboxylic acid derivatives (such as esters, amides[155] or – more specifically – Evans-auxiliary[156]) or by Wittig reaction.[157] Secondly, they are accessible *via* catalytic functionalizations, e.g. thiocarbonylation[133, 158] or coupling of thiocarboxylic acids[159] further incentivizing late stage introduction. Thirdly, thioesters are comparably stable and can be stored for a long period of time on shelf without decomposition and do not necessitate immediate conversion. Lastly, the released thiolate can be exploited, e.g. in reactions such as Michael-addition[139] or subsequent cross-coupling[160].

An inherent property of thioesters is their ease in activation under transition metal-catalysis. This is due to a poorer orbital overlap with the more diffuse *S*-orbitals leading to a more reactive ester moiety.[133] With pioneering examples from Fukuyama, thioesters **93** have been employed in either ketone synthesis using organozinc reagents (Fukuyama cross-coupling, FCC, Scheme 3.30) [146a, 161] or reduction with silanes furnishing aldehydes (Fukuyama reduction, FR)[162] under palladium-catalysis. In case of the FCC, very mild conditions and short reaction times allowed for a tolerance of functional groups such as esters, aldehydes or olefins.

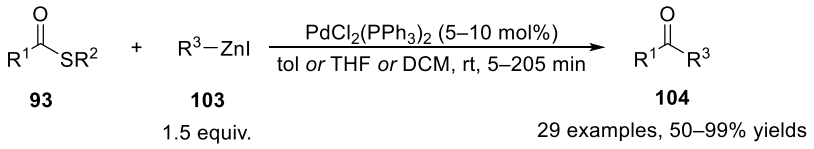

Scheme 3.30. Original FCC procedure to synthesize ketones from thioesters and organozinc iodides.[161]

Therefore, this reaction was later successfully employed in the synthesis of biotin.[163] FCC has also proven valuable in pharmaceutical compound synthesis such as isoprekinamycin[164], eribulin[165] or SLGT2 inhibitors[166].[167] As an example, within the synthesis of anthramycin, thioester derivative **106** (Scheme 3.31) was demonstrated to undergo Stille-coupling at the vinyl iodide moiety under palladium catalysis which demonstrates a remarkable chemoselectivity.[156a]

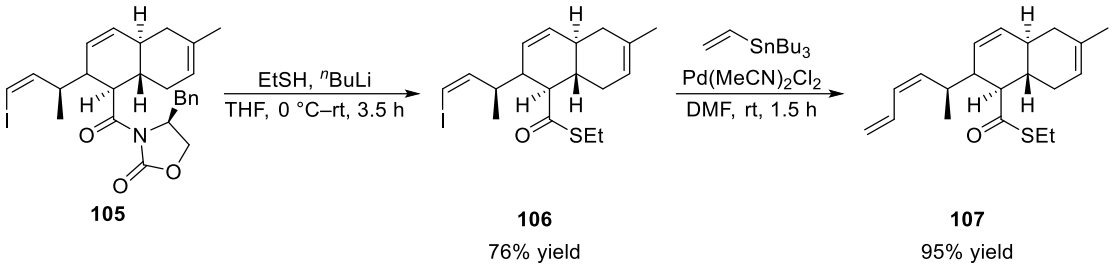

Scheme 3.31. Chemoselective Stille-coupling during the synthesis of antharamycin.[156a]

Further reports on palladium-catalyzed FCC included a phosphine-free reaction[146b], the employment on Pd-nanoparticles[168] or an enantioconvergent synthesis by coupling of racemic benzylic organozinc reagents with thioesters using bulky TADDOL-derived phosphoramidite ligands.[146c] Efforts also have been devoted to the utilization of carbon organometalloids as it incentivizes more versatile methods. Therefore, the scope of FCC has been broadened by the employment of boronic esters (Liebeskind-Srogl coupling)[169], organostannanes[170] and organoindium compounds[171]. However, as a disadvantage, the mentioned methods rely on stochiometric copper additives.

Replacement of palladium with more cost-efficient base metals have also been examined in case of FCC. A pioneering example for this is the utilization of nickel acetyl acetonate as precatalyst.[172] Despite its simplicity, the method suffered from high amounts of biphenyl byproduct which is a liability especially during purification. In solving this problem, efforts of the Fleischer group have resulted in the utilization of an air and moisture stable nickel precatalyst **C1** which suppressed the homo-coupling reaction (Scheme 3.32).[173]

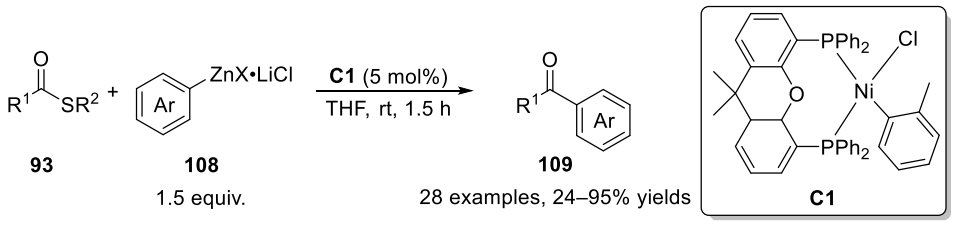

Scheme 3.32. Ni-catalyzed FCC utilizing an air- and moisture stable precatalyst to synthesize phenones.[173]

With nickel present, the reaction additionally exhibited isomerization reactivity as well as activation of aryl chlorides. The latter enabled the formal insertion of a phenyl moiety in the thioester C-S bond by first FCC and a subsequent C-S cross-coupling. In another study, the more active *S*-(2-pyridyl)thioesters **84** were shown to react with excess aryl zinc pivalates **110** under cobalt catalysis (Scheme 3.33).[174] However, both methodologies are limited to the synthesis of phenones as alkyl zinc reagents could not be utilized in these cross-couplings. Then again, rare examples of alkynylations were achieved *via* palladium-catalysis employing alkynyl pivalates.[175]

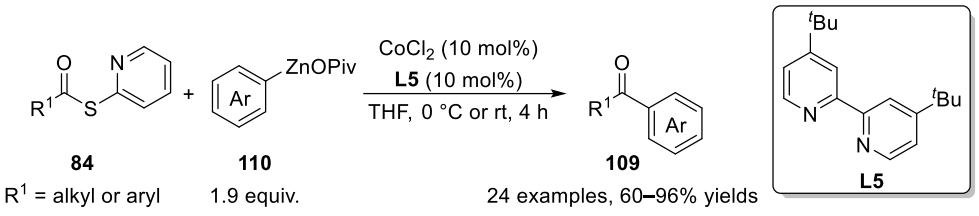

Scheme 3.33. Cobalt-catalyzed cross-coupling of organozinc pivalates with thioesters.[174]

Recent efforts in cross-electrophile coupling have constituted another potential application of thioesters. With their propensity for activation, thioesters could be leveraged in a nickel-catalyzed cross-electrophile-coupling with *N*-hydroxyphthalimide (NHP) esters.[176] In view of these literature reports, the acylation of organometallic reagents with first-row transition metal-catalysts has been less explored. This further incentivizes studies that furnish target structures with a higher degree of functionalization than phenones.

3.2 Aims of This Chapter

Recent reports for the cross-coupling of thioesters with organometallic reagents have often been limited by the reactivity of the transmetalation reagent. Typically, Grignard reagents frequently lead to side product formation and organozinc reagents possess limitations due to their lower reactivity, which incentivized further research.

Such potential liabilities make organomanganese reagents, known for their intermediary reactivity, predestined for the synthesis of a broad range of functionalized molecules. Since organomanganese reagents were less commonly studied in previous literature on cross-coupling reactions, the development of an iron-catalyzed acylation was coveted as both transition metals are highly abundant, low in toxicity and possesses low carbon footprints. Furthermore, the acylation by thioesters was determined to be beneficial due to their stability on shelf under air and moisture conditions as well as purification by normal phase chromatography. In view of these advantages, the study should: i) investigate the synthesis and reactivity of organomanganese reagents; ii) include a wide exploration of thioesters substrates expanding the scope known in literature; and iii) scrutinize potential intermediates, thereby gaining further insights in iron-catalyzed cross-coupling in the absence of additional ligands.

3.3 Results and Discussion

3.3.1 Synthesis of Organomanganese Reagents

Alkyl manganese halides synthesized from the manganese chloride precursor were mainly employed in this study. The utilization of chloride precursor **111** was due to previous descriptions in literature with a reported ease in synthesis and comparably high temperature stability.[5e] Aliphatic manganese chlorides possessing β-hydrogen atoms were reported to react at temperatures up to rt, although, only in presence of 1-methylpyrrolidin-2-one (NMP).[21] Surprisingly, the synthesis of ethyl manganese bromide lithium chloride complex (**112**) was observed to proceed in acceptable yields only at -20 °C (Scheme 3.34). Moreover, warming solutions of **112** to rt led to effervescence, the formation of black colloids and almost complete loss of reactivity. Hence, optimization of the synthesis was desired.

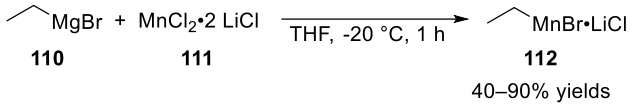

Scheme 3.34. Synthesis of ethyl manganese bromide lithium chloride complex.

Previous studies on cross-coupling reactions recognized an influence of polar co-solvents like 1,3-dimethylimidazolidin-2-one (DMI) or NMP on reagents such as organomagnesium or organozinc reagents as discussed previously (see chapter **2.1.1**, p. 23).[49b, 54, 115] In terms of manganese reagents, catalytic conversions have been reported employing NMP as co-solvent at up to ambient temperatures.[21] Experimental observations with organomanganese solutions indicated differences with or without NMP, as only the latter visibly degraded faster to black tar. To probe this, decomposition of both solutions was monitored *via* Knochel iodometric titration (Scheme 3.35).[177] In three separate experiments with varying amounts of NMP, concentration was measured with increased temperature to monitor the decomposition of reagent **112**.[177] The results indicated decomposition to occur almost independently of co-solvent and amount thereof. Measured equivalents of iodine consumed by titration, slightly increased at 40 °C for measurements with excess NMP. While the measurement is prone to error especially at such low concentrations, it was hypothesized to be complicated by decomposition products.

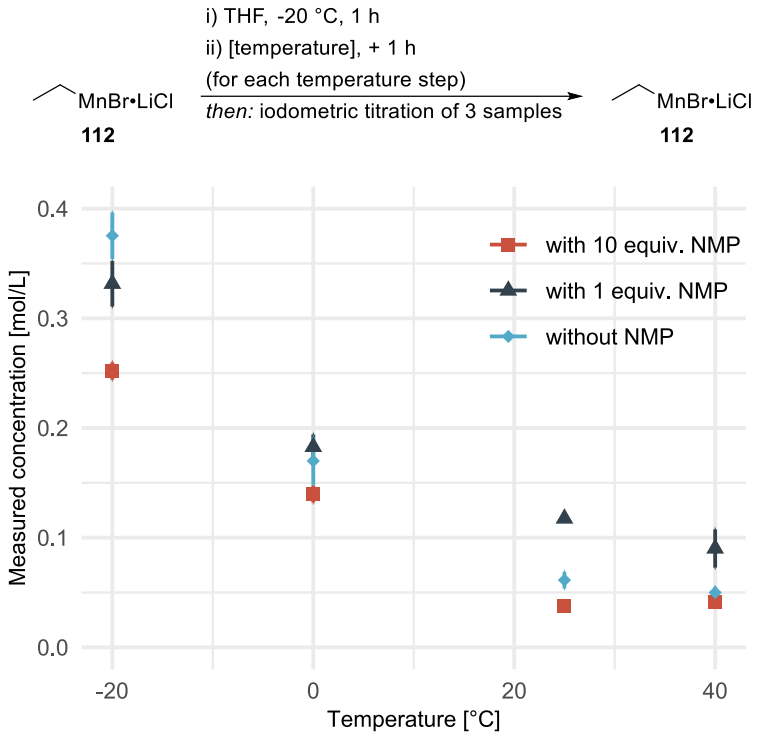

Scheme 3.35 Measured concentration of organomanganese reagent in solution by Knochel iodometric titration. Each point represents the average and standard deviation of three titrations from the same solution.

The forming suspension (with or without NMP) likely contained reduced manganese(0) particles **113d** due to β-hydrogen elimination or homo-coupling. Potentially formed **113d** would react with iodine and result in measurement errors (Scheme 3.36). Therefore, it was not possible to reliably determine whether the employment of NMP as co-solvent might circumvent the necessary cooling to -20 °C.

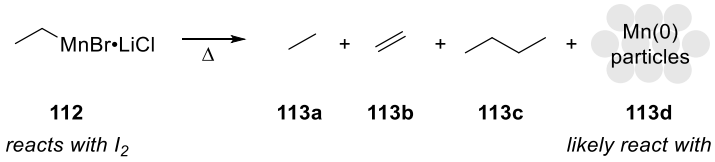

Scheme 3.36. Potential decomposition reactions for aliphatic manganese reagents.

Subsequently, the experiment was adapted: Separate reaction solutions of *n*-octyl manganese bromide (**114**) with or without NMP were quenched with an excess of iodine and products were quantified *via* GC-FID (Scheme 3.37). As a major advantage, the experiment allowed for the detection of multiple decomposition products such as homo-coupling and β-hydrogen elimination. In view of the isothermal results at -20 °C **(D)**, a rise in 1-octene concentration **(A)** as well as a loss of organomanganese reagent **(B)** were detected. The decomposition proceeded seemingly independent to the rise of temperature from –20 to 5 °C **(D)**. Interestingly, the concentration of **(A)** was observed to decrease at elevated temperatures, potentially forming another side product. At 0 °C–rt an increased concentration loss was confirmed, which remarkably ceased at a certain threshold **(B)**.

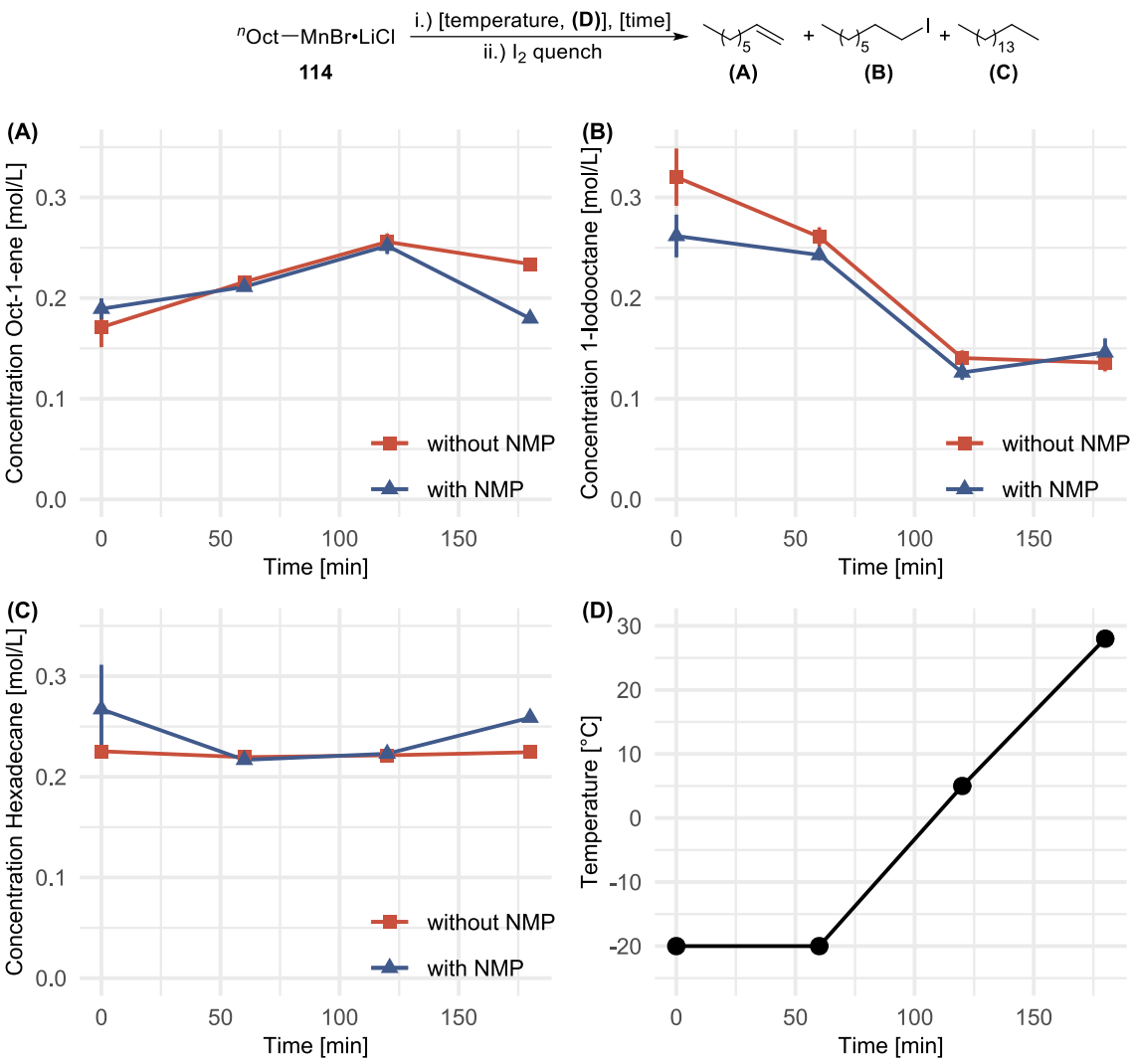

Scheme 3.37. Quantification of decomposition products of *n*-octyl manganese halide dependent on temperature. Each measuring point reflects the average and standard deviation of three separate samples from the same stock solution.

A third peak was identified *via* GC-MS as hexadecane which would likely be formed by homo-coupling of **114**. Seemingly, **(C)** is not affected by increased temperatures except for the reaction with NMP. Therefore, it was assumed that the concentration is likely originating from the synthesis of Grignard reagent and/or initial side reactions of the transmetalation reaction.

Similarly problematic to the unsolved issue of reagent decay, repeatedly no appreciable amount of organomanganese halide was afforded *via* transmetalation. The reaction yield was observed to be susceptible to experimental parameters such as the use of - at best - freshly purchased stirring bars. Therefore, it was attempted to modify the transmetalation procedure. Firstly, bypassing the ate complex **111** by using only manganese dichloride in a suspension and slow addition of Grignard reagent furnished no yield and reacted with strong effervescence (Table 3.4 – Entry 1). In comparison to literature examples, similar transmetalation conditions were described to be successful, lithium reagents were employed at low temperatures[8] or - in a recent report - with a freshly milled manganese salt in a anisole slurry which was limited to the synthesis of methyl manganese.[178] The addition of TMEDA to

previously low-yielding ate complexes led only to similar diminished yields (Table 3.4 – Entry 2). Furthermore, manganese(II) acetyl acetonate (acac) as slightly soluble precursor failed (Table 3.4 - Entry 3). Related to Cahiez's procedure employment of tetra-*n*-butyl ammonium halide salt instead of lithium chloride did not furnish any meaningful transmetalation yield (Table 3.4 – Entry 4).[179] Additionally, highly reactive Rieke metals were probed.[180] However, even with these reactive metallic particles, the synthesis of organomanganese reagent did not proceed (Table 3.4 – Entry 5). This was reasoned by the mandatory low temperature (-20 °C), which conflicts the ambient conditions usually applied when synthesizing them from Rieke metals. However, the results stand in contrast to literature reports in which β-hydrogen containing alkyl bromides could be converted with Rieke manganese. Then again, the literature method was relying on excess amount of bromide and 1,2-dibromoethane additive.[9]

Table 3.4. Attempts in synthesis of ethyl manganese reagent.

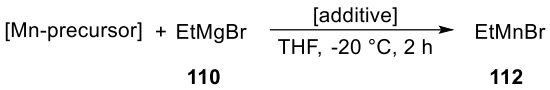

Entry	Manganese precursor	Further deviation	Yield (%)[b]
1	$MnCl_2$	Slow addition	✗
2	$MnCl_2$•2 LiCl	TMEDA (10 mol%)	✗
3	$Mn(acac)_2$		✗
4	$MnCl_2$•2 $N(^nBu)_4I$		✗
5	From Mn(0)*	instead EtBr	✗
6	$Mn_6(O)_2(OPiv)_{10}$	-50 °C–rt	✗

In one literature report, the utilization of manganese pivalates was mentioned with reagents such as $(PivO)_2(Bu)MnLi$ but their synthesis was not reported.[16] Even though, pivalate ligation were hypothesized to be able to stabilize manganese reagents alike to the corresponding organozinc reagents.[181] In an attempt to synthesize manganese pivalates only oligonuclear Mn^{II+}/Mn^{III+} clusters were obtained in presence of oxygen which were described literature.[182] To obtain preliminary results, manganese pivalate cluster was exposed to Grignard reagents at low temperatures and slowly warmed up to rt (Table 3.4 – Entry 6) which did not afford any meaningful yield. Then again, the manganese precursor contained Mn^{+III} which could have facilitated the loss in yield.

Although organomanganese reagents have been optimized in the last decades to become a synthetically useful option, the synthesis of non-stabilized β-hydrogen containing manganese reagents still suffers from the necessity of ate complex synthesis, which can cause problems in terms of yield and reproducibility. Moreover, the synthesized reagents suffer from an observable overall decomposition and therefore rely on daily new synthesis and concentration determination.

3.3.2 Initial Screening

The designated reaction was already investigated in the authors Master Thesis.[183] Therein, the reaction was probed for a potential Ni-catalyzed reaction, however, did not furnish yields above 60%. During these studies, iron was already identified as a potential transition metal catalyst, but reaction optimizations were not finalized. Reinvestigation of the reaction was conducted by screening other potentially catalytically active transition metals (Table 3.5).

Table 3.5. Metal-screening for the cross-coupling of thioester **115a** with ethyl manganese reagent **112**.[a]

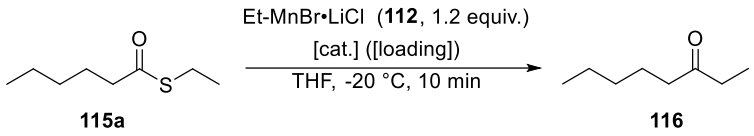

115a **116**

Entry	Deviation from std. conditions	Loading (mol%)	Conversion (%)[b]	Yield (%)[b]
1	No catalyst	-	18	0
2	$Ni(acac)_2$	5	95	52
3	$CoCl_2$	10	81	64
4	$Mn(acac)_3$	5	62	5[a]
5	CuI	10	44	37
6	$PdCl_2(PPh_3)_2$	5	26	18
7	$FeCl_2$	10	92	82
8	$Fe(acac)_2$	5	quant.	89
9	$FeCl_3$	10	99	84
10	$Fe(acac)_3$	5	quant.	91
11	$Fe(acac)_3$	1	99	86
12	$Fe_2(tmeda)_3$	5	99	89

[a]: Reaction conditions: **115a** (53.4 mg, 333 µmol, 1 equiv.), EtMnCl•LiCl (400 µmol, 1.2 equiv. based on titre in THF), dry THF (1 mL), -20 °C, 10 min. [b]: Quantification *via* GC-FID measurement using *n*-pentadecane (100 µL) as internal standard.

The reaction did not afford product without any catalyst present (Table 3.5 – Entry 1). This further confirms that the organomanganese reagent itself or any impurities stemming from manganese precursor do not potentially catalyze the reaction. Other late first-row transition metal salts reproducibly only afforded poor to good yields (Table 3.5 – Entries 2–5). It is important to point out, that mediocre yields were obtained employing a copper precatalyst, as instances are known in literature in which supposed iron-catalyzed reactions were enabled by copper impurities.[56j, 184] The palladium precatalyst from Fukuyama's original cross-coupling procedure performed only poorly, although reaction times of both reactions are similarly short (Table 3.5 – Entry 6).[161] Gratifyingly, results with iron led to very good yields under the applied conditions. The reaction exhibited similar very good yields independent of initial iron oxidation state or anion (Table 3.5 – Entries 8+10). Lower catalyst loading led to slightly decreased yields, but with irreproducible results. Additionally, iron-tmeda-precatalyst known for

C(sp^2)-C(sp^3) cross-coupling performed similarly well (Table 3.5 – Entries 12).[67] Conveniently, any utilization of ligands (e.g. Bipy or Xantphos) resulted in lower yields.

Due to persisting differences of conversion and yield of ca. 10%, the catalytic reaction was further investigated. The difference was associated with the occurrence of an inseparable side product. This side product could not be fully characterized but led to separation problems on small scale. Since the reactivity of manganese reagent constituted a key aspect of the reaction, alternative transmetalation reagents were screened as the synthesis was repeatedly affording low yields - *vide supra*.

As a starting point, Grignard reagent was utilized, which showed precipitation in the reaction solution and afforded medium yields (Table 3.6 – Entry 1). Subsequent employment of soluble Knochel Grignard reagent performed similarly in terms of yields but exhibited lower conversions (Table 3.6 – Entry 2). Although, upon longer reaction times side products of 1,2-addition **117** and Grignard reduction **118** were observed as competition reactions (Scheme 3.38).

Table 3.6. Optimization of iron-catalyzed cross-coupling of organometallic reagents.[a]

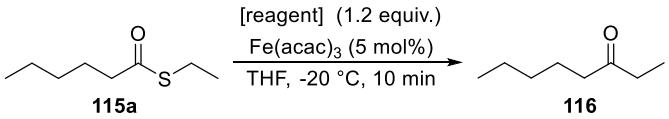

Entry	Reagent	Conversion (%)[b]	Yield (%)[b]
1	Instead EtMgBr	79	48
2	Instead EtMgBr•LiCl	59	54
3	Instead EtMgBr + 10 mol% $MnCl_2$•2 LiCl	81	67
4	Instead EtZnBr•LiCl	12	0
5	Instead Et_2Zn	48	34
6	Instead $Et_4Mn(MgBr)_2$,- 79 °C, 2 h	30	19
7	Instead Et_2Mn, -79 °C, 2 h	49	37

[a]: Reaction conditions: **115a** (53.4 mg, 333 µmol, 1 equiv.), transmetalation reagent (400 µmol, 1.2 equiv. based on titre in THF), $Fe(acac)_3$ (5.9 mg, 16.7 µmol, 0.05 equiv.), dry THF (1 mL), -20 °C, 10 min. [b]: Quantification *via* GC-FID measurement using *n*-pentadecane (100 µL) as internal standard.

Additional catalytic amounts of manganese ate complex led to increased yields, however, performed comparably worse than preformed organomanganese halide (Table 3.6 – Entry 3). Utilization of ethyl zinc halide lithium chloride complex showed no product yield as described in the preceding studies by Gehrtz et al.[173] Surprisingly, *in situ* prepared diethyl zinc yielded designated ketone, though in poor yields (Table 3.6 – Entry 5). To a similar end, manganate and diethyl manganese were used at lower temperatures due to a potential thermal decay during synthesis (Table 3.6 – Entry 6+7). Both reagents led to unsatisfactory yields. In comparison, the more reactive diethyl manganese performed better than tetraalkylmanganate, which formed a brown precipitate under the reaction conditions.

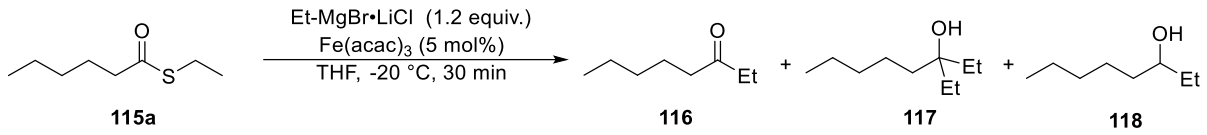

Scheme 3.38. Side products of the cross-coupling reaction with Grignard reagents observed *via* GC-MS.

As the screening on transmetalation reagents did not lead to a higher yield, different solvents were screened (Table 3.7). The results indicated that the influence of ethereal solvent was low, as THF, 2-methyl THF, 1,4-dioxane and diethyl ether all afforded **116** in very good yields (Table 3.7 – Entries 1-4). In view of reports on the influence of NMP as promoter in iron-catalyzed cross-coupling, the co-solvent was also probed.[60] However, the utilization led to slightly decreased yields (Table 3.7 – Entry 5). In line with previous literature, solvents like ethyl acetate, acetonitrile and even DCM could be used (Table 3.7 – Entries 6–8).[1a, 38] This result supports a completed transmetalation, as Grignard reagents are incompatible with these solvents.

Table 3.7. Optimization of solvents for iron-catalyzed cross-coupling of organomanganese reagent **112**.[a]

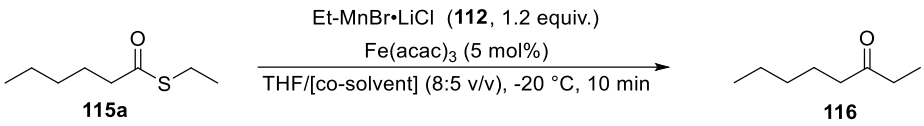

Entry	Deviation from std. conditions	Conversion (%)[a]	Yield (%)[a]
1	THF	quant.	91
2	2-MeTHF	99	93
3	1,4-dioxane[c]	98	90
4	Et_2O	99	88
5	NMP	90	84
6	EtOAc	quant.	92
7	ACN	98	78
8	DCM	83	71
9	THF[d]	quant.	98

[a]: Reaction conditions: **115a** (53.4 mg, 333 µmol, 1 equiv.), EtMnBr•LiCl (400 µmol, 1.2 equiv. based on titre in THF), $Fe(acac)_3$ (5.9 mg, 16.7 µmol, 0.05 equiv.), dry THF (1 mL), -20 °C, 10 min. [b]: Quantification *via* quantitative GC-FID measurement using *n*-pentadecane (100 µL) as internal standard. [c]: Reaction formed a slurry. [d]: THF was not degassed.

Serendipitously, an experiment was conducted employing THF with traces of oxygen present leading to quantitative yield (Table 3.7 – Entry 9). The traces of oxygen were usually obtained by only drying the solvent over molecular sieves. Albeit, bubbling air through dry and degassed THF achieved a similar increase in yield.

With optimized conditions at hand, first product **116** was isolated with 78% yield. The decreased yield was attributed to the volatility of the product and verified by an observable decrease of product amount under applied work-up conditions. While degradation was never observed during substrate

screening, exposition of pure product to reaction conditions was examined. Under applied conditions no 1,2-addition or Grignard reduction was observable with **116** (Scheme 3.39). In contrast, starting from **115a** in presence of an excess of manganese reagent (1.5 equiv.) and increased reaction times, 1,2-addition was observed.

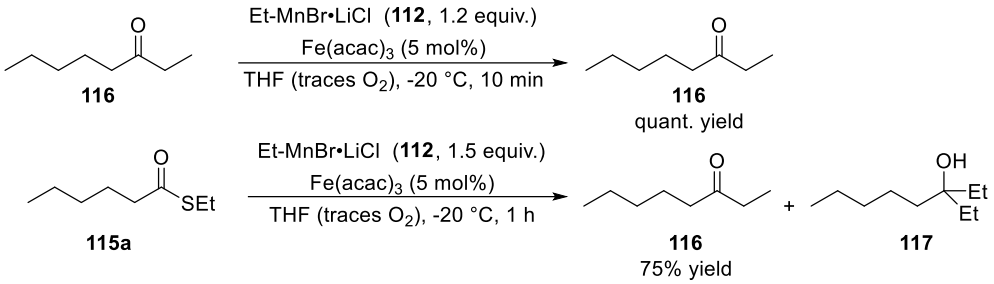

Scheme 3.39. Experiments investigating side product formation due to subsequent 1,2-addition under catalytic conditions.

Considering the complexity of the employed catalytic system, a potential influence of the thiol moiety of the thioesters was examined before substrate screening. The results exemplify an order of reactivity prim~aryl>sec>>tert (Scheme 3.40). The tertiary thiolate thioester **115d** furnished medium conversion and mediocre yields. This indicates that steric demands of the thiol scaffold can inhibit the catalysis and is in line to previous reports on thioesters being influenced by sterics.[185] Furthermore, dithioester **115e** was probed and showed only traces of side product formation. Utilization of this type of dithioester starting materials can be incentivized for low weight acyl moieties.

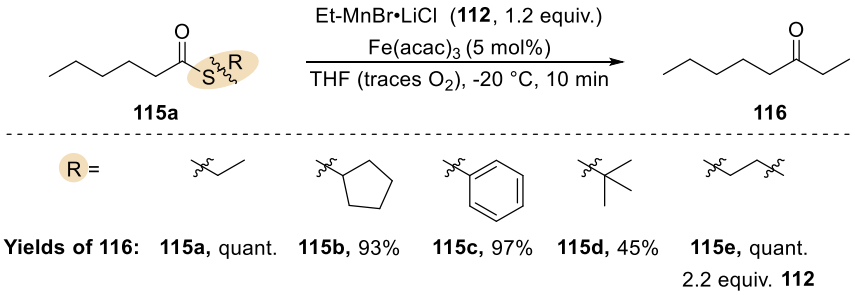

Scheme 3.40. Screening of the influence of the thiol moiety on the product yield.

3.3.3 Substrate Scope

Following reaction optimization, a substrate screening was conducted. Mainly sparsely functionalized thioesters were screened first (Scheme 3.41). Due to the volatility of low weight ketones leading to reduced yields, some substrates were converted using *n*-hexyl manganese chloride lithium chloride complex (**121**). Compound **120a** could be afforded in excellent yields and showed only slight decrease upon higher scale. The loss in yield was attributed to practical impediments such as addition and stirring speed, as the reagent is known to decompose at rt. For substrates with moieties that will be deprotonated by organometallic reagent, e.g. **120b**, additional equivalents of manganese reagent were added, which led to full conversions. As the reaction displayed a strong effervescence after quenching, it can be assumed that not all extra manganese reagent was consumed in a respective acid-base reactions. Therefore, the reaction would likely proceed with less excess of **112**.

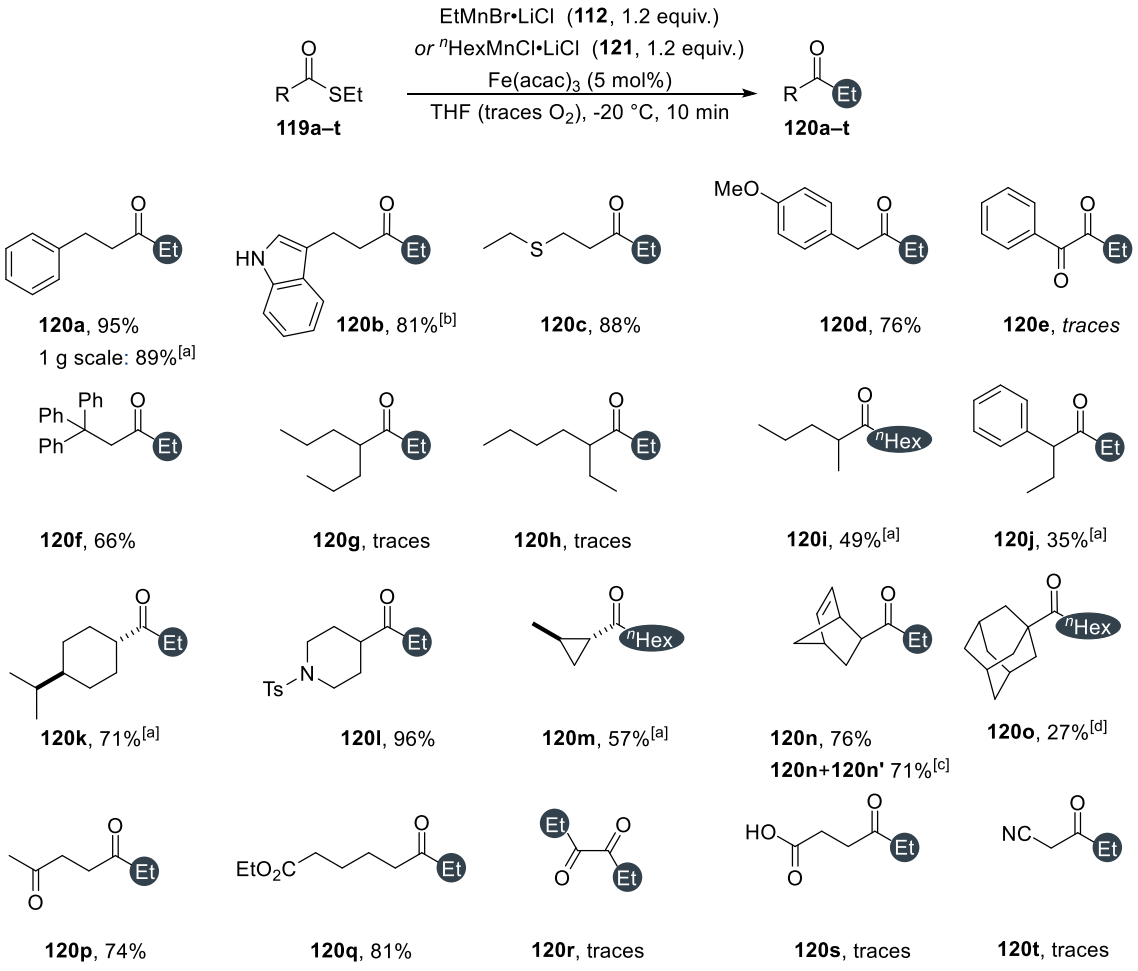

Scheme 3.41. Coupling of various thioesters with ethyl manganese bromide. Isolated yields are displayed unless stated otherwise. Reaction conditions: thioester **115a** (1 mmol, 1 equiv.), EtMnBr•LiCl or ^{n}HexMnCl•LiCl (1.2 mmol, 1.2 equiv. based on titre, usually ≤ 0.3 M in not degassed THF), $Fe(acac)_3$ (17.7 mg, 50 µmol, 0.05 equiv.), dry THF (3 mL, not degassed), -20 °C, 10 min. [a]: 15 min. [b]: EtMnBr•LiCl (2.2 mmol, 2.2 equiv. based on titre, usually ≤ 0.3 M in THF). [c]: Mixture of isomers: *endo*/*exo* = 5:3. [d]: NMR yield. [e]: EtMnBr•LiCl (3.2 mmol, 3.2 equiv. based on titre, usually ≤ 0.3 M in THF).

Thioethers **119c** were tolerated as well as benzylic substrates **119d, 119j**. No decarbonylation was observed for these substrates, while **119e** decarbonylated side products were detected by GC-MS. Increased bulk in β-position furnished 66% isolated yield **120f**, whereas secondary thioesters led to remarkably different results depending on the substituent in α-position. Interestingly, while branched substrates with methyl- or phenyl-substituents led to decreased yields, α-substituents longer than ethyl afforded only traces of product **120g**–**120j**. In stark contrast, 6-membered cyclic substrates were converted **119k, 119i** in good to excellent yields. In terms of cyclic compounds, cyclopropyl and norbornene derived thioesters furnished the products in medium to good yields **120m**, **120n**. For the latter substrate, two reactions were performed, i) with a mixed *endo/exo* diastereomers and ii) with a pure *endo* diastereomer. Both showed similar yields and no change in *endo/exo* ratio was observed. Next, the product **120o** could not be separated from the starting material and was therefore quantified *via* NMR spectroscopy. Lastly, the tolerance of a carbonyl moiety was observed for ketones and esters, but not for 1,2-dithioesters, carboxylic acids or alkyl nitriles **119p**–**119t**. Iron-catalyzed thiolysis of esters, which was described in literature for specific *O*-aryl esters with defined iron-carbonyl complexes, was not observed for any carboxylic acid derivative.[186]

The preference of primary *versus* secondary thioesters was verified in a regioselectivity experiment (Scheme 3.42). It is important to add that the conversion with 1.2 equiv. of organomanganese reagent was mainly yielding **123**, minor amounts of **124** were observed.

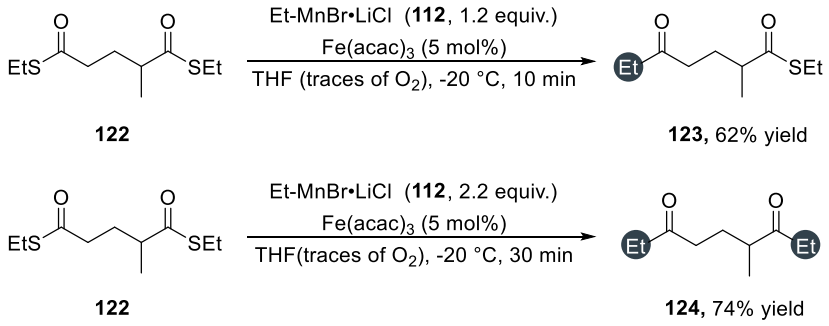

Scheme 3.42. Sequential reactivity of primary and secondary thioesters exemplifying regioselectivity. Isolated yields are displayed.

A similar reactivity could not be obtained when a phenyl group occupied the α-position to the secondary thioester group (Scheme 3.43). Both mono- and disubstituted products were observed, as well as a strong effervescence indicating unreacted ethyl manganese reagent. Possibly, the α-phenyl moiety might lead to deactivation of the catalyst leading to an incomplete consumption of manganese reagent, because multiple reproductions all showed strong effervescence during quenching even after prolonged reaction time or higher catalyst loading.

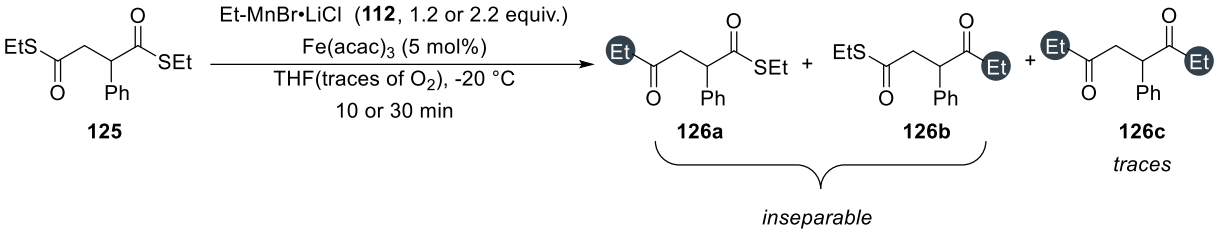

Scheme 3.43. Unsuccessful regioselectivity experiment of α-phenyl dithioester **125**.

To gain a deeper understanding, the conversion of thioesters with different steric bulk was monitored. Remarkably, differences in reaction speed were very large (Scheme 3.44). Further resolution of primary substrates was difficult to obtain. Lower reaction temperatures (-40 °C, orange) did not lead to a sufficiently higher resolution and at even lower temperatures (-79 °C) solubility issues were complicating the reaction.

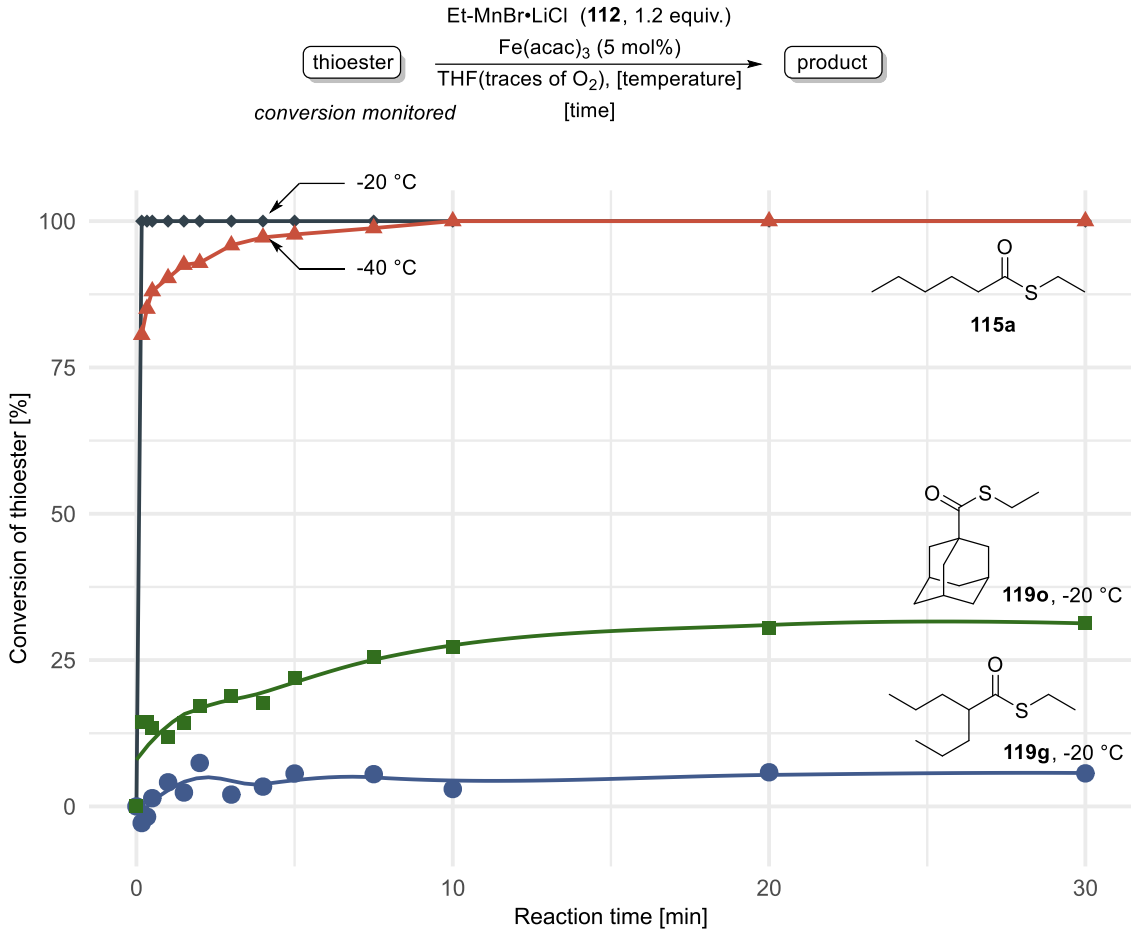

Scheme 3.44. Conversion of thioesters with different sterical demands close to the thioester moiety.

In view of the obtained trace amount of **120g**, it was hypothesized that activation of thioester might be impeded. To this end, easier activation has been recognized in literature for *S*-phenyl in comparison to *S*-ethyl thioesters.[185] This trend was confirmed as substrate **127** displayed increased reactivity and led to 50% yield based on GC-MS integral.

Scheme 3.45. Observed reaction yield of **120g** by utilization of aryl thiolates.

Next, it was elucidated whether the reaction proceeds either due to a more facile activation or due to an aryl thiolate furnishing a potentially more reactive iron species. Therefore, the synthesis of aryl iron thiolate **128** was conducted following a procedure from Cahiez and co-workers (Scheme 3.46) and it was probed as catalysts.[86] With no yield of target product observable *via* GC-MS, the results indicate that the increased reactivity of **120g** was likely enabled by a favored activation step, not due to a formation of a more active iron aryl thiolate species.

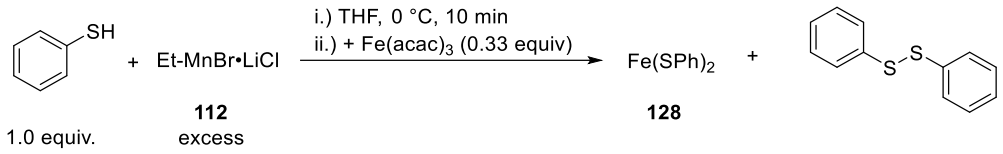

Scheme 3.46. Synthesis of employed aryl thiolate iron complexes analogously to Cahiez's studies.[86]

In comparison to primary thioesters, tertiary thioester **119o** afforded poor yields. Due to the effervescence when quenching the reaction, it was assumed that the substrate might poison the catalyst due to its steric bulk. Experimentally, this was indicated in reaction progress experiments, during which the conversion stagnated (Scheme 3.44). To probe this assumption, extra amount of precatalyst was added after prolonged reaction time, which led to further conversion of the starting material (Scheme 3.47). Therefore, a potential poisoning of the catalyst was substantiated as both coupling partners persisted in solution and side reaction was observed. Higher conversions of **119o** were obtained in this experiment than in previous reaction progress study. This was attributed to dependence of yield on concentration of organomanganese reagent and swiftness of the addition as well as mixing phenomena which led to slightly different yields in reproductions.

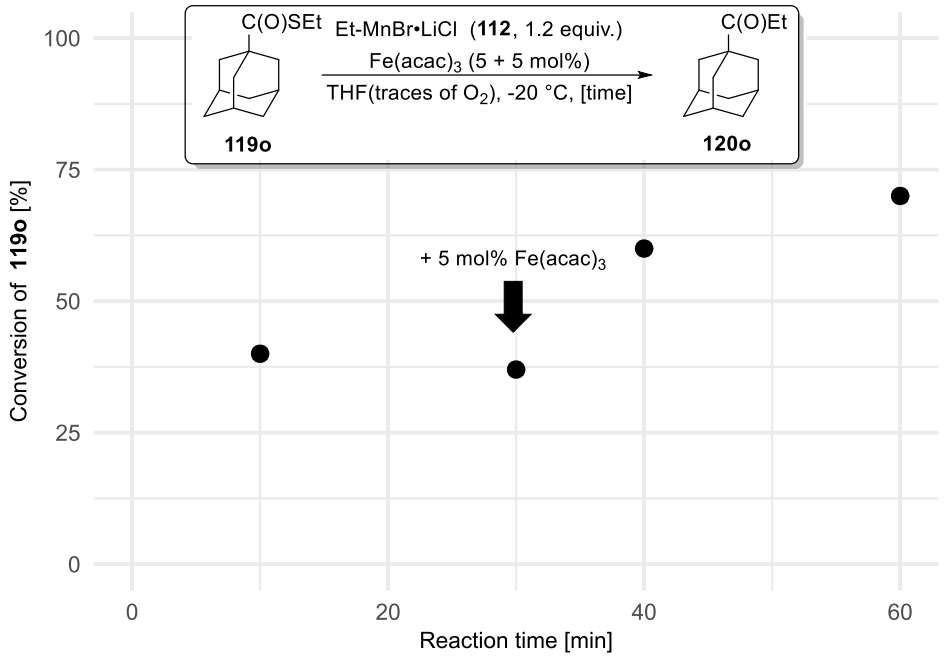

Scheme 3.47. Validation of the catalyst poisoning by readministration of iron-precatalyst.

In comparison to the previous nickel-catalyzed FCC of the Fleischer group, the methodology tolerated benzoic acid-derived thioesters (Scheme 3.48). While substituents such as Me- or MeO- were tolerated in very good to excellent yields **130b, 130c**, the reaction was possible for a range of (pseudo-)halide-substituents in medium to good yields **130d–130h**.

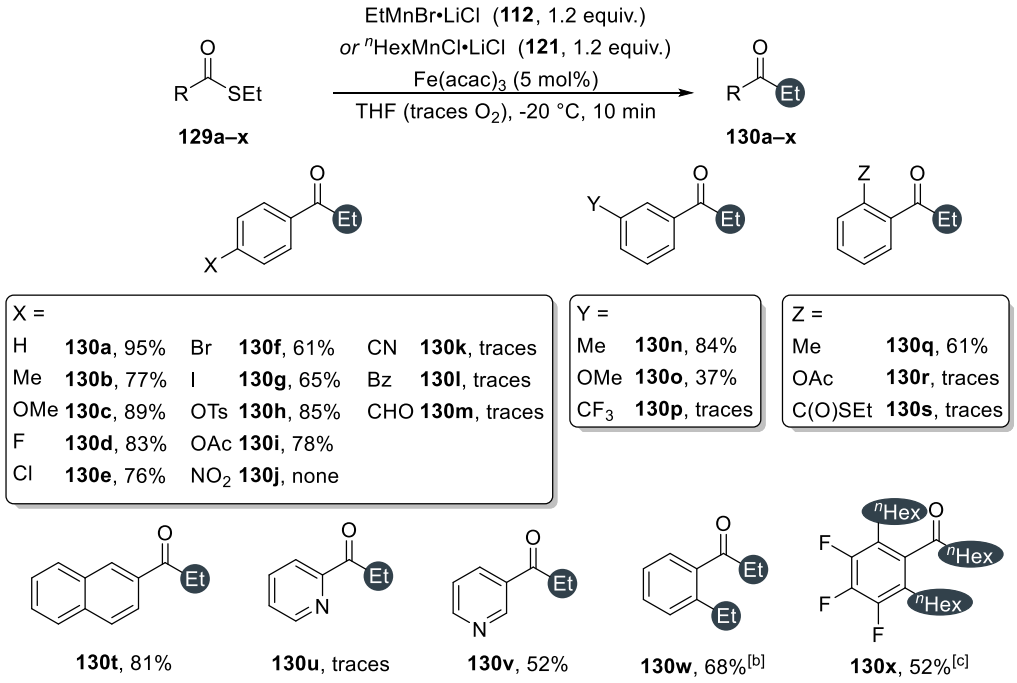

Scheme 3.48. Coupling of various aryl thioesters with ethyl manganese bromide. Isolated yields are displayed unless stated otherwise. Reaction conditions: thioester (1 mmol, 1 equiv.), EtMnBr•LiCl or ^{n}HexMnCl•LiCl (1.2 mmol, 1.2 equiv. based on titre, usually ≤ 0.3 M in not degassed THF), $Fe(acac)_3$ (17.7 mg, 50 µmol, 0.05 equiv.), dry THF (3 mL, not degassed), -20 °C, 10 min. [a]: 15 min. [b]: EtMnBr•LiCl (2.2 mmol, 2.2 equiv. based on titre, usually ≤ 0.3 M in THF). [c]: EtMnBr•LiCl (3.2 mmol, 3.2 equiv. based on titre, usually ≤ 0.3 M in THF).

While most of the substrates showed traces of subsequent Kumada coupling, even the reactive aryl iodide moiety was affording feasible yields. *Para*-sulfonate and acetate were tolerated in good to very good yields affording **130h** and **130i**. Traces of Kumada-coupling were observed for the tosylated thioester which, similar to the well performing aryl chloride, contrasts results found in literature describing the activation of these (pseudo-)halides.[61]

Not surprisingly, nitro group-containing substrate **129j** afforded only poor yields, forming a variety of side products such as anilines. However, nitriles exhibited a complete loss in yield without any formed side products which might be caused by a similar behavior as in case of **119t**. In this example, poisoning was hypothesized, as well. Therefore, to a reaction solution of **129k** standard substrate **115a** with further manganese reagent was added (Scheme 3.49). As almost no yields were observed for both thioesters, this validates a likely poisoning of the catalyst due to the nitrile group. Notably, this contrasts the results of the optimization screening in which acetonitrile as solvent performed with acceptable yields. Other substituents, which suppressed the desired reactivity, were benzoyl- and formyl moieties. Not surprisingly, the formyl moiety led to 1,2-addition and subsequent products, whereas **129l** exhibited no formation of target product.

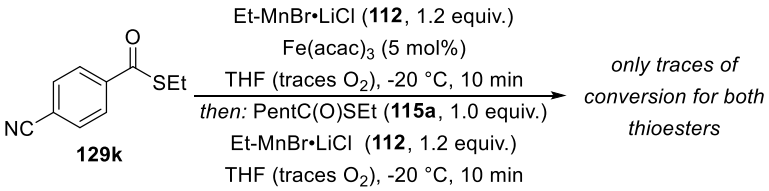

Scheme 3.49. Poisoning experiment of nitrile-containing compounds.

Interestingly, thioesters with *meta*-substituents such as **129o** or **129p** performed poorly whereas a **129n** led to good yields. Multiple reproductions for **129p** revealed that side products such as 1,2-addition and subsequent elimination resulted in diminished yields. With regards to the diminished reactivity, no clear trend could be concluded. *Ortho*-substituted compounds such as **129q** afforded decreased yields, but further exhibited decreased conversion *via* GC-MS. *Ortho*-carbonyl substituents such as esters or thioesters gave a multitude of side products, in case of **129r** and **129s**, which were not further investigated. Next, **129t** performed similarly well in comparison to the benzoic acid derived substrates and even electron-poor 3-pyridyl moiety was tolerated in medium yields of **130v**, whereas 2-pyridyl **129u** was not yielding product.

In view of the influence of the *ortho*-position, *ortho*-fluorinated compounds were employed under the reaction conditions. For this, a second substitution of the fluoro-group with another ethyl moiety was observed. Not surprisingly, this reactivity is known for reagents such as organolithium or Grignard reagents, but also for organomanganese compounds in case of chlorides, bromides and iodides.[17] In case of the studied reaction, this reactivity was additionally found applicable to every halide in *ortho*-position. Notably, the substitution was found independent of any transition metal-catalyst.

Considering potential applications of the reaction, the substrate scope was further explored with derivatives of natural and pharmaceutical products. Less complex natural compound-derived thioesters such as **131a** or **131b** performed in medium to good yields. Other functionalized natural products such as **131c–g** demonstrated that not only complex carbonyl-containing molecules are tolerated but also amines, *exo*-cyclic double bonds or molecules containing more than one protic hydrogen if excess manganese reagent is used. In case of **131d,** 1,2- or 1,4-addition was observed to be a competition reaction in minor extent.

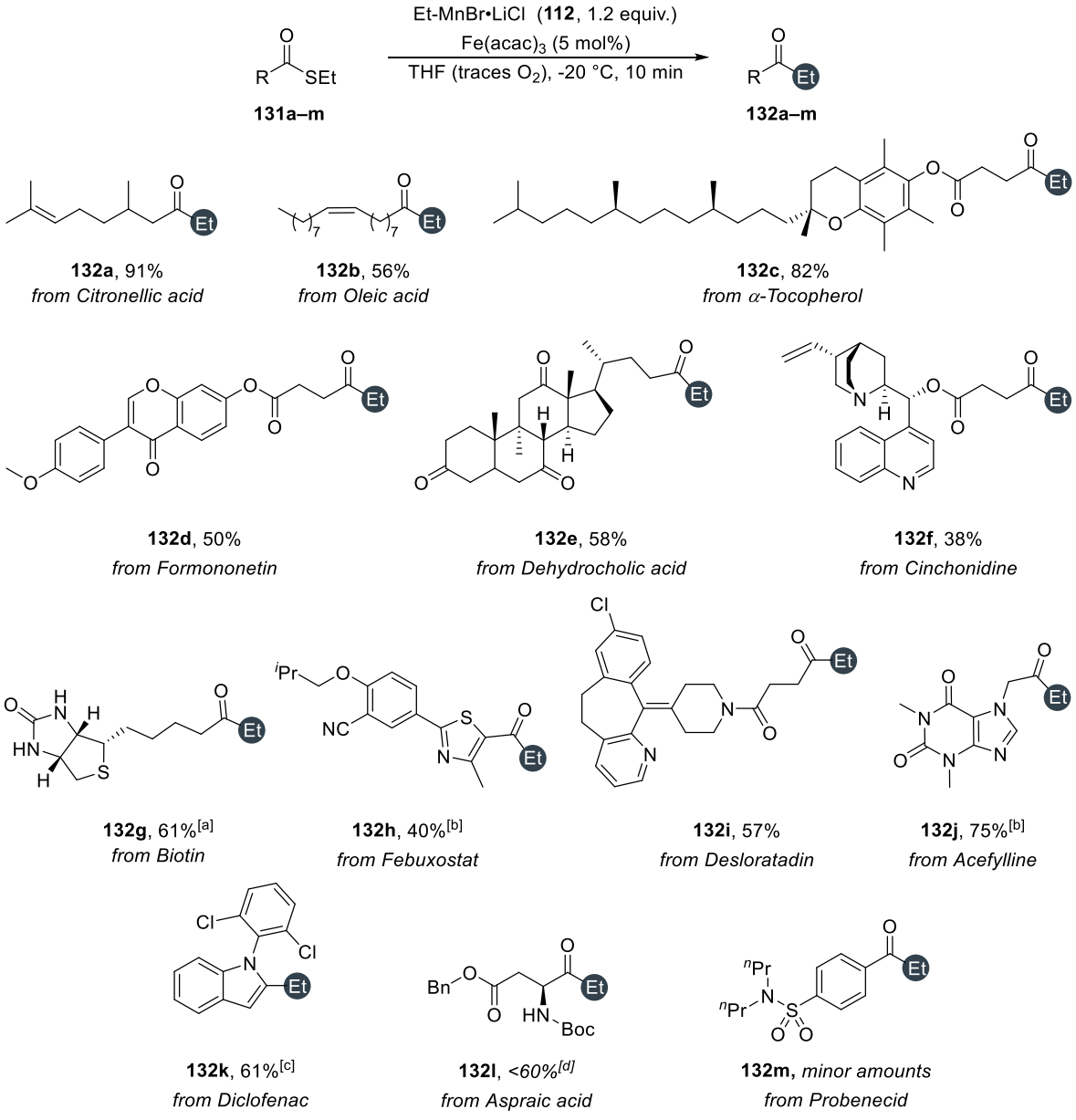

Scheme 3.50. Coupling of various aryl thioesters with ethyl manganese bromide. Isolated yields are displayed unless stated otherwise. Reaction conditions: thioester (1 mmol, 1 equiv.), EtMnBr•LiCl (1.2 mmol, 1.2 equiv. based on titre, usually ≤ 0.3 M in not degassed THF), $Fe(acac)_3$ (17.7 mg, 50 µmol, 0.05 equiv.), dry THF (3 mL, not degassed), -20 °C, 10 min. [a]: EtMnBr•LiCl (3.2 mmol, 3.2 equiv. based on titre, usually ≤ 0.3 M in THF). [b]: 15 min. [c]: EtMnBr•LiCl (2.2 mmol, 2.2 equiv. based on titre, usually ≤ 0.3 M in THF). [d]: impure yields.

Pharmaceutical compounds **131h**–**131k** could be converted in medium to good yields. Noticeably, the nitrile-containing ketone **132h** could be produced, which was attributed to either the absence of

electronic influence on the thioester or to the sterically demanding alkyl chain close to the nitrile moiety. Besides these, the low yield of **132l**, which was contaminated with impurities and therefore not further pursued as results indicated a mediocre tolerance of a carbamate protecting group. Generally, carbamates were observed to undergo thiolysis under the applied conditions. Another substrates that led to poor yields were **131m**.

During the synthesis of starting materials for this screening several coupling methodologies have been employed: Steglich esterifications with *N,N'*-dicyclohexylcarbodiimide (DCC) or *N,N'*-di(propan-2-yl)methanediimine (DIC), synthesis *via* acyl chloride or fluoride, coupling using *iso*-butyl chloroformate (IBCF), cyanuric chloride (CC) or 2-chloro-4,6,-dimethoxy-1,3,5-triazine (CDMT). Generally, Steglich esterifications afforded the thioesters in medium to good yields, although, with more functional groups present, the listed methodologies were probed for specific substrates. To summarize, while some substrates led to very poor yields due to likely steric or unknown chemical reasons, e.g. **133a+b**, thiolation of conjugated bonds, such in case of **133c**, affected the synthesis of starting materials, as well (representative examples in Scheme 3.51).

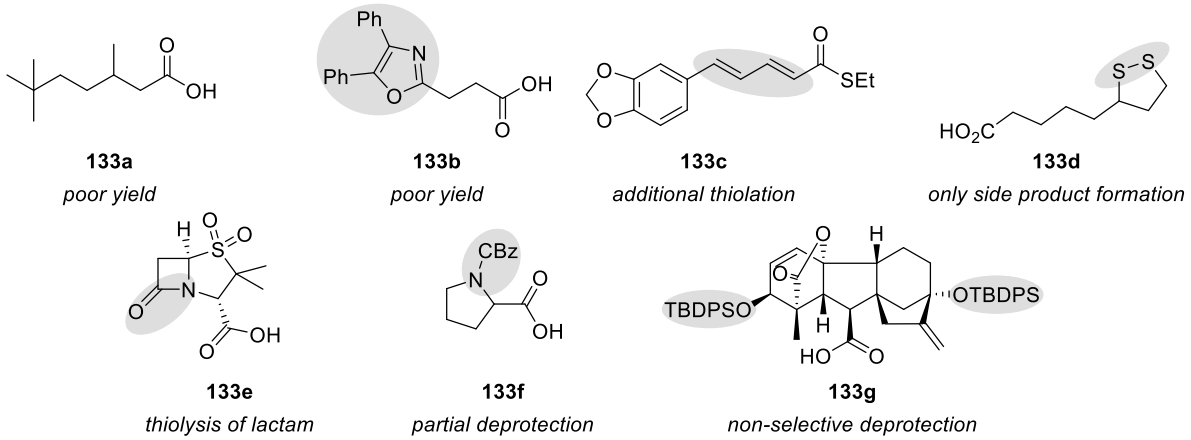

Scheme 3.51. Excerpt of substrates with unsuccessful thioester synthesis; shaded are the moieties probably causing difficulties in synthesis of thioester during coupling reaction.

For natural compounds, their known biochemical reactivity was found to be reflected in their reactions in presence of thiols, e.g. ring-opening of liponic acid **133d** and thiolysis of β-lactam **133e**. Often, side reactions were observed, which were associated with a high thiolate concentration. For instance, under Steglich conditions thiolytic cleavage of benzyloxycarbonyl (CBz) and *tert*-butyldiphenylsilyl (TBDPS) protection groups were observed **133f, 133g** and the respective byproducts were identified *via* GC-MS, likely rendering these functionalities problematic for the designated catalytic reaction. To resolve these issues, some of the natural compounds have been synthesized as respective succinoates **131c, 131d, 131f, 131i**. The advantages of these succinyl-linked thioesters were the available linker compound on higher scale **119s** as well as suppression of side reactivities associated with the presence of thiolate in solution. Generally, this stratagem can be employed as an alternative estimate for synthetic applicability of a catalytic method (Figure 3.5).

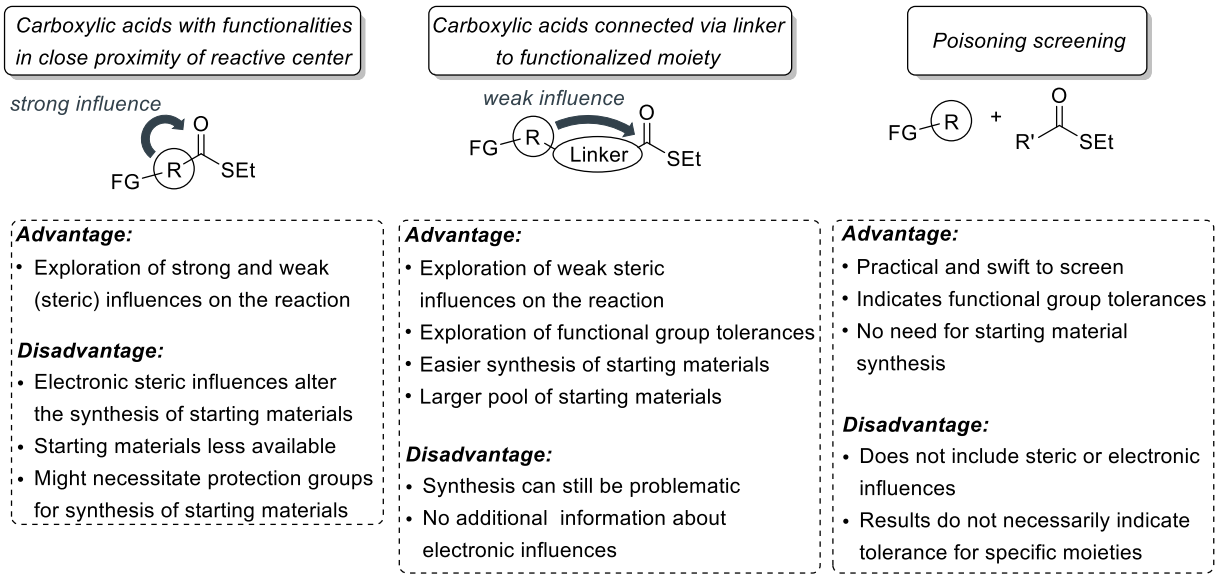

Figure 3.5. Overview of potential advantages and disadvantages of methodologies to evaluate substrate scope.

While the succinyl-linker in this case certainly decreases the informative value over influences such as electron-withdrawing or -donating aryl substituents or Lewis-acidic or -basic functionalities close to the thioester moiety, the broader pool of starting materials enabled screenings of highly functionalized molecules. In literature, another alternative to explore reactivities and robustness of a method is a poisoning screening during which a standardized reaction is probed with a range of additives.[187] Even so, this methodology led to contradicting results in the studied cases, therefore, only linker-type substrates were included for the evaluation of the substrate scope. However, even the synthesis of complex linker-type substrates was not always successful *via* the acid chloride **134** and different coupling reactions with the carboxylic acid **119s** were screened in these instances (Scheme 3.52). Commonly, elimination was the main competition reaction, e.g. likely formation of **136a** and **136b** from their starting materials.

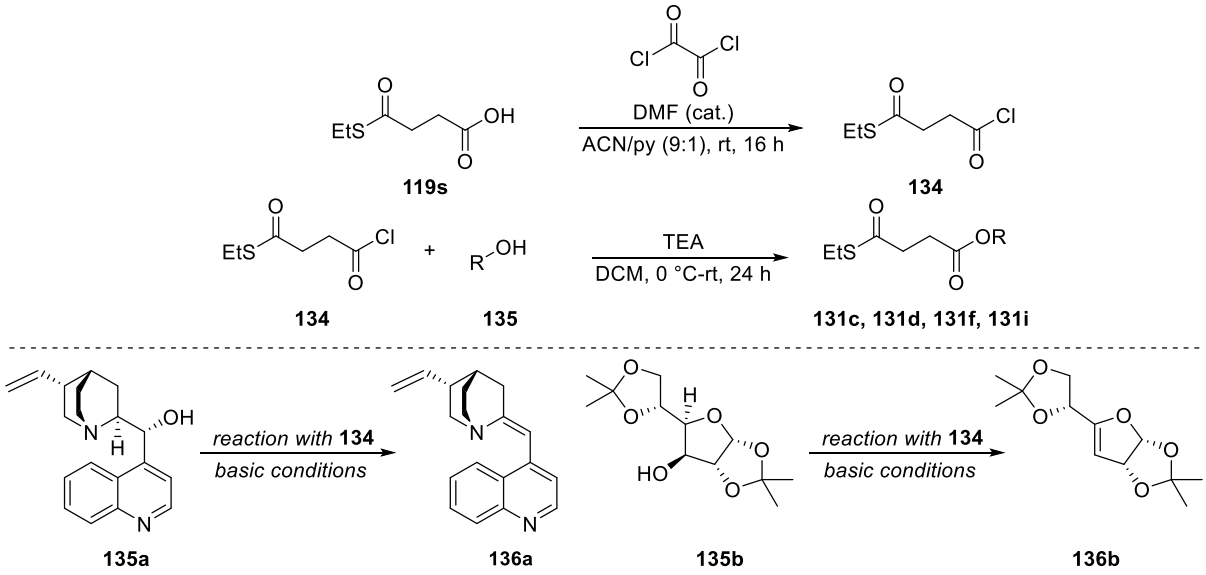

Scheme 3.52. Side products of the synthesis of linker-type substrates identified *via* NMR analysis.

Next to the exploration of highly functionalized substrates, the reaction was employed in the synthesis of dihydrojasmone, a terpenoide natural product starting from thioester **119p.** The reaction furnished higher yields than in case of substrate **120p** which was attributed to more efficient column separation. The subsequent aldol reaction was performed after a literature procedure and not further optimized, yielding 51% of dihydrojasmone.

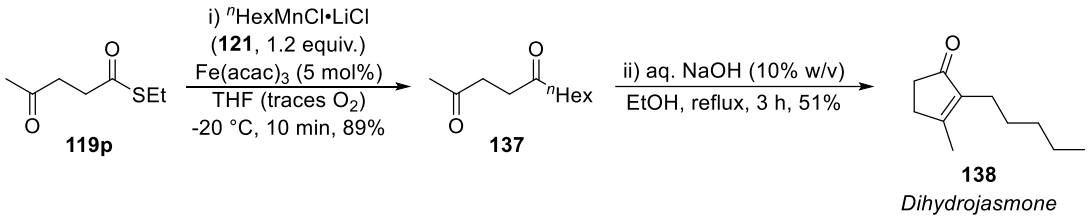

Scheme 3.53. Synthesis of dihydrojasmone (**138**) using the iron-catalyzed Fukuyama cross-coupling.

Besides, utilization of dithioesters and thiocyanates were attempted. Dithioester **139** did not exhibit any conversion of starting materials to respective thiones or otherwise. However, decyanation of thiocyanate **140** was observable in GC-MS analysis due to the likely formation of cyanide as well as benzyl thiol and benzyl disulfide during the reaction. The employment of other C(O)-S building blocks will be discussed in following chapters.

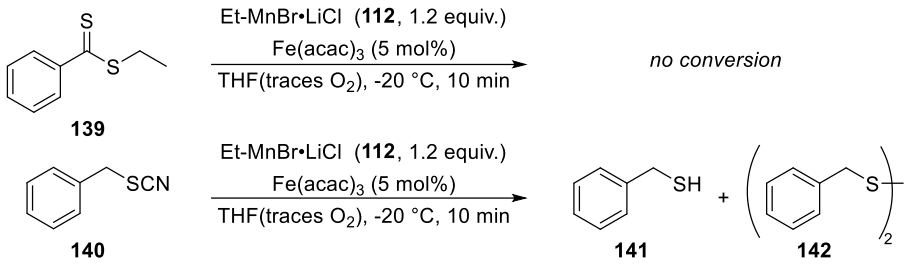

Scheme 3.54. Attempted conversion of other thio-based electrophilic building blocks.

3.3.4 Scope of Organomanganese Reagents

As a central goal for this investigation, the employment of different organomanganese reagents was studied. Thioester **119a** was used as the aliphatic moiety since the corresponding products are non-volatile (Scheme 3.55).

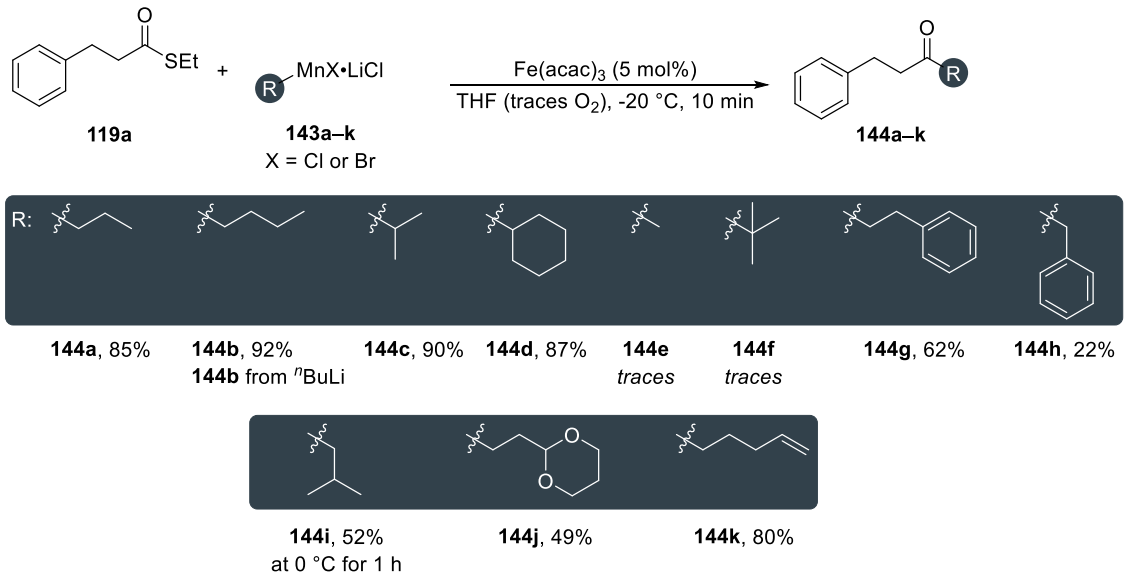

Scheme 3.55. Coupling of various aryl thioesters with different organomanganese reagents. Isolated yields are displayed unless stated otherwise. Reaction conditions: **119a** (194.3 mg, 1 mmol, 1 equiv.), organomanganese reagent **143a**–**143k** (1.2 mmol, 1.2 equiv. based on titre, usually ≤ 0.3 M in not degassed THF), $Fe(acac)_3$ (17.7 mg, 50 µmol, 0.05 equiv.), dry THF (3 mL, not degassed), -20 °C, 10 min.

n-Propyl manganese chloride (**143a**) afforded similar very good yields compared to ethyl manganese bromide. The reaction furnished slightly increased yields with *n*-butyl manganese bromide synthesized from *n*-butyl lithium. Thus, transmetalation reagents are unlikely to be influenced by residual Mg^{2+} ions. In terms of ion influences, it has to be pointed out, that the bromide anions (and traces of iodide from Grignard activation) are not mandatory. This was exemplified in the synthesis of **120i** or **120m** using *n*-hexyl manganese chloride instead of bromide. Therefore, no strong anion influence can be assumed.

More reactive, secondary manganese reagents were converted to **144c** with very good yields. However, only traces of product were obtained from methyl and *tert*-butyl manganese reagents (**144e**, **144f**). Yields could be slightly increased by the addition of NMP (only for Me-), prolonged reaction times and increased temperatures. Still, resulting GC yields never exceeded 20%. At this point, the reactivity was considered to rely on (sterically-) accessible β-hydrogen atoms for catalyst activation. Previous literature has drawn attention to similar observations of iron-catalyzed cross-coupling of Grignard reagents, in which absence of β-hydrogen atoms is often connected to decreased yields.[116] Surprisingly, the product of non-β-hydrogen containing manganese reagents could be isolated in case of **144h**, even though in poor yields with high amounts of homo-coupled product. In contrast, homo-coupling was never determined to be a major side reaction for alkyl manganese reagents. Observed traces were associated with the synthesis of organomanganese reagents, not the catalytic reaction.

Moreover, 2-methyl-propyl manganese halide, which was originally examined for a synthesis of another natural compound **147**, did only furnish trace yield under standard conditions with thioester **146** and **119a**. After adjusting the reaction conditions to 0 °C and prolonged stirring, 52% yield of **144i** were isolated (Scheme 3.56).

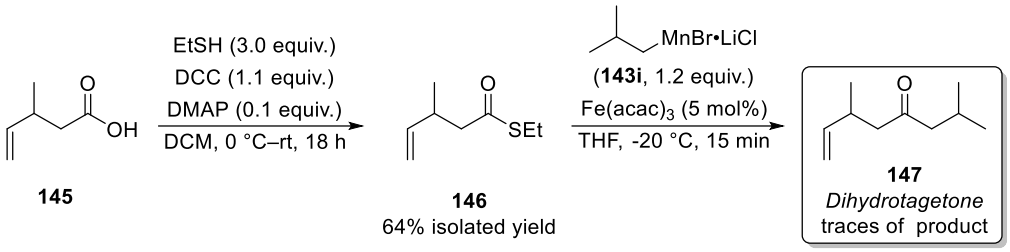

Scheme 3.56. Attempted synthesis of dihydrotagetone yielding only traces of product.

This deviation was attributed to a potential influence of β-hydrogen atoms as these are sterically less available due to the shielding methyl groups. In view of the medium yields obtained for **144i**, likely necessitating further optimization for synthesis of **147,** further synthesis was not attempted.

Attempts to utilize aryl manganese reagents were unsuccessful as only homo-coupling was observed (Scheme 3.57). This is in line with reports of iron-catalyzed cross-coupling of aryl Grignard reagents with aryl or alkyl halides.[67, 69] These are usually relying on specific ligands, strongly coordinating anions or on electronic properties of the electrophile. Then again, a spectrum of different reactivities is readily accessible with manganese reagents. Therefore, a screening was conducted comparing an iron-precatalyst, which showed comparably good results in preliminary experiments, with a Ni-xantphos system. The Ni-catalysis was chosen based on the previous works by Gehrtz et al.[173, 188] and served as a control to verify that the reagent solutions were capable of transmetalation. Iron-catalysis was unable to furnish cross-coupled products and usually led to biphenyl (10–30%). The Ni-catalyzed reaction led to medium yields with similar amounts of biphenyl. Both results indicate a catalyzed homo-coupling as competition reaction. Similar results were obtained when using dimethyl manganese, bisvinyl manganese or bisalkynyle manganese, all of which led to only homo-coupling product. Then again, in these cases, no verification of the synthesis of manganese reagents was conducted other than iodometric titration.

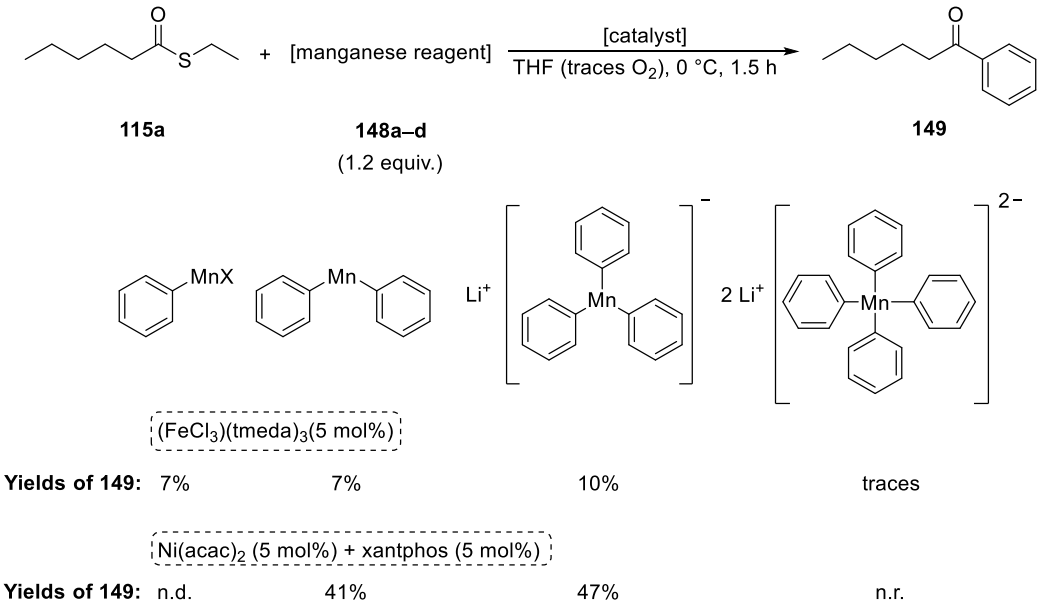

Scheme 3.57. Comparison of Fe- and Ni-catalyzed Fukuyama cross-coupling when utilizing different aromatic organomanganese reagents.

3.3.5 Comparative Studies

Competition reactions have been conducted to gain a better understanding of corresponding reactivities of thioesters. While it is generally accepted that *S*-aryl thioester are easier to activate[133, 185], a competition experiment with an alkyl *versus* aryl thioester indicated a slight preference for the conversion of *S*-alkyl thioester (Scheme 3.58). The results might serve as a rough approximation demonstrating that disregarding easier activation, **115c** is not a favored electrophile. Nevertheless, scrambling of thioesters cannot be excluded.

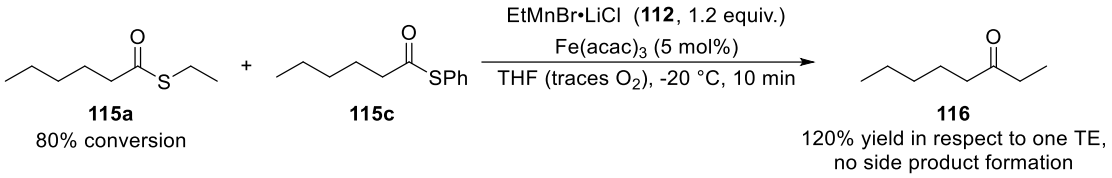

Scheme 3.58. Competition experiment between *S*-alkyl and *S*-aryl thioesters.

A closely related system to the studied reaction is the iron-catalyzed cross-coupling utilizing acyl halides and Grignard reagents.[96] Reproduction of the original procedure with small deviations led to observations of interfering Grignard reduction and 1,2-addition, though with certain exceptions. No such side products were yielded when replacing Grignard with organomanganese reagent under the same conditions. To a similar end, reproduction of a non-catalytic acylation of organomanganese reagents did not lead to the expected high yields and high selectivity.[34] In the experiment, mainly 1,2-addition was observed with 1.2 equiv. of **112** exemplifying the limitation of this method.

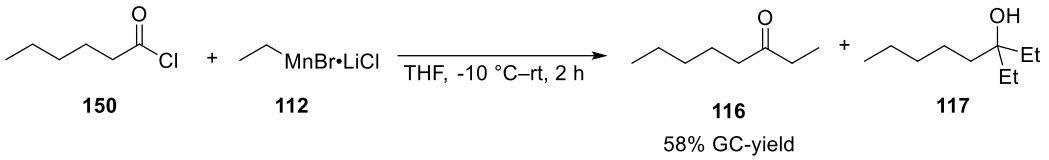

Scheme 3.59. Non-catalytic ketones synthesis utilizing organomanganese reagents.

Since both mentioned experimental procedures employed acyl chlorides, competition between acid chlorides and thioesters was briefly studied. In a first attempt, benzoyl and acyl halides were converted (Scheme 3.60).

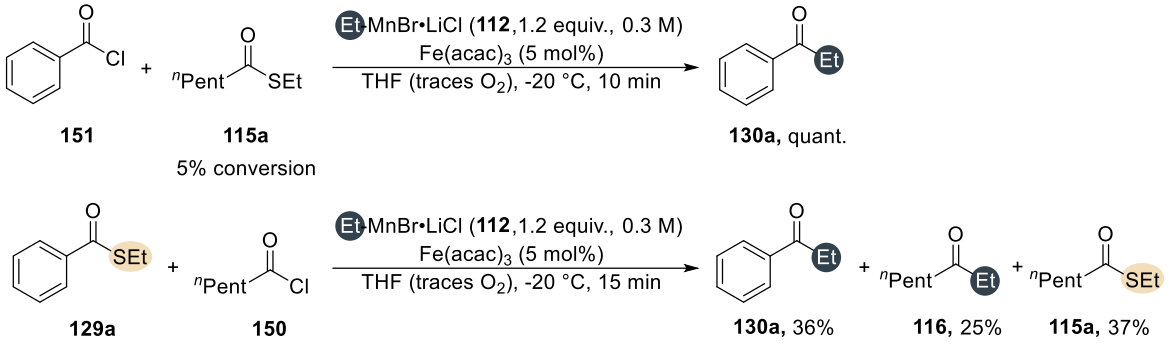

Scheme 3.60. Competition experiments between thioesters and acyl halides employing benzoyl and acetyl moieties with respective yields quantified by GC-FID.

Obtained results indicate a difference between benzoyl and acetyl moiety which impacts the cross-coupling reaction. However, this deviation is not reflected in previous substrate scopes for the iron-catalyzed cross-coupling with manganese reagents. Additionally, the seemingly more reactive benzoyl chloride (**151**) promoted the formation of thioester **115a**. In view of reactivity differences, the comparability of the results was impeded. Therefore, an adapted competition experiment was conducted using hexanoyl chloride (**150**) and *S*-ethyl pentanoyl thioate (**151**) (Scheme 3.61). The reaction was performed at -40 °C and at -78 °C.

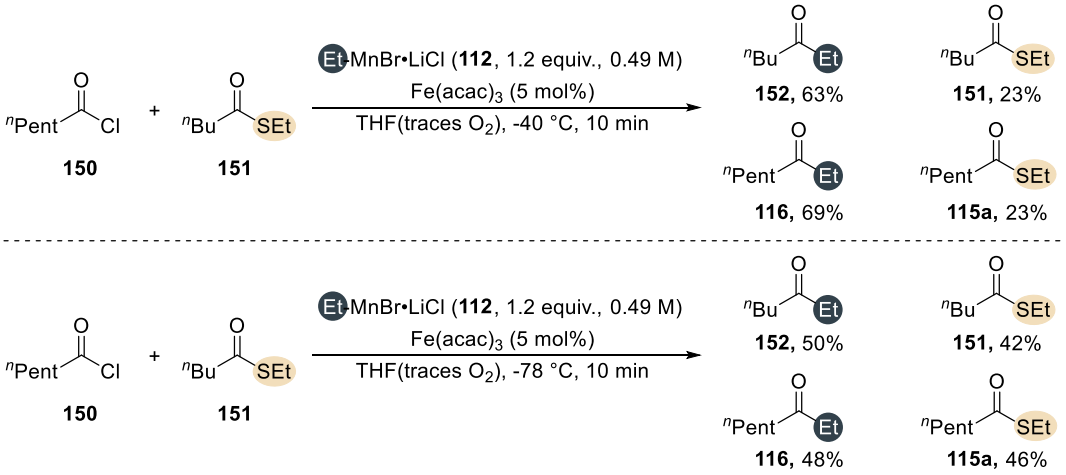

Scheme 3.61. Competition experiments between acyl halides and thioesters under catalytic conditions with respective yields of products quantified by GC-FID.

Observed ketone yields **152**:**116** closely resemble a 1:1 ratio at both temperatures. Therefore, neither coupling partner is favored under the catalytic conditions. Subsequently, this contradicts a general approximation of higher reactivity of acyl halides compared to thioesters. This is especially remarkable as the results of secondary branched thioesters were seemingly hindered by the activation step. Additionally, like the preceding experiment, a thioester formed from the acyl halide. At lower temperatures the thioester formation occurs almost in a 1:1 ratio of liberated thiolate. It is pertinent to consider that this formation of **115a** from acyl halide and thiolate, while accessible under non-catalytic conditions, usually proceeds much slower. Thus, the formation might be indicative of an *in situ* formed iron thiolate.

3.3.6 Further Mechanistic Investigation

The multitude of parameters influencing this reaction prompted further studies. Firstly, the reaction was monitored in presence and absence of oxygen (Scheme 3.62).

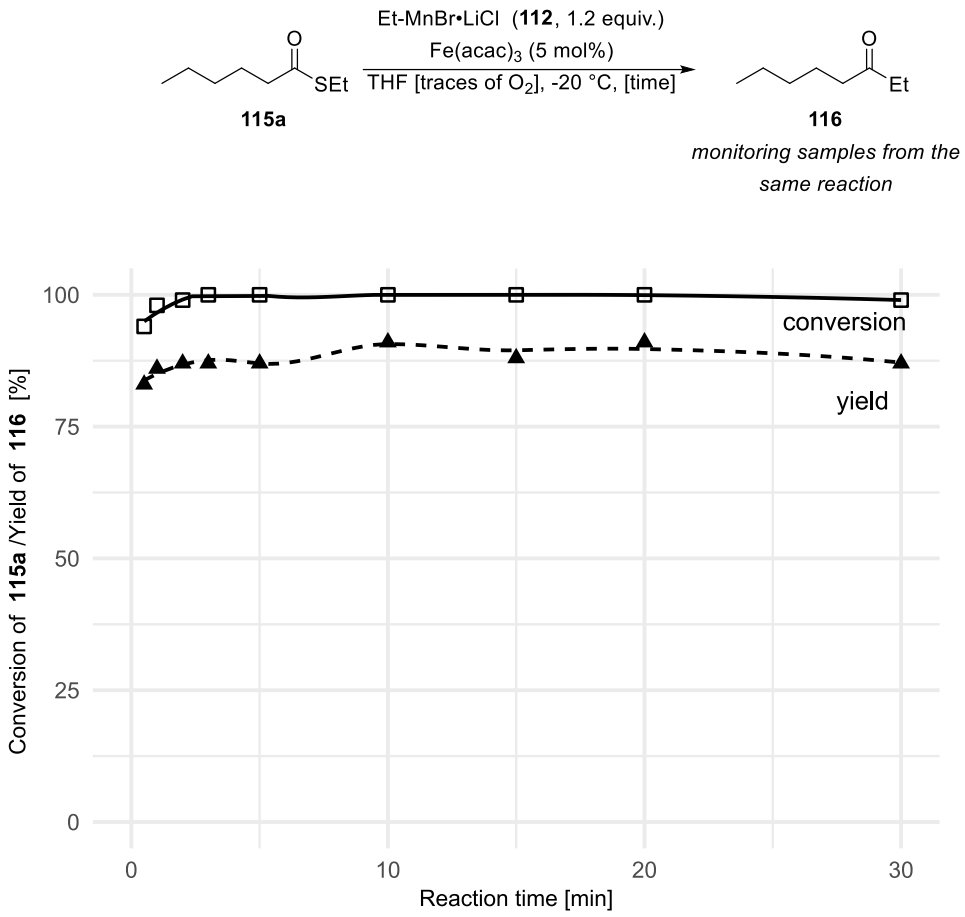

Scheme 3.62. Monitoring the synthesis of **116** under catalytic conditions in presence and absence of trace oxygen.

Notably, the side reaction responsible for a ca. 10% difference in yield seems to occur early in the catalytic reaction. Unfortunately, the side product could never be sufficiently separated to elucidate an underlying reactivity but can be observed *via* GC. This side reaction occurred independently of the added organomanganese or catalyst equivalents.

Then, *tert*-butyl manganese chloride was used as a probe to gain insights into a possible oxygen coordination. This was due to strong color change when treated with traces of oxygen. An electron paramagnetic resonance (EPR) spectrum was measured with and without oxygen in frozen solutions (Figure 3.6). The spectra manifested that present oxygen in solution influences the manganese species. However, likely several manganese species are present in solution which rendered further simulation and interpretation unsuccessful.

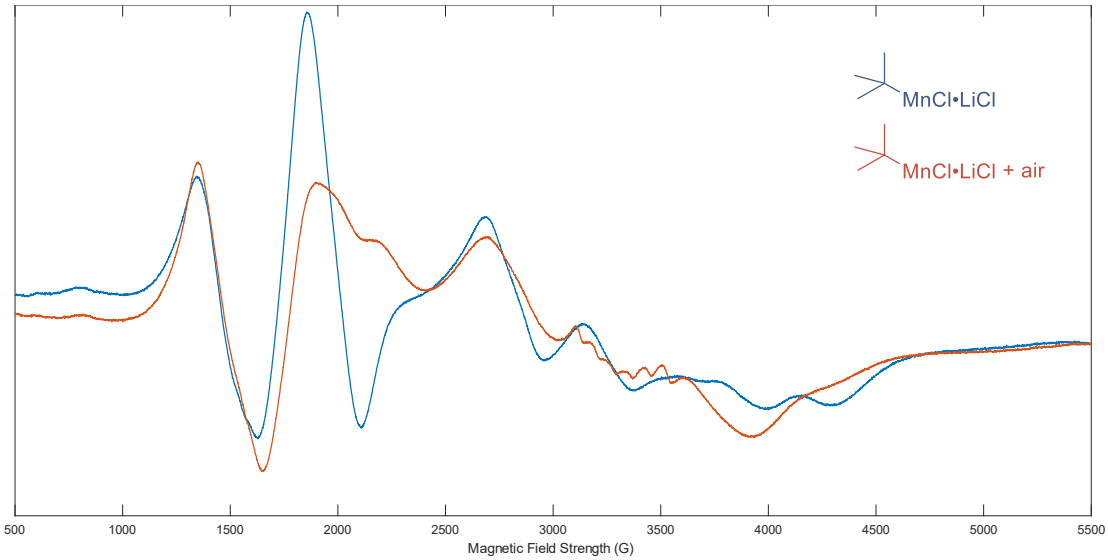

Figure 3.6. EPR spectra (X-band, 9.324 GHz, 1:1 2-MeTHF/THF, 120 K) of *tert*-butyl manganese chloride with (orange) and without (blue) trace oxygen.

The coordination of oxygen with organomanganese reagents has been mainly studied in reports on the homo-coupling of aryl-, vinyl- or alkynyl Grignard reagents.[84c, 189] As literature suggests both manganese or iron are capable of oxidative homo-coupling, it was considered that a loss of alkyl species might play a role. Thus, the decay of iron catalyst mixed with manganese reagent was monitored. For this, iron-precatalyst was treated with manganese reagent and **115a** was added to the reaction (Scheme 3.63). The results indicate that unlike reports on an iron-catalyzed decomposition of bisalkyl manganese reagents no swift loss of **112** was observed.[5a] For this experiment, it has to be mentioned that the change in addition sequence gave rise to ca. 10% difference between conversion and yield, forming a side product. Not surprisingly, iron-catalyst was observed to decompose slowly when exposed to manganese reagents, however, much slower compared to reactions with Grignard reagents.[118] Verifying this, the reaction was repeated by stirring for 1 h but adding more manganese reagent to exclude a loss of **112** which led to similar low yields and conversion. Thus, traces of oxygen likely inhibit the formation of an early minor alkyl iron-species which forms a side product early in the reaction. To this end, it is not unlikely that the established oxygen-coordinating ability of manganese allow for a more efficient deliverance from metal to metal.

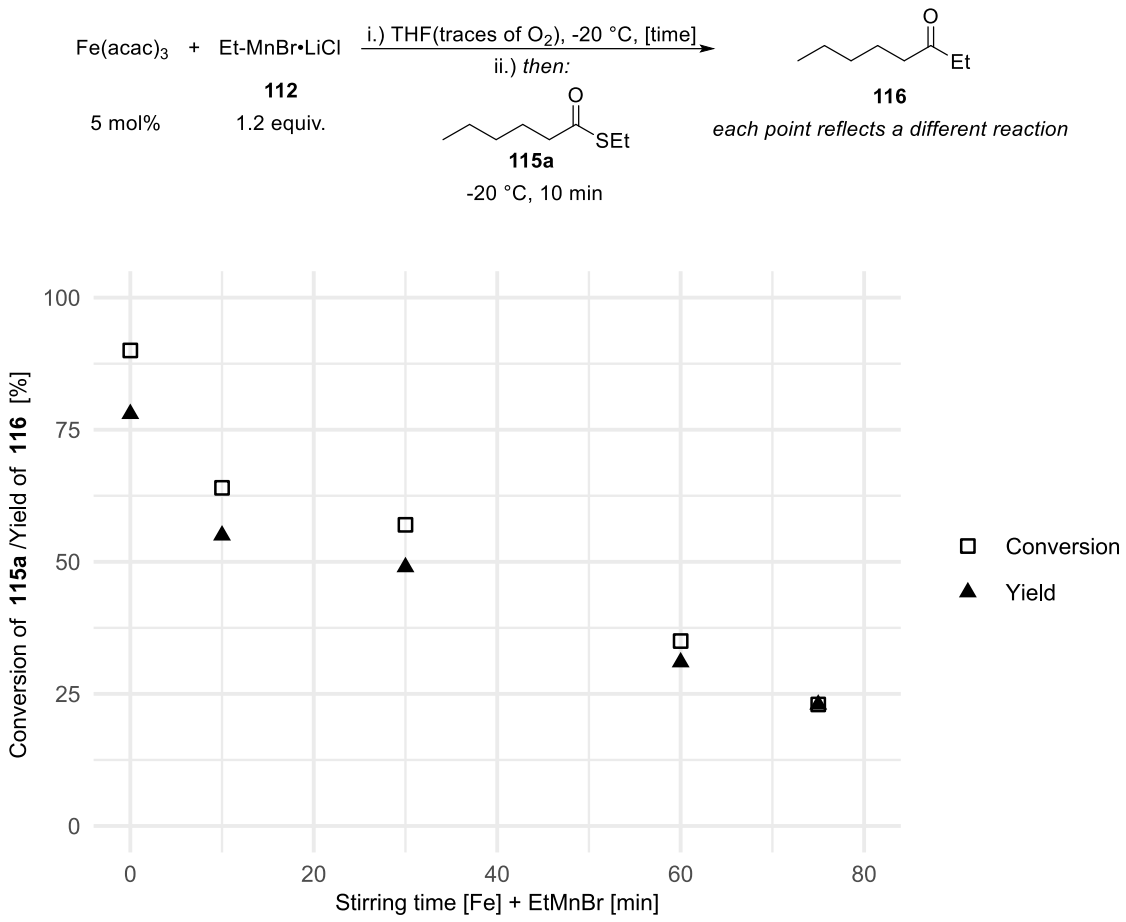

Scheme 3.63. Observation of catalyst decomposition by exposition to manganese reagent **112**.

Since oxygen plays a minor role in terms of yields, single-electron transfer steps might be relevant in the underlying mechanism. Often, iron-catalyzed cross-couplings of Grignard regents have been postulated to occur *via* a radical pathway.[122] Hence, radical scavengers were employed (Table 3.8). Scavengers such as 2,2,6,6-tetramethylpiperidinyloxyl (TEMPO)- and 4-[(3,5-di-*tert*-butyl-4-oxocyclohexa-2,5-dien-1-ylidene)methyl]-2,6-di-*tert*-butylphenoxyl (Galvinoxyl)-free radical led to unmeaningful results (Table 3.8 – Entry 1–4). As both likely reacted stoichiometrically with organomanganese reagent to afford the ethylated product, no other potential intermediates could be isolated (Scheme 3.64). Similar reactivity is known for aryl and alkynyl Grignard and alkyl lithium reagents and exemplifies a potentially limited use of these scavengers for this reaction.[190]

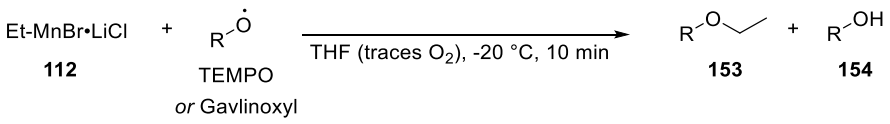

Scheme 3.64. Side reactions observed with oxyl-free radical scavengers.[190]

Table 3.8. Results of radical scavenger experiments on the catalytic reaction.[a]

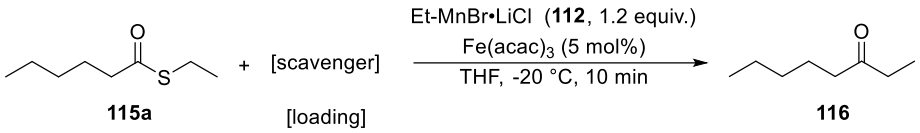

Entry	Scavenger	Scavenger Loading	Conversion (%)[b]	Yield (%)[b]	Side product formation
1	TEMPO	30 mol%	93	80	✓
2	TEMPO	2 equiv.	17	0	✓✓
3	Galvinoxyl	30 mol%	81	75	✓
4	Galvinoxyl	2 equiv.	-	0	✓✓
5	BHT	30 mol%	quant.	94	✗
6	BHT	2 equiv.	21	21	✗
7	Dihydroanthracene	30 mol%	quant.	95	✗
8	Dihydroanthracene	2 equiv.	quant.	94	✓

[a]: Reaction conditions: **115a** (53.4 mg, 333 µmol, 1 equiv.), EtMnCl•LiCl (400 µmol, 1.2 equiv. based on titre in THF), dry THF (1 mL), -20 °C, 10 min. [b]: Quantification *via* GC-FID measurement using *n*-pentadecane (100 µL) as internal standard.

Next, 2,6-di-*tert*-butyl-4-methylphenol (BHT) likely reacts with **112** in an acid-base reaction which slightly lowers the yields with low loading and shuts down reactivity in stochiometric amount (Table 3.8 – Entry 5+6). Lastly, dihydroanthracene did not exhibit a strong influence (Table 3.8 – Entry 7+8). With stochiometric amounts, traces of anthracene were observed as side product in GC-MS. Further experiments using Michael acceptors such as ethyl acrylate or 1,1-diphenyl ethene did not result in observed and characterizable side products.

Freeze-quenched reaction solutions were studied *via* electron-paramagnetic resonance (Figure 3.7). However, in view of the spectra of pure manganese compound, overlapping strong signals likely diminish trace signals appearing upon pretreatment of manganese reagent with iron precatalyst. Previous studies of manganese reagents mainly focused on tetraalkyl/-aryl manganates, which complicated simulations due to a lack in reference systems.[5b, 191] Therefore, no solid conclusion could be drawn from obtained EPR spectra other than being unsuited for reaction monitoring.

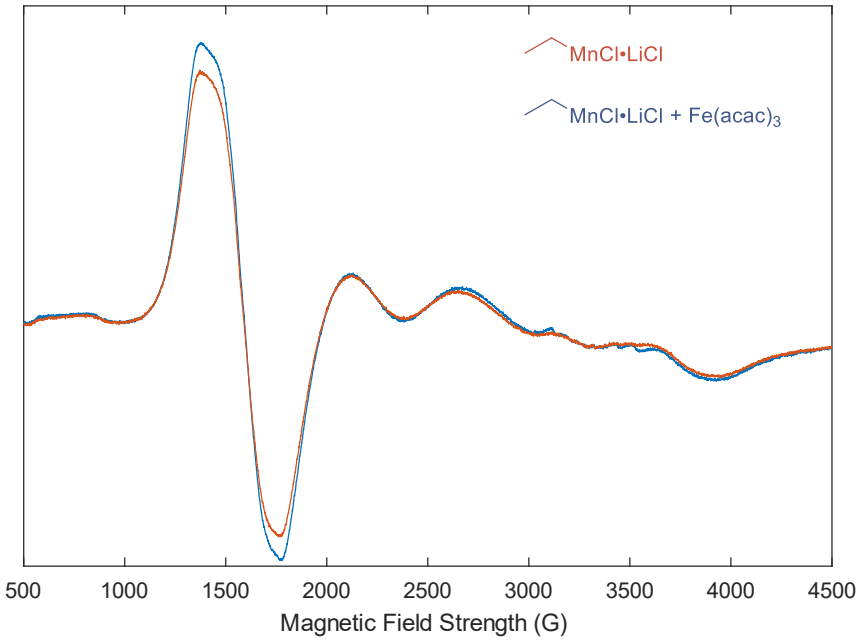

Figure 3.7. EPR spectra (X-band, 9.324 GHz, 1:1 2-MeTHF/THF, 120 K) of ethyl manganese halide with (blue) and without (orange) treatment with $Fe(acac)_3$.

Subsequently, paramagnetic ^1H NMR was employed as alternative to EPR measurements. However, this was only enabled by substituting organomanganese with corresponding Grignard reagents as the paramagnetism of manganese prohibited any acquisition of NMR data. Measuring a standard reaction, the occurrence of the typical $Fe(acac)_3$ peak (21 ppm (broad)) was not observable. Instead, a broad signal appeared after 2 minutes with a downfield shift of $\delta \approx 160$ ppm with $\Delta\nu \approx 660$ Hz in presence of thioester or thiolate (Scheme 3.65). Comparable peaks have been reported, e.g. in works of Chirik and co-workers (δ = 150 ppm, $\Delta\nu \approx 555$ Hz)[192], or Wernecke and co-workers (δ = 166 ppm)[193] for low-spin Fe^{+II}-alkyl species containing β-hydrogen atoms. These results suggest that released thiolate in solution might stabilize intermediary alkyl ferrate compounds **155**.

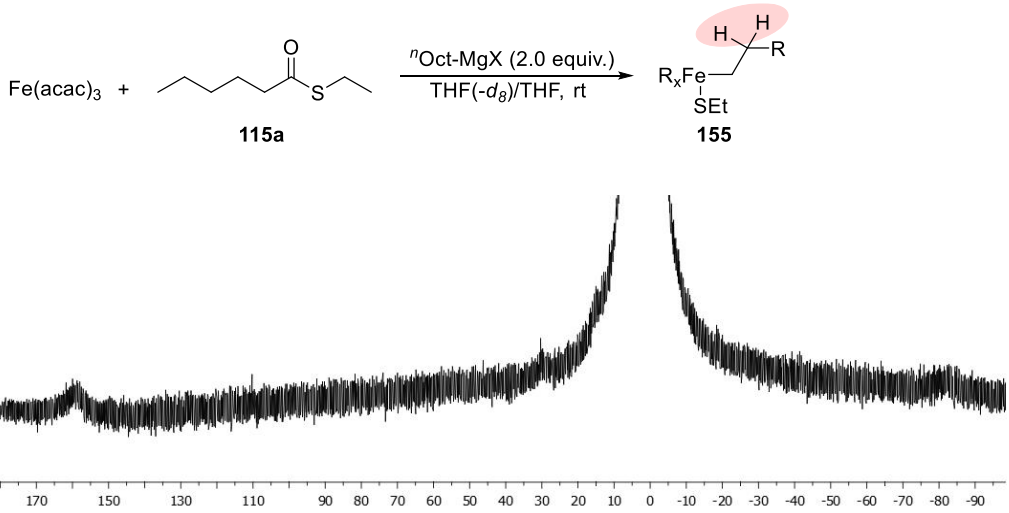

Scheme 3.65. Measured ^1H NMR spectrum exemplifying a downfield peak indicative of low-spin Fe^{+II} intermediates.

This potential iron-thiolate interaction seems counterintuitive in view of the readily accessible thiolate homo-coupling catalyzed by iron. Namely, this proneness to homo-coupling prohibited the synthesis of Fe^{+II} or Fe^{+III} thiolate complexes, furnishing only iron tar and disulfides. Thus, the decomposition *via* sulfide homo-coupling likely constitutes only a slow process.

Further studies of the iron-catalyzed cross-coupling were conducted with an $Fe(Mes)_3^-$ probe (**56**) in order to verify the reactivity with thiolates *in situ* (Figure 3.8). Upon treatment of the ferrate complex with thiolate or thioester, mesityl signals progressively decreased (framed red). Concomitantly, two sets of signals appeared. These were attributed to Fe^{+II} species with an intermediary spin (S = 1) or as oligonuclear intermediates. The conversion of thioester was verified by obtaining respective mesitylated ketone. Upon addition of extra mesityl magnesium bromide, $[Fe(Mes)_3]^-$ peaks reemerged. This strongly suggests that the generation of iron-thiolates is a reversible process.

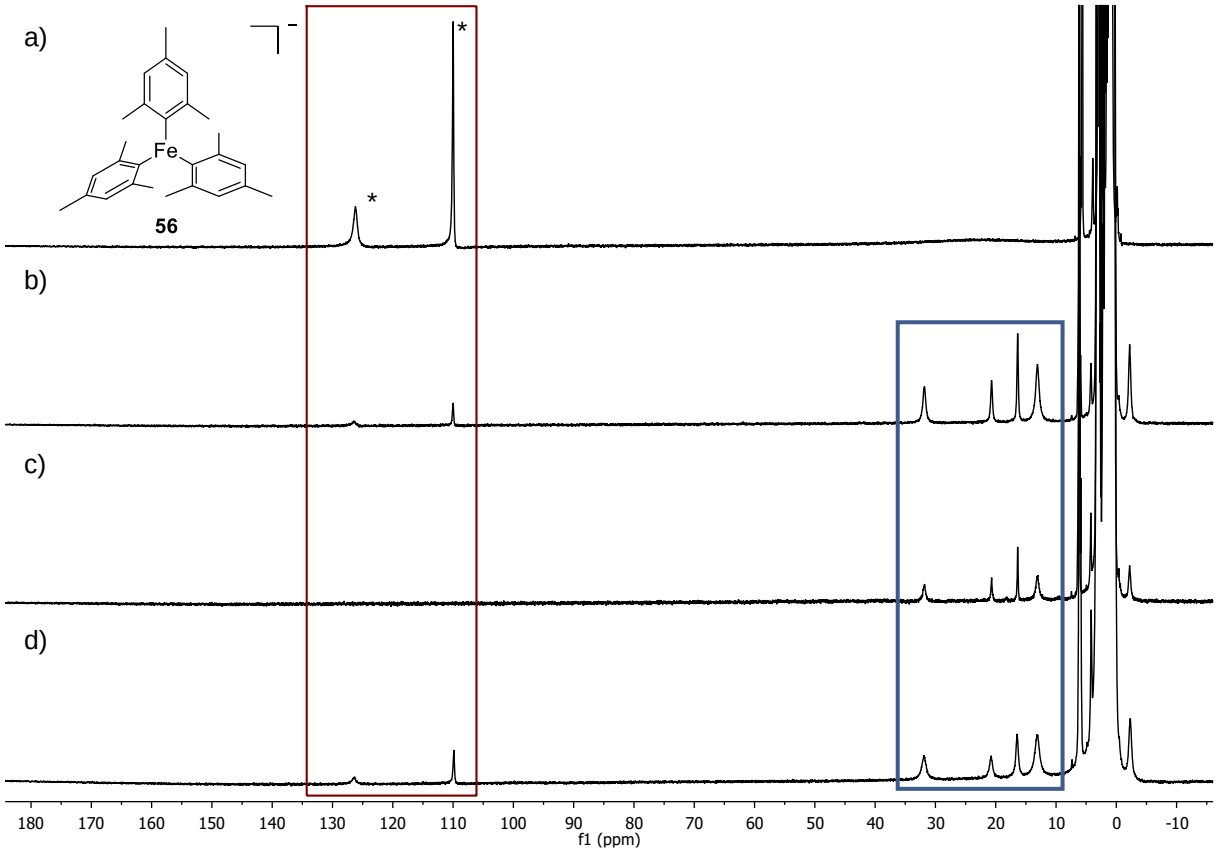

Figure 3.8. ^{1}H-NMR studies of $[Fe(Mes)_3]^-$ in THF-d_8: a) Mixture of MesMgBr (3.2 equiv.) and $FeCl_2$ at 20 °C. b) Treatment with **115a** (8 equiv.) after 20 min. c) after 2 h. d) Addition of further MesMgBr (2 equiv.); the asterisk peaks (*) in the red box belong to $[Fe(Mes)_3]^-$; The blue box is marking the peaks of potentially two intermediary iron species.

Subsequent studies on stochiometric scale indicated that higher amounts of iron also yielded higher amounts of side product with less yield of **116** (Table 3.9 – Entry 1).

Table 3.9. Reaction yields of stochiometric iron catalyst with and without thiolate additive.[a]

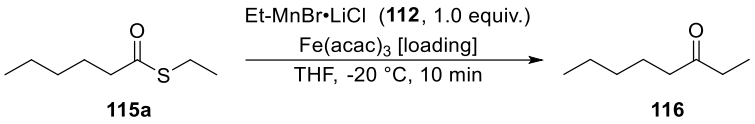

Entry	$Fe(acac)_3$ (equiv.)	LiSEt (equiv.)	Yield (%)[b]
1	1	0	67
2	1	1	63
3	1	3	66

[a]: Reaction conditions: **115a** (53.4 mg, 333 µmol, 1 equiv.), EtMnCl•LiCl (400 µmol, 1.2 equiv. based on titre in THF), dry THF (1 mL), -20 °C, 10 min. [b]: Quantification *via* GC-FID measurement using *n*-pentadecane (100 µL) as internal standard.

However, presence of excess of thiolate anion did not diminish the yields (Table 3.9 – Entries 2+3). This further substantiates that oxidation of thiolate is a slower process and thus an unlikely poisoning pathway. It rather crucially enables the stabilization of the catalytically active species *via* coordination. Importantly, such stabilizations have been reported for $C(sp^2)$-$C(sp^2)$ iron-catalyzed cross-coupling utilizing fluorides or alcoholates as coordinating anions.[69–70] Based on these findings, a hypothetical mechanism was formulated (Scheme 3.66).

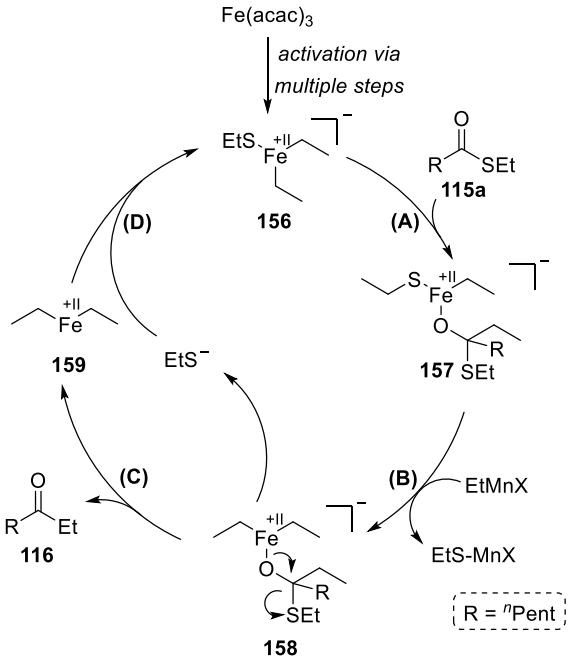

Scheme 3.66. Hypothetical catalytic cycle of the iron-catalyzed cross-coupling reaction.

It suggests that iron precatalyst is converted into active catalyst *via* β-hydrogen elimination of the coordinated alkyl chain and subsequent redox reactions. As the influence of oxygen was observed to occur early in the reaction, suppression of other reduced iron-species or facilitated generation of active

iron-catalyst might be promoted. The generation of an active thiolate-stabilized Fe^{+II} species **156** is validated by the paramagnetic NMR studies. Based upon theoretical studies on the substitution of acyl halides, an oxidative addition-reductive elimination pathway was not considered. Strong influences of sterics are reflected in a 1,2-type addition to furnish **157**, which would be inhibited by increased steric demands. This intermediate might be susceptible to poisoning with donors such as α-phenyl groups by either steric influences or π-coordination. Transmetalation and subsequent elimination of thiolate furnish the product and might occur either as a two-step process **(C)** or intramolecularly **(D)** or, in case of the former, the neutral dialkyl iron-species is potentially stabilized by thiolate coordination, due to a strong Fe-S interaction.

In order to substantiate the existence of a potential species, **157** or **158**, this hypothesized intermediate would be a suitable target to scavenge, since a mixed acetal (Scheme 3.67) would indicate a 1,2- addition-type. To this end, the organometallic hemiacetal was thought to be likely the responsible species for the poisoning effects observed for **119j**. Since especially this thioester led to poor yields, scavenging experiments were enabled with higher catalyst loading which would increase the amount of potentially scavenged product **160**. In order to obtain this scavenged mixed acetal TMS-Cl and IBCF were employed. However, high amounts of thiolate favored the reaction with employed scavengers. Mostly, thiolation of the electrophile was obtained with only minute amounts of side products which were not suited for NMR analysis. Further attempts in monitoring the reaction *via in situ* IR analysis failed due to low concentration and a too high reaction rate.

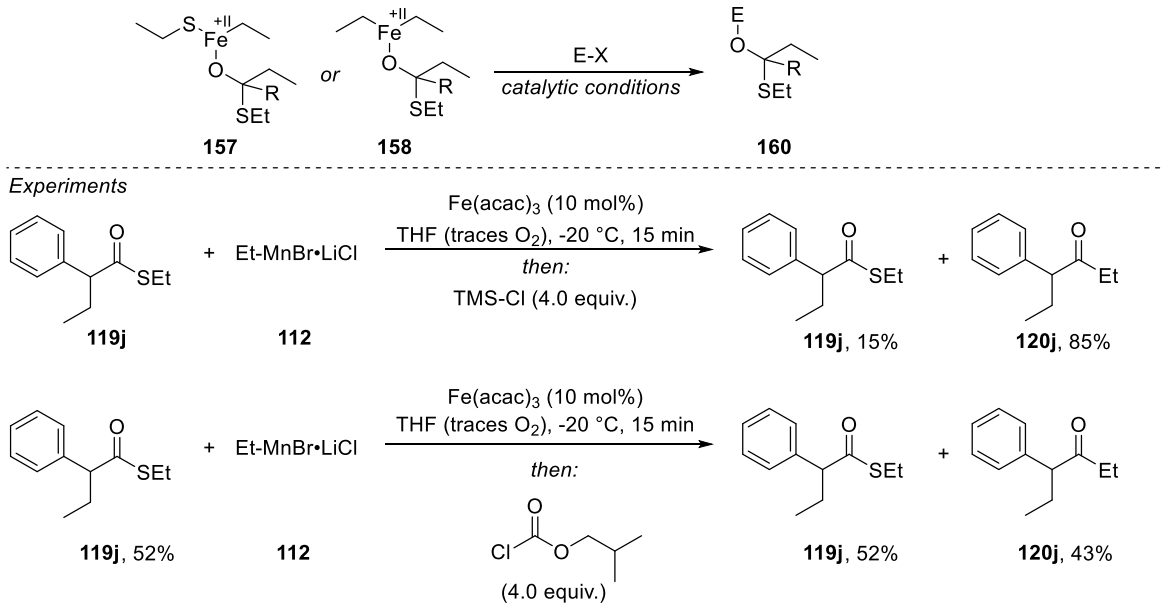

Scheme 3.67. Attempted scavenging experiments using reactive electrophiles. Yields displayed reflect GC-MS integral ratios.

3.4 Conclusion and Outlook

In summary, an iron-catalyzed cross-coupling of thioesters with non-stabilized alkyl organomanganese reagents was developed (Scheme 3.68). The synthetic method tolerated a broad spectrum of functional groups, e.g. (sulfon-)amides, ketones, esters or aryl halide groups, which led to the synthesis and isolation of 52 substrates including derivatives of pharmaceutical and natural compounds. To widen the substrate scope, a linker-type strategy was developed to simplify the evaluation of functional group tolerance. The reaction was successfully employed in the synthesis of the natural compound dihydrojasmone. Further experiments revealed an influence by steric demands of the carboxylic-, thiol- as well as organomanganese moiety. Based on the steric dependence, selective transformation for specific thioester motifs were demonstrated, enabling regioselectivity. By modification of *S*-substituent, it was exemplified that an unreactive sterically more demanding substrate can be converted to the respective product. Furthermore, in competition experiments, *S*-alkyl thioesters were shown to be similar in reactivity to *S*-aryl thioesters or acyl chlorides in case of non-functionalized alkyl starting materials. Attempts to optimize the synthesis and stability of manganese reagents did not afford beneficial synthetic approaches and the employed reagents were studied on their thermal decomposition. Additionally, the cross-coupling reaction was found to be influenced by trace oxygen, which was hypothesized to suppress initial side product formation. Paramagnetic NMR studies on model compounds gave insights into the possible participation of high-spin alkyl Fe^{+II} thiolates for which the formation was found to be likely reversible.

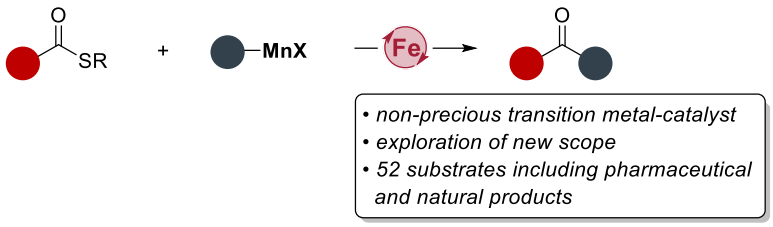

Scheme 3.68. Overview of the general iron-catalyzed cross-coupling of thioesters with alkyl manganese halides.

The interplay between thiolate and iron was associated with a higher stability of reactive iron species. Future studies might focus on the iron-sulfur interaction by ligand development implementing thiolate moieties. Lastly, the studies on organomanganese reagents exemplified vast potential for optimization. Since these reagents possess a synthetically attractive functional group tolerance, the study of their equilibria and counterion influences might enable an easier synthesis and higher temperature stability.

3.5 References

[1] a) G. Cahiez, C. Duplais, J. Buendia, *Chem. Rev.* **2009**, *109*, 1434–1476; b) G. Cahiez, A. Moyeux, in *Grignard Reagents and Transition Metal Catalysts, Formation of C-C Bonds by Cross-Coupling* (Ed.: J. Cossy), De Gruyter, Berlin/Boston, **2016**, pp. 210–243; c) G. Cahiez, O. Gager, in *Patai's Chemistry of Functional Groups* (Ed.: I. M. Zvi Rapopport), John Wiley & Sons Inc, **2011**.

[2] H. Gilman, J. C. Bailie, *J. Org. Chem.* **1937**, *02*, 84–94.

[3] H. Gilman, R. H. Kirby, *J. Am. Chem. Soc.* **1941**, *63*, 2046–2048.

[4] a) R. Riemschneider, H.-G. Kassahn, W. Schneider, *Z. Naturforsch.* **1960**, *15 b*, 547–551; b) C. Beermann, K. Clauss, *Angew. Chem.* **1959**, *71*, 627.

[5] a) M. Tamura, J. Kochi, *J. Organomet. Chem.* **1971**, *29*, 111–129; b) R. A. Andersen, E. Carmona-Guzman, J. F. Gibson, G. Wilkinson, *J. Chem. Soc., Dalton Trans.* **1976**, 2204–2211; c) G. Cahiez, D. Bernard, J. F. Normant, *Synthesis* **1977**, *1977*, 130–133; d) F. Keigo, N. Shigeki, O. Koichiro, U. Kiitiro, N. Hitosi, *Chem. Lett.* **1986**, *15*, 869–870; e) G. Cahiez, M. Alami, *Tetrahedron* **1989**, *45*, 4163–4176.

[6] E. J. Corey, G. H. Posner, *Tetrahedron Lett.* **1970**, *11*, 315–318.

[7] G. Cahiez, J. F. Normant, *Tetrahedron Lett.* **1977**, *18*, 3383–3384.

[8] M. Uzelac, P. Mastropierro, M. de Tullio, I. Borilovic, M. Tarrés, A. R. Kennedy, G. Aromí, E. Hevia, *Angew. Chem. Int. Ed.* **2021**, *60*, 3247–3253.

[9] S.-H. Kim, M. V. Hanson, R. D. Rieke, *Tetrahedron Lett.* **1996**, *37*, 2197–2200.

[10] Z. Peng, P. Knochel, *Org. Lett.* **2011**, *13*, 3198–3201.

[11] P. Quinio, A. D. Benischke, A. Moyeux, G. Cahiez, P. Knochel, *Synlett* **2015**, *26*, 514–518.

[12] S. H. Wunderlich, M. Kienle, P. Knochel, *Angew. Chem. Int. Ed.* **2009**, *48*, 7256–7260.

[13] G. Cahiez, B. Figadere, *Tetrahedron Lett.* **1986**, *27*, 4445–4448.

[14] G. Cahiez, A. Alexakis, J. F. Normant, *Synthetic Commun.* **1979**, *9*, 639–645.

[15] G. Cahiez, *Tetrahedron Lett.* **1981**, *22*, 1239–1242.

[16] C. Boucley, G. Cahiez, S. Carini, V. Cerè, M. Comes-Franchini, P. Knochel, S. Pollicino, A. Ricci, *J. Organomet. Chem.* **2001**, *624*, 223–228.

[17] G. Cahiez, D. Luart, F. Lecomte, *Org. Lett.* **2004**, *6*, 4395–4398.

[18] J. Hibino, S. Nakatsukasa, K. Fugami, S. Matsubara, K. Oshima, H. Nozaki, *J. Am. Chem. Soc.* **1985**, *107*, 6416–6417.

[19] M. Hojo, H. Harada, *Chem. Commun.* **1997**, 2077–2078.

[20] J. Nakao, R. Inoue, H. Shinokubo, K. Oshima, *J. Org. Chem.* **1997**, *62*, 1910–1911.

[21] G. Cahiez, S. Marquais, *Pure Appl. Chem.* **1996**, *68*, 53–60.

[22] a) M. S. Hofmayer, J. M. Hammann, G. Cahiez, P. Knochel, *Synlett* **2018**, *29*, 65–70; b) M. S. Hofmayer, J. M. Hammann, D. Haas, P. Knochel, *Org. Lett.* **2016**, *18*, 6456–6459.

[23] A. D. Benischke, A. Desaintjean, T. Juli, G. Cahiez, P. Knochel, *Synthesis* **2017**, *49*, 5396–5412.

[24] R. Giovannini, T. Stüdemann, G. Dussin, P. Knochel, *Angew. Chem. Int. Ed.* **1998**, *37*, 2387–2390.

[25] a) A. Desaintjean, S. Belrhomari, L. Rousseau, G. Lefèvre, P. Knochel, *Org. Lett.* **2019**, *21*, 8684–8688; b) L. Rousseau, A. Desaintjean, P. Knochel, G. Lefèvre, *Molecules* **2020**, *25*, 723.

[26] A. D. Benischke, A. J. A. Breuillac, A. Moyeux, G. Cahiez, P. Knochel, *Synlett* **2016**, *27*, 471–476.

[27] A. Leleu, Y. Fort, R. Schneider, *Adv. Synth. Catal.* **2006**, *348*, 1086–1092.

[28] R. D. Rieke, Y. Suh, S.-H. Kim, *Tetrahedron Lett.* **2005**, *46*, 5961–5964.

[29] G. Cahiez, A. Martin, T. Delacroix, *Tetrahedron Lett.* **1999**, *40*, 6407–6410.

[30] E. Riguet, M. Alami, G. Cahiez, *Tetrahedron Lett.* **1997**, *38*, 4397–4400.

[31] G. Cahiez, S. Marquais, *Tetrahedron Lett.* **1996**, *37*, 1773–1776.

[32] G. Cahiez, P.-Y. Chavant, E. Metais, *Tetrahedron Lett.* **1992**, *33*, 5245–5248.

[33] G. Cahiez, M. Alami, *Tetrahedron Lett.* **1990**, *31*, 7423–7424.

[34] G. Cahiez, B. Laboue, *Tetrahedron Lett.* **1989**, *30*, 7369–7372.

[35] G. Cahiez, M. Alami, *Tetrahedron Lett.* **1989**, *30*, 3541–3544.

[36] G. Cahiez, M. Alami, *Tetrahedron Lett.* **1989**, *30*, 7365–7368.

[37] S. Reformatsky, *Ber. Dtsch. Chem. Ges.* **1887**, *20*, 1210–1211.

[38] G. Cahiez, P.-Y. Chavant, *Tetrahedron Lett.* **1989**, *30*, 7373–7376.
[39] a) *Shanghai Metals Market (SMM) Spot prices*, https://www.metal.com/, (accessed 14.06.2022); b) Prices were calculated with a USD/Euro = 0.9574.
[40] *Safety Data Sheet - Magnesiumchlorid-Hexahydrat*, https://www.merckmillipore.com/DE/de/product/msds/MDA_CHEM-102367?Origin=PDP, (accessed 17.07.2022).
[41] *Safety Data Sheet - Mangan(II)-chlorid-Tetrahydrat*, https://www.sigmaaldrich.com/DE/de/sds/sigald/221279, (accessed 17.07.2022).
[42] *Safety Data Sheet - Zinkchlorid*, https://www.sigmaaldrich.com/DE/de/sds/sigald/208086, (accessed 18.07.2022).
[43] C. Tantardini, A. R. Oganov, *Nat. Commun.* **2021**, *12*, 2087.
[44] P. Knochel, R. D. Singer, *Chem. Rev.* **1993**, *93*, 2117–2188.
[45] M. Zhou, J. Tsien, T. Qin, *Angew. Chem. Int. Ed.* **2020**, *59*, 7372–7376.
[46] P. Knochel, W. Dohle, N. Gommermann, F. F. Kneisel, F. Kopp, T. Korn, I. Sapountzis, V. A. Vu, *Angew. Chem. Int. Ed.* **2003**, *42*, 4302–4320.
[47] M. Balkenhohl, P. Knochel, *Chem. Eur. J.* **2020**, *26*, 3688–3697.
[48] a) C. Lichtenberg, T. P. Spaniol, I. Peckermann, T. P. Hanusa, J. Okuda, *J. Am. Chem. Soc.* **2013**, *135*, 811–821; b) M. Hatano, T. Matsumura, K. Ishihara, *Org. Lett.* **2005**, *7*, 573–576.
[49] a) Y. Kato, C. M. Williams, M. Uchiyama, S. Matsubara, *Org. Lett.* **2019**, *21*, 473–475; b) T. D. Bluemke, W. Clegg, P. García-Alvarez, A. R. Kennedy, K. Koszinowski, M. D. McCall, L. Russo, E. Hevia, *Chem. Sci.* **2014**, *5*, 3552–3562.
[50] F. F. Kneisel, M. Dochnahl, P. Knochel, *Angew. Chem. Int. Ed.* **2004**, *43*, 1017–1021.
[51] a) S.-H. Kim, R. D. Rieke, *J. Org. Chem.* **2000**, *65*, 2322–2330; b) R. D. Rieke, P. T.-J. Li, T. P. Burns, S. T. Uhm, *J. Org. Chem.* **1981**, *46*, 4323–4324; c) S. Kudret, J. D. Haen, L. Lutsen, D. Vanderzande, W. Maes, *Adv. Synth. Catal.* **2013**, *355*, 569–575.
[52] R. Nast, H. Griesshammer, *Chem. Lett.* **1957**, *90*, 1315–1320.
[53] L. C. McCann, H. N. Hunter, J. A. C. Clyburne, M. G. Organ, *Angew. Chem. Int. Ed.* **2012**, *51*, 7024–7027.
[54] P. Eckert, S. Sharif, M. G. Organ, *Angew. Chem. Int. Ed.* **2021**, *60*, 12224–12241.
[55] L. C. McCann, M. G. Organ, *Angew. Chem. Int. Ed.* **2014**, *53*, 4386–4389.
[56] a) S. Sandl, A. Jacobi von Wangelin, *Angew. Chem. Int. Ed.* **2020**, *59*, 5434–5437; b) C. Bolm, J. Legros, J. Le Paih, L. Zani, *Chem. Rev.* **2004**, *104*, 6217–6254; c) B. D. Sherry, A. Fürstner, *Acc. Chem. Res.* **2008**, *41*, 1500–1511; d) W. M. Czaplik, M. Mayer, J. Cvengroš, A. J. von Wangelin, *ChemSusChem* **2009**, *2*, 396–417; e) G. Manolikakes, in *Comprehensive Organic Synthesis II (Second Edition)* (Ed.: P. Knochel), Elsevier, Amsterdam, **2014**, pp. 392–464; f) R. B. Bedford, *Acc. Chem. Res.* **2015**, *48*, 1485–1493; g) O. M. Kuzmina, A. K. Steib, A. Moyeux, G. Cahiez, P. Knochel, *Synthesis* **2015**, *47*, 1696–1705; h) A. Fürstner, *ACS Cent. Sci.* **2016**, *2*, 778–789; i) A. Guérinot, J. Cossy, *Top. Curr. Chem.* **2016**, *374*, 49; j) T. L. Mako, J. A. Byers, *Inorg. Chem. Front.* **2016**, *3*, 766–790; k) T. Parchomyk, K. Koszinowski, *Synthesis* **2017**, *49*, 3269–3280; l) J. D. Sears, P. G. N. Neate, M. L. Neidig, *J. Am. Chem. Soc.* **2018**, *140*, 11872–11883; m) A. Fürstner, *Bull. Chem Soc. Jpn.* **2021**, *94*, 666–677; n) M. L. Neidig, S. H. Carpenter, D. J. Curran, J. C. DeMuth, V. E. Fleischauer, T. E. Iannuzzi, P. G. N. Neate, J. D. Sears, N. J. Wolford, *Acc. Chem. Res.* **2019**, *52*, 140–150.
[57] M. Tamura, J. K. Kochi, *J. Am. Chem. Soc.* **1971**, *93*, 1487–1489.
[58] R. S. Smith, J. K. Kochi, *J. Org. Chem.* **1976**, *41*, 502–509.
[59] G. A. Molander, B. J. Rahn, D. C. Shubert, S. E. Bonde, *Tetrahedron Lett.* **1983**, *24*, 5449–5452.
[60] G. Cahiez, H. Avedissian, *Synthesis* **1998**, *1998*, 1199–1205.
[61] A. Fürstner, A. Leitner, *Angew. Chem. Int. Ed.* **2002**, *41*, 609–612.
[62] a) C. E. I. Knappke, A. Jacobi von Wangelin, *Chem. Soc. Rev.* **2011**, *40*, 4948–4962; b) C. Torborg, M. Beller, *Adv. Synth. Catal.* **2009**, *351*, 3027–3043.
[63] R. B. Bedford, D. W. Bruce, R. M. Frost, J. W. Goodby, M. Hird, *Chem. Commun.* **2004**, 2822–2823.
[64] R. Martin, A. Fürstner, *Angew. Chem. Int. Ed.* **2004**, *43*, 3955–3957.
[65] T. Nagano, T. Hayashi, *Org. Lett.* **2004**, *6*, 1297–1299.
[66] M. Nakamura, K. Matsuo, S. Ito, E. Nakamura, *J. Am. Chem. Soc.* **2004**, *126*, 3686–3687.
[67] G. Cahiez, V. Habiak, C. Duplais, A. Moyeux, *Angew. Chem. Int. Ed.* **2007**, *46*, 4364–4366.

[68] a) W. M. Czaplik, M. Mayer, S. Grupe, A. J. v. Wangelin, *Pure Appl. Chem.* **2010**, *82*, 1545–1553; b) W. M. Czaplik, M. Mayer, A. Jacobi von Wangelin, *Angew. Chem. Int. Ed.* **2009**, *48*, 607–610.

[69] T. Hatakeyama, M. Nakamura, *J. Am. Chem. Soc.* **2007**, *129*, 9844–9845.

[70] Y.-Y. Chua, H. A. Duong, *Chem. Commun.* **2014**, *50*, 8424–8427.

[71] Y. Yoshitaka, A. Hiroaki, N. Makoto, H. Hideto, I. Takashi, A. Masatoshi, *Chem. Lett.* **2011**, *40*, 983–985.

[72] K. Bica, P. Gaertner, *Org. Lett.* **2006**, *8*, 733–735.

[73] R. R. Chowdhury, A. K. Crane, C. Fowler, P. Kwong, C. M. Kozak, *Chem. Commun.* **2008**, 94–96.

[74] G. Bauer, C. W. Cheung, X. Hu, *Synthesis* **2015**, *47*, 1726–1732.

[75] R. B. Bedford, M. Betham, D. W. Bruce, A. A. Danopoulos, R. M. Frost, M. Hird, *J. Org. Chem.* **2006**, *71*, 1104–1110.

[76] L. Adak, T. Hatakeyama, M. Nakamura, *Bull. Chem Soc. Jpn.* **2021**, *94*, 1125–1141.

[77] S. Kawamura, M. Nakamura, *Chem. Lett.* **2013**, *42*, 183–185.

[78] a) T. Hatakeyama, T. Hashimoto, K. K. A. D. S. Kathriarachchi, T. Zenmyo, H. Seike, M. Nakamura, *Angew. Chem. Int. Ed.* **2012**, *51*, 8834–8837; b) R. Agata, S. Kawamura, K. Isozaki, M. Nakamura, *Chem. Lett.* **2019**, *48*, 238–241; c) K. G. Dongol, H. Koh, M. Sau, C. L. L. Chai, *Adv. Synth. Catal.* **2007**, *349*, 1015–1018.

[79] M. Jin, L. Adak, M. Nakamura, *J. Am. Chem. Soc.* **2015**, *137*, 7128–7134.

[80] J. L. Kneebone, V. E. Fleischauer, S. L. Daifuku, A. A. Shaps, J. M. Bailey, T. E. Iannuzzi, M. L. Neidig, *Inorg. Chem.* **2016**, *55*, 272–282.

[81] T. Hatakeyama, Y. Yoshimoto, T. Gabriel, M. Nakamura, *Org. Lett.* **2008**, *10*, 5341–5344.

[82] Y. Deng, X.-J. Wei, X. Wang, Y. Sun, T. Noël, *Chem. Eur. J.* **2019**, *25*, 14532–14535.

[83] X.-J. Wei, I. Abdiaj, C. Sambiagio, C. Li, E. Zysman-Colman, J. Alcázar, T. Noël, *Angew. Chem. Int. Ed.* **2019**, *58*, 13030–13034.

[84] a) J. Périchon, C. Cosmini, in *Handbook of Functionalized Organometallics*, **2005**, pp. 629–653; b) X. Xu, D. Cheng, W. Pei, *J. Org. Chem.* **2006**, *71*, 6637–6639; c) G. Cahiez, A. Moyeux, J. Buendia, C. Duplais, *J. Am. Chem. Soc.* **2007**, *129*, 13788–13789.

[85] a) E. Bisz, M. Szostak, *Green Chem.* **2017**, *19*, 5361–5366; b) E. Bisz, M. Koston, M. Szostak, *Green Chem.* **2021**, *23*, 7515–7521.

[86] G. Cahiez, O. Gager, J. Buendia, C. Patinote, *Chem. Eur. J.* **2012**, *18*, 5860–5863.

[87] a) A. S. Wong, B. Zhang, B. Li, M. L. Neidig, J. A. Byers, *Org. Process Res. Dev.* **2021**, *25*, 2461–2472; b) C. C. Tyrol, N. S. Yone, C. F. Gallin, J. A. Byers, *Chem. Commun.* **2020**, *56*, 14661–14664; c) M. P. Crockett, A. S. Wong, B. Li, J. A. Byers, *Angew. Chem. Int. Ed.* **2020**, *59*, 5392–5397.

[88] a) A. D. Benischke, M. Leroux, I. Knoll, P. Knochel, *Org. Lett.* **2016**, *18*, 3626–3629; b) T. Hatakeyama, N. Nakagawa, M. Nakamura, *Org. Lett.* **2009**, *11*, 4496–4499.

[89] Z. Jia, Q. Liu, X.-S. Peng, H. N. C. Wong, *Nat. Commun.* **2016**, *7*, 10614.

[90] T. Iwasaki, R. Akimoto, H. Kuniyasu, N. Kambe, *Chem. Asian J.* **2016**, *11*, 2834–2837.

[91] V. E. Fleischauer, S. B. Muñoz Iii, P. G. N. Neate, W. W. Brennessel, M. L. Neidig, *Chem. Sci.* **2018**, *9*, 1878–1891.

[92] Z. Mo, Q. Zhang, L. Deng, *Organometallics* **2012**, *31*, 6518–6521.

[93] R. B. Bedford, D. W. Bruce, R. M. Frost, M. Hird, *Chem. Commun.* **2005**, 4161–4163.

[94] T. Hatakeyama, Y. Okada, Y. Yoshimoto, M. Nakamura, *Angew. Chem. Int. Ed.* **2011**, *50*, 10973–10976.

[95] C. W. Cheung, P. Ren, X. Hu, *Org. Lett.* **2014**, *16*, 2566–2569.

[96] B. Scheiper, M. Bonnekessel, H. Krause, A. Fürstner, *J. Org. Chem.* **2004**, *69*, 3943–3949.

[97] D. Gärtner, A. L. Stein, S. Grupe, J. Arp, A. Jacobi von Wangelin, *Angew. Chem. Int. Ed.* **2015**, *54*, 10545–10549.

[98] B.-J. Li, L. Xu, Z.-H. Wu, B.-T. Guan, C.-L. Sun, B.-Q. Wang, Z.-J. Shi, *J. Am. Chem. Soc.* **2009**, *131*, 14656–14657.

[99] A. C. P. Rivera, R. Still, D. E. Frantz, *Angew. Chem. Int. Ed.* **2016**, *55*, 6689–6693.

[100] K. Itami, S. Higashi, M. Mineno, J.-i. Yoshida, *Org. Lett.* **2005**, *7*, 1219–1222.

[101] T. Agrawal, S. P. Cook, *Org. Lett.* **2014**, *16*, 5080–5083.

[102] A. Fürstner, A. Leitner, M. Méndez, H. Krause, *J. Am. Chem. Soc.* **2002**, *124*, 13856–13863.

[103] Z. Li, L. Liu, H.-m. Sun, Q. Shen, Y. Zhang, *Dalton T.* **2016**, *45*, 17739–17747.

[104] T. Agrawal, S. P. Cook, *Org. Lett.* **2013**, *15*, 96–99.
[105] A. L. Silberstein, S. D. Ramgren, N. K. Garg, *Org. Lett.* **2012**, *14*, 3796–3799.
[106] X. Chen, Z.-J. Quan, X.-C. Wang, *Appl. Organomet. Chem.* **2015**, *29*, 296–300.
[107] T. Xing, Z. Zhang, Y.-X. Da, Z.-J. Quan, X.-C. Wang, *Asian J. Org. Chem.* **2015**, *4*, 538–544.
[108] M. Carril, A. Correa, C. Bolm, *Angew. Chem. Int. Ed.* **2008**, *47*, 4862–4865.
[109] C. Duplais, F. Bures, I. Sapountzis, T. J. Korn, G. Cahiez, P. Knochel, *Angew. Chem. Int. Ed.* **2004**, *43*, 2968–2970.
[110] C. Cardellicchio, V. Fiandanese, G. Marchese, L. Ronzini, *Tetrahedron Lett.* **1985**, *26*, 3595–3598.
[111] E. Zhou, P. Chourreu, N. Lefèvre, M. Ahr, L. Rousseau, C. Herrero, E. Gayon, G. Cahiez, G. Lefèvre, *ACS Org. Inorg. Au* **2022**.
[112] A. Fürstner, R. Martin, H. Krause, G. Seidel, R. Goddard, C. W. Lehmann, *J. Am. Chem. Soc.* **2008**, *130*, 8773–8787.
[113] M. H. Al-Afyouni, K. L. Fillman, W. W. Brennessel, M. L. Neidig, *J. Am. Chem. Soc.* **2014**, *136*, 15457–15460.
[114] S. B. Muñoz, S. L. Daifuku, W. W. Brennessel, M. L. Neidig, *J. Am. Chem. Soc.* **2016**, *138*, 7492–7495.
[115] S. B. Muñoz, S. L. Daifuku, J. D. Sears, T. M. Baker, S. H. Carpenter, W. W. Brennessel, M. L. Neidig, *Angew. Chem. Int. Ed.* **2018**, *57*, 6496–6500.
[116] A. Fürstner, H. Krause, C. W. Lehmann, *Angew. Chem. Int. Ed.* **2006**, *45*, 440–444.
[117] B. Heggen, W. Thiel, *J. Organomet. Chem.* **2016**, *804*, 42–47.
[118] J. D. Sears, S. B. Muñoz III, S. L. Daifuku, A. A. Shaps, S. H. Carpenter, W. W. Brennessel, M. L. Neidig, *Angew. Chem. Int. Ed.* **2019**, *58*, 2769–2773.
[119] R. B. Bedford, P. B. Brenner, E. Carter, P. M. Cogswell, M. F. Haddow, J. N. Harvey, D. M. Murphy, J. Nunn, C. H. Woodall, *Angew. Chem. Int. Ed.* **2014**, *53*, 1804–1808.
[120] T. Parchomyk, S. Demeshko, F. Meyer, K. Koszinowski, *J. Am. Chem. Soc.* **2018**, *140*, 9709–9720.
[121] B. Bogdanović, M. Schwickardi, *Angew. Chem. Int. Ed.* **2000**, *39*, 4610–4612.
[122] N. J. Bakas, J. D. Sears, W. W. Brennessel, M. L. Neidig, *Angew. Chem. Int. Ed.* **2022**, *61*, e202114986.
[123] H. Takaya, S. Nakajima, N. Nakagawa, K. Isozaki, T. Iwamoto, R. Imayoshi, N. J. Gower, L. Adak, T. Hatakeyama, T. Honma, et al., *Bull. Chem Soc. Jpn.* **2015**, *88*, 410–418.
[124] J. L. Kneebone, W. W. Brennessel, M. L. Neidig, *J. Am. Chem. Soc.* **2017**, *139*, 6988–7003.
[125] A. Hedström, Z. Izakian, I. Vreto, C.-J. Wallentin, P.-O. Norrby, *Chem. Eur. J.* **2015**, *21*, 5946–5953.
[126] a) A. Bekhradnia, P.-O. Norrby, *Dalton T.* **2015**, *44*, 3959–3962; b) J. A. Przyojski, K. P. Veggeberg, H. D. Arman, Z. J. Tonzetich, *ACS Catal.* **2015**, *5*, 5938–5946.
[127] T. Parchomyk, K. Koszinowski, *Chem. Eur. J.* **2016**, *22*, 15609–15613.
[128] T. Parchomyk, K. Koszinowski, *Chem. Eur. J.* **2018**, *24*, 16342–16347.
[129] R. B. Bedford, P. B. Brenner, D. Elorriaga, J. N. Harvey, J. Nunn, *Dalton T.* **2016**, *45*, 15811–15817.
[130] P. G. N. Neate, M. D. Greenhalgh, W. W. Brennessel, S. P. Thomas, M. L. Neidig, *Angew. Chem. Int. Ed.* **2020**, *59*, 17070–17076.
[131] V. Wowk, L. Rousseau, G. Lefèvre, *Organometallics* **2021**, *40*, 3253–3266.
[132] X.-j. Wang, L. Zhang, X. Sun, Y. Xu, D. Krishnamurthy, C. H. Senanayake, *Org. Lett.* **2005**, *7*, 5593–5595.
[133] V. Hirschbeck, P. H. Gehrtz, I. Fleischer, *Chem. Eur. J.* **2017**, *24*, 7092–7107.
[134] S. Nahm, S. M. Weinreb, *Tetrahedron Lett.* **1981**, *22*, 3815–3818.
[135] H. A. Staab, E. Jost, *Liebigs Ann. Chem.* **1962**, *655*, 90–94.
[136] A. R. Akhbar, V. Chudasama, R. J. Fitzmaurice, L. Powell, S. Caddick, *Chem. Commun.* **2014**, *50*, 743–746.
[137] P. Sureshbabu, S. Azeez, N. Muniyappan, S. Sabiah, J. Kandasamy, *J. Org. Chem.* **2019**, *84*, 11823–11838.
[138] T. Mukaiyama, M. Araki, H. Takei, *J. Am. Chem. Soc.* **1973**, *95*, 4763–4765.
[139] V. Hirschbeck, M. Böldl, P. H. Gehrtz, I. Fleischer, *Org. Lett.* **2019**, *21*, 2578–2582.

[140] a) D. Djukanovic, B. Heinz, F. Mandrelli, S. Mostarda, P. Filipponi, B. Martin, P. Knochel, *Chem. Eur. J.* **2021**, *27*, 13977–13981; b) B. Heinz, D. Djukanovic, M. A. Ganiek, B. Martin, B. Schenkel, P. Knochel, *Org. Lett.* **2020**, *22*, 493–496.
[141] a) G. Cahiez, B. Laboue, *Tetrahedron Lett.* **1992**, *33*, 4439–4442; b) R. J. Anderson, C. A. Henrick, L. D. Rosenblum, *J. Am. Chem. Soc.* **1974**, *96*, 3654–3655.
[142] K. Colas, A. C. V. D. dos Santos, A. Mendoza, *Org. Lett.* **2019**, *21*, 7908–7913.
[143] V. V. Bykov, D. N. Korolev, N. A. Bumagin, *Russ. Chem. B+* **1997**, *46*, 1631–1632.
[144] a) Y. Zhang, T. Rovis, *J. Am. Chem. Soc.* **2004**, *126*, 15964–15965; b) Y. Ogiwara, D. Sakino, Y. Sakurai, N. Sakai, *Eur. J. Org. Chem.* **2017**, *2017*, 4324–4327.
[145] a) Q. Chen, X.-H. Fan, L.-P. Zhang, L.-M. Yang, *RSC Adv.* **2014**, *4*, 53885–53890; b) L. J. Gooßen, K. Ghosh, *Angew. Chem. Int. Ed.* **2001**, *40*, 3458–3460.
[146] a) H. Tokuyama, S. Yokoshima, T. Yamashita, S. C. Lin, L. P. Li, T. Fukuyama, *J. Braz. Chem. Soc.* **1998**, *9*, 381–387; b) K. Kunchithapatham, C. C. Eichman, J. P. Stambuli, *Chem. Commun.* **2011**, *47*, 12679–12681; c) R. Oost, A. Misale, N. Maulide, *Angew. Chem. Int. Ed.* **2016**, *55*, 4587–4590.
[147] H. Tatamidani, F. Kakiuchi, N. Chatani, *Org. Lett.* **2004**, *6*, 3597–3599.
[148] A. Chatupheeraphat, H.-H. Liao, W. Srimontree, L. Guo, Y. Minenkov, A. Poater, L. Cavallo, M. Rueping, *J. Am. Chem. Soc.* **2018**, *140*, 3724–3735.
[149] B. J. Simmons, N. A. Weires, J. E. Dander, N. K. Garg, *ACS Catal.* **2016**, *6*, 3176–3179.
[150] G. Meng, M. Szostak, *Org. Lett.* **2015**, *17*, 4364–4367.
[151] R. K. Dieter, *Tetrahedron* **1999**, *55*, 4177–4236.
[152] L. Shi, B. P. Tu, *Curr. Opin. Cell Biol.* **2015**, *33*, 125–131.
[153] S. Trefely, C. D. Lovell, N. W. Snyder, K. E. Wellen, *Mol. Metab.* **2020**, *38*, 100941.
[154] I. Buhaescu, H. Izzedine, *Clin. Biochem.* **2007**, *40*, 575–584.
[155] a) Y. Shi, X. Liu, H. Cao, F. Bie, Y. Han, P. Yan, R. Szostak, M. Szostak, C. Liu, *Org. Biomol. Chem.* **2021**, *19*, 2991–2996; b) M. M. Rahman, G. Li, M. Szostak, *Synthesis* **2020**, *52*, 1060–1066.
[156] a) E. K. Davison, J. L. Freeman, W. Zhang, W. M. Wuest, D. P. Furkert, M. A. Brimble, *Org. Lett.* **2020**, *22*, 5550–5554; b) C. Steinborn, R. E. Wildermuth, D. M. Barber, T. Magauer, *Angew. Chem. Int. Ed.* **2020**, *59*, 17282–17285.
[157] a) A. Riefert, M. E. Maier, *Synthesis* **2018**, *50*, 3131–3145; b) S. Loscher, R. Schobert, *Chem. Eur. J.* **2013**, *19*, 10619–10624.
[158] a) V. Hirschbeck, P. H. Gehrtz, I. Fleischer, *J. Am. Chem. Soc.* **2016**, *138*, 16794–16799; b) X. Qi, Z.-P. Bao, X.-T. Yao, X.-F. Wu, *Org. Lett.* **2020**, *22*, 6671–6676; c) Y. Feng, S. Yang, S. Zhao, D.-P. Zhang, X. Li, H. Liu, Y. Dong, F.-G. Sun, *Org. Lett.* **2020**.
[159] N. Sawada, T. Itoh, N. Yasuda, *Tetrahedron Lett.* **2006**, *47*, 6595–6597.
[160] P. H. Gehrtz, V. Geiger, T. Schmidt, L. Sršan, I. Fleischer, *Org. Lett.* **2019**, *21*, 50–55.
[161] H. Tokuyama, S. Yokoshima, T. Yamashita, T. Fukuyama, *Tetrahedron Lett.* **1998**, *39*, 3189–3192.
[162] H. Tokuyama, S. Yokoshima, S. C. Lin, L. P. Li, T. Fukuyama, *Synthesis* **2002**, 1121–1123.
[163] T. Shimizu, M. Seki, *Tetrahedron Lett.* **2000**, *41*, 5099–5101.
[164] S.-Q. Tang, J. Bricard, M. Schmitt, F. Bihel, *Org. Lett.* **2019**, *21*, 844–848.
[165] J. H. Lee, Y. Kishi, *J. Am. Chem. Soc.* **2016**, *138*, 7178–7186.
[166] J. Talode, D. Kato, H. Nagae, H. Tsurugi, M. Seki, K. Mashima, *J. Org. Chem.* **2020**, *85*, 12382–12392.
[167] S. Sikandar, A. F. Zahoor, S. Naheed, B. Parveen, K. G. Ali, R. Akhtar, *Mol. Divers.* **2022**, *26*, 589–628.
[168] Y. Mori, M. Seki, *Adv. Synth. Catal.* **2007**, *349*, 2027–2038.
[169] Y. Yu, L. S. Liebeskind, *J. Org. Chem.* **2004**, *69*, 3554–3557.
[170] R. Wittenberg, J. Srogl, M. Egi, L. S. Liebeskind, *Org. Lett.* **2003**, *5*, 3033–3035.
[171] B. W. Fausett, L. S. Liebeskind, *J. Org. Chem.* **2005**, *70*, 4851–4853.
[172] T. Shimizu, M. Seki, *Tetrahedron Lett.* **2002**, *43*, 1039–1042.
[173] P. H. Gehrtz, P. Kathe, I. Fleischer, *Chem. Eur. J.* **2018**, *24*, 8774–8778.
[174] F. H. Lutter, L. Grokenberger, M. S. Hofmayer, P. Knochel, *Chem. Sci.* **2019**, *10*, 8241–8245.
[175] Y.-H. Chen, C. P. Tüllmann, M. Ellwart, P. Knochel, *Angew. Chem. Int. Ed.* **2017**, *56*, 9236–9239.

[176] J. Wang, B. P. Cary, P. D. Beyer, S. H. Gellman, D. J. Weix, *Angew. Chem. Int. Ed.* **2019**, *58*, 12081–12085.
[177] A. Krasovskiy, P. Knochel, *Synthesis* **2006**, 0890–0891.
[178] W. Tong, G. Zhou, J. H. Waldman, *Org. Process Res. Dev.* **2022**, *26*, 1184–1190.
[179] G. Cahiez, L. Razafintsalama, B. Laboue, F. Chau, *Tetrahedron Lett.* **1998**, *39*, 849–852.
[180] E. M. Hanada, T. K. S. Tagawa, M. Kawada, S. A. Blum, *J. Am. Chem. Soc.* **2022**, *144*, 12081–12091.
[181] A. Hernán-Gómez, E. Herd, E. Hevia, A. R. Kennedy, P. Knochel, K. Koszinowski, S. M. Manolikakes, R. E. Mulvey, C. Schnegelsberg, *Angew. Chem. Int. Ed.* **2014**, *53*, 2706–2710.
[182] E. Y. Fursova, V. I. Ovcharenko, A. S. Bogomyakov, G. V. Romanenko, *J. Struct. Chem.* **2013**, *54*, 164–167.
[183] V. Geiger, Master Thesis, University of Tübingen, **2018**.
[184] S. L. Buchwald, C. Bolm, *Angew. Chem. Int. Ed.* **2009**, *48*, 5586–5587.
[185] Y. Tian, L. Wang, H.-Z. Yu, *RSC Adv.* **2016**, *6*, 61996–62004.
[186] S. Magens, B. Plietker, *Chem. Eur. J.* **2011**, *17*, 8807–8809.
[187] T. Gensch, M. Teders, F. Glorius, *J.Org. Chem.* **2017**, *82*, 9154-9159.
[188] P. H. Gehrtz, Doctoral Thesis, University of Tübingen, **2018**.
[189] G. Cahiez, C. Duplais, J. Buendia, *Angew. Chem. Int. Ed.* **2009**, *48*, 6731–6734.
[190] a) M. S. Maji, A. Studer, *Synthesis* **2009**, *2009*, 2467–2470; b) G. M. Whitesides, T. L. Newirth, *J. Org. Chem.* **1975**, *40*, 3448.
[191] M. Uzelac, P. Mastropierro, M. de Tullio, I. Borilovic, M. Tarrés, A. R. Kennedy, G. Aromí, E. Hevia, *Angew. Chem. Int. Ed.*, **2021**, *60*, 3247–3253.
[192] R. J. Trovitch, E. Lobkovsky, P. J. Chirik, *J. Am. Chem. Soc.* **2008**, *130*, 11631–11640.
[193] C. G. Werncke, J. Pfeiffer, I. Müller, L. Vendier, S. Sabo-Etienne, S. Bontemps, *Dalton T.* **2019**, *48*, 1757–1765.

4.1 Introduction

4.1.1 Cobalt-Catalyzed Cross-Coupling

4.1.1.1 Early Developments

Next to palladium-, nickel- or iron-catalyzed cross-couplings, cobalt has been advanced as a transition metal-catalyst for similar transformations.[1] Despite the significant progress in this field, cobalt is attributed with toxicity problematic for pharmaceutical applications and with a rising market price due to battery materials.[2]

As a pioneering example on cobalt-catalyzed couplings, this transition metal was part of a study conducted by Gilman. Therein, substochiometric cobalt-additive mediated a homo-coupling of phenyl magnesium bromide (**45**) forming biphenyl (**153**) quantitatively, similarly to iron or nickel (Scheme 4.1).[3]

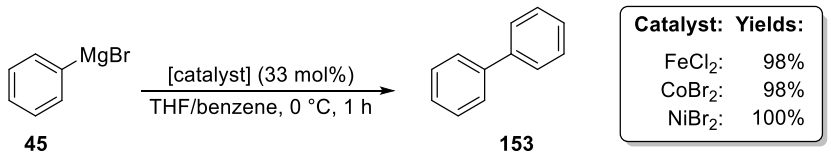

Scheme 4.1. Gilman's study on the influence of transition metal halide salts on Grignard reagents.[3]

Following studies of Kharasch and co-workers on transition metal-catalyzed cross-coupling with Grignard reagents were also investigating cobalt-catalysis.[4] To this end, a similar homo-coupling of phenyl magnesium halide was observed to occur with additional oxidants such as ethyl bromide or *iso*-propyl chloride.[4a] Elaborating on Gilman's studies, cross-coupling reactions with methyl magnesium bromide (**34**) were probed in which styryl halide or alkynyl halide were converted (Scheme 4.2).[5]

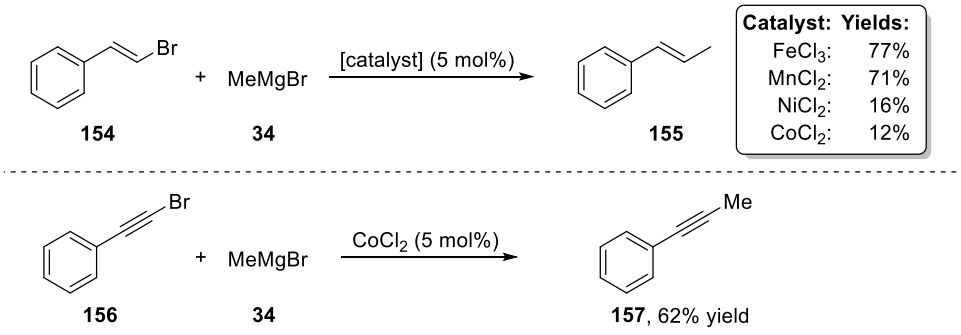

Scheme 4.2 Excerpt from Kharasch studies on styryl or alkynyl halides with different transition metal salts.[5]

The coupling of styryl halides with cobalt-catalyst performed poorly in comparison to other transition metals, whereas methylation of alkynyl bromides led to comparably good yields. Indeed, later reports demonstrated that stochiometric amounts of methyl(cyano-)cobalatates are suitable methylation reagents for a range of organic compounds, e.g. styryl bromides[6], alkenyl chlorides[7], acyl halides[8] or

aryl halides[9].[10] Shortly after, activation of vinyl halides, **35** or **160**, was optimized with the utilization of NMP as co-solvent, leading to the development of catalytic alkenylation of organomagnesium or organozinc reagents, and arylation in case of Mg (Scheme 4.3).[11] However, similar to studies on iron-catalysis[12], other polar co-solvents also possessed a positive influence. The reaction with less reactive alkyl zinc reagent proceeded much more sluggishly and necessitated higher catalyst loadings and excess organometallic reagent. It is important to point out that generally cobalt-catalyzed cross-coupling reactions perform similarly independent of the initial oxidation state.

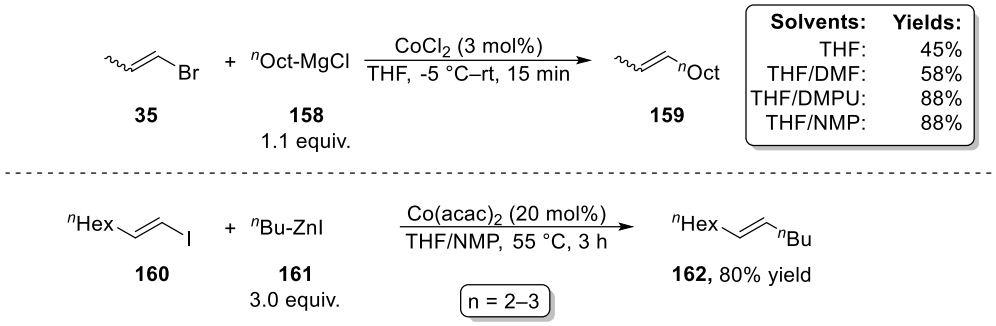

Scheme 4.3. Co-catalyzed alkenylation of organomagnesium- or organozinc reagents.[11]

Other early reports demonstrated that cobalt can be utilized to catalyze the synthesis of aryl zinc reagents from metallic zinc.[13]

4.1.1.2 Modern cobalt-catalyzed cross-couplings

Over decades, cobalt-catalyzed cross-couplings have evolved as a reliable tool for the transformations of a broad spectrum of organic electrophiles and organomagnesium[14], -aluminium[15], -zinc[16] or -manganese[17] reagents (Table 4.1). Likewise, a lot of progress has been achieved in cobalt-catalyzed Suzuki-Miyaura-type couplings, leading to the development of more optimal ligands for difficult transformations.[18] The incentive to utilize cobalt-catalysts is especially due to a sought-after activation of C(sp^3)-electrophiles. Namely, this activation is coveted due to a lower competition of β-hydrogen elimination pathways which can be problematic for nickel- or palladium-catalysts.[1c–e, 19] Nevertheless, cobalt-catalysts have been reported to promote dehydrohalogenation reactions.[20]

Table 4.1. Overview of different cobalt-catalyzed or -mediated C-C cross-couplings with different organometallic compounds (Mg, Al, Zn, ZnOPiv, Mn) – omitted are Suzuki-Miyaura couplings. The table does not depict all the researched methodologies in full. Hybridizations corresponds to the organic (pseudo-)halide.

Organometallic reagent	Alkyl (sp^3) 	Aryl (sp^2) 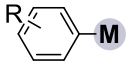	Alkynyl (sp) 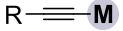
Electrophile:			
Alkyl (sp^3) 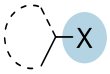	**$sp^3_{(prim.)}$**-F[21]/Br[22]/I[22b, 23]	**$sp^3_{(prim.)}$**-Cl[24]/Br[15, 24–25]/I[26]	**sp^3**-Cl[27]/Br[27–28]
	$sp^3_{(sec.)}$-Br[22]/I[22b, 23]	**$sp^3_{(sec.)}$**-Cl[29]/Br[14a, 15, 16b, 25, 29–30]/I[14b, 17, 26, 31]	**$sp^3_{(sec.)}$**-Br[28]/I[28, 32]
	$sp^3_{(tert.)}$-Cl[22b]/Br[22b]		
	$sp^3_{(allyl)}$-Cl[33]/Br[16b, 34]/ OP(O)(OEt)$_2$[33]/OMe[35]	**$sp^3_{(allyl)}$**-OR[35]	
Alkenyl, aryl (sp^2) 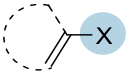	**$sp^2_{(vinyl)}$**-Cl[36]/Br[11b, 36]/I[11b]	**$sp^2_{(vinyl)}$**-Br[11, 37]/I[11a, 37]/OTf[38]/ OAc[39]/OTs[39]/OPiv[39]	**$sp^2_{(vinyl)}$**-OTf[40]
	$sp^2_{(hetero-, aryl)}$-Cl[16a]/ Br[16a, 41]/OTs[42]/OMs[42]/ phosphonium[43]	**$sp^2_{(hetero-, aryl)}$**-F[44]/Cl[37, 45]/Br[15, 37, 45a]/I[37]/OTs[42]/OMs[42]/	**$sp^2_{(hetero-, aryl)}$**-Cl[46]/ Br[46]/I[46]
Alkynyl (sp) 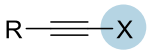	**$sp_{(alkynyl)}$**-Br[47]	**$sp_{(alkynyl)}$**-Br[37, 47]	

As a major advantage, cobalt-catalyzed cross-couplings usually proceed without racemization of a stereogenic center, enabling diastereoselective C(sp^2)-C(sp^3) cross-couplings.[17, 28–29, 30a] This strategy was applied in the synthesis of (−)-isoaltholactone (**165,** natural product from *Goniothalamus malayanus*)[29b, 48] (Scheme 4.4), intermediates for NK_1-agonists[14b], derivation of bromo-β-lactams[29a] as well as an enantioselective synthesis of natural compounds such as (*S*)-preclamol.[14a, 49]

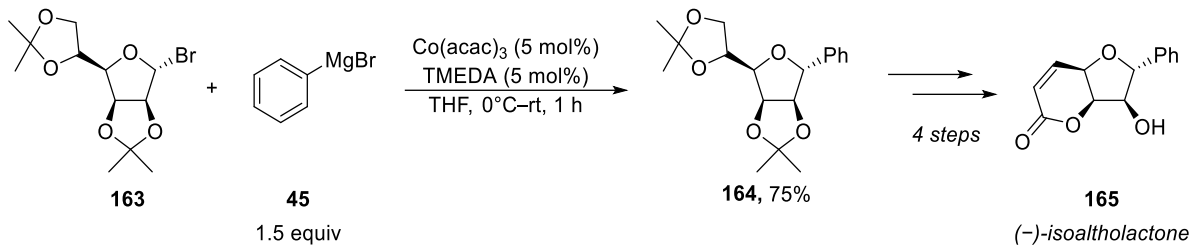

Scheme 4.4. Synthesis of natural product (−)-isoaltholactone *via* a cobalt-catalyzed diastereoselective arylation.[29b]

In general, these transformations are postulated to occur *via* a Co^{+I}-intermediate with activation of the electrophile proceeding *via* SET-processes.[15] The formation of Co^{+I}-species was supported by radical clock experiments[14a, 19b], EPR spin-trapping[50] and ESI-MS studies[19c]. The ESI-MS measurements revealed that the formation of the Co^{+I} intermediate occurs concomitantly to the generation of low-valent Co-species. The initially formed intermediate **166** is likely first transmetalated to the electron-rich species **167** (Scheme 4.5). Subsequently, SET-activation leads to the formation of Co^{+II} complex which then depending on the proposed cycle either recombines (cycle I) or activates (cycle II) the organohalide. In favor of a cycle I-pathway, studied diaryl Co^{+II} complexes were reported to perform reductive elimination much more readily in gas-phase fragmentation reactions than diaryl Co^{+III} species.[19c] Other literature examples have substantiated catalytic capabilities of Co^{+II} bisorganyles.[24, 51] Conversely, studies have demonstrated a mostly concerted reductive elimination pathway from dimethyl Co^{+III}-complexes.[52]

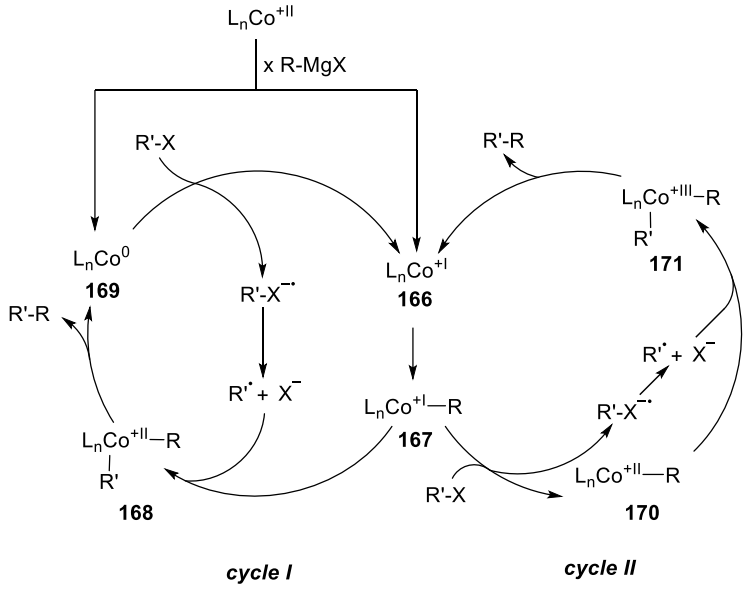

Scheme 4.5. Proposed catalytic cycles for cross-coupling reactions with either a Co^0/Co^{+II} or Co^{+I}/Co^{+III} catalytic cycle.[19c]

Besides, radical intermediates generated by cobalt -catalysis have been leveraged to perform radical 5-exo-trig cyclizations.[19b, 25, 53] One application has been reported in the enantioselective synthesis of AH13205 (**175**, prostanoid EP_2-receptor agonist, anti-inflammatory[54], reduces intraocular pressure[55]) which utilized a cyclization and arylation with a simple chiral cyclohexadiamine-based ligand.[30c]

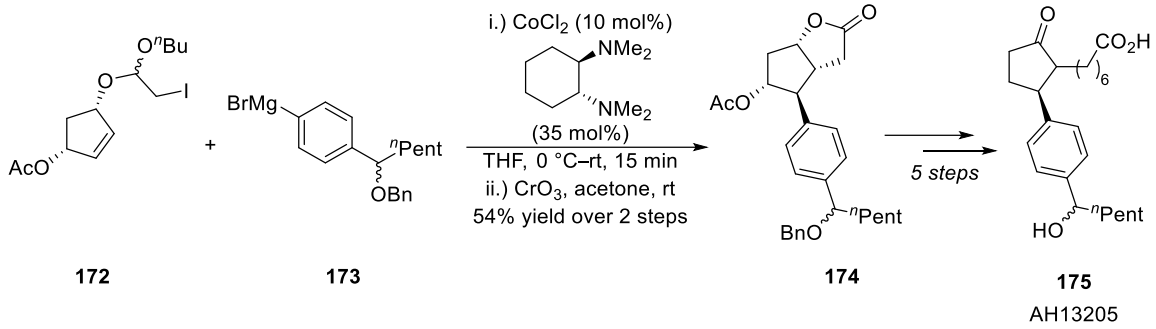

Scheme 4.6 Steps in the synthesis of AH13205 by cobalt-catalyzed activation of an alkyl iodide and subsequent ring-formation with high stereoselectivity.[30c]

Similarly, the propensity of cobalt for radical generation was key in the activation of electrophiles using cobalamin or similar substrates, e.g. in dual catalytic methodologies.[56] Additionally, these radical pathways allowed for decarboxylative cross-couplings of compounds such as *N*-hydroxyphthalimide (NHP) esters which were demonstrated to couple aryl, vinyl and alkynyl zinc reagents (Scheme 4.7).[57]

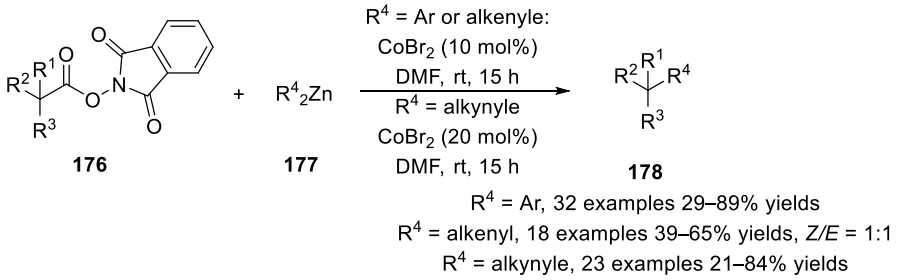

Scheme 4.7. Radical decarboxylation and cross-coupling of NHP esters yielding quaternary carbon centers.[57]

In terms of coupling of aryl halides, cobalt-catalyzed cross-couplings have been associated with slower reactions.[58] Later on, literature examples demonstrated a beneficial reactivity for such transformations with additives such as quinoline for Kumada-type coupling or sodium formate for Negishi-type couplings (Scheme 4.8).[45a, 59]

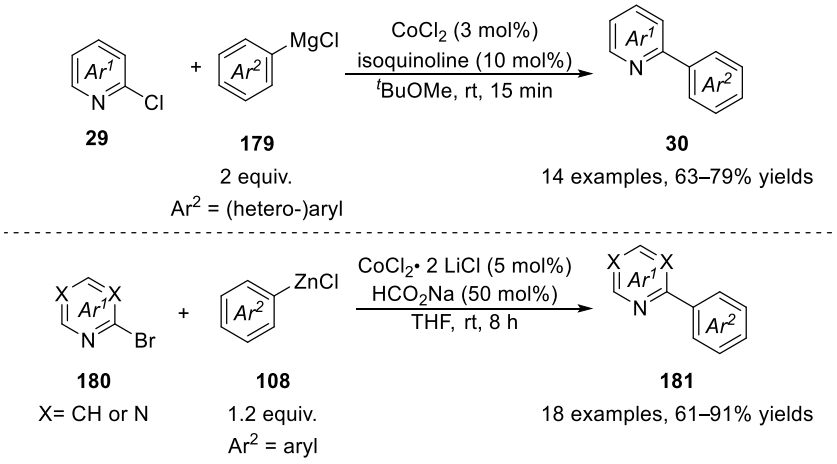

Scheme 4.8. C(sp^2)-C(sp^2) cross-coupling with organomagnesium or -zinc reagents employing additives to promote the reaction.[45a, 59]

Interestingly, the utilization of alkyl instead of aryl zinc reagents furnished high yields without formate additive.[16a] Then again, the reaction of aryl halides could also be achieved with the aid of directing groups in such as *ortho*-olefins, -ketones as well as 2-pyridyls.[45a, 45b, 60] Similar to the studies on iron-catalyzed C(sp^2)-C(sp^2) cross-couplings, the methodology can be promoted with stronger coordinating anions such as fluorides.[45c]

As one major advantage, cobalt-catalysis can enable the synthesis of Grignard reagents from aryl (pseudo-)halides[61] as well as of organozinc reagents.[61a, 61b, 62] In practice, *in situ* generated organometallic species are directly converted in a subsequent cross-coupling reaction.[47, 60a, 63] Recently, even less reactive aryl (thio-)ethers have been converted to corresponding Grignard reagents with a Co^{+II}-catalyst.[64] Such reactivities demonstrate the aptitude of cobalt-catalysts for reductive cross-electrophile couplings[45d, 65] with or without preformed organometallic reagents.[41a] In one report, reactive aryl (pseudo-)halides have been coupled with less reactive aryl halides (Scheme 4.9). However, the method was necessitating 2 equivalents of less reactive component, high amounts of reductant – even with prior activation – and high amounts of cobalt. Nevertheless, the circumvention of the synthesis and storage of highly reactive organometallic reagents is a crucial advantage in terms of availability.

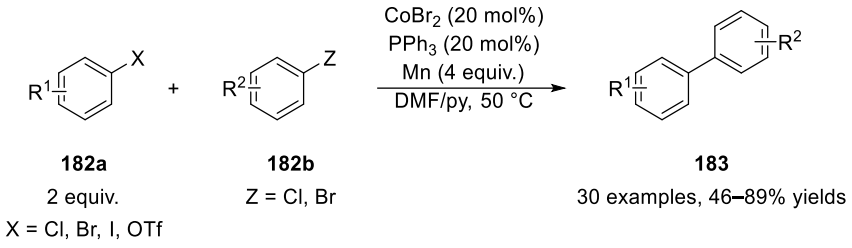

Scheme 4.9. Cobalt-assisted cross-electrophile-coupling synthesizing biaryls by utilizing metallic reductant.[45d]

Other recent applications for cobalt-catalyzed cross-couplings relate to the relative ease of coupling organozinc pivalates. These organometallic reagents are considered more air and moisture resistant in contrast to organozinc halides and can be stored as a solid for a prolonged period.[66] Compared to other transition metals, cobalt-catalysis has been most commonly employed in the cross-coupling of these reagents.[46, 67] A recent example demonstrating high functional group tolerance is the fluoroalkylarylation of alkenes (Scheme 4.10).

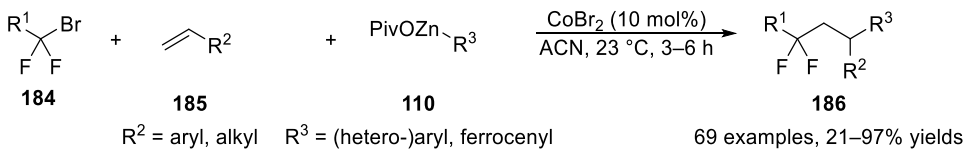

Scheme 4.10. Cobalt-catalyzed fluoroalkylarylation of alkenes employing organozinc pivalates.[50]

Such a transformation is sought after since fluorinated compounds often possess coveted properties for pharmaceutical applications.[68] The reported mechanistic studies demonstrated that aryl zinc pivalates enable the formation of a Co^{+I}-species which then undergoes SET-reactions.

4.1.1.3 Cobalt-catalyzed acylation

In terms of acylations, early studies by Knochel and co-workers led to the development of cobalt-catalyzed methodologies utilizing bisalkyl- or bisarylzinc under CO atmosphere in a THF/NMP mixture.[33, 69] Moreover, the reaction was applicable to simple acid chlorides, e.g. **100**, which gave rise to a potentially wider synthetic scope (Scheme 4.11). In parallel to these publications, the methylation of acyl chlorides was reported, although, with stochiometric amounts of methyl cobaltate.[10]

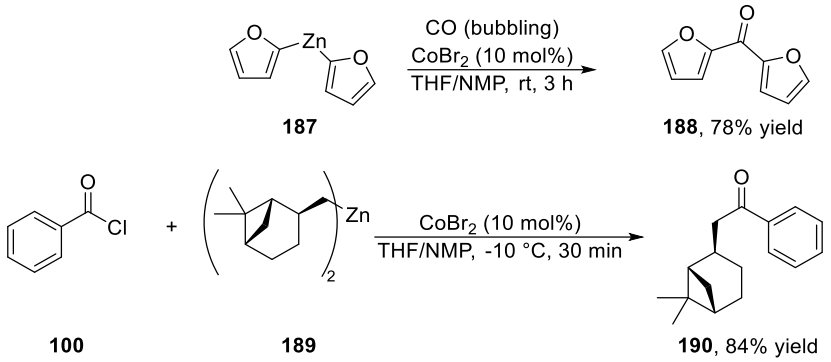

Scheme 4.11. Synthesis of ketones by cobalt-catalyzed acylation of bisorganozinc reagents.[33, 69]

As mentioned previously, the ability of cobalt to catalyze the synthesis organozinc reagents is an often-exploited advantage of the transition metal. In electrochemical studies, sacrificial Zn anodes were utilized under cobalt-catalytic conditions to generate **108**, which further reacted with acyl chlorides (Scheme 4.12).[70] Interestingly, the synthesis of zinc reagents did not exhibit a strong dependance on electron-withdrawing substituents, indicating a potentially broad synthetic applicability. A similar reaction was later developed for acid anhydrides.[71] In case of the anhydrides, zinc dust was used as reductant, circumventing an electrochemical setup but necessitating substochiometric allyl chloride and triflic acid additives to sufficiently activate the metallic reductant.

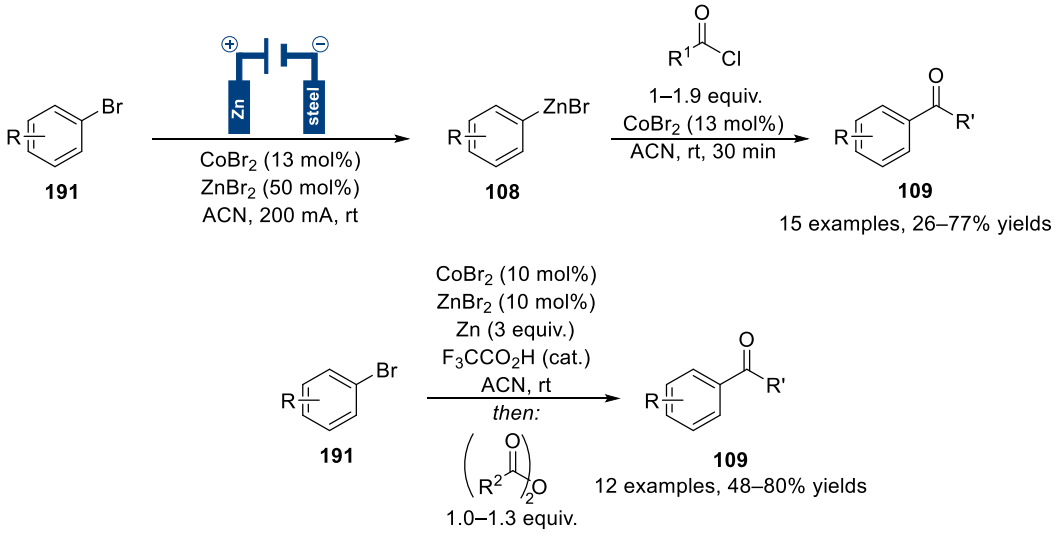

Scheme 4.12. Cobalt-catalyzed (electro-)chemical synthesis of aryl zinc reagents with subsequent cross-coupling.[70–71]

As a more recent examples, another synthesis of symmetrical diaryl ketones was reported.[72] Ethyl chloroformates reacted with *in situ* generated organozinc reagents in presence of a cobalt precatalyst and reductant (Scheme 4.13).

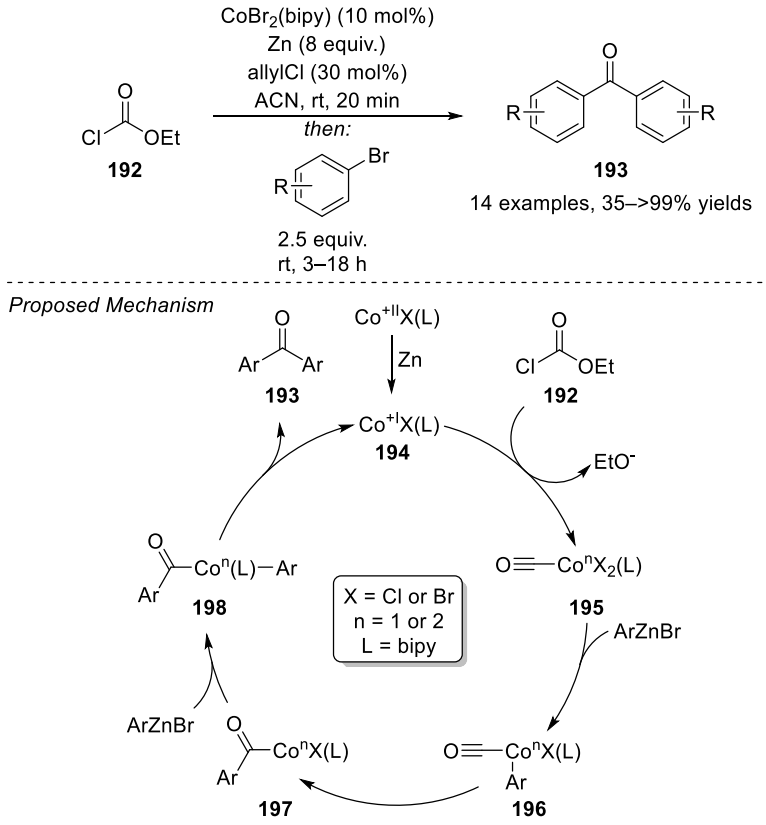

Scheme 4.13. Conversion of ethyl chloroformates to form symmetrical-substituted ketones *via* a cobalt-carbonyl intermediate.[72]

For this reaction a mechanism with a cobalt-carbonyl intermediate, **195** or **196**, was postulated which was proposed due to carbonyl bands observed *via* IR spectroscopy. This is followed by transmetalation, migratory insertion and second transmetalation with a reductive elimination.[72] Although the scope of substrates is limited to benzophenone-derivatives for this reaction system, the intermediary formation of cobalt carbonyls indicates a key property of the transition metal: To enable coordination and transfer of CO ligand for cross-coupling methodologies.

Enabling access to unsymmetrical ketones, thiopyridyl esters were employed in a cobalt-catalyzed acylation reaction with organozinc pivalates furnishing phenones which has been discussed in a previous chapter (see Chapter **2.1.3**, p. 40)[73] Moreover, *N*-acyl glutarimides **199** have been increasingly employed as acyl donors due to their increased reactivity.[74] Employing Co-catalysis, **199** were coupled with *in situ* synthesized organozinc reagents.[63] In a later report, a similar reaction system was applicable to the less reactive alkyl zinc reagents which were not generated *in situ*. However, the method relied on high catalyst loadings of 20 mol% and 2.0 equivalents of organometallic reagent decreasing the efficiency of the conversion and was limited to the synthesis of phenones.[75]

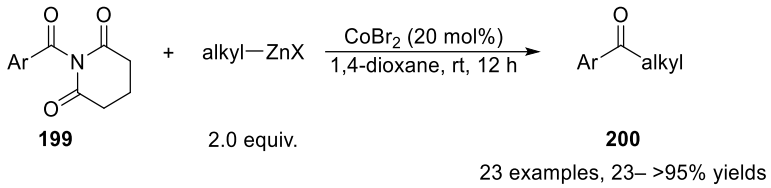

Scheme 4.14. Cross-coupling of *N*-acyl glutarimides with alkyl zinc reagents utilizing cobalt-catalysis.[75]

In view of these literature examples of cobalt-catalyzed cross-couplings, the disadvantages of a comparable higher price to other first-row transition metals and its toxicity come with the advantages of activation of difficult electrophiles, available *in situ* synthesis of organometallic reagents for cross-electrophile couplings as well as suitably fast acylation chemistry under mild conditions.

4.1.2 Carbonyl-Sulfur Building Blocks in Catalysis

Bivalent sulfur constitutes an important moiety in natural compounds. Next to thioethers or disulfides, the carbonyl-sulfur bond is another common motif in biochemistry with the most prominent example of acetyl CoA (Figure 4.1, **201**). This thioacetate is only one example of acyl CoA-metabolites which are associated with key biochemical pathways (oxidative decarboxylation, β-oxidation, TCA cycle) and processing of xenobiotic carboxylic acids.[76] Additionally, examples of natural products or drugs are known to incorporate carbonyl-sulfur motifs, e.g. suncheonosides[77] (**202**), benzoxacystol (**203**)[78], formicin A or fluticasone.[79] This is not limited to thioesters, but extents to thiocarbamates and thiocarbonates which have been incorporated in drugs (pioglitazone, **204**; rosiglitazone)[80], drug candidates (oxathiazole-2-one GL5, **205**[81]) or have been discovered from natural sources **206** (Figure 4.1).[79b, 80, 82]

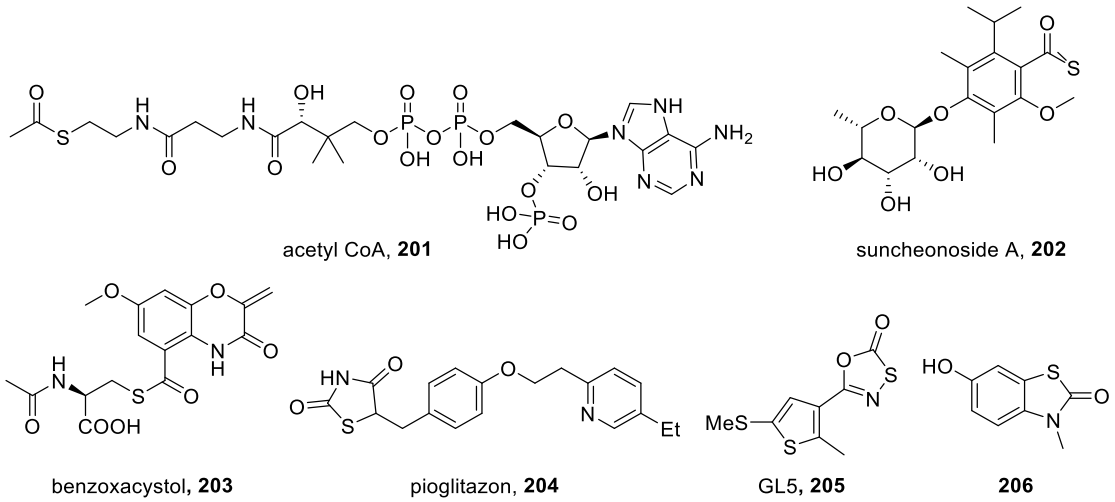

Figure 4.1. Examples of carbonyl-sulfur motif in natural or pharmaceutical compounds.[76a, 79b]

In view of bond dissociation energies (BDE), the differences between thioester, thioformate and thiocarbamate seem negligible when compared to the impact of the thiol moiety, **210** vs. **212**, (Figure 4.2). In terms of these approximations, thiocarbonates **209** and dithiocarbonates **207** do deviate, but to a lesser extent than the influence of the thiol moiety. Although the approximative nature of this comparison prohibits deductions about their reactivity, the utilization of these compounds as sulfur-based building blocks can be considered to relate to the corresponding thioesters.

Particularly, transition metal-catalysis is known to enable activation of C(O)-S bonds by oxidative addition or similar processes. Albeit, the generated thiolates are often considered catalyst poisons, especially for Pd- or Pt-catalysts.[83] Then again, many examples of catalytic conversion of thiolates validate the potential in synthesis of sulfur based-building blocks which has been summarized in multiple reviews.[84]

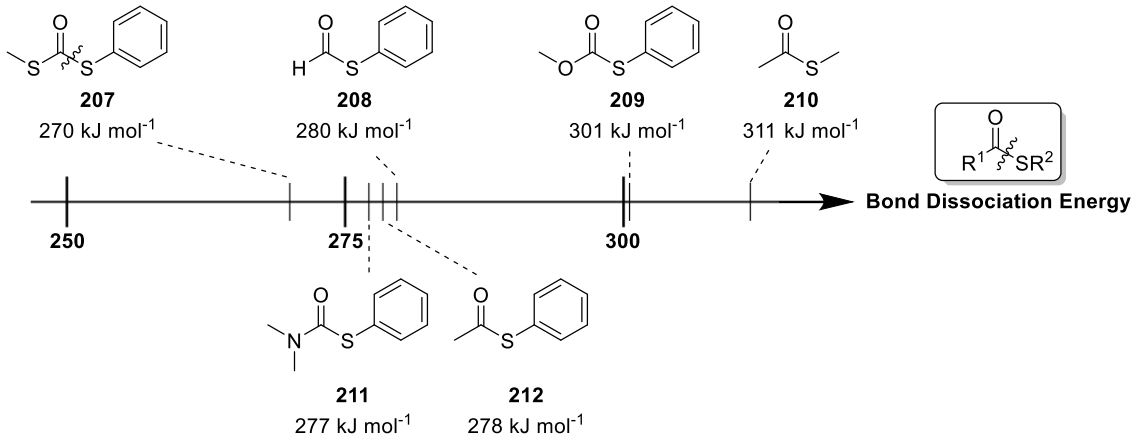

Figure 4.2. Bond dissociation energies calculated using ALFABET estimator (machine learning-based).[85] The values of thioesters **210** and **212** are close (<8 kJ mol^{-1}) to reported DFT-based results.[86]

4.1.2.1 Thioesters

Thioesters have mainly been utilized as acyl donors with catalytic applications connected to the Fukuyama cross-coupling (FCC) [87] or Fukuyama reduction reaction (FRR)[88] – which have been discussed in case of FCC in previous chapters of this thesis with the focus on the catalytic reactions with organometallic reagents (see chapter **2.1.3** p. 39).[84c, 89] Historically, the capability of thioesters for acylation reactions has been established prior to Fukuyama's reports, e.g. in non-catalytic reactions with organocopper reagents.[90] An advantage of thioesters for synthetic purposes is that the reactivity can be efficiently altered by the thiol substituent. Namely, they can be categorized from highest to lowest reactivity as such: 2-pyridyl>aryl>alkyl.[91] Implementing this, recent research on this topic leveraged high reactivity of 2-pyridyl thioesters in a Ni-catalyzed, reductive, decarboxylative cross-electrophile coupling with *N*-hydroxyphthalimide esters (NHP) (Scheme 4.15).[92] Therein, thioesters constituted the acyl donors and NHP esters the decarboxylated radical precursors. Not surprisingly, the method possessed the advantage of being able to couple NHP esters with protic moieties or aryl/- alkyl halides, which furnishes products difficult to obtain *via* FCC or similar methodologies.

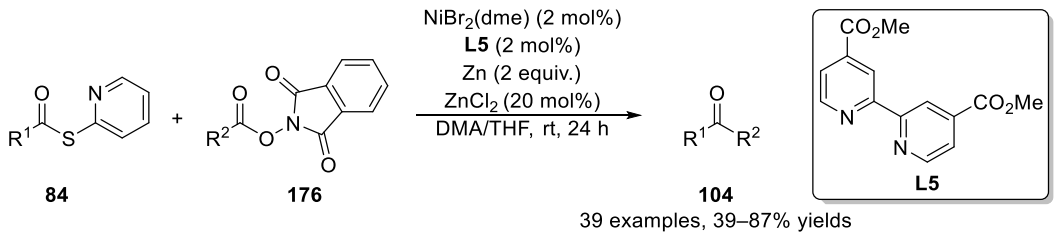

Scheme 4.15. Reductive cross-electrophile coupling of NHP esters with thiopyridyl esters.[92]

It is important to point out that while thioesters have been postulated to be activated *via* SET-reactions under Ni-catalysis[93], in this instance, radical generation was far more accessible for the NHP esters ($E_{1/2}$(NHP ester) = -1.7 V; $E_{1/2}$(2-pyridyl thioester) = -2.8 V *vs* Fc/Fc$^+$ in DMF)[92]. However, *S*-pyridyl thioesters have been exemplified to react as acyl radical donors.[94] Indeed, similar to the bond dissociation energies discussed in this chapter, reported reduction potentials reveal the influence of the

carbonyl as well as thiol and even substituents on an aryl thiol moiety (Figure 4.3).[92, 95] Thus, the reactivity of thioesters can be manipulated for reaction purposes, e.g. catalytic acylations.

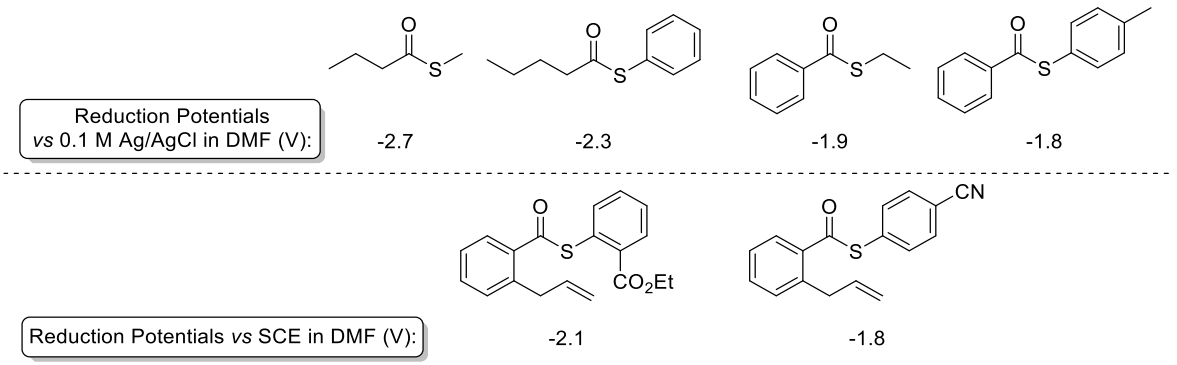

Figure 4.3. Reported values of reduction potentials of thioesters demonstrating the influences of the carbonyl and thiol substituents.[95a, 95b]

Notwithstanding the utility of the acylation utilizing thioesters, the thiol moiety constitutes a valuable fragment for synthetic applications as well, especial for pharmaceutical applications. This is due to beneficial properties of thioethers in comparison to oxoethers such as higher lipophilicity or different metabolism of the compounds.[96] Nevertheless, poisoning of transition metal-catalysts by thiols or thiolates is a common problem for catalytic synthesis. Therefore, thioesters enable catalytic transformations as released thiolate is directly converted, suppressing side reactions such as disulfide formation. Namely, thioacetates[97] or thiobenzoates have been used as thiol surrogates. Recently, thiobenzoates **213** were employed in the synthesis of functionalized vinyl thioethers reacting with *N*-tosylhydrazones **214** (Scheme 4.16).[98]

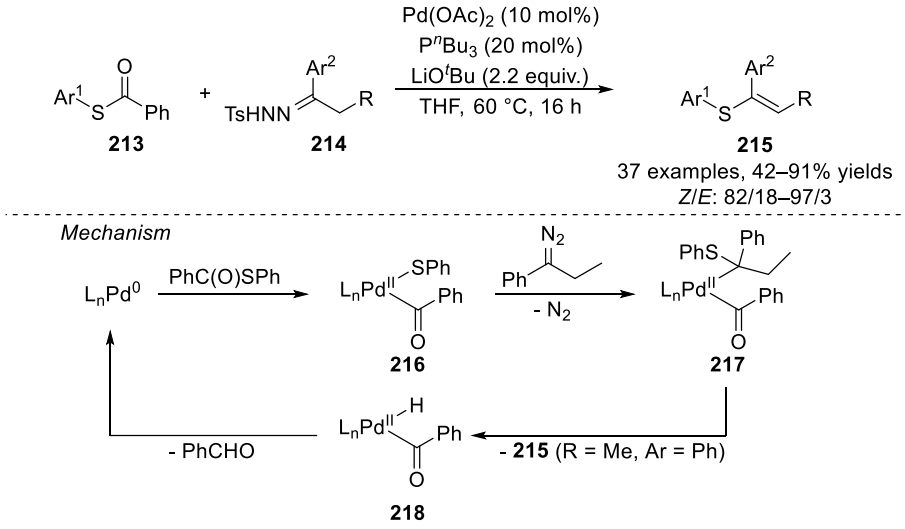

Scheme 4.16. Denitrogenative cross-coupling of protected thiolates with *N*-tosylhydrazones.[98]

The utilization of the thiol surrogate proceeded similarly to FCC by oxidative addition to form species **216**, which reacted with hydrazone **214** to **217**. Then, the facile β-hydride elimination of palladium from **217** and subsequent reductive elimination of **218** furnished aryl vinyl thioethers and aryl aldehydes as

by-product. Most notably, this methodology demonstrates that thioesters can be leveraged not only in the synthesis of ketones, but also of complex thioethers by utilization of known reactivities.

Of course, efforts to affix both, acyl and thiolate moiety, have been made with the most general example being a formal insertion of an unsaturated bond into the C(O)-S bond affording thioacylation products. Examples of such reactions are scarce, mostly palladium-catalyzed and necessitate medium to high catalyst loadings (Scheme 4.17).[95a, 99] Similar reactions have also been realized for the corresponding iminothiolation of alkynes.[100]

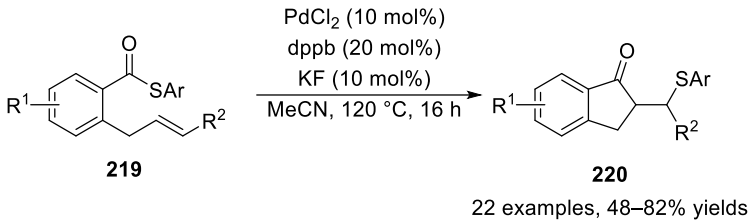

Scheme 4.17. Pd-catalyzed intramolecular thioacylation furnishing indanone thioethers.[99]

More complex examples have been studied with a tandem FCC-Migita reaction[101] constituting a formal insertion of a phenyl moiety into the thioester. Similarly, the employment of 1,2,3-triazoles was reported utilizing Rh-catalysis which is known to give rise to Rh-carbene intermediates (Scheme 4.18, **(B)**) In return, this enabled the synthesis of thiazepines (**223**), an important class of pharmaceutical products.[102] These examples reflect the multitude of fragments that can be formally inserted into C(O)-S bonds.

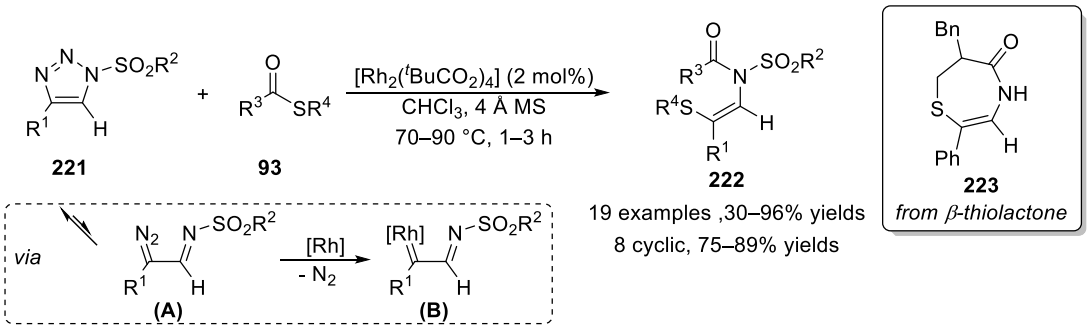

Scheme 4.18. Thioacylation of activated triazoles enabling ring-expansion of thiolactones.[102]

Thioesters can also be converted to furnish formal insertion into the C(O)-C bond. A recent study has exemplified that such a transformation can be achieved by nickel-catalysis (Scheme 4.19).[103] For this, an activation of aryl iodide **224** is followed by a cyclization leading to an intermediate that can oxidatively add a thioester furnishing species **227**. In the postulated mechanism a migratory de- and reinsertion of CO allows for the formation of species **229** which then furnishes the valuable thioester products **226** by reductive elimination.

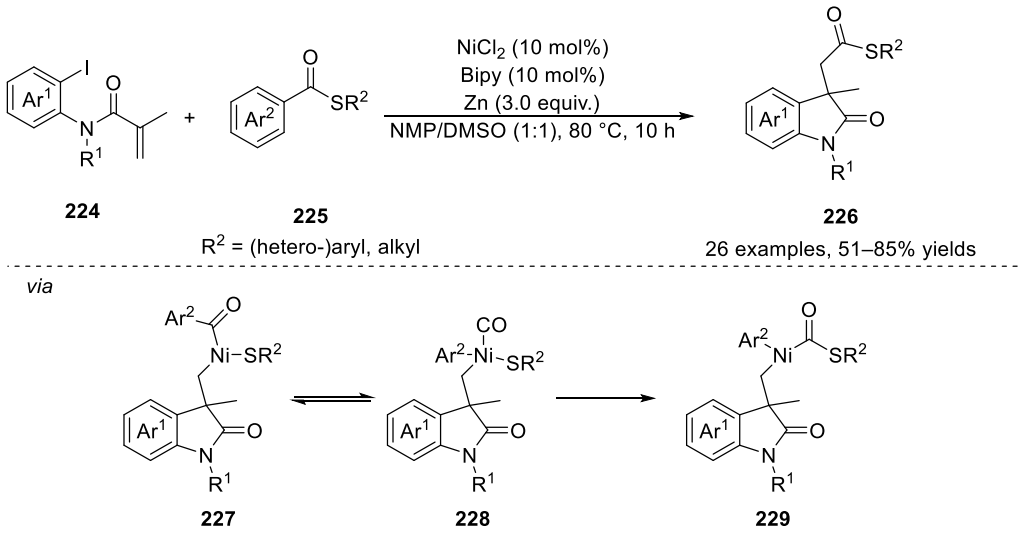

Scheme 4.19. Nickel-catalyzed thioesterification of alkenes by a postulated transfer of the carbonyl group.[103]

As demonstrated in the above example, decarbonylation is a common reactivity for acyl donor fragments and the plethora of transformations connected with this process have been summarized in recent reviews.[104] In case of thioesters, early reports demonstrated decarbonylation by palladium-catalysts or stochiometric amounts of rhodium or nickel.[105] Seeking a catalytic method, four working groups published almost concurrently similar Ni-catalyzed decarbonylations.[106] In the first report, a comparative study demonstrated the difference in yield and selectivity for Ni- and Pd-catalysis (Scheme 4.20).

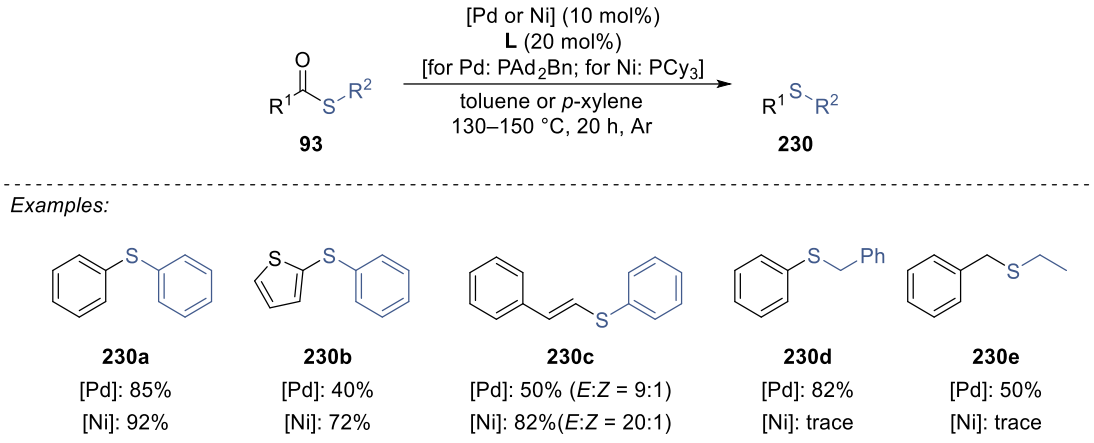

Scheme 4.20. Comparative examples for the Ni- and Pd-catalyzed decarbonylative thioether synthesis from thioesters.[106a]

Interestingly, the Ni-catalyzed reaction was more suitable for the coveted bisaryl thioethers. While other reports disclosed the increase the yields for alkyl thiolates, e.g. **230d** or **230e**, enabled by different ligand choice, the reported methodologies generally relied on the utilization of benzoyl-based starting materials.[106b] Ensuing reports also leveraged this reaction for the synthesis of fluorinated thioethers, decarbonylative borylation[107] or selective single- and double decarbonylation *via* nickel-catalysis.[108]

4.1.2.2 Thioformates

Much less known substrates for transition metal-catalysis are thioformates which have been more explored in biochemistry-related research.[109] Only recently, an application of these reagents has been reported establishing their potential in FCC-type reactions. In a palladium-catalyzed reaction, the formylation of aryl zinc halides was achieved, leading to respective aryl aldehydes (Scheme 4.21).[110]

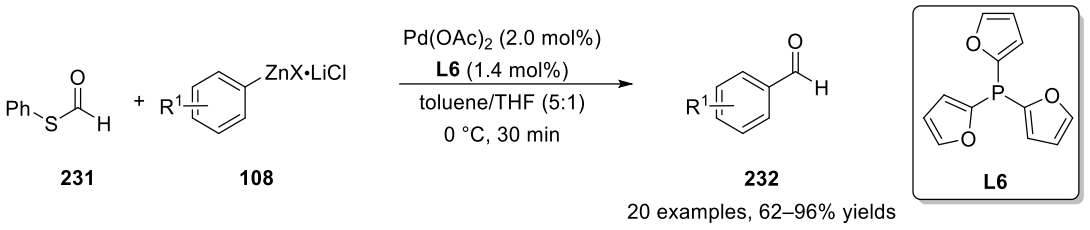

Scheme 4.21. Formylation of aryl zinc reagents using *S*-thioformates as carbonyl source.[110]

The reaction necessitated the utilization of a very specific metal-to-ligand ratio, which reportedly had a significant influence. However, the method could convert a range of organozinc reagents under mild conditions, tolerating functionalities such as nitriles, esters or phenols. In a subsequent study, the procedure was adapted to convert styryl zinc reagents.[111] Due to a decreased reactivity, the method required the use of more reactive thioformates **233** and $ZnBr_2$ additive (Scheme 4.22). The salt additive is known for Negishi-type couplings to promote transmetalation and therefore increase the overall reaction yields.[112] Additionally, *S*-thioformates have also been employed in non-transition metal-catalyzed synthesis of tertiary aldehydes.[113]

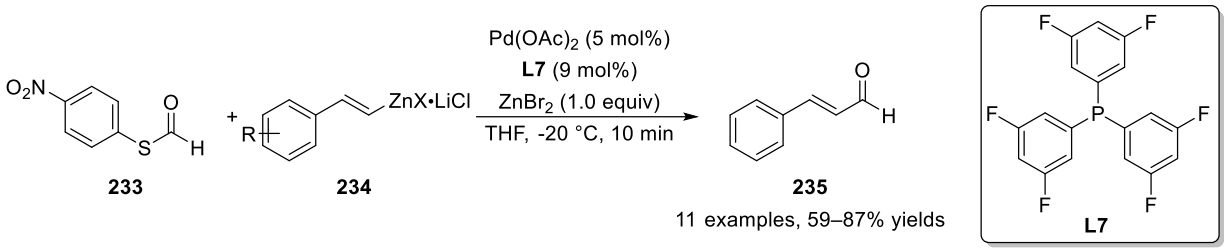

Scheme 4.22. Synthesis of 3-phenyl acroleins by palladium-catalysis utilizing *S*-phenyl thioformates as formyl source.[111]

When comparing the synthetic applications of thioformates for the synthesis of aldehydes, all reactions featured low temperatures and short reaction times and the use of additives or specific ligands was essential to furnish meaningful yields.

4.1.2.3 Thiocarbonates and thiocarbamates

Other examples of C(O)-S motifs are thiocarbonates and thiocarbamates, which can also be utilized as suitable building blocks for catalytic reactions. This potential was demonstrated in recent literature examples. For instance, a palladium-catalyzed Liebeskind-Srogl-type coupling of boronic acid esters was shown to proceed with thiocarbonates leading to the methoxycarbonylated products.[114] Additionally to thioesters or -formates, thiocarbonates are able to undergo decarboxylation under catalytic conditions, which has been reported for Ru-catalyzed synthesis of highly-substituted allyl thioethers (Scheme 4.23).[115]

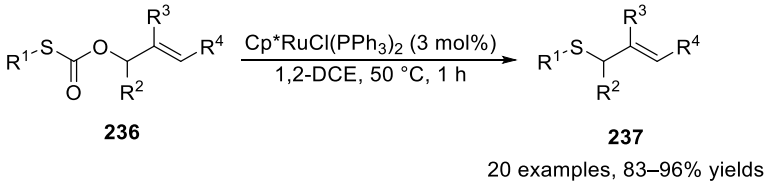

Scheme 4.23. Ru-catalyzed decarboxylation of allyl thiocarbamates furnishing highly functionalized allyl thioethers.[115]

Similarly, decarboxylative reactions have also been investigated with palladium-based catalysts. In a recent example, abundant cyclic carbonates were converted to allyl thioethers with high *Z/E*-ratios (Scheme 4.24).[116]

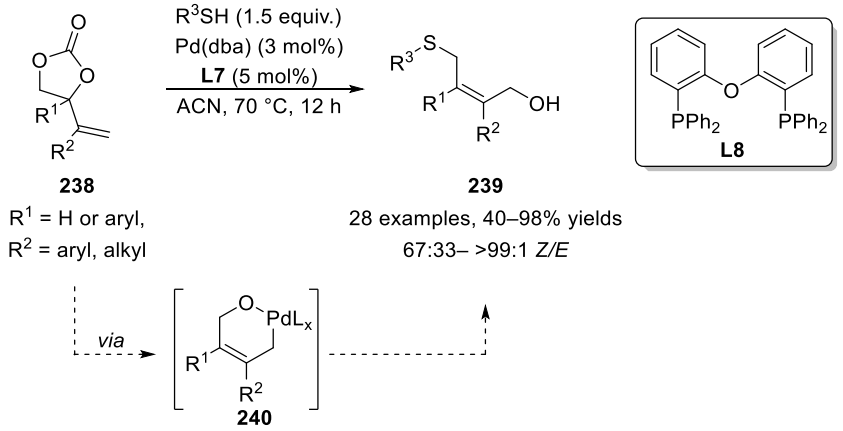

Scheme 4.24. Palladium-catalyzed conversion of vinyl cyclic carbonates with thiols yielding highly functionalized allyl thiols.[116]

Therein, the products were either synthesized as allyl thioethers **239** or oxidized to the respective sulfones. Mechanistically, the reaction was proposed to proceed *via* a 6-membered palladacycle **240**, based upon previous studies from the same group.[117] Although, other reports indicate that thiocarbonates are easily generated *via* thiolysis under similar reaction conditions from cyclic carbonates without catalyst.[118] Therefore, the discussed synthesis of allyl thioethers might proceed *via* thiocarbamate intermediates. Noticeably, the discussed decarboxylations proceed under much milder conditions in comparison to the decarbonylations, which is reflected in a broader tolerance of functional

groups. Although, in view of the current repertoire of methodologies, a precious metal-catalyst is necessary.

Further developments of this chemistry highlight the still underexplored potential of sulfur-containing carbonate derivatives, namely, an activation at the C(O)-O bond instead of the C(O)-S bond.[119] Such a transformation was enabled by the bulk of a *tert*-butoxy group on the thiocarbamate substrate. A nickel-catalyzed reductive cross-coupling with aryl triflates led to the synthesis of benzoic acid thioesters under comparably mild conditions for electron-poor substrates or slightly elevated temperatures for electron-rich substrates (Scheme 4.25). In this report, no further activation of the thioester was mentioned.

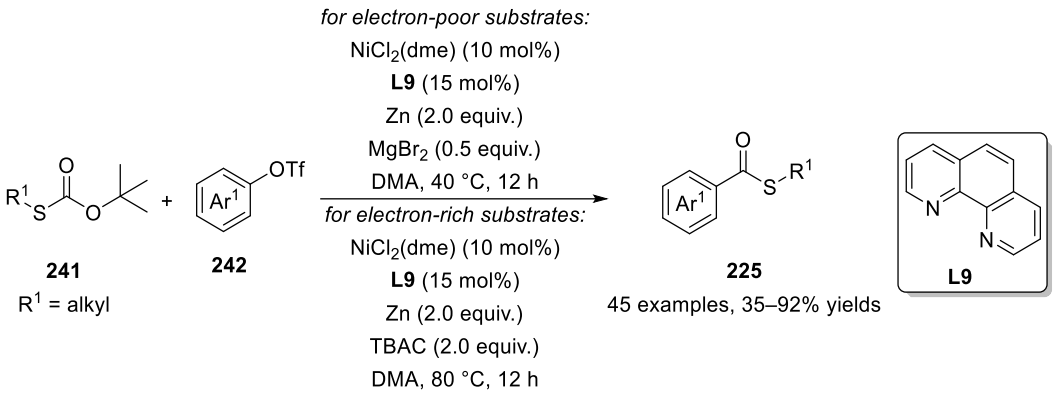

Scheme 4.25. Nickel-catalyzed reductive cross-coupling reaction of vinyl triflates and thiocarbonates.[119]

As an analogue to thiocarbonates, thiocarbamates are most commonly known as intermediates in the synthesis of complex thiophenols *via* Newmann-Kwart rearrangement.[120] However, their reactivity in transition metal-catalyzed reactions is seldomly explored. For instance - similar to thioacylations - a nickel-catalyzed formal insertion of alkynes **244** into the C(O)-S bond of thiocarbamates **243** was reported (Scheme 4.26).[121]

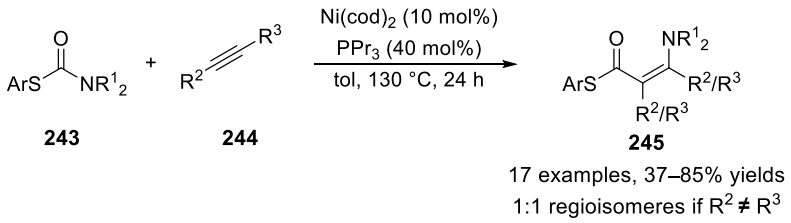

Scheme 4.26. Aminothioesterification of alkynes employing nickel-catalysis.[121]

The reaction was shown to convert internal alkynes with (hetero-)aryl thiolates leading to the *syn*-product, although employing high catalyst and ligand loadings as well as high reaction temperatures. The *N*-substituents were not limited to methyl groups, but sterically demanding substituents decreased reaction yields.

In summary, aside from thioesters, other C(O)S-building blocks have rarely been explored with transition metal-catalysis. However, enough proof-of-concept studies exist to incentivize further

research. Especially, the stability of C(O)-S building blocks but also the available synthesis *via* thiolysis, such as thiocarabamates as well as the potential application in thioether synthesis are promising properties for further research.

4.2 Aims of this chapter

Recent literature examples have established the use of thioformates as formyl donors for catalytic cross-coupling reactions with organozinc halides furnishing aldehydes. However, no example of a first-row transition metal has been reported, limiting the catalytic utilizations to palladium-catalysts. Also, reported literature procedures necessitate specific conditions (metal-to-ligand ratio, choice of ligand, functionalized thioformates), which render this reaction difficult to apply in organic synthesis. Such potential liabilities of this approach were incentivizing the study of late first-row transition metals as catalysts for the synthesis of aldehydes, which would be feasible for electron-poor highly functionalized building blocks. For this, the potential (side-)reactivities of thioformates with organometallic reagents and thiolates should be studied in depth to gain a better understanding for their application in organic synthesis.

Furthermore, the reactivities of building blocks containing a C(O)-S moieties (e.g. thioformates, thiocarbamates) should be probed for potential applications apart from catalytic cross-coupling reactions such as thiolations or thiofunctionalizations. For this, several approaches should be tested, e.g. slow-release of thiolate by Grignard reagent or by reduction to furnish diaryl sulfides or reaction with styrenes under first-row transition metal-catalysis.

4.3 Results and Discussion

4.3.1 Cobalt-Catalyzed Formylation of Organozinc Reagents

In preceding research, the catalytic conversion of *S*-phenyl thioformate was studied under nickel- and iron-catalytic conditions.[122] During these screenings, a competition reaction was observed leading to high amounts of decarbonylated starting material even in absence of a transition metal. Additionally, the method was determined to be the limited to aryl zinc reagents and unable to employ magnesium- or manganese reagents as these favored subsequent 1,2-addition. Overall, only trace amounts of product were observed for both transition metals. After these experiments, cobalt was found to be able to furnish minor yields of product **247**. Thus, a ligand screening with cobaltous chloride was conducted (Table 4.2).

Table 4.2. Ligand screening for the Co-catalyzed formylation of organozinc reagents.[a,b]

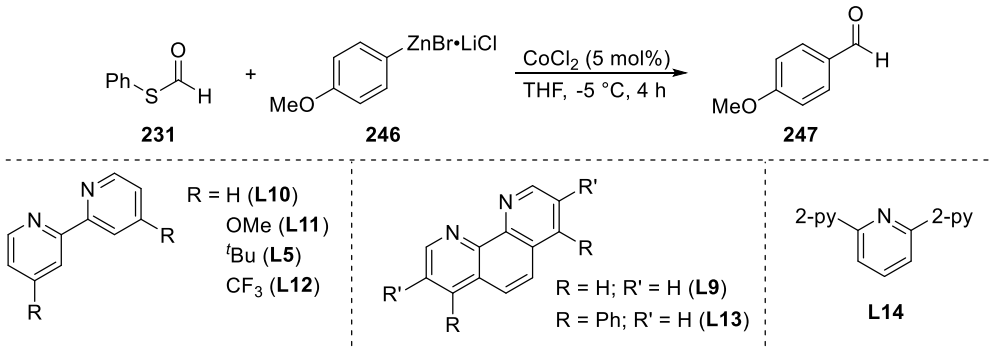

Entry	Deviation from standard conditions	Conversion (%)[c]	Yield (%)[c]
1	-	quant.	6
2	blank	84	traces
3	$Co(acac)_2$	98	6
4	+**L10** (5 mol%)	98	46
5	+**L11** (5 mol%)	quant.	32
6	+**L5** (5 mol%)	quant.	24
7	+**L12** (5 mol%)	quant.	21
8	+**L9** (5 mol%)	quant.	39
9	+**L13** (5 mol%)	quant.	40
10	+**L14**(5 mol%)	quant.	traces
11	$CoCl_2$ (2 mol%) + **L10** (2.0 mol%)	quant.	8
12	**+L10**(10 mol%)	quant.	51

[a]: Reaction conditions: **231** (46.0 mg, 333 µmol, 1 equiv.), **246** (400 µmol, 1.2 equiv.), dry THF (330 µL), -20 °C, 4 h. [b]: Screenings were conducted in supervised Bachelor thesis.[123] [c]: Quantification *via* GC-FID measurement using *n*-pentadecane (100 µL) as internal standard.

In line with previous results, starting material was still converted in the absence of catalyst (Table 4.2 - Entry 2). This might indicate that a decarbonylation competition reaction is occurring under

the applied conditions as no other side product could be identified. One possible explanation would be a deprotonation of the thioformate and subsequent decarbonylation. In literature, such a reactivity has been reported recently, whereby, *S*-thioformates acted as CO source in reaction with amine bases (Scheme 4.27).[124]

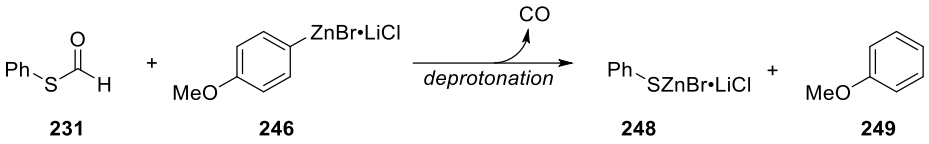

Scheme 4.27. Hypothesized deprotonation of *S*-phenyl thioformates by organozinc reagents.[124]

The observed overall high conversion in the screening can be reasoned by such a side reaction. In terms of ligand performance, simple bipyridine (**L10**) performed best (Table 4.2 – Entry 4) with 46% yield. In contrast, substituted bipyridine-type ligands did not exhibit any increase in yield, but higher solubilization was observed in some instances (Table 4.2 – Entry 6). Furthermore, phenanthroline-type ligands performed similarly well to **L10** with approximately 40% yield for **L9** and **L13** (Table 4.2 – Entries 8+9). The ligand **L14** led to traces of yield (Table 4.2 – Entry 10). In addition, varying catalyst or ligand loadings were probed for the simplest ligand, **L10** (Table 4.2 – Entries 4, 11, 12). Not surprisingly, lower catalyst and ligand loading led to diminished yields, while an increased ligand:metal ratio slightly increased the yield.

Nevertheless, different classes of ligands were screened to gain an overview of potential alternatives or influences. DMEDA (**L15**) or TMEDA (**L16**) (Table 4.3. – Entries 1+2) led to 5% of yield, although, the conversion of **231** was decreased. Phosphine ligands did not promote the reaction with triphenylphosphine (**L17**) leading to 9% of yield (Table 4.3. – Entry 5) and the ligand employed in the palladium-catalyzed formylation of organozinc reagents **L6** gave only traces of yield (Table 4.3. – Entry 4). However, the ligands **L6** and **L4** strongly reduced the competing conversion of starting material (Table 4.3. – Entries 3+4). Other more complex imine-type ligands, **L18** or **L19**, did not give rise to yields close to the results of bispyridyl-type ligands, as well as the electron-rich NHC **L20** which only led to traces of product (Table 4.3. – Entries 6–8).

Table 4.3. Ligand screening of the Co-catalyzed formylation of organozinc reagents.[a,b]

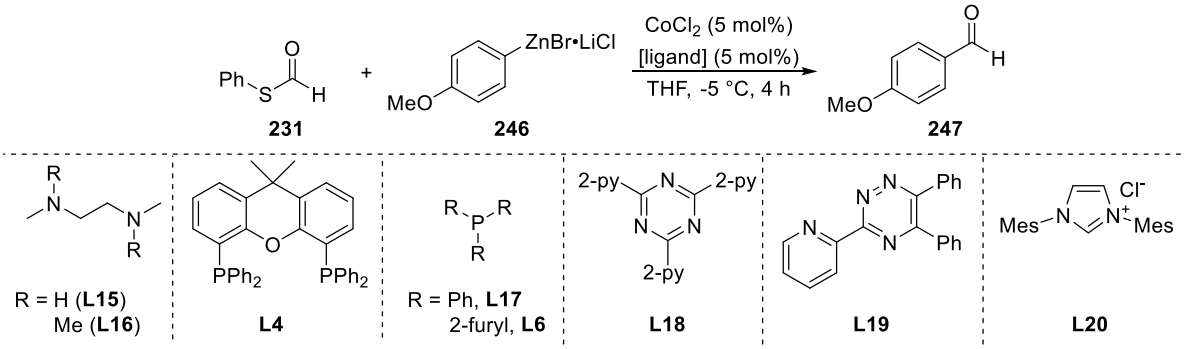

Entry	Deviation from std. conditions	Conversion (%)[c]	Yield (%)[c]
1	+**L15**	85	5
2	+**L16**	72	5
3	+**L4**[d]	23	none
4	+**L6**[d]	45	traces
5	+**L17**	quant.	9
6	+**L18**	81	8
7	+**L19**	81	8
8	+**L20**	83	5

[a]: Reaction conditions: **231** (46.0 mg, 333 µmol, 1 equiv.), **246** (400 µmol, 1.2 equiv.), dry THF (330 µL), -20 °C, 4 h. [b]: Screenings were conducted in supervised Bachelor theses.[123, 125] [c]: Quantification *via* GC-FID measurement using *n*-pentadecane (100 µL) as internal standard. [d]: Percentages were determined by ratio of GC-MS integrals.

Next, a narrow solvent screening was conducted to monitor the potential impact on the reaction (Table 4.4). All the screened solvents led to decreased yields, although, DCM resulted in only a small deviation in consideration of the quantification error of the GC-FID (Table 4.4 – Entry 2).

Table 4.4. Solvent screening for the cobalt-catalyzed formylation of organozinc reagents.[a,b]

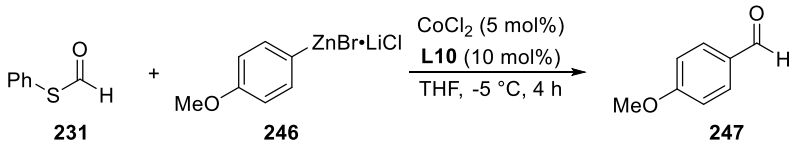

Entry	Deviation from standard conditions	Conversion (%)[c]	Yield (%)[c]
1	none	quant.	51
2	THF/DCM	quant.	44
3	THF/NMP	quant.	15
4	THF/Et_2O	quant.	16

[a]: Reaction conditions: **231** (46.0 mg, 333 µmol, 1 equiv.), **246** (400 µmol, 1.2 equiv.), **L10** (5.2 mg, 33 µmol, 0.1 equiv.), dry THF (330 µL), -20 °C, 4 h. [b]: Screenings were conducted in supervised Bachelor thesis.[123] [b]: Quantification *via* GC-FID measurement using *n*-pentadecane (100 µL) as internal standard.

The polar co-solvent NMP, known for its influence on the equilibria of organometallic species, led only to minor yields (Table 4.4 – Entry 3). Similarly, Et_2O furnished 15%, which might be due to the low solubility of organozinc halides in the solvent (Table 4.4 – Entry 4).

In view of the insights about metal salts, ligands, solvents and transmetalation reagents, the source of formate was varied. Reportedly, substituents with strong electronic influence on the *S*-aryl moiety can promote higher reaction yields.[111] However, this was determined to necessitate more specific starting materials for the conversion, likely limiting the substrate scope. Therefore, only formats from available thiols, e.g. *O*-aryl formate **250a** or benzylic or alkyl, *S*-thioformates **250b+c** were probed (Table 4.5).

Table 4.5. Alternative (thio-)formates screened for the cobalt-catalyzed formylations.[a,b]

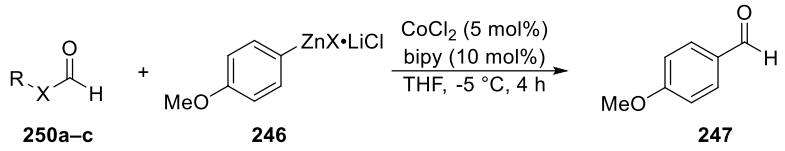

Entry	R =	X =	Yield(%)[c]
1	Ph	O	traces
2	Bn	S	traces
3	^{n}Hept	S	4

[a]: Reaction conditions: **231** (46.0 mg, 333 µmol, 1 equiv.), **246** (400 µmol, 1.2 equiv.), dry THF (330 µL), -5 °C, 4 h. [b]: Screenings were conducted in supervised Bachelor thesis.[123] [c]: Quantification *via* GC-FID measurement using *n*-pentadecane (100 µL) as internal standard.

Thus far, the method provided unsatisfactory yields for a substrate screening. Attempts for substrate isolation with different aryl zinc halides led to similar mediocre yields and were impaired by difficult separations of by- and side products. In order to gain a deeper understanding of the underlying difficulties, a 1.5 mmol-scale reaction was performed with isolation of all potential side products (Scheme 4.28).

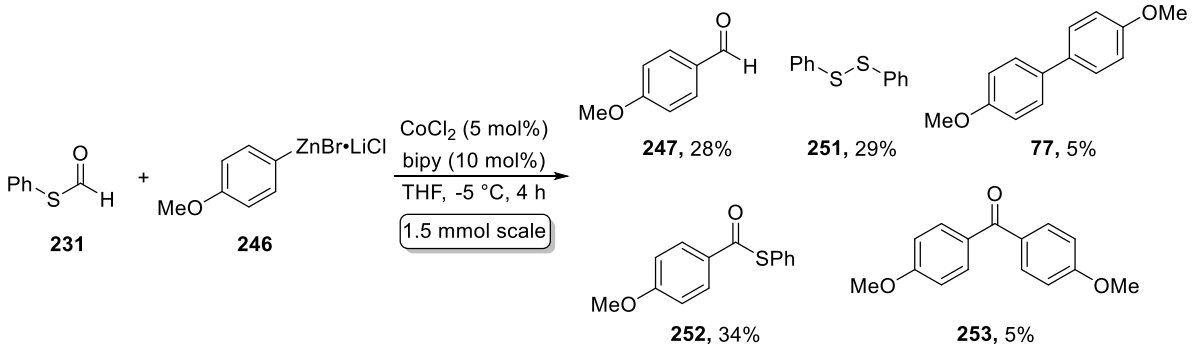

Scheme 4.28. Isolated yields of the cobalt-catalyzed formylation with all by- and side products.

Next to target aldehyde **247**, disulfide **251** was isolated in almost 1:1 ratio with 29% isolated yield. The high yield of this side product might be attributed to a resilience of *in situ* generated cobalt species against poisoning by free thiolates as multiple turnovers seem to proceed. Next to this, homo-coupled

bisphenyl **77** was observed in low amounts, which could result from catalyst activation. Surprisingly, thioester **252** was isolated in even higher yields than the target product. This corresponded to an undetermined side product observed during previous screenings. Moreover, the thioester underwent a FCC to form **253**, which is in line with the results of the previous chapter (chapter **3.2.2**, p. 47), which showed that cobalt was able to catalyze FCC.

The formation of the thioester was associated to cause the low yields observed for the reaction, however, the sum (by-)products only accounted for 67% of converted **231** which reflects a likely competing decarbonylation reaction. For the formation of **252**, two pathways were hypothesized (Scheme 4.29).

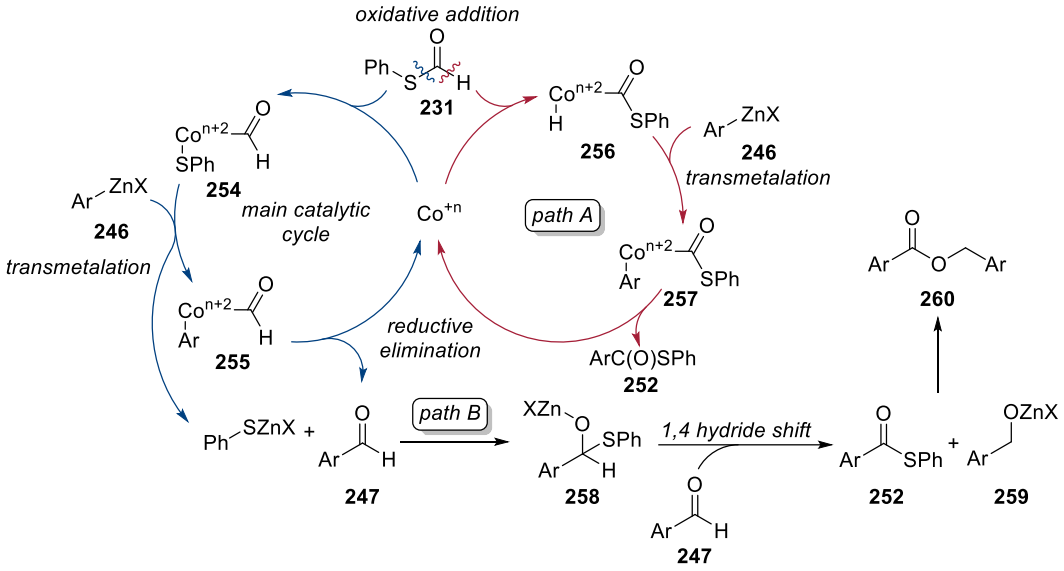

Scheme 4.29. Hypothesized pathways for the formation of side product **252** by either activation of the formate or a Tishchenko-type reaction.

Next to the main catalytic cycle, the activation of **231** could potentially occur at the formate C-H bond to form species **256** (path A). This would lead to the formation of **257** which subsequently forms the observed side product **252**. Path B is related to reported literature of Tishchenko-type reactions employing benzylic magnesium thiolates as catalysts to convert aryl aldehydes to products of type **260**.[126] Therein, the thiolate salt forms a mixed hemiacetal **258** with the aldehyde, which then undergoes a hydride shift, consuming 2 equivalents of aldehyde in both steps and forming **252** in the process. In the literature study, the 1,4-hydride shift was postulated to be faster than the subsequent step which would be the alcoholysis of **252** by **259** to form **260**. Validation of path A, *via* potential hydrothioesterification or similar hydrofunctionalization reactions failed in every attempt. Nevertheless, the electron-rich bidentate phosphine showed very low decarbonylation yields, which could be associated to the favored formation and stabilization of the hydride intermediate **256**. In favor of path B, side products were observed which might substantiate the formation of **259** or **260** *via* GC-MS. However, due to separation issues these side products could never be further verified and only fragmental MS peaks were observed.

Based upon the discussed results, it was hypothesized that starting material decomposition could be decreased with slower addition. However, the conducted experiments showed this approach to be unproductive (Scheme 4.30).

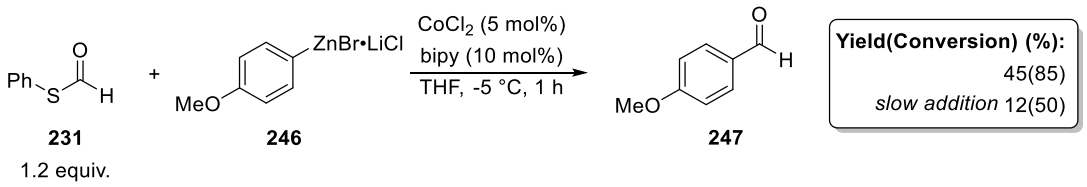

Scheme 4.30. Attempts to decrease the extent of decarbonylation by increase of the amount of thioformate **231** and slower addition speed.

Following, a second screening of metal sources was conducted to obtain insights into potential counterion influences (Table 4.6). It was observed that the cobalt halide possesses an influence on the reaction outcome with cobalt bromide performing best with 58% yield (Table 4.6 – Entry 3). Interestingly, cobalt iodide performed worse with 36% yield, which might be attributed to impurities as this salt is very sensitive to air (Table 4.6 – Entry 4). The addition of tetra-*n*-butyl ammonium acetate (TBAA) led to a visible increase in solubilization of the precatalyst but did not increase reaction yields (Table 4.6 – Entry 5).

Table 4.6. Screening of counterion influence by probing different cobalt precatalysts.

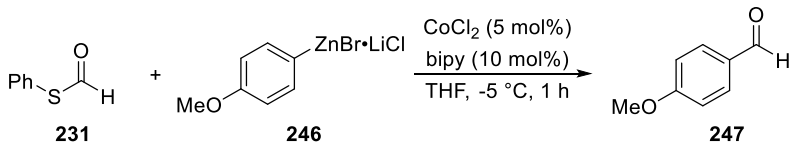

Entry	Deviation from std. conditions	Conversion (%)[b]	Yield (%)[b]
1	none	85	45
2	Instead $Co(OAc)_2$	quant.	32
3	Instead $CoBr_2$	97	58
4	Instead CoI_2	n.d.	36
5	+ 20 mol% TBAA	95	46

[a]: Reaction conditions: **231** (46.0 mg, 333 µmol, 1 equiv.), **246** (400 µmol, 1.2 equiv.), dry THF (1 mL), -5 °C, 1 h. [b]: Quantification *via* GC-FID measurement using *n*-pentadecane (100 µL) as internal standard.

In view of the comparably higher cost of cobaltous bromide, the chloride salt was still a focus of following experiments (Table 4.7). Subsequent screenings explored a potential influence of dilution and other less polar solvents (Table 4.7 – Entries 1, 3, 4). While higher dilutions or the utilization of co-solvent led to decreased yields, the results exhibited a lower conversion.

Table 4.7. Variation of solvation by dilution or use of co-solvent.[a]

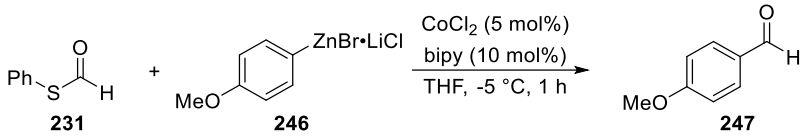

Entry	Deviation from std. conditions	Conversion (%)[b]	Yield (%)[b]
1	THF (0.08 M)	74	33
2	THF/xylene (slurry, to rt)	100	14
3	THF/toluene	61	32
4	THF/toluene[c]	98	20

[a]: Reaction conditions: **231** (46.0 mg, 333 µmol, 1 equiv.), **246** (400 µmol, 1.2 equiv.), solvent (1 mL), -5 °C, 1 h. [b]: Quantification *via* GC-FID measurement using *n*-pentadecane (100 µL) as internal standard. [c]: Zinc reagent was not added dropwise (ca. 1 min of complete addition), but swiftly (ca. 1 second of complete addition).

Other means to influence solubilization of cobalt precatalyst were reported in previous literature which exemplified the use of cobalt ate complexes.[22a] With this precursor, the bipyridyl complex was observed to immediately precipitate after addition of ligand which ensured complexation. Therefore, an additional ligand screening was performed (Table 4.8). In terms of ligands, the visibly soluble complexes of **L5** and **L21** performed the best with up to 51% yield (Table 4.8 – Entries 2+4). However, following optimization with **L21** did not lead to any meaningful increase in yield.

Table 4.8. Screening employing a soluble cobalt ate complex as precatalyst.[a]

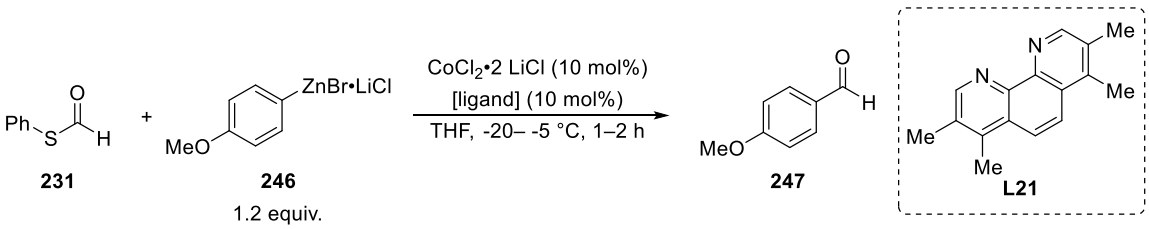

Entry	Deviation from std. conditions	Conversion (%)[b]	Yield (%)[b]
1	**L10**	84	33
2	**L5**	78	40
3	**L9**	90	28
4	**L21**	95	51
5	**L13**	66	7

[a]: Reaction conditions: **231** (46.0 mg, 333 µmol, 1 equiv.), **246** (400 µmol, 1.2 equiv.), dry THF (330 µL), -20– -5 °C, 1–2 h. [b]: Quantification *via* GC-FID measurement using *n*-pentadecane (100 µL) as internal standard.

All things considered, higher metal loadings, utilization of toluene and higher dilutions were identified to potentially furnish higher yields. When combined, resulting experiments demonstrated the positive influence of these parameters with an overall maximum yield of 66%. Still, the results reflect loss of product or starting material to competing side reactions. Notably, the change from $CoCl_2$ to $CoBr_2$ does not indicate a strong influence of halide counterions during this screening.

Table 4.9. Higher metal loadings combined with successful ligands performing best for the catalytic formylation.[a]

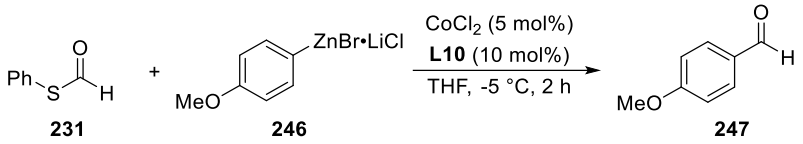

Entry	Deviation from std. conditions	Conversion (%)[b]	Yield (%)[b]
1	none	85	45
2	$CoCl_2$ (10 mol%)	quant.	62
3	$CoBr_2$ (10 mol%)	quant.	44
4	$CoCl_2$ (10 mol%), +toluene (1 mL)	quant.	66
5	$CoCl_2$ (10 mol%), **L5** (10 mol%), +toluene (1 mL)	quant.	67

[a]: Reaction conditions: **231** (46.0 mg, 333 µmol, 1 equiv.), **246** (400 µmol, 1.2 equiv.), dry THF (330 µL), -5 °C, 2 h. [b]: Quantification *via* GC-FID measurement using *n*-pentadecane (100 µL) as internal standard.

In an attempt to circumvent the decarbonylation by likely deprotonation, a reductive cross-electrophile approach was considered. Cobalt-catalysis was reported to be able to perform similar reactions such as conversion of aryl bromides to the corresponding aryl zinc reagents catalytically[61b], therefore, a formylation of aryl bromide was probed (Scheme 4.31).

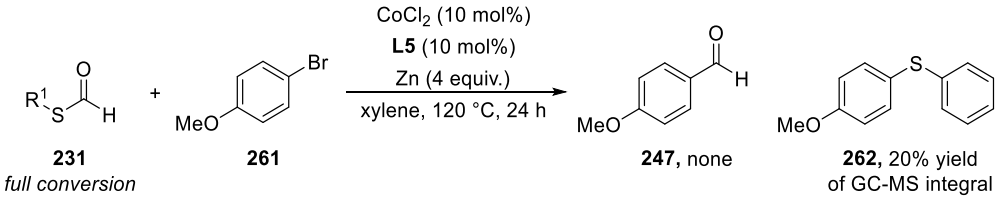

Scheme 4.31. Attempted formylation of aryl bromides by a cobalt-catalyzed cross-electrophile-type coupling.

In this experiment, no formation of target product was observed. However, yields of thioether **262** were identified. Thus, a Migita-type coupling is promoted under the applied condition with thiolate likely generated by decarbonylation of thioformate, though in poor yields. High amounts of bromide starting material were recovered indicating that an *in situ* formation of organozinc reagents, as reported in multiple instances, likely necessitates metal surface activating reagents.[61b]

4.3.2 Investigations towards the Reactivity of Thiocarbamates for Cross-Coupling Reactions

Discussed experiments have demonstrated thioformates as potential starting materials for the synthesis of bisaryl thioethers. This class of sulfur compounds is especially coveted as their synthesis is generally difficult, e.g. cross-coupling reactions, can be challenging.

Therefore, the potential of this approach was examined. Ultimately, the application of thiocarbamates was considered as starting materials since their conversion at elevated temperatures was reported without defunctionalization.[121] The following results were acquired to establish potential reactivities of thiocarbamates under catalytic conditions for ongoing or future research. Therefore, the results reflect the initial development of a panel of potential target applications rather than optimization of single methodologies.

The first experiments focused on the synthesis of thioethers by reaction of **263** with aryl halides which was enabled by the utilization of strong bases to release the thiolate *in situ*. Similar to previous studies of the Fleischer working group a nickel-xantphos precatalyst **C1** was exploited.[101, 127] Most importantly, other screened transition metals (Ti, Fe, Co) did not furnish any yields and were therefore not further tested (Scheme 4.32).[101, 127]

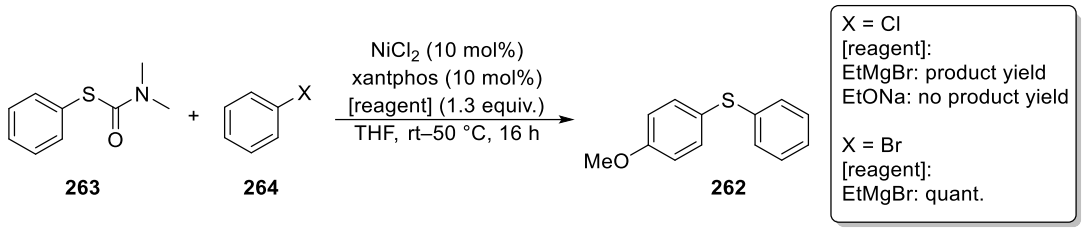

Scheme 4.32. Nickel-catalyzed synthesis of thioethers by cross-coupling of *S*-aryl thiocarbamates.

While alcoholate base was unable to promote product generation, the employment of alkyl Grignard reagent led to the formation of target product. However, quantification of the results was flawed as **262** and **263** overlapped in the gas chromatographic determination of yield. Then again, the conversion proceeded almost quantitatively with no starting material **263** left when employing aryl bromides instead of chlorides. This reaction was hypothesized to be enabled by a slow reaction of Grignard reagent **with 263** which gradually releases thiolates that swiftly undergoes cross-coupling. Therefore, overall concentration of aryl thiolate was kept low, which suppressed the connected poisoning reactions.

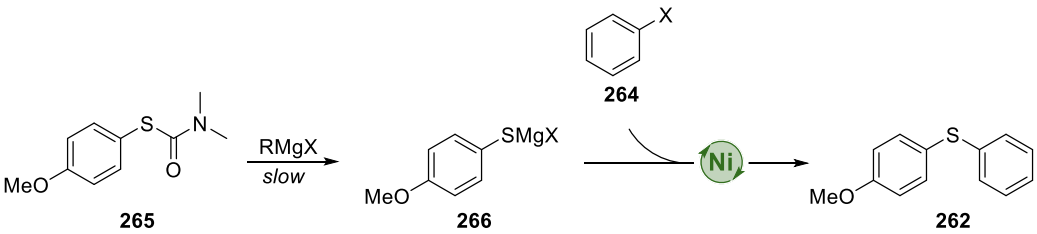

Scheme 4.33. Hypothesized slow release of thiolate enabling the synthesis of bisaryl sulfides.

To this end, further investigations into this stratagem of a slow release of aryl thiolates was continued as a Master Thesis in the group and will not be discussed in this Thesis any further.[128]

To additionally explore potential reactions of thiocarbamates, the utilization of *S*-alkyl thioesters as coupling partners was probed. In view of the multitude of decarbonylative reaction of thioesters, their

reactivity was suited for the designated reaction, circumventing the utilization of organometallic reagents. The initial reactions were closely related to reported literature utilizing 1,3-bis(diphenylphosphino)propane (Dppp, **L22**) as ligand. The results indicated that the activation and decarbonylation proceeded under the applied conditions and minor yields could be gained (Scheme 4.34).

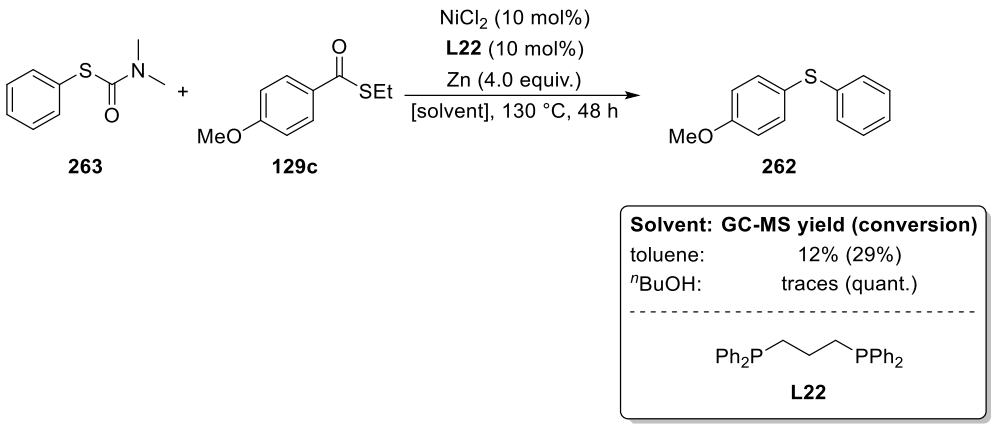

Scheme 4.34. Reductive decarbonylative cross-electrophile coupling of thioesters and thiocarbamates to furnish bisaryl thioethers.

Alternatively, thiocarbamate **265** was explored for potential reactions with styrenes, as literature examples of thiocarbamyolation would be a desirable conversion if possible under milder reaction conditions than previous studies.[121] A short study revealed a surprisingly complex reaction behavior, as xantphos (**L4**) furnished hydrothiolation product **268** and a coupling of released thiolate with thiocarbamate reacting as electrophile by aryl-S(carbamate) bond scission (**269**, Scheme 4.35). Similar pseudohalide activations are known with *O*-aryl carbamates.[129]

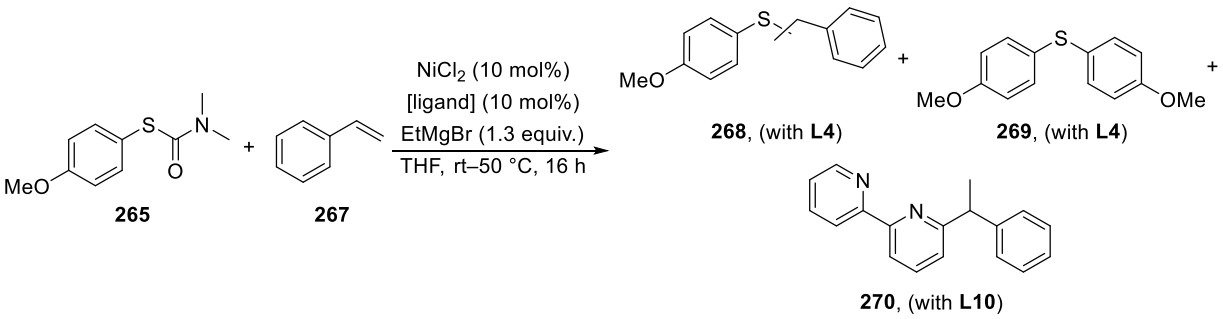

Scheme 4.35. Minor products in nickel-catalyzed reactions of thiocarbamates in presence of styrene.

When **L10** was used as a ligand, product **270** was isolated in minor yields, for which the change in precatalyst from nickel chloride to cobalt chloride increased the yield slightly. Seminal attempts to exchange bipyridine with pyridines as coveted substrates for *ortho*-functionalization, afforded target product in traces (3% isolated yield), thereby, either indicating a non-catalytic reaction or the necessity of thiolate ligation for the observed reactivity.

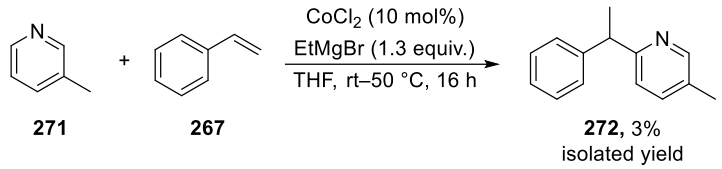

Scheme 4.36. α-Functionalization of pyridines under cobalt catalytic conditions with styrene.

Since the use of cobalt-catalyst led to a favored formation of the product **272**, a complex mixture screening (CMS) was conducted to gain further insights, as a multitude of side products were observed. In previous publications similar types of screenings have been employed to increase the efficiency of the reaction optimization process.[130] This is achieved by enabling larger amounts of reactants, e.g. ligands, to be initially probed by screening not singular but groups of reactants, i.e. multiple – in this case five - similar ligands are added to one reaction. This allows for larger amounts of ligands to be screened initially in groups which are then deconvoluted in later steps of the optimization to identify a suitable target ligand(s), thereby, significantly reducing the number of experiments from "classic" linear screenings, e.g. 25 (CMS) *vs.* 384 (linear)[130a] or 72 (CMS) *vs.* 624 (linear)[131]. In the case of the reactivity of thiocarbamates, this approach was employed not only to gain more rapidly insights into potential ligands, but also to obtain an overview of potential targets of the reaction.

Making use of the broader range of ligands and potential targets covered by a screening, three groups were defined by bisimine-type ligands (group A), (bis-)phosphine ligands (group B) and ligands with protic groups (group C, Scheme 4.37). The results showed that similarly to the cobalt-catalyzed formylation, the homo-coupling proceeds in high yields independently of ligand group, indicating a general low poisoning effect of thiolates. Interestingly, the likely formation of amide **275** was observed. The constitution of this product was determined by independent synthesis of *anti*-Markovnikov product which differed in retention time and fragmentation of a sample of Markovnikov-product. The formation of **275** was hypothesized to be connected to the formation of reduced species **273** enabled by group B or C. In view of the formation of **275** and **273** the reactions were thought to be indicative of a hydromagnesiation reaction.

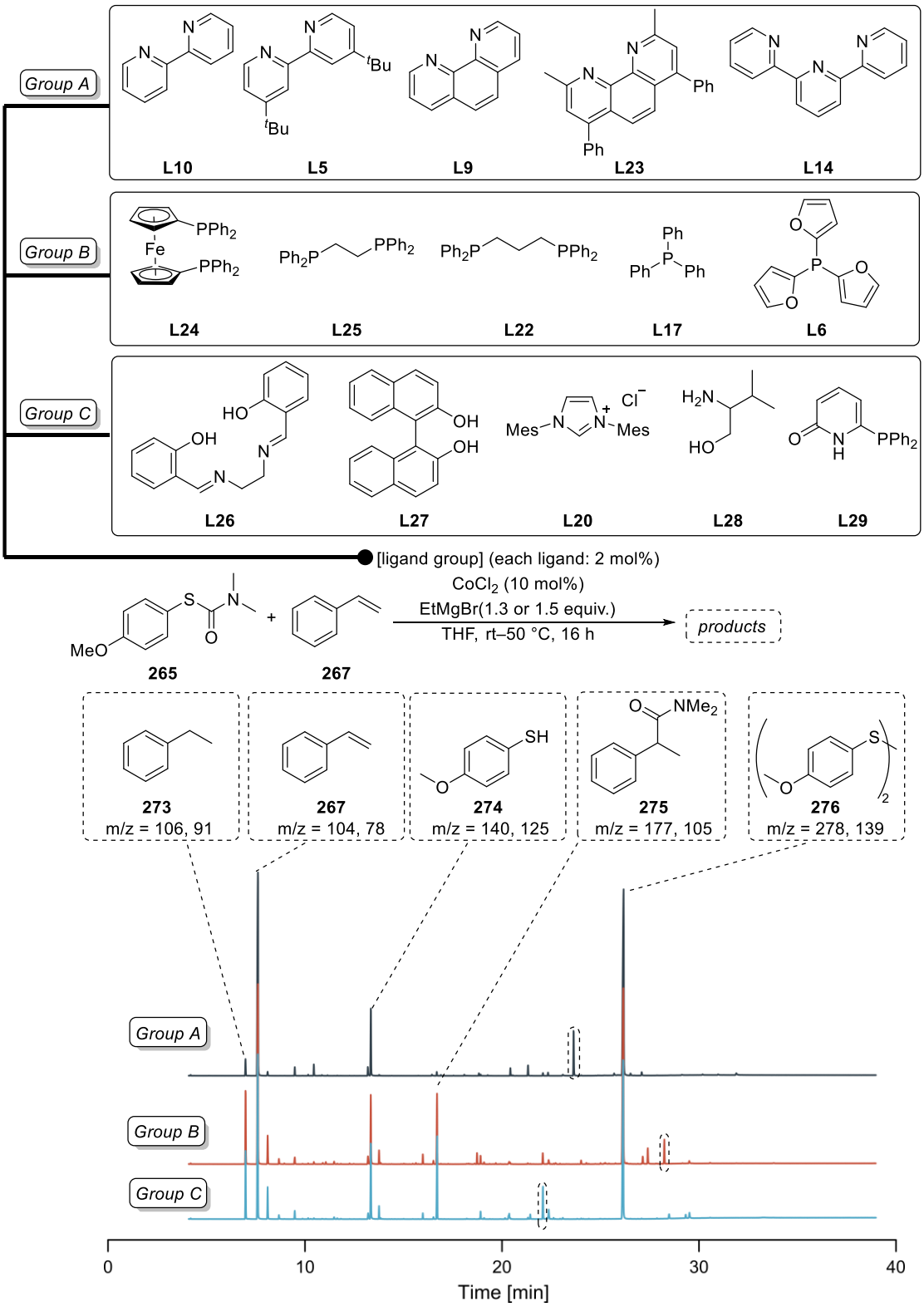

Scheme 4.37. Screening of ligand groups for potential target products. The circled peaks reflect potential products only enabled by certain ligand groups.

Such a catalytic hydromagnesiation of styrene would be closely related to reported reactivity of iron-catalysts, furnishing **278**, which - in this case - would subsequently undergoes a FCC reaction (Scheme 4.38). Since the results were associated to already well studied reactivities of Fe-catalysis, these observations were not further pursued.

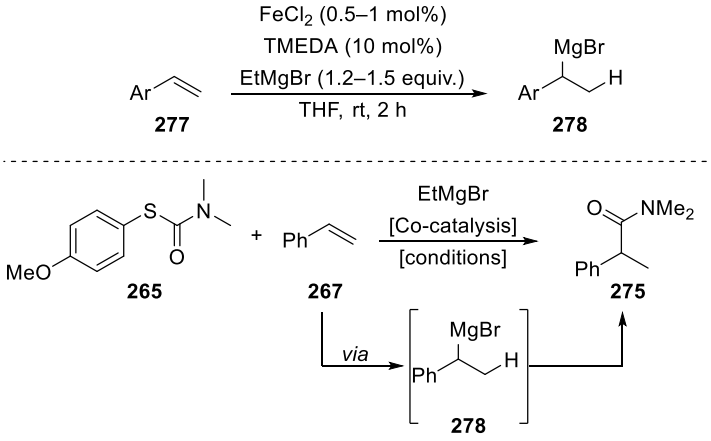

Scheme 4.38. Top: Reported iron-catalyzed hydromagnesiation of styrenes.[132] Bottom: Hypothesized cobalt-catalyzed steps for the synthesis of **275**.

The results revealed that next to the expected cleavage of the thiolate from starting material **265** by organometallic reagent, a hydromagnesiation can likely be promoted by cobalt-catalysis. Other findings indicate that thiocarbamates can sluggishly react as leaving group in cross-coupling chemistry and that these building blocks can react in FCC-type reactions.

4.4 Conclusion and Outlook

In summary, two classes of C(O)-S starting materials were studied: *S*-aryl thioformates and *S*-aryl thiocarbamates. Firstly, a cobalt-catalyzed formylation of organozinc halides with *S*-aryl thioformates was optimized with yields up to 67%. Conveniently, the optimization revealed that simple bisimine-type ligands performed superiorly with bipyridyl affording the highest yields. During screenings, decreased yields were observed to be related to competing non-catalytic decarbonylation and the formation of a thioester side product *via* catalytic or non-catalytic pathways. To suppress such reactions, various parameters (addition speed, co-solvents or additives) were examined, indicating that solubility of the precatalytic complex or a higher dilution and non-polar solvent mixtures were beneficial. To further optimize this method, the role of potential Tishchenko-type reaction should be studied more in depth and either further optimization of reaction parameters or scavenging of thiolate might enable higher yields.

Secondly, screenings for the utilization of thiocarbamates in catalytic reactions exemplified their potential use as masked thiolates, thereby, suppressing poisoning of transition metal catalysts. Initial results were obtained for a nickel-xantphos reaction system. In this case, thiocarbamates were shown to enable the synthesis of bisaryl sulfides starting from aryl halides by slow activation of the thiocarbamate with Grignard reagent. In separate experiments with styrene, a multitude of side products suggested a potential reactivity of cobalt-catalysts for hydromagnesiations.

For both studied C(O)-S starting materials, the utilization of cobalt-catalysis exhibited a high tolerance for the thiolate byproducts. Therefore, this transition metal might be considered in future applications, e.g. with aryl thiolates or other C(O)-S starting materials such as thioacetates, or thiocarbonates.

4.5 References

[1] a) C. Gosmini, J.-M. Bégouin, A. Moncomble, *Chem. Commun.* **2008**, 3221–3233; b) W. Hess, J. Treutwein, G. Hilt, *Synthesis* **2008**, *2008*, 3537–3562; c) G. Cahiez, A. Moyeux, *Chem. Rev.* **2010**, *110*, 1435–1462; d) G. Manolikakes, in *Comprehensive Organic Synthesis II (Second Edition)* (Ed.: P. Knochel), Elsevier, Amsterdam, **2014**, pp. 392–464; e) A. Rérat, C. Gosmini, in *Grignard Reagents and Transition Metal Catalysts, Formation of C-C Bonds by Cross-Coupling* (Ed.: J. Cossy), De Gruyter, Berlin/Boston, **2016**, pp. 152–209; f) J. M. Hammann, M. S. Hofmayer, F. H. Lutter, L. Thomas, P. Knochel, *Synthesis* **2017**, *49*, 3887–3894; g) S. H. Kyne, G. Lefèvre, C. Ollivier, M. Petit, V.-A. Ramis Cladera, L. Fensterbank, *Chem. Soc. Rev.* **2020**, *49*, 8501–8542; h) K. Juhász, Á. Magyar, Z. Hell, *Synthesis* **2021**, *53*, 983–1002; i) O. Planas, C. J. Whiteoak, X. Ribas, in *Non-Noble Metal Catalysis*, **2019**, pp. 297–328; j) F. H. Lutter, S. Graßl, L. Grokenberger, M. S. Hofmayer, Y. H. Chen, P. Knochel, *ChemCatChem* **2019**; k) A. Guérinot, J. Cossy, *Acc. Chem. Res.* **2020**, *53*, 1351–1363; l) Y. Nassar, F. Rodier, V. Ferey, J. Cossy, *ACS Catal.* **2021**, 5736–5761.

[2] a) K. S. Egorova, V. P. Ananikov, *Organometallics* **2017**, *36*, 4071–4090; b) Editorial, *Nat. Energy* **2020**, *5*, 825–825.

[3] H. Gilman, M. Lichtenwalter, *J. Am. Chem. Soc.* **1939**, *61*, 957–959.

[4] a) M. S. Kharasch, E. K. Fields, *J. Am. Chem. Soc.* **1941**, *63*, 2316–2320; b) M. S. Kharasch, D. C. Sayles, *J. Am. Chem. Soc.* **1942**, *64*, 2972–2975; c) M. S. Kharasch, M. Kleiman, *J. Am. Chem. Soc.* **1943**, *65*, 491–493; d) M. S. Kharasch, D. W. Lewis, W. B. Reynolds, *J. Am. Chem. Soc.* **1943**, *65*, 498–500; e) M. S. Kharasch, W. Nudenberg, S. Archer, *J. Am. Chem. Soc.* **1943**, *65*, 495–498; f) M. S. Kharasch, W. B. Reynolds, *J. Am. Chem. Soc.* **1943**, *65*, 501–504; g) W. H. Urry, M. S. Kharasch, *J. Am. Chem. Soc.* **1944**, *66*, 1438–1440; h) M. S. Kharasch, W. H. Urry, *J. Org. Chem* **1948**, *13*, 101–109; i) M. S. Kharasch, R. L. Huang, *J. Org. Chem* **1952**, *17*, 669–677.

[5] M. S. Kharasch, F. L. Lambert, W. H. Urry, *J. Org. Chem* **1945**, *10*, 298–306.

[6] T. Kauffmann, G. Hopp, B. Laarmann, D. Stegemann, D. Wingbermühle, *Tetrahedron Lett.* **1990**, *31*, 511–514.

[7] T. Kauffmann, R. Sälker, K.-U. Voß, *Chem. Ber.* **1993**, *126*, 1447–1452.

[8] T. Kauffmann, K.-U. Voß, G. Neiteler, *Chem. Ber.* **1993**, *126*, 1453–1459.

[9] T. Kauffmann, H. Nienaber, *Synthesis* **1995**, *1995*, 207–211.

[10] T. Kauffmann, *Angew. Chem. Int. Ed.* **1996**, *35*, 386–403.

[11] a) H. Avedissian, L. Bérillon, G. Cahiez, P. Knochel, *Tetrahedron Lett.* **1998**, *39*, 6163–6166; b) G. Cahiez, H. Avedissian, *Tetrahedron Lett.* **1998**, *39*, 6159–6162.

[12] G. Cahiez, H. Avedissian, *Synthesis* **1998**, *1998*, 1199–1205.

[13] C. Gosmini, Y. Rollin, J. Y. Nédélec, J. Périchon, *J. Org. Chem* **2000**, *65*, 6024–6026.

[14] a) Y. Zhou, L. Wang, G. Yuan, S. Liu, X. Sun, C. Yuan, Y. Yang, Q. Bian, M. Wang, J. Zhong, *Org. Lett.* **2020**, *22*, 4532–4536; b) J. M. Hammann, A. K. Steib, P. Knochel, *Org. Lett.* **2014**, *16*, 6500–6503.

[15] G. Dilauro, F. Messa, F. Bona, S. Perrone, A. Salomone, *Chem. Commun.* **2021**, *57*, 10564–10567.

[16] a) F. H. Lutter, L. Grokenberger, P. Spieß, J. M. Hammann, K. Karaghiosoff, P. Knochel, *Angew. Chem. Int. Ed.* **2020**, *59*, 5546–5550; b) M. M. Lorion, V. Koch, M. Nieger, H.-Y. Chen, A. Lei, S. Bräse, J. Cossy, *Chem. Eur. J.* **2020**, *26*, 13163–13169.

[17] M. S. Hofmayer, J. M. Hammann, D. Haas, P. Knochel, *Org. Lett.* **2016**, *18*, 6456–6459.

[18] a) L. R. Mills, D. Gygi, J. R. Ludwig, E. M. Simmons, S. R. Wisniewski, J. Kim, P. J. Chirik, *ACS Catal.* **2022**, *12*, 1905–1918; b) J. R. Ludwig, E. M. Simmons, S. R. Wisniewski, P. J. Chirik, *Org. Lett.* **2021**, *23*, 625–630; c) H. A. Duong, W. Wu, Y.-Y. Teo, *Organometallics* **2017**, *36*, 4363–4366; d) S. Asghar, S. B. Tailor, D. Elorriaga, R. B. Bedford, *Angew. Chem. Int. Ed.* **2017**, *56*, 16367–16370; e) J. M. Neely, M. J. Bezdek, P. J. Chirik, *ACS Cent. Sci.* **2016**, *2*, 935–942.

[19] a) J. Diccianni, Q. Lin, T. Diao, *Acc. Chem. Res.* **2020**, *53*, 906–919; b) T. Tsuji, H. Yorimitsu, K. Oshima, *Angew. Chem. Int. Ed.* **2002**, *41*, 4137–4139; c) F. Kreyenschmidt, S. E. Meurer, K. Koszinowski, *Chem. Eur. J.* **2019**, *25*, 5912–5921.

[20] T. Kobayashi, H. Ohmiya, H. Yorimitsu, K. Oshima, *J. Am. Chem. Soc.* **2008**, *130*, 11276–11277.
[21] T. Iwasaki, K. Yamashita, H. Kuniyasu, N. Kambe, *Org. Lett.* **2017**, *19*, 3691–3694.
[22] a) G. Cahiez, C. Chaboche, C. Duplais, A. Giulliani, A. Moyeux, *Adv. Synth. Catal.* **2008**, *350*, 1484–1488; b) H. Ohmiya, T. Tsuji, H. Yorimitsu, K. Oshima, *Chem. Eur. J.* **2004**, *10*, 5640–5648.
[23] C. Andersen, V. Ferey, M. Daumas, P. Bernardelli, A. Guérinot, J. Cossy, *Org. Lett.* **2019**.
[24] J. A. Killion, W. T. Darrow, M. R. Brennan, C. A. Leahy, A. R. Fout, *Organometallics* **2022**, *41*, 1769–1776.
[25] H. Ohmiya, K. Wakabayashi, H. Yorimitsu, K. Oshima, *Tetrahedron* **2006**, *62*, 2207–2213.
[26] J. M. Hammann, D. Haas, P. Knochel, *Angew. Chem. Int. Ed.* **2015**, *54*, 4478–4481.
[27] A. Kuno, N. Saino, T. Kamachi, S. Okamoto, *Tetrahedron Lett.* **2006**, *47*, 2591–2594.
[28] H. Ohmiya, H. Yorimitsu, K. Oshima, *Org. Lett.* **2006**, *8*, 3093–3096.
[29] a) V. Koch, M. M. Lorion, E. Barde, S. Bräse, J. Cossy, *Org. Lett.* **2019**; b) L. Nicolas, E. Izquierdo, P. Angibaud, I. Stansfield, L. Meerpoel, S. Reymond, J. Cossy, *J. Org. Chem* **2013**, *78*, 11807–11814.
[30] a) M. S. Hofmayer, A. Sunagatullina, D. Brösamlen, P. Mauker, P. Knochel, *Org. Lett.* **2020**, *22*, 1286–1289; b) G. Cahiez, C. Chaboche, C. Duplais, A. Moyeux, *Org. Lett.* **2009**, *11*, 277–280; c) H. Ohmiya, H. Yorimitsu, K. Oshima, *J. Am. Chem. Soc.* **2006**, *128*, 1886–1889.
[31] B. Barré, L. Gonnard, R. Campagne, S. Reymond, J. Marin, P. Ciapetti, M. Brellier, A. Guérinot, J. Cossy, *Org. Lett.* **2014**, *16*, 6160–6163.
[32] J. M. Hammann, D. Haas, C.-P. Tüllmann, K. Karaghiosoff, P. Knochel, *Org. Lett.* **2016**, *18*, 4778–4781.
[33] C. K. Reddy, P. Knochel, *Angew. Chem. Int. Ed.* **1996**, *35*, 1700–1701.
[34] R. Frlan, M. Sova, S. Gobec, G. Stavber, Z. Časar, *J. Org. Chem* **2015**, *80*, 7803–7809.
[35] H. Yasui, K. Mizutani, H. Yorimitsu, K. Oshima, *Tetrahedron* **2006**, *62*, 1410–1415.
[36] T. Kamachi, A. Kuno, C. Matsuno, S. Okamoto, *Tetrahedron Lett.* **2004**, *45*, 4677–4679.
[37] J. M. Hammann, F. H. Lutter, D. Haas, P. Knochel, *Angew. Chem. Int. Ed.* **2017**, *56*, 1082–1086.
[38] S. Eiji, I. Yusuke, H. Tamio, *Chem. Lett.* **2008**, *37*, 654–655.
[39] J. Li, P. Knochel, *Angew. Chem. Int. Ed.* **2018**, *57*, 11436–11440.
[40] E. Shirakawa, T. Sato, Y. Imazaki, T. Kimura, T. Hayashi, *Chem. Commun.* **2007**, 4513–4515.
[41] a) A. D. Benischke, I. Knoll, A. Rérat, C. Gosmini, P. Knochel, *Chem. Commun.* **2016**, *52*, 3171–3174; b) H. Hiroyuki, U. Minoru, Y. Hiroto, Y. Hideki, O. Koichiro, *Chem. Lett.* **2008**, *37*, 1178–1179.
[42] A. Piontek, W. Ochędzan-Siodłak, E. Bisz, M. Szostak, *ChemCatChem* **2021**, *13*, 202–206.
[43] X. Zhang, A. McNally, *ACS Catal.* **2019**, *9*, 4862–4866.
[44] J. Wei, K.-M. Liu, X.-F. Duan, *J. Org. Chem* **2017**, *82*, 1291–1300.
[45] a) D. Haas, J. M. Hammann, F. H. Lutter, P. Knochel, *Angew. Chem. Int. Ed.* **2016**, *55*, 3809–3812; b) S. Gülak, O. Stepanek, J. Malberg, B. R. Rad, M. Kotora, R. Wolf, A. Jacobi von Wangelin, *Chem. Sci.* **2013**, *4*, 776–784; c) T. Hatakeyama, S. Hashimoto, K. Ishizuka, M. Nakamura, *J. Am. Chem. Soc.* **2009**, *131*, 11949–11963; d) M. Amatore, C. Gosmini, *Angew. Chem. Int. Ed.* **2008**, *47*, 2089–2092.
[46] J. M. Hammann, L. Thomas, Y.-H. Chen, D. Haas, P. Knochel, *Org. Lett.* **2017**, *19*, 3847–3850.
[47] M. Corpet, X.-Z. Bai, C. Gosmini, *Adv. Synth. Catal.* **2014**, *356*, 2937–2942.
[48] S. M. Colegate, L. B. Din, A. Latiff, K. M. Salleh, M. W. Samsudin, B. W. Skelton, K.-I. Tadano, A. H. White, Z. Zakaria, *Phytochemistry* **1990**, *29*, 1701–1704.
[49] a) Z. Li, X.-Y. Cheng, N.-Y. Yang, J.-J. Chen, W.-Y. Tang, J.-Q. Bian, Y.-F. Cheng, Z.-L. Li, Q.-S. Gu, X.-Y. Liu, *Organometallics* **2021**, *40*, 2215–2219; b) Y. Zhou, C. Liu, L. Wang, L. Han, S. Hou, Q. Bian, J. Zhong, *Synlett* **2019**, *30*, 860–862.
[50] X. Cheng, X. Liu, S. Wang, Y. Hu, B. Hu, A. Lei, J. Li, *Nat. Commun.* **2021**, *12*, 4366.
[51] J. A. Przyojski, H. D. Arman, Z. J. Tonzetich, *Organometallics* **2013**, *32*, 723–732.
[52] H. Xu, W. H. Bernskoetter, *J. Am. Chem. Soc.* **2011**, *133*, 14956–14959.
[53] a) K. Wakabayashi, H. Yorimitsu, K. Oshima, *J. Am. Chem. Soc.* **2001**, *123*, 5374–5375; b) T. Fujioka, T. Nakamura, H. Yorimitsu, K. Oshima, *Org. Lett.* **2002**, *4*, 2257–2259; c) H. Someya, H. Ohmiya, H. Yorimitsu, K. Oshima, *Org. Lett.* **2007**, *9*, 1565–1567; d) H. Someya, A. Kondoh, A. Sato, H. Ohmiya, H. Yorimitsu, K. Oshima, *Synlett* **2006**, *2006*, 3061–3064.

[54] A. T. Nials, C. J. Vardey, L. H. Denyer, M. Thomas, S. J. Sparrow, G. D. Shepherd, R. A. Coleman, *Cardiovasc. Drug Rev.* **1993**, *11*, 165–179.
[55] M. Richter, A. H.-P. Krauss, D. F. Woodward, E. Lütjen-Drecoll, *Invest. Ophth. Vis. Sci.* **2003**, *44*, 4419–4426.
[56] a) K. Komeyama, T. Michiyuki, I. Osaka, *ACS Catal.* **2019**; b) L. K. G. Ackerman, L. L. Anka-Lufford, M. Naodovic, D. J. Weix, *Chem. Sci.* **2015**, *6*, 1115–1119.
[57] X.-G. Liu, C.-J. Zhou, E. Lin, X.-L. Han, S.-S. Zhang, Q. Li, H. Wang, *Angew. Chem. Int. Ed.* **2018**, *57*, 13096–13100.
[58] T. J. Korn, G. Cahiez, P. Knochel, *Synlett* **2003**, *2003*, 1892–1894.
[59] O. M. Kuzmina, A. K. Steib, J. T. Markiewicz, D. Flubacher, P. Knochel, *Angew. Chem. Int. Ed.* **2013**, *52*, 4945–4949.
[60] a) J.-M. Bégouin, C. Gosmini, *J. Org. Chem* **2009**, *74*, 3221–3224; b) J.-M. Begouin, M. Rivard, C. Gosmini, *Chem. Commun.* **2010**, *46*, 5972–5974.
[61] a) M.-Y. Jin, N. Yoshikai, *J. Org. Chem.* **2011**, *76*, 1972–1978; b) H. Fillon, C. Gosmini, J. Périchon, *J. Am. Chem. Soc.* **2003**, *125*, 3867–3870; c) C. Gosmini, M. Amatore, S. Claudel, J. Périchon, *Synlett* **2005**, *2005*, 2171–2174.
[62] L. Melzig, C. R. Diène, C. J. Rohbogner, P. Knochel, *Org. Lett.* **2011**, *13*, 3174–3177.
[63] C. Dorval, E. Dubois, Y. Bourne-Branchu, C. Gosmini, G. Danoun, *Adv. Synth. Catal.* **2019**, *361*, 1777–1780.
[64] E. Pietrasiak, S. Ha, S. Jeon, J. Jeong, J. Lee, J. Seo, E. Lee, *J. Org. Chem* **2022**, *87*, 8380–8389.
[65] a) Y. Cai, A. D. Benischke, P. Knochel, C. Gosmini, *Chem. Eur. J.* **2017**, *23*, 250–253; b) S. Pal, S. Chowdhury, E. Rozwadowski, A. Auffrant, C. Gosmini, *Adv. Synth. Catal.* **2016**, *358*, 2431–2435; c) C. E. I. Knappke, S. Grupe, D. Gärtner, M. Corpet, C. Gosmini, A. Jacobi von Wangelin, *Chem. Eur. J.* **2014**, *20*, 6828–6842; d) M. Amatore, C. Gosmini, J. Périchon, *Eur. J. Org. Chem.* **2005**, *2005*, 989–992.
[66] a) S. Bernhardt, G. Manolikakes, T. Kunz, P. Knochel, *Angew. Chem. Int. Ed.* **2011**, *50*, 9205–9209; b) A. Hernán-Gómez, E. Herd, E. Hevia, A. R. Kennedy, P. Knochel, K. Koszinowski, S. M. Manolikakes, R. E. Mulvey, C. Schnegelsberg, *Angew. Chem. Int. Ed.* **2014**, *53*, 2706–2710.
[67] X. Liu, J. Wang, J. Li, *Synlett* **2022**.
[68] M. Inoue, Y. Sumii, N. Shibata, *ACS Omega* **2020**, *5*, 10633–10640.
[69] A. Devasagayaraj, P. Knochel, *Tetrahedron Lett.* **1995**, *36*, 8411–8414.
[70] H. Fillon, C. Gosmini, J. Périchon, *Tetrahedron* **2003**, *59*, 8199–8202.
[71] I. Kazmierski, M. Bastienne, C. Gosmini, J.-M. Paris, J. Périchon, *J. Org. Chem* **2004**, *69*, 936–942.
[72] A. Rérat, C. Michon, F. Agbossou-Niedercorn, C. Gosmini, *Eur. J. Org. Chem.* **2016**, *2016*, 4554–4560.
[73] F. H. Lutter, L. Grokenberger, M. S. Hofmayer, P. Knochel, *Chem. Sci.* **2019**, *10*, 8241–8245.
[74] M. M. Rahman, C. Liu, E. Bisz, B. Dziuk, R. Lalancette, Q. Wang, H. Chen, R. Szostak, M. Szostak, *J. Org. Chem* **2020**, *85*, 5475–5485.
[75] C. Dorval, O. Stetsiuk, S. Gaillard, E. Dubois, C. Gosmini, G. Danoun, *Org. Lett.* **2022**, *24*, 2778–2782.
[76] a) R. Leonardi, Y.-M. Zhang, C. O. Rock, S. Jackowski, *Prog. Lipid Res.* **2005**, *44*, 125–153; b) M. Darnell, K. Breitholtz, E. M. Isin, U. Jurva, L. Weidolf, *Chem. Res. Toxicol.* **2015**, *28*, 886–896.
[77] B. Shin, S. Ahn, M. Noh, J. Shin, D.-C. Oh, *J. Nat. Prod.* **2015**, *78*, 1390–1396.
[78] J. Nachtigall, K. Schneider, C. Bruntner, A. T. Bull, M. Goodfellow, H. Zinecker, J. F. Imhoff, G. Nicholson, E. Irran, R. D. Süssmuth, et al., *J. Antibiot.* **2011**, *64*, 453–457.
[79] a) X. Wang, Z.-B. Dong, *Eur. J. Org. Chem.* **2022**, *2022*, e202200452; b) Y. Hai, M.-Y. Wei, C.-Y. Wang, Y.-C. Gu, C.-L. Shao, *Mar. Life Sci. Technol.* **2021**, *3*, 488–518.
[80] K. A. Scott, J. T. Njardarson, *Top. Curr. Chem.* **2018**, *376*, 5.
[81] G. Lin, D. Li, L. P. S. de Carvalho, H. Deng, H. Tao, G. Vogt, K. Wu, J. Schneider, T. Chidawanyika, J. D. Warren, et al., *Nature* **2009**, *461*, 621–626.
[82] A. A. Stierle, J. H. Cardellina, F. L. Singleton, *Tetrahedron Lett.* **1991**, *32*, 4847–4848.
[83] a) T. Itoh, T. Mase, *J. Org. Chem* **2006**, *71*, 2203–2206; b) B. Zeysing, C. Gosch, A. Terfort, *Org. Lett.* **2000**, *2*, 1843–1845; c) R. H. Crabtree, *Chem. Rev.* **2015**, *115*, 127–150.
[84] a) S. Otsuka, K. Nogi, H. Yorimitsu, *Top. Curr. Chem.* **2018**, *376*, 13; b) V. Hirschbeck, P. H. Gehrtz, I. Fleischer, *Chem. Eur. J.* **2017**, *24*, 7092–7107; c) F. Pan, Z.-J. Shi, *ACS Catal.* **2014**,

4, 280–288; d) S. G. Modha, V. P. Mehta, E. V. Van Der Eycken, *Chem. Soc. Rev.* **2013**, *42*, 5042–5055; e) V. J. Geiger, R. M. Oechsner, P. H. Gehrtz, I. Fleischer, *Synthesis* **2022**, DOI: 10.1055/a–1914–1231.
[85] P. C. St. John, Y. Guan, Y. Kim, S. Kim, R. S. Paton, *Nat. Commun.* **2020**, *11*, 2328.
[86] Y. Tian, L. Wang, H.-Z. Yu, *RSC Adv.* **2016**, *6*, 61996–62004.
[87] H. Tokuyama, S. Yokoshima, T. Yamashita, T. Fukuyama, *Tetrahedron Lett.* **1998**, *39*, 3189–3192.
[88] T. Fukuyama, S. C. Lin, L. Li, *J. Am. Chem. Soc.* **1990**, *112*, 7050.
[89] a) S. Sikandar, A. F. Zahoor, S. Naheed, B. Parveen, K. G. Ali, R. Akhtar, *Mol. Divers.* **2022**, *26*, 589–628; b) J. Lou, Q. Wang, P. Wu, H. Wang, Y.-G. Zhou, Z. Yu, *Chem. Soc. Rev.* **2020**.
[90] R. J. Anderson, C. A. Henrick, L. D. Rosenblum, *J. Am. Chem. Soc.* **1974**, *96*, 3654–3655.
[91] Y. Tian, L. Wang, H.-Z. Yu, *RSC Adv.* **2016**, *6*, 61996–62004.
[92] J. Wang, B. P. Cary, P. D. Beyer, S. H. Gellman, D. J. Weix, *Angew. Chem. Int. Ed.* **2019**, *58*, 12081–12085.
[93] P. H. Gehrtz, P. Kathe, I. Fleischer, *Chem. Eur. J.* **2018**, *24*, 8774–8778.
[94] M. Ociepa, O. Baka, J. Narodowiec, D. Gryko, *Adv. Synth. Catal.* **2017**, *359*, 3560–3565.
[95] a) S. Ozaki, M. Adachi, S. Sekiya, R. Kamikawa, *J. Org. Chem.* **2003**, *68*, 4586–4589; b) M. Weïwer, S. Olivero, E. Duñach, *Tetrahedron* **2005**, *61*, 1709–1714; c) J. Gruber, F. Ferraz Camilo, *J. Chem. Soc. Perk. T 1* **1999**, 127–130.
[96] F. Zaragoza Dörwald, *Lead Optimization for Medicinal Chemists*, Wiley-VCH, Weinheim, **2013**.
[97] a) X.-B. Xu, J. Liu, J.-J. Zhang, Y.-W. Wang, Y. Peng, *Org. Lett.* **2013**, *15*, 550–553; b) N. Park, K. Park, M. Jang, S. Lee, *J. Org. Chem.* **2011**, *76*, 4371–4378.
[98] K. Ishitobi, K. Muto, J. Yamaguchi, *ACS Catal.* **2019**, *9*, 11685–11690.
[99] J. Wu, W.-H. Xu, H. Lu, P.-F. Xu, *Adv. Synth. Catal.* **2021**, *363*, 3013–3017.
[100] Y. Minami, H. Kuniyasu, A. Sanagawa, N. Kambe, *Org. Lett.* **2010**, *12*, 3744–3747.
[101] P. H. Gehrtz, V. Geiger, T. Schmidt, L. Sršan, I. Fleischer, *Org. Lett.* **2019**, *21*, 50–55.
[102] T. Miura, Y. Fujimoto, Y. Funakoshi, M. Murakami, *Angew. Chem. Int. Ed.* **2015**, *54*, 9967–9970.
[103] Y. Feng, S. Yang, S. Zhao, D.-P. Zhang, X. Li, H. Liu, Y. Dong, F.-G. Sun, *Org. Lett.* **2020**.
[104] F. Bie, X. Liu, H. Cao, Y. Shi, T. Zhou, M. Szostak, C. Liu, *Org. Lett.* **2021**, *23*, 8098–8103.
[105] a) K. Osakada, T. Yamamoto, A. Yamamoto, *Tetrahedron Lett* **1987**, *28*, 6321–6324; b) E. Wenkert, D. Chianelli, *J. Chem. Soc., Chem. Commun.* **1991**, 627–628.
[106] a) N. Ichiishi, C. A. Malapit, Ł. Woźniak, M. S. Sanford, *Org. Lett.* **2018**, *20*, 44–47; b) K. Ishitobi, R. Isshiki, K. K. Asahara, C. Lim, K. Muto, J. Yamaguchi, *Chem. Lett.* **2018**, *47*, 756–759; c) S.-C. Lee, H.-H. Liao, A. Chatupheeraphat, M. Rueping, *Chem. Eur. J.* **2018**, *24*, 3608–3612; d) C. Liu, M. Szostak, *Chem. Commun.* **2018**, *54*, 2130–2133.
[107] H. Ochiai, Y. Uetake, T. Niwa, T. Hosoya, *Angew. Chem. Int. Ed.* **2017**, *56*, 2482–2486.
[108] Z.-J. Zheng, C. Jiang, P.-C. Shao, W.-F. Liu, T.-T. Zhao, P.-F. Xu, H. Wei, *Chem. Commun.* **2019**, *55*, 1907–1910.
[109] S. Jonsson, S. Ricagno, Y. Lindqvist, N. G. J. Richards, *J. Biol. Chem.* **2004**, *279*, 36003–36012.
[110] R. Haraguchi, S.-g. Tanazawa, N. Tokunaga, S.-i. Fukuzawa, *Org. Lett.* **2017**, *19*, 1646–1649.
[111] R. Haraguchi, S. g. Tanazawa, N. Tokunaga, S. i. Fukuzawa, *Eur. J. Org. Chem.* **2018**, *2018*, 1761–1764.
[112] L. C. McCann, M. G. Organ, *Angew. Chem. Int. Ed.* **2014**, *53*, 4386–4389.
[113] R. Haraguchi, A. Kusakabe, N. Mizutani, S.-i. Fukuzawa, *Org. Lett.* **2018**, *20*, 1613–1616.
[114] Y.-F. Cao, L.-J. Li, M. Liu, H. Xu, H.-X. Dai, *J. Org. Chem* **2020**, *85*, 4475–4481.
[115] R.-H. Zheng, H.-C. Guo, T.-T. Chen, Q. Huang, G.-B. Huang, H.-J. Jiang, *RSC Adv.* **2018**, *8*, 25123–25126.
[116] J. E. Gómez, W. Guo, A. W. Kleij, *Org. Lett.* **2016**, *18*, 6042–6045.
[117] W. Guo, L. Martínez-Rodríguez, E. Martin, E. C. Escudero-Adán, A. W. Kleij, *Angew. Chem. Int. Ed.* **2016**, *55*, 11037–11040.
[118] F. Ouhib, B. Grignard, E. Van Den Broeck, A. Luxen, K. Robeyns, V. Van Speybroeck, C. Jerome, C. Detrembleur, *Angew. Chem. Int. Ed.* **2019**, *58*, 11768–11773.
[119] Z. Zhu, Y. Gong, W. Tong, W. Xue, H. Gong, *Org. Lett.* **2021**, *23*, 2158–2163.
[120] T. Broese, A. F. Roesel, A. Prudlik, R. Francke, *Org. Lett.* **2018**, *20*, 7483–7487.
[121] T. Inami, T. Kurahashi, S. Matsubara, *Chem. Commun.* **2015**, *51*, 1285–1288.

[122] V. Geiger, Master Thesis, University of Tübingen, **2018**.
[123] J. Riedmaier, Bachelor Thesis, University of Tübingen, **2019**.
[124] C. A. DeSimone, S. L. Naqvi, S. Z. Tasker, *Chem. Eur. J.* **2022**, *28*, e202201326.
[125] N. Kehl, Bachelor Thesis, University of Tübingen, **2020**.
[126] S. P. Curran, S. J. Connon, *Angew. Chem. Int. Ed.* **2012**, *51*, 10866–10870.
[127] R. M. Oechsner, J. P. Wagner, I. Fleischer, *ACS Catalysis* **2022**, *12*, 2233–2243.
[128] R. Richter, Master Thesis, University of Tübingen, **2022**.
[129] A. L. Silberstein, S. D. Ramgren, N. K. Garg, *Org. Lett.* **2012**, *14*, 3796–3799.
[130] a) E. Wolf, E. Richmond, J. Moran, *Chem. Sci.* **2015**, *6*, 2501–2505; b) E. Richmond, J. Moran, *Synlett* **2016**, *27*, 2637–2643; c) E. Richmond, J. Moran, *J. Org. Chem.* **2015**, *80*, 6922–6929.
[131] J. M. Fordham, P. Kollmus, M. Cavegn, R. Schneider, M. Santagostino, *J. Org. Chem.* **2022**, *87*, 4400–4414.
[132] a) P. Neate, M. D. Greenhalgh, W. W. Brennessel, S. P. Thomas, M. L. Neidig, *J. Am. Chem. Soc.* **2019**; b) P. G. N. Neate, M. D. Greenhalgh, W. W. Brennessel, S. P. Thomas, M. L. Neidig, *Angew. Chem. Int. Ed.* **2020**, *59*, 17070–17076.

5. EXPERIMENTAL PART

5.1 General Information

5.1.1 Chemicals

LiCl, CoCl 6 H_2O, magnesium turnings (p.A. grade) were supplied by the central chemical desk of the University of Tübingen. $MnCl_2$ was supplied by Acros Organics (99+%) and $ZnCl_2$ was supplied by Merck Millipore (98+%), both chemicals were stored in a screw-capped plastic bottles. Iron(III) acetyl acetonate used for the catalytic reaction was supplied by either Acros Organics (99+% in some cases of the initial optimization reactions) or Sigma Aldrich (≥99.9% for optimization reactions and substrate screening). Other chemicals were purchased from abcr, Acros, BLDChem, Carbolution Chemicals, Fluka, Fluorochem, Merck, Sigma-Aldrich or TCI.

NMR analysis of used thiols was performed prior, especially for ethanethiol (mainly supplied from Acros Organics). If not sufficiently pure, thiols were usually distilled prior to use, degassed and stored at -10 °C in Schlenk vessels under inert gas. Thioesters were handled under air and stored at 0 °C, although, decomposition of thioesters was only observed at rt in rare instances.

Solvents for chromatography, thin-layer chromatography, reaction work-up and recrystallization were either HPLC grade purity or were distilled prior to use.

5.1.2 General Techniques

5.1.2.1 Reaction set-up

All reactions with organometallic reactants and catalyst were carried out under Ar or N_2 atmosphere with predried glassware using common air-free techniques, unless noted otherwise. Dry THF was stored in a Schlenk-round bottom flask (RBF) under inert gas over 3 Å MS (20% w/v, at least 3 days storage). Before, the solvent was distilled over Na/benzophenone. Activation of 3 Å MS was achieved by either microwave-activation or heating under vacuum (280 °C, 7 mBar, 1 h). The non-degassed THF used in catalytic reactions was obtained by adding predistilled THF (stored over freshly crushed KOH for at least 2 days)[1] through a filter into a container under inert gas with activated 3 Å MS (50% v/v, at least 5 days storage).

As ethanethiol possesses a high vapour pressure, therefore, connection to an inert gas line led to high contaminations of the inert gas. Due to this, a separate line was used for reactions with volatile thiols or the line purged before other reactions were conducted.

The catalytic reactions were mainly conducted using a Julabo FT902 Cryostate with an acetone bath. The cryostat was set to -15 °C achieving a cooling bath temperature range from -20 °C to -15 °C.

5.1.2.2 Liquid Chromatography

Column chromatography was carried out either manually or by a Puriflash system (Interchim XS420) using silica gel (0.04–0.063 mm) from Machery&Nagel unless noted otherwise. TLC analysis was carried out using aluminium-backed plates coated with silica 60 F_{254} (0.2 mm thickness) and the compounds detected under ultraviolet (UV) light (254 nm). Alternatively, the plates were stained with a $KMnO_4$ or anisaldehyde TLC dip solution and gently heated or by treated with iodine vapours. In case of the anisaldehyde stain often colors were observable, which are mentioned for respective compounds.

Definition of "gradient" used below: In separations using the Puriflash system, a gradient was developed around a suitable binary eluent combination X:Y (latter is the strong solvent, X + Y = 100). The eluent programs are given for each respective compound. In any given volumetric ratio for TLC or (flash-)LC, the reported ratios reflect a volume/volume (v/v)-ratio.

Dry-column vacuum chromatography (DCVC) was performed following literature procedure.[2] Silica employed for these separation was supplied by Merck (Silica Gel 60 0.015–0.040 mm) and samples were subjected to wet loading by injection into a layer of *n*-hexane (Hex) or petroleum ether 60/90 (PE) layer during column flow.

5.1.3 Analytical Techniques

5.1.3.1 Nuclear Magnetic Resonance spectroscopy (NMR)

NMR spectra were recorded using a Bruker Avance 400, a Bruker Avance III HD 300 NanoBay, a Bruker Avance III HDX 600 or a Bruker Avance III HDX 700, ^{13}C-NMR and ^{31}P-NMR experiments were performed in proton-decoupled mode, which is not noted explicitly. Chemical shifts are reported in parts per million relative to the residual NMR solvent signals[3] (chloroform: ^{1}H δ = 7.26 ppm and ^{13}C δ = 77.16 ppm; dichloromethane: ^{1}H δ = 5.32 and ^{13}C δ = 53.84; methanol: ^{1}H δ = 3.31 and ^{13}C δ = 49.00; acetonitrile: ^{1}H δ = 1.94 and ^{13}C δ = 118.26) and the *J*-coupling constants are given in Hertz with the usual designations for splitting patterns (s = singlet, d = doublet, t = triplet, q = quartet, quin = quintet, hept = heptet, m = multiplet, br = broad).

5.1.3.2 Electron Paramagnetic Resonance spectroscopy (EPR)

EPR measurements were carried out by the NMR department of the Institute of Organic Chemistry, University of Tübingen on a Bruker EMXmicro with PremiumX microwave-bridge. The samples were prepared in the EPR tube (3 mm outer diameter) at -20 °C in a mixture 2-MeTHF/THF (1:1, 0.3 M). After addition of reagents, the samples were carefully tapped for 1 min and frozen in liquid nitrogen. The spectra were acquired at 120 K.

5.1.3.3 High Resolution Mass Spectrometry (HR-MS)

HR-MS (ESI, APCI, EI) measurements were carried out by the mass spectrometry department of the Institute of Organic Chemistry, University of Tübingen. Measurements were carried out using maXis 4G from Bruker (ESI, APCI) or by a MAT95 from Finnegan (EI).

5.1.3.4 Gas Chromatography (GC-MS or GC-FID)

GC-LR-MS (EI) analysis was carried out by our standard GC/MS method. For this, an Agilent 7820A GC equipped with a190915-433UI column (30 m × 250 µm × 0.25 µm) and 7820MSD was used. Program: Heating from 50 °C to 280 °C within 15 minutes. Also, samples were measured by the MS-department of the University of Tübingen with an 8890 GC system and 5977B MSD. For these measurements, temperature program started by holding 3 min at 40 °C, then heating to 320 °C within 32 min and holding for 10 min at the same temperature. These measurements are marked with 'method B'.

GC-FID (flame ionization detection) analysis was carried out on an Agilent 7820A system using dry hydrogen or nitrogen as carrier gas. For this, an Agilent 19091J-431 column (30 m × 320 µm × 0.25 µm) was used. Program 50-280M12 (N_2): Heating from 50 °C to 280 °C with 20 °C/min and hold for 0.5 min; Program 50-280M15 (H_2): Heating from 50 °C to 280 °C with 20 °C/min and hold for 3 min.

5.1.3.5 Infrared Spectroscopy(IR)

FT-IR spectra were recorded using a Cary 630 FTIR by applying the sample neat on a diamond ATR (attenuated total reflection) sampler. The spectra were automatically processed, and intensities assigned in R. The processing code is appended to this thesis (see Appendix, p.225).

5.1.3.6 Melting Point Determination

Melting point determination was achieved by using a MPM HV 3 machine with a visual detection (heating rate 1 °C/min). If a solid possessed a melting point close to rt, it is assigned "ambient temperature".

5.1.4 Starting materials

Syntheses of thioesters **115a, 115b, 115c, 119b, 119h, 129j, 129l, 119o, 119q, 131b, 131e, 131l, 250b, 250c** were reported in previous publications or theses of our group.[4]

Starting materials of substrates unsuccessful in the substrate screening **119e**[5], **119r**[6], **140**[7], **129k**[8], **131m**[8] were synthesized by either cited literature procedure or respective general procedures and purity verified by NMR, GC-MS and IR analysis. Unknown starting materials were fully characterized and are included below.

5.2 General Procedures (GP)

General Procedure A–Synthesis of thioesters *via* Steglich esterification

The reaction was conducted following a modified literature procedure.[9] In a round bottom flask (RBF) equipped with a stirring bar, carboxylic acid (10 mmol) was dissolved in dichloromethane (DCM) and ethanethiol (2.2 mL, 30 mmol, 3 equiv.) was added. The solution was cooled to 0 °C and 4-dimethylaminopyridine (DMAP) was added (0.1 equiv.). Over a period of 2 min *N*,*N*'-dicyclohexylcarbodiimide (DCC) or *N*,*N*'-diisopropylcarbodiimide (DIC) (1.1 equiv.) was added in portions at the same temperature. The reaction was allowed to warm to room temperature (rt) and stirred overnight. Then, the suspension was filtered and the crude solution reduced *in vacuo*. Further work-up steps are given for each respective compound.

General remark:

Even if purification was attempted by filtration through a silica plug, as is mentioned in several literature procedures[10], residue signals in the ^{1}H and ^{13}C NMR-spectra can be observe, likely originating from either from a dialkylurea byproduct or rearrangement side product. These impurities were observed to cause problems with column separations and even bulb-to-bulb distillation. In order to remove these impurities, extraction of most products after filtration through a small silica plug was achieved by subsequent extraction of DCM solution with 3 × 6 M HCl, which made column separation obsolete in most cases.

General Procedure B–Synthesis of thioesters from acid chlorides

In a RBF equipped with a stirring bar, ethanethiol (1.2 equiv.) was dissolved in DCM (0.5 M in respect to the acid chloride), put under an Ar-atmosphere and cooled to 0 °C. Then, TEA (1.0 equiv.) was added. A solution of acid chloride (usually 10 mmol) in DCM (2 M or until homogeneous) was slowly added *via* syringe (over 5 min) to the vigorously stirred solution of thiol. After 30 min at 0 °C, the mixture was stirred at rt until no more starting material was observed (reaction monitoring by TLC - usually after 1-4 h). Water was added to the reaction mixture and the solution was extracted with aq. HCl (6 M), sat. aq. $NaHCO_3$ and brine. The combined organic layers were dried over anhydrous $MgSO_4$ and solvent was evaporated *in vacuo*.

General Procedure C–Synthesis of organomanganese halides

Synthesis of Grignard reagents:

In a Schlenk RBF equipped with a stirring bar and septum, magnesium turnings (1.3 equiv.) were dried using a propane torch under high vacuum. The flask was allowed to cool to rt under vacuum, then flushed with inert gas. A crumb of iodine was added and gently heated until vapours emerged. The inert gas tap was closed, and the turnings were stirred in iodine vapour for 5 min. After this, an ice bath was put under

the flask and the turnings were stirred for another 5 min or until complete resublimation of iodine. Then, the inert gas tab was opened, and anhydrous tetrahydrofuran (THF) was added at once (aimed concentration was 1.3 M in respect of aryl bromide). A few drops of organobromide (1.0 equiv.) were added until a visible change in color and emergence of reaction heat were observable. The mixture was cooled with a water-ice bath (ca. 10 °C) and further organobromide was added slowly. After no strong heat generation was observable, the cooling bath was removed and the reaction was stirred overnight at rt. Quantification was achieved by Knochel iodometric titration.[11]

Synthesis of the soluble manganese precursor:

The ate complex was synthesized according to a modified literature procedure.[12] In a Schlenk-RBF equipped with stirring bar and septum, LiCl (3.56 g, 84 mmol, 2.1 equiv.) was dried with a heat gun under vacuum, allowed to cool and put under an Ar atmosphere. Then, manganese dichloride tetrahydrate (7.92 g, 40 mmol, 1 equiv.) was added and the salts were dried under high vacuum at 70 °C for 1 h and at 120 °C then 4 h. Afterwards, the RBF was allowed to cool to rt and anhydrous degassed THF was added (40 mL). The suspension was stirred until a homogenous yellow solution was obtained (at least 24 h and up to 5 d).

Synthesis of the organomanganese halide:

The reaction was conducted according to a modified literature procedure.[13] In a Schlenk-RBF equipped with stirring bar and septum manganese ate complex (1.2 equiv.) was diluted with anhydrous THF (designated concentration was 0.25 M of the organomanganese halide). The reaction mixture was cooled in a cooling bath to at least -5 °C and Grignard reagent (1.0 equiv. based on titre) was slowly added. The mixture was stirred for 2 h at the same temperature, titrated (iodometric) and then used the same day.

General remark:

Depending on the supplier and batch of the manganese chloride, reproducibility issues for the synthesis of ate complex occurred. This can lead to ethyl manganese reagents that decompose over various time frames (yields <10% after 1 h or even complete loss of concentration). These problems were solved by using manganese dichloride with a higher purity grade and/or freshly purchased stirring bars. It was therefore concluded that the difference in batches is the presence of metal impurities as well as trace iron impurities leaching from stirring bars that catalyse the decomposition of the reagent, as is known for dialkyl manganese compounds.[14]

From experience, the drying of LiCl can be achieved using a propane torch or better heat gun. However, manganese dichloride should not be heated over 150 °C as observable color changes occur (with propane torch to green/turquoise). This led to very low, if any, transmetalation yields by the ate complex solution and irreproducible results in subsequent reactions. In case of low yields, it is strongly recommended to

use newly purchased stirring bars and weighing with separate new spatulas or glass spatulas. After the appropriate time of stirring, the color of the ate complex solution varies from citrus yellow (optimal) to orange (showed reduced yields). Purchased $MnCl_2$•2 LiCl complex solutions from chemical vendors cannot be recommended which – in case of our sample – contained impurities which led to catalysis without catalyst necessary. Detailed pictures showing the colors of the ate complex and the manganese reagents are included below.

General Procedure D–Monitoring of Organomanganese reagent by iodometric titration

A solution of ethyl manganese reagent was synthesized according to GP-C. The solution was divided in 3 × 12 mL to which NMP was added (none, 0.5 mL or 5 mL for the different solutions). The solutions stirred for 1 h at each temperature step before the titration was performed. For each data point three iodometric titrations after literature procedure were conducted.[11]

General Procedure E–Monitoring of Organomanganese reagent by quenched solution

Two Schlenk-RBF equipped with septum and stirring bar were heated with a propane torch and 3 × evacuated/flushed with argon. Then, ate complex (6 mL, 6 mmol, 1 M in THF, 1.3 equiv.) was added and the flasks cooled to -20 °C. After this, *n*-octyl magnesium bromide (7.2 mL, 4.7 mmol, 0.65 M in THF) was added slowly and the solution mixed with *n*-pentadecane (820 µL) and either THF (2 mL) or NMP (2 mL). The mixtures were stirred for 1 h at each temperature step (-20 °C, -20 °C, 5 °C, rt) and for each data point three samples (each 0.5 mL) were drawn *via* syringe and quenched immediately by addition into a I_2 solution (THF). The quenched solution was shaken after addition of a few drops of sat. aq. $Na_2S_2O_3$ solution and EA (~ 2 mL). The organic layer was separated, filtered through a pad of anhydrous $MgSO_4$, basic Al_2O_3 and Celite in a Pasteur pipette before analysis *via* GC-FID.

General Procedure F–Optimization of iron-catalyzed Fukuyama coupling of alkyl manganese reagents

In a flame-dried Schlenk-tube equipped with a stirring bar and septum iron(III) acetyl acetonate ($Fe(acac)_3$) (5.9 mg, 16.7 µmol, 5 mol%) was added and vacuum applied. After flushing with Ar, the precatalyst was dissolved in 1 mL of THF (dried over 50% v/v 3 Å preactivated molecular sieves for 1 week, not degassed) and cooled to -20 °C. Thioester **115a** (53.4 mg, 333 µmol) was added to the mixture. Then, organomanganese reagent prepared according to GP-C (1.2 mmol; 0.18–0.30 M in THF based on titre) was added and the mixture was stirred for 10 min. Before quenching, the internal standard *n*-pentadecane (100 µL) was added. The reaction was quenched using sat. aq. NH_4Cl solution (ca. 1 mL) and the organic layer was diluted with 3 mL of organic solvent (Et_2O or EA). The organic layer was separated, filtered through a pad of anhydrous $MgSO_4$, basic Al_2O_3 and Celite in a Pasteur pipette before diluting with DCM and analysis *via* GC-FID.

General Procedure G–Iron-catalyzed Fukuyama coupling of ethyl/hexyl manganese reagents

In a flame-dried Schlenk-tube equipped with a stirring bar and septum, $Fe(acac)_3$ (17.7 mg, 50 µmol, 5 mol%) was added and vacuum applied for 10 min. After flushing with Ar, the catalyst was dissolved in 3 mL of THF (dried over 50% v/v 3 Å preactivated molecular sieves for 1 week, not degassed) and cooled to -20 °C. Thioester (1.0 mmol) was added to the mixture. Then, ethyl or hexyl manganese reagent prepared according to GP-C (1.2 mmol; 0.18–0.32 M in THF based on titre) was added and the mixture was stirred for 10 min. The reaction was quenched using sat. NH_4Cl solution (ca. 2 mL), the organic layer was diluted with 10 mL of organic solvent (Et_2O or EA) and the aqueous layer extracted (4 × 10 mL of respective solvent). The combined organic layers were dried over anhydrous $MgSO_4$ and the solvent removed under reduced pressure.

General remark:

For the catalytic conversion of substrates, it is recommended to utilize anisaldehyde stain for TLC analysis in case of less functionalized substrates. Although most aliphatic thioesters can be observed by UV-detection with 254 nm (weak extinction), anisaldehyde staining is able to distinguish between starting material (yellow color – fades within 30 minutes) and product (blue color – fades after hours).

General Procedure H–Iron-catalyzed Fukuyama coupling of different alkyl manganese reagents

In a flame-dried Schlenk-tube equipped with a stirring bar and septum, $Fe(acac)_3$ (17.7 mg, 50 µmol, 5 mol%) was added and vacuum applied for 10 min. After flushing with Ar, the precatalyst was dissolved in 3 mL of THF (dried over 50% v/v 3 Å preactivated molecular sieves for 1 week, not degassed) and cooled to -20 °C. Thioester **119a** (194 mg, 1.00 mmol) was added to the mixture. Then, organomanganese reagent prepared according to GP-C (1.2 mmol; 0.20–0.28 M in THF based on titre) was added and the mixture stirred for 10 min. The reaction was quenched using sat. NH_4Cl solution (ca. 2 mL), the organic layer was diluted with 10 mL of organic solvent (Et_2O or EA) and the aqueous layer was extracted (4 × 10 mL of respective solvent). The combined organic layers were dried over anhydrous $MgSO_4$ and the solvent was removed under reduced pressure.

General Procedure I–Reaction progress monitoring of iron-catalyzed Fukuyama coupling of alkyl manganese reagents

In a flame-dried Schlenk-tube equipped with a stirring bar and septum $Fe(acac)_3$ (13.2 mg, 37.5 µmol, 5 mol%) was added and vacuum applied. After flushing with Ar, the precatalyst was dissolved in of THF (2 mL, dried over 50% v/v 3 Å preactivated molecular sieves for 1 week, not degassed) and cooled to -20 °C. Then, thioester (750 µmol) and *n*-pentadecane (100 µL) were added. Organomanganese reagent prepared according to GP-C (1.2 mmol; 0.18–0.33 M in THF based on titre) was added. Samples (~200 µL) were withdrawn from the reaction solution using separate syringes, which were inertized in a separate vessel. The samples were quenched by addition of sat. aq. NH_4Cl solution (ca. 1 mL) and the

organic layer was diluted with 0.5 mL of organic solvent (EA). The organic layer was filtered through a pad of $MgSO_4$, basic Al_2O_3 and Celite in a Pasteur pipette before diluting with DCM and analysis *via* GC-FID.

General Procedure J–Reaction observation of catalyst decomposition

In a flame-dried Schlenk-tube equipped with a stirring bar and septum $Fe(acac)_3$ (5.9 mg, 16.7 µmol, 5 mol%) was added and vacuum applied. After flushing with Ar, the precatalyst was dissolved in THF (1 mL, dried over 50% v/v 3 Å preactivated molecular sieves for 1 week, not degassed) and cooled to -20 °C. Organomanganese reagent prepared according to GP-C (1.2 mmol; 0.20–0.28 M in THF based on titre) was added and the mixture was stirred for a specific time (10 min, 30 min or 60 min). Then, thioester **115a** (53.4 mg, 333 µmol) was added and the mixture was stirred for 10 min at the same temperature. Before quenching, *n*-pentadecane (100 µL) was added. The reaction was quenched using sat. aq. NH_4Cl solution (ca. 1 mL) and the organic layer diluted with EA (1 mL). The organic layer was filtered through a pad of anhydrous $MgSO_4$, basic Al_2O_3 and Celite in a Pasteur pipette before diluting with DCM and analysis *via* GC-FID.

General Procedure K (GP-K)–Synthesis of thiosuccinoates

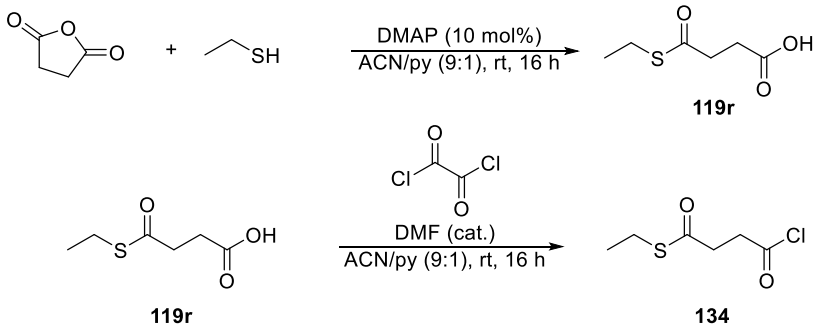

*Synthesis of 4-(ethylthio)-4-oxobutanoic acid (**119r**):*

The compound was synthesized according to a modified literature procedure.[15] Succinic anhydride (10.0 g, 100 mmol) and DMAP (1.22 g, 10.0 mmol, 0.1 equiv.) were dissolved in a mixture of acetonitrile/anhydrous pyridine (125 mL, 9:1 v/v). Ethanethiol (16.3 mL, 220 mmol, 2.2 equiv.) was added at once and the mixture was stirred over night at rt. Then, the solvents and leftover thiol were evaporated *in vacuo* and the crude compound was dissolved in EA (ca. 100 mL). The mixture was extracted with aq. HCl (3 × 20 mL, 1 M) and demin.water (3 × 20 mL) before drying over anhydrous $MgSO_4$. The solvents were evaporated *in vacuo* yielding a colorless smelly oil with no need for further purification (13.6 g, 84.2 mmol, 84%).

*Synthesis of S-ethyl 4-chloro-4-oxobutanethioate (**134**):*

Crude thioester **119r** (3.24 g, 20.0 mmol) was dissolved in Et_2O (50 mL) under Ar atmosphere and the solution was cooled to 0 °C. Then, oxalyl chloride (1.9 mL, 22 mmol, 1.1 equiv.) and a drop of dry DMF

were added and the mixture was stirred at 0 °C for 30 min and afterwards for 1 h at rt. The solvent was evaporated *in vacuo* in a heating bath at 30 °C. The reaction yielded a crude orange colored oil (3.47 g, 96% crude yield), which was used without any further purification. The acid chloride was synthesized freshly whenever used.

Synthesis of succinoate thioester:

The procedures are noted for each substrate **131c**, **131d, 131f** and **131i** respectively.

General Procedure L–Synthesis of organozinc halides

The reaction was conducted according to a modified literature procedure.[4d] In a predried Schlenk-RBF equipped with stirring bar and septum, Grignard reagent (1.0 equiv. based on titre) was slowly added to a zinc chloride solution (1 M in THF, 1.2 equiv.) at rt. The mixture was stirred for at least 1 h at the same temperature before use. Titration usually confirmed quantitative yield.

General Procedure M–Optimization of cobalt-catalyzed Fukuyama coupling of aryl zinc reagents

In a flame-dried Schlenk-tube equipped with a stirring bar and septum cobaltous chloride hexahydrate ($CoCl_2 \cdot 6\ H_2O$) (7.9 mg, 33 µmol, 0.1 equiv.) was added and vacuum applied while heating with a heat gun until a complete change in color was observed (purple to blue). After three cycles of vacuum/flushing with Ar, ligand (33 µmol, 0.1 equiv.) was added followed by three cycles of vacuum/flushing with Ar. The solids were dissolved in dry degassed solvent (usually THF, 1 mL) and gently heated with a heat gun for 1 min or until a change in color was observable. After this, the mixture was cooled to -20 °C and thioformate **231** (46.0 mg, 333 µmol) added. Then, organozinc reagent prepared according to GP-L (400 µmol, 0.2–0.5 M in THF, 1.2 equiv.) was added and the mixture was stirred for 1–4 h at -20 °C. Before quenching, the internal standard *n*-pentadecane (100 µL) was added. The reaction was quenched using sat. aq. NH_4Cl solution (ca. 1 mL) and the organic layer was diluted with EA (3 mL). The organic layer was separated, filtered through a pad of anhydrous $MgSO_4$, basic Al_2O_3 and Celite in a Pasteur pipette before diluting with DCM and analysis *via* GC-FID.

5.3 General Procedures - Pictures

Figure 4.1. Left: $MnCl_2 \cdot 2\ LiCl$ furnishing high yields in transmetalation. Right: Ate complex with likely impurities of $MnCl_2$ leading to diminished yields in transmetalation.

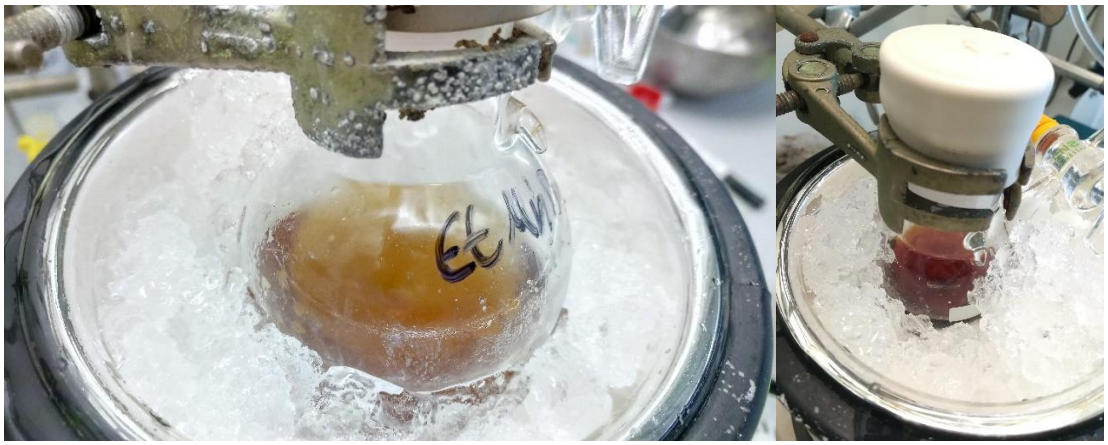

Figure 4.2. Ethyl manganese reagent color depending on purity and oxygen content from orange to orange-red.

Figure 4.3. Oxygenated manganese reagent solutions from left to right: 2-Methylpropyl-(**143j**), *iso*-propyl (**143c**), *tert*-butyl (**143f**) and benzyl (**143h**) manganese halide (colors from left to right: brown-purple, wine red, ink blue, black-green).

5.4 Synthesis and Analytical Data of Thioesters

S-(*tert*-butyl) hexanethioate (**115d**)

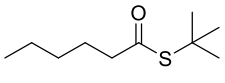

115d

According to GP-A, the product **115ad** was synthesized using hexanoic acid (1.3 mL, 10.0 mmol, 1.0 equiv.), 2-methylpropane-2-thiol (2.2 mL, 30 mmol, 3 equiv.), DMAP (122 mg, 1.00 mmol, 0.1 equiv.) and DCC (2.27 g, 11.0 mmol, 1.1 equiv.). Purification was achieved by filtration through a short silica plug using *n*-hexane (Hex)/ethylacetate (EA) (8:2). The filtrate was washed with aq. HCl (2 × 20 mL, 6 M), aq. KOH (1 × 20 mL, 10% w/v), sat. aq. $NaHCO_3$ (1 × 20 mL) and brine (1 × 20 mL), then dried over anhydrous $MgSO_4$. The product was yielded as a colorless oil (1.53 g, 8.12 mmol, 81%).

$C_{10}H_{20}OS$ (188.33 g/mol)

R_f: 0.23 (Hex) [$KMnO_4$, UV].

^{1}H NMR (400 MHz, $CDCl_3$): δ = 2.42 (t, *J* = 7.6 Hz, 2H), 1.65–1.55 (m, 2H), 1.49–1.39 (m, 9H, $C(CH_3)_3$), 1.31 –1.26 (m, 4H), 0.87 (t, *J* = 7.1, 3H, CH_3).

^{13}C NMR (101 MHz, $CDCl_3$): δ = 200.7 (*C*(O)SEt), 47.8, 44.7, 31.2, 30.0, 25.5, 22.5, 14.0.

GC-MS (EI): t_r = 4.57 min, m/z(%) = 131 (22, [$M^{+\bullet}$-$C_4H_9^\bullet$]), 99 (89, [$M^{+\bullet}$-$SC_4H_9^\bullet$]), 71 (42, [$M^{+\bullet}$-$SC_4H_9^\bullet$-CO]), 57 (100, [$C_4H_9^{+\bullet}$]).

HR-MS (EI): m/z calc. for $[M]^+$ 188.122937, found 188.12047.

IR (ATR, $\tilde{\nu}$ [cm^{-1}]): 2991 (w, C-H_{aliph}), 2955 (m, C-H_{aliph}), 2924 (m), 2864 (w), 1683 (s, C=O), 1456 (m), 1418 (w), 1388 (w), 1362 (m), 1337 (w), 1300 (w), 1210 (w), 1164 (m), 1120 (m), 1071 (w), 1027 (m), 1004 (m), 956 (m), 919 (w), 736 (w), 699 (w).

S,*S*'-(ethane-1,2-diyl) dihexanethioate (**115e**)

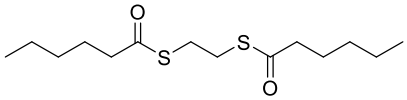

115e

According to modified GP-B, the product **115e** was synthesized using hexanoyl chloride (2.8 mL, 20 mmol, 1 equiv.), ethane-1,2-dithiol (840 µL, 10 mmol, 0.5 equiv.) and TEA (2.8 mL, 20 mmol, 1 equiv.). in $CHCl_3$ (40 mL). Purification was achieved by washing the solution with aq. HCl (2 x 20 mL, 1 M), aq. KOH (3 × 20 mL, 10% w/v), sat. $NaHCO_3$ (1 × 20 mL) and brine (1 × 20 mL). The organic layer was dried over anhydrous $MgSO_4$ and solvent evaporated under reduced pressure.

Further purification was achieved by manual column chromatography (isocratic Hex/EA = 97:3) to yield a colourless liquid with a characteristic unpleasant smell (1.55 g, 5.34 mmol, 53%).

$C_{14}H_{26}O_2S_2$ (290.48 g/mol)

R_f: 0.54 (Hex/EA = 95:5) [UV].

^{1}H NMR (400 MHz, $CDCl_3$): δ = 3.04 (s, 4H), 2.54 (t, *J* = 7.5 Hz, 4H), 1.72–1.53 (m, 4H), 1.38–1.21 (m, 8H), 0.95–0.78 (m, 6H).

^{13}C NMR (101 MHz, $CDCl_3$): δ = 199.1 (*C*(O)SEt), 44.2, 31.2, 28.9, 25.4, 22.4, 14.0.

HR-MS (ESI): m/z calc. for $[M+Na]^+$ 313.12664, found 313.12702.

IR (ATR, $\tilde{\nu}$ [cm^{-1}]): 2951 (m, C-H_{aliph}), 2928 (m, C-H_{aliph}), 2861 (w), 1690 (vs, C=O), 1459 (w), 1410 (w), 1374 (w), 1340 (w), 1269 (w), 1236 (w), 1203 (w), 1120 (m), 1068 (w), 1022 (m), 1007 (m), 963 (s), 922 (m), 844 (w), 736 (m), 699 (w).

S-ethyl 3-phenylpropanethioate (**119a**)

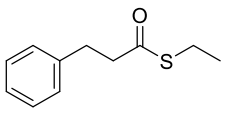

119a

According to GP-A, the product **119a** was synthesized using 3-phenylpropanoic acid (3.75 g, 25 mmol, 1.0 equiv.), ethanethiol (5.4 mL, 75 mmol, 3 equiv.), DMAP (305.4 mg, 2.5 mmol, 0.1 equiv.) and DCC (5.67 g, 27.5 mmol, 1.1 equiv.). Purification was achieved by filtration through a short silica plug using Hex/EA (8:2) and washing the filtrate with aq. HCl (2 × 10 mL, 6 M), sat. aq. $NaHCO_3$ (1 × 10 mL) and brine (1 × 10 mL) as well as drying over anhydrous $MgSO_4$. The product was yielded as a colorless oil (3.86 g, 19.87 mmol, 79%). The analytical data is in good accordance to reported literature.[16]

$C_{11}H_{14}OS$ (194.29 g/mol)

R_f: 0.30 (Hex/Et_2O = 9:1) [anis - yellow, UV].

^{1}H NMR (400 MHz, $CDCl_3$): δ = 7.36–7.30 (m, 2H, $C_{Ar}H$), 7.27–7.23 (m, 3H, $C_{Ar}H$), 3.05–3.02 (m, 2H), 2.96–2.89 (m, 4H), 1.30 (t, *J* = 7.4 Hz, 3H).

^{13}C NMR (101 MHz, $CDCl_3$): δ = 198.8 (*C*(O)SEt), 140.2 (C_{Ar}), 128.6 (C_{Ar}), 128.4 (C_{Ar}), 126.4 (C_{Ar}), 45.6, 31.6, 23.4, 14.9.

IR (ATR, $\tilde{\nu}$ [cm^{-1}]): 3062 (w, C-H_{arom}), 3025 (w, C-H_{arom}), 2965 (w, C-H_{arom}), 2928 (w, C-H_{arom}), 2868 (w, C-H_{arom}), 1683 (vs, C=O), 1601 (w), 1493 (w), 1448 (m), 1411 (w), 1373 (w), 1345 (w), 1262 (w), 1172 (w), 1045 (s), 967 (s), 878 (w), 840 (w), 740 (s), 695 (s).

S-ethyl 3-(ethylthio)propanethioate (**119c**)

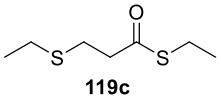

119c

(The product was unanticipatedly synthesized.) The product **119c** was synthesized from 3-chloropropanoic acid (1.09 g, 10.0 mmol), which was dissolved in acetone (20 mL). Then, 2-chloro-4,6-dimethoxy-1,3,5-triazine (2.11 g, 12.0 mmol, 1.2 equiv.) and TEA (4.2 mL, 30 mmol, 3 equiv.) were added. A precipitation of white solid was observed. The reaction was stirred at rt for 1 h. After this, ethanethiol (815 µL, 11.0 mmol, 1.1 equiv.) was added and the reaction was stirred further for 2 h at rt. Purification was achieved by evaporation of solvent under reduced pressure and dilution of the crude product in EA (60 mL). The organic layer was washed with aq. HCl (3 × 10 mL, 6 M), sat. aq. $NaHCO_3$ (1 × 10 mL) and brine (1 × 10 mL) and dried over anhydrous Na_2SO_4. The product was obtained as a colorless oil with a distinct strong odor (551 mg, 3.09 mmol, 56% - in respect to thiol).

$C_7H_{14}OS_2$ (178.05 g/mol)

R_f: 0.08 (Hex) [$KMnO_4$].

^{1}H NMR (400 MHz, $CDCl_3$): δ = 2.89 (q, *J* = 7.4 Hz, 2H), 2.81 (s, 4H), 2.55 (q, *J* = 7.4 Hz, 2H), 1.25 (t, *J* = 7.4 Hz, 6H).

^{13}C NMR (101 MHz, $CDCl_3$): δ = 198.0 (*C*(O)SEt), 44.3, 26.9, 26.2, 23.5, 14.81, 14.76.

GC-MS (EI): t_r = 5.43 min, m/z(%) = 178 (17, [$M^{+\bullet}$]), 149 (15, [$M^{+\bullet}$-$C_2H_5^{\bullet}$]), 117 (20, [$M^{+\bullet}$-$SC_2H_5^{\bullet}$]), 89 (71, [$M^{+\bullet}$-$SC_2H_5^{\bullet}$-CO]), 75 (100, [$M^{+\bullet}$-$SC_2H_5^{\bullet}$-CO-CH_2]).

HR-MS (ESI): m/z calc. for $[M+Na]^+$ 201.03783, found 201.03810.

IR (ATR, $\tilde{\nu}$ [cm^{-1}]): 2965 (w, C-H_{aliph}), 2924 (w, C-H_{aliph}), 2872 (w, C-H_{aliph}), 1683 (vs, C=O), 1448 (m), 1415 (m), 1374 (w), 1329 (w), 1262 (m), 1225 (w), 1164 (w), 1037 (s), 957 (s), 870 (w), 759 (w), 699 (m).

S-ethyl 2-(4-methoxyphenyl)ethanethioate (**119d**)

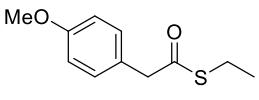

119d

According to GP-A, **119d** was synthesized using *para*-methoxy phenyl acetic acid (1.69 g, 10.0 mmol, 1.0 equiv.), ethanethiol (2.2 mL, 30 mmol, 3 equiv.), DMAP (122 mg, 1.00 mmol, 0.1 equiv.) and DCC (2.27 g, 11.0 mmol, 1.1 equiv.). Purification was achieved by filtration through a short silica plug using Hex/EA (9:1), washing the filtrate with aq. HCl (2 × 20 mL, 6 M), sat. $NaHCO_3$ (1 × 20 mL) and brine

(1 × 20 mL) as well as drying over anhydrous $MgSO_4$. The product was obtained as a pale-yellow oil (1.71 g, 8.13 mmol, 81%).

$C_{11}H_{14}O_2S$ (210.29 g/mol)

R_f: 0.51 (Hex/Et_2O = 9:1) [$KMnO_4$, UV].

^{1}H NMR (400 MHz, $CDCl_3$): δ = 7.25–7.11 (m, 2H, $C_{Ar}H$), 6.94–6.79 (m, 2H, $C_{Ar}H$), 3.80 (s, 3H, OCH_3), 3.74 (s, 2H, $PhCH_2$), 2.85 (q, *J* = 7.4 Hz, 2H, $C(O)SCH_2CH_3$), 1.22 (t, *J* = 7.4 Hz, 3H, $C(O)SCH_2CH_3$).

^{13}C NMR (101 MHz, $CDCl_3$): δ = 198.2 (*C*(O)), 159.0 (C_{Ar}), 130.8 (C_{Ar}), 125.9 (C_{Ar}), 114.1 (C_{Ar}), 55.3 (OCH_3), 49.8 ($ArCH_2$), 23.7 ($C(O)SCH_2CH_3$), 14.7 ($C(O)SCH_2CH_3$).

GC-MS (EI): t_r = 5.53 min, m/z(%) = 210 (1, [$M^{+\bullet}$]), 121 (100, [$M^{+\bullet}$-$C_3H_5OS^{\bullet}$]).

HR-MS (ESI): m/z calc. for $[M+Na]^+$ 233.06067, found 233.06103.

IR (ATR, $\tilde{\nu}$ [cm^{-1}]): 3062 (w, C-H_{arom}), 3032 (w, C-H_{arom}), 2962 (w, C-H_{aliph}), 2928 (w, C-H_{aliph}), 2834 (w, C-H_{aliph}), 1679 (s, C=O), 1608 (m), 1582 (w), 1508 (s), 1453 (m), 1418 (w), 1377 (w), 1299 (w), 1243 (vs, C-O), 1176 (s), 1109 (w), 1027 (s), 923 (w), 818 (m), 774 (s), 721 (w), 691 (m).

S-ethyl 3,3,3-triphenylpropanethioate (**119f**)

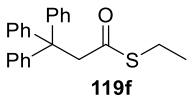

119f

According to GP-A, **119f** was synthesized using 3,3,3-triphenyl propionic acid (3.02 g, 10 mmol, 1.0 equiv.), ethanethiol (2.2 mL, 30.0 mmol, 3 equiv.), DMAP (122.2 mg, 1 mmol, 0.1 equiv.) and DCC (2.27 g, 11 mmol, 1.1 equiv.). Purification was achieved by fritting through a small silica plug using Hexane/EA (9:1). The product was recrystallized as white crystalline solid (Hex/THF =9:1) (924.1 mg, 2.67 mmol, 27%). The analytical data is in good accordance to reported literature values.[4d]

$C_{23}H_{22}OS$ (346.49 g/mol)

R_f: 0.27 (PE/EA = 98:2) [UV].

^{1}H NMR (400 MHz, $CDCl_3$): δ = 7.35–7.27 (m, 7H, $C_{Ar}H$), 7.27–7.20 (m, 8H, $C_{Ar}H$), 4.02 (s, 2H, Ph_3CCH_2), 2.71 (q, *J* = 7.6 Hz, 2H, $C(O)SCH_2CH_3$), 1.07 (t, *J* = 7.6 Hz, 3H, $C(O)SCH_2CH_3$).

^{13}C NMR (101 MHz, $CDCl_3$): δ = 196.8 (*C*(O)), 146.5 (C_{Ar}), 129.4 (C_{Ar}), 128.0 (C_{Ar}), 126.4 (C_{Ar}), 55.0 (Ph_3CCH_2), 23.7 ($C(O)SCH_2CH_3$), 14.8 ($C(O)SCH_2CH_3$).

GC-MS (EI): t_r = 11.97 min, m/z(%) = 243 (100, [$Ph_3C^{+\bullet}$]), 165 (157, [$Ph_3C^{+\bullet}$-C_6H_6]).

IR (ATR, $\tilde{\nu}$ [cm^{-1}]): 3058 (w, C-H$_{arom}$), 3021 (w, C-H$_{arom}$), 2928 (w, C-H$_{aliph}$), 2854 (w, C-H$_{aliph}$), 1694 (m, C=O), 1664 (w), 1593 (w), 1519 (w), 1489 (m), 1441 (m), 1404 (w), 1377 (w), 1333 (w), 1258 (w), 1220 (w), 1187 (w), 1161 (w), 1113 (w), 1083 (w), 1027 (m), 953 (m), 818 (w), 781 (w), 777 (w), 751 (m), 695 (s).

S-ethyl 2-propylpentanethioate (**119g**)

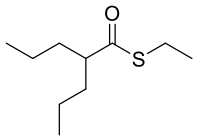

119g

According to GP-A, **119g** was synthesized using valproic acid (1.60 mL, 10.0 mmol, 1.0 equiv.), ethanethiol (2.2 mL, 30 mmol, 3 equiv.), DMAP (122 mg, 1.00 mmol, 0.1 equiv.) and DCC (2.27 g, 11.0 mmol, 1.1 equiv.). Purification was achieved by filtration through a short silica plug (Hex/EA = 9:1) and washing the solution with aq. HCl (2 × 20 mL, 6 M), aq. KOH (1 × 20 mL, 10% w/v), sat. $NaHCO_3$ (1 × 20 mL) and brine (1 × 20 mL). The organic layer was dried over anhydrous $MgSO_4$ and the solvent evaporated under reduced pressure to yield the target compound as a colorless oil (1.59 g, 8.44 mmol, 84%).

$C_{10}H_{20}OS$ (188.33 g/mol)

R_f: 0.65 (PE/EA = 97:3) [UV, anis - yellow].

^{1}H NMR (400 MHz, $CDCl_3$): δ = 2.84 (qd, *J* = 7.4, 2.2 Hz, 2H), 2.60–2.44 (m, 1H), 1.72–1.54 (m, 2H), 1.45–1.09 (m, 9H), 0.91–0.82 (m, 6H).

^{13}C NMR (101 MHz, $CDCl_3$): δ = 203.9 (*C*(O)SEt), 54.2, 35.3, 23.2, 20.6, 15.0, 14.2.

GC-MS (EI): t_r = 4.79 min, m/z(%) = 127 (9, [$M^{+\bullet}$-$C_2H_5S^{\bullet}$]), 99 (5, [$M^{+\bullet}$-$C_2H_5S^{\bullet}$-CO]), 57 (100).

HR-MS (APCI): m/z calc. for $[M+H]^+$ 189.13076, found 189.13114.

IR (ATR, $\tilde{\nu}$ [cm^{-1}]): 2958 (m, C-H$_{aliph}$), 2928 (m, C-H$_{aliph}$), 2869 (m, C-H$_{aliph}$), 1683 (vs, C=O), 1456 (m), 1377 (w), 1265 (w), 1232 (w), 1151 (w), 1116 (w), 1053 (w), 997 (s), 941 (m), 900 (m), 870 (w), 766 (m), 710 (w), 688 (w).

S-ethyl 2-methylpentanethioate (**119i**)

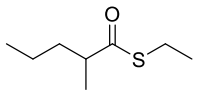

119i

According to GP-A, **119i** was synthesized using 2-methylvaleric acid (1.25 mL, 10.0 mmol, 1.0 equiv.), ethanethiol (2.2 mL, 30 mmol, 3.0 equiv.), DMAP (122 mg, 1.00 mmol, 0.1 equiv.) and DCC (2.27 g, 11.0 mmol, 1.1 equiv.). Purification was achieved by filtration through a short silica plug (Hex/EA = 30:1) and washing the gained diluted solution with aq. HCl (3 × 20 mL, 6 M), sat. aq. $NaHCO_3$ (2 × 20 mL) and brine (1 × 20 mL). The organic layer was dried over anhydrous $MgSO_4$ and solvent evaporated under reduced pressure. The product was obtained as a colorless oil (1.22 g, 7.61 mmol, 76%).

$C_8H_{16}OS$ (160.28 g/mol)

R_f: 0.57 (PE/EA = 97:3) [$KMnO_4$].

^{1}H NMR (400 MHz, $CDCl_3$): 2.85 (q, *J* = 7.3 Hz, 2H, C(O)SC*H*$_2$CH$_3$), 2.69–2.55 (m, 1H), 1.76–1.60 (m, 1H), 1.45–1.17 (m, 6H), 1.15 (d, *J* = 6.9 Hz, 3H, CHC*H*$_3$), 0.90 (t, *J* = 7.3 Hz, 3H).

^{13}C NMR (101 MHz, $CDCl_3$): 204.2 (*C*(O)SEt), 48.5, 36.4, 23.1, 20.5, 17.8, 15.0, 14.2.

HR-MS (APCI): m/z calc. for $[M+H]^+$ 161.09946, found 161.09972.

GC-MS (EI): t_r = 3.53 min, m/z(%) = 131 (12, $[M^{+\bullet}]$), 99 (32, $[M^{+\bullet}\text{-}C_2H_5S^{\bullet}]$), 71, (100, $[M^{+\bullet}\text{-}C_2H_5S^{\bullet}\text{-}CO]$).

IR (ATR, $\tilde{\nu}$ [cm^{-1}]): 2962 (m, C-H_{aliph}), 2928 (m, C-H_{aliph}), 2872 (w, C-H_{aliph}), 1684 (vs, C=O), 1455 (m), 1418 (w), 1377 (w), 1344 (w), 1265 (w), 1232 (w), 1161 (w), 1103 (w), 1098 (w), 1031 (w), 997 (w), 960 (vs), 908 (m), 870 (w), 755 (w), 695 (w).

S-ethyl 2-phenylbutanethioate (**119j**)

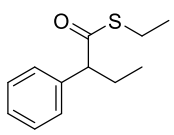

119j

According to GP-A, **119j** was synthesized using 2-phenylbutyric acid (1.64 g, 10.0 mmol, 1.0 equiv.), ethanethiol (2.2 mL, 30 mmol, 3.0 equiv.), DMAP (122 mg, 1.00 mmol, 0.1 equiv.) and DCC (2.27 g, 11.0 mmol, 1.1 equiv.). Purification was achieved by filtration through a short silica plug using a solvent mixture (Hex/EA = 30:1). The product was obtained as a colorless oil (1.93 g, 9.26 mmol, 93%).

$C_{12}H_{16}OS$ (208.32 g/mol)

R_f: 0.27 (Hex/Et_2O = 30:1) [$KMnO_4$].

^{1}H NMR (400 MHz, $CDCl_3$): δ = 7.32–7.17 (m, 5H, $C_{Ar}H$), 3.58 (t, *J* = 7.6 Hz, 1H), 2.88–2.69 (m, 2H), 2.12 (dt, *J* = 13.5, 7.3 Hz, 1H), 1.79 (dt, *J* = 13.6, 7.4 Hz, 1H), 1.15 (t, *J* = 7.4 Hz, 3H), 0.84 (t, *J* = 7.4 Hz, 3H).

^{13}C NMR (101 MHz, $CDCl_3$): 200.7 (*C*(O)SEt), 138.7 (C_{Ar}), 128.7 (C_{Ar}), 128.3 (C_{Ar}), 127.5(C_{Ar}), 62.3, 26.7, 23.1, 14.7, 12.2.

GC-MS (EI): t_r = 6.54 min, m/z(%) = 208 (2, [$M^{+\bullet}$]), 147 (7, [$M^{+\bullet}$-$C_2H_5S^{\bullet}$]), 119, (37, [$M^{+\bullet}$-$C_2H_5S^{\bullet}$-CO]), 91 (100, [$Bn^{+\bullet}$]).

HR-MS (ESI): m/z calc. for $[M+Na]^+$ 231.08141, found 231.08181.

IR (ATR, $\tilde{\nu}$ [cm^{-1}]): 3062 (w, C-H_{arom}), 3028 (w, C-H_{arom}), 2965 (w, C-H_{aliph}), 2928 (w, C-H_{aliph}), 2872 (w, C-H_{aliph}), 2116 (w), 1682 (s, C=O), 1597 (w), 1493 (w), 1452 (m), 1415 (w), 1377 (w), 1340 (w), 1299 (w), 1261 (w), 1113 (w), 977 (s), 909 (w), 840 (w), 814 (m), 736 (m), 699 (s).

S-ethyl *trans*-4-*iso*-propylcyclohexane-1-carbothioate (**119k**)

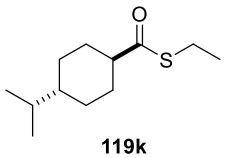

119k

According to GP-A, **119k** was synthesized using *trans*-4-*iso*-propylcyclohexane carboxylic acid (1.70 g, 10.0 mmol, 1.0 equiv.), ethanethiol (2.2 mL, 30 mmol, 3.0 equiv.), DMAP (122 mg, 1.00 mmol, 0.1 equiv.) and DCC (2.27 g, 11.0 mmol, 1.1 equiv.). Purification was achieved by filtration through a short silica plug (Hex/EA = 8:2) and washing the filtrate with aq. HCl (2 × 100 mL, 6 M), sat. $NaHCO_3$ (1 × 100 mL) and brine (1 × 100 mL). The organic layer was dried over anhydrous $MgSO_4$ and solvent evaporated under reduced pressure. The product was obtained as a colorless oil (1.47 g, 6.86 mmol, 69%).

$C_{12}H_{22}OS$ (214.37 g/mol)

R_f: 0.44 (Hex/EA = 98:2) [anis - blue, UV].

^{1}H NMR (400 MHz, $CDCl_3$): δ = 2.85 (q, *J* = 7.4 Hz, 2H, S$CH_2$$CH_3$), 2.40 (tt, *J* = 12.2, 3.5 Hz, 1H, C*H*C(O)SEt), 2.04–1.93 (m, 2H), 1.83–1.75 (m, 2H), 1.53–1.35 (m, 3H), 1.24 (t, *J* = 7.4 Hz, 3H, S$CH_2$$CH_3$), 1.13–0.93 (m, 3H), 0.86 (d, *J* = 6.8 Hz, 6H, CH_3CHCH_3).

^{13}C NMR (101 MHz, $CDCl_3$): δ = 203.3 (*C*(O)SEt), 53.1, 43.3, 32.8, 29.8, 29.0, 22.9, 19.8, 14.9.

GC-MS (EI): t_r = 6. 86 min, m/z(%) = 153 (15, [$M^{+\bullet}$-$C_2H_5S^{\bullet}$-CO]), 81 (100).

HR-MS (ESI): m/z calc. for $[M+Na]^+$ 237.12836, found 237.12858.

IR (ATR, $\tilde{\nu}$ [cm^{-1}]): 2928 (s, C-H_{aliph}), 2860 (m, C-H_{aliph}), 1683 (s, C=O), 1448 (m), 1415 (w), 1370 (w), 1311 (w), 1265 (w), 1232 (w), 1163 (w), 1146 (w), 1112 (w), 1053 (m), 980 (s), 934 (m), 897 (w), 878 (w), 874 (w), 837 (w), 807 (s), 759 (w), 706 (w).

S-ethyl 1-tosylpiperidine-4-carbothioate (**119l**)

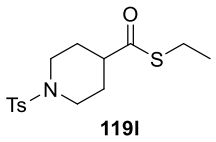

119l

According to GP-A, **119l** was synthesized using 1-tosylpiperidine-4-carboxylic acid (2.83 g, 10.0 mmol, 1.0 equiv.), ethanethiol (2.2 mL, 30 mmol, 3.0 equiv.), DMAP (122 mg, 1.00 mmol, 0.1 equiv.) and DCC (2.27 g, 11.0 mmol, 1.1 equiv.). Purification was achieved by filtration through a short silica plug (Hex/EA = 9:1). The product was recrystallized from pure Et_2O to yield colorless crystals (2.31 g, 7.05 mmol, 71%). The data is in accordance with reported literature.[16]

$C_{15}H_{21}NO_3S_2$ (327.46 g/mol)

R_f: 0.14 (Hex/EA = 9:1) [$KMnO_4$, UV].

^{1}H NMR (400 MHz, $CDCl_3$): δ = 7.64–7.62 (m, 2H, $C_{Ar}H$), 7.40–7.27 (m, 2H, $C_{Ar}H$), 3.82–3.65 (m, 2H), 2.84 (q, *J* = 7.4 Hz, 2H), 2.43–2.33 (m, 6H), 1.99–1.77 (m, 4H), 1.21 (t, *J* = 7.4 Hz, 3H).

^{13}C NMR (101 MHz, $CDCl_3$): δ = 201.1 (*C*(O)SEt), 143.8 (C_{Ar}), 133.1 (C_{Ar}), 129.8 (C_{Ar}), 127.8 (C_{Ar}), 49.2, 45.6, 28.1, 23.2, 21.7, 14.8.

IR (ATR, $\tilde{\nu}$ [cm^{-1}]): 2937 (w, C-H_{aliph}), 2831 (w, C-H_{aliph}), 1683 (m, C=O), 1594 (w), 1493 (w), 1448 (w), 1377 (w), 1346 (w), 1329 (w), 1299 (w), 1254 (w), 1221 (w), 1155 (m), 1120 (w), 1094 (w), 1064 (w), 984 (w), 975 (w), 922 (m), 828 (w), 803 (m), 721 (m).

S-ethyl *trans*-2-methylcyclopropane-1-carbothioate (**119m**)

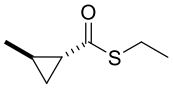

119m

According to GP-A, **119m** was synthesized using 2-methylcyclopropane-1-carboxylic acid (0.97 mL, 10.0 mmol, 1.0 equiv.), ethanethiol (2.2 mL, 30 mmol, 3.0 equiv.), DMAP (122 mg, 1.00 mmol, 0.1 equiv.) and DCC (2.27 g, 11.0 mmol, 1.1 equiv.). Purification was achieved by dry column vacuum chromatography (Hex). The product was obtained as a colorless oil (751.4 mg, 5.21 mmol, 52%). The analytical data is in good accordance to previously published literature.[17]

$C_7H_{12}OS$ (144.23 g/mol)

trans/cis= 10:1

R_f: 0.26 (Hex) [UV, anis - yellow].

^{1}H NMR (400 MHz, $CDCl_3$, mixture): 2.86 (q, *J* = 7.4 Hz, 2H, SC*H*$_2$), 1.71 (dt, *J* = 8.3, 4.3 Hz, 1H), 1.57–1.45 (m, 1H), 1.43–1.26 (m, 1H), 1.23 (t, *J* = 7.4 Hz, 3H, SCH_2CH_3), 1.10 (d, *J* = 6.1 Hz, 3H, $CHCH_3$), 0.77–0.73 (m, 1H).

^{13}C NMR (101 MHz, $CDCl_3$, mixture): 198.8 (*C*(O)SEt), 31.4, 23.4, 19.8, 19.2, 18.1, 15.0.

HR-MS (EI): m/z calc. for $[M]^+$ 144.060337, found 144.05855.

GC-MS (EI, method B): t_r = 11.03 min, m/z(%) = 144 (10, $[M^{+\bullet}]$), 83 (100, $[M^{+\bullet}\text{-}C_2H_5S^{\bullet}]$).

IR (ATR, $\tilde{\nu}$ [cm^{-1}]): 2961 (w, C-H_{aliph}), 2928 (w, C-H_{aliph}), 2872 (w, C-H_{aliph}), 1675 (vs, C=O), 1445 (m), 1399 (m), 1374 (m), 1314 (w), 1265 (w), 1180 (w), 1060 (s), 1027 (s), 952 (s), 903 (s), 843 (w), 777 (w), 743 (s), 662 (w).

S-ethyl (1*S**,2*S**,4*S**)-bicyclo[2.2.1]hept-5-ene-2-carbothioate (**119n**) and a mixture with diastereomer (**119n+119n'**)

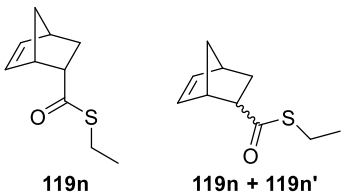

119n **119n + 119n'**

According to GP-A, both products were synthesized using bicyclo[2.2.1]hept-5-ene-2-carboxylic acid (1.38 g, 10.0 mmol, 1.0 equiv.), ethanethiol (2.2 mL, 30 mmol, 3.0 equiv.), DMAP (122 mg, 1.00 mmol, 0.1 equiv.) and DCC (2.27 g, 11.0 mmol, 1.1 equiv.). Purification was achieved by flash column chromatography (23 g SiO_2, isocratic Hex/EA = 98:2, 15 CV). The separation yielded pure *endo*-product

(**119n**) as well as a mixture of *endo*- and *exo*-product (**119n**+**119n'**). The products were obtained as a colorless oil (sum of products: 837.1 mg, 4.59 mmol, 46%).

$C_{10}H_{14}OS$ (182.28 g/mol)

R_f: 0.20 (PE/EA = 98:2) [$KMnO_4$, anis, UV].

119n: ^{1}H NMR (400 MHz, $CDCl_3$): 6.20 (dd, *J* = 5.7, 3.1 Hz, 1H, $C_{alkene}H$), 5.93 (dd, *J* = 5.7, 2.8 Hz, 1H, $C_{alkene}H$), 3.27 (tq, *J* = 3.1, 1.5 Hz, 1H), 3.18 (dt, *J* = 9.0, 3.9 Hz, 1H), 2.95–2.74 (m, 3H), 1.86 (ddd, *J* = 11.8, 9.1, 3.7 Hz, 1H), 1.59–1.39 (m, 2H), 1.35–1.17 (m, 4H).

119n: ^{13}C NMR (101 MHz, $CDCl_3$): 201.0 (*C*(O)SEt), 137.9 (C_{alkene}), 132.0 (C_{alkene}), 53.0, 49.7, 47.3, 42.9, 29.5, 23.3, 15.0.

d.r. (**119n** + **119n'**) = 5 (*endo*) : 3 (*exo*)

1m + 1m': ^{1}H NMR (400 MHz, $CDCl_3$): 6.23–6.07 (m, $C_{alkene}H$), 5.92 (dd, *J* = 5.7, 2.8 Hz, $C_{alkene}H$), 3.26 (tq, *J* = 3.3, 1.6 Hz), 3.17 (dt, *J* = 9.0, 3.9 Hz), 3.04 (ddt, *J* = 3.3, 2.3, 1.2 Hz), 2.96–2.75 (m), 2.45 (ddd, *J* = 8.2, 4.5, 1.9 Hz), 1.98–1.80 (m), 1.62–1.17 (m).

119n + 119n': ^{13}C NMR (101 MHz, $CDCl_3$): 202.6 (*C*(O)SEt), 201.0 (*C*(O)SEt), 138.6 (C_{alkene}), 137.9 (C_{alkene}), 135.8 (C_{alkene}), 132.0 (C_{alkene}), 53.0, 52.6, 49.6, 47.9, 47.3, 46.4, 42.9, 41.9, 30.8, 29.4, 23.5, 23.3, 15.00, 14.98.

HR-MS (ESI): m/z calc. for $[M+Na]^+$ 205.06576, found 205.06614.

GC-MS (EI): t_r = 5.48 min, m/z(%) = 182 (12, $[M^{+\bullet}-SC_2H_5^{\bullet}]$), 121 (37, $[M^{+\bullet}-SC_2H_5^{\bullet}]$), 55 (100).

IR (**119n**, ATR, $\tilde{\nu}$ [cm^{-1}]): 3062 (w, C-H_{arom}), 2969 (m, C-H_{aliph}), 2935 (w, C-H_{aliph}), 2869 (w, C-H_{aliph}), 1683 (s, C=O), 1448 (w), 1415 (w), 1374 (w), 1333 (w), 1262 (m), 1224 (w), 1176 (w), 1131 (w), 1126 (w), 1065 (s), 1030 (m), 1000 (s), 966 (w), 920 (m), 844 (s), 807 (m), 777 (m), 747 (m), 706 (vs).

<u>*S*-ethyl 4-oxopentanethioate (**119p**)</u>

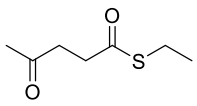

119p

According to GP-A, **119p** was synthesized using levulinic acid (2.1 mL, 20 mmol, 1 equiv.), ethanethiol (5.9 mL, 80 mmol, 4.0 equiv.), DMAP (244 mg, 2.00 mmol, 0.1 equiv.) and DCC (4.54 g, 22.0 mmol, 1.1 equiv.). Purification was achieved by manual column chromatography (Hex/Et_2O = 7:3). The product was obtained as a colorless oil with a sweet smell (1.23 g, 7.68 mmol, 38%).

$C_7H_{12}O_2S$ (160.23 g/mol)

R_f: 0.26 (Hex/Et_2O = 7:3) [$KMnO_4$].

^{1}H NMR (400 MHz, $CDCl_3$): δ = 2.73–2.63 (m, 6H), 2.02 (s, 3H, C(O)CH_3), 1.07 (t, *J* = 7.4 Hz, 3H, C(O)SCH_2CH_3).

^{13}C NMR (101 MHz, $CDCl_3$): δ = 205.8 (*C*(O)$_{ketone}$), 198.0 (*C*(O)$_{thioester}$), 37.7 37.2, 29.5, 23.0, 14.5.

GC-MS (EI): t_r = 4.67 min, m/z(%) = 99 (100, [$M^{+\bullet}$-$C_2H_5S^{\bullet}$]).

HR-MS (ESI): m/z calc. for $[M+Na]^+$ 183.04502, found 183.04536.

IR (ATR, $\tilde{\nu}$ [cm^{-1}]): 2969 (w, C-H$_{aliph}$), 2928 (w, C-H$_{aliph}$), 2876 (w, C-H$_{aliph}$), 1716 (s, C=O$_{ketone}$), 1682 (vs, C=O$_{thioester}$), 1448 (w), 1407 (m), 1361 (m), 1292 (w), 1262 (w), 1224 (w), 1191 (w), 1161 (m), 1071 (m), 989 (s), 953 (s), 855 (w), 740 (w), 703 (w).

S-ethyl 2-cyanoethanethioate (**119t**)

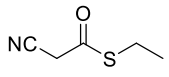

119t

According to GP-A, the product **119t** was synthesized using cyanoacetic acid (1.28 g, 15 mmol, 1.0 equiv.), ethanethiol (3.3 mL, 45 mmol, 3.0 equiv.), DMAP (183 mg, 1.5 mmol, 0.1 equiv.) and DCC (3.40 g, 16.5 mmol, 1.1 equiv.). Purification was achieved by manual column chromatography (Hex/Et2O = 7:3) The product was obtained as a colorless oil (742 mg, 5.74 mmol, 38%).

C_5H_7NOS (129.18 g/mol)

R_f: 0.44 (Hex/Et_2O = 7:3) [$KMnO_4$].

^{1}H NMR (400 MHz, $CDCl_3$): δ = 3.60 (s, 2H, NCCH_2C(O)SEt), 2.98 (q, *J* = 7.4 Hz, 2H, C(O)S$CH_2$$CH_3$), 1.29 (t, *J* = 7.4 Hz, 3H, C(O)SCH_2CH_3).

^{13}C NMR (101 MHz, $CDCl_3$): δ = 187.4 (*C*(O)SEt), 113.0 (N*C*CH_2C(O)SEt), 32.5, 24.6, 14.4.

GC-MS (EI): t_r = 3.82 min, m/z = 129 (41, [$M^{+\bullet}$]), 101(9), 89 (55, [$M^{+\bullet}$-$C_2H_sN^{\bullet}$]), 68 (100, [$M^{+\bullet}$-$C_2H_5S^{\bullet}$]), 62, 61 (32, [$C_2H_5S^{+\bullet}$]).

HR-MS (ESI): m/z calc. for $[M+Na]^+$ 152.01406, found 152.01417.

IR (ATR, $\tilde{\nu}$ [cm^{-1}]): 2968 (w, C-H$_{aliph}$), 2927 (w, C-H$_{aliph}$), 2879 (w, C-H$_{aliph}$), 2259 (w, C≡N), 1746 (w), 1682 (vs, C=O), 1452 (w), 1385 (m), 1306 (w), 1266 (m), 1195 (w), 1083 (m), 1015 (s), 971 (m), 907 (s), 788 (m), 758 (w), 673 (w).

S,*S*-diethyl 2-methylpentanebis(thioate) (**122**)

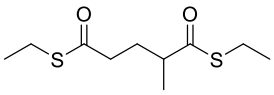

122

According to GP-A, **122** was synthesized using 2-methyl glutaric acid (1.46 g, 10.0 mmol, 1.0 equiv.), ethanethiol (3.6 mL, 50.0 mmol, 5.0 equiv.), DMAP (244 mg, 2 mmol, 0.1 equiv.) and DCC (4.54 g, 22 mmol, 2.2 equiv.). Purification achieved by filtration through a silica plug (PE/EA = 9:1). The combined organic layers were extracted solution with aq. HCl (2 × 30 mL, 6 M), aq. KOH (2 × 30 mL, 10% w/v), sat. $NaHCO_3$ (1 × 20 mL) and brine (1 × 20 mL). The organic layer was dried over anhydrous $MgSO_4$ and solvent evaporated under reduced pressure. The product was yielded as a colorless oil (2.00 g, 8.56 mmol, 86%). The analytical data is in good accordance to literature examples.[18]

$C_{10}H_{18}O_2S_2$ (234.37 g/mol)

R_f: 0.67 (Hex/EA = 9:1) [$KMnO_4$, anis - yellow, UV].

^{1}H NMR (400 MHz, $CDCl_3$): δ = 2.83 (*pseudo*-qd, *J* = 7.4, 0.7 Hz, 4H), 2.70–2.46 (m, 3H), 2.06–1.91 (m, 1H), 1.83–1.71 (m, 1H), 1.25–1.10 (m, 9H).

^{13}C NMR (101 MHz, $CDCl_3$): δ = 203.0 (*C*(O)SEt), 198.8 (*C*(O)SEt), 47.5, 41.4, 29.3, 23.4, 23.2, 17.8, 14.8.

HR-MS (ESI): m/z calc. for $[M+Na]^+$ 257.06404, found 257.06442.

GC-MS (EI, method B): t_r = 19.14 min, m/z(%) = 173 (100, $[M^{+\bullet}- C_2H_5S^\bullet]$), 145 (39, $[M^{+\bullet}-C_2H_5S^\bullet-CO]$), 89 (56, $[C_3H_5OS^\bullet]$).

IR (ATR, $\tilde{\nu}$ [cm^{-1}]): 2969 (w, C-H_{aliph}), 2931 (w, C-H_{aliph}), 2872 (w, C-H_{aliph}), 1679 (vs, C=O), 1452 (m), 1414 (w), 1374 (w), 1314 (w), 1262 (w), 1191 (w), 1127 (w), 1049 (m), 1020 (m), 957 (vs), 892 (m), 814 (w), 741 (m), 691 (w).

S,*S*-diethyl 2-phenylbutanebis(thioate) (**125**)

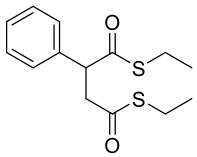

125

According to GP-A, **125** was synthesized using phenylsuccinic acid (1.94 g, 10.0 mmol, 1.0 equiv.), ethanethiol (3.6 mL, 50 mmol, 5.0 equiv.), DMAP (244 mg, 2 mmol, 0.2 equiv.) and DCC (4.54 g, 22.0 mmol, 2.2 equiv.). Purification was achieved by fritting through a small silica plug (Hex/EA = 90:1) and washing the solution with aq. HCl (2 × 20 mL, 6 M), demin. water (1 × 20 mL), aq. KOH (2 × 20 mL, 10% w/v) and brine (1 × 20 mL). The organic layer was dried over anhydrous $MgSO_4$ and solvent evaporated under reduced pressure. Further purification was achieved by evaporation of residual impurities by Kugelrohr distillation (120 °C, 50 mBar) to yield a colorless oil. (1.80 g, 6.37 mmol, 64%).

$C_{14}H_{18}O_2S_2$ (282.42 g/mol)

R_f: 0.38 (Hex/EA = 97:3) [UV].

^{1}H NMR (400 MHz, $CDCl_3$): δ = 7.29–7.15 (m, 5H, $C_{Ar}H$), 4.25 (dd, *J* = 8.5, 6.1 Hz, 1H), 3.40 (dd, *J* = 16.3, 8.5 Hz, 1H), 2.87 (dd, *J* = 16.3, 6.1 Hz, 1H), 2.82–2.67 (m, 4H), 1.15–1.03 (m, 6H).

^{13}C NMR (101 MHz, $CDCl_3$): δ = 199.0 (*C*(O)SEt), 196.9 (*C*(O)SEt), 137.2 (C_{Ar}), 128.9 (C_{Ar}), 128.2 (C_{Ar}), 127.9 (C_{Ar}), 55.5, 46.7, 23.8, 23.5, 14.7, 14.4.

HR-MS (ESI): m/z calc. for $[M+Na]^+$ 305.06404, found 305.06447.

GC-MS (EI): t_r = 9.341 min, m/z(%) = 221 (23, $[M^{+\bullet}-SC_2H_5]$), 151 (28), 104 (100).

IR (ATR, $\tilde{\nu}$ [cm^{-1}]): 3062 (w, C-H_{arom}), 3028 (w, C-H_{arom}), 2968 (w, C-H_{aliph}), 2928 (w, C-H_{aliph}), 2872 (w, C-H_{aliph}), 1676 (vs, C=O), 1597 (w), 1493 (w), 1448 (m), 1406 (w), 1377 (w), 1338 (w), 1333 (w), 1307 (w), 1258 (m), 1232 (w), 1195 (w), 1082 (w), 1050 (m), 990 (s), 973 (s), 933 (s), 866 (w), 717 (s), 699 (s).

S-phenyl 2-propylpentanethioate (**127**)

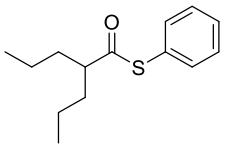

127

According to GP-A, **127** was synthesized using valproic acid (1.44 g, 10.0 mmol, 1.0 equiv.), thiophenol (3.1 mL, 30 mmol, 3.0 equiv.), DMAP (122 mg, 1.0 mmol, 0.1 equiv.) and DIC (1.7 mL, 11.0 mmol, 1.1 equiv.) in DCM (20 mL). Purification was achieved by washing the solution with aq. HCl (2 × 20 mL, 6 M), aq. KOH (2 × 20 mL, 10% w/v), sat. $NaHCO_3$ (1 × 20 mL) and brine (1 × 20 mL). The organic layer was dried with anhydrous $MgSO_4$ and solvent evaporated under reduced pressure to yield the product as colorless oil (626 mg, 265 mmol, 27%).

$C_{14}H_{20}OS$ (236.37 g/mol)

R_f: 0.65 (Hex) [UV].

^{1}H NMR (400 MHz, $CDCl_3$): δ = 7.45–7.36 (m, 5H, $C_{Ar}H$), 2.75–2.64 (m, 1H), 1.80–1.63 (m, 2H), 1.55-1.32 (m, 6H), 0.94 (t, *J* = 7.2 Hz, 6H).

^{13}C NMR (101 MHz, $CDCl_3$): δ = 201.6 (*C*(O)SEt), 134.5 (C_{Ar}), 129.3 (C_{Ar}), 129.2 (C_{Ar}), 128.2 (C_{Ar}), 54.1, 35.3, 20.7, 14.3.

HR-MS (ESI): m/z calc. for $[M+Na]^+$ 259.11271, found 259.11310.

GC-MS (EI, method B): t_r = 19.88 min, m/z = 127 (73, $[M^{+\bullet}\text{-}SC_6H_5^{\bullet}]$), 109 (27, $[C_6H_5S^{+\bullet}\text{-}CO]$), 99 (25, $[M^{+\bullet}\text{-}SC_6H_5^{\bullet}\text{-}CO]$).

IR (ATR, $\tilde{\nu}$ [cm^{-1}]): 3062 (w, C-H_{arom}), 2957 (m, C-H_{aliph}), 2928 (m, C-H_{aliph}), 2868 (w, C-H_{aliph}), 1701 (s, C=O), 1582 (w), 1463 (m), 1444 (m), 1377 (w), 1338 (w), 1232 (w), 1146 (w), 1113 (w), 1064 (w), 989 (s), 937 (m), 889 (s), 740 (s), 687 (s).

S-ethyl benzothioate (**129a**)

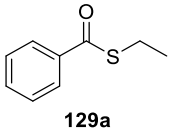

129a

According to GP-B, **129a** was synthesized using benzoyl chloride (2.2 mL, 20 mmol), ethanethiol (1.8 mL, 24 mmol, 1.2 equiv.) and TEA (2.8 mL, 20 mmol, 1 equiv.). Purification was achieved by bulb-to-bulb distillation (4 mbar, 160 °C). The product was obtained as a light yellow oil (2.90 g, 17.4 mmol, 87%). The NMR spectra are in accordance to previous literature values.[19]

$C_9H_{10}OS$ (166.24 g/mol)

R_f: 0.44 (Hex/EA = 30:1) [UV].

^{1}H NMR (400 MHz, $CDCl_3$): δ = 7.98–7.88 (m, 2H, $C_{Ar}H$), 7.59–7.49 (m, 1H, $C_{Ar}H$), 7.46–7.36 (t, *J* = 7.7 Hz, 2H, $C_{Ar}H$), 3.07 (q, *J* = 7.4 Hz, 2H, SCH_2CH_3), 1.35 (t, *J* = 7.4 Hz, 3H, SCH_2CH_3).

^{13}C NMR (101 MHz, $CDCl_3$): δ = 192.1 (*C*(O)SEt), 137.3 (C_{Ar}), 133.3 (C_{Ar}), 128.6 (C_{Ar}), 127.2 (C_{Ar}), 23.5 (SCH_2CH_3), 14.9 (SCH_2CH_3).

GC-MS (EI): t_r = 5.61 min, m/z(%) = 166 (12, [$M^{+\bullet}$]), 105 (100, [$M^{+\bullet}$-$C_2H_5S^{\bullet}$]), 77 (35, [$M^{+\bullet}$-$C_2H_5S^{\bullet}$-CO]).

HR-MS (APCI): m/z calc. for $[M+H]^+$ 167.05251, found 167.05286.

IR (ATR, $\tilde{\nu}$ [cm^{-1}]): 3059 (w, C-H_{arom}), 3032 (w, C-H_{arom}), 2969 (w, C-H_{aliph}), 2928 (w, C-H_{aliph}), 2872 (w, C-H_{aliph}), 1657 (vs, C=O), 1584 (m), 1485 (w), 1448 (m), 1414 (w), 1374 (w), 1310 (w), 1266 (w), 1239 (w), 1202 (vs), 1172 (s), 1101 (w), 1069 (w), 1027 (w), 997 (w), 971 (w), 904 (vs), 770 (s), 684 (vs).

S-ethyl 4-methylbenzothioate (**129b**)

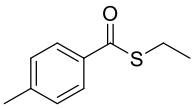

129b

According to GP-B, **129b** was synthesized using 4-methylbenzoyl chloride (1.3 mL, 10.0 mmol, 1.0 equiv.), ethanethiol (790 µL, 11.0 mmol, 1.1 equiv.) and TEA (1.4 mL, 10 mmol, 1 equiv.). The product was purified by DCVC (PE/EA = 98:2). The product was obtained as a colorless oil (1.44 g, 7.99 mmol, 80%). The analytical data is in good accordance to reported literature.[20]

$C_{10}H_{12}OS$ (180.27 g/mol)

R_f: 0.41 (PE/EA = 98:2) [$KMnO_4$, anis].

^{1}H NMR (400 MHz, $CDCl_3$): δ = 7.90–7.82 (m, 2H, $C_{Ar}H$), 7.23 (d, *J* = 8.0 Hz, 2H, $C_{Ar}H$), 3.06 (q, *J* = 7.4 Hz, 2H, CH_2CH_3), 2.40 (s, 3H, $ArCH_3$), 1.34 (t, *J* = 7.4 Hz, 3H, CH_2CH_3).

^{13}C NMR (101 MHz, $CDCl_3$): δ = 191.8 (*C*(O)SEt), 144.1 (C_{Ar}), 134.8 (C_{Ar}), 129.3 (C_{Ar}), 127.3 (C_{Ar}), 23.4, 21.8, 14.9.

GC-MS (EI, method B): t_r = 17.22 min, m/z(%) = 180 (6, [$M^{+\bullet}$]), 119 (100, [$M^{+\bullet}$-$C_2H_5S^{\bullet}$]), 91 (35, [$M^{+\bullet}$-$C_2H_5S^{\bullet}$-CO]).

IR (ATR, $\tilde{\nu}$ [cm^{-1}]): 3029 (w, C-H$_{arom}$), 2965 (w, C-H$_{aliph}$), 2924 (w, C-H$_{aliph}$), 2869 (w, C-H$_{aliph}$), 2820 (w, C-H$_{aliph}$), 1702 (w), 1654 (vs, C=O), 1604 (s), 1571 (w), 1504 (w), 1448 (m), 1410 (w), 1374 (w), 1303 (w), 1265 (w), 1243 (w), 1207 (vs), 1172 (s), 1113 (w), 1047 (w), 971 (w), 945 (w), 907 (vs), 818 (s), 785 (m), 717 (m).

S-ethyl 4-methoxybenzothioate (**129c**)

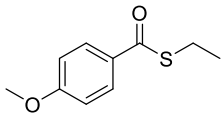

129c

According to GP-B, **129c** was synthesized using 4-methylbenzoyl chloride (1.4 mL, 10.0 mmol, 1.0 equiv.), ethanethiol (790 µL, 11.0 mmol, 1.1 equiv.) and TEA (1.4 mL, 10 mmol, 1 equiv.). The product was purified by DCVC (PE:EA = 98:2) and was obtained as a colorless oil (1.44 g, 8.00 mmol, 80%). The analytical data is in good accordance to previously published literature.[18]

$C_{10}H_{12}O_2S$ (196.26 g/mol)

R_f: 0.24 (PE/EA = 98:2) [UV, $KMnO_4$].

^{1}H NMR (300 MHz, $CDCl_3$): δ = 7.99–7.88 (m, 2H, $C_{Ar}H$), 6.97–6.85 (m, 2H, $C_{Ar}H$), 3.85 (s, 3H, O-CH_3), 3.05 (q, *J* = 7.4 Hz, 2H, CH_2CH$_3$), 1.34 (t, *J* = 7.4 Hz, 3H, CH$_2$CH_3).

^{13}C NMR (75 MHz, $CDCl_3$): δ = 190.7 (*C*(O)SEt), 163.8 (C_{Ar}), 130.3 (C_{Ar}), 129.4 (C_{Ar}), 113.8 (C_{Ar}), 55.6 (O*C*H$_3$), 23.4 (*C*H$_2$CH$_3$), 15.0 (CH$_2$*C*H$_3$).

GC-MS (EI, method B): t_r = 19.30 min, m/z(%) = 196 (7, [M$^{+\bullet}$]), 135 (100, [M$^{+\bullet}$-C$_2$H$_5$S$^\bullet$]), 107 (10, [M$^{+\bullet}$-C$_2$H$_5$S$^\bullet$-CO]).

IR (ATR, $\tilde{\nu}$ [cm^{-1}]): 2965 (w, C-H$_{aliph}$), 2928 (w, C-H$_{aliph}$), 2872 (w, C-H$_{aliph}$), 2838 (w, C-H$_{aliph}$), 1650 (s, C=O), 1597 (vs), 1504 (s), 1452 (m), 1415 (w), 1307 (m), 1255 (s), 1213 (vs, C$_{arom}$-O$_{ether}$), 1161 (vs C$_{aliph}$-O$_{ether}$), 1113 (m), 1057 (w), 1027 (s), 971 (w), 948 (w), 907 (vs), 833 (vs), 792 (m), 732 (w).

S-ethyl 4-fluorobenzothioate (**129d**)

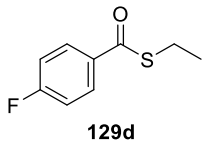

129d

According to GP-A, **129d** was synthesized using 4-fluorobenzoic acid (1.40 g, 10.0 mmol, 1.0 equiv.), ethanethiol (2.2 mL, 30 mmol, 3 equiv.), DMAP (122 mg, 1.00 mmol, 0.1 equiv.) and DCC (2.27 g, 11.0 mmol, 1.1 equiv.). Purification was achieved by filtration through a short silica plug using DCM and washing the filtrate with aq. HCl (2 × 20 mL, 6 M), sat. $NaHCO_3$ (1 × 20 mL) and brine (1 × 20 mL). The organic layer was dried with anhydrous $MgSO_4$ and solvent evaporated under reduced pressure to yield the product as a colorless oil (1.41 g, 7.65 mmol, 77%). The spectral data is in accordance to reported literature.[18]

C_9H_9FOS (184.23 g/mol)

R_f: 0.49 (Hex/EA = 30:1) [$KMnO_4$].

^{1}H NMR (600 MHz, $CDCl_3$): δ = 8.01–7.95 (m, 2H, $C_{Ar}H$), 7.15–7.08 (m, 2H, $C_{Ar}H$), 3.07 (q, *J* = 7.4 Hz, 2H), 1.35 (t, *J* = 7.4 Hz, 3H).

^{13}C NMR (151 MHz, $CDCl_3$): δ = 190.7 (*C*(O)SEt), 166.0 (d, J^1_{C-F} = 254.6 Hz, C_{Ar}F), 133.7 (d, J^4_{C-F} = 3.1 Hz, C_{Ar}C(O)SEt), 129.8 (d, J^3_{C-F} = 9.3 Hz, C_{Ar}CCF), 115.8 (d, J^2_{C-F} = 22.1 Hz, C_{Ar}CF), 23.7 (S*C*H$_2$), 14.9 (SCH$_2$*C*H$_3$).

^{19}F NMR (565 MHz, $CDCl_3$): δ = -105.1 (m).

GC-MS (EI, method B): t_r = 15.21 min, m/z(%) = 184 (9, [$M^{+\bullet}$]), 123 (100, [$M^{+\bullet}$-$C_2H_5S^{\bullet}$]), 95 (32, [$M^{+\bullet}$-$C_2H_5S^{\bullet}$-CO]).

IR (ATR, $\tilde{\nu}$ [cm^{-1}]): 2973 (w, C-H$_{aliph}$), 2935 (w, C-H$_{aliph}$), 2875 (w, C-H$_{aliph}$), 1653 (s, C=O), 1594 (s, C-F), 1541 (w), 1500 (s), 1448 (w), 1407 (w), 1295 (w), 1228 (vs), 1202 (vs), 1150 (s), 1098 (w), 1057 (w), 1008 (w), 967 (w), 945 (w), 915 (vs), 840 (vs), 811 (s), 729 (w).

S-ethyl 4-chlorobenzothioate (**129e**)

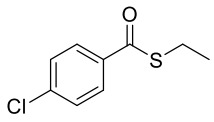

129e

According to GP-A, **129e** was synthesized using 4-chlorobenzoic acid (1.57 g, 10.0 mmol, 1.0 equiv.), ethanethiol (2.2 mL, 30 mmol, 3 equiv.), DMAP (122 mg, 1.00 mmol, 0.1 equiv.) and DIC (1.7 mL, 11 mmol, 1.1 equiv.). Purification was achieved by DCVC (Hex/EA = 30:1) and product was obtained as a colorless oil (1.18 g, 5.88 mmol, 59%).

C_9H_9ClOS (200.68 g/mol)

R_f: 0.38 (Hex/EA = 99:1) [UV].

^{1}H NMR (400 MHz, $CDCl_3$): δ = 7.91−7.88 (m, 2H, $C_{Ar}H$), 7.43−7.40 (m, 2H, $C_{Ar}H$), 3.08 (q, *J* = 7.4 Hz, 2H, CH_2CH_3), 1.35 (t, *J* = 7.4 Hz, 3H, CH_2CH_3).

^{13}C NMR (101 MHz, $CDCl_3$): δ = 191.1 (*C*(O)SEt), 139.7 (C_{Ar}), 135.7 (C_{Ar}), 129.0 (C_{Ar}), 128.6 (C_{Ar}), 23.7 (SCH_2CH_3), 14.8 (SCH_2CH_3).

GC-MS (EI): t_r = 6.66 min, m/z(%) = 202 (2, $[M^{+\bullet}]$), 200 (5, $[M^{+\bullet}]$), 141 (32, $[M^{+\bullet}\text{-}C_2H_5S^{\bullet}]$), 139 (100, $[M^{+\bullet}\text{-}C_2H_5S^{\bullet}]$), 113 (9, $[M^{+\bullet}\text{-}C_2H_5S^{\bullet}\text{-}CO]$), 111 (27, $[M^{+\bullet}\text{-}C_2H_5S^{\bullet}\text{-}CO]$).

HR-MS (EI): m/z calc. for $[M]^+$ 200.005714, found 200.00387.

IR (ATR, $\tilde{\nu}$ [cm^{-1}]): 3088 (w, C-H_{arom}), 3062 (w, C-H_{arom}), 2969 (w, C-H_{aliph}), 2928 (w, C-H_{aliph}), 2872 (w, C-H_{aliph}), 1658 (vs, C=O), 1583 (s), 1482 (m), 1448 (w), 1396 (m), 1270 (w), 1202 (vs), 1169 (s), 1090 (s), 1012 (w), 971 (w), 908 (vs), 830 (vs), 726 (m).

S-ethyl 4-bromobenzothioate (**129f**)

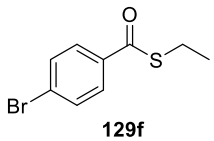

129f

According to GP-A, **129f** was synthesized using 4-bromobenzoic acid (2.01 g, 10.0 mmol, 1.0 equiv.), ethanethiol (2.2 mL, 30 mmol, 3 equiv.), DMAP (122 mg, 1.0 mmol, 0.1 equiv.) and DIC (1.7 mL, 11 mmol, 1.1 equiv.). Purification was achieved by filtration through a silica plug (Hex/EA = 99:1) and subsequent distillation of side product (4 mbar, 155 °C) yielded the product as a colorless oil (1.87 g, 7.63 mmol, 76%, 95% purity). The analytical data is in good accordance to reported literature.[10]

C_9H_9BrOS (245.13 g/mol)

R_f: 0.32 (Hex/EA = 99:1) [UV].

^{1}H NMR (400 MHz, $CDCl_3$): δ = 7.82−7.78 (m, 2H, $C_{Ar}H$), 7.57−7.54 (m, 2H, $C_{Ar}H$), 3.06 (q, *J* = 7.4 Hz, 2H, CH_2CH_3), 1.33 (t, *J* = 7.4 Hz, 3H, CH_2CH_3).

^{13}C NMR (101 MHz, $CDCl_3$): δ = 191.3 (*C*(O)SEt), 136.1 (C_{Ar}), 132.0 (C_{Ar}), 128.8 (C_{Ar}), 128.4 (C_{Ar}), 23.7 (SCH_2CH_3), 14.8 (SCH_2CH_3).

GC-MS (EI): t_r = 7.26 min, m/z(%) = 246 (6, [$M^{+\bullet}$]), 244 (6, [$M^{+\bullet}$]), 185 (100, [$M^{+\bullet}$-$SC_2H_5^{\bullet}$]), 183 (100, [$M^{+\bullet}$-$SC_2H_5^{\bullet}$]), 157 (28, [$M^{+\bullet}$-$SC_2H_5^{\bullet}$-CO]), 155 (28, [$M^{+\bullet}$-$SC_2H_5^{\bullet}$-CO]).

IR (ATR, $\tilde{\nu}$ [cm^{-1}]): 3084 (w, C-H_{arom}), 3058 (w, C-H_{arom}), 2965 (w, C-H_{aliph}), 2928 (w, C-H_{aliph}), 2868 (w, C-H_{aliph}), 1720 (w), 1657 (vs, C=O), 1579 (s), 1478 (m), 1451 (w), 1392 (m), 1269 (m), 1202 (vs), 1169 (s), 1102 (w), 1064 (s), 1008 (m), 967 (w), 945 (w), 941 (w), 905 (vs), 826 (vs), 755 (w), 714 (s), 677 (w).

S-ethyl 4-iodobenzothioate (**129g**)

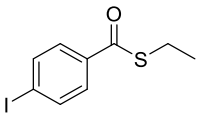

129g

According to GP-A, **129g** was synthesized using 4-iodobenzoic acid (2.48 g, 10.0 mmol, 1.0 equiv.), ethanethiol (2.2 mL, 30 mmol, 3 equiv.), DMAP (122 mg, 1.00 mmol, 0.1 equiv.) and DIC (1.7 mL, 11 mmol, 1.1 equiv.). Purification was achieved by filtration through a silica plug (Hex/EA = 99:1) and yielded the product as an orange oil (2.31 g, 7.91 mmol, 79%, 95% purity). The spectral data matches reported literature examples.[10]

C_9H_9IOS (292.12 g/mol)

R_f: 0.31 (Hex/EA = 99:1) [UV].

Melting point: 58.9–60.0 °C (EA).

^{1}H NMR (400 MHz, $CDCl_3$): δ =7.92–7.73 (m, 2H, $C_{Ar}H$), 7.71–7.55 (m, 2H, $C_{Ar}H$), 3.07 (q, *J* = 7.4 Hz, 2H, CH_2CH_3), 1.35 (t, *J* = 7.4 Hz, 3H, CH_2CH_3).

^{13}C NMR (101 MHz, $CDCl_3$): δ = 191.6 (*C*(O)SEt), 138.0 (C_{Ar}), 136.7 (C_{Ar}), 128.7 (C_{Ar}), 101.1 (C_{Ar}I), 23.7 (CH_2CH_3), 14.8 (CH_2CH_3).

GC-MS (EI): t_r = 8.01 min, m/z(%) = 293 (1, [$M^{+\bullet}$]), 292 (12, [$M^{+\bullet}$]), 232 (9, [$M^{+\bullet}$-$SC_2H_5^{\bullet}$]), 231 (100, [$M^{+\bullet}$-$SC_2H_5^{\bullet}$-CO]), 204 (3, [$M^{+\bullet}$-$SC_2H_5^{\bullet}$-CO]), 203 (24, [$M^{+\bullet}$-$SC_2H_5^{\bullet}$-CO]).

IR (ATR, $\tilde{\nu}$ [cm^{-1}]): 2965 (w, C-H$_{aliph}$), 2927 (w, C-H$_{aliph}$, C-H$_{aliph}$), 2868 (w, C-H$_{aliph}$), 1717 (w), 1656 (vs, C=O), 1575 (s), 1474 (w), 1448 (w), 1415 (w), 1385 (m), 1269 (m), 1202 (s), 1172 (s), 1102 (m), 1053 (m), 1004 (m), 971 (w), 904 (vs), 822 (vs), 751 (m), 710 (s).

S-ethyl 4-(tosyloxy)benzothioate (**129h**)

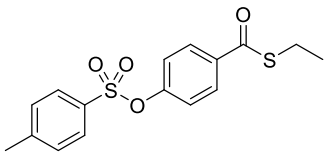

129h

According to GP-A, **129h** was synthesized using 4-(tosyloxy)benzoic acid (1.17 g, 4 mmol, 1.0 equiv.), ethanethiol (890 µL, 30.0 mmol, 3 equiv.), DMAP (49 mg, 400 µmol, 0.1 equiv.) and DCC (909 mg, 4.40 mmol, 1.1 equiv.). Purification was achieved by filtration through a short silica plug (Hex/EA = 8:2) and washing the filtrate with aq. HCl (2 × 100 mL, 6 M), aq. KOH (1 × 100 mL, 10% w/v), sat. $NaHCO_3$ (1 × 100 mL) and brine (1 × 100 mL). The organic layer was dried over anhydrous $MgSO_4$ and solvent evaporate *in vacuo*. The product was obtained as a colorless solid (868 mg, 2.71 mmol, 68%). The spectral data is in good accordance to previously reported literature examples.[18]

$C_{16}H_{16}O_3S_2$ (320.05 g/mol)

R_f: 0.58 (Hex/EA = 8:2) [UV].

^{1}H NMR (400 MHz, $CDCl_3$): δ = 7.93–7.85 (m, 2H, C$_{Ar}$*H*), 7.74–7.66 (m, 2H, C$_{Ar}$*H*), 7.35–7.27 (m, 2H, C$_{Ar}$*H*), 7.10–7.01 (m, 2H, C$_{Ar}$*H*), 3.06 (q, *J* = 7.4 Hz, 2H, C*H*$_2$CH$_3$), 2.44 (s, 3H, ArC*H*$_3$), 1.33 (t, *J* = 7.4 Hz, 3H, CH$_2$C*H*$_3$).

^{13}C NMR (101 MHz, $CDCl_3$): δ = 190.9 (*C*(O)SEt), 153.2 (*C*$_{Ar}$), 145.9 (*C*$_{Ar}$), 135.9 (*C*$_{Ar}$), 132.1 (*C*$_{Ar}$), 130.0 (*C*$_{Ar}$), 128.9 (*C*$_{Ar}$), 128.6 (*C*$_{Ar}$), 122.6 (*C*$_{Ar}$), 23.8, 21.9, 14.8.

IR (ATR, $\tilde{\nu}$ [cm^{-1}]): 2962 (w, C-H$_{aliph}$), 2928 (w, C-H$_{aliph}$), 2872 (w, C-H$_{aliph}$), 1653 (m, C=O), 1590 (w), 1493 (w), 1451 (w), 1407 (w), 1374 (m), 1295 (w), 1273 (w), 1202 (s), 1150 (s), 1090 (m), 1012 (w), 964 (w), 912 (m), 858 (s), 807 (m), 751 (s), 717 (s), 673 (s).

4-((ethylthio)carbonyl)phenyl acetate (**129i**)

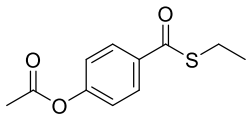

129i

According to GP-A, **129i** was synthesized using 4-acetoxybenzoic acid (3.60 g, 20.0 mmol, 1.0 equiv.), ethanethiol (7.2 mL, 100 mmol, 5.0 equiv.), DMAP (244 mg, 2.00 mmol, 0.1 equiv.) and DCC (4.54 g, 22.0 mmol, 1.1 equiv.). Purification was achieved by DCVC (Hex/EA = 9:1). The product was obtained as a slightly yellow-colored oil (1.21 g, 5.40 mmol, 54%).

$C_{11}H_{12}O_3S$ (224.27 g/mol)

R_f: 0.06 (Hex/EA = 9:1) [$KMnO_4$, UV].

^{1}H NMR (400 MHz, $CDCl_3$): δ = 8.04–7.95 (m, 2H, $C_{Ar}H$), 7.22–7.13 (m, 2H, $C_{Ar}H$), 3.07 (q, *J* = 7.4 Hz, 2H, CH_2CH_3), 2.32 (s, 3H, $CH_3C(O)O$), 1.35 (t, *J* = 7.4 Hz, 3H, CH_2CH_3).

^{13}C NMR (101 MHz, $CDCl_3$): δ = 191.0 (*C*(O)SEt), 168.9 (*C*(O)OAr), 154.6 (C_{Ar}), 134.9 (C_{Ar}), 128.8 (C_{Ar}), 121.9 (C_{Ar}), 23.7, 21.3, 14.9.

GC-MS (EI, method B): t_r = 20.41 min, m/z(%) = 224 (3, [$M^{+\bullet}$]), 163 (58, [$M^{+\bullet}$-$C_2H_5S^{\bullet}$]), 122 (9), 121 (100).

HR-MS (ESI): m/z calc. for $[M+Na]^+$ 247.03994, found 247.04014.

IR (ATR, $\tilde{\nu}$ [cm^{-1}]): 3062 (w, C-H_{arom}), 2969 (w, C-H_{aliph}), 2928 (w, C-H_{aliph}), 2872 (w, C-H_{aliph}), 1754 (m, C=O_{ester}), 1650 (m, C=$O_{thioester}$), 1589 (w), 1493 (w), 1448 (w), 1433 (w), 1407 (w), 1369 (w), 1295 (w), 1179 (s), 1150 (m), 1101 (m), 1049 (w), 1005 (m), 969 (w), 907 (s), 848 (s), 803 (m), 759 (w), 732 (m), 681 (m).

S-ethyl 4-cyanobenzothioate (**129k**)

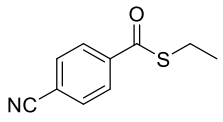

129k

According to GP-A, **129k** was synthesized using 4-cyanobenzoic acid (1.91 g, 10.0 mmol, 1.0 equiv.), ethanethiol (2.2 mL, 30 mmol, 3 equiv.), DMAP (122 mg, 1.00 mmol, 0.1 equiv.) and DCC (2.27 g, 11.0 mmol, 1.1 equiv.). Purification was achieved by filtration through a short silica plug (Hex/EA = 9:1) and washing the filtrate with 6 M HCl (2 × 20 mL), 10% aq. KOH (1 × 20 mL), sat. $NaHCO_3$ (1 × 20 mL) and brine (1 × 20 mL). The combined organic layers were dried over anhydrous $MgSO_4$ and solvent evaporated *in vacuo.* The product was yielded as colorless solid (1.45 g, 7.58 mmol, 76%). The data is in accordance with reported literature.[18]

$C_{10}H_9NOS$ (191.25 g/mol)

R_f: 0.30 (Hex/Et_2O = 9:1) [$KMnO_4$].

^{1}H NMR (400 MHz, $CDCl_3$): δ = 8.12–7.95 (m, 2H, $C_{Ar}H$), 7.79–7.71 (m, 2H, $C_{Ar}H$), 3.12 (q, *J* = 7.4 Hz, 2H, SCH_2CH_3), 1.37 (t, *J* = 7.4 Hz, 3H, SCH_2CH_3).

^{13}C NMR (75 MHz, $CDCl_3$): δ = 190.9 (*C*(O)SEt), 140.4 (C_{Ar}), 132.6 (C_{Ar}), 127.8 (C_{Ar}), 118.0 (*C*N), 116.6 (C_{Ar}), 24.1 (SCH_2CH_3), 14.7 (SCH_2CH_3).

GC-MS (EI): t_r = 7.29 min, m/z(%) = 191 (6, [$M^{+\bullet}$]), 130 (100, [$M^{+\bullet}$-$C_2H_5S^{\bullet}$]), 102 (28, [$M^{+\bullet}$-$C_2H_5S^{\bullet}$-CO]).

IR (ATR, $\tilde{\nu}$ [cm^{-1}]): 3085 (w, C-H_{arom}), 2968 (w, C-H_{aliph}), 2928 (w, C-H_{aliph}), 2872 (w, C-H_{aliph}), 2220 (w, C≡N), 1646 (s, C=O), 1560 (w), 1500 (w), 1452 (w), 1403 (m), 1377 (w), 1278 (w), 1198 (s), 1161 (m), 1113 (w), 1057 (w), 1016 (w), 964 (w), 914 (s), 833 (s), 829 (s), 763 (s), 733 (m).

S-ethyl 4-formylbenzothioate (**129m**)

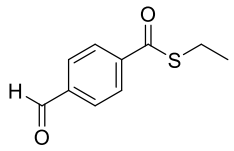

129m

According to GP-A, **129m** was synthesized using 4-formyl benzoic acid (1.50 g, 10 mmol, 1.0 equiv.), ethanethiol (2.2 mL, 30.0 mmol, 3 equiv.), DMAP (122 mg, 1 mmol, 0.1 equiv.) and DCC (2.27 g, 11 mmol, 1.1 equiv.). Purification was achieved by manual column chromatography (Hex/Et_2O = 95:5-9:1) which led to an impure product which was further purified by flash column chromatography (23 g SiO_2, gradient from Hex/EA = 95:5–80:20 over 15 CV). The product was gained as a colorless solid which melts at ambient temperature (368 mg, 246 µmol, 25%).

$C_{10}H_{10}O_2S$ (194.25 g/mol)

R_f: 0.24 (Hex/EA = 9:1) [UV].

Melting point: ambient temperature.

^{1}H NMR (400 MHz, $CDCl_3$): δ = 10.08 (s, 1H, C*H*(O)), 8.22–7.91 (m, 4H, $C_{Ar}H$), 3.10 (q, *J* = 7.4 Hz, 2H, SCH_2CH_3), 1.36 (t, *J* = 7.4 Hz, 3H, SCH_2CH_3).

^{13}C NMR (101 MHz, $CDCl_3$): δ = 191.6, 191.5, 141.6 (C_{Ar}), 139.3 (C_{Ar}), 129.9 (C_{Ar}), 127.8 (C_{Ar}), 24.0 (SCH_2CH_3), 14.7 (SCH_2CH_3).

HR-MS (ESI): m/z calc. for $[M+MeOH+Na]^+$ 249.05559, found 249.05552.

GC-MS (EI): t_r = 7.30 min, m/z(%) =194 (5, $[M^{+\bullet}]$), 133 (100, $[M^{+\bullet}-SC_2H_5^{\bullet}]$), 105 (23, $[M^{+\bullet}\ SC_2H_5^{\bullet}-CO]$), 77 (29, $[C_6H_5^{+\bullet}]$).

IR (ATR, $\tilde{\nu}$ [cm^{-1}]): 2969 (w, C-H_{aliph}), 2928 (w, C-H_{aliph}), 2868 (w, C-H_{aliph}), 2832 (w, C-H_{aliph}), 1701 (vs, C=$O_{aldehyde}$), 1653 (vs, C=$O_{thioester}$), 1571 (w), 1500 (w), 1451 (w), 1411 (w), 1378 (m), 1299 (w), 1266 (w), 1243 (w), 1195 (vs), 1105 (w), 1053 (w), 1008 (w), 971 (w), 912 (vs), 819 (vs), 725 (m), 684 (m).

S-ethyl 3-methylbenzothioate (**129n**)

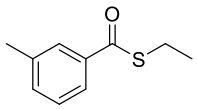

129n

According to GP-B, **129n** was synthesized using 3-methyl benzoyl chloride (1.32 g, 10.0 mmol, 1.0 equiv.), ethanethiol (790 µL, 11.0 mmol, 1.1 equiv.) and TEA (1.4 mL, 10 mmol, 1 equiv.). Purification was achieved by filtration through a short silica plug (Hex/EA = 98:2) and washing the filtrate with aq. HCl (2 × 30 mL, 6 M) and brine (1 × 30 mL). Then, the combined organic layers were dried over anhydrous $MgSO_4$ and solvent evaporated under reduced pressure. The product was obtained as a colorless oil (1.49 g, 8.27 mmol, 83%).

$C_{10}H_{12}OS$ (180.27 g/mol)

R_f: 0.41 (PE/EA = 98:2) [$KMnO_4$].

^{1}H NMR (400 MHz, CD_2Cl_2): δ = 7.81–7.72 (m, 2H, $C_{Ar}H$), 7.44–7.30 (m, 2H, $C_{Ar}H$), 3.06 (q, *J* = 7.4 Hz, 2H, SCH_2CH_3), 2.41 (s, 3H, CH_3), 1.34 (t, *J* = 7.4 Hz, 3H, SCH_2CH_3).

^{13}C NMR (101 MHz, CD_2Cl_2): δ = 192.2 (*C*(O)SEt), 139.0 (C_{Ar}), 137.7 (C_{Ar}), 134.4 (C_{Ar}), 128.8 (C_{Ar}), 127.9 (C_{Ar}), 124.6 (C_{Ar}), 23.8, 21.4, 15.0.

HR-MS (APCI): m/z calc. for $[M+H]^+$ 181.06816, found 181.06865.

GC-MS (EI): t_r = 6.23 min, m/z(%) = 180 (8, $[M^{+\bullet}]$), 119 (100, $[M^{+\bullet}-C_2H_5S^{\bullet}]$), 91 (58, $[M^{+\bullet}-C_2H_5S^{\bullet}-CO]$).

IR (ATR, $\tilde{\nu}$ [cm^{-1}]): 3043 (w, C-H_{arom}), 2965 (w, C-H_{aliph}), 2925 (w, C-H_{aliph}), 2868 (w, C-H_{aliph}), 1657 (vs, C=O), 1591 (m), 1478 (w), 1448 (m), 1418 (w), 1377 (w), 1243 (s), 1151 (s), 1094 (w), 1049 (w), 1008 (w), 945 (s), 889 (w), 833 (s), 792 (vs), 691 (s).

S-ethyl 3-methoxybenzothioate (**129o**)

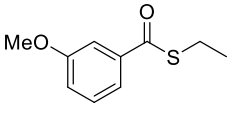

129o

According to GP-A, **129o** was synthesized using 3-methoxybenzoic acid (1.52 g, 10.0 mmol, 1.0 equiv.), ethanethiol (2.2 mL, 30 mmol, 3 equiv.), DMAP (122 mg, 1.00 mmol, 0.1 equiv.) and DCC (2.27 g, 11.0 mmol, 1.1 equiv.). Purification was achieved by filtration through a short silica plug using Hexane/EA (9:1) and washing the filtrate with aq. HCl (2 × 20 mL, 6 M), sat. $NaHCO_3$ (1 × 20 mL) and brine (1 × 20 mL). The product was obtained as a colorless oil (1.61 g, 8.21 mmol, 82%).

$C_{10}H_{12}O_2S$ (196.26 g/mol)

R_f: 0.58 (Hex/EA = 9:1) [UV].

^{1}H NMR (400 MHz, $CDCl_3$): δ = 7.56 (ddd, *J* = 7.7, 1.6, 1.0 Hz, 1H, $C_{Ar}H$), 7.45 (dd, *J* = 2.6, 1.6 Hz, 1H, $C_{Ar}H$), 7.33 (t, *J* = 8.1 Hz, 1H, $C_{Ar}H$), 7.09 (ddd, *J* = 8.1, 2.6, 1.0 Hz, 1H, $C_{Ar}H$), 3.83 (s, 3H, OCH_3), 3.06 (q, *J* = 7.4 Hz, 2H, CH_2CH_3), 1.34 (t, *J* = 7.4 Hz, 3H, CH_2CH_3).

^{13}C NMR (101 MHz, $CDCl_3$): δ = 192.0 (*C*(O)SEt), 159.8 (C_{Ar}), 138.6 (C_{Ar}), 129.7 (C_{Ar}), 119.8(C_{Ar}), 119.3 (C_{Ar}), 111.5 (C_{Ar}), 55.5 (OCH_3), 23.6 (CH_2CH_3), 14.8 (CH_2CH_3).

GC-MS (EI, method B): t_r = 18.69 min, m/z(%) = 196 (17, [$M^{+\bullet}$]), 135 (100, [$M^{+\bullet}$-$C_2H_5S^{\bullet}$]), 107 (100, [$M^{+\bullet}$-$C_2H_5S^{\bullet}$-CO]).

HR-MS (ESI): m/z calc. for $[M+Na]^+$ 219.04502, found 219.04545.

IR (ATR, $\tilde{\nu}$ [cm^{-1}]): 3070 (w, C-H_{arom}), 2969 (w, C-H_{aliph}), 2932 (w, C-H_{aliph}), 2875 (w, C-H_{aliph}), 2835 (w, C-H_{aliph}), 1735 (m), 1660 (s, C=O), 1588 (m), 1481 (m), 1455 (m), 1429 (m), 1370 (w), 1318 (w), 1288 (w), 1249 (vs, C_{arom}-O_{ether}), 1191 (m), 1158 (s), 1090 (w), 1042 (s), 967 (m), 941 (s), 874 (w), 833 (m), 789 (vs), 695 (s).

S-ethyl 3-(trifluoromethyl)benzothioate (**129p**)

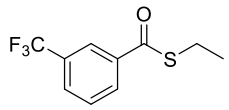

129p

According to GP-B, **129p** was synthesized using 3-(trifluoromethyl)benzoyl chloride (1.5 mL, 10.0 mmol, 1.0 equiv.), ethanethiol (790 µL, 11.0 mmol, 1.1 equiv.) and TEA (1.4 mL, 10 mmol, 1 equiv.). Purification was achieved by bulb-to-bulb distillation (4 mbar, 180 °C). The product was obtained as a yellow oil (1.74 g, 7.43 mmol, 74%).

$C_{10}H_9F_3OS$ (234.24 g/mol)

R_f: 0.30 (Hex) [UV, anis].

^{1}H NMR (300 MHz, CDCl3): δ = 8.24–8.16 (m, 1H, $C_{Ar}H$), 8.15–8.09 (m, 1H, $C_{Ar}H$), 7.84–7.77 (m, 1H, $C_{Ar}H$), 7.62–7.55 (m, 1H, $C_{Ar}H$), 3.11 (q, *J* = 7.4 Hz, 2H, CH_2CH_3), 1.36 (t, *J* = 7.4 Hz, 3H, CH_2CH_3).

^{13}C NMR (75 MHz, $CDCl_3$): δ = 191.0 (*C*(O)SEt), 137.9, 131.4 (q, J^2_{C-F} = 33.0 Hz, C_{Ar}-CF_3), 130.5, 129.7 (q, J^3_{C-F} = 3.7 Hz, C_{Ar}), 125.5 (q, J^1_{C-F} = 271.5 Hz, CF_3), 124.15 (q, J^3_{C-F} = 3.9 Hz, C_{Ar}), 23.86 (CH_2CH_3), 14.74 (CH_2CH_3).

^{19}F-NMR (377 MHz, $CDCl_3$): δ = –62.9 (s).

GC-MS (EI, method B): t_r = 15.07 min, m/z(%) = 234 (9, [$M^{+\bullet}$]), 173 (100, [$M^{+\bullet}$-$C_2H_5S^{\bullet}$]), 145 (45, [$M^{+\bullet}$-$C_2H_5S^{\bullet}$-CO]).

HR-MS (APCI): m/z calc. for $[M+H]^+$ 235.03990, found 235.04022.

IR (ATR, $\tilde{\nu}$ [cm^{-1}]): 3040 (w, C-H_{arom}), 2995 (w, C-H_{aliph}), 2951 (w, C-H_{aliph}), 2891 (w, C-H_{aliph}), 2813 (w, C-H_{aliph}), 1560 (s, C=O), 1452 (s, C-CF_3), 1344 (s), 1198(s, CF_3), 1109 (s, CF_3), 934(m), 807 (s).

S-ethyl 2-methylbenzothioate (**129q**)

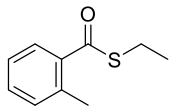

129q

According to GP-A, **129q** was synthesized using 2-methylbenzoic acid (1.36 g, 10.0 mmol, 1.0 equiv.), ethanethiol (2.2 mL, 45 mmol, 3 equiv.), DMAP (122 mg, 1.00 mmol, 0.1 equiv.) and DCC (2.27 g, 11.0 mmol, 1.1 equiv.). Purification was achieved by filtration through a short silica plug using DCM and washing the obtained solution with aq. HCl (1 × 20 mL, 6 M), aq. HCl (1 × 20 mL, 1 M), sat. $NaHCO_3$ (1 × 20 mL) and brine (1 × 20 mL). The combined organic layers were dried over anhydrous $MgSO_4$ and solvents evaporated under reduced pressure. The product was obtained as a colorless oil (860 mg, 4.77 mmol, 48%). The analytical data is in good accordance to reported literature.[10]

$C_{10}H_{12}OS$ (180.27 g/mol)

R_f: 0.46 (Hex/EA = 9:1) [$KMnO_4$, anis, UV].

^{1}H NMR (400 MHz, $CDCl_3$): δ = 7.86 (dd, *J* = 8.1, 1.4 Hz, 1H, $C_{Ar}H$), 7.47 (td, *J* = 7.5, 1.4 Hz, 1H, $C_{Ar}H$), 7.38–7.30 (m, 2H, $C_{Ar}H$), 3.15 (q, *J* = 7.4 Hz, 2H, SCH_2CH_3), 2.59 (s, 3H, $PhCH_3$), 1.46 (t, *J* = 7.4 Hz, 3H, SCH_2CH_3).

^{13}C NMR (101 MHz, $CDCl_3$): δ = 194.7 (*C*(O)SEt), 137.9 (C_{Ar}), 136.8 (C_{Ar}), 131.6 (C_{Ar}), 131.6 (C_{Ar}), 128.5 (C_{Ar}), 125.8 (C_{Ar}), 24.1 (SCH_2CH_3), 20.7 ($ArCH_3$), 14.9 (SCH_2CH_3).

GC-MS (EI): t_r = 5.95 min, m/z(%) = 119 (100, [$M^{+\bullet}$-$C_2H_5S^{\bullet}$]), 91 (27, [$M^{+\bullet}$-$C_2H_5S^{\bullet}$-CO]).

IR (ATR, $\tilde{\nu}$ [cm^{-1}]): 3062 (w, C-H_{arom}), 3018 (w, C-H_{arom}), 2968 (w, C-H_{aliph}), 2928 (w, C-H_{aliph}), 2872 (w, C-H_{aliph}), 1660 (vs, C=O), 1601 (w), 1597 (w), 1568 (w), 1481 (w), 1452 (m), 1377 (w), 1288 (w), 1284 (w), 1265 (w), 1191 (s), 1123 (w), 1047 (w), 971 (w), 945 (w), 900 (vs), 762 (s), 721 (s), 680 (s).

2-((ethylthio)carbonyl)phenyl acetate (**129r**)

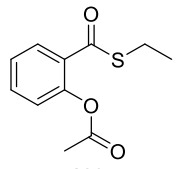

129r

The compound **129r** was synthesized by dissolving acetylsalicylic acid (1.80 g, 10.0 mmol, 1.0 equiv.) and oxalyl chloride (1.0 mL, 12 mmol, 1.2 equiv.) in DCM (60 mL). After a drop of dry DMF was added to the mixture, the reaction was stirred for 30 min at rt. The solvent was evaporated and residual oxalyl chloride was distilled off *in vacuo*. The crude acid chloride was suspended in DCM (40 mL) and solution of ethanethiol (940 µL, 13.0 mmol, 1.3 equiv.) and TEA (1.5 mL, 11 mmol, 1.1 equiv.) in DCM (40 mL) were added dropwise at 0 °C. The reaction was stirred at rt for 16 h. Then, the reaction was quenched with demin. water (ca. 10 mL) after which a white solid precipitated. Purification was achieved by washing the filtrate with aq. KOH solution (3 × 20 mL, 10% w/v), aq. HCl (3 × 20 mL, 6 M), sat. aq. $NaHCO_3$ (1 × 20 mL) and brine (1 × 20 mL). The organic phase was dried over anhydrous $MgSO_4$ and solvents evaporated *in vacuo* to yield a yellow oil (1.88 g, 8.38 mmol, 84%).

$C_{11}H_{12}O_3S$ (224.27 g/mol)

R_f: 0.41 (Hex/EA = 9:1) [UV].

^{1}H NMR (400 MHz, $CDCl_3$): δ = 7.92 (dd, *J* = 8.0, 1.7 Hz, 1H, $C_{Ar}H$), 7.53 (td, *J* = 7.8, 1.7 Hz, 1H, $C_{Ar}H$), 7.31 (td, *J* = 7.8, 1.2 Hz, 1H, $C_{Ar}H$), 7.11 (dd, *J* = 8.0, 1.2 Hz, 1H, $C_{Ar}H$), 3.02 (q, *J* = 7.4 Hz, 2H, SCH_2CH_3), 2.34 (s, 3H, $H_3CC(O)O$), 1.33 (t, *J* = 7.4 Hz, 3H, SCH_2CH_3).

^{13}C NMR (101 MHz, $CDCl_3$): δ = 190.4 (*C*(O)SEt), 169.5 (H_3CC(O)O), 148.0 (C_{Ar}), 133.5 (C_{Ar}), 130.5 (C_{Ar}), 129.7 (C_{Ar}), 126.2 (C_{Ar}), 124.0 (C_{Ar}), 24.0, 21.2, 14.7.

HR-MS (ESI): m/z calc. for $[M+Na]^+$ 247.03994, found 247.04034.

GC-MS (EI): t_r = 7.26, m/z = 163 (64), 121 (100).

IR (ATR, $\tilde{\nu}$ [cm^{-1}]): 3070 (w, C-H_{arom}), 2972 (w, C-H_{aliph}), 2931 (w, C-H_{aliph}), 2872 (w, C-H_{aliph}), 1765 (s, C=O_{ester}), 1660 (s, C=$O_{thioester}$), 1601 (w), 1575 (w), 1478 (w), 1445 (w), 1366 (m), 1266 (w), 1179 (vs), 1108 (m), 1042 (w), 1008 (m), 919 (s), 897 (vs), 863 (s), 814 (m), 762 (s), 684 (m).

S,*S*-diethyl benzene-1,2-bis(carbothioate) (1**29s**)

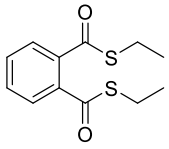

129s

According to GP-A, **129s** was synthesized using phthalic acid (3.32g, 20 mmol, 1.0 equiv.), ethanethiol (11.2 mL, 160 mmol, 8.0 equiv.), DMAP (489 mg, 4.0 mmol, 0.2 equiv.) and DCC (9.08 g, 44.0 mmol, 2.2 equiv.). Solid side products were filtered off, the organic layer was dried over anhydrous $MgSO_4$ and solvent evaporated under reduced pressure. Further purification was achieved by flash column chromatography (23 g SiO_2, isocratic Hex for 4 CV, then gradient to Hex/Et_2O = 8:2 over 2 CV and hold for 4 CV)) to yield a colorless oil (1.03 g, 4.29 mmol, 21%).

$C_{12}H_{14}O_2S_2$ (254.36 g/mol)

R_f: 0.38 (PE/Et_2O = 8:2) [UV]

^{1}H NMR (400 MHz, $CDCl_3$): δ = 7.67 (dd, *J* = 5.7, 3.3 Hz, 2H, $C_{Ar}H$), 7.56–7.46 (m, 2H, $C_{Ar}H$), 3.06 (q, *J* = 7.4 Hz, 4H, 2 × C(O)SC$H_2$$CH_3$), 1.35 (t, *J* = 7.4 Hz, 6H, 2 × C(O)SCH_2CH_3).

^{13}C NMR (101 MHz, $CDCl_3$): δ = 193.2 (*C*(O)SEt), 137.6 (C_{Ar}), 131.2 (C_{Ar}), 128.2 (C_{Ar}), 24.3 (C(O)S*C*$H_2$$CH_3$), 14.5 (C(O)S$CH_2$*C*$H_3$).

HR-MS (ESI): m/z calc. for $[M+Na]^+$ 277.03274, found 277.03299.

GC-MS (EI): t_r = 9.10, m/z(%) = 193 (97, $[M^{+\bullet}\text{-}SC_2H_5^{\bullet}]$), 165 (100, $[M^{+\bullet}\text{-}C_2H_5^{\bullet}\text{-}SC_2H_5^{\bullet}\text{-}CO]$).

IR (ATR, $\tilde{\nu}$ [cm^{-1}]): 3064 (w, C-H_{arom}), 2968 (w, C-H_{aliph}), 2928 (w, C-H_{aliph}), 2872 (w, C-H_{aliph}), 1660 (vs, C=O), 1590 (w), 1571 (w), 1448 (m), 1414 (w), 1374 (w), 1291 (w), 1262 (m), 1194 (vs), 1112 (m), 1053 (w), 966 (w), 910 (vs), 766 (s), 703 (vs), 656 (s).

S-ethyl naphthalene-2-carbothioate (**129t**)

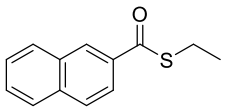

129t

Naphthoic acid (1.72 g, 10 mmol) was dissolved in DCM (50 mL) and 2-chloro-4,6-dimethoxy-1,3,5-triazine (2.11 g, 12.0 mmol, 1.2 equiv.) as well as TEA (4.0 mL, 30 mmol, 3.0 equiv.) were added. The reaction mixture was stirred at rt for 2 h. Then, ethanethiol (0.94 mL, 13 mmol, 1.3 equiv.) was added and the reaction was stirred for 1 h. Afterwards, the crude reaction mixture was extracted with aq. HCl (2 × 20 mL, 6 M), sat. aq. $NaHCO_3$ (1 × 20 mL) and brine (1 × 20 mL). The organic layer was dried over anhydrous $MgSO_4$ and solvent evaporated under reduced pressure. The product was yielded as a colorless solid (1.04 g, 4.81 mmol, 48%, 95% purity). The spectral data is in good accordance with reported literature.[18]

$C_{13}H_{12}OS$ (216.30 g/mol)

R_f: 0.45 (PE/EA = 97:3) [$KMnO_4$, anis, UV].

^{1}H NMR (400 MHz, $CDCl_3$): δ = 8.56–8.50 (m, 1H, $C_{Ar}H$), 8.04–7.93 (m, 2H, $C_{Ar}H$), 7.92–7.84 (m, 2H, $C_{Ar}H$), 7.64–7.51 (m, 2H, $C_{Ar}H$), 3.14 (q, *J* = 7.4 Hz, 2H, C(O)SCH_2), 1.40 (t, *J* = 7.4 Hz, 3H, C(O)SCH_2CH_3).

^{13}C NMR (101 MHz, $CDCl_3$): δ = 192.2 (*C*(O)SEt), 135.8 (C_{Ar}), 134.7 (C_{Ar}), 132.6 (C_{Ar}), 129.7 (C_{Ar}), 128.63 (C_{Ar}), 128.56 (C_{Ar}), 128.5 (C_{Ar}), 127.9 (C_{Ar}), 127.0 (C_{Ar}), 123.3 (C_{Ar}), 23.7 (S*C*$H_2$$CH_3$), 15.0 (SC$H_2$*C*$H_3$).

GC-MS (EI): t_r = 8.96 min, m/z(%) = 216 (9, [$M^{+\bullet}$]), 155 (100, [$M^{+\bullet}$-$C_2H_5S^\bullet$]), 127 (69, [$M^{+\bullet}$-$C_2H_5S^\bullet$-CO]).

IR (ATR, $\tilde{\nu}$ [cm^{-1}]): 3055 (w, C-H_{arom}), 2961 (w, C-H_{aliph}), 2924 (w, C-H_{aliph}), 2868 (w, C-H_{aliph}), 2820 (w, C-H_{aliph}), 1642 (s, C=O), 1571 (w), 1452 (w), 829 (w).

S-ethyl pyridine-2-carbothioate (**129u**)

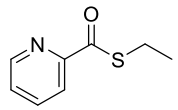

129u

According to GP-A, **129u** was synthesized using picolinic acid (1.23 g, 10 mmol, 1.0 equiv.), ethanethiol (2.2 mL, 30.0 mmol, 3 equiv.), DMAP (122 mg, 1 mmol, 0.1 equiv.) and DCC (2.27 g, 11 mmol, 1.1 equiv.). Purification was achieved by twice filtration through a small silica plug (Hex/EA = 9:1) and washing the resulting solution with aq. HCl (2 × 20 mL, 6 M), aq. KOH (1 × 20 mL, 10% w/v), sat. $NaHCO_3$ (1 × 20 mL) and brine (1 × 20 mL). The organic layer was dried over anhydrous $MgSO_4$ and solvent evaporated under reduced pressure. The product was obtained as a colorless oil (1.01 g, 6.05 mmol, 61%).

C_8H_9NOS (167.23 g/mol)

R_f: 0.56 (Hex/EA = 9:1) [UV].

^{1}H NMR (400 MHz, $CDCl_3$): δ = 8.72–8.66 (m, 1H, $C_{Ar}H$), 8.00–7.94 (m, 1H, $C_{Ar}H$), 7.87–7.82 (m, 1H, $C_{Ar}H$), 7.59–7.42 (m, 1H, $C_{Ar}H$), 3.04 (q, *J* = 7.5, 0.7 Hz, 2H), 1.35 (t, *J* = 7.5, 0.7 Hz, 3H).

^{13}C NMR (101 MHz, $CDCl_3$): δ = 193.8 (*C*(O)SEt), 152.2 (C_{Ar}), 149.3 (C_{Ar}), 137.4 (C_{Ar}), 127.9 (C_{Ar}), 120.5 (C_{Ar}), 23.2, 14.6.

GC-MS (EI): t_r = 6.04 min, m/z(%) = 139 (11), 111 (6), 107 (14), 106 (21, $[M^{+\bullet}\text{-}C_2H_5S^{\bullet}]$), 79 (38, $[M^{+\bullet}]$), 78 (100, $[M^{+\bullet}\text{-}C_2H_5S^{\bullet}\text{-}CO]$), 51 (39).

HR-MS (APCI): m/z calc. for $[M+H]^+$ 168.04776, found 168.04807.

IR (ATR, $\tilde{\nu}$ [cm^{-1}]): 3054 (w, C-H_{arom}), 2968 (w, C-H_{aliph}), 2928 (w, C-H_{aliph}), 2872 (w, C-H_{aliph}), 1661 (vs, C=O), 1578 (m), 1456 (m), 1433 (m), 1374 (w), 1292 (w), 1262 (s), 1217 (s), 1146 (w), 1087 (w), 1049 (w), 993 (w), 971 (w), 920 (vs), 792 (s), 740 (s), 710 (s).

S-ethyl pyridine-3-carbothioate (**129v**)

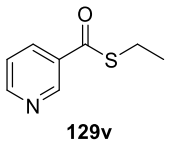

129v

According to GP-A, **129v** was synthesized using nicotinic acid (1.23 g, 10.0 mmol, 1.0 equiv.), ethanethiol (2.2 mL, 30 mmol, 3 equiv.), DMAP (122 mg, 1.00 mmol, 0.1 equiv.) and DCC (2.27 g, 11.0 mmol, 1.1 equiv.). Purification was achieved by filtration through a short silica plug (Hex/EA = 9:1) and washing the filtrate with aq. HCl (2 × 20 mL, 6 M). The aqueous layer was neutralized with aq. KOH solution (10% w/v – pH = 9) and extracted with EA (4 × 25 mL). Then, the combined organic layers were washed with brine (1 × 20 mL) and yielded the product as a slightly yellow-colored oil (436 mg, 2.76 mmol, 28%). The analytical data is in accordance with reported literature.[10]

C_8H_9NOS (167.23 g/mol)

R_f: 0.35 (Hex/EA = 9:1) [$KMnO_4$, UV].

^{1}H NMR (400 MHz, $CDCl_3$): δ = 9.17 (d, *J* = 2.2 Hz, 1H, $C_{Ar}H$), 8.78 (dd, *J* = 4.9, 1.7 Hz, 1H, $C_{Ar}H$), 8.25–8.17 (m, 1H, $C_{Ar}H$), 7.41 (ddt, *J* = 7.1, 4.9, 1.1 Hz, 1H, $C_{Ar}H$), 3.12 (q, *J* = 7.4 Hz, 2H), 1.37 (t, *J* = 7.4 Hz, 3H).

^{13}C NMR (101 MHz, $CDCl_3$): δ = 190.7 (*C*(O)SEt), 153.6 (C_{Ar}), 148.4 (C_{Ar}), 134.8(C_{Ar}), 133.0 (C_{Ar}), 123.7 (C_{Ar}), 23.7, 14.8.

GC-MS (EI): t_r = 5.86 min, m/z(%) = 167 (10, [$M^{+\bullet}$]), 106 (100, [$M^{+\bullet}$-$C_2H_5S^{\bullet}$]), 78 (66, [$M^{+\bullet}$-$C_2H_5S^{\bullet}$-CO]).

IR (ATR, $\tilde{\nu}$ [cm^{-1}]): 3039 (w, C-H_{arom}), 2969 (w, C-H_{aliph}), 2928 (w, C-H_{aliph}), 2872 (w, C-H_{aliph}), 1657 (vs, C=O), 1578 (s), 1452 (w), 1414 (s), 1377 (w), 1325 (w), 1269 (w), 1214 (vs), 1116 (w), 1086 (w), 1029 (w), 968 (w), 908 (vs), 811 (s), 777 (w), 702 (vs), 664 (m).

S-ethyl 2-fluorobenzothioate (**129w**)

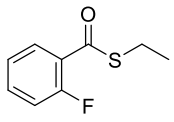

129w

According to GP-A, **129w** was synthesized using 2-fluorobenzoic acid (701 mg, 5.00 mmol, 1.0 equiv.), ethanethiol (1.1 mL, 15.0 mmol, 3 equiv.), DMAP (61 mg, 500 µmol, 0.1 equiv.) and DCC (1.13 g, 5.50 mmol, 1.1 equiv.). Purification was achieved by filtration through a short silica plug using DCM and washing the filtrate with aq. HCl (2 × 20 mL, 6 M), sat. $NaHCO_3$ (1 × 20 mL) and brine (1 × 20 mL). The organic layer was dried over anhydrous $MgSO_4$ and solvent evaporated under reduced pressure. The product was obtained as a colorless oil (812 mg, 4.40 mmol, 88%).

C_9H_9FOS (184.23 g/mol)

R_f: 0.44 (Hex/EA = 30:1) [UV].

^{1}H NMR (400 MHz, $CDCl_3$): δ = 7.84 (td, *J* = 7.5, 1.8 Hz, 1H, $C_{Ar}H$), 7.49 (dddd, *J* = 8.2, 7.3, 5.0, 1.8 Hz, 1H, $C_{Ar}H$), 7.20 (td, *J* = 7.6, 1.1 Hz, 1H, $C_{Ar}H$), 7.13 (ddd, *J* = 10.8, 8.3, 1.1 Hz, 1H, $C_{Ar}H$), 3.07 (q, *J* = 7.4 Hz, 2H), 1.35 (t, *J* = 7.4 Hz, 3H).

^{13}C NMR (75 MHz, $CDCl_3$): δ = 189.1 (d, J^3_{C-F} = 4.5 Hz), 160.4 (d, J^1_{C-F} = 257.6 Hz, $C_{Ar}F$), 134.2 (d, J^3_{C-F} = 8.9 Hz), 129.8 (d, J^4_{C-F} = 1.7 Hz), 125.9 (d, J^2_{C-F} = 11.4 Hz), 124.3 (d, J^3_{C-F} = 3.7 Hz), 117.0 (d, J^2_{C-F} = 22.3 Hz), 23.9 (CH_2CH_3), 14.6(CH_2CH_3).

^{19}F NMR (376 MHz, $CDCl_3$): δ = -111.1 (s).

GC-MS (EI): t_r = 5.65 min, m/z(%) = 184 (6, [$M^{+\bullet}$]), 123 (100, [$M^{+\bullet}$-$C_2H_5S^\bullet$]), 95 (26, [$M^{+\bullet}$-$C_2H_5S^\bullet$-CO]).

HR-MS (ESI): m/z calc. for $[M+Na]^+$ 207.02503, found 207.02529.

IR (ATR, $\tilde{\nu}$ [cm^{-1}]): 3074 (w, C-H_{arom}), 3040 (w, C-H_{arom}), 2972 (w, C-H_{aliph}), 2931 (w, C-H_{aliph}), 2872 (w, C-H_{aliph}), 1668 (s, C=O), 1645 (s), 1605 (s), 1579 (w), 1481 (s, C-F), 1448 (s), 1414 (w), 1377 (w), 1266 (s), 1225 (m), 1195 (s), 1153 (m), 1105 (m), 971 (w), 912 (vs), 807 (m), 759 (vs).

S-ethyl 2,3,4,5,6-pentafluorobenzothioate (**129x**)

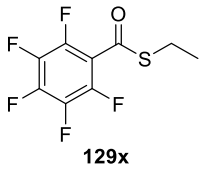

129x

The compound **129x** was synthesized after a modified GP-B. Ethanethiol (790 µL, 11.0 mmol, 1.1 equiv.) and TEA (1.39 mL, 10.0 mmol, 1.0 equiv.) were dissolved in *n*-hexane (50 mL). After cooling the mixture to 0 °C, 2,3,4,5,6-pentafluorobenzoyl chloride (1.44 mL, 10.0 mmol) was added slowly over 5 min to the reaction mixture. The reaction was allowed to warm to rt and stirred for 12 h. The reaction mixture was quenched with the addition of demin. water (10 mL). The organic layer was extracted with sat. $NaHCO_3$ solution (2 × 30 mL) and brine (1 × 30 mL). The organic layer was dried over anhydrous $MgSO_4$. The product was obtained as a colorless oil (1.92 g, 7.49 mmol, 75%).

$C_9H_{15}F_5OS$ (256.19 g/mol)

R_f: 0.36 (Hex) [$KMnO_4$, UV].

^{1}H NMR (600 MHz, $CDCl_3$): δ = 3.14 (q, *J* = 7.4 Hz, 2H, C(O)SC*H*$_2$CH$_3$), 1.39 (td, *J* = 7.4, 0.9 Hz, 3H, C(O)SCH$_2$C*H*$_3$).

^{13}C NMR (151 MHz, $CDCl_3$): δ = 183.3 (*C*(O)SEt), 143.8 (dddd, *J* = 255.1, 15.6, 7.5, 4.4 Hz, *C*$_{Ar}$F), 142.9 (dtt, *J* = 258.8, 13.2, 4.4 Hz, *C*$_{Ar}$F), 137.7 (dddd, *J* = 254.4, 16.7, 13.2, 5.1 Hz, *C*$_{Ar}$F), 25.0 (S*C*H$_2$CH$_3$), 14.3 (SCH$_2$H$_3$).

^{19}F NMR (376 MHz, $CDCl_3$): δ = -139.7–-142.1 (m), -149.7 (tt, *J* = 20.8, 3.3 Hz), -159.8–-160.0 (m).

HR-MS (APCI): m/z calc. for $[M+H]^+$ 257.00540, found 257.00565.

GC-MS (EI): t_r = 5.37 min, m/z(%) = 256 (53, $[M^{+\bullet}]$), 195 (100, $[M^{+\bullet}$-$C_2H_5S^{\bullet}]$), 167 (32, $[M^{+\bullet}$-$C_2H_5S^{\bullet}$-CO]).

IR (ATR, $\tilde{\nu}$ [cm^{-1}]): 2976 (w, C-H$_{aliph}$), 2936 (w, C-H$_{aliph}$), 2879 (w, C-H$_{aliph}$), 1668 (s, C=O), 1492 (vs, C-F), 1414 (m), 1377 (w), 1314 (s), 1265 (w), 1131 (vs), 1053 (w), 979 (vs), 811 (vs), 770 (s), 725 (s).

S-ethyl 3,7-dimethyloct-6-enethioate (**131a**)

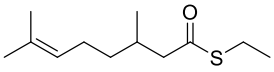

131a

According to GP-A, **131a** was synthesized using citronellic acid (1.8 mL, 10.0 mmol, 1.0 equiv.), ethanethiol (2.2 mL, 30.0 mmol, 3.0 equiv.), DMAP (122 mg, 1.00 mmol, 0.1 equiv.) and DCC (2.27 g, 11.0 mmol, 1.1 equiv.). Purification was achieved by filtration through a short silica plug using DCM and washing the filtrate with aq. HCl (2 × 20 mL, 6 M), sat. $NaHCO_3$ (1 × 20 mL) and brine (1 × 20 mL). A second filtration through a silica plug was necessary to remove trace impurities. The product was obtained as a colorless oil (1.56 g, 7.28 mmol, 73%). The spectral data is in good accordance to previously reported literature.[21]

$C_{12}H_{22}OS$ (214.37 g/mol)

R_f: 0.26 (Hex) [anis].

^{1}H NMR (400 MHz, $CDCl_3$): δ = 5.11–5.02 (m, 1H, $CH_2CHC(CH_3)_2$), 2.86 (q, *J* = 7.4 Hz, 2H, $C(O)SCH_2CH_3$), 2.53 (dd, *J* = 14.4, 5.9 Hz, 1H), 2.33 (dd, *J* = 14.4, 8.2 Hz, 1H), 2.10–1.89 (m, 3H), 1.66 (d, *J* = 1.7 Hz, 3H), 1.58 (d, *J* = 1.5 Hz, 3H), 1.41–1.12 (m, 5H), 0.93 (d, *J* = 6.7 Hz, 3H).

^{13}C NMR (101 MHz, $CDCl_3$): δ 199.3 ($C(O)SEt$), 131.7 ($CH_2CHC(CH_3)_2$), 124.3 ($CH_2CHC(CH_3)_2$), 51.4, 36.8, 30.9, 25.8, 25.5, 23.4, 19.5, 17.8, 14.9.

GC-MS (EI): t_r = 6.30 min, m/z(%) = 152 (19, $[M^{+\bullet}\text{-}C_2H_5S^{\bullet}]$), 69 (100, $[C_5H_9^{+\bullet}]$).

IR (ATR, $\tilde{\nu}$ [cm^{-1}]): 2962 (m, C-H_{aliph}), 2922 (m, C-H_{aliph}), 2872 (w, C-H_{aliph}), 2863 (w, C-H_{aliph}), 1687 (s, C=O), 1451 (m), 1377 (w), 1348 (w), 1265 (w), 1236 (w), 1209 (w), 1169 (w), 1107 (w), 1046 (w), 1004 (s), 938 (w), 889 (w), 826 (w), 753 (m), 688 (w).

(R)-2,5,7,8-tetramethyl-2-((4*R*,8*R*)-4,8,12-trimethyltridecyl)chroman-6-yl-4-(ethylthio)-4-oxobutanoate (**131c**)

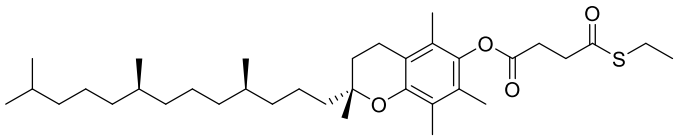

131c

α-Tocopherol (2.15 g, 5.00 mmol) and DMAP (31 mg, 250 µmol, 0.05 equiv.) were dissolved in a tin foil wrapped RBF flask equipped with a stirring bar in a DCM (30 mL)/anhydrous pyridine (3 mL) mixture to which TEA (700 µL, 5.00 mmol, 1.0 equiv.) was added. The solution was cooled to 0 °C after which a solution of acid chloride **134** (prepared according to GP-K; 1.17 g crude compound, 6.50 mmol, 1.3 equiv.) diluted in dry DCM (1 mL) was added *via* syringe pump (0.15 mL/min) while the mixture was vigorously stirred. After 30 min at 0 °C, the mixture was allowed to warm to rt and stirred for additional 23 h. The reaction was quenched by adding aq. KOH solution (ca. 15 mL, 10% w/v) and extracted with aq. KOH solution (2 × 10 mL, 10% w/v), sat. aq. NH_4Cl solution (3 × 10 mL) and brine (1 × 10 mL). The organic layer was dried over anhydrous $MgSO_4$. Evaporation of solvents yielded a viscous red oil which was purified by manual column chromatography (Hex/EA = 97:3–95:5). Due to the viscosity of the product, residue solvent was distilled off *via* Kugelrohr distillation (100 °C, 5 mbar, 1 h), yielding a colorless oil (1.87 g, 65%, not light-sensitive).

$C_{35}H_{58}O_4S$ (574.91 g/mol)

R_f: 0.68 (Hex/EA = 8:2) [UV, anis - black].

^{1}H NMR (400 MHz, $CDCl_3$): δ = 3.07–2.97 (m, 4H), 2.97–2.88 (m, 2H), 2.70–2.55 (m, 2H), 2.10 (s, 3H), 2.03 (s, 3H), 1.99 (s, 3H), 1.90–1.81 (m, 2H), 1.64–1.00 (m, 27H), 0.97–0.77 (m, 12H).

^{13}C NMR (101 MHz, $CDCl_3$): δ = 197.3 (*C*(O)SEt), 170.5 (CH_2CH_2*C*(O)O), 149.3 (C_{Ar}), 140.4 (C_{Ar}), 126.6 (C_{Ar}), 124.8 (C_{Ar}), 122.9 (C_{Ar}), 117.2 (C_{Ar}), 74.9 (O$C_{aliphat}$), 39.4, 38.3, 37.5, 37.4, 37.4, 37.3, 32.7, 32.6, 31.1, 28.6, 28.0, 24.8, 24.4, 23.3, 22.7, 22.6, 21.0, 20.6, 19.8, 19.7, 19.62, 19.59, 14.8, 12.9, 12.0, 11.8.

HR-MS (ESI): m/z calc. for $[M+Na]^+$ 597.39480, found 597.39485.

IR (ATR, $\tilde{\nu}$ [cm^{-1}]): 2924 (m, C-H_{aliph}), 2861 (w, C-H_{aliph}), 1754 (m, C=O_{ester}), 1690 (m, C=$O_{thioester}$), 1456 (m), 1411 (w), 1370 (m), 1337 (w), 1303 (w), 1247 (w), 1221 (w), 1194 (m), 1146 (s, C-O-C), 1105 (m), 1066 (s), 969 (m), 941 (m), 861 (w), 729 (w), 680 (w).

3-(4-methoxyphenyl)-4-oxo-4*H*-chromen-7-yl 4-(ethylthio)-4-oxobutanoate **(131d)**

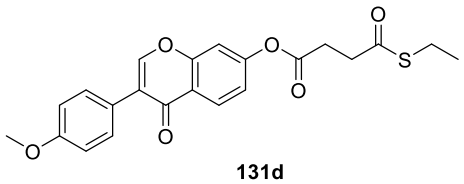

131d

Formononetin (2.68 g, 10.0 mmol) was dissolved in a RBF flask equipped with a stirring bar in a DCM/THF (100 mL, 3:2 v/v) mixture to which TEA (1.8 mL, 13 mmol, 1.3 equiv.) was added. The solution was cooled to 0 °C after which acid chloride **134** (prepared according to GP-K; 2.35 g crude compound, 13.0 mmol, 1.3 equiv.) was carefully added. After 1 h at 0 °C, the mixture was allowed to warm to rt and stirred at this temperature for 40 h. The reaction was quenched by adding demin. water (ca. 40 mL). The aqueous layer was extracted with DCM (3 × 20 mL) and the combined organic layers evaporated *in vacuo*. Then, the crude red-brown oil was diluted in EA (60 mL) and extracted with aq. KOH solution (4 × 20 mL, 10% w/v), demin. water (1 × 20 mL) and brine (1 × 20 mL). The organic layer was dried over anhydrous Na_2SO_4 and solvent was evaporated to yield a crude light-red solid. The product was purified *via* recrystallization from pure EtOH (2 × in 15 mL). The product was obtained as rosé colored scales (2.63 g, 6.38 mmol, 64%).

$C_{22}H_{20}O_6S$ (412.46 g/mol)

R_f: 0.63 (Hex/EA = 7:3) [anis].

Melting point: 110.9–112.1 °C (EtOH).

^{1}H NMR (400 MHz, $CDCl_3$): δ = 8.32 (d, *J* = 8.7 Hz, 1H, C(O)$_{ketone}$C$_{Ar}$C$_{Ar}$*H*), 7.97 (s, 1H, OC*H*CAr), 7.61–7.44 (m, 2H, C$_{Ar}$-*H*), 7.31 (d, *J* = 2.1 Hz, 1H, O$_{ester}$C$_{Ar}$C*H*), 7.17 (dd, *J* = 8.8, 2.2 Hz, 1H, C(O)$_{ketone}$C$_{Ar}$C$_{Ar}$HC$_{Ar}$*H*), 7.01–6.83 (m, 2H), 3.84 (s, 3H, OC*H*$_3$), 3.08–2.99 (m, 2H), 2.98–2.84 (m, 4H, C*H*$_2$CH$_3$ and C*H*$_2$CH$_2$), 1.28 (t, *J* = 7.4 Hz, 3H, CH$_2$C*H*$_3$).

^{13}C NMR (101 MHz, $CDCl_3$): δ 197.7 (*C*(O)SEt), 175.9 (*C*(O)$_{ketone}$), 170.1 (CH$_2$*C*(O)O), 159.9 (*C*$_{Ar}$), 156.8 (*C*$_{Ar}$), 154.4 (*C*$_{Ar}$), 152.7 (*C*$_{Ar}$), 130.2 (*C*$_{Ar}$), 128.0 (*C*$_{Ar}$), 125.3 (*C*$_{Ar}$), 123.9 (*C*$_{Ar}$), 122.5 (*C*$_{Ar}$), 119.5 (*C*$_{Ar}$), 114.2 (*C*$_{Ar}$), 111.0 (*C*$_{Ar}$), 55.5 (ArO*C*H$_3$), 38.3, 29.6, 23.7, 14.8.

HR-MS (ESI): m/z calc. for $[M+Na]^+$ 435.08728, found 435.08789.

IR (ATR, $\tilde{\nu}$ [cm^{-1}]): 3088 (w, C-H$_{arom}$), 3048 (w, C-H$_{arom}$), 3017 (w, C-H$_{arom}$), 2965 (w, C-H$_{aliph}$), 2928 (w, C-H$_{aliph}$), 2838 (w, C-H$_{aliph}$), 1754 (m, C=O$_{ester}$), 1672 (m, C=O$_{thioester}$), 1635 (m), 1605 (m), 1564 (w), 1508 (w), 1437 (m), 1414 (m), 1374 (w), 1291 (m), 1251 (w), 1220 (m), 1167 (m), 1120 (s), 1068 (s), 1016 (m), 971 (s), 933 (m), 863 (m), 826 (m), 800 (s), 766 (s), 736 (m), 695 (s).

(R)-quinolin-4-yl*((1S,2S,4S,5R)*-5-vinylquinuclidin-2-yl)methyl 4-(ethylthio)-4-oxobutanoate **(131f)**

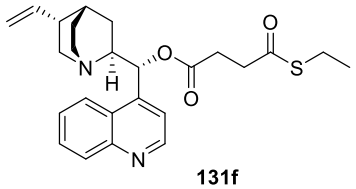

131f

The product **131f** was synthesized by a modified literature procedure.[22] In a RBF equipped with a stirring bar, thioester **134** (1.14 g, 7.00 mmol) was dissolved in THF (30 mL) and cooled to –20 °C. Then, TEA (980 µL, 7.00 mmol, 1 equiv.) and *iso*-butyl chloroformate (910 µL, 7.00 mmol, 1 equiv.) were added and the mixture was stirred for 30 min. Then, Cinchonidine (2.06 g, 7.00 mmol, 1.0 equiv.) was added and the reaction was stirred for 8 h at -20 °C. The reaction was quenched with the addition of demin. water (20 mL). The mixture was diluted with EA (30 mL) and the aqueous layer was extracted with EA (3 × 10 mL). The combined organic layers were washed with sat aq. $NaHCO_3$ (1 × 20 mL) and brine (1 × 20 mL). Purification was achieved by manual column chromatography (Hex/EtOH = 3.5:1–1:3.5). The product was yielded as a colorless solid (1.50 g, 3.4 mmol, 49%).

$C_{25}H_{30}N_2O_3S$ (438.59 g/mol)

R_f: 0.63 (Hex/EtOH = 1:3.5) [UV, anis].

Melting point: 73.4–79.0 °C (EtOH).

^{1}H NMR (400 MHz, $CDCl_3$): δ = 8.84 (d, *J* = 4.5 Hz, 1H, $C_{Ar}H$), 8.75–8.67 (m, 1H, $C_{Ar}H$), 8.16–8.02 (m, 1H, $C_{Ar}H$), 7.72 (tt, *J* = 7.0, 5.2 Hz, 2H, $C_{Ar}H$), 7.32 (d, *J* = 4.5 Hz, 1H, $C_{Ar}H$), 7.20 (s, 1H, $C_{Ar}H$), 5.60 (ddd, *J* = 17.1, 10.3, 6.6 Hz, 1H, C*H*CH_2), 5.02 (dd, *J* = 14.0, 3.8 Hz, 2H), 3.75–3.60 (m, 1H), 3.58–3.39 (m, 2H), 3.24 (s, 1H), 3.09–2.94 (m, 1H), 2.90–2.75 (m, 6H), 2.73–2.53 (m, 1H), 2.18–2.01 (m, 3H), 1.91 (d, *J* = 13.2 Hz, 1H), 1.70 (ddd, *J* = 13.1, 8.2, 5.1 Hz, 1H), 1.18 (t, *J* = 7.4 Hz, 3H, SCH_2CH_3).

^{3}C NMR (101 MHz, $CDCl_3$): δ 197.9 (*C*(O)SEt), 170.0 (CH_2C(O)O), 149.7 (C_{Ar}), 148.5 (C_{Ar}), 142.5 (C_{Ar}), 137.7 (C_{Ar}), 130.3 (C_{Ar}), 129.9 (C_{Ar}), 128.2 (C_{Ar}), 124.8 (C_{Ar}), 123.9 (C_{Ar}), 117.4, 117.1, 71.1, 58.9, 55.0, 43.2, 38.1, 37.2, 29.2, 27.1, 25.0, 23.5, 20.5, 14.7.

HR-MS (ESI): m/z calc. for $[M+H]^+$ 439.20499, found 439.20531.

IR (ATR, $\tilde{\nu}$ [cm^{-1}]): 3056 (w, C-H_{arom}), 2928 (w, C-H_{aliph}), 2876 (w, C-H_{aliph}), 2322 (br, w), 1745 (m, C=O_{ester}), 1679 (m, C=$O_{thioester}$), 1590 (w), 1567 (w), 1508 (w), 1455 (w), 1407 (w), 1366 (w), 1347 (w), 1306 (w), 1235 (w), 1198 (w), 1149 (m), 1064 (m), 971 (m), 925 (m), 855 (m), 810 (m), 762 (m), 725 (m).

S-ethyl 5-((3aS,4S,6aR)-2-oxohexahydro-1*H*-thieno[3,4-*d*]imidazol-4-yl)pentanethioate (**131g**)

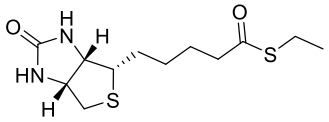

131g

According to GP-A, **131g** was synthesized using biotin (1.47 g, 6.00 mmol, 1.0 equiv.), ethanethiol (1.3 mL, 18.0 mmol, 3.0 equiv.), DMAP (73 mg, 600 µmol, 0.1 equiv.) and DIC (1.0 mL, 6.6 mmol, 1.1 equiv.) by using dry DMF (35 mL) as solvent. The reaction was stirred for 72 h at rt. Purification was achieved by solvent evaporation and dilution with EA (30 mL) and demin. water (30 mL). The aqueous layer was extracted with EA (3 × 15 mL). Afterwards, the combined organic layers were washed with aq. LiCl solution (4 × 20 mL) and brine (1 × 20 mL). The organic layer was dried over anhydrous Na_2SO_4. Purification was achieved by washing the solids with hot *n*-hexane, followed by a manual column chromatography (DCM/MeOH = 30:1–20:1) and recrystallization from pure ACN. The product was obtained as a colorless solid (886 mg, 3.07 mmol, 51%).

$C_{12}H_{20}N_2O_2S_2$ (288.42 g/mol)

R_f: 0.36 (DCM/MeOH = 25:1) [UV, anis - yellow].

Melting point: 152.4–154.7 °C (MeOH).

^{1}H NMR (600 MHz, MeOD-d_4): δ = 4.49 (ddd, *J* = 7.9, 5.0, 1.0 Hz, 1H, NHC*H*CH$_2$S), 4.30 (dd, *J* = 7.9, 4.4 Hz, 1H, NHC*H*CHS), 3.20 (ddd, *J* = 9.0, 5.7, 4.4 Hz, 1H, NHCHC*H*S), 2.93 (dd, *J* = 12.8, 5.0 Hz, 1H, NHCHCH_AH$_B$S), 2.87 (q, *J* = 7.4 Hz, 2H, C(O)SCH_2CH$_3$), 2.71 (d, *J* = 12.8 Hz, 1H, NHCHCH$_A$$H_B$S), 2.58 (t, *J* = 7.4 Hz, 2H), 1.78–1.64 (m, 3H), 1.62–1.55 (m, 1H), 1.49–1.42 (m, 2H), 1.23 (t, *J* = 7.4 Hz, 3H, C(O)SCH$_2$CH_3).

^{13}C NMR (151 MHz, MeOD-d_4): δ = 201.2 (*C*(O)SEt), 166.1(NH*C*(O)NH), 63.4, 61.6, 56.9, 44.5, 41.0, 29.5, 29.4, 26.7, 24.0, 15.2.

HR-MS (ESI): m/z calc. for $[M+Na]^+$ 311.08584, found 311.08625.

IR (ATR, $\tilde{\nu}$ [cm^{-1}]): 3208 (w, N-H), 2928 (w, C-H$_{aliph}$), 2861 (w, C-H$_{aliph}$), 1696 (vs, C=O$_{thioester}$), 1649 (s, C=O$_{urea}$), 1459 (m), 1421 (m), 1377 (w), 1318 (w), 1258 (m), 1154 (m), 1116 (w), 1053 (w), 1008 (m), 975 (m), 945 (w), 915 (w), 870 (w), 822 (w), 725 (m), 695 (m).

S-ethyl 2-(3-cyano-4-isobutoxyphenyl)-4-methylthiazole-5-carbothioate (**131h**)

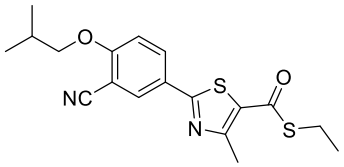

131h

According to GP-A, **131h** was synthesized using febuxostat (2.21 g, 7.0 mmol, 1.0 equiv.), ethanethiol (1.6 mL, 21 mmol, 3 equiv.), DMAP (86 mg, 700 µmol, 0.1 equiv.) and DIC (1.2 mL, 7.7 mmol, 1.1 equiv.). Purification was achieved by filtration through a silica pad (PE/Et_2O = 1:1) and recrystallization from pure Et_2O. The product was yielded as slightly yellow crystals (685 mg, 1.90 mmol, 27%). The analytical data is in good accordance to literature examples.[18]

$C_{18}H_{20}N_2O_2S_2$ (360.49 g/mol)

R_f: 0.32 (Hex/Et_2O = 8:2) [UV].

^{1}H NMR (400 MHz, $CDCl_3$): δ = 8.19 (d, *J* = 2.3 Hz, 1H, $C_{Ar}H$), 8.10 (dd, *J* = 8.9, 2.3 Hz, 1H, $C_{Ar}H$), 7.01 (d, *J* = 8.9 Hz, 1H, $C_{Ar}H$), 3.90 (d, *J* = 6.5 Hz, 2H), 3.09 (q, *J* = 7.4 Hz, 2H), 2.77 (s, 3H), 2.28–2.13 (m, 1H), 1.37 (t, *J* = 7.4 Hz, 3H), 1.09 (d, *J* = 6.7 Hz, 6H).

^{13}C NMR (101 MHz, $CDCl_3$): δ = 183.3 (*C*(O)SEt), 166.7 (C_{Ar}), 162.8 (C_{Ar}), 158.3 (C_{Ar}), 132.8 (C_{Ar}), 132.3 (C_{Ar}), 130.4 (C_{Ar}), 125.8 (C_{Ar}), 115.5 (C_{Ar}), 112.8 (C_{Ar}), 103.2 (C_{Ar}), 75.8, 28.3, 24.8, 19.2, 18.4, 14.9.

IR (ATR, $\tilde{\nu}$ [cm^{-1}]): 3084 (w, C-H_{arom}), 2965 (w, C-H_{aliph}), 2928 (w, C-H_{aliph}), 2869 (w, C-H_{aliph}), 2227 (w, C≡N), 1642 (m, C=O), 1597 (w), 1500 (m), 1467 (w), 1426 (m), 1366 (m), 1288 (s), 1262 (m), 1191 (s), 1124 (m), 1028 (w), 989 (s), 956 (m), 911 (w), 870 (s), 826 (s), 766 (m), 718 (m), 673 (m).

S-ethyl 4-(4-(8-chloro-5,6-dihydro-11*H*-benzo[5,6]cyclohepta[1,2-*b*]pyridin-11-ylidene)piperidin-1-yl)-4-oxobutanethioate **(131i)**

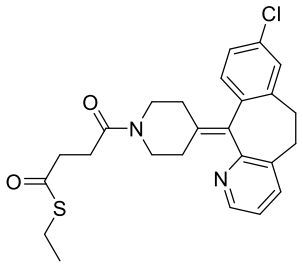

131i

Desloratadin (*free* base; 466.2 mg, 1.50 mmol) was dissolved in a RBF flask, equipped with a stirring bar, in DCM (10 mL) to which TEA (230 µL, 1.65 mmol, 1.1 equiv.) was added. The solution was cooled to 0 °C and acid chloride **134** (prepared according to GP-K; 325 mg crude compound, 1.80 mmol, 1.2 equiv.) was added. After 1 h at 0 °C, the mixture was allowed to warm to rt and stirred for 40 h. The reaction was quenched by addition of demin. water (ca. 5 mL) and the solution was diluted with distilled DCM (10 mL). The organic layer was extracted with aq. HCl (3 × 5 mL, 6 M), sat. $NaHCO_3$ (1 × 5 mL) and brine (1 × 5 mL). The organic layer was dried over anhydrous Na_2SO_4 and solvent was evaporated. The product was purified by flash column chromatography (23 g SiO_2, gradient Hex/EtOH from pure Hex to 85:15 over 5 CV, hold for 2 CV, then gradient to 70:30 over 4 CV). The product was obtained as a colorless foam (473 mg, 1.04 mmol, 69%).

$C_{25}H_{27}ClN_2O_2S$ (455.01 g/mol)

R_f: 0.76 (Hex/EtOH = 1:1) [UV, anis].

Melting point: 57.8–59.7 °C (EA).

^{1}H NMR (400 MHz, $CDCl_3$, mixture of isomers): δ = 8.51 (dd, *J* = 4.6, 1.7 Hz, 1H, $C_{Ar}H$), 7.55 (dt, *J* = 7.8, 2.1 Hz, 1H, $C_{Ar}H$), 7.29–7.17 (m, 4H, $C_{Ar}H$), 4.30–4.00 (m, 1H, $C_{Ar}H$), 3.86–3.72 (m, 1H), 3.59–3.19 (m, 4H), 3.10–2.86 (m, 6H), 2.80 (t, *J* = 6.7 Hz, 2H), 2.74–2.56 (m, 1H), 2.55–2.36 (m, 3H), 1.34 (t, *J* = 7.4 Hz, 3H, SCH_2CH_3).

^{13}C NMR (101 MHz, $CDCl_3$, mixture of isomers): δ 198.7, 169.1, 169.0, 156.7, 156.6, 146.6, 146.5, 139.5, 139.4, 137.5, 137.44, 137.35, 136.69, 136.66, 134.4, 133.3, 133.1, 132.82, 132.80, 130.32, 130.28, 128.88, 128.85, 126.04, 125.99, 122.2, 45.9, 42.7, 42.6, 38.7, 31.53, 31.50, 31.34, 31.31, 31.0, 30.8, 30.3, 30.1, 27.98, 27.95, 23.1, 14.6.

HR-MS (ESI): m/z calc. for $[M+Na]^+$ 477.13740, found 477.13782.

IR (ATR, $\tilde{\nu}$ [cm^{-1}]): 2965 (w, C-H_{aliph}), 2915 (w, C-H_{aliph}), 2861 (w, C-H_{aliph}), 1683 (w, C=$O_{thioester}$), 1638 (m, C=O_{amid}), 1586 (w), 1560 (w), 1429 (m), 1360 (w), 1325 (w), 1266 (w), 1205 (m), 1172 (w), 1087 (w), 1060 (w), 1023 (w), 986 (m), 971 (m), 885 (w), 825 (m), 780 (w), 720 (w).

S-ethyl 2-(1,3-dimethyl-2,6-dioxo-1,2,3,6-tetrahydro-7-purin-7-yl)ethanethioate (**131j**)

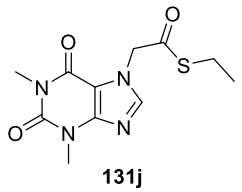

131j

In a RBF equipped with a stirring bar, theophylline-7-acetic acid (2.82 g, 10.0 mmol, 1.0 equiv.) was dissolved in DCM (80 mL) and oxalyl chloride (1.0 mL, 12 mmol, 1.2 equiv.) added. After the addition of a drop of dry DMF, the reaction was stirred for 30 min at rt. The solvent was evaporated and residual oxalyl chloride was distilled off *in vacuo*. The crude acid chloride was suspended in DCM (40 mL) and a solution of ethanethiol (790 µL, 11.0 mmol, 3 equiv.) and TEA (1.5 mL, 11 mmol, 1.1 equiv.) in DCM (40 mL) was added dropwise at 0 °C. The reaction was allowed to warm to rt and stirred for 16 h. The reaction was quenched by addition of demin. water (ca. 10 mL) after which a white solid precipitated. Addition of sat. aq. Na_2CO_3 sol. (ca. 20 mL) led to a clear biphasic solution. The aqueous layer was extracted with DCM (3 × 20 mL,). The combined organic layers were dried over anhydrous $MgSO_4$ and solvent evaporated under reduced pressure. The product was recrystallized in a mixture (Hex/DCM = 1:1) as a white solid (635 mg, 2.25 mmol, 23%).

$C_{11}H_{14}N_4O_3S$ (282.32 g/mol)

R_f: 0.13 (Hex/EA = 1:1) [$KMnO_4$].

Melting point: 101.2–101.9 °C (DCM).

^{1}H NMR (400 MHz, $CDCl_3$): δ = 7.60 (s, 1H, NC*H*N), 5.22 (s, 2H, NCH_2C(O)SEt), 3.58 (s, 3H, CH_3), 3.36 (s, 3H, CH_3), 2.95 (q, *J* = 7.4 Hz, 2H, SCH_2CH$_3$), 1.25 (t, *J* = 7.4 Hz, 3H, SCH$_2$CH_3).

^{13}C NMR (101 MHz, $CDCl_3$): δ = 193.4 (*C*(O)SEt), 155.3, 151.7, 148.7, 142.2, 107.2, 54.5, 29.9, 28.1, 23.8, 14.4.

HR-MS (ESI): m/z calc. for $[M+Na]^+$305.06788, found 305.06787.

IR (ATR, $\tilde{\nu}$ [cm^{-1}]): 3099 (w, C-H_{arom}), 2982 (w, C-H_{aliph}), 2940 (w, C-H_{aliph}), 2880 (w, C-H_{aliph}), 1653 (s, C=$O_{thioester}$), 1604 (m), 1542 (m), 1448 (m), 1400 (m), 1370 (m), 1337 (w), 1281 (w), 1228 (m), 1184 (m), 1053 (w), 1023 (m), 968 (m), 885 (w), 822 (w), 799 (w), 740 (s).

S-ethyl 2-(2-((2,6-dichlorophenyl)amino)phenyl)ethanethioate (**131k**)

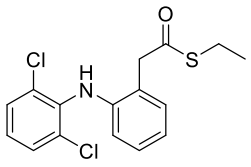

131k

According to GP-A, **131k** was synthesized using diclofenac (2.96 g, 10.0 mmol, 1.0 equiv.), ethanethiol (2.2 mL, 30 mmol, 3.0 equiv.), DMAP (122 mg, 1.00 mmol, 0.1 equiv.) and DCC (2.27 g, 11.0 mmol, 1.1 equiv.). Purification was achieved by fritting through a silica plug (Hex/EA = 1:1 + few drops TEA). Afterwards, the solvents were evaporated under reduced pressure. Then, the crude solid was redissolved in EA (ca. 20 mL) and extracted with aq. HCl (2 × 20 mL, 6 M). The organic layer was reduced *in vacuo* and Hex added. The hydrochloride salt crystallized at –20 °C. The solids were separated from the solvent, washed with Hex and afterwards redissolved in EA (ca. 40 mL). After this, the solution was extracted with aq. KOH solution (10% w/v) and solvents evaporated. The product was gained as a lightly brown solid (599 mg, 1.76 mmol, 18%).

$C_{16}H_{15}Cl_2NOS$ (340.26 g/mol)

R_f: 0.20 (Hex/Et_2O = 8:2) [UV].

Melting point: 77.0–77.7 °C (EA).

^{1}H NMR (600 MHz, $CDCl_3$): δ = 7.34 (d, *J* = 8.0 Hz, 2H, $C_{Ar}H$), 7.23 (dd, *J* = 7.5, 1.5 Hz, 1H, $C_{Ar}H$), 7.13 (td, *J* = 7.8, 1.6 Hz, 1H, $C_{Ar}H$), 7.02–6.94 (m, 2H, $C_{Ar}H$), 6.92 (br s, *J* = 5.1 Hz, 1H, N*H*), 6.54 (dd, *J* = 8.0, 1.1 Hz, 1H, $C_{Ar}H$), 4.00 (s, 2H, ArCH_2), 2.92 (q, *J* = 7.4 Hz, 2H, CH_2CH_3), 1.26 (t, *J* = 7.4 Hz, 3H, CH_2CH_3).

^{13}C NMR (151 MHz, $CDCl_3$): 199.0 (*C*(O)SEt), 142.9 (C_{Ar}), 137.9 (C_{Ar}), 131.1 (C_{Ar}), 129.7 (C_{Ar}), 129.0 (C_{Ar}), 128.3 (C_{Ar}), 124.6 (C_{Ar}), 124.2 (C_{Ar}), 122.1 (C_{Ar}), 118.3 (C_{Ar}), 47.8 (ArCH_2C(O)), 24.0 (C(O)SCH_2CH_3), 14.7 (C(O)SCH_2CH_3).

HR-MS (ESI): m/z calc. for $[M+Na]^+$ 362.01436, found 362.01450.

GC-MS (EI): t_r = 11.36 min, m/z(%) = 339 (6, $[M^{+\bullet}]$), 278 (53, $[M^{+\bullet}-SC_2H_5^{\bullet}]$), 214 (100).

IR (ATR, $\tilde{\nu}$ [cm^{-1}]): 3290 (w, br, N-H), 2924 (w, C-H_{aliph}), 1735 (w), 1661 (m, C=O), 1575 (w), 1500 (m), 1448 (m), 1410 (w), 1292 (w), 1243 (w), 1195 (w), 1169 (w), 1095 (w), 1042 (w), 1012 (m), 971 (w), 915 (w), 870 (w), 837 (w), 769 (m), 743 (s), 703 (m), 672 (m).

HR-MS (APCI): m/z calc. for $[M+H]^+$ 159.08381, found 159.08403.

GC-MS (EI): t_r = 3.43, m/z =130 (14, $[M^{+\bullet}-C_2H_4]$), 97 (33, $[M^{+\bullet}-C_2H_5S^{\bullet}]$), 69 (100, $[M^{+\bullet}-C_2H_5S^{\bullet}-CO]$).

IR (ATR, $\tilde{\nu}$ [cm^{-1}]): 3077 (w, C-H_{alkene}), 2965 (w, C-H_{aliph}), 2931 (w, C-H_{aliph}), 2875 (w, C-H_{aliph}), 1686 (vs, C=O), 1642 (w), 1452 (w), 1415 (w), 1374 (w), 1336 (w), 1262 (w), 1217 (w), 1152 (w), 1109 (w), 1053 (m), 996 (s), 915 (s), 833 (w), 800 (w), 751 (m), 672 (w).

5.5 Synthesis and Analytical Data of Ketones

octan-3-one (**116**)

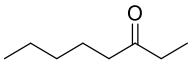

116

According to GP-G, **116** was synthesized using ethyl manganese bromide lithium chloride complex (4.80 mL, 1.20 mmol, 0.25 M, 1.2 equiv.) and *S*-ethyl hexanethioate ester **115a** (160 mg, 1.00 mmol). Purification was achieved by column chromatography (Hex/Et_2O = 30:1). The product was obtained as a colorless oil with a pleasant flowery smell (100 mg, 780 µmol, 78%). The analytical data is in good accordance to reported literature.[23]

$C_8H_{16}O$ (128.22 g/mol)

R_f: 0.47 (Hex/Et_2O = 30:1) [anis - blue].

^{1}H NMR (300 MHz, $CDCl_3$): δ = 2.46–2.34 (m, 4H), 1.62–1.52 (m, 2H), 1.38–1.17 (m, 4H), 1.04 (t, *J* = 7.4 Hz, 3H), 0.87 (t, *J* = 6.8 Hz, 3H).

^{13}C NMR (75 MHz, $CDCl_3$): δ = 212.0 (*C*(O)), 42.5, 35.9, 31.5, 23.7, 22.5, 14.0, 7.9.

GC-MS (EI): t_r = 2.80 min, m/z(%) = 128 (3, [$M^{+\bullet}$]), 99 (40, [$M^{+\bullet}$-$C_2H_5^{\bullet}$]), 57 (100).

IR (ATR, $\tilde{\nu}$ [cm^{-1}]): 2973 (w, C-H_{aliph}), 2939 (w, C-H_{aliph}), 2909 (w, C-H_{aliph}), 2835 (w, C-H_{aliph}), 1683 (s, C=O), 1586 (s), 1482 (m), 1456 (m), 1429 (m), 1344 (m), 1322 (m), 1284 (m), 1251 (s), 1198 (s), 1169 (s), 1083 (w), 1042 (s), 967 (m), 874 (w), 837 (m), 777 (s), 728 (w), 684 (s).

1-phenylpentan-3-one (**120a**)

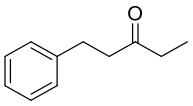

120a

According to GP-G, **120a** was synthesized using ethyl manganese bromide lithium chloride complex (4.3 mL, 1.2 mmol, 0.28 M, 1.2 equiv.) and *S*-ethyl 3-phenylpropanethioate **119a** (194 mg, 1.00 mmol). Purification was achieved by column chromatography (Hex/Et_2O = 9:1). The product was obtained as a colorless oil (154 mg, 950 µmol, 95%). The analytical data is in good accordance with the reported literature.[24]

Upscale Experiment:

The reaction was set up with the following changes: *S*-ethyl 3-phenylpropanethioate **119a** (1.00 g, 5.15 mmol), iron(III) acetyl acetonate (90.9 mg, 257 µmol, 0.05 equiv.) were dissolved in THF (15 mL not degassed) and cooled to -20 °C. Then, ethyl manganese bromide lithium chloride complex (0.22 M, 28 mL, 6.2 mmol, 1.2 equiv.) was added in 3 portions and the reaction stirred for 10 min at the same temperature. The reaction was quenched with aq. sat. NH_4Cl solution (30 mL). The solution was diluted with ethyl acetate (20 mL) and the aq. layer extracted with the same solvent (3 × 30 mL). Purification was achieved by manual column chromatography (Hex/EA = 98:2) to yield a colorless oil (742 mg, 4.57 mmol, 89%).

$C_{11}H_{14}O$ (162.23 g/mol)

R_f: 0.30 (Hex/Et_2O = 9:1) [$KMnO_4$].

^{1}H NMR (400 MHz, $CDCl_3$): δ = 7.22–7.16 (m, 2H, $C_{Ar}H$), 7.13– 7.07 (m, 3H, $C_{Ar}H$), 2.84–2.79 (m, 2H), 2.67– 2.63 (m, 2H), 2.31 (q, *J* = 7.3 Hz, 2H), 0.95 (t, *J* = 7.3 Hz, 3H).

^{13}C NMR (101 MHz, $CDCl_3$): δ = 210.6 (*C*(O)), 141.2 (C_{Ar}), 128.5 (C_{Ar}), 128.4 (C_{Ar}), 126.1 (C_{Ar}), 43.9, 36.2, 29.9, 7.8 (CH_2CH_3).

GC-MS (EI): t_r = 5.37 min, m/z(%) = 162 (49, [$M^{+\bullet}$]), 133 (39,[$M^{+\bullet}$-$C_2H_5^{\bullet}$]), 105 (95, [$M^{+\bullet}$-$C_2H_5^{\bullet}$-CO]), 91 (100, $Bn^{+\bullet}$), 77, 57.

IR (ATR, $\tilde{\nu}$ [cm^{-1}]): 3062 (w, C-H_{arom}), 3025 (w, C-H_{arom}), 2973 (w, C-H_{aliph}), 2935 (w, C-H_{aliph}), 2905 (w, C-H_{aliph}), 1709 (s, C=O), 1601 (w), 1493 (w), 1452 (m), 1411 (m), 1367 (m), 1265 (w), 1163 (w), 1112 (m), 1079 (w), 1053 (w), 1031 (w), 974 (w), 948 (w), 788 (w), 744 (s), 699 (s).

1-(*1H*-indol-3-yl)pentan-3-one (**120b**)

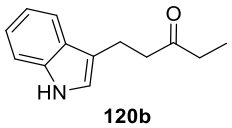

120b

According to GP-G, **120b** was synthesized using ethyl manganese bromide lithium chloride complex (11 mL, 2.2 mmol, 0.20 M, 2.2 equiv.) and *S*-ethyl 3-(1*H*-indol-2-yl)propanethioate **119b** (233 mg, 1.00 mmol). Purification was achieved by flash column chromatography (14 g SiO_2, 1 CV 9:1 = Hex/EA, then gradient over 10 CV to 6:4 = Hex/EA, then hold for 3 CV). The product was obtained as a colorless crystalline solid (163 mg, 810 µmol, 81%). The analytical data is in good accordance with the reported literature.[25]

$C_{13}H_{15}NO$ (201.27 g/mol)

R_f: 0.32 (Hex/Et_2O = 8:2) [$KMnO_4$].

^{1}H NMR (400 MHz, $CDCl_3$): δ = 8.00 (br s, N*H*, 1H), 7.65–7.57 (m, 1H, $C_{Ar}H$), 7.36 (dt, *J* = 8.2, 0.9 Hz, 1H, $C_{Ar}H$), 7.20 (ddd, *J* = 8.2, 7.0, 1.2 Hz, 1H, $C_{Ar}H$), 7.13 (ddd, *J* = 8.0, 7.0, 1.2 Hz, 1H, $C_{Ar}H$), 7.02-6.94 (m, 1H, $C_{Ar}H$), 3.07 (t, *J* = 7.3 Hz, 2H), 2.83 (t, *J* = 7.3 Hz, 2H), 2.42 (q, *J* = 7.3 Hz, C(O)CH_2CH$_3$,2H), 1.05 (t, *J* = 7.3 Hz, C(O)CH_2CH_3, 3H).

^{13}C NMR (101 MHz, $CDCl_3$): δ = 211.6 (*C*(O)), 136.4 (C_{Ar}), 127.3 (C_{Ar}), 122.1 (C_{Ar}), 121.6 (C_{Ar}), 119.4 (C_{Ar}), 118.8 (C_{Ar}), 115.5 (C_{Ar}), 111.3 (C_{Ar}), 42.9, 36.2, 19.6, 7.9.

GC-MS (EI): t_r = 9.07 min, m/z(%) = 201 (30, [$M^{+\bullet}$]), 144 (39, [$M^{+\bullet}$-$C_3H_5O^{\bullet}$]), 130 (100, [$M^{+\bullet}$-$C_5H_9O^{\bullet}$]).

IR (ATR, $\tilde{\nu}$ [cm^{-1}]): 3315 (w, br, N-H), 2972 (w, C-H_{aliph}), 2931 (w, C-H_{aliph}), 2894 (w, C-H_{aliph}), 2885 (w, C-H_{aliph}), 2846 (w, C-H_{aliph}), 1698 (m, C=O), 1616 (w), 1558 (w), 1443 (w), 1407 (w), 1377 (m), 1332 (m), 1265 (w), 1217 (m), 1105 (m), 1042 (m), 1005 (w), 974 (w), 919 (w), 855 (w), 807 (w), 777 (w), 729 (s).

1-*S*-(ethylthio)pentan-3-one (**120c**)

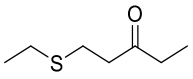

120c

According to GP-G, **120c** was synthesized using ethyl manganese bromide lithium chloride complex (4.7 mL, 1.2 mmol, 0.25 M, 1.2 equiv.) and 3-*S*-(ethylthio)-propylcarboxylic acid *S*-ethyl thioester **119c** (178 mg, 1.00 mmol). Purification was achieved by filtration of the crude product through a pad of silica (Hex/Et_2O = 95:5). The product was obtained as a yellow oil with an unpleasant smell (128.2 mg, 877 µmol, 88%).

$C_7H_{14}OS$ (146.25 g/mol)

R_f: 0.24 (PE/EA = 97:3) [anis].

^{1}H NMR (400 MHz, $CDCl_3$): δ = 2.83–2.65 (m, 4H), 2.54 (q, *J* = 7.4 Hz, 2H), 2.45 (q, *J* = 7.3 Hz, 2H), 1.25 (t, *J* = 7.4 Hz, 3H), 1.06 (t, *J* = 7.3 Hz, 3H).

^{13}C NMR (101 MHz, $CDCl_3$): δ = 209.9 (*C*(O)), 42.5, 36.4, 26.4, 25.6, 14.9, 7.8.

GC-MS (EI): t_r = 4.11 min, m/z (%) = 146 (39, [$M^{+\bullet}$]), 117 (15, [$M^{+\bullet}$-$C_2H_5^{\bullet}$]), 89 (47, [$M^{+\bullet}$-$C_2H_5^{\bullet}$-CO]), 57 (100, [$C_3H_5O^{+\bullet}$]).

HR-MS (EI): m/z calc. for [M]$^+$ 146.075987, found 146.07375.

IR (ATR, $\tilde{\nu}$ [cm^{-1}]): 2969 (m, C-H_{aliph}), 2928 (m, C-H_{aliph}), 1710 (s, C=O), 1452 (m), 1414 (m), 1355 (m), 1262 (m), 1191 (w), 1165 (w), 1109 (m), 1059 (w), 971 (w), 945 (w), 882 (w), 785 (w), 740 (w).

1-(4-*para*-anisyl)butan-2-one (**120d**)

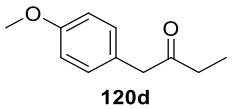

120d

According to GP-G, **120d** was synthesized using ethyl manganese bromide lithium chloride complex (7.1 mL, 1.2 mmol, 0.17 M, 1.2 equiv.) and *S*-ethyl 2-(4-methoxyphenyl)ethanethioate **119d** (210 mg, 1.00 mmol). Purification was achieved by manual column chromatography (Hex/EA = 30:1). The product was obtained as a brown oil (135 mg, 757 µmol, 76%). The analytical data is in good accordance to reported literature.[26]

$C_{11}H_{14}O_2$ (178.23 g/mol)

R_f: 0.25 (Hex/EA = 30:1) [anis].

^{1}H NMR (400 MHz, $CDCl_3$): δ = 7.16–7.08 (m, 2H, $C_{Ar}H$), 6.90–6.82 (m, 2H, $C_{Ar}H$), 3.79 (s, 3H, OCH_3), 3.62 (s, 2H, $PhCH_2$), 2.46 (q, *J* = 7.3 Hz, 2H, $C(O)CH_2CH_3$), 1.02 (t, *J* = 7.3 Hz, 3H, $C(O)CH_2CH_3$).

^{13}C NMR (101 MHz, $CDCl_3$): δ = 209.6 (*C*(O)), 158.7 (C_{Ar}), 130.5 (C_{Ar}), 126.6 (C_{Ar}), 114.2 (C_{Ar}), 55.4, 49.0, 35.2 (CH_2CH_3), 7.9 (CH_2CH_3).

GC-MS (EI): t_r = 6.31 min, m/z(%) = 178 (12, [$M^{+\bullet}$]), 121 (100, [$M^{+\bullet}$-$C_3H_5^{\bullet}$]).

1,1,1-triphenylpentan-3-one (**120f**)

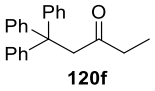

120f

According to GP-G, **120f** was synthesized using ethyl manganese bromide lithium chloride complex (4.4 mL, 1.2 mmol, 0.27 M, 1.2 equiv.) and *S*-ethyl 3,3,3-triphenylpropanethioate **119f** (210 mg, 1.00 mmol). Purification was achieved by flash column chromatography (23 g SiO_2, 8 CV pure PE to PE/EA = 92:8). The product was obtained as colorless solid (206 mg, 655 µmol, 66%).

$C_{23}H_{22}O$ (314.43 g/mol)

R_f: 0.22 (PE/EA = 30:1) [UV].

Melting point: 89.7–90.1 °C (EA).

GC-MS (EI): t_r = 11.18 min, m/z(%) = 243 (100, [$M^{+\bullet}$]), 165 (76, [$M^{+\bullet}$-$C_6H_6^{\bullet}$]).

^{1}H NMR (400 MHz, $CDCl_3$): δ = 7.34–7.18 (m, 15H, $C_{Ar}H$), 3.86 (s, 2H, Ph_3CCH_2), 2.16 (q, *J* = 7.2 Hz, 2H, $C(O)CH_2$), 0.87 (t, *J* = 7.2 Hz, 3H, $C(O)CH_2CH_3$).

^{13}C NMR (101 MHz, $CDCl_3$): δ = 209.0 (*C*(O)Et), 146.9 ($C_{Ar,}$), 129.3 ($C_{Ar,}$), 128.0 (C_{Ar}), 126.3 ($C_{Ar,}$), 56.2, 53.2, 38.2 (CH_2CH_3), 7.8 (CH_2CH_3).

IR (ATR, $\tilde{\nu}$ [cm^{-1}]): 3058 (w, C-H_{arom}), 3021 (w, C-H_{arom}), 2928 (w, C-H_{aliph}), 2854 (w, C-H_{aliph}), 1694 (m, C=O), 1664 (w), 1593 (w), 1519 (w), 1489 (m), 1441 (m), 1404 (w), 1377 (w), 1333 (w), 1258 (w), 1220 (w), 1187 (w), 1161 (w), 1113 (w), 1083 (w), 1027 (m), 953 (m), 818 (w), 781 (w), 777 (w), 751 (m), 695 (s).

4-methylundecan-5-one (**120i**)

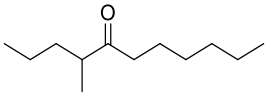

120i

According to GP-G, **120i** was synthesized using *n*-hexyl manganese bromide lithium chloride complex (4.1 mL, 1.2 mmol, 0.29 M, 1.2 equiv.) and *S*-ethyl 2-methylpentanethioate **119i** (160 mg, 1.00 mmol). Purification was achieved by manual column chromatography (15–60 µm SiO_2 - Merck, Hex/EA = 99:1). The product was obtained as a colorless oil (91 mg, 491 µmol, 49%).

$C_{12}H_{24}O$ (184.32 g/mol)

R_f: 0.34 (Hex/EA =99:1) [anis].

^{1}H NMR (400 MHz, $CDCl_3$): δ = 2.57–2.45 (m, 1H), 2.44–2.35 (m, 2H), 1.69–1.48 (m, 3H), 1.36–1.19 (m, 9H), 1.04 (d, *J* = 6.9 Hz, 3H, C(O)CHC*H*$_3$), 0.93–0.83 (m, 6H).

^{13}C NMR (101 MHz, $CDCl_3$): δ = 215.3 (*C*(O)), 46.2, 41.3, 35.3, 31.8, 29.1, 23.8, 22.7, 20.6, 16.5, 14.3, 14.2.

GC-MS (EI): t_r = 3.53 min, m/z(%) = 131 (17, [$M^{+\bullet}$-$C_5H_{11}^{\bullet}$]), 99 (38, [$M^{+\bullet}$-$C_6H_{13}^{\bullet}$]), 71 (100, [$M^{+\bullet}$-$C_6H_{13}^{\bullet}$-CO]), 55.

HR-MS (EI, 45 eV): m/z calc. for $[M]^+$ 184.182166, found 184.18068.

IR (ATR, $\tilde{\nu}$ [cm^{-1}]): 2957 (m, C-H_{aliph}), 2927 (s, C-H_{aliph}), 2863 (m, C-H_{aliph}), 1709 (s, C=O), 1459 (m), 1407 (w), 1373 (w), 1306 (w), 1261 (w), 1232 (w), 1191 (w), 1165 (w), 1101 (w), 1057 (w), 1016 (w), 870 (w), 803 (w), 731 (w).

4-phenylhexan-3-one (**120j**)

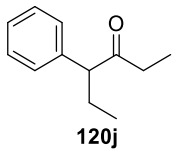

120j

According to GP-G, **120j** was synthesized using ethyl manganese bromide lithium chloride complex (6.0 mL, 1.2 mmol, 0.2 M, 1.2 equiv.) and *S*-ethyl 2-phenylbutanethioate **119j** (208 mg, 1.00 mmol). Purification was achieved by manual column chromatography (Hex/EA = 98:2). The product was obtained as a colorless oil (62 mg, 353 µmol, 35%). The analytical data is in good accordance to reported literature.[27]

$C_{12}H_{16}O$ (176.26 g/mol)

R_f: 0.67 (Hex/EA = 30:1) [$KMnO_4$].

^{1}H NMR (300 MHz, $CDCl_3$): δ = 7.32–7.10 (m, 5H, $C_{Ar}H$), 3.48 (t, J = 7.4 Hz, 1H, PhC*H*), 2.47–2.19 (m, 2H), 2.12–1.91 (m, 1H), 1.80–1.56 (m, 1H), 0.91 (t, *J* = 7.4 Hz, 3H), 0.77 (t, *J* = 7.4 Hz, 3H).

^{13}C NMR (75 MHz, $CDCl_3$): δ = 211.3 (*C*(O)), 139.3 (C_{Ar}), 128.9 (C_{Ar}), 128.3 (C_{Ar}), 127.2 (C_{Ar}), 60.6 (Ph*C*H), 35.2, 25.4, 12.2, 8.0 (CH_3).

GC-MS (EI): t_r = 5.22 min, m/z(%) = 176 (6, [$M^{+\bullet}$]), 119 (31, [$M^{+\bullet}$-$C_3H_5O^{\bullet}$]), 91 (100, [$Bz^{+\bullet}$]).

IR (ATR, $\tilde{\nu}$ [cm^{-1}]): 3062 (w, C-H_{arom}), 3025 (w, C-H_{arom}), 2973 (w, C-H_{aliph}), 2935 (w, C-H_{aliph}), 2905 (w, C-H_{aliph}), 1709 (s, C=O), 1601 (w), 1493 (w), 1452 (m), 1411 (m), 1367 (m), 1265 (w), 1163 (w), 1112 (m), 1079 (w), 1053 (w), 1031 (w), 974 (w), 948 (w), 788 (w), 744 (s), 699 (s).

1-(*trans*-4-*iso*propylcyclohexyl)propan-1-one (**120k**)

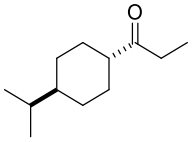

120k

According to GP-G, **120k** was synthesized using ethyl manganese bromide lithium chloride complex (5.5 mL, 1.2 mmol, 0.22 M, 1.2 equiv.) and *S*-ethyl *trans*-4-*iso*-propylcyclohexane-1-carbothioate **119k** (214 mg, 1.00 mmol). The reaction was stirred for 15 min at -20 °C. Purification was achieved by manual column chromatography (Hex/EA = 98:2). The product was obtained as a colorless oil (130 mg, 713 µmol, 71%).

$C_{12}H_{22}O$ (182.31 g/mol)

R_f: 0.44 (Hex/EA = 98:2) [anis].

^{1}H NMR (400 MHz, $CDCl_3$): δ = 2.45 (q, *J* = 7.3 Hz, 2H, C(O)CH_2), 2.27 (tt, *J* = 12.2, 3.4 Hz, 1H), 1.94–1.73 (m, 4H), 1.48–1.20 (m, 3H), 1.07–0.91 (m, 6H), 0.85 (d, *J* = 6.8 Hz, 6H, CH(CH_3)$_2$).

^{13}C NMR (101 MHz, $CDCl_3$): δ = 215.1 (*C*(O)), 51.0, 43.5, 33.9, 32.9, 29.2, 28.9, 19.9, 7.9.

GC-MS (EI): t_r = 6.66 min, m/z(%) = 182 (13, [$M^{+\bullet}$]), 164 (17), 153 (16, [$M^{+\bullet}$-$C_2H_5^{\bullet}$]), 125 (49, [$M^{+\bullet}$-$C_2H_5^{\bullet}$-CO]), 110 (21, [$M^{+\bullet}$-$C_2H_5^{\bullet}$-CO-$CH_3^{\bullet}$]), 83 (46, [$C_6H_{11}^{+\bullet}$]), 69 (100, [$C_5H_9^{+\bullet}$]).

HR-MS (ESI): m/z calc. for $[M+Na]^+$ 205.15629, found 205.15666.

IR (ATR, $\tilde{\nu}$ [cm^{-1}]): 2928 (s, C-H_{aliph}), 2857 (m, C-H_{aliph}), 1706 (s, C=O), 1452 (m), 1411 (w), 1373 (m), 1340 (w), 1229 (w), 1173 (w), 1143 (w), 1116 (w), 1076 (w), 1054 (w), 1012 (w), 982 (w), 941 (w), 897 (w), 852 (w), 796 (w).

1-(1-tosylpiperidin-4-yl)propan-1-one (**120l**)

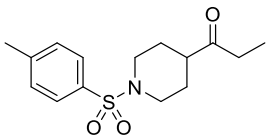

120l

According to GP-G, **120l** was synthesized using ethyl manganese bromide lithium chloride complex (5.7 mL, 1.2 mmol, 0.21 M, 1.2 equiv.) and *S*-ethyl 1-tosylpiperidine-4-carbothioate **119l** (327 mg, 1.00 mmol). Purification was achieved by manual column chromatography (Hex/EA = 8:2). The product was obtained as a colorless solid (283 mg, 958 µmol, 96%).

$C_{15}H_{21}NO_3S$ (295.40 g/mol)

R_f: 0.38 (Hex/EA = 8:2) [UV, anis].

Melting point: 107.9–108.5 °C (EA).

^{1}H NMR (400 MHz, $CDCl_3$): δ = 7.68–7.60 (m, 2H, $C_{Ar}H$), 7.32 (d, *J* = 8.0 Hz, 2H, $C_{Ar}H$), 3.77–3.66 (m, 2H), 2.47–2.34 (m, 7H), 2.31–2.19 (m, 1H), 1.94–1.83 (m, 2H), 1.80–1.65 (m, 2H), 1.01 (t, *J* = 7.2 Hz, 3H, C(O)CH_2C*H*$_3$).

^{13}C NMR (101 MHz, $CDCl_3$): δ = 212.1 (*C*(O)), 143.7 (C_{Ar}), 133.2 (C_{Ar}), 129.8 (C_{Ar}), 127.83 (C_{Ar}), 47.3, 45.7, 33.7, 27.2, 21.7, 7.8 (*C*H_3).

HR-MS (ESI): m/z calc. for $[M+Na]^+$ 318.11344, found 318.11371.

IR (ATR, $\tilde{\nu}$ [cm^{-1}]): 2972 (w, C-H_{aliph}), 2920 (w, C-H_{aliph}), 2846 (w, C-H_{aliph}), 1702 (m, C=O), 1661 (w), 1593 (w), 1445 (w), 1410 (w), 1377 (w), 1322 (m), 1284 (m), 1243 (m), 1157 (s), 1127 (m), 1094 (m), 1053 (m), 1020 (w), 979 (w), 926 (m), 866 (w), 833 (w), 807 (w), 759 (w), 722 (m), 699 (m).

trans-1-(2-methylcyclopropyl)heptan-1-one (**120m**)

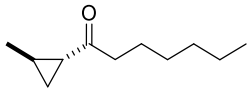

120m

According to GP-G, **120m** was synthesized using *n*-hexyl manganese bromide lithium chloride complex (4.1 mL, 1.2 mmol, 0.29 M, 1.2 equiv.) and *S*-ethyl 2-methylcyclopropane-1-carbothioate **119m** (144 mg, 1.00 mmol). Purification was achieved by manual column chromatography (Hex/Et_2O = 99:1 to 7:3). The product was obtained as a colorless oil (96 mg, 572 µmol, 57%).

$C_{11}H_{20}O$ (168.28 g/mol)

R_f: 0.08 (Hex/EA = 99:1) [anis - yellow].

^{1}H NMR (400 MHz, $CDCl_3$): δ = 2.50 (t, *J* = 7.5 Hz, 2H), 1.69–1.54 (m, 3H), 1.47–1.14 (m, 8H), 1.10 (d, *J* = 6.0 Hz, 3H), 0.92–0.83 (m, 3H), 0.68 (ddd, *J* = 7.7, 6.3, 3.5 Hz, 1H).

^{13}C NMR (101 MHz, $CDCl_3$): δ = 210.9 (*C*(O)), 43.8, 31.8, 29.7, 29.1, 24.2, 22.7, 20.0, 19.3, 18.3, 14.2.

GC-MS (EI): t_r = 4.78 min, m/z(%) = 168 (1, [$M^{+\bullet}$]), 98 (53, [$M^{+\bullet}$-C_5H_{10}]), 83 (100, [$M^{+\bullet}$-C_5H_{10}-$CH_3^\bullet$]), 55.

HR-MS (EI, 45 eV): m/z calc. for $[M]^+$ 168.15123, found 168.150866.

IR (ATR, $\tilde{\nu}$ [cm^{-1}]): 2954 (m, C-H_{aliph}), 2927 (m, C-H_{aliph}), 2861 (m, C-H_{aliph}), 1694 (s, C=O), 1456 (m), 1403 (m), 1377 (m), 1355 (w), 1351 (w), 1325 (w), 1262 (w), 1202 (w), 1161 (w), 1131 (w), 1082 (s), 1034 (m), 960 (w), 938 (w), 855 (m), 807 (w), 762 (w), 725 (w).

1-((1*S**,2*S**,4*S**)-bicyclo[2.2.1]hept-5-en-2-yl)propan-1-one (**120n**) and a mixture with diastereomer (**120n+120n'**)

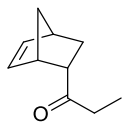

120n

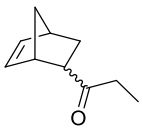

120n + 120n'

According to GP-G, the products **120n** as well as **120n +120n** were synthesized using ethyl manganese bromide lithium chloride complex (7.1 mL, 1.2 mmol, 0.17 M, 1.2 equiv.) and *S*-ethyl (1*S*,2*R*,4*S*)-bicyclo[2.2.1]hept-5-ene-2-carbothioate **119n** or the mixture **119n + 119n'** (182 mg, 1.00 mmol). Both purifications were achieved by manual column chromatography (Hex/EA = 9:1). Additional purification was necessary which in both cases was achieved by bulb-to-bulb distillation (165 °C, 200 mbar). **120n** was obtained as a colorless oil (113 mg, 752 µmol, 75%) and mixture **120n + 120n'** also as colorless oil (106 mg, 706 µmol, 71%, d.r. = 5(**120n**):3(**120n'**)).

$C_{10}H_{14}O$ (150.22 g/mol)

R_f: 0.30 (PE/EA = 98:2) [anis - yellow].

120n: ^{1}H NMR (400 MHz, $CDCl_3$): δ = 6.15 (dd, *J* = 5.7, 3.1 Hz, 1H, $C_{alkene}H$), 5.83 (dd, *J* = 5.7, 2.8 Hz, 1H, $C_{alkene}H$), 3.25–3.20 (m, 1H), 3.01 (dt, *J* = 9.1, 4.0 Hz, 1H), 2.92–2.87 (m, 1H), 2.44 (qd, *J* = 7.3, 3.3 Hz, 1H), 1.75 (ddd, *J* = 11.8, 9.1, 3.7 Hz, 1H), 1.54–1.40 (m, 2H), 1.32 (dt, *J* = 8.2, 1.6 Hz, 1H), 1.02 (t, *J* = 7.4 Hz, 3H).

120n: ^{13}C NMR (101 MHz, $CDCl_3$): δ = 211.8 (*C*(O)Et), 137.9 (C_{alkene}), 131.5 (C_{alkene}), 51.4, 50.1, 46.1, 42.8, 35.0, 27.6, 8.1.

120n + 120n ‘: ^{1}H NMR (400 MHz, $CDCl_3$): δ = 6.17–6.07 (m), 5.81 (dd, *J* = 5.8, 2.7 Hz, 1H), 3.21 (s), 3.05–2.85 (m), 2.63–2.32 (m), 1.85 (dt, *J* = 11.5, 4.1 Hz, 1H), 1.73 (ddd, *J* = 12.3, 8.9, 3.7 Hz, 1H), 1.51–1.17 (m), 1.10–0.96 (m).

120n + 120n ‘: ^{13}C NMR (101 MHz, $CDCl_3$): δ = 213.6 (*C*(O)Et), 211.7 (*C*(O)Et), 138.3 (C_{alkene}), 137.8 (C_{alkene}), 136.0 (C_{alkene}), 131.4 (C_{alkene}), 51.4, 50.5, 50.0, 46.08, 46.0, 45.8, 42.7, 41.8, 35.9, 35.0, 29.4, 27.6, 8.2, 8.0.

HR-MS (ESI): m/z calc. for $[M+Na]^+$ 173.09369, found 173.09396.

GC-MS (EI, mixture): t_r = 4.04 min, m/z(%) = 150 (10, $[M^{+\bullet}]$), 66 (100, $[C_5H_6^{+\bullet}]$); t_r = 4.20 min, m/z(%) = 150 (12, $[M^{+\bullet}]$), 66 (100, $[C_5H_6^{+\bullet}]$).

IR (**3m**, ATR, $\tilde{\nu}$ [cm^{-1}]): 3136 (w, C-H_{arom}), 3062 (w, C-H_{arom}), 2969 (m, C-H_{aliph}), 2935 (w, C-H_{aliph}), 2869 (w, C-H_{aliph}), 1683 (s, C=O), 1448 (w), 1415 (w), 1374 (w), 1333 (w), 1262 (m), 1224 (w), 1176 (w), 1131 (w), 1126 (w), 1065 (s), 1030 (m), 1000 (s), 966 (w), 920 (m), 844 (s), 807 (m), 777 (m), 747 (m), 706 (vs).

1-(adamantan-1-yl)heptan-1-one (**120o**)

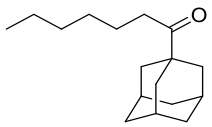

120o

According to GP-G, **120o** was synthesized using *n*-hexyl manganese bromide lithium chloride complex (4.4 mL, 0.27 M, 1.2 mmol, 1.2 equiv.) and *S*-ethyl adamantane-1-carbothioate **119o** (224 mg, 1 mmol). The yield was calculated by determination of the relative composition R of the ethyl thioate and ethyl ketone group in the ^{1}H NMR spectrum (298 µmol, 30%).

The sample concentration was determined by the formula:

$$R = \frac{n_p}{n_{SM}} = \frac{I_P}{N_p} / \frac{I_{SM}}{N_{SM}} = \frac{0.495}{1.00} = 0.5$$

$$m_{total} = M_P * n_P + M_{SM} * \frac{n_P}{R}$$

$$n_P = \frac{m_{total}}{\left(\frac{M_{SM}}{R}\right) + M_P} = \frac{191\ mg}{\left(\frac{224.36 \frac{g}{mol}}{0.49}\right) + 192.3\ \frac{g}{mol}} = 298\ \mu mol$$

R: relative composition
I_p: Integral of product
I_{SM}: Integral starting material
n_P: amount of product
n_{SM}: amount of starting material
N_P: nuclei count of product
N_{SM}: nuclei count of starting material
M_P: molecular mass of the product
M_{SM}: molecular mass of the starting material

$C_{13}H_{20}O$ (192.30 g/mol)

R_f: 0.35 (Hex/ACN = 99:1) [anis].

2,5-heptadione (**120p**)

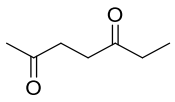

120p

According to GP-G, **120p** was synthesized using ethyl manganese bromide lithium chloride complex (4.8 mL, 1.2 mmol, 0.25 M, 1.2 equiv.) and *S*-ethyl 4-oxopentanethioate **119p** (160 mg, 1.00 mmol). Purification was achieved by column chromatography (Hex/Et_2O = 1:1). The product was obtained as a yellow oil (95 mg, 739 µmol, 74%). The spectral data is in good accordance to previous literature.[28]

$C_7H_{12}O_2$ (128.17 g/mol)

R_f: 0.32 (Hex/Et_2O = 1:1) [$KMnO_4$].

^{1}H NMR (400 MHz, $CDCl_3$): δ = 2.76–2.62 (m, 4H), 2.47 (q, *J* = 7.3 Hz, C(O)C*H*$_2$CH$_3$, 2H), 2.17 (s, C(O)CH$_3$, 3H), 1.04 (t, *J* = 7.3, C(O)CH$_2$C*H*$_3$, 3H).

^{13}C NMR (101 MHz, $CDCl_3$): δ = 210.1 (*C*(O)), 207.5 (*C*(O)), 37.1, 36.0, 35.8, 30.1, 7.9.

GC-MS (EI): t_r = 3.07 min, m/z(%) = 99 (100, [$M^{+\bullet}$-$C_2H_5^{\bullet}$]).

HR-MS (ESI): m/z calc. for $[M+Na]^+$ 151.07295, found 151.07319.

IR (ATR, $\tilde{\nu}$ [cm^{-1}]): 2976 (w, C-H$_{aliph}$), 2939 (w, C-H$_{aliph}$), 2879 (w, C-H$_{aliph}$), 1713 (s, C=O), 1455 (w), 1415 (w), 1370 (m), 1246 (m), 1176 (s), 1112 (m), 1028 (m), 971 (w), 859 (w), 796 (w), 766 (w).

ethyl 6-oxooctanoate (**120q**)

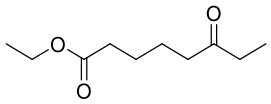

120q

According to GP-G, **120q** was synthesized using ethyl manganese bromide lithium chloride complex (4.3 mL, 1.2 mmol, 0.28 M, 1.2 equiv.) and ethyl 6-(ethylthio)-6-oxohexanoate **119q** (218 mg, 1.00 mmol). Purification was achieved by manual column chromatography (Hex/Et$_2$O = 7:3). The product was obtained as a colorless oil (150 mg, 805 µmol, 81%).

$C_{10}H_{18}O_3$ (186.25 g/mol)

R_f: 0.31 (Hex/Et$_2$O = 7:3) [$KMnO_4$].

^{1}H NMR (400 MHz, $CDCl_3$): δ = 4.10 (q, *J* = 7.2, 1.1 Hz, 2H), 2.42–2.37 (m, 4H), 2.32–2.23 (m, 2H), 1.65–1.52 (m, 4H), 1.23 (t, *J* = 7.2, 1.1 Hz, 3H), 1.03 (t, *J* = 7.4, 1.1 Hz, 3H).

^{13}C NMR (101 MHz, $CDCl_3$): δ = 211.3 (*C*(O)Et), 173.5 (*C*(O)OEt), 60.4, 42.0, 36.0, 34.2, 24.6, 23.4, 14.3, 7.9 (C(O)CH_2*C*H_3).

GC-MS (EI): t_r = 5.59 min, m/z(%) = 157 (10, [$M^{+\bullet}$-$C_2H_5^{\bullet}$]), 115 (21, [$M^{+\bullet}$-$C_4H_7O^{\bullet}$]), 110 (69), 101 (23, [$M^{+\bullet}$-$C_5H_9O^{\bullet}$]), 57 (100, [$H_5C_2O^{+\bullet}$ or $H_9C_4^{+\bullet}$]).

HR-MS (ESI): m/z calc. for [M+Na]$^+$ 209.11482, found 209.11522.

IR (ATR, $\tilde{\nu}$ [cm^{-1}]): 2976 (w, C-H$_{aliph}$), 2939 (w, C-H$_{aliph}$), 2879 (w, C-H$_{aliph}$), 1730 (s, C=O$_{ester}$), 1712 (s, C=O$_{ketone}$), 1455 (w), 1414 (w), 1370 (m), 1243 (m), 1176 (s), 1113 (m), 1028 (m).

S-ethyl 2-methyl-5-oxoheptanethioate (**123**)

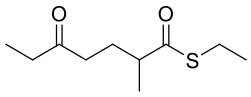

123

According to GP-G, **123** was synthesized using ethyl manganese bromide lithium chloride complex (4.6 mL, 1.2 mmol, 0.26 M, 1.2 equiv.) and *S*,*S*-diethyl 2-methylpentanebis(thioate) **122** (234 mg, 1.00 mmol). Purification was achieved by column chromatography (Hex/EA = 97:3). The product was obtained as a colorless oil (126 mg, 623 µmol, 62%).

$C_{10}H_{18}O_2S$ (202.31 g/mol)

R_f: 0.39 (Hex/EA = 97:3) [anis].

^{1}H NMR (300 MHz, $CDCl_3$): δ = 2.85 (q, *J* = 7.4 Hz, 2H), 2.72–2.51 (m, 1H), 2.48–2.33 (m, 4H), 2.03–1.63 (m, 2H), 1.24 (t, *J* = 7.4 Hz, 3H), 1.17 (d, *J* = 6.9 Hz, 3H), 1.04 (t, *J* = 7.3 Hz, 3H).

^{13}C NMR (75 MHz, $CDCl_3$): δ = 210.7 (Et*C*(O)CH_2), 203.6 (*C*(O)SEt), 47.8, 39.6, 36.1, 27.9, 23.2, 18.0, 14.9, 8.0.

GC-MS (EI): t_r = 6.09 min, m/z(%) = 141 (20, [$M^{+\bullet}$-$C_2H_5S^{\bullet}$]), 57 (100, [$M^{+\bullet}$-$C_7H_{13}OS^{\bullet}$]).

HR-MS (ESI): m/z calc. for $[M+Na]^+$ 225.09197, found 225.09236.

IR (ATR, $\tilde{\nu}$ [cm^{-1}]): 2972 (w, C-H_{aliph}), 2932 (w, C-H_{aliph}), 2879 (w, C-H_{aliph}), 1713 (s, C=O_{ketone}), 1679 (s, C=$O_{thioester}$), 1452 (m), 1414 (w), 1370 (m), 1262 (w), 1194 (w), 1112 (w), 1049 (w), 1019 (w), 956 (s), 897 (w), 822 (w), 736 (w), 695 (w).

4-methylnona-3,6-dione (**124**)

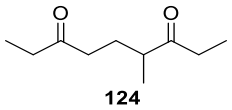

124

According to GP-G, **124** was synthesized using ethyl manganese bromide lithium chloride complex (4.8 mL, 2.2 mmol, 0.20 M, 1.2 equiv.) and *S*,*S*-diethyl 2-methylpentanebis(thioate) **122** (234 mg, 1.00 mmol). Purification was achieved by manual column chromatography (Hex/EA = 9:1). The product was obtained as a colorless oil (135 mg, 793 µmol, 79%).

$C_{10}H_{18}O_2$ (170.25 g/mol)

R_f: 0.08 (Hex/EA = 9:1) [anis].

^{1}H NMR (400 MHz, $CDCl_3$): δ = 2.58–2.26 (m, 7H), 1.97–1.83 (m, 1H), 1.72–1.56 (m, 1H), 1.11–0.93 (m, 9H).

^{13}C NMR (101 MHz, $CDCl_3$): δ = 214.9 (*C*(O)), 211.2 (*C*(O)), 45.23, 39.7, 36.0, 34.3, 26.7, 16.7, 7.94, 7.90.

GC-MS (EI, method B): t_r = 14.20 min, m/z(%) = 170 (10, [$M^{+\bullet}$]), 141 (11, [$M^{+\bullet}$-$C_2H_5^{\bullet}$]), 141 (11, [$M^{+\bullet}$-$C_2H_5^{\bullet}$-C_2H_4]), 57 (100, [$C_3H_5O^{+\bullet}$]).

HR-MS (ESI): m/z calc. for $[M+Na]^+$ 193.11990, found 193.12016.

IR (ATR, $\tilde{\nu}$ [cm^{-1}]): 2972 (m, C-H_{aliph}), 2932 (m, C-H_{aliph}), 2885 (w, C-H_{aliph}), 1709 (vs, C=O), 1456 (m), 1411 (w), 1370 (m), 1254 (w), 1191 (w), 1106 (m), 1030 (w), 971 (w).

propiophenone (**130a**)

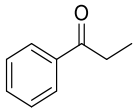

130a

According to GP-G, **130a** was synthesized using ethyl manganese bromide lithium chloride complex (4.1 mL, 1.2 mmol, 0.29 M, 1.2 equiv.) and *S*-ethyl benzothioate **129a** (166 mg, 1.00 mmol). Purification was achieved by column chromatography (Hex/Et_2O = 95:5). The product was obtained as a yellow oil with a characteristic smell (128 mg, 954 µmol, 95%). The spectral data matches the data given by the chemical vendors (e.g. Sigma Aldrich).

$C_9H_{10}O$ (134.18 g/mol)

R_f: 0.38 (Hex/Et_2O = 95:5) [$KMnO_4$].

^{1}H NMR (400 MHz, $CDCl_3$): δ = 7.95 (dt, *J* = 8.7, 1.6 Hz, 2H, $C_{Ar}H$), 7.58–7.49 (m, 1H, $C_{Ar}H$), 7.45–7.37 (m, 2H, Ar*H*), 2.99 (q, *J* = 7.3, 2H, C(O)CH_2CH$_3$), 1.21 (t, *J* = 7.3, 3H, C(O)CH$_2$CH_3).

^{13}C NMR (101 MHz, $CDCl_3$): δ = 200.9 (*C*(O)), 137.0 (C_{Ar}), 132.9 (C_{Ar}), 128.6 (C_{Ar}), 128.0 (C_{Ar}), 31.9 (C(O)*C*H$_2$CH$_3$), 8.3(C(O)CH$_2$*C*H$_3$).

1-(*p*-tolyl)propan-1-one (**130b**)

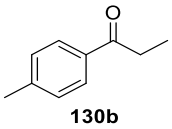

130b

According to GP-G, **130b** was synthesized using ethyl manganese bromide lithium chloride complex (4.4 mL, 1.2 mmol, 0.27 M, 1.2 equiv.) and *S*-ethyl 4-methylbenzothioate **129b** (148 mg, 1.00 mmol). Purification was achieved by manual column chromatography (Hex/Et_2O = 98:2). The product was obtained as a colorless oil with a distinct smell (114 mg, 766 µmol, 77%). The spectral data matches previous literature examples.[29]

$C_{10}H_{12}O$ (148.21 g/mol)

R_f: 0.17 (Hex/Et_2O = 98:2) [anis].

^{1}H NMR (300 MHz, $CDCl_3$): δ = 7.92–7.81 (m, 2H, $C_{Ar}H$), 7.31–7.20 (m, 2H, $C_{Ar}H$), 2.98 (q, *J* = 7.3 Hz, 2H, CH_2), 2.41 (s, 3H, ArCH_3), 1.22 (t, *J* = 7.3 Hz, 3H, CH$_2$CH_3).

^{13}C NMR (75 MHz, $CDCl_3$): δ = 200.6 (*C*(O)Et), 143.7 (C_{Ar}), 134.5 (C_{Ar}), 129.3 (C_{Ar}), 128.2 (C_{Ar}), 31.8 (*C*H$_2$CH$_3$), 21.8 (Ar*C*H$_3$), 8.5 (CH$_2$*C*H$_3$).

GC-MS (EI): t_r = 4.91 min, m/z(%) = 148 (11, [$M^{+\bullet}$]), 119 (100, [$M^{+\bullet}$-$C_2H_5^{\bullet}$]), 91 (50, [$M^{+\bullet}$-$C_2H_5^{\bullet}$-CO]).

IR (ATR, $\tilde{\nu}$ [cm^{-1}]): 3032 (w, C-H_{arom}), 2976 (w, C-H_{aliph}), 2935 (w, C-H_{aliph}), 2879 (w, C-H_{aliph}), 1679 (vs, C=O), 1605 (s), 1571 (w), 1452 (m), 1407 (m), 1351 (m), 1318 (w), 1280 (w), 1219 (s), 1180 (s), 1116 (w), 1083 (w), 1015 (m), 948 (s), 833 (w), 785 (s), 736 (w).

1-(4-methoxyphenyl)propan-1-one (**130c**)

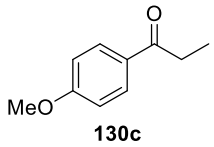

130c

According to GP-G, **130c** was synthesized using ethyl manganese bromide lithium chloride complex (4.4 mL, 1.2 mmol, 0.27 M, 1.2 equiv.) and *S*-ethyl 4-methoxybenzothioate **129c** (196 mg, 1.00 mmol). Purification was achieved by manual column chromatography (PE/EA = 97:3). The product was obtained as a yellow oil (147 mg, 892 µmol, 89%). The analytical data is in good accordance to reported literature.[30]

$C_{10}H_{12}O_2$ (164.20 g/mol)

R_f: 0.13 (Hex/Et_2O = 30:1) [anis].

^{1}H NMR (300 MHz, $CDCl_3$): δ = 8.01–7.89 (m, 2H, $C_{Ar}H$), 6.99–6.87 (m, 2H, $C_{Ar}H$), 3.86 (s, 3H, OCH_3), 2.95 (q, *J* = 7.3 Hz, 2H, $C(O)CH_2CH_3$), 1.21 (t, *J* = 7.3 Hz, 3H, $C(O)CH_2CH_3$).

^{13}C NMR (75 MHz, $CDCl_3$): δ = 199.6 (*C*(O)), 163.4 (C_{Ar}), 130.4 (C_{Ar}), 130.2 (C_{Ar}), 113.8 (C_{Ar}), 55.6 (OCH_3), 31.6 (CH_2CH_3), 8.6 (CH_2CH_3).

GC-MS (EI): t_r = 6.04 min, m/z(%) = 164 (16, [$M^{+\bullet}$]), 135 (100, [$M^{+\bullet}$-$C_2H_5^{\bullet}$]), 107(13, [$M^{+\bullet}$-$C_2H_5^{\bullet}$-CO]).

IR (ATR, $\tilde{\nu}$ [cm^{-1}]): 2972 (w, C-H_{aliph}), 2935 (w, C-H_{aliph}), 2909 (w, C-H_{aliph}), 2839 (w, C-H_{aliph}), 1675 (s, C=O), 1597 (s), 1508 (m), 1456 (m), 1415 (m), 1351 (m), 1310 (m), 1254 (s), 1224 (vs, C_{arom}-O_{ether}-C), 1168 (vs), 1109 (m), 1021 (s, C-O-C_{asymm}), 948 (s), 841 (s), 796 (s), 733 (w).

1-(4-fluorophenyl)propan-1-one (**130d**)

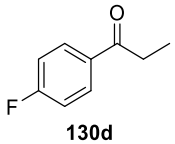

130d

According to GP-G, **130d** was synthesized using ethyl manganese bromide lithium chloride complex (5.7 mL, 1.2 mmol, 0.21 M, 1.2 equiv.) and *S*-ethyl 4-fluorobenzothioate **129d** (184 mg, 1.00 mmol). Purification was achieved by column chromatography (Hex/Et_2O= 98:2). Due to compound volatility, evaporation of solvent was fully achieved by bulb-to-bulb-distillation (90 °C, 500 mbar). The product was obtained as a colorless oil (126 mg, 829 µmol, 83%). The analytical data is in good accordance previous literature examples.[31]

C_9H_9FO (152.17 g/mol)

R_f: 0.33 (Hex/Et_2O = 98:2) [anis].

^{1}H NMR (300 MHz, $CDCl_3$): δ = 7.97 (ddd, *J* = 8.9, 5.4, 1.4 Hz, 2H, $C_{Ar}H$), 7.17–7.02 (m, 2H, $C_{Ar}H$), 2.95 (q, *J* = 7.3, 2H, C(O)CH_2CH$_3$), 1.20 (t, *J* = 7.3, 3H, C(O)CH$_2$CH_3).

^{13}C NMR (101 MHz, $CDCl_3$): δ = 199.2 (*C*(O)), 165.7 (d, J^1_{C-F} = 254.2 Hz), 133.4 (d, J^4_{C-F} = 3.1 Hz), 130.7 (d, J^3_{C-F} = 9.2 Hz), 115.7 (d, J^2_{C-F} = 21.8 Hz), 31.8 (*C*H$_2$CH$_3$), 8.3 (CH$_2$*C*H$_3$).

^{19}F NMR (282 MHz, $CDCl_3$): δ = -105.8 (s).

GC-MS (EI): t_r = 4.00 min, m/z(%) = 152(14, [$M^{+\bullet}$]), 123 (100, [$M^{+\bullet}$-$C_2H_5^\bullet$]), 95 (3, [$M^{+\bullet}$-$C_2H_5^\bullet$-CO]).

IR (ATR, $\tilde{\nu}$ [cm^{-1}]): 3065 (w, C-H$_{arom}$), 3025 (w, C-H$_{arom}$), 2969 (w, C-H$_{aliph}$), 2935 (w, C-H$_{aliph}$), 2905 (w, C-H$_{aliph}$), 2876 (w, C-H$_{aliph}$), 1709 (s), 1687 (s, C=O), 1597 (m), 1500 (m), 1455 (m, C-F), 1410 (w), 1374 (w), 1348 (m), 1305 (w), 1273 (w), 1221 (s), 1154 (m), 1131 (w), 1101 (w), 1016 (w), 986 (w), 952 (w), 904 (w), 848 (m), 800 (m), 751 (m), 699 (s).

1-(4-chlorophenyl)propan-1-one (**130e**)

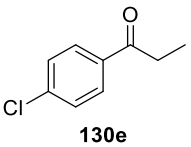

130e

According to GP-G, **130e** was synthesized using ethyl manganese bromide lithium chloride complex (4.6 mL, 1.2 mmol, 0.26 M, 1.2 equiv.) and *S*-ethyl 4-chlorobenzothioate **129e** (234 mg, 1.00 mmol). Purification was achieved by manual column chromatography (Hex) The product was obtained as a colorless solid (128 mg, 759 µmol, 76%). The analytical data matches previously reported literature.[32]

C_9H_9ClO (168.62 g/mol)

R_f: 0.18 (Hex/EA = 99:1) [anis].

^{1}H NMR (400 MHz, $CDCl_3$): δ = 7.95–7.86 (m, 2H, $C_{Ar}H$), 7.47–7.39 (m, 2H, $C_{Ar}H$), 2.98 (q, *J* = 7.2 Hz, 2H, CH_2CH_3), 1.23 (t, *J* = 7.2 Hz, 3H, CH_2CH_3).

^{13}C NMR (101 MHz, $CDCl_3$): δ = 199.7 (*C*(O)), 139.4 (C_{Ar}), 135.3 (C_{Ar}), 129.5 (C_{Ar}), 129.0 (C_{Ar}), 31.4 (CH_2CH_3), 8.3 (CH_2CH_3).

GC-MS (EI): t_r = 5.35 min, m/z(%) = 170 (3, [$M^{+\bullet}$]), 168 (10, [$M^{+\bullet}$]), 141 (31, [$M^{+\bullet}$-$C_2H_5^{\bullet}$]), 139 (100, [$M^{+\bullet}$-$C_2H_5^{\bullet}$]).

IR (ATR, $\tilde{\nu}$ [cm^{-1}]): 3065 (w, C-H_{arom}), 2977 (w, C-H_{aliph}), 2936 (w, C-H_{aliph}), 2905 (w, C-H_{aliph}), 2879 (w, C-H_{aliph}), 1683 (vs, C=O), 1616 (w), 1586 (s), 1482 (w), 1455 (w), 1400 (m), 1348 (m), 1314 (w), 1277 (w), 1213 (s), 1176 (w), 1090 (s), 1008 (s), 948 (s), 841 (m), 792 (s), 762 (m).

1-(4-bromophenyl)propan-1-one (**130f**)

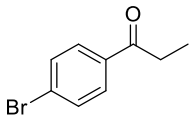

130f

According to GP-G, **130f** was synthesized using ethyl manganese bromide lithium chloride complex (4.6 mL, 1.2 mmol, 0.27 M, 1.2 equiv.) and *S*-ethyl 4-bromobenzothioate **129f** (245 mg, 1.00 mmol). Purification was achieved by manual column chromatography (Hex/Et_2O = 99:1) The product was obtained as a colorless solid (131 mg, 614 µmol, 61%). The spectral data is in good accordance to previous literature.[33]

C_9H_9BrO (213.07 g/mol)

R_f: 0.19 (Hex/EA = 99:1) [anis].

^{1}H NMR (400 MHz, $CDCl_3$): δ = 7.87–7.79 (m, 2H, $C_{Ar}H$), 7.64–7.56 (m, 2H, $C_{Ar}H$), 2.97 (q, *J* = 7.2 Hz, 2H, $C(O)SCH_2CH_3$), 1.22 (t, *J* = 7.2 Hz, 3H, $C(O)SCH_2CH_3$).

^{13}C NMR (101 MHz, $CDCl_3$): δ = 199.9 (*C*(O)), 135.7 (C_{Ar}), 132.0 (C_{Ar}), 129.7 (C_{Ar}), 128.1 (C_{Ar}), 31.9 ($C(O)SCH_2CH_3$), 8.3 ($C(O)SCH_2CH_3$).

GC-MS (EI): t_r = 5.98 min, m/z(%) = 214 (11, [$M^{+\bullet}$]), 212 (13, [$M^{+\bullet}$]), 185 (95, [$M^{+\bullet}$-$C_2H_5^{\bullet}$]), 183 (100, [$M^{+\bullet}$-$C_2H_5^{\bullet}$]), 157 (23, [$M^{+\bullet}$-$C_2H_5^{\bullet}$-CO]), 155 (25, [$M^{+\bullet}$-$C_2H_5^{\bullet}$-CO]).

IR (ATR, $\tilde{\nu}$ [cm^{-1}]): 2969 (w, C-H$_{aliph}$), 2928 (w, C-H$_{aliph}$), 2872 (w, C-H$_{aliph}$), 1680 (s, C=O), 1579 (m), 1482 (w), 1452 (w), 1392 (m), 1351 (m), 1292 (w), 1265 (w), 1210 (s), 1172 (m), 1105 (w), 1064 (m), 1004 (m), 949 (s), 837 (m), 814 (w), 784 (s), 759 (m), 673 (w).

1-(4-iodophenyl)propan-1-one (**130g**)

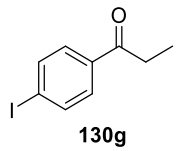

130g

According to GP-G, **130g** was synthesized using ethyl manganese bromide lithium chloride complex (4.6 mL, 1.2 mmol, 0.27 M, 1.2 equiv.) and *S*-ethyl 4-iodobenzothioate **129g** (292 mg, 1.00 mmol). Purification was achieved by manual column chromatography (Hex/Et$_2$O = 99:1). The product was obtained as a slightly orange solid (169 mg, 651 µmol, 65%).

C_9H_9IO (260.07 g/mol)

R_f: 0.24 (Hex/Et$_2$O = 99:1) [anis].

Melting point: 58.9–60.0 °C (EA).

^{1}H NMR (400 MHz, $CDCl_3$): δ = 7.92–7.72 (m, 2H, C$_{Ar}$*H*), 7.72–7.49 (m, 2H, C$_{Ar}$*H*), 2.96 (q, *J* = 7.2 Hz, 2H, C(O)SC*H*$_2$CH$_3$), 1.21 (t, *J* = 7.2 Hz, 3H, C(O)SCH$_2$C*H*$_3$).

^{13}C NMR (101 MHz, $CDCl_3$): δ = 200.1 (*C*(O)SEt), 138.0 (*C*$_{Ar}$), 136.2 (*C*$_{Ar}$), 129.5 (*C*$_{Ar}$), 100.9 (*C*$_{Ar}$), 31.9 (*C*H$_2$CH$_3$), 8.2 (CH$_2$*C*H$_3$).

GC-MS (EI): t_r = 6.74 min, m/z(%) = 260 (23, [M$^{+\bullet}$]), 231 (100, [M$^{+\bullet}$-C$_2$H$_5$S$^\bullet$]), 203 (19, [M$^{+\bullet}$-C$_2$H$_5$S$^\bullet$-CO]).

HR-MS (ESI): m/z calc. for [M+Na]$^+$ 282.95903, found 282.95900.

IR (ATR, $\tilde{\nu}$ [cm^{-1}]): 2969 (w, C-H$_{aliph}$), 2931 (w, C-H$_{aliph}$), 2898 (w, C-H$_{aliph}$), 2868 (w, C-H$_{aliph}$), 1676 (s, C=O), 1571 (m), 1478 (w), 1449 (w), 1385 (m), 1344 (m), 1269 (w), 1210 (m), 1176 (m), 1105 (w), 1083 (w), 1053 (w), 1027 (w), 997 (m), 945 (s), 840 (m), 784 (s), 751 (m), 666 (w).

4-propionylphenyl 4-methylbenzenesulfonate (**130h**)

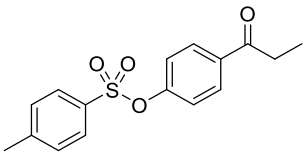

130h

According to GP-G, **130h** was synthesized using ethyl manganese bromide lithium chloride complex (6.0 mL, 1.2 mmol, 0.2 M, 1.2 equiv.) and *S*-ethyl 4-(tosyloxy)benzothioate **129h** (336 mg, 1.00 mmol). Purification was achieved by manual column chromatography (Hex/EA = 9:1) The product was obtained as a colorless soild (258 mg, 848 µmol, 85%).

$C_{16}H_{16}O_4S$ (304.36 g/mol)

R_f: 0.23 (Hex/EA = 9:1) [UV].

Melting point: 76.8–77.2 °C (EA).

^{1}H NMR (400 MHz, $CDCl_3$): δ = 7.95–7.86 (m, 2H, $C_{Ar}H$), 7.75–7.67 (m, 2H, $C_{Ar}H$), 7.35–7.28 (m, 2H, $C_{Ar}H$), 7.12–7.04 (m, 2H, $C_{Ar}H$), 2.96 (q, *J* = 7.1 Hz, 2H, $COCH_2CH_3$), 2.45 (s, 3H, $ArCH_3$), 1.21 (t, *J* = 7.1 Hz, 3H, $C(O)CH_2CH_3$).

^{13}C NMR (101 MHz, $CDCl_3$): δ = 199.5 (*C*(O)), 152.9 (C_{Ar}), 145.9 (C_{Ar}), 135.6 (C_{Ar}), 132.2 (C_{Ar}), 130.0 (C_{Ar}), 129.8 (C_{Ar}), 128.6 (C_{Ar}), 122.6 (C_{Ar}), 32.0, 21.9, 8.2.

HR-MS (ESI): m/z calc. for $[M+Na]^+$ 327.06615, found 327.06592.

IR (ATR, $\tilde{\nu}$ [cm^{-1}]): 2972 (w, $C\text{-}H_{aliph}$), 2932 (w, $C\text{-}H_{aliph}$), 2880 (w, $C\text{-}H_{aliph}$), 1713 (s), 1679 (vs, C=O), 1452 (m), 1414 (w), 1373 (m, S=O), 1262 (w), 1191 (w), 1112 (w), 1049 (w), 1023 (w), 956 (s), 897 (w), 822 (w), 733 (w), 695 (w).

4-propionylphenyl acetate (**130i**)

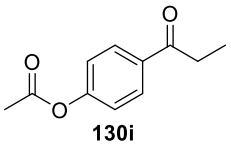

130i

According to GP-G, **130i** was synthesized using ethyl manganese bromide lithium chloride complex (5.2 mL, 1.2 mmol, 0.23 M, 1.2 equiv.) and 4-((ethylthio)carbonyl)phenyl acetate **129i** (224 mg, 1.00 mmol). Purification was achieved by column chromatography (Hex/EA = 9:1). The product was obtained as a colorless solid (150 mg, 781 µmol, 78%).

$C_{11}H_{12}O_3$ (192.13 g/mol)

R_f: 0.57 (Hex/EA = 9:1) [anis].

Melting point: 56.9–57.7 °C (EA).

^{1}H NMR (400 MHz, $CDCl_3$): δ = 8.02–7.99 (m, 2H, $C_{Ar}H$) 7.26–7.17 (m, 2H, $C_{Ar}H$), 2.99 (q, *J* = 7.2 Hz, 2H, C(O)CH_2CH$_3$), 2.33 (s, 3H, CH_3C(O)OPh), 1.22 (t, *J* = 7.2 Hz, 3H, C(O)CH$_2$CH_3).

^{13}C NMR (101 MHz, $CDCl_3$): δ = 199.7 (*C*(O)CH$_2$CH$_3$), 169.1 (*C*(O)OAr), 154.3 (C_{Ar}), 134.7 (C_{Ar}), 129.7 (C_{Ar}), 121.9 (C_{Ar}), 31.9 (C(O)*C*H$_2$CH$_3$), 21.3 (*C*H$_3$C(O)OPh), 8.4 (C(O)CH$_2$*C*H$_3$).

GC-MS (EI): t_r = 6.70 min, m/z(%) = 192 (7, [$M^{+\bullet}$]), 163 (9, [$M^{+\bullet}$-$C_2H_5^{\bullet}$]), 150 (7), 134 (16), 121 (100).

HR-MS (ESI): m/z calc. for $[M+Na]^+$ 215.06786, found 215.06803.

IR (ATR, $\tilde{\nu}$ [cm^{-1}]): 3047 (w, C-H$_{arom}$), 2976 (w, C-H$_{aliph}$), 2935 (w, C-H$_{aliph}$), 1750 (s, C=O$_{ketone}$), 1676 (s, C=O$_{ester}$), 1593 (m), 1504 (w), 1459 (w), 1407 (m), 1366 (m), 1296 (w), 1198 (s), 1157 (s), 1105 (m), 1083 (w), 1079 (w), 1046 (w), 1009 (m), 953 (m), 912 (s), 863 (m), 859 (m), 818 (m), 788 (s), 744 (w), 714 (w), 661 (w).

1-(*m*-tolyl)propan-1-one (**130n**)

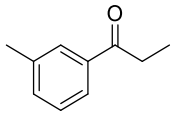

130n

According to GP-G, **130n** was synthesized using ethyl manganese bromide lithium chloride complex (4.8 mL, 1.2 mmol, 0.25 M, 1.2 equiv.) and *S*-ethyl 3-methylbenzothioate **129n** (180 mg, 1.00 mmol). Purification was achieved by manual column chromatography (Hex/Et_2O = 98:2). The product was obtained as a colorless oil (124.5 mg, 840 µmol, 84%). The analytical data is in accordance to previous literature examples.[30]

$C_{10}H_{12}O$ (148.21 g/mol)

R_f: 0.15 (Hex/Et_2O = 98:2) [anis].

^{1}H NMR (400 MHz, $CDCl_3$): δ = 7.80–7.72 (m, 2H, $C_{Ar}H$), 7.41–7.29 (m, 2H, $C_{Ar}H$), 2.99 (q, *J* = 7.3 Hz, 2H, C(O)CH_2CH$_3$), 2.41 (s, 3H, CH_3Ph), 1.22 (t, *J* = 7.3 Hz, 3H, C(O)CH$_2$CH_3).

^{13}C NMR (101 MHz, $CDCl_3$): δ = 201.2 (*C*(O)), 138.5 (C_{Ar}), 137.1 (C_{Ar}), 133.7 (C_{Ar}), 128.6 (C_{Ar}), 128.5 (C_{Ar}), 125.3 (C_{Ar}), 32.0 (Ph*C*H$_3$), 21.5 (*C*H$_2$CH$_3$), 8.5 (CH$_2$*C*H$_3$).

GC-MS (EI): t_r = 4.82 min, m/z(%) = 148 (14, [$M^{+\bullet}$]), 119 (100, [$M^{+\bullet}$-$C_2H_5^{\bullet}$]), 91 (55, [$M^{+\bullet}$-$C_2H_5^{\bullet}$-CO]).

IR (ATR, $\tilde{\nu}$ [cm^{-1}]): 3032 (w, C-H_{arom}), 2976 (w, C-H_{aliph}), 2935 (w, C-H_{aliph}), 2879 (w, C-H_{aliph}), 1683 (s, C=O), 1586 (w), 1455 (m), 1418 (w), 1348 (m), 1314 (w), 1280 (w), 1247 (s), 1165 (s), 1083 (w), 1034 (w), 1009 (w), 964 (m), 915 (w), 863 (w), 859 (w), 837 (w), 773 (s), 729 (m), 688 (s).

1-(3-methoxyphenyl)propan-1-one (**130o**)

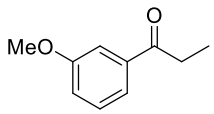

130o

According to GP-G, **130o** was synthesized using ethyl manganese bromide lithium chloride complex (6.3 mL, 1.2 mmol, 0.19 M, 1.2 equiv.) and *S*-ethyl 3-methoxybenzothioate **129o** (196 mg, 1.00 mmol). Extraction of the compound was achieved by utilizing Et_2O as solvent. Purification was achieved by manual column chromatography (Hex/Et_2O = 98:2). The product was obtained as a colorless oil (61 mg, 368 µmol, 37%). The analytical data matches previous reports.[34]

$C_{10}H_{12}O_2$ (164.20 g/mol)

R_f: 0.11 (Hex/Et_2O = 98:2) [anis].

^{1}H NMR (300 MHz, $CDCl_3$): δ = 7.59–7.45 (m, 2H, $C_{Ar}H$), 7.35 (*pseudo*-t, *J* = 7.9 Hz, 1H, $C_{Ar}H$), 7.09 (ddd, *J* = 8.2, 2.6, 0.9 Hz, 1H, $C_{Ar}H$), 3.85 (s, 3H, OCH_3), 2.98 (q, *J* = 7.2 Hz, 2H, $C(O)CH_2CH_3$), 1.22 (t, *J* = 7.2 Hz, 3H, $C(O)CH_2CH_3$).

^{13}C NMR (75 MHz, $CDCl_3$): δ = 200.7 (*C*(O)), 159.9 (C_{Ar}), 138.4 (C_{Ar}), 129.6 (C_{Ar}), 120.7 (C_{Ar}), 119.4 (C_{Ar}), 112.4 (C_{Ar}), 55.5(OCH_3), 32.0 (CH_2CH_3), 8.4 (CH_2CH_3).

GC-MS (EI): t_r = 5.73 min, m/z(%) = 164 (31, [$M^{+\bullet}$]), 135 (100, [$M^{+\bullet}$-$C_2H_5^{\bullet}$]), 107 (30, [$M^{+\bullet}$-$C_2H_5^{\bullet}$-CO]).

1-(*o*-tolyl)propan-1-one (**130q**)

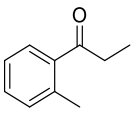

130q

According to GP-G, **130q** was synthesized using ethyl manganese bromide lithium chloride complex (4.7 mL, 1.2 mmol, 0.25 M, 1.2 equiv.) and *S*-ethyl 2-methylbenzothioate **129q** (180 mg, 1.00 mmol). Purification was achieved by manual column chromatography (Hex/EA = 30:1). The product was obtained as a yellow oil (91 mg, 615 µmol, 62%). The analytical data is in good accordance with the reported literature.[35]

$C_{10}H_{12}O$ (148.21 g/mol)

R_f: 0.21 (Hex) [anis].

^{1}H NMR (400 MHz, $CDCl_3$): δ = 7.66–7.58 (m, 1H, $C_{Ar}H$), 7.40–7.31 (m, 1H, $C_{Ar}H$), 7.29–7.20 (m, 2H, $C_{Ar}H$), 2.91 (q, *J* = 7.3 Hz, 2H, CH_2CH_3), 2.49 (s, 3H, $ArCH_3$), 1.19 (t, *J* = 7.3 Hz, 3H, CH_2CH_3).

^{13}C NMR (101 MHz, $CDCl_3$): δ = 205.2 (*C*(O)), 138.2 (C_{Ar}), 138.0 (C_{Ar}), 132.0 (C_{Ar}), 131.1 (C_{Ar}), 128.4 (C_{Ar}), 125.7 (C_{Ar}), 34.8, 21.4, 8.5.

GC-MS (EI): t_r = 4.57 min, m/z(%) = 148 (12, [$M^{+\bullet}$]), 119 (100, [$M^{+\bullet}$-$C_2H_5^{\bullet}$]), 91 (55, [$M^{+\bullet}$-$C_2H_5^{\bullet}$-CO]).

IR (ATR, $\tilde{\nu}$ [cm^{-1}]): 3062 (w, C-H_{arom}), 3021 (w C-H_{arom}), 2973 (w, C-H_{aliph}), 2932 (w, C-H_{aliph}), 2879 (w, C-H_{aliph}), 1683 (s, C=O), 1597 (w), 1568 (w), 1482 (w), 1452 (m), 1415 (w), 1377 (w), 1343 (m), 1288 (w), 1213 (s), 1131 (w), 1076 (w), 1038 (w), 1009 (w), 944 (s), 796 (w), 747 (s).

1-(naphthalen-2-yl)propan-1-one (**130t**)

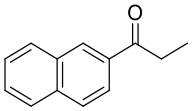

130t

According to GP-G, **130t** was synthesized using ethyl manganese bromide lithium chloride complex (4.5 mL, 1.2 mmol, 0.27 M, 1.2 equiv.) and *S*-ethyl naphthalene-2-carbothioate **129t** (216 mg, 1.00 mmol). Purification was achieved by manual column chromatography (Hex/EA = 99:1). The product was obtained as a colorless solid (150 mg, 814 µmol, 81%). The analytical data is in good accordance with the reported literature.[36]

$C_{13}H_{12}O$ (184.21 g/mol)

R_f: 0.17 (Hex/EA = 99:1) [UV].

Melting point: 58.9–60.1 °C (EA).

^{1}H NMR (400 MHz, $CDCl_3$): δ = 8.51–8.46 (m, 1H, $C_{Ar}H$), 8.05 (dd, *J* = 8.6, 1.7 Hz, 1H, $C_{Ar}H$), 8.00-7.84 (m, 3H, $C_{Ar}H$), 7.58 (dddd, *J* = 18.7, 8.1, 6.9, 1.4 Hz, 2H, $C_{Ar}H$), 3.15 (q, *J* = 7.3 Hz, 2H, CH_2CH_3), 1.29 (t, *J* = 7.3 Hz, 3H, CH_2CH_3).

^{13}C NMR (101 MHz, CDCl3): δ= 200.9 (*C*(O)Et), 135.6 (C_{Ar}), 134.4 (C_{Ar}), 132.7 (C_{Ar}), 129.7 (C_{Ar}), 128.5 (C_{Ar}), 128.5 (C_{Ar}), 127.9 (C_{Ar}), 126.8 (C_{Ar}), 124.0 (C_{Ar}), 32.02 ($C(O)CH_2$), 8.6 ($C(O)CH_2CH_3$).

GC-MS (EI, method B): t_r = 19.91 min, m/z(%) = 184 (34, [$M^{+\bullet}$]), 155 (100, [$M^{+\bullet}$-$C_2H_5^{\bullet}$]), 127 (61, [$M^{+\bullet}$-$C_2H_5^{\bullet}$-CO]).

1-(pyridin-3-yl)propan-1-one (**130v**)

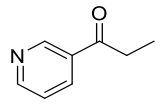

130v

According to GP-G, **130v** was synthesized using ethyl manganese bromide lithium chloride complex (5.2 mL, 1.2 mmol, 0.23 M, 1.2 equiv.) and *S*-ethyl pyridine-3-carbothioate **129v** (167 mg, 1.00 mmol). Quenching of the reaction was performed with brine (5 mL). Purification was achieved by manual column chromatography (PE/EA = 8:2). The product was obtained as a yellow oil (70.1 mg, 519 µmol, 52%).

C_8H_9NO (135.17 g/mol)

R_f: 0.37 (PE/EA = 8:2) [UV, anis].

^{1}H NMR (400 MHz, $CDCl_3$): δ = 9.15 (s, 1H, $C_{Ar}H$), 8.75 (d, *J* = 5.2 Hz, 1H, $C_{Ar}H$), 8.21 (dd, *J* = 8.1, 3.5 Hz, 1H, $C_{Ar}H$), 7.40 (dt, *J* = 8.1, 3.5 Hz, 1H, $C_{Ar}H$), 3.07–2.95 (m, 2H, CH_2CH_3), 1.27–1.17 (m, 3H, CH_2CH_3).

^{13}C NMR (101 MHz, $CDCl_3$): δ = 199.6 (*C*(O)), 153.5 (C_{Ar}), 149.7 (C_{Ar}), 135.4 (C_{Ar}), 132.2 (C_{Ar}), 123.8 (C_{Ar}), 32.3 (CH_2CH_3), 8.0 (CH_2CH_3).

GC-MS (EI): t_r = 13.22 min, m/z(%) = 135 (31, [$M^{+\bullet}$]), 106 (100, [$M^{+\bullet}$-$C_2H_5^\bullet$]), 78 (51, [$M^{+\bullet}$-$C_2H_5^\bullet$-CO]).

HR-MS (ESI): m/z calc. for $[M+H]^+$ 136.07569, found 136.07570.

IR (ATR, $\tilde{\nu}$ [cm^{-1}]): 3043 (w, C-H_{arom}), 2977 (w, C-H_{aliph}), 2939 (w, C-H_{aliph}), 2905 (w, C-H_{aliph}), 1687 (vs, C=O), 1582 (s), 1456 (w), 1415 (m), 1355 (m), 1280 (w), 1225 (s), 1191 (w), 1116 (w), 1086 (w), 1016 (m), 945 (s), 826 (w), 785 (s), 702 (s), 669 (w).

1-(2-ethylphenyl)propan-1-one (**130w**)

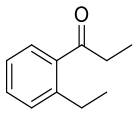

130w

According to GP-G, **130w** was synthesized using ethyl manganese bromide lithium chloride complex (11 mL, 2.2 mmol, 0.20 M, 2.2 equiv.) and *S*-ethyl 2-fluorobenzothioate **129w** (184 mg, 1.00 mmol). Purification was achieved by column chromatography (Hex/Et_2O = 98:2). The product was obtained as a colorless oil (110 mg, 678 µmol, 68%).

$C_{11}H_{14}O$ (162.23 g/mol)

R_f: 0.32 (Hex/EA = 30:1) [anis].

^{1}H NMR (400 MHz, $CDCl_3$): δ = 7.51 (dd, *J* = 7.7, 1.3 Hz, 1H, $C_{Ar}H$), 7.40–7.31 (m, 1H, $C_{Ar}H$), 7.29–7.17 (m, 2H, $C_{Ar}H$), 2.93–2.73 (m, 4H), 1.23–1.12 (m, 6H).

^{13}C NMR (101 MHz, $CDCl_3$): δ = 205.9 (*C*(O)Et), 143.7 (C_{Ar}), 138.6 (C_{Ar}), 131.1 (C_{Ar}), 130.4 (C_{Ar}), 128.0 (C_{Ar}), 125.7 (C_{Ar}), 35.4, 27.1, 16.2, 8.5.

GC-MS (EI): t_r = 14.43 min, m/z(%) = 162 (19, [$M^{+\bullet}$]), 133 (100, [$M^{+\bullet}$-$C_2H_5^{\bullet}$]), 105 (100, [$M^{+\bullet}$-$C_2H_5^{\bullet}$-CO]).

HR-MS (ESI): m/z calc. for $[M+Na]^+$ 185.09369, found 185.09362.

IR (ATR, $\tilde{\nu}$ [cm^{-1}]): 3066 (w, C-H_{arom}), 2973 (w, C-H_{aliph}), 2935 (w, C-H_{aliph}), 2876 (w, C-H_{aliph}), 1686 (vs, C=O), 1608 (m), 1575 (w), 1478 (m), 1451 (s), 1411 (w), 1348 (m), 1310 (w), 1269 (m), 1206 (s), 1150 (w), 1109 (w), 1070 (w), 1012 (w), 948 (s), 826 (w), 755 (vs).

1-(3,4,5-trifluoro-2,6-dihexylphenyl)heptan-1-one (**130x**)

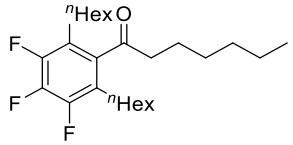

130x

According to GP-G, **130x** was synthesized using *n*-hexyl manganese chloride lithium chloride complex (5.9 mL, 3.2 mmol, 0.27 M, 3.2 equiv.) and *S*-ethyl 2,3,4,5,6-pentafluorobenzothioate **129x** (128 mg, 500 µmol). Purification was achieved by flash column chromatography (23 g - 15 µm spherical SiO_2, pure Hex, 2 CV). The product was obtained as a colorless oil (108 mg, 262 µmol, 52%).

$C_{25}H_{39}F_3O$ (412.58 g/mol)

R_f: 0.15 (Hex) [UV].

^{1}H NMR (400 MHz, $CDCl_3$): δ = 2.66 (t, *J* = 7.3 Hz, 2H, C(O)CH_2), 2.45–2.36 (m, 4H), 1.76–1.64 (m, 2H), 1.54–1.44 (m, 4H), 1.43–1.19 (m, 18H), 0.94–0.84 (m, 9H, 3 × CH_3).

^{13}C NMR (101 MHz, $CDCl_3$): δ = 206.5 ,147.8 (ddd, *J* = 247.8, 10.0, 3.4 Hz), 139.8 (dd, *J* = 251.3, 16.1 Hz), 137.3 (dd, *J* = 3.4 Hz), 122.3 (dd, *J* = 12.4, 6.1 Hz), 45.8, 31.7, 31.4, 30.6, 29.4, 28.8, 26.9, 23.2, 22.5, 14.0.

^{19}F NMR (376 MHz, $CDCl_3$): δ = -140.61 (d, J^3_{F-F} = 20.7 Hz), -160.24 (t, J^3_{F-F} = 20.7 Hz).

HR-MS (EI): m/z calc. for $[M]^+$ 412.294751, found 412.29544.

GC-MS (EI): t_r = 10.69 min, m/z(%) = 327 (100, [$M^{+\bullet}$-$C_6H_{13}^{\bullet}$]).

IR (ATR, $\tilde{\nu}$ [cm^{-1}]): 2954 (m, C-H_{aliph}), 2924 (s, C-H_{aliph}), 2858 (m, C-H_{aliph}), 1705 (m, C=O), 1616 (w), 1489 (m, C-F), 1456 (s, C-F), 1404 (w), 1359 (m), 1180 (w), 1124 (m), 1090 (m), 1045 (w), 1001 (w), 971 (w), 926 (w), 889 (w), 848 (w), 822 (w), 759 (w), 725 (w), 684 (w), 665 (w).

5,9-dimethyldec-8-en-3-one (**132a**)

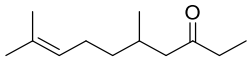

132a

According to GP-G, **132a** was synthesized using ethyl manganese bromide lithium chloride complex (4.6 mL, 1.2 mmol, 0.26 M, 1.2 equiv.) and citronellic acid *S*-ethylthioester **131a** (214 mg, 1.00 mmol). Purification was achieved by column chromatography (Hex/Et_2O= 98:2 to pure Et_2O). The product was obtained as a colorless oil with a pleasant smell (165 mg, 906 µmol, 91%). The analytical data is in accordance to reported literature.[30]

$C_{12}H_{22}O$ (182.17 g/mol)

R_f: 0.24 (Hex/Et_2O = 98:2) [anis - blue].

^{1}H NMR (400 MHz, $CDCl_3$): δ = 5.12–5.02 (m, 1H, $C_{alkene}H$), 2.45–2.31 (m, 3H), 2.20 (dd, *J* = 15.7, 8.2 Hz, 1H), 2.08–1.87 (m, 3H), 1.66 (s, 3H), 1.58 (s, 3H), 1.38–1.10 (m, 2H), 1.03 (t, *J* = 7.3 Hz, 3H), 0.88 (d, *J* = 6.6 Hz, 3H).

^{13}C NMR (101 MHz, $CDCl_3$): δ = 211.8 (*C*(O)Et), 131.6 (C_{alkene}), 124.5 (C_{alkene}), 50.0, 37.1, 36.6, 29.1, 25.8, 25.6, 19.9, 17.8, 7.9.

GC-MS (EI): t_r = 5.13 min, m/z(%) = 182 (7, [$M^{+\bullet}$]), 110 (45, [$C_8H_{14}^{+\bullet}$]), 57 (100, [$C_3H_5O^{+\bullet}$]).

IR (ATR, $\tilde{\nu}$ [cm^{-1}]): 2965 (m, C-H_{aliph}), 2920 (m, C-H_{aliph}), 2880 (w, C-H_{aliph}), 1709 (s, C=O), 1455 (m), 1411 (w), 1371 (m), 1280 (w), 1228 (w), 1146 (w), 1112 (m), 1027 (w), 975 (w), 941 (w), 890 (w), 822 (w).

(*Z*)-icos-11-en-3-one (**132b**)

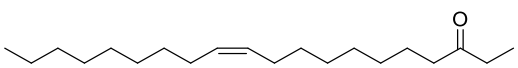

132b

According to GP-G, **132b** was synthesized using ethyl manganese bromide lithium chloride complex (4.6 mL, 1.2 mmol, 0.26 M, 1.2 equiv.) and *S*-ethyl (*Z*)-octadec-9-enethioate **131b** (214 mg, 1.00 mmol). Purification was achieved by column chromatography (Hex/Et_2O= 98:2 to pure Et_2O). The product was obtained as a colorless oil (165 mg, 560 µmol, 56%).

$C_{20}H_{38}O$ (294.52 g/mol)

R_f: 0.38 (Hex/EA = 9:1) [anis].

^{1}H NMR (400 MHz, $CDCl_3$): δ = 5.43–5.28 (m, 2H, C*H*), 2.47–2.34 (m, 4H), 2.08–1.92 (m, 4H), 1.62–1.54 (m, 2H), 1.38–1.22 (m, 20H), 1.05 (t, *J* = 7.3 Hz, 3H), 0.93–0.82 (m, 3H).

^{13}C NMR (101 MHz, $CDCl_3$): δ = 212.2 (*C*(O)), 130.1 (C_{alkene}), 129.9 (C_{alkene}), 42.6, 36.0, 32.1, 29.9, 29.9, 29.7, 29.5, 29.4, 29.1, 27.4, 27.3, 24.1, 22.8, 14.3, 8.0.

HR-MS (EI): m/z calc. for $[M]^+$ 294.291717, found 294.28958.

IR (ATR, $\tilde{\nu}$ [cm^{-1}]): 3002 (w, C-H_{alkene}), 2921 (s, C-H_{aliph}), 2853 (m, C-H_{aliph}), 1716 (m, C=O), 1459 (m), 1411 (w), 1370 (w), 1314 (w), 1273 (w), 1251 (w), 1169 (w), 1109 (w), 1030 (w), 967 (w), 721 (w).

(*R*)-2,5,7,8-tetramethyl-2-((4*R*,8*R*)-4,8,12-trimethyltridecyl)chroman-6-yl 4-oxohexanoate (**132c**)

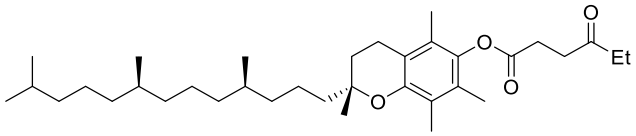

132c

According to GP-G, **132c** was synthesized using ethyl manganese bromide lithium chloride complex (7.1 mL, 1.2 mmol, 0.17 M, 1.2 equiv.) and (*R*)-2,5,7,8-tetramethyl-2-((4*R*,8*R*)-4,8,12-trimethyltridecyl)chroman-6-yl 4-(ethylthio)-4-oxobutanoate **131c** (287 mg, 500 µmol). Purification was achieved by manual column chromatography (CyH/EA = 95:5). The product was obtained as a colorless viscous oil (224 mg, 412 µmol, 82%).

$C_{35}H_{58}O_4$ (542.85 g/mol)

R_f: 0.55 (Hex/EA = 9:1) [anis - brown, UV].

^{1}H NMR (400 MHz, $CDCl_3$): δ = 3.15–2.77 (m, 4H), 2.58 (t, *J* = 6.8 Hz, 2H), 2.51 (q, *J* = 7.3 Hz, 2H), 2.08 (s, 3H), 2.01 (s, 3H), 1.98 (s, 3H), 1.86–1.68 (m, 2H), 1.59–1.46 (m, 4H), 1.41–0.99 (m, 23H), 0.90–0.80 (m, 12H).

^{13}C NMR (101 MHz, $CDCl_3$): δ = 209.4 (*C*(O)Et), 171.7 (CH_2CH_2C(O)O), 149.5 (C_{Ar}), 140.6 (C_{Ar}), 126.9 (C_{Ar}), 125.1 (C_{Ar}), 123.1 (C_{Ar}), 117.5 (C_{Ar}), 75.2 (CO*C*R), 39.5, 37.71, 37.69, 37.6, 37.6, 37.4, 36.7, 36.2, 32.94, 32.85, 28.1, 27.9, 27.1, 25.0, 24.6, 22.9, 22.8, 21.2, 20.7, 19.9, 19.84, 19.81, 13.1, 12.2, 12.0, 8.0.

HR-MS (ESI): m/z calc. for $[M+Na]^+$ 566.42273, 565.42334.

IR (ATR, $\tilde{\nu}$ [cm^{-1}]): 2924 (m, C-H$_{aliph}$), 2861 (w, C-H$_{aliph}$), 1753 (m, C=O$_{ester}$), 117 (m, C=O$_{ketone}$), 1456 (m), 1411 (m), 1368 (m), 1247 (w), 1221 (w), 1194 (m), 1146 (s, C-O-C), 1109 (s), 1083 (m), 1019 (w), 982 (w), 931 (w), 861 (w), 736 (m).

3-(4-methoxyphenyl)-4-oxo-4-chromen-7-yl 4-oxohexanoate **(132d)**

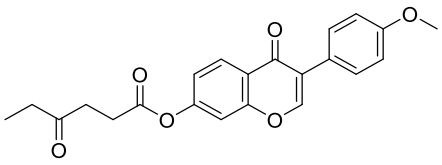

132d

According to GP-G, **132d** was synthesized using ethyl manganese bromide lithium chloride complex (2.1 mL, 0.60 mmol, 0.28 M, 1.2 equiv.) and 3-(4-methoxyphenyl)-4-oxo-4*H*-chromen-7-yl 4-(ethylthio)-4-oxobutanoate **131d** (206 mg, 1.00 mmol). Purification was achieved by flash column chromatography (23 SiO_2, gradient from Hex/EA = 95:5 to 48:52 over 16 CV, then pure EA for 3 CV). The product was further purified by recrystallization in pure EtOH. The product was obtained as a colorless solid (95 mg, 250 µmol, 50%).

$C_{22}H_{20}O_6$ (380.40 g/mol)

R_f: 0.26 (Hex/EA = 7:3) [UV, anis - purple].

Melting point: 126.6–126.8 °C (EA).

^{1}H NMR (400 MHz, $CDCl_3$): δ = 8.30 (d, *J* = 8.7 Hz, 1H, C$_{ketone}$(O)C$_{Ar}$C$_{Ar}$*H*), 7.96 (s, 1H, OC*H*CAr), 7.57–7.44 (m, 2H), 7.29 (d, *J* = 2.1 Hz, 1H, O$_{ester}$C$_{Ar}$C*H*), 7.16 (dd, *J* = 8.8, 2.2 Hz, 1H, C(O)$_{ketone}$C$_{Ar}$C$_{Ar}$HC$_{Ar}$*H*), 7.05–6.83 (m, 2H), 3.83 (s, 3H, OC*H*$_3$), 2.89–2.84 (m, 4H), 2.52 (q, *J* = 7.3 Hz, 2H, C*H*$_2$CH$_3$), 1.11 (t, *J* = 7.3 Hz, 3H, CH$_2$C*H*$_3$).

^{13}C NMR (101 MHz, $CDCl_3$): δ 209.1 (*C*(O)CH$_2$CH$_3$), 175.9 (*C*(O)$_{ketone}$C$_{Ar}$), 170.9 (CH$_2$*C*(O)O), 159.8 (*C*$_{Ar}$), 156.7 (*C*$_{Ar}$), 154.6 (*C*$_{Ar}$), 152.7 (*C*$_{Ar}$), 130.2 (*C*$_{Ar}$), 127.9 (*C*$_{Ar}$), 125.2 (*C*$_{Ar}$), 123.9 (*C*$_{Ar}$), 122.4 (*C*$_{Ar}$), 119.5 (*C*$_{Ar}$), 114.1 (*C*$_{Ar}$), 111.0 (*C*$_{Ar}$), 55.5 (ArO*C*H$_3$), 36.6, 36.0, 28.3, 7.9.

HR-MS (ESI): m/z calc. for $[M+Na]^+$ 403.11521, found 403.11566.

IR (ATR, $\tilde{\nu}$ [cm^{-1}]): 3006 (w, C-H$_{arom}$), 2965 (w, C-H$_{aliph}$), 2928 (w, C-H$_{aliph}$), 2872 (w, C-H$_{aliph}$), 2835 (w, C-H$_{aliph}$), 1747 (w, C=O$_{ketone}$), 1698 (m), 1645 (m), 1609 (m), 1571 (w), 1508 (m), 1463 (w), 1433 (m), 1355 (w), 1288 (m), 1228 (s), 1173 (m), 1146 (s), 1105 (m), 1053 (m), 1023 (s), 953 (m), 930 (m), 917 (w), 913 (w), 876 (m), 837 (s), 807 (s), 777 (m), 747 (w), 718 (w), 691 (w).

(5*S*,8*R*,9*S*,10*S*,13*S*,14*S*,17*R*)-10,13,17-trimethyl-17-((*R*)-5-oxoheptan-2-yl)dodecahydro-3*H*-cyclopenta[a]phenanthrene-3,7,12(2*H*,4*H*)-trione (**132e**)

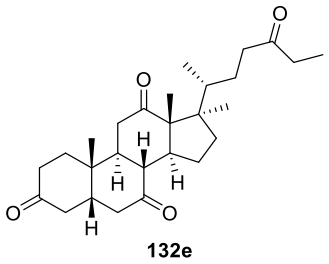

132e

According to GP-G, **132e** was synthesized using ethyl manganese bromide lithium chloride complex (7.1 mL, 1.2 mmol, 0.17 M, 1.2 equiv.) and S-ethyl (*R*)-4-((5*S*,8*R*,9*S*,10*S*,13*S*,14*S*,17*R*)-10,13,17-trimethyl-3,7,12-trioxohexadecahydro-1*H*-cyclopenta[*a*]phenanthren-17-yl)pentanethioate **131e** (223 mg, 500 µmol). Purification was achieved by flash column chromatography (Hex/EA = 9:1 to 40:60 and hold for 2 CV). The product was obtained as a colorless solid (120 mg, 290 µmol, 58%).

$C_{26}H_{38}O_4$ (414.59 g/mol)

R_f: 0.33 (Hex/EA = 1:1) [anis].

Melting point: 215 °C (decomp.).

^{1}H NMR (400 MHz, $CDCl_3$): δ = 3.02–2.74 (m, 4H), 2.56–1.91 (m, 15H), 1.90–1.71 (m, 2H), 1.67–1.55 (m, 1H), 1.43–1.17 (m, 8H), 1.08–0.99 (m, 6H), 0.88–0.78 (m, 3H).

^{13}C NMR (101 MHz, $CDCl_3$): δ = 212.24 (*C*(O)), 212.21 (*C*(O)), 209.2 (*C*(O)), 208.9 (*C*(O)), 57.0, 51.9, 49.1, 47.0, 45.7, 45.7, 45.1, 42.9 39.4, 38.8, 36.6, 36.1, 36.1, 35.5, 35.4, 29.3, 27.7, 25.3, 22.0, 18.9, 12.0, 8.0.

HR-MS (ESI): m/z calc. for $[M+Na]^+$ 437.26623, found 437.26600.

IR (ATR, $\tilde{\nu}$ [cm^{-1}]): 2965 (w, C-H_{aliph}), 2913 (w, C-H_{aliph}), 2868 (w, C-H_{aliph}), 1705 (s, C=O), 1454 (w), 1432 (w), 1381 (w), 1343 (w), 1295 (w), 1273 (w), 1240 (w), 1184 (w), 1124 (w), 1120 (w), 1105 (w), 1072 (w), 1027 (w), 1004 (w), 952 (w), 930 (w), 896 (w), 870 (w), 833 (w), 803 (w), 777 (w), 725 (w), 684 (w).

(*R*)-quinolin-4-yl((1*S*,2*S*,4*S*,5*R*)-5-vinylquinuclidin-2-yl)methyl 4-oxohexanoate **(132f)**

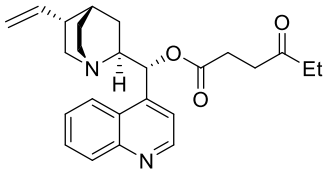

132f

According to GP-G, **132f** was synthesized using ethyl manganese bromide lithium chloride complex (2.1 mL, 0.60 mmol, 0.28 M, 1.2 equiv.) and *(R)*-quinolin-4-yl*((1S,2S,4S,5R)*-5-vinylquinuclidin-2-yl)methyl 4-(ethylthio)-4-oxobutanoate **131f** (219 mg, 1.00 mmol). Purification was achieved by flash column chromatography (23 g SiO_2, gradient DCM/MeOH from pure DCM to 90:10 over 15 CV). The product was obtained as a colorless solid (77 mg, 190 µmol, 38%).

$C_{25}H_{30}N_2O_3$ (406.53 g/mol)

R_f: 0.29 (DCM/MeOH = 35:1) [UV].

^{1}H NMR (400 MHz, $CDCl_3$): δ = 8.87 (d, *J* = 4.5 Hz, 1H, $C_{Ar}H$), 8.23–8.15 (m, 1H, $C_{Ar}H$), 8.10 (dd, *J* = 8.5, 1.3 Hz, 1H, $C_{Ar}H$), 7.68 (ddd, *J* = 8.3, 6.8, 1.3 Hz, 1H, $C_{Ar}H$), 7.56 (ddd, *J* = 8.4, 6.9, 1.4 Hz, 1H, $C_{Ar}H$), 7.38 (d, *J* = 4.5 Hz, 1H, $C_{Ar}H$), 6.49 (d, *J* = 7.1 Hz, 1H), 5.81 (ddd, *J* = 16.8, 10.4, 7.4 Hz, 1H, C*H*CH_2), 5.02–4.93 (m, 2H, CHCH_2), 3.38–3.28 (m, 1H), 3.15–3.05 (m, 1H), 3.00 (dd, *J* = 13.8, 10.0 Hz, 1H), 2.76–2.50 (m, 6H), 2.39 (q, *J* = 7.6 Hz, 2H), 2.29–2.20 (m, 1H), 1.92–1.80 (m, 2H), 1.76–1.65 (m, 1H), 1.58–1.47 (m, 2H), 1.01 (t, *J* = 7.3 Hz, 3H, C(O)CH_2CH_3).

^{13}C NMR (101 MHz, $CDCl_3$): δ 209.0 (*C*(O)Et), 172.0 (CH_2*C*(O)O), 150.1 (C_{Ar}), 148.7 (C_{Ar}), 145.3 (C_{Ar}), 141.8 (C_{Ar}), 130.5 (C_{Ar}), 129.2 (C_{Ar}), 126.9 (C_{Ar}), 126.0 (C_{Ar}), 123.3 (C_{Ar}), 118.7, 114.5, 74.4, 59.8, 56.7, 42.5, 39.8, 36.4, 35.9, 28.1, 27.8, 27.6, 24.4, 7.8.

HR-MS (ESI): m/z calc. for $[M+H]^+$ 407.23292, found 407.23363.

IR (ATR, $\tilde{\nu}$ [cm^{-1}]): 3070 (w, C-H_{arom}), 2935 (w, C-H_{aliph}), 2869 (w, C-H_{aliph}), 1738 (m, C=O_{ester}), 1713 (s, C=O_{ketone}), 1634 (w), 1590 (w), 1568 (w), 1508 (w), 1456 (w), 1411 (w), 1357 (w), 1314 (w), 1234 (w), 1198 (m), 1158 (s), 1112 (m), 1080 (w), 1046 (w), 986 (m), 945 (w), 911 (s), 852 (w), 811 (m), 759 (m), 726 (vs), 672 (w).

(3a*S*,4*S*,6a*R*)-4-(5-oxoheptyl)tetrahydro-1*H*-thieno[3,4-*d*]imidazol-2(3*H*)-one (**132g**)

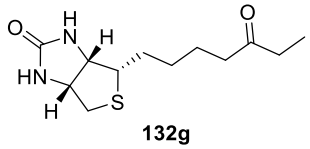

132g

According to GP-G, **132g** was synthesized using ethyl manganese bromide lithium chloride complex (11.4 mL, 3.20 mmol, 0.28 M, 3.2 equiv.) and *S*-ethyl 5-((3aS,4S,6aR)-2-oxohexahydro-1*H*-thieno[3,4-*d*]imidazol-4-yl)pentanethioate **131g** (288 mg, 1.00 mmol). Purification was achieved by flash column chromatography (23 SiO_2, gradient DCM/MeOH from pure DCM to 92:8 over 10 CV, then to 75:25 over 3 CV, hold for 1 CV, then gradient to 50:50 over 1 CV). The product was obtained as a colorless viscous oil (156 mg, 609 µmol, 61%).

$C_{12}H_{20}N_2O_2S$ (256.36 g/mol)

R_f: 0.46 (DCM/MeOH = 20:1) [anis - brown].

Melting point: 145.5–147.5 °C (EA).

^{1}H NMR (700 MHz, CD_3CN): δ = 4.70 (s, 1H, N*H*), 4.51 (s, 1H, N*H*), 3.19 (s, 1H, SC*H*), 2.94 (d, *J* = 7.5 Hz, 1H, SC*H*HCH), 2.67 (*J* = 12.9 Hz, 1H, SCH*H*CH), 2.48–2.34 (m, 4H), 2.26–2.06 (m, 2H), 1.66 (*pseudo*-s, 1H), 1.55 (*pseudo*-s, 3H), 1.35 (*pseudo*-s, 2H), 0.96 (t, *J* = 7.2 Hz, 3H, CH_2CH_3).

^{13}C NMR (176 MHz, CD_3CN): δ = 212.2 (*C*(O)CH_2CH_3), 62.6 (NHC*H*), 61.1(NHC*H*), 56.7 (SC*H*), 42.5, 41.6, 36.2, 29.4, 29.3, 24.5, 8.1.

^{1}H NMR (400 MHz, D_3COD): δ = 4.53 (s, 1H, N*H*), 4.34 (s, 1H, N*H*), 3.31 (s, 1H, SC*H*), 3.20 (s, 1H), 2.98–2.88 (m, 1H), 2.69 (d, *J* = 12.5 Hz, 1H), 1.79–1.67 (m, 1H), 1.59 (dt, *J* = 13.2, 6.8 Hz, 2H), 1.49–1.36 (m, 2H), 1.01 (t, *J* = 7.2 Hz, 3H).

^{13}C NMR (101 MHz, MeOD-d_4): δ = 214.4 (*C*(O)CH_2CH_3), 101.3 (NH*C*(O)NH), 63.4 (NHC*H*), 61.7 (NHC*H*), 57.0 (SC*H*), 42.8, 41.1, 36.5, 29.8, 29.6, 24.8, 8.1.

HR-MS (ESI): m/z calc. for $[M+Na]^+$ 279.11377, found 279.11391.

IR (ATR, $\tilde{\nu}$ [cm^{-1}]): 3261 (w, N-H), 3191 (w, N-H), 2974 (w, C-H_{aliph}), 2932 (m, C-H_{aliph}), 2909 (m, C-H_{aliph}), 2849 (w, C-H_{aliph}), 2365 (m), 1683 (s, C=$O_{thioester}$), 1515 (w), 1448 (m), 1422 (m), 1366 (m), 1308 (m), 1256 (w), 1206 (m), 1161 (w), 1113 (m), 1060 (w), 1021 (w), 978 (m), 926 (m), 859 (m), 822 (m), 792 (w), 788 (w), 758 (s), 721 (s), 684 (m).

1-(2-(3-cyano-4-*iso*butoxyphenyl)-4-methylthiazyl)propanone (**132h**)

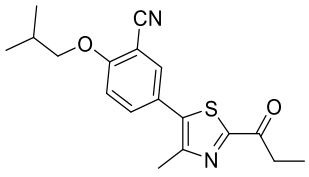

132h

According to GP-G, **132h** was synthesized using ethyl manganese bromide lithium chloride complex (2.5 mL, 1.2 mmol, 0.24 M, 1.2 equiv.) and *S*-ethyl 2-(3-cyano-4-isobutoxyphenyl)-4-methylthiazole-5-carbothioate **131h** (180 mg, 0.5 mmol). Purification was achieved by flash liquid chromatography (23 g SiO_2, gradient Hex/EA from 95:5 to 85:15 over 15 CV, then gradient to 50:50 over 1 CV, hold for 5 CV). The product was obtained as a slightly yellow solid (65 mg, 198 µmol, 40%).

$C_{18}H_{20}N_2O_2S$ (328.43 g/mol)

R_f: 0.40 (Hex/EA = 9:1) [anis, UV].

Melting point: 157.8–158.3 °C (EA).

^{1}H NMR (400 MHz, $CDCl_3$): δ = 8.18 (d, *J* = 2.3 Hz, 1H, $C_{Ar}H$), 8.11 (dd, *J* = 8.9, 2.3 Hz, 1H, $C_{Ar}H$), 7.01 (d, *J* = 8.9 Hz, 1H, $C_{Ar}H$), 3.90 (d, *J* = 6.5 Hz, 2H), 2.87 (q, *J* = 7.2 Hz, 2H), 2.77 (s, 3H), 2.28–2.13 (m, 1H, C*H*), 1.23 (*t*, *J* = 7.2 Hz, 3H), 1.09 (d, *J* = 6.7 Hz, 6H).

^{13}C NMR (101 MHz, $CDCl_3$): δ = 193.6 (*C*(O)Et), 166.3 (C_{Ar}), 162.7 (C_{Ar}), 159.6 (C_{Ar}), 132.8 (C_{Ar}), 132.3 (C_{Ar}), 130.7 (C_{Ar}), 126.0 (C_{Ar}), 115.5 (C_{Ar}), 112.8 (C_{Ar}), 103.1, 75.8, 36.5, 28.3, 19.2, 18.6, 8.3.

GC-MS (EI): t_r = 12.60 min, m/z(%) = 328 (12, [$M^{+\bullet}$]), 272 (27), 243 (100), 215(10).

HR-MS (ESI): m/z calc. for $[M+Na]^+$ 351.11377, found 351.11376.

IR (ATR, $\tilde{\nu}$ [cm^{-1}]): 2973 (w, C-H_{aliph}), 2935 (w, C-H_{aliph}), 2909 (w, C-H_{aliph}), 2872 (w, C-H_{aliph}), 2225 (w, C≡N), 1645 (m, C=O), 1597 (w), 1504 (w), 1463 (w), 1422 (m), 1381 (w), 1377 (w), 1355 (w), 1288 (m), 1217 (m), 1168 (m), 1124 (m), 1064 (w), 1042 (w), 1038 (w), 1005 (m), 963 (m), 911 (w), 878 (w), 818 (m), 762 (w), 724 (w), 664 (w).

1-(4-(8-chloro-5,6-dihydro-11*H*-benzo[5,6]cyclohepta[1,2-*b*]pyridin-11-ylidene)piperidin-1-yl)hexane-1,4-dione **(132i)**

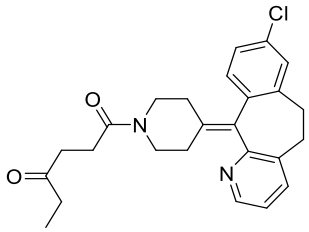

132i

According to GP-G, **132i** was synthesized using ethyl manganese bromide lithium chloride complex (2.1 mL, 0.60 mmol, 0.28 M, 1.2 equiv.) and *S*-ethyl 4-(4-(8-chloro-5,6-dihydro-11*H*-benzo[5,6]cyclohepta[1,2-*b*]pyridin-11-ylidene)piperidin-1-yl)-4-oxobutanethioate **131i** (227 mg, 1.00 mmol). Purification was achieved by flash column chromatography (23 SiO_2, gradient from Hex/EtOH = 90:10 to 66:34 over 6 CV, hold for 2 CV, gradient over 1 CV to 30:70, then gradient over 2 CV to 20:80). The product was obtained as a colorless foam (120 mg, 283 µmol, 57%).

$C_{25}H_{27}ClN_2O_2$ (422.95 g/mol)

R_f: 0.64 (Hex/EtOH = 1:1) [anis].

Melting point: 54.8–56.0 °C (EtOH).

^{1}H NMR (400 MHz, $CDCl_3$, mixture of isomers): δ = 8.39 (dd, *J* = 4.8, 1.7 Hz, 1H, $C_{Ar}H$), 7.43 (dt, *J* = 8.0, 2.0 Hz, 1H, $C_{Ar}H$), 7.20–7.01 (m, 4H, $C_{Ar}H$), 4.09–3.86 (m, 1H), 3.80–3.63 (m, 1H), 3.47–3.03 (m, 4H), 2.91–2.26 (m, 12H), 1.05 (t, *J* = 7.3 Hz, 3H, $C(O)CH_2CH_3$).

^{13}C NMR (101 MHz, $CDCl_3$, mixture of isomers): δ = 210.8, 170.2, 170.2, 157.1, 157.0, 146.9, 146.8, 139.7, 139.6, 137.8, 137.7, 137.7, 137.6, 137.1, 137.0, 134.7, 133.5, 133.4, 133.1, 133.1, 130.6, 130.6, 129.1, 129.1, 126.4, 126.3, 122.4, 46.2, 46.2, 43.0, 42.9, 36.9, 36.3, 31.8, 31.8, 31.6, 31.6, 31.3, 31.0, 30.6, 30.3, 27.1, 27.1, 7.9.

HR-MS (ESI): m/z calc. for $[M+H]^+$ 423.18338, found 423.18363.

IR (ATR, $\tilde{\nu}$ [cm^{-1}]): 3042 (w, C-H_{arom}), 2972 (w, C-H_{aliph}), 2903 (w, C-H_{aliph}), 1709 (m, C=O_{ketone}), 1637 (s, C=O_{amide}), 1586 (w), 1560 (w), 1430 (s), 1366 (m), 1325 (w), 1269 (w), 1206 (m), 1172 (m), 1109 (m), 1023 (w), 990 (m), 915 (w), 893 (w), 889 (w), 825 (m), 785 (w), 726 (s).

1,3-dimethyl-7-(2-oxobutyl)-3,7-dihydro-1*H*-purine-2,6-dione (**132j**)

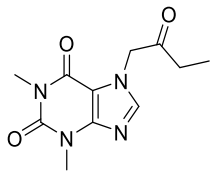

132j

According to GP-G, **132j** was synthesized using ethyl manganese bromide lithium chloride complex (4.6 mL, 1.2 mmol, 0.26 M, 1.2 equiv.) and *S*-ethyl 2-(1,3-dimethyl-2,6-dioxo-1,2,3,6-tetrahydro-7-purin-7-yl)ethanethioate **131j** (282 mg, 1.00 mmol). The reaction stirred for 15 min at -20 °C. Purification was achieved by filtering the crude product through a pad of silica (DCM/MeOH = 40:1). Then, the product was further purified by recrystallization (Hex/EtOH = 5:3) and obtained as a colorless solid (188 mg, 751 µmol, 75 %).

$C_{11}H_{14}N_4O_3$ (250.26 g/mol)

R_f: 0.18 (DCM/MeOH = 20:1) [UV, anis].

Melting point: 148.2–149.2 °C (EtOH).

^{1}H NMR (400 MHz, $CDCl_3$): δ = 7.52 (s, 1H, NC*H*), 5.12 (s, 2H, NCH_2C(O)), 3.57 (s, 3H, NCH_3), 3.34 (s, 3H, NCH_3), 2.61 (q, *J* = 7.4 Hz, 2H, C(O)CH_2CH$_3$), 1.14 (t, *J* = 7.4 Hz, 3H, C(O)CH$_2$CH_3).

^{13}C NMR (101 MHz, $CDCl_3$): δ = 202.5 (*C*(O)), 155.5 (N*C*(O)), 151.7 (N*C*(O)), 148.6, 142.1, 107.0, 54.2 (N*C*H$_2$C(O)), 33.5 (*C*H$_2$CH$_3$), 29.9 (N*C*H$_3$), 28.0 (NCH$_3$), 7.4 (CH$_2$*C*H$_3$).

HR-MS (ESI): m/z calc. for $[M+Na]^+$ 273.09581, found 273.09588.

IR (ATR, $\tilde{\nu}$ [cm^{-1}]): 3125 (w, C-H$_{heterocyclic}$), 2965 (w, C-H$_{aliph}$), 2939 (w, C-H$_{aliph}$), 2887 (w, C-H$_{aliph}$), 1731 (w), 1693 (m, C=O$_{ketone}$), 1649 (s, C=O$_{amide}$), 1542 (m, C=O$_{amide}$), 1455 (m), 1429 (m), 1400 (m), 1370 (m), 1336 (w), 1292 (w), 1237 (m), 1187 (m), 1116 (m), 1072 (w), 1027 (m), 978 (w), 930 (w), 904 (w), 856 (w), 810 (w), 766 (m), 740 (m), 673 (w).

1-(2,6-dichlorophenyl)-2-ethyl-1*H*-indole (**132k**)

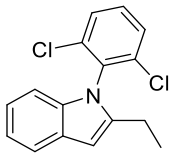

132k

According to GP-G, **132k** was synthesized using ethyl manganese bromide lithium chloride complex (4.8 mL, 1.2 mmol, 0.25 M, 1.2 equiv.) and *S*-ethyl 2-(2-((2,6-dichlorophenyl)-amino)phenyl)ethanethioate **131k** (170 mg, 500 µmol). Purification was achieved by column chromatography (Hex/EA = 9:1). The product was obtained as a brown oil (88 mg, 303 µmol, 61%).

$C_{16}H_{13}Cl_2N$ (290.19 g/mol)

R_f: 0.67 (Hex/EA = 9:1) [UV].

^{1}H NMR (400 MHz, $CDCl_3$): δ = 7.67–7.56 (m, 1H, $C_{Ar}H$), 7.53 (d, *J* = 8.3 Hz, 2H, $C_{Ar}H$), 7.40 (dd, *J* = 8.7, 7.5 Hz, 1H, $C_{Ar}H$), 7.18–7.03 (m, 2H, $C_{Ar}H$), 6.78 (d, *J* = 7.5 Hz, 1H, $C_{Ar}H$), 6.49 (d, *J* = 1.8 Hz, 1H, $C_{Ar}H$), 2.48 (q, *J* = 7.5 Hz, 2H, CH_2CH_3), 1.28 (t, *J* = 7.5 Hz, 3H, CH_2CH_3).

^{13}C NMR (101 MHz, $CDCl_3$): δ = 143.1 (C_{Ar}), 136.8 (C_{Ar}), 136.7 (C_{Ar}), 133.9 (C_{Ar}), 130.4 (C_{Ar}), 129.0 (C_{Ar}), 128.6 (C_{Ar}), 121.6 (C_{Ar}), 120.5 (C_{Ar}), 120.1 (C_{Ar}), 109.4 (C_{Ar}), 99.9 (C_{Ar}), 20.2, 12.5.

HR-MS (ESI): m/z calc. for $[M+Na]^+$ 312.03173, found 312.03181.

2,5-undecadion (**137**)

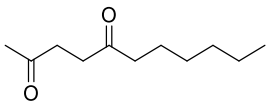

137

According to GP-G, **137** was synthesized using *n*-hexyl manganese bromide lithium chloride complex (4.8 mL, 1.2 mmol, 0.25 M, 1.2 equiv.) and *S*-ethyl 4-oxopentanethioate **120p** (160 mg, 1.00 mmol). Purification was achieved by bulb-to-bulb distillation (155 °C, 5 mbar). The product was obtained as a colorless oil which solidified after exposure to sonification (164 mg, 890 µmol, 89%). The spectral data is in good accordance to previous literature.[37]

$C_{11}H_{20}O_2$ (184.28 g/mol)

R_f: 0.27 (Hex/EA = 9:1) [anis].

^{1}H NMR (400 MHz, $CDCl_3$): δ = 2.70–2.64 (m, 4H), 2.42 (t, *J* = 7.4 Hz, 2H), 2.17 (s, 3H), 1.61–1.51 (m, 2H), 1.30–1.18 (m, 6H), 0.85 (t, *J* = 6.7 Hz, 3H).

^{13}C NMR (101 MHz, $CDCl_3$): δ = 209.8 (*C*(O)), 207.4 (*C*(O)), 42.9, 37.0, 36.1, 31.7, 30.1, 29.0, 23.9, 22.6, 14.1.

dihydrojasmone (**138**)

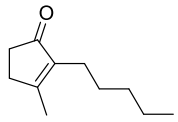

138

The compound **137** (151 mg, 819 µmol) was dissolved in ethanol (10 mL) and an aq. NaOH solution (2 mL, 10% w/v) was added. The reaction was heated to reflux and stirred for 3 h. Afterwards, the reaction was allowed to cool, the crude solution was diluted with brine (5 mL) and was extracted with EA (4 × 10 mL). The combined organic layers were dried over anhydrous $MgSO_4$ and solvent reduced *in vacuo*. The compound was yielded by bulb-to-bulb distillation (120 °C, 10 mbar) as a colorless oil with a distinct smell of jasmine flowers (70 mg, 421 µmol, 51%). The spectral data is in good accordance to previous literature.[38]

$C_{11}H_{18}O$ (166.26 g/mol)

R_f: 0.16 (PE/EA = 97:3) [anis].

^{1}H NMR (400 MHz, $CDCl_3$): δ = 2.51–2.43 (m, 2H), 2.42–2.30 (m, 2H), 2.14 (t, *J* = 7.6 Hz, 2H), 2.03 (s, 3H, CC*H*$_3$), 1.41–1.16 (m, 6H), 0.86 (t, *J* = 7.0 Hz, 3H).

^{13}C NMR (101 MHz, $CDCl_3$): δ = 209.8 (*C*(O)), 170.1 (C_{alkene}), 140.9 (C_{alkene}), 34.5, 31.9, 31.6, 28.2, 23.1, 22.6, 17.4, 14.2.

1-phenyl-hexan-3-one (**144a**)

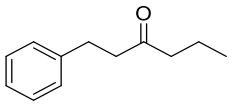

144a

According to GP-H, **144a** was synthesized using *n*-propyl manganese bromide lithium chloride complex (0.21 M, 5.7 mL, 1.2 mmol, 1.2 equiv.) and *S*-ethyl 3-phenylpropanethioate **119a** (194 mg, 1.00 mmol). Purification was achieved by column chromatography (Hex/EA = 30:1). The product was obtained as a colorless oil with a sweet pleasant smell (149.5 mg, 848 µmol, 85%). The data is in good accordance to reported literature.[24]

$C_{12}H_{16}O$ (176.26 g/mol)

R_f: 0.24 (Hex/EA = 30:1) [$KMnO_4$].

^{1}H NMR (400 MHz, $CDCl_3$): δ = 7.30–7.25 (m, 2H, $C_{Ar}H$), 7.21–7.17 (m, 3H, $C_{Ar}H$), 2.90 (t, *J* = 7.7 Hz, 2H, C(O)CH_2CH_2Ph), 2.72 (t, *J* = 7.7 Hz, 2H, C(O)CH_2CH_2Ph), 2.37 (t, *J* = 7.3 Hz, 2H, C(O)$CH_2CH_2CH_3$), 1.59 (h, *J* = 7.4 Hz, 2H, CH_2CH_3), 0.90 (t, *J* = 7.4 Hz, 3H, CH_2CH_3).

^{13}C NMR (101 MHz, $CDCl_3$): δ = 210.3 (*C*(O)), 141.3 (C_{Ar}), 128.6 (C_{Ar}), 128.4 (C_{Ar}), 126.2 (C_{Ar}), 45.1, 44.4, 29.9, 17.3, 13.9 (CH_3).

IR (ATR, $\tilde{\nu}$ [cm^{-1}]): 3062 (w, C-H_{arom}), 3025 (w, C-H_{arom}), 2958 (m, C-H_{aliph}), 2932 (w, C-H_{aliph}), 2875 (w, C-H_{aliph}), 1709 (s, C=O), 1601 (w), 1493 (w), 1452 (m), 1407 (w), 1369 (m), 1288 (w), 1275 (w), 1161 (w), 1124 (w), 1063 (w), 1031 (w), 1001 (w), 900 (w), 747 (s), 699 (s).

1-phenylheptan-3-one (**144b**)

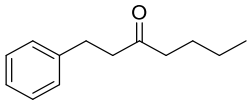

119a

The organomanganese reagent was synthesized by diluting $MnCl_2$·LiCl solution prepared after GP-C (3.6 mL, 1M in THF, 1.2 equiv.) with THF (7 mL) and slowly adding *n*-butyl lithium solution (1.2 mL, 3.0 mmol, 2.5 M in hexanes) at -79°C.[1] The solution was stirred for 1.5 h while warming up to -20 °C. Similar to GP-H, **144b** was synthesized using the prepared *n*-butyl manganese chloride lithium chloride complex (6 mL, 1.2 mmol, 0.2 M, 2 equiv.) and *S*-ethyl 3-phenylpropanethioate **119a** (194 mg, 1.00 mmol). Purification was achieved by column chromatography (Hex/Et_2O = 99:1). The product was obtained as a colorless oil with a sweet smell (175 mg, 920 µmol, 92%). Analytical data is in good accordance to reported literature.[39]

$C_{13}H_{18}O$ (190.26 g/mol)

R_f: 0.26 (Hex/Et_2O = 99:1) [UV].

^{1}H NMR (400 MHz, $CDCl_3$): δ = 7.30–7.27 (m, 2H, $C_{Ar}H$), 7.20–7.17 (m, 3H, $C_{Ar}H$), 2.90 (t, *J* = 7.4 Hz, 2H), 2.73 (t, *J* = 7.4 Hz, 2H), 2.38 (t, *J* = 7.4 Hz, 2H), 1.62–1.47 (m, 2H), 1.35–1.20 (m, 2H), 0.89 (t, *J* = 7.3 Hz, 3H).

^{13}C NMR (101 MHz, $CDCl_3$): δ = 210.5 (*C*(O)), 141.3 (C_{Ar}), 128.6 (C_{Ar}), 128.4 (C_{Ar}), 126.2 (C_{Ar}), 44.4, 42.9, 29.9, 26.0, 22.5, 14.0 (CH_3).

GC-MS (EI): t_r = 6.59 min, m/z(%) = 190 (9, [$M^{+\bullet}$]), 148 (16, [$M^{+\bullet}$-C_3H_6]), 105 (74, [$M^{+\bullet}$-C_3H_6 -CO]), 91 (100, [$Bn^{+\bullet}$]).

[1] The concentration of this reagent could not be determined as the color change for iodometric titration was observed to be much slower in absence of Mg-cations. The hydrolysis of the reagent therefore prohibits accurate determination of the concentration.

IR (ATR, $\tilde{\nu}$ [cm^{-1}]): 3062 (w, C-H_{arom}), 3025 (w, C-H_{arom}), 2954 (m, C-H_{aliph}), 2928 (m, C-H_{aliph}), 2868 (w, C-H_{aliph}), 1709 (s, C=O), 1601 (w), 1493 (w), 1452 (m), 1407 (w), 1369 (m), 1262 (w), 1202 (w), 1161 (w), 1124 (w), 1063 (w), 1031 (w), 971 (w), 911 (w), 744 (s), 699 (s).

4-methyl-1-phenylpentan-3-one (**144c**)

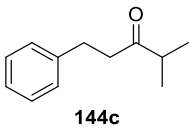

144c

According to GP-H, **144c** was synthesized using *iso*-propyl manganese bromide lithium chloride complex (4.1 mL, 1.2 mmol, 0.29 M, 1.2 equiv.) and *S*-ethyl 3-phenylpropanethioate **119a** (194 mg, 1.00 mmol). Purification was achieved by column chromatography (Hex/EA = 95:5). The product was obtained as a colorless oil with a sweet smell (158 mg, 896 µmol, 90%). The analytical data is in good accordance with the reported literature.[30]

$C_{12}H_{16}O$ (176.26 g/mol)

R_f: 0.33 (Hex/Et_2O = 95:5) [UV].

^{1}H NMR (400 MHz, $CDCl_3$): δ 7.30–7.26 (m, 2H, $C_{Ar}H$), 7.20–7.17 (m, 3H, $C_{Ar}H$), 2.89 (t, *J* = 7.8, 2H), 2.79–2.75 (m, 2H), 2.62–2.52 (hept, *J* = 6.9 Hz, 1H), 1.08–1.06 (d, *J* = 6.9 Hz, 6H).

^{13}C NMR (101 MHz, $CDCl_3$): δ = 213.9 (*C*(O)), 141.5 (C_{Ar}), 128.6 (C_{Ar}), 128.5 (C_{Ar}), 126.2 (C_{Ar}), 42.1, 41.2, 30.0, 18.3 (CH_3).

GC-MS (EI): t_r = 5.67 min, m/z(%) = 176 (19, [$M^{+\bullet}$]), 133 (40, [$M^{+\bullet}$-$C_3H_7^{\bullet}$]), 105 (100, [$M^{+\bullet}$-$C_3H_7^{\bullet}$-CO]), 91 (97, [$Bn^{+\bullet}$]).

IR (ATR, $\tilde{\nu}$ [cm^{-1}]): 3062 (w, C-H_{arom}), 3025 (w, C-H_{arom}), 2966 (m, C-H_{aliph}), 2928 (w, C-H_{aliph}), 2875 (w, C-H_{aliph}), 1709 (s, C=O), 1601 (w), 1493 (w), 1456 (m), 1407 (w), 1362 (w), 1284 (w), 1262 (w), 1183 (w), 1066 (m), 1031 (w), 997 (w), 964 (w), 926 (w), 747 (s), 699 (s).

1-cyclohexyl-3-phenylpropan-1-one (**144d**)

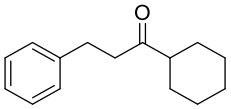

144d

According to GP-H, **144d** was synthesized using cyclohexyl manganese bromide lithium chloride complex (3.8 mL, 1.2 mmol, 0.32 M, 1.2 equiv.) and *S*-ethyl 3-phenylpropanethioate **119a** (194 mg, 1.00 mmol). Purification was achieved by column chromatography (PE/EA = 30:1). The product was obtained as a colorless oil (188 mg, 896 µmol, 87%). The analytical data is in good accordance with the reported literature.[40]

$C_{15}H_{20}O$ (216.32 g/mol)

R_f: 0.14 (PE/EA = 30:1) [UV].

^{1}H NMR (400 MHz, $CDCl_3$): δ = 7.32–7.24 (m, 2H, $C_{Ar}H$), 7.23–7.14 (m, 3H, $C_{Ar}H$), 2.89 (t, *J* = 7.8 Hz, 2H, C(O)CH_2CH_2Ph), 2.76 (t, *J* = 7.8 Hz, 2H, C(O)CH_2CH_2Ph), 2.31 (tt, *J* = 11.1, 3.4 Hz, 1H, C(O)C*H*), 1.83–1.74 (m, 4H, Cy*H*), 1.67–1.14 (m, 6H, Cy*H*).

^{13}C NMR (101 MHz, $CDCl_3$): δ = 213.3 (*C*(O)), 141.6 (C_{Ar}), 128.7 (C_{Ar}), 128.5 (C_{Ar}), 126.1 (C_{Ar}), 51.1, 42.4, 29.9, 28.5, 25.6, 25.8.

GC-MS (EI): t_r = 8.09, m/z(%) = 216 (27, [$M^{+\bullet}$]), 133 (41, [$M^{+\bullet}$-$C_6H_{11}^{\bullet}$]), 111 (23, [$M^{+\bullet}$-$C_8H_9^{\bullet}$]), 105 (74, [$M^{+\bullet}$-$C_6H_{11}^{\bullet}$-CO]), 91 (100, [$Bz^{+\bullet}$]), 83 (100, [$Cy^{+\bullet}$]).

IR (ATR, $\tilde{\nu}$ [cm^{-1}]): 3059 (w, C-H_{arom}), 3025 (w, C-H_{arom}), 2924 (s, C-H_{aliph}), 2853 (m, , C-H_{aliph}), 1705 (s, C=O), 1601 (w), 1493 (w), 1448 (m), 1407 (w), 1370 (w), 1319 (w), 1314 (w), 1297 (w), 1262 (w), 1187 (w), 1142 (w), 1083 (w), 1027 (w), 989 (m), 889 (w), 744 (m), 699 (s).

1,5-diphenylpentan-3-one (**144g**)

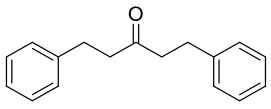

144g

According to GP-H, **144g** was synthesized using 2-phenylethyl manganese bromide lithium chloride complex (5.7 mL, 1.2 mmol, 0.21 M, 1.2 equiv.) and *S*-ethyl 3-phenylpropanethioate **119a** (194 mg, 1.00 mmol). Purification was achieved by flash column chromatography (23 g SiO_2, gradient from pure Hex to Hex/Et_2O 90:10 over 14 CV and hold for 3 CV). The product was obtained as a colorless oil with a sweet smell (148 mg, 621 µmol, 62%). The analytical data is in good accordance with the reported literature.[41]

$C_{17}H_{18}O$ (238.33 g/mol)

R_f: 0.47 (Hex/Et_2O = 9:1) [UV].

^{1}H NMR (400 MHz, $CDCl_3$): δ = 7.26– 7.04 (m, 10H, $C_{Ar}H$), 2.82 (t, *J* = 7.6 Hz, 1H), 2.64 (t, *J* = 7.6 Hz, 1H).

^{13}C NMR (101 MHz, $CDCl_3$): δ = 209.3 (*C*(O)), 141.1 (C_{Ar}), 128.6 (C_{Ar}), 128.5 (C_{Ar}), 126.3 (C_{Ar}), 44.7 (Ph*C*H_2), 29.9 (PhCH_2*C*H_2).

GC-MS (EI): t_r = 9.33 min, m/z(%) = 238 (9, [$M^{+\bullet}$]), 133 (24, [$M^{+\bullet}$-$C_8H_9^{\bullet}$]), 105 (55, [$C_8H_9^{+\bullet}$]), 91 (100, [$Bn^{+\bullet}$]).

IR (ATR, $\tilde{\nu}$ [cm^{-1}]): 3058 (w, C-H_{arom}), 3025 (w, C-H_{arom}), 2924 (w, C-H_{aliph}), 2861 (w, C-H_{aliph}), 2801 (w, C-H_{aliph}), 1709 (s, C=O), 1601 (w), 1493 (m), 1448 (m), 1407 (m), 1366 (m), 1284 (w), 1183 (w), 1090 (m), 1027 (w), 978 (w), 911 (w), 744 (s), 695 (vs).

1,4-diphenylbutan-2-one (**144h**)

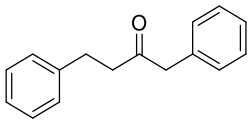

144h

According to GP-H, **144h** was synthesized using benzyl manganese bromide lithium chloride complex (4.4 mL, 1.2 mmol, 0.27 M, 1.2 equiv.) and *S*-ethyl 3-phenylpropanethioate **119a** (194 mg, 1.00 mmol). Purification was achieved by column chromatography (Hex/Et_2O = 95:5). The product was obtained as a colorless oil with a sweet smell (49 mg, 218 µmol, 22%). The analytical data is in good accordance with the reported literature.[42]

$C_{16}H_{16}O$ (224.30 g/mol)

R_f: 0.21 (Hex/Et_2O = 98:2) [UV].

^{1}H NMR (400 MHz, $CDCl_3$): δ = 7.34–7.14 (m, 5H, $C_{Ar}H$), 7.14–7.00 (m, 5H, $C_{Ar}H$), 3.59 (s, 2H, PhCH_2C(O)), 2.84–2.75 (m, 2H), 2.75–2.65 (m, 2H).

^{13}C NMR (101 MHz, $CDCl_3$): δ = 207.6 (*C*(O)), 141.1 (C_{Ar}), 134.2 (C_{Ar}), 129.5 (C_{Ar}), 128.9 (C_{Ar}), 128.6 (C_{Ar}), 128.5 (C_{Ar}), 127.2 (C_{Ar}), 126.2 (C_{Ar}), 50.5, 43.6, 29.9.

GC-MS (EI): t_r = 8.67 min, m/z(%) = 224 (1, [$M^{+\bullet}$]), 133 (12, [$M^{+\bullet}$-$Bn^{\bullet}$]), 105 (22, [$M^{+\bullet}$-$Bn^{\bullet}$-CO]), 91 (100, [$Bn^{+\bullet}$]).

IR (ATR, $\tilde{\nu}$ [cm^{-1}]): 3062 (w, C-H_{arom}), 3028 (w, C-H_{arom}), 2924 (w, C-H_{aliph}), 1701 (s, C=O), 1601 (w), 1493 (w), 1448 (w), 1411 (m), 1359 (w), 1280 (m), 1217 (m), 1153 (m), 1072 (w), 1027 (w), 997 (w), 934 (w), 914 (w), 833 (w), 781 (w), 744 (m), 695 (s).

5-methyl-1-phenylhexan-3-one (**144i**)

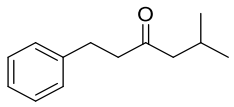

144i

According to GP-H with minor deviations, **144i** was synthesized using *iso*-butyl manganese bromide lithium chloride complex (4.4 mL, 1.2 mmol, 0.27 M, 1.2 equiv.) and *S*-ethyl 3-phenylpropanethioate **119a** (194 mg, 1 mmol). Purification was achieved by flash column chromatography (23 g SiO_2, 15 µm spherical, Hex/ACN = 99:1). The product was obtained as a colorless oil with a fruitful smell (99 mg, 522 µmol, 52%). The analytical data is in good accordance to reported literature.[43]

$C_{13}H_{18}O$ (190.29 g/mol)

R_f: 0.14 (Hex/ACN = 50:1) [anis - blue].

^{1}H NMR (400 MHz, $CDCl_3$): δ = 7.37–7.28 (m, 2H, $C_{Ar}H$), 7.28–7.19 (m, 3H, $C_{Ar}H$), 2.94 (t, *J* = 7.6 Hz, 2H), 2.75 (t, *J* = 7.6 Hz, 2H), 2.31 (d, *J* = 6.8 Hz, 2H, C(O)CH_2C$(CH_3)_2$), 2.24–2.10 (m, 1H), 0.94 (d, *J* = 6.8 Hz, 6H, CH(C$H_3)_2$).

^{13}C NMR (101 MHz, $CDCl_3$): δ = 210.1 (*C*(O)Et), 141.3 (C_{Ar}), 128.6 (C_{Ar}), 128.5(C_{Ar}), 126.2(C_{Ar}), 52.2, 44.9, 29.8, 24.7, 22.7.

1-(1,3-dioxan-2-yl)-5-phenylpentan-3-one (**144j**)

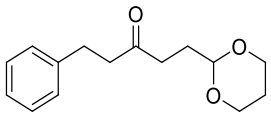

144j

According to GP-H, **144j** was synthesized using (1,3-dioxan-2-ylethyl) manganese bromide lithium chloride complex (5.7 mL, 1.2 mmol, 0.21 M, 1.2 equiv.) and *S*-ethyl 3-phenylpropanethioate **119a** (194 mg, 1.00 mmol). Quenching the reaction was achieved by addition of brine (ca. 2 mL). Purification was achieved by column chromatography (Hex/Et_2O = 1:1). The product was obtained as a colorless oil with a sweet smell (121 mg, 487 µmol, 49%).

$C_{15}H_{20}O_3$ (248.32 g/mol)

R_f: 0.45 (Hex/Et = 30:1) [$KMnO_4$].

^{1}H NMR (400 MHz, $CDCl_3$): δ = 7.29–7.26 (m, 2H, $C_{Ar}H$), 7.20–7.17 (m, 3H, $C_{Ar}H$), 4.55 (t, *J* = 4.9 Hz, 1H), 4.06 (dt, *J* = 11.8 Hz, 5.0 Hz, 2H), 3.72 (dt, *J* = 12.2 Hz, 2.5 Hz, 2H), 2.91–2.88 (m, 2H), 2.76–2.72 (m, 2H), 2.52 (t, *J* = 7.2 Hz, 2H), 1.88 (dt, *J* = 7.2 Hz, 4.9 Hz, 2H), 1.43–1.24 (m, 2H).

^{13}C NMR (101 MHz, $CDCl_3$): δ = 209.6 (*C*(O)), 141.3 (C_{Ar}), 128.6 (C_{Ar}), 128.5 (C_{Ar}), 126.2 (C_{Ar}), 101 (O*C*HO), 67.0(*C*H_2OCHO), 44.4, 37.0, 29.9, 29.1, 25.9 (CH_2CH_3).

GC-MS (EI): t_r = 9.29 min, m/z(%) = 247 (3, [$M^{+\bullet}$]), 191 (6, [$M^{+\bullet}$-C_3H_5O]), 172 (42), 100 (100).

HR-MS (ESI): m/z calc. for $[M+Na]^+$ 271.13047, found 271.13055.

IR (ATR, $\tilde{\nu}$ [cm^{-1}]): 3059 (w, C-H_{arom}), 3025 (w, C-H_{arom}), 2958 (w, C-H_{aliph}), 2932 (w, C-H_{aliph}), 2850 (w, C-H_{aliph}), 1709 (s, C=O), 1601 (w), 1493 (w), 1448 (w), 1407 (w), 1370 (m), 1281 (w), 1240 (w), 1209 (w), 1176 (w), 1139 (s, C_{aliph}-O_{ether}-C), 1092 (m), 1042 (m), 1004 (m), 923 (w), 889 (w), 848 (w), 747 (m), 699 (s).

1-phenyloct-7-en-3-one (**144k**)

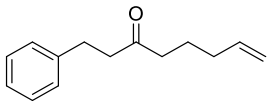

144k

According to GP-H, **144k** was synthesized using pent-4-enyle manganese bromide lithium chloride complex (4.0 mL, 1.2 mmol, 0.3 M, 1.2 equiv.) and *S*-ethyl 3-phenylpropanethioate **119a** (194 mg, 1.00 mmol). Purification was achieved by column chromatography (PE/EA = 30:1). The product was obtained as a colorless oil (161 mg, 796 µmol, 80%). The analytical data is in good accordance with the reported literature.[44]

$C_{14}H_{18}O$ (202.30 g/mol)

R_f: 0.29 (PE/EA = 30:1) [anis, $KMnO_4$, UV].

^{1}H NMR (400 MHz, $CDCl_3$): δ = 7.37–7.28 (m, 2H, $C_{Ar}H$), 7.26–7.19 (m, 3H, $C_{Ar}H$), 5.79 (ddt, *J* = 16.9, 10.2, 6.7 Hz, 1H, $C_{alkene}HCH_2$), 5.15–4.81 (m, 2H, $CHC_{alkene}H_2$), 2.94 (t, *J* = 7.6 Hz, 2H, PhCH_2CH_2), 2.77 (t, *J* = 7.6, 2H, $PhCH_2CH_2$), 2.44 (t, *J* = 7.4 Hz, 2H), 2.13–1.99 (m, 2H), 1.71 (p, *J* = 7.4 Hz, 2H).

^{13}C NMR (101 MHz, $CDCl_3$): δ = 210.1 (*C*(O)), 141.3 (C_{Ar}), 138.1 ($C_{alkene}HCH_2$), 128.6 (C_{Ar}), 128.5 (C_{Ar}), 126.2 (C_{Ar}), 115.4 ($CHC_{alkene}H_2$), 44.5, 42.3, 33.2, 29.9, 22.9.

GC-MS (EI): t_r = 7.05 min, m/z(%) = 202 (5, [$M^{+\bullet}$]), 133 (28, [$M^{+\bullet}$-$C_5H_9^{\bullet}$]), 105 (58, [$M^{+\bullet}$-$C_5H_9^{\bullet}$-CO]), 91(100, [$Bz^{+\bullet}$]).

IR (ATR, $\tilde{\nu}$ [cm^{-1}]): 3068 (w, C-H_{arom}), 3025 (w, C-H_{arom}), 2931 (w, C-H_{aliph}), 2865 (w, C-H_{aliph}), 1709 (s, C=O), 1638 (w), 1601 (w), 1493 (w), 1448 (m), 1408 (w), 1366 (m), 1300 (w), 1209 (w), 1187 (w), 1153 (w), 1083 (w), 1027 (w), 994 (m), 911 (s), 744 (m), 699 (s).

5.6 Reaction Procedures for Ferrates

All samples were prepared at 25 °C in a recirculating Jacomex Campus inert atmosphere (Ar) glovebox and vacuum Schlenk lines. Glassware was dried overnight at 120 °C before use. Deuterated solvents were thoroughly degassed and dried overnight on 4 Å molecular sieves. All non-deuterated solvents were dried over a Na/benzophenone mixture and distilled before use; NMR tubes equipped with a J. Young valve were used for all ^{1}H NMR experiments. All chemicals were used as purchased, unless specified otherwise. The synthesized thioester **115a** was degassed and dried on molecular sieves prior to use in ^{1}H NMR experiments.

NMR spectra were obtained using a Magritek benchtop 60 MHz Spinsolve spectrometer. Chemical shifts for ^{1}H NMR spectra were referenced to solvent non-deuterated impurities (herein THF).

*Typical procedure for probing reactivity of $[FeMes_3]^-$ with **56**:*

In a glovebox, a J. Young NMR tube was charged with $FeCl_2$ (2 mg, 16 µmol) in THF-d_8. 3.1 equiv. (50 µmol, 50 µL) of a 1 M THF solution of MesMgBr was then added; the solution turned to pale yellow. In order to ensure full conversion of $FeCl_2$, the tube was sonicated during 30 min. ^{1}H NMR monitoring confirmed formation of $[FeMes_3]^-$. In a second experiment, an excess of **115a** was added (22.4 mg, 140 µmol, 8.8 equiv.). ^{1}H NMR spectrum was recorded after 10 min at room temperature.

^{1}H NMR monitoring of reaction between $[FeMes_3]^-$ and EtSMgBr

In a glovebox, a J. Young NMR tube was charged with $FeCl_2$ (2 mg, 16 µmol) in THF-d_8. 3.1 equiv. (50 µmol, 50 µL) of a 1 M THF solution of MesMgBr was then added; the solution turned to pale yellow. In order to ensure full conversion of $FeCl_2$, the tube was sonicated during 30 min. ^{1}H NMR monitoring confirmed formation of $[FeMes_3]^-$. In a second experiment, 0.3 equiv. of *in situ* generated EtSMgBr (dissolved in ca. 100 µL of d_8 THF) was added. ^{1}H NMR spectrum was recorded after 10 min at room temperature.

5.7 Miscellaneous Syntheses

ethyl benzodithioate (**139**)

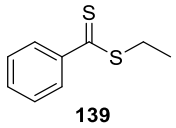

139

The product was synthesized by a modified literature procedure.[45] Lawesson's reagent (3.03 g, 7.50 mmol, 0.75 equiv.) was dissolved in degassed toluene (100 mL) and thioester **129a** (1.66 g, 10.0 mmol, 1.0 equiv.) added at once. The reaction was heated to reflux for 8 h. After cooling, the mixture was concentrated by evaporation of solvent. The crude product was purified by manual column chromatography (Hex) to yield a intense red colored oil (987 mg, 5.41 mmol, 54%)

$C_9H_{10}S_2$ (182.30 g/mol)

R_f: 0.54 (Hex) [Vis].

^{1}H NMR (400 MHz, $CDCl_3$): δ = 8.05–7.94 (m, 2H, $C_{Ar}H$), 7.59–7.47 (m, 1H, $C_{Ar}H$), 7.43–7.34 (m, 2H, $C_{Ar}H$), 3.39 (q, *J* = 7.5 Hz, 2H, SCH_2CH_3), 1.42 (t, *J* = 7.5 Hz, 3H, SCH_2CH_3).

^{13}C NMR (101 MHz, $CDCl_3$): δ = 145.3 (*C*(S)SEt), 132.3 (C_{Ar}), 128.7 (C_{Ar}), 128.4 (C_{Ar}), 126.9 (C_{Ar}), 31.6 (SCH_2CH_3), 12.4 (SCH_2CH_3).

HR-MS (APCI): m/z calc. for $[M+H]^+$ 183.02967, found. 183.03003.

GC-MS (EI): t_r = 6.96, m/z(%) = 182 (23, $[M^{+\bullet}]$), 121 (100, $[M^{+\bullet}\text{-}SC_2H_5^{\bullet}]$), 91 (29).

IR (ATR, $\tilde{\nu}$ [cm^{-1}]): 3055 (w, C-H_{arom}), 2924 (w, C-H_{aliph}), 1735 (w), 1661 (m), 1575 (w), 1500 (m), 1448 (m), 1410 (w), 1292 (w), 1243 (w), 1195 (w), 1169 (w), 1095 (w), 1042 (w), 1012 (m), 971 (w), 915 (w), 870 (w), 837 (w), 769 (m), 743 (s), 703 (m), 672 (m).

S-Phenyl thioformate (**231**)

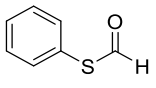

231

The product was synthesized by a modified literature procedure.[46] Formic acid (11.3 mL, 300 mmol, 6.0 equiv.) and acetic anhydride (18.9 mL, 200 mmol, 4.0 equiv.) were stirred at 60 °C for 2 h in a RBF equipped with stirring bar and drying tube. Then, the mixture was allowed to cool to rt and thiophenol (5.1 mL, 50 mmol, 1.0 equiv.) and pyridine (400 µL, 5 mmol, 0.1 equiv.) added. The reaction stirred 18 h at rt. Afterwards, the reaction was quenched by addition on demin. water (ca. 15 mL) and diluted with EA (50 mL). The aq. layer was extracted with EA (3 × 30 mL). Afterwards, the organic layer was extracted with aq. KOH (3 × 20 mL, 10% w/v), sat. aq. $NaHCO_3$ (1 × 20 mL) and brine (1 × 20 mL) before drying over anhydrous Na_2SO_4. The organic layer was dried over anhydrous Na_2SO_4. The purification was achieved by bulb-to-bulb distillation of residual thiophenol (120 °C, 10 mBar) and vacuum distillation of product (70 °C, 0.7 mBar) to yield a colorless oil with a characteristic unpleasant smell (5.70 g, 41.3 mmol, 83%)[Lit.[46]: 93%]. The analytical data is in accordance to reported literature.[46]

C_7H_6OS (138.18 g/mol)

R_f: 0.53 (Hex/EA = 30:1) [UV]

^{1}H NMR (400 MHz, $CDCl_3$): δ = 10.24 (s, 1H, *H*C(O)SAr), 7.55–7.41 (m, 5H, $C_{Ar}H$).

^{13}C NMR (101 MHz, $CDCl_3$): δ = 190.1 (H*C*(O)SAr), 134.4 (C_{Ar}), 130.1 (C_{Ar}), 129.8 (C_{Ar}), 126.3 (C_{Ar}).

S-phenyl dimethylcarbamothioate (**263**)

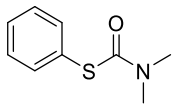

263

The thiocarbamate **263** was synthesized by an adapted procedure.[47] In a RBF equipped with a stirring bar, thiophenol (1.3 mL, 13.1 mmol, 1.0 equiv.) was dissolved in THF (14 mL) and sodium hydride (580 mg, 14.4 mmol, 1.1 equiv.) added in portions at 0 °C. After 30 min, dimethylcarbamoyl chloride (1.6 mL, 17.2 mmol, 1.3 equiv.) was carefully added at the same temperature. The reaction was allowed to stir for 18 h while warming to rt. The reaction mixture was quenched with aq. sat. NH_4Cl sol. and ethereal solvent evaporated from the biphasic system under reduced pressure. Then, the suspension was diluted with DCM and the aqueous layer extracted with DCM (5 × 10 mL). The organic phase was dried over anhydrous $MgSO_4$, concentrated under reduced pressure and the gained oil stored at 4 °C which led to crystallization of target product. The precipitate was recrystallized from Et_2O and washed with cold pentane (4 × 3 mL) to obtain *S*-phenyl-*N*,*N*-dimethylthiocarbamate **263** (2.19 g, 12.1 mmol, 92%)[Lit.[47]: 59%] as colorless aciculate crystals. The analytical data in accordance with the reported literature.[47]

$C_9H_{11}NOS$ (181.25 g/mol)

R_f: 0.25 (PE/EA = 5:1) [UV]

Melting point = 44–47 °C (Et_2O).

^{1}H NMR (400 MHz, $CDCl_3$): δ = 7.55–7.45 (m, 2H, $C_{Ar}H$), 7.43–7.33 (m, 3H, $C_{Ar}H$), 3.12–3.01 (m, 6H, $N(CH_3)_2$).

^{13}C NMR (101 MHz, $CDCl_3$): δ = 167.0 (CO), 135.8 (C_{Ar}), 129.2 (C_{Ar}), 129.0 (C_{Ar}), 128.9 (C_{Ar}), 37.0 ($N(CH_3)_2$).

S-(4-methoxyphenyl) dimethylcarbamothioate (**265**)

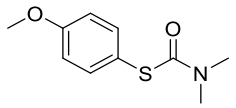

265

The thiocarbamate **265** was synthesized by an adapted procedure.[47] In a RBF equipped with a stirring bar, *p*-methoxythiophenol (7.0 mL, 57.1 mmol, 1.0 equiv.) was dissolved in and THF (80 mL). Then, sodium hydride (2.51 g, 62.8 mmol, 1.1 equiv.) was added in portions at 0 °C. After 30 min. dimethylcarbamoyl chloride (6.8 mL, 71.2 mmol, 1.3 equiv.) was carefully added at the same temperature. The reaction was allowed to stir for 18 h while warming to rt. After quenching the reaction mixture with sat. aq. NH_4Cl solution (15 mL), THF was evaporated under reduced pressure. The remaining white sludge was dissolved in EA (150 mL) and washed with demin. water (1 × 100 mL), aq. KOH sol. (3 × 75 mL, 10% w/v), sat. $NaHCO_3$ sol. (1 × 100 mL) and brine (1 × 100 mL). The organic phase was dried over anhydrous $MgSO_4$, filtered and evaporated to receive the crude product as a white solid. After recrystallization from EtOAc (10 mL) the *S*-(4-methoxyphenyl) dimethylcarbamothioate **265** (10.14 g, 48.0 mmol. 84%) [Lit.[48]: 79%] is obtained as colorless aciculate crystals. The analytical data aligns with the reported literature.[48]

$C_{10}H_{13}NO_2S$ (211.28 g/mol)

R_f: 0.15 (PE/EA = 5:1) [UV]

Melting point = 91–92 °C (EA).

^{1}H NMR (400 MHz, $CDCl_3$): δ =7.43–7.36 (m, 2 H, $C_{Ar}H$), 6.95– 6.88 (m, 2 H, $C_{Ar}H$), 3.81 (s, 3 H, OCH_3), 3.17–2.92 (m, 6 H, $N(CH_3)_2$).

^{13}C NMR (101 MHz, $CDCl_3$): δ = 167.8 (*C*O), 160.7 ($C_{Ar}OCH_3$), 137.5 (C_{Ar}), 119.5 (C_{Ar}), 114.7 (C_{Ar}), 55.5 (OCH_3), 37.0 ($N(CH_3)_2$).

5.8 References

[1] D. B. G. Williams, M. Lawton, *J. Org. Chem.* **2010**, *75*, 8351–8354.
[2] D. S. Pedersen, C. Rosenbohm, *Synthesis* **2001**, *2001*, 2431–2434.
[3] H. E. Gottlieb, V. Kotlyar, A. Nudelman, *J. Org. Chem.* **1997**, *62*, 7512–7515.
[4] a) V. Hirschbeck, M. Böldl, P. H. Gehrtz, I. Fleischer, *Org. Lett.* **2019**, *21*, 2578–2582; b) J. Riedmaier, Bachelor Thesis, University of Tübingen, **2019**; c) V. Geiger, Master Thesis, University of Tübingen, **2018**; d) P. H. Gehrtz, P. Kathe, I. Fleischer, *Chem. Eur. J.* **2018**, *24*, 8774–8778.
[5] M. Wang, Z. Dai, X. Jiang, *Nat. Commun.* **2019**, *10*, 2661.
[6] I. Mizota, C. Ueda, Y. Tesong, Y. Tsujimoto, M. Shimizu, *Org. Lett.* **2018**, *20*, 2291–2296.
[7] N. Iranpoor, H. Firouzabadi, H. Shaterian, *Synlett* **2000**, *2000*, 65–66.
[8] H. Ochiai, Y. Uetake, T. Niwa, T. Hosoya, *Angew. Chem. Int. Ed.* **2017**, *56*, 2482–2486.
[9] B. Neises, W. Steglich, *Angew. Chem. Int. Ed.* **1978**, *17*, 522–524.
[10] K. Kunchithapatham, C. C. Eichman, J. P. Stambuli, *Chem. Commun.* **2011**, *47*, 12679-12681.
[11] A. Krasovskiy, P. Knochel, *Synthesis* **2006**, 0890–0891.
[12] L. Rousseau, A. Desaintjean, P. Knochel, G. Lefèvre, *Molecules* **2020**, *25*, 723.
[13] G. Cahiez, M. Alami, *Tetrahedron* **1989**, *45*, 4163–4176.
[14] M. Tamura, J. Kochi, *J. Organomet. Chem.* **1971**, *29*, 111–129.
[15] X. Zhang, P. Sun, L. Huangshan, B.-H. Hu, P. B. Messersmith, *Chem. Commun.* **2015**, *51*, 9662–9665.
[16] P. H. Gehrtz, P. Kathe, I. Fleischer, *Chem. Eur. J.* **2018**, *24*, 8774–8778.
[17] D. V. Avilov, M. G. Malusare, E. Arslancan, D. C. Dittmer, *Org. Lett.* **2004**, *6*, 2225–2228.
[18] H. Ochiai, Y. Uetake, T. Niwa, T. Hosoya, *Angew. Chem. Int. Ed.* **2017**, *56*, 2482–2486.
[19] X. Qi, Z.-P. Bao, X.-T. Yao, X.-F. Wu, *Org. Lett.* **2020**, *22*, 6671–6676.
[20] J. B. Azeredo, M. Godoi, R. S. Schwab, G. V. Botteselle, A. L. Braga, *Eur. J. Org. Chem.* **2013**, *2013*, 5188–5194.
[21] N. Li, J. Ou, M. Miesch, P. Chiu, *Org. Biomol. Chem.* **2011**, *9*, 6143–6147.
[22] D. C. B. Siebert, R. Sommer, D. Pogorevc, M. Hoffmann, S. C. Wenzel, R. Müller, A. Titz, *Beilstein J. Org. Chem.* **2019**, *15*, 2922–2929.
[23] T. Xia, Z. Wei, B. Spiegelberg, H. Jiao, S. Hinze, J. G. de Vries, *Chem. Eur. J.* **2018**, *24*, 4043-4049.
[24] M. V. Laktsevich-Iskryk, N. A. Varabyeva, V. V. Kazlova, V. N. Zhabinskii, V. A. Khripach, A. L. Hurski, *Eur. J. Org. Chem.* **2020**, *2020*, 2431–2434.
[25] T. C. Wabnitz, J.-Q. Yu, J. B. Spencer, *Chem. Eur. J.* **2004**, *10*, 484–493.
[26] N. J. Clegg, S. Paruthiyil, D. C. Leitman, T. S. Scanlan, *J. Med. Chem.* **2005**, *48*, 5989–6003.
[27] T. Miyoshi, T. Miyakawa, M. Ueda, O. Miyata, *Angew. Chem. Int. Ed.* **2011**, *50*, 928–931.
[28] K. Mori, J. Tabata, *Tetrahedron* **2017**, *73*, 6530–6541.
[29] M. Liu, Z. Hyder, Y. Sun, W. Tang, L. Xu, J. Xiao, *Org. Biomol. Chem.* **2010**, *8*, 2012–2015.
[30] E. Erbing, A. Vázquez-Romero, A. Bermejo Gómez, A. E. Platero-Prats, F. Carson, X. Zou, P. Tolstoy, B. Martín-Matute, *Chem. Eur. J.* **2016**, *22*, 15659–15663.
[31] Z. Hyder, J. Ruan, J. Xiao, *Chem. Eur. J.* **2008**, *14*, 5555–5566.
[32] Y. Li, D. Xue, W. Lu, C. Wang, Z.-T. Liu, J. Xiao, *Org. Lett.* **2014**, *16*, 66–69.
[33] B. Scheiper, M. Bonnekessel, H. Krause, A. Fürstner, *J. Org. Chem.* **2004**, *69*, 3943–3949.
[34] L. K. M. Chan, D. L. Poole, D. Shen, M. P. Healy, T. J. Donohoe, *Angew. Chem. Int. Ed.* **2014**, *53*, 761–765.
[35] M. Uyanik, D. Suzuki, T. Yasui, K. Ishihara, *Angew. Chem. Int. Ed.* **2011**, *50*, 5331–5334.
[36] A. K. Ghosh, J. Takayama, Y. Aubin, K. Ratia, R. Chaudhuri, Y. Baez, K. Sleeman, M. Coughlin, D. B. Nichols, D. C. Mulhearn, et al., *J. Med. Chem.* **2009**, *52*, 5228–5240.
[37] P. B. Cranwell, M. O'Brien, D. L. Browne, P. Koos, A. Polyzos, M. Peña-López, S. V. Ley, *Org. Biomol. Chem.* **2012**, *10*, 5774–5779.
[38] M. Hayashi, M. Shibuya, Y. Iwabuchi, *Org. Lett.* **2012**, *14*, 154–157.
[39] R. Hu, F.-J. Chen, X. Zhang, M. Zhang, W. Su, *Nat. Commun.* **2019**, *10*, 3681.
[40] G. S. Lee, J. Won, S. Choi, M.-H. Baik, S. H. Hong, *Angew. Chem. Int. Ed.* **2020**, *59*, 16933-16942.

[41] Y. Qin, J. Lu, Z. Zou, H. Hong, Y. Li, Y. Li, L. Chen, J. Hu, Y. Huang, *Org. Chem. Front.* **2020**, *7*, 1817–1822.
[42] C. Zhao, X. Jia, X. Wang, H. Gong, *J. Am. Chem. Soc.* **2014**, *136*, 17645–17651.
[43] B. S. Pilgrim, A. E. Gatland, C. H. A. Esteves, C. T. McTernan, G. R. Jones, M. R. Tatton, P. A. Procopiou, T. J. Donohoe, *Org. Biomol. Chem.* **2016**, *14*, 1065–1090.
[44] G. C. Tay, N. Sizemore, S. D. Rychnovsky, *Org. Lett.* **2016**, *18*, 3050–3053.
[45] R. J. Hewitt, M. J. H. Ong, Y. W. Lim, B. A. Burkett, *Eur. J. Org. Chem.* **2015**, *2015*, 6687-6700.
[46] R. Haraguchi, S.-g. Tanazawa, N. Tokunaga, S.-i. Fukuzawa, *Org. Lett.* **2017**, *19*, 1646–1649.
[47] A. F. Roesel, M. Ugandi, N. T. T. Huyen, M. Májek, T. Broese, M. Roemelt, R. Francke, *J. Org. Chem.* **2020**, *85*, 8029–8044.
[48] J. D. Moseley, R. F. Sankey, O. N. Tang, J. P. Gilday, *Tetrahedron* **2006**, *62*, 4685–4689.

6. SUMMARY/ZUSAMMENFASSUNG

This thesis deals with catalytic conversions of carbonyl-sulfur building blocks using late transition metal-catalysts to provide valuable transformations for organic syntheses, by exploiting selective C-S bond activation under mild conditions. For this, cross-coupling reactions are crucial transformations in small to large scale organic syntheses and usually employ late transition metal-catalysts. While palladium is still an important catalyst for such conversions, replacement of this precious metal by iron, cobalt or nickel is incentivized by a favorable cost-efficiency, abundance or carbon-footprint, which was presented in chapter 1 of this thesis. To this end, historical developments, overviews of current state-of-the-art methodologies and mechanistic studies of iron- and cobalt-catalyzed cross-couplings of Grignard reagents were reviewed in respective chapters.

In chapter 2, the iron-catalyzed cross-coupling of thioesters with alkyl manganese reagents was developed. These reagents enabled the reaction to proceed under mild conditions, short reaction times, medium catalyst loadings of a cheap iron-precatalyst while only necessitating low excess of manganese reagent. This led to the synthesis of a broad scope of ketones with examples of highly functionalized compounds such as derivatives of natural or pharmaceutical compounds. The regioselectivity of the method as well as the tolerance of aryl (pseudo-)halides allowed for beneficial orthogonal reactivity. Furthermore, the observed formation of iron thiolates during the reaction demonstrated an advantage of thio-based building blocks on the overall reaction such as the stabilization of potential alkyl iron intermediates in presence of thiolate.

In chapter 3, the transition metal-catalyzed (Co, Ni) conversions of *S*-aryl thioformates or *S*-aryl thiocarbamates was studied. The carbonyl-sulfur building blocks were probed for reactions with organometallic reagents under catalytic conditions. The formylation of organozinc reagents by employing *S*-thioformates as formyl donors, was found to be promoted by cobalt-catalysis. With only fair yields, the results exhibited a complex reactivity of the starting materials as well as the aldehyde products. Additionally, both building blocks were studied as masked thiolate sources for the synthesis of thioethers, which proceeded with varying yields under reductive or cross-coupling conditions. For thiocarbamates, the cobalt-catalyzed cross-coupling reaction also proceeded in the presence of styrene *via* hydromagnesiation.

Diese Arbeit befasst sich mit den katalytischen Umwandlungen von Carbonyl-Schwefel-Bausteinen unter Verwendung von späten Übergangsmetallkatalysatoren, welche wertvolle Umwandlungen für organische Synthesen mittels selektiver Aktivierung von C-S-Bindungen unter milden Bedingungen ermöglichen. Hierfür wurden Kreuzkupplungsreaktionen erforscht, da diese entscheidende Reaktionen bei organischen Synthesen darstellen in kleinem oder großem Maßstab und bei denen in der Regel späte Übergangsmetallkatalysatoren eingesetzt werden. Palladium ist zwar immer noch ein wichtiges Katalysatormetall für solche Umwandlungen, aber der Ersatz dieses Edelmetalls durch Eisen, Kobalt oder Nickel wird durch eine günstigere Kosteneffizienz, höheres natürliches Vorkommen oder den geringeren Kohlenstoff-Fußabdruck der Metalle begünstigt, was in Kapitel 1 dieser Arbeit erläutert wurde. Zu diesem Zweck wurden in nachfolgenden Kapiteln historische Entwicklungen, Zusammenfassungen über aktuelle Methoden und mechanistische Details von eisen- und kobaltkatalysierten Kreuzkupplungen von Grignard-Reagenzien diskutiert.

In Kapitel 2 wurde eine eisenkatalysierte Kreuzkupplung von Thioestern mit Alkylmangan-Reagenzien entwickelt. Diese Reagenzien ermöglichten die Reaktion unter sehr milden Bedingungen, kurzen Reaktionszeiten und mittleren Katalysatorladungen eines preisgünstigen Eisen-Präkatalysators, während nur ein geringer Überschuss des Manganreagenzes erforderlich war. Dies führte zur Synthese eines breiten Spektrums von Ketonen mit Beispielen von hochfunktionalisierten Verbindungen, wie Naturstoff- oder pharmazeutische Derivate. Die Regioselektivität der Methode sowie die Toleranz gegenüber Aryl(pseudo)halogeniden ermöglichten eine vorteilhafte orthogonale Reaktivität. Darüber hinaus verdeutlichte die beobachtete Bildung von intermediären Eisenthiolaten während der Reaktion einen Vorteil von Schwefel-basierten Bausteinen für die Gesamtreaktion, wie eine Stabilisierung intermediärer Alkyleisen-Spezies durch die Thiolatanionen.

In Kapitel 3 wurde die Übergangsmetall-katalysierte (Co, Ni) Umwandlung von *S*-Arylthioformiaten in *S*-Arylthiocarbamate untersucht. Die Carbonyl-Schwefel-Bausteine wurden für Reaktionen mit organometallischen Reagenzien unter Übergangsmetall-katalytischen Bedingungen untersucht. Es wurde festgestellt, dass die Formylierung von Organozinkreagenzien unter Verwendung von *S*-Thioformaten als Formyl-Donatoren durch Kobalt-Katalyse ermöglicht wird. Die Ergebnisse zeigten eine komplexe Reaktivität der Ausgangsstoffe und der Aldehydprodukte bei mittleren Ausbeuten. Zusätzlich wurden beide Bausteine als maskierte Thiolatquelle für die Synthese von Thioethern untersucht, die unter reduktiven oder Kreuzkupplungsbedingungen unterschiedlichen Ausbeuten ergaben. Bei den Thiocarbamaten erfolgte die kobaltkatalysierte Kreuzkupplungsreaktion auch mit zusätzlichem Styrol über eine mögliche Hydromagnesiierungsreaktion.

7. APPENDIX

7.1 Code

The following code was used in the data processing of the IR spectra. The code is written in R and was last executed 27.08.2022.

```
################################################################################
###R Statistics: https://www.r-project.org/ ###
###README:
###For execution the file path has to be adjusted AND the .spc files from the spectrometer have to be
###converted to .csv. For this, spectragryph was used. The loop will convert any .csv spectrum into a
###.txt with wavenumber and intensity. A .png will be created with circled peaks for peak verification.
################################################################################

##############################################Packages#################################
###Load packages
	library(tibble)
	library(dplyr)
	library(ggplot2)
	library(hyperSpec)
	library(tidyr)
	library(reshape2)

##############################################File-readout#############################
###Reading of the folder data
	labor <- "*\path" #Change path to working path, e.g. C:\\User\\...
	setwd(labor) #Change of working directory. The files will be generated in this folder.
		filelist <- list.files(path=labor, pattern="*.csv") #Generate list of .csv files
		filelist1<-gsub(".csv", "", filelist) # List for naming w/o .csv

#################################Local Maxima Minima Function#####################
###find_peaks function from:
#https://github.com/stasg/findPeaks/blob/66eb57cd25e7b4ccc87e7da75f273629cc83588b/find_peaks.
R
###From: Stasia Grinberg, Last update 28.08.2022
	find_peaks <- function (x, m = 3){
		shape <- diff(sign(diff(x, na.pad = FALSE)))
		pks <- sapply(which(shape < 0), FUN = function(i){
			z <- i - m + 1
			z <- ifelse(z > 0, z, 1)
			w <- i + m + 1
			w <- ifelse(w < length(x), w, length(x))
			if(all(x[c(z : i, (i + 2) : w)] <= x[i + 1])) return(i + 1) else return(numeric(0))
		})
		pks <- unlist(pks)
		pks
		}

################################################################################
###Start of Loop:
for (i in 1:NROW(filelist)){

	################################Import data in R################################
	#Data read-out for .csv files. The values are ";" separated.
```

```
p= read.csv(filelist[i], header = FALSE, stringsAsFactors = FALSE, sep=";")
p1<-p[-c(1,2),-3] #Optional: cut out header and additional column added by spectragryph
pflip<- p1[dim(p1)[1]:1,] #invert sequence of rows for hyperSpec

###Data type manipulations to numerical and bind to data frame
pWN<- as.numeric(gsub(",", ".", gsub("\\.", "", pflip$V1))) #Saves Wavenumbers as pWN
pTM<- as.numeric(gsub(",", ".", gsub("\\.", "", pflip$V2))) #Saves Transmission values as pTN
spc1 <- new ("hyperSpec", spc = pTM, wavelength= pWN) #creating spc for hyperref

############################Hyper spec manipulations##########################
###Smoothing the Spectrum
smooth <- spc.smooth.spline (spc1 [,, c (1850~2100,2200 ~ 2400, 2500 ~ 2825, 3150 ~
max)],wl (spc1 [,, 650 ~ max]),df = 4, spar = 1) # smoother, values are set manually but can
lead to errors.
spc1 <- (spc1-smooth)+100
spc1 <- spc.loess (spc1, c(seq (650, 4000, 1)))

###Convert back into a data frame for local minima function
WN<-spc1@wavelength # smoothed wavenumbers are put in variable WN
spc1@data[["spc"]]->TM
TM<-as.numeric(as.character(TM))

###Formating the spectrum for the right sequence direction.
TM[TM>100] <- 100# Cut-off nonsensical values
spectruminv = data.frame(WN,TM) #Bind to new data frame
spectrum<- spectruminv[dim(spectruminv)[1]:1,] #Change Direction of Peaks back

#####################################Peak finding#############################
###Make data frame of local minima and maxima
ds_min = find_peaks(-spectrum$TM) #Find peaks fnct with "-" to get local minima
x_all<-spectrum$WN[ds_min] #x-values in data frame
y_all<-spectrum$TM[ds_min] #y-values in data frame
allmin<-as.data.frame(cbind(x_all,y_all)) #bind x- and y- values

###Criteria for weak, medium, strong. A mean of all values is generated and the baseline
#difference is used as measure of general differences in intensity to balance arbitrarily assigned
#values of m, s, vs.
        crit<-mean(spectrum$TM)# Mean of spectrum intensity is generated
                diffcrit=100-crit # determination of correction factor.
                medium = 90-(2*diffcrit) # Medium is below 90% with correction
                strong = 75-(2*diffcrit) # Strong is below 75% with correction
                vstrong= 50-(2*diffcrit) # Very strong is below 50% with correction

###Applying criteria to all local minima values
allmin_cmplt_peaks = allmin %>%
        #Filter has to be applied since the local minimas of C-H_arom are very small.
        filter(if_else(x_all>2800&x_all<3150, y_all < (100-(0.33*(100-crit))), y_all < crit))
        #Peak intensity is added to the text output
        allmin_cmplt = allmin_cmplt_peaks %>%
                mutate(x_all = paste(x_all," (",ifelse(y_all<vstrong, "vs)",
                        ifelse(y_all<strong, "s)",
                        ifelse(y_all<medium, "m)", "w)"))),sep=""))
# The Peak vector gets converted to text and a dot added at the last value.
ds3<-gsub(last(allmin_cmplt$x_all),paste(last(allmin_cmplt$x_all),".", sep =
""),allmin_cmplt$x_all, fixed = TRUE)
```

```
        ################################Creating Output files#############################
        ###Output: Write the values as .txt.
                table<- matrix(ds3, nrow=1)
                write.table(matrix(ds3, nrow=1), file=paste("IRPeaks-",filelist1[i],"-.txt", sep = ""), sep
                = ", ", row.names=FALSE, quote=FALSE, col.names = FALSE)
        ###Saves the Plot with the selected Peaks for verifications
                png(paste("IRPeaks-",filelist1[i],"-.png", sep = ""),width=1400,height=900, units =
                "px", pointsize = 30)
                plot(allmin_cmplt_peaks, col ="red",
                xlim=c(3900,500),ylim=c(0.0,100.0),xlab="Wavenumber", ylab="Transmission",
                smoother = FALSE, grid = FALSE, lwd = 2) # Plots circled peaks
                lines(spectrum, col ="black", lwd = 2) # Plots the spectrum
                dev.off()
}
#############################################################################################
```

7.2 List of Abbreviations

Ac	Acetyl
acac	Acetylacetonate
acetyl-CoA	Acetyl coenzyme A
ACN	Acetontirile
Ad	Adamantly-
ALFABET	A machine-learning derived, fast, accurate bond dissociation enthalpy tool
APCI	Atmospheric pressure chemical ionization
aq	Aqueous
Ar	Aryl
AT	Atom transfer
ATR	Attenuated total reflection
BHT	2,6-Di-*tert*-butyl-4-methylphenol
bipy	2,2′-Bipyridine
Bn	Benzyl-
Boc	*tert*-Butyloxycarbonyl
CBz	Benzyloxycarbonyl
CC	Cyanuric chloride
CDMT	2-Chloro-4,6,-dimethoxy-1,3,5-triazine
COD	Cycloocta-1,5-dien
cms	Complex mixture screening
Cy	Cyclohexyl-
CV	Column volume(s)
d	Doublet (NMR)
δ	Chemical shift (NMR)
DCC	*N,N'*-Dicyclohexylcarbodiimid
DCE	1,2-Dichloroethane
DCM	Dichloromethane
DFT	Density-functional theory
DIC	*N,N'*-Diisopropylcarbodiimid
DMA	*N*,*N*-Dimethylacetamide
DMAP	4-*N*,*N*-dimethylaminopyridine
DME	1,2-Dimethoxyethane
DMF	*N*,*N*-Dimethylformamide
DMI	1,3-Dimethyl-2-imidazolidinone

DMPU	1,3-Dimethyl-1,3-diazinan-2-one
dppb	1,2-Bis(diphenylphosphino)butane
dppbz	1,2-Bis(diphenylphosohino)benzene
dppe	1,2-Bis(diphenylphosphino)ethane
dppp	1,2-Bis(diphenylphosphino)propane
EI	Electron ionization
EN	(Pauling) Electronegativity
EP_2	Prostaglandin E2 receptor 2
EPR	Electron paramagnetic resonance
equiv.	Equivalent
ESI	Electrospray ionization
EA	Ethylacetate
Fc	Ferrocen(yl-)
FCC	Fukuyama cross-coupling
FID	Flameionization detection
FRR	Fukuyama reaction
galvinoxyl	4-[(3,5-Di-*tert*-butyl-4-oxocyclohexa-2,5-dien-1-ylidene)methyl]-2,6-di-*tert*-butylphenoxyl
GC	Gas chromatography
GP	General procedure
Hal	Halide
HMTA	Hexamethylenetetraamine
Hz	Hertz
IBCF	*iso*-Butyl chloroformate
IGR	Inogranic Grignard reagents
IR	Infrared
J	Coupling constant (NMR)
Lit.	Literature value
m	Multiplet (NMR)
M	Molar
Mes	Mesityl
MP	Metling point
MS	Mass spectrometry
Ms	Mesylate
NHC	N-Heterocyclic carbenes
NHP	N-Hydroxyphthalimide esters

NK_1	Neurokinin 1 receptor
NMP	*N*-Methyl-2-pyrrolidone
NMR	Nuclear magnetic resonance
OA	Oxidative addition
PEPPSI	Pyridine-enhanced precatalyst preparation stabilization and initiation
Piv	Pivaloyl
ppm	Parts per million
prim	Primary
py	Pyridyl
R	Response factor
Rf	Retardation factor
rt	Room temperature
s	Singlet
Sat.	Saturated
SCE	Saturated calomel electrode
SciOPP	1,2-Bis[bis(3,5-di(*tert*-butyl)phenyl)phosphino]benzene
sec	Secondary
SET	Single-electron transfer
t	Triplet (NMR)
TADDOL	α,α,α',α'-Tetraaryl-1,3-dioxolan-4,5-dimethanol
TBAA	Tetra-*n*-butylammonium acetate
TBAC	Tetra-*n*-butylammonium chloride
TBDPS	*tert*-Butyldiphenylsilyl
TCA	tricarboxylic acid cycle
TE	Thioester
TEA	Triethylamine
TEMPO	(2,2,6,6-Tetramethylpiperidin-1-yl)oxyl
tert	Tertiary
Tf	Triflate
THF	Tetrahydrofuran
TLC	Thin-layer chromatography
TMEDA	N,N,N',N'Tetramethylethylenediamine
TMS	Trimethylsilyl-
Ts	Tosyl
UV	Ultraviolet

ν	Peak width
Xant(phos)	(9,9-Dimethyl-9*H*-xanthene-4,5-diyl)bis(diphenylphosphane)

7.3 Glossary

This glossary includes descriptions for commonly used depictions, terms or descriptions which were not conclusively defined in IUPAC guidelines.

Depictions	
Bracket with charge superscript: 	A bracket [] or abbreviated bracket with a non-circled charge indicates the overall charge of a molecule.
Circled charges: 	The circled charge symbol is indicating formal charge on the atom its located.
Miniature catalytic cycle 	A miniature catalytic cycle indicates a catalytic conversion with the displayed transition metal (M) without further specification of ligand, additive or experimental conditions.
Edge brackets on reaction arrow: 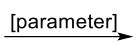	Besides the notation of chemical complexes, edge brackets on a reaction arrow enclose a changing parameter of a screening.
Terms	
C(sp^x)-C(sp^y) cross-coupling	For carbon-carbon bond forming cross-couplings, this notation is describing the C(nucleophile)-C(electrophile) with the heuristically used hybridization description.
Pseudohalides	Moieties which react similar to the respective halide moiety - often oxidative addition or other activation processes - are referred to as pseudohalides, e.g. tosylates, triflates, etc.
Oligoorganylmetallat(±X)	The number in brackets of *oligoorganylmetallates* is referring to the oxidation state of the transition metal, e.g. trismesitylferrate(+II) for Fe^{+II}.
Organometalloid	Organometalloids are referring to chemical compounds with at least one carbon atom bonded to B, Si, Ge, As, Sb or Te.
Side product and *byproduct*	Side product is referring to compounds that form due to alternative pathways, thereby consuming starting material in a non-productive way. Byproducts refer to compounds that result from designated reaction in parallel to the target product.
Description of Yields	
Traces (Yield)	Traces of yield is referring to GC-MS integral or quantitative GC-FID yields below 5%, due to GC-error and noise of measurement.
Quantitative (Yield)	Quantitative yield is referring to experimentally meaningful quantified GC-FID yields higher than 98%.
Yields	Reaction yields are described as the following: 100–90% excellent, 90–80% very good, 80–70% good, 70–50% fair, 50–30% mediocre or medium, <30% poor yields. Since these measures do not take into account the difficulty of certain compounds, descriptions are also made with e.g. *comparably good* yields, which does not correspond to a set range of values.

Writing Styles	
Ligandnames, or -abbreviations	Coordinated ligands or solvents are written with only lower case letters (e.g. $NiCl_2(thf)_4$). Free ligands are either written with a first capital letter or – in case of true acronyms – only with capital letters (e.g. TMEDA, Bipy or SciOPP). This does not apply to NHCs (e.g. IMes, SIPr), organyl groups (e.g Et_2Mg, Cp_2Fe), or non-abbreviated ligands (aminoketonates, phosphines).
Organyl groups	Abbreviated organyl groups are written with an initial capital latter (^{n}BuLi, ^{n}OctMgBr), when written out with an initial lower case letter (^{n}octyl-MgBr, mesityl-$FeBr_2$).

7.4 NMR Spectra of Thioesters

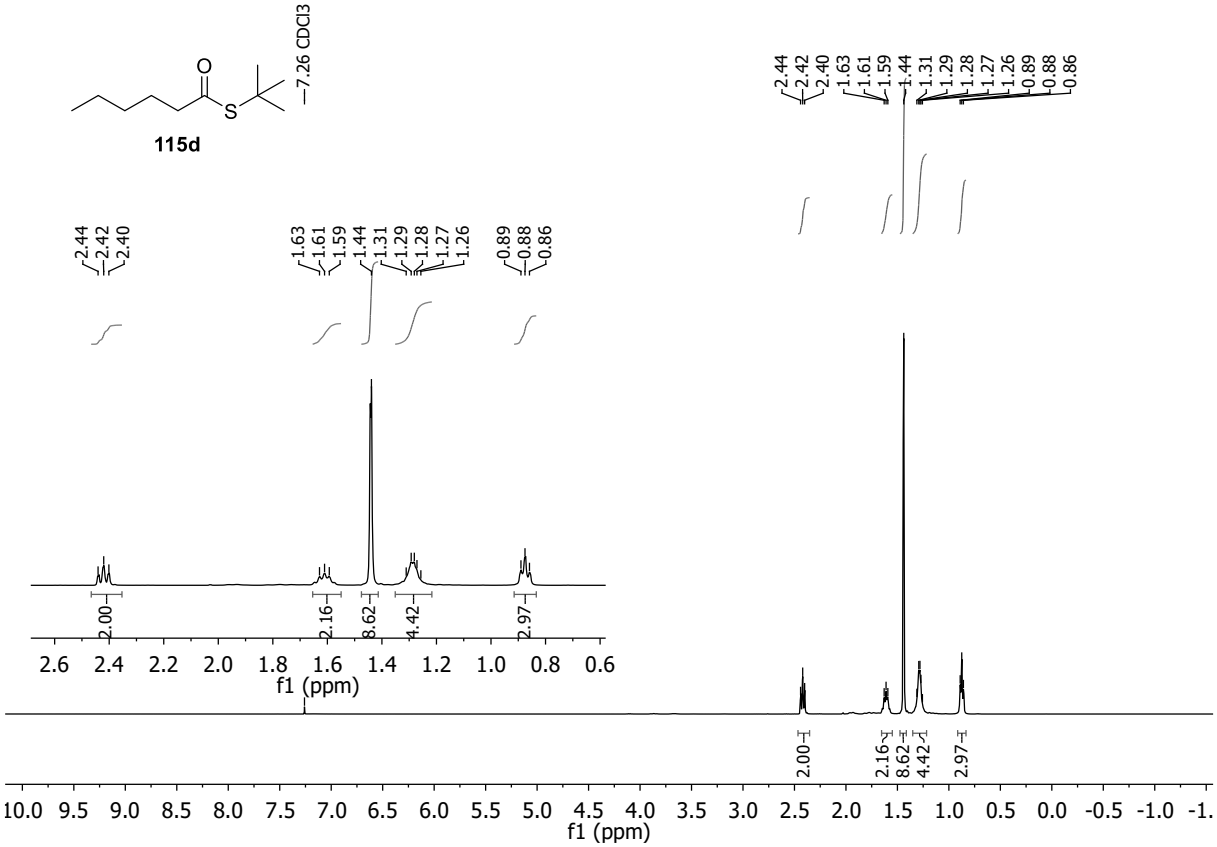

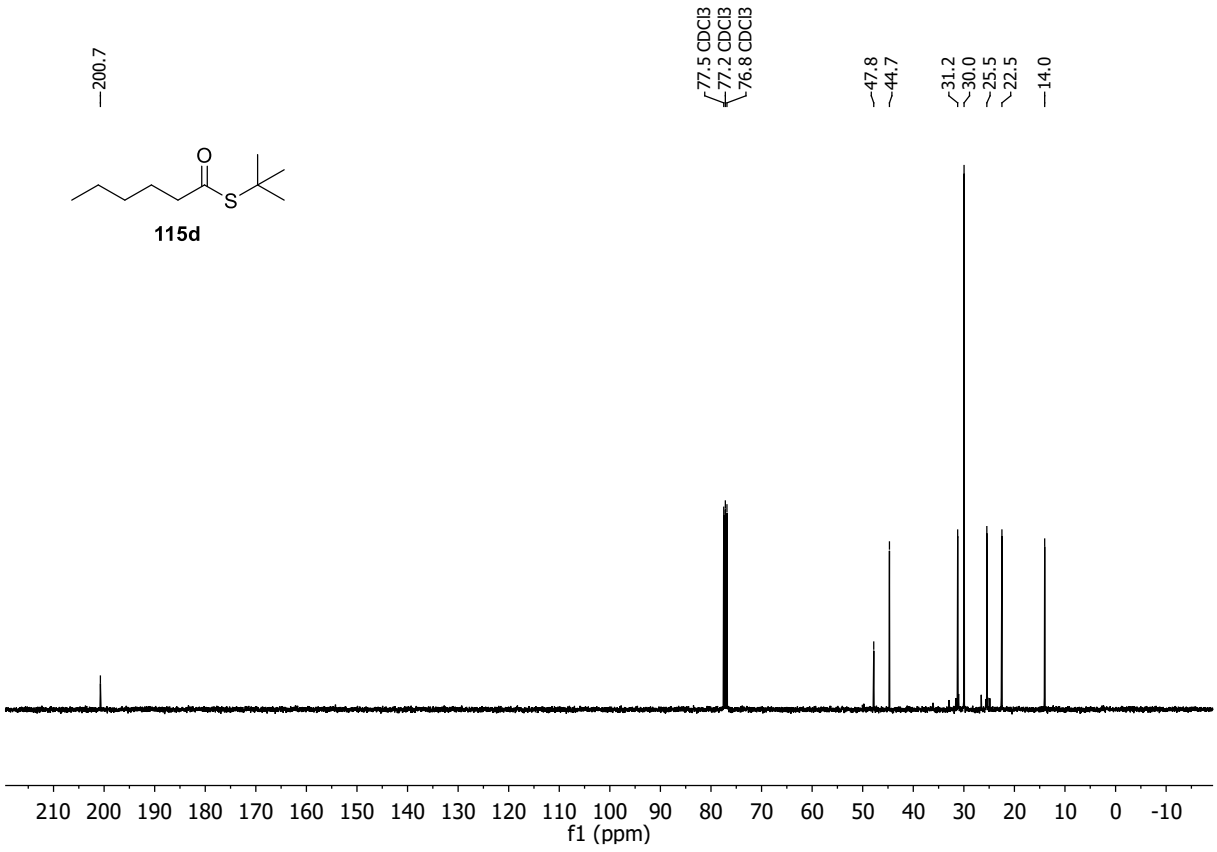

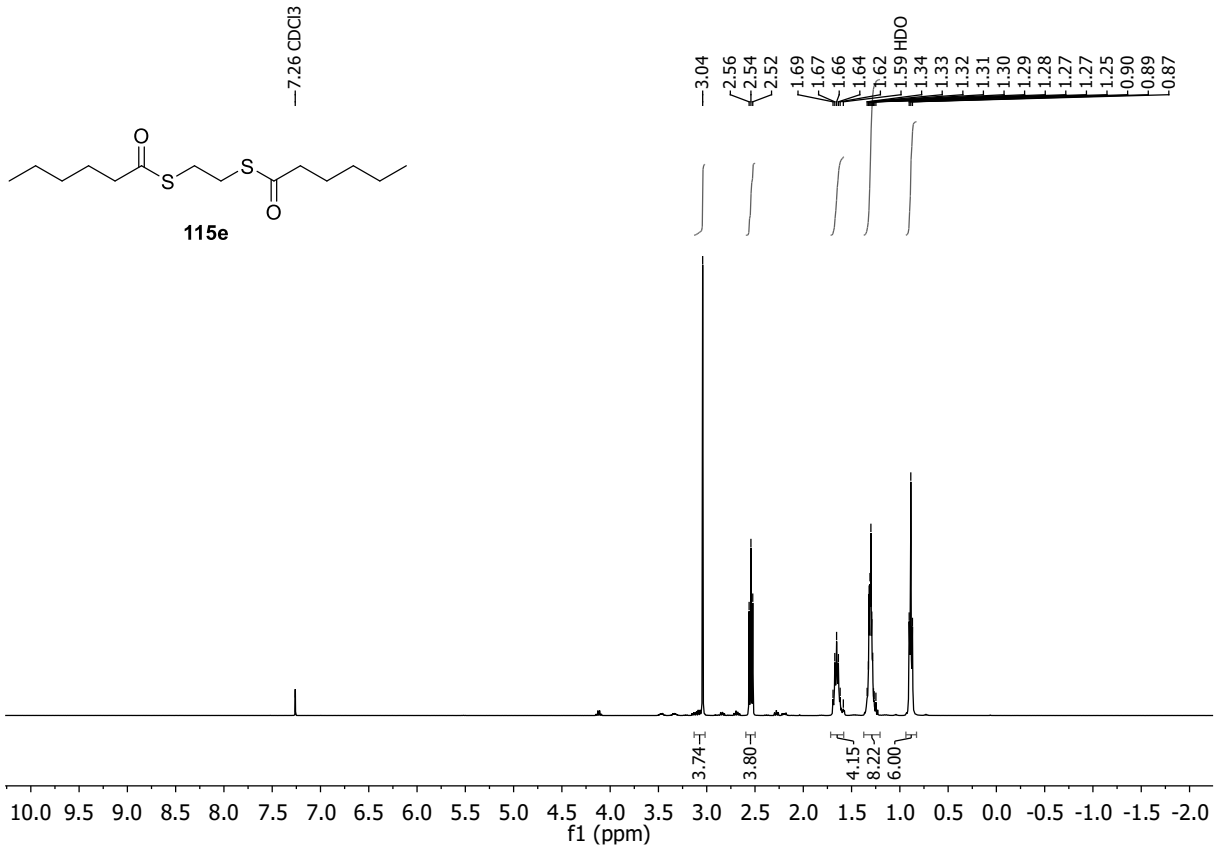
7.26 CDCl3
3.04
2.56
2.54
2.52
1.69
1.67
1.66
1.64
1.62
1.59 HDO
1.34
1.33
1.32
1.31
1.30
1.29
1.28
1.27
1.27
1.25
0.90
0.89
0.87
3.74
3.80
4.15
8.22
6.00
f1 (ppm)

115e

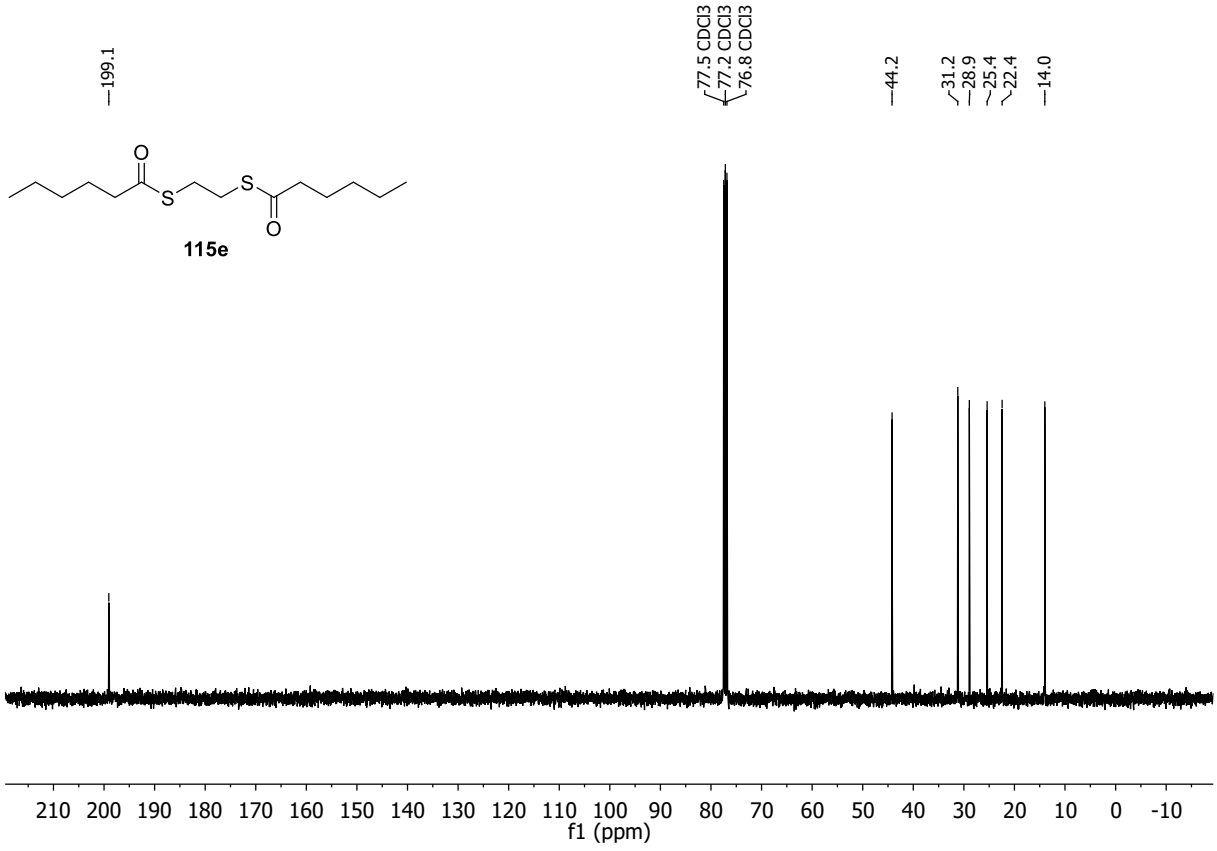
199.1
77.5 CDCl3
77.2 CDCl3
76.8 CDCl3
44.2
31.2
28.9
25.4
22.4
14.0
f1 (ppm)

115e

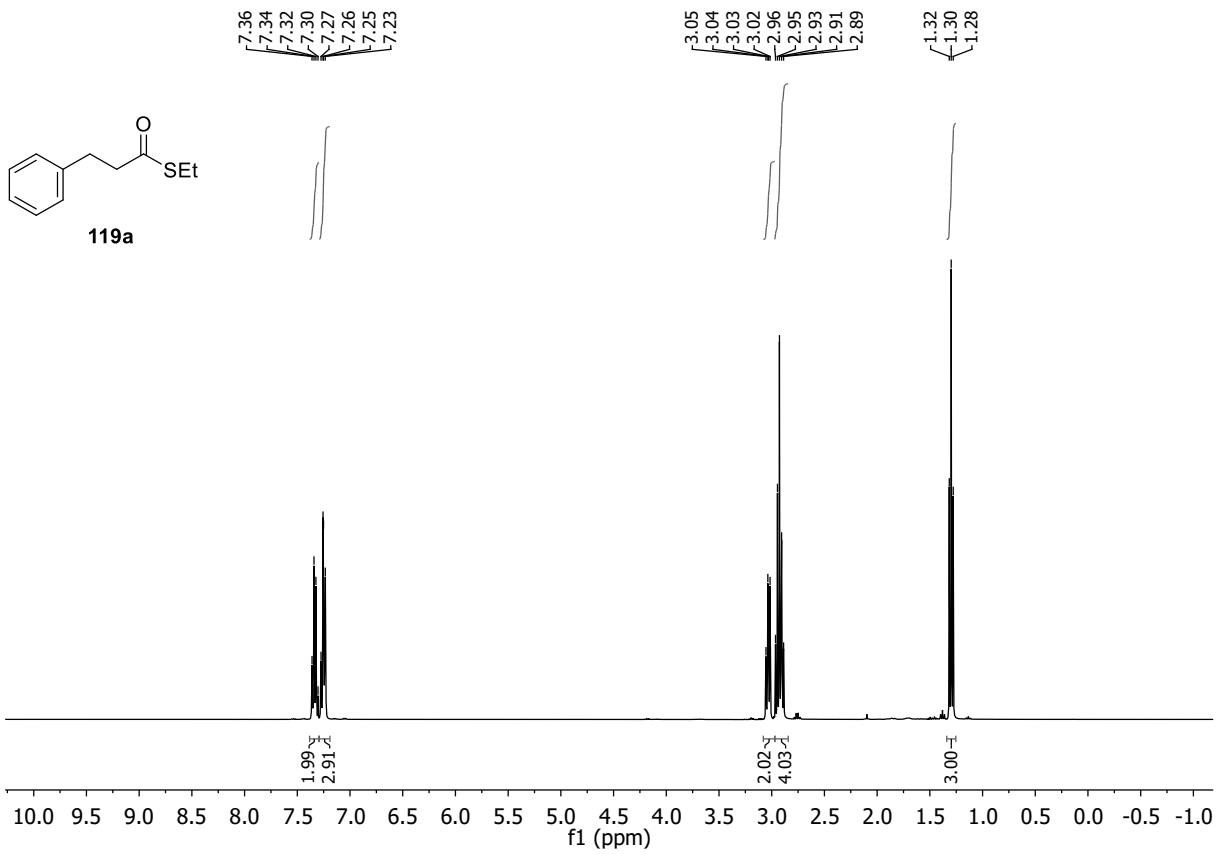
7.36
7.34
7.32
7.30
7.27
7.26
7.25
7.23
3.05
3.04
3.03
3.02
2.96
2.95
2.93
2.91
2.89
1.32
1.30
1.28
O
SEt
119a
1.99
2.91
2.02
4.03
3.00
10.0 9.5 9.0 8.5 8.0 7.5 7.0 6.5 6.0 5.5 5.0 4.5 4.0 3.5 3.0 2.5 2.0 1.5 1.0 0.5 0.0 -0.5 -1.0
f1 (ppm)

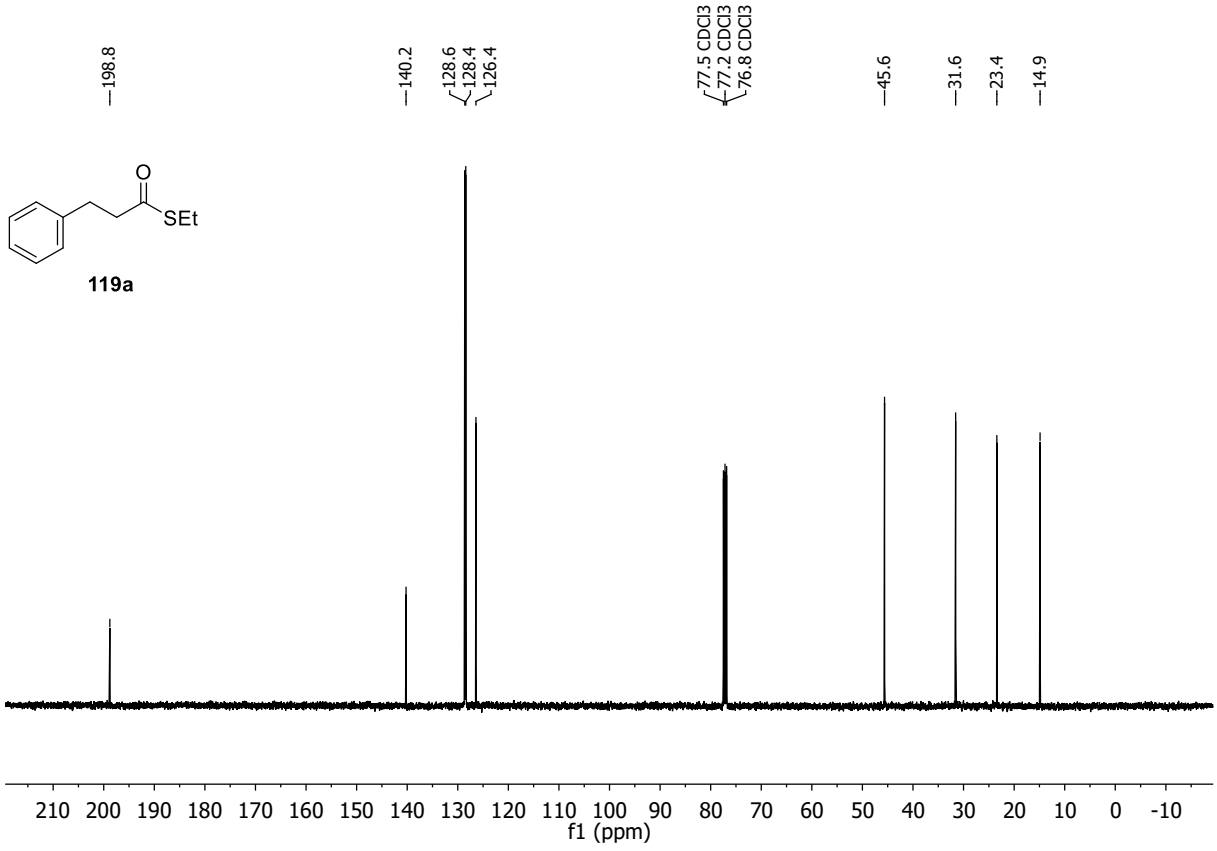
198.8
140.2
128.6
128.4
126.4
77.5 CDCl3
77.2 CDCl3
76.8 CDCl3
45.6
31.6
23.4
14.9
O
SEt
119a
210 200 190 180 170 160 150 140 130 120 110 100 90 80 70 60 50 40 30 20 10 0 -10
f1 (ppm)

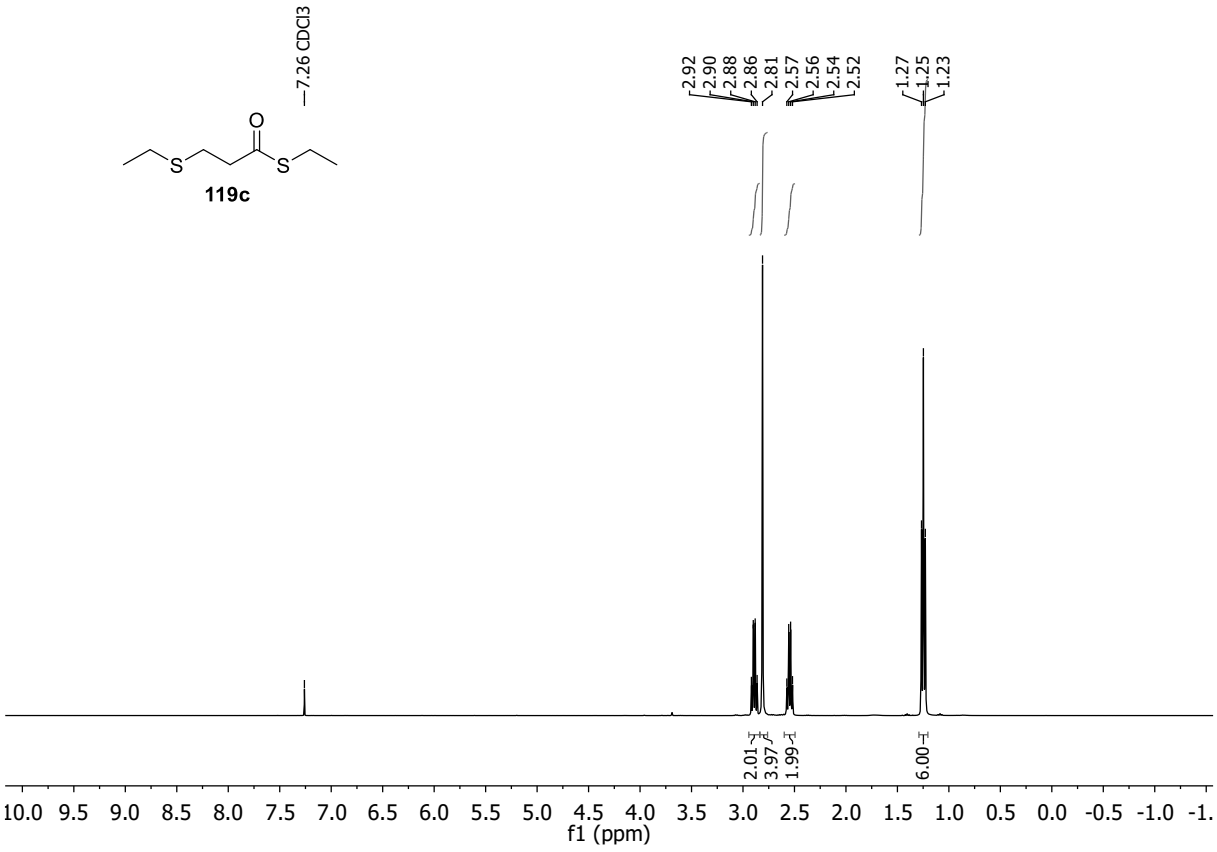
7.26 CDCl3
2.92
2.90
2.88
2.86
2.81
2.57
2.56
2.54
2.52
1.27
1.25
1.23
119c
2.01
3.97
1.99
6.00
f1 (ppm)

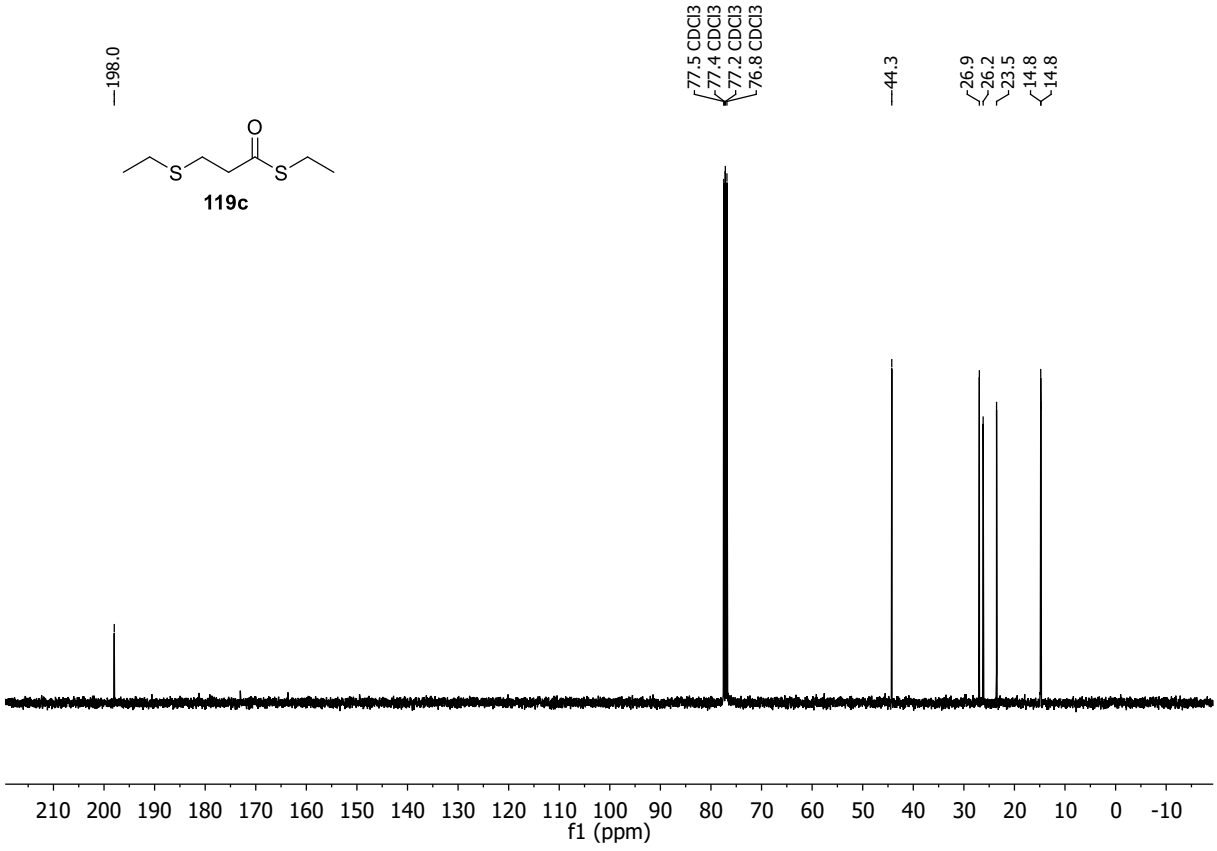
198.0
77.5 CDCl3
77.4 CDCl3
77.2 CDCl3
76.8 CDCl3
44.3
26.9
26.2
23.5
14.8
14.8
119c
f1 (ppm)

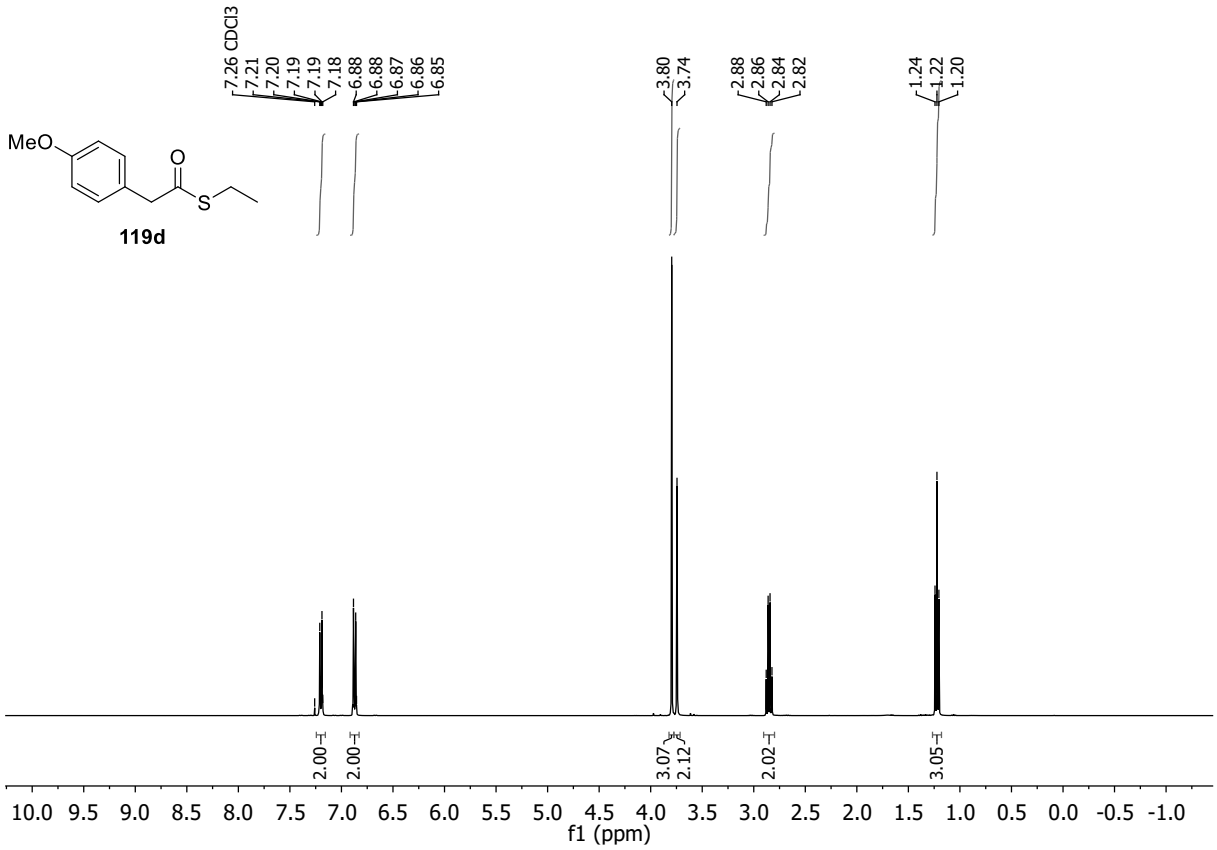
7.26 CDCl3
7.21
7.20
7.19
7.19
7.18
6.88
6.88
6.87
6.86
6.85
3.80
3.74
2.88
2.86
2.84
2.82
1.24
1.22
1.20
MeO
O
S
119d
2.00
2.00
3.07
2.12
2.02
3.05
10.0 9.5 9.0 8.5 8.0 7.5 7.0 6.5 6.0 5.5 5.0 4.5 4.0 3.5 3.0 2.5 2.0 1.5 1.0 0.5 0.0 -0.5 -1.0
f1 (ppm)

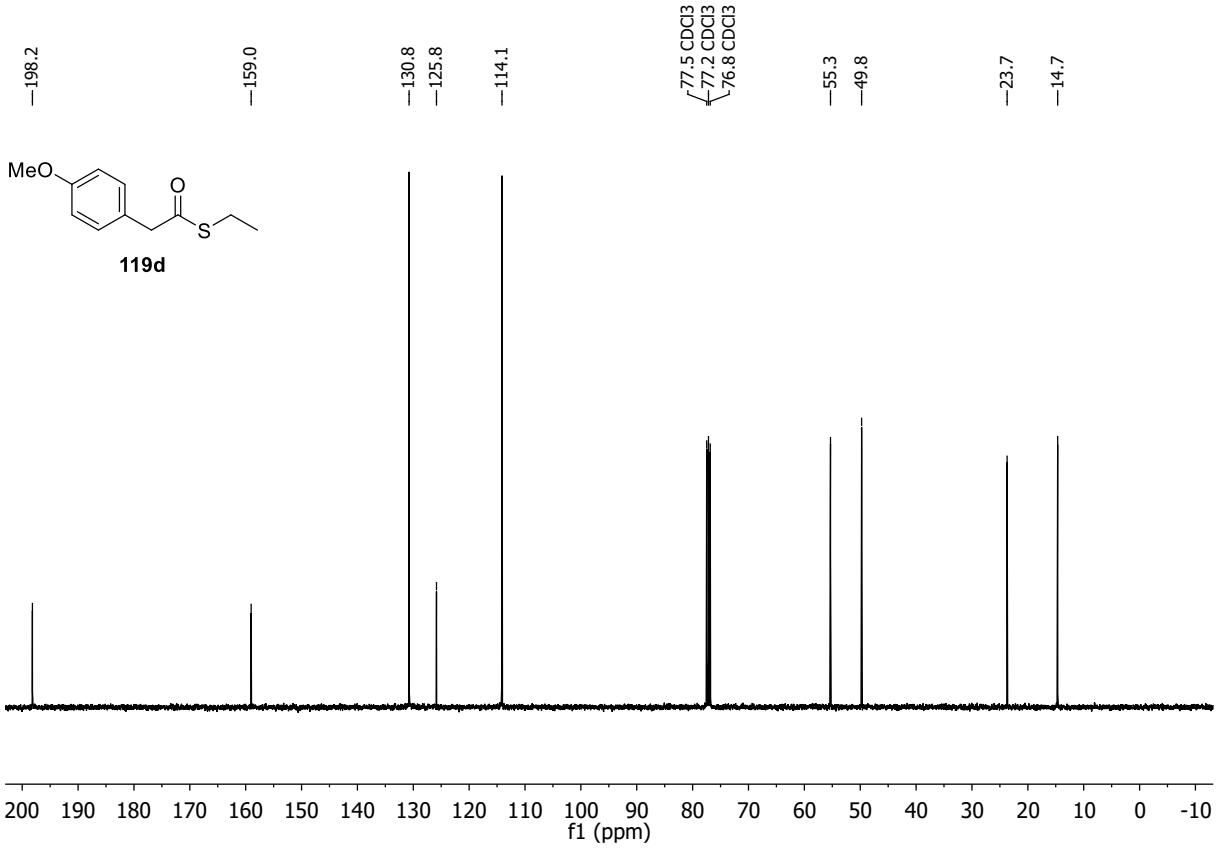
198.2
159.0
130.8
125.8
114.1
77.5 CDCl3
77.2 CDCl3
76.8 CDCl3
55.3
49.8
23.7
14.7
MeO
O
S
119d
200 190 180 170 160 150 140 130 120 110 100 90 80 70 60 50 40 30 20 10 0 -10
f1 (ppm)

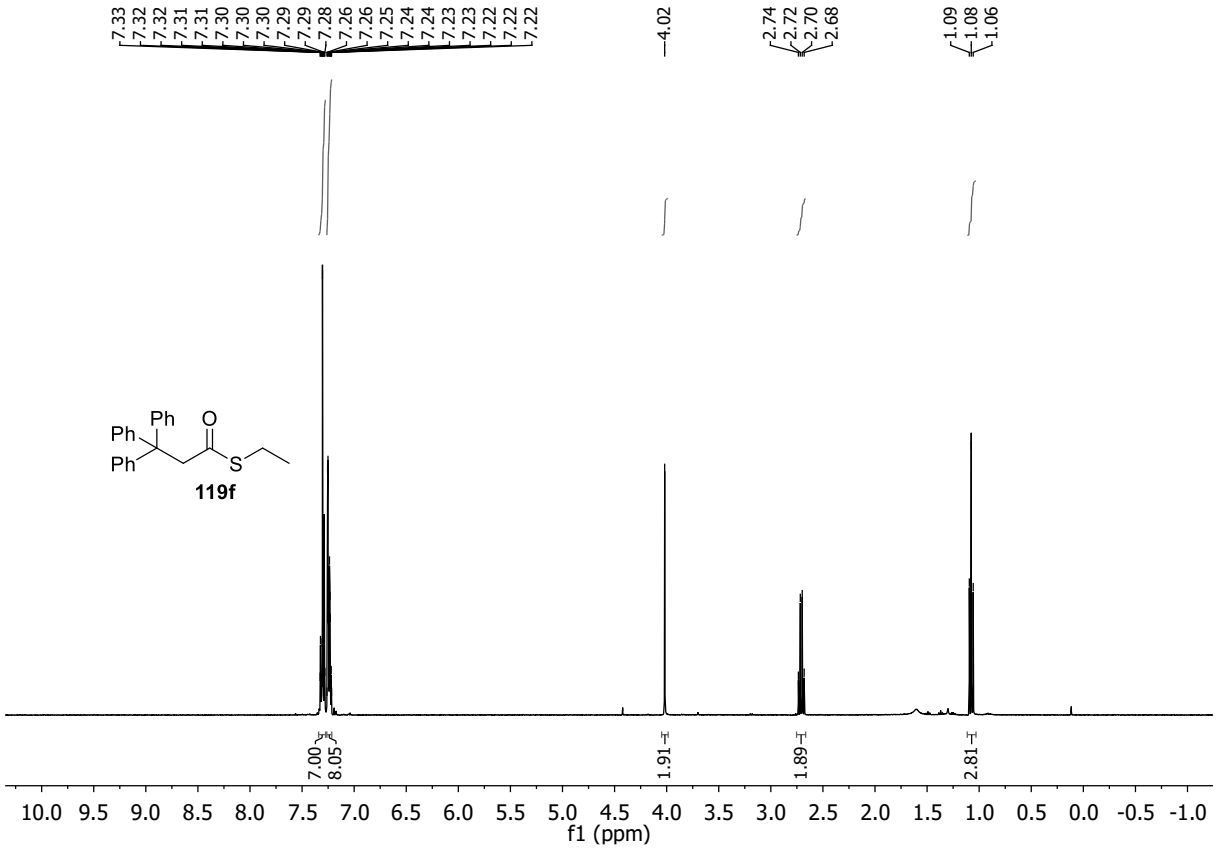
7.33
7.32
7.32
7.31
7.31
7.30
7.30
7.30
7.29
7.29
7.28
7.26
7.26
7.25
7.24
7.24
7.23
7.23
7.22
7.22
7.22
4.02
2.74
2.72
2.70
2.68
1.09
1.08
1.06
Ph
Ph
O
S
119f
7.00
8.05
1.91
1.89
2.81
10.0 9.5 9.0 8.5 8.0 7.5 7.0 6.5 6.0 5.5 5.0 4.5 4.0 3.5 3.0 2.5 2.0 1.5 1.0 0.5 0.0 -0.5 -1.0
f1 (ppm)

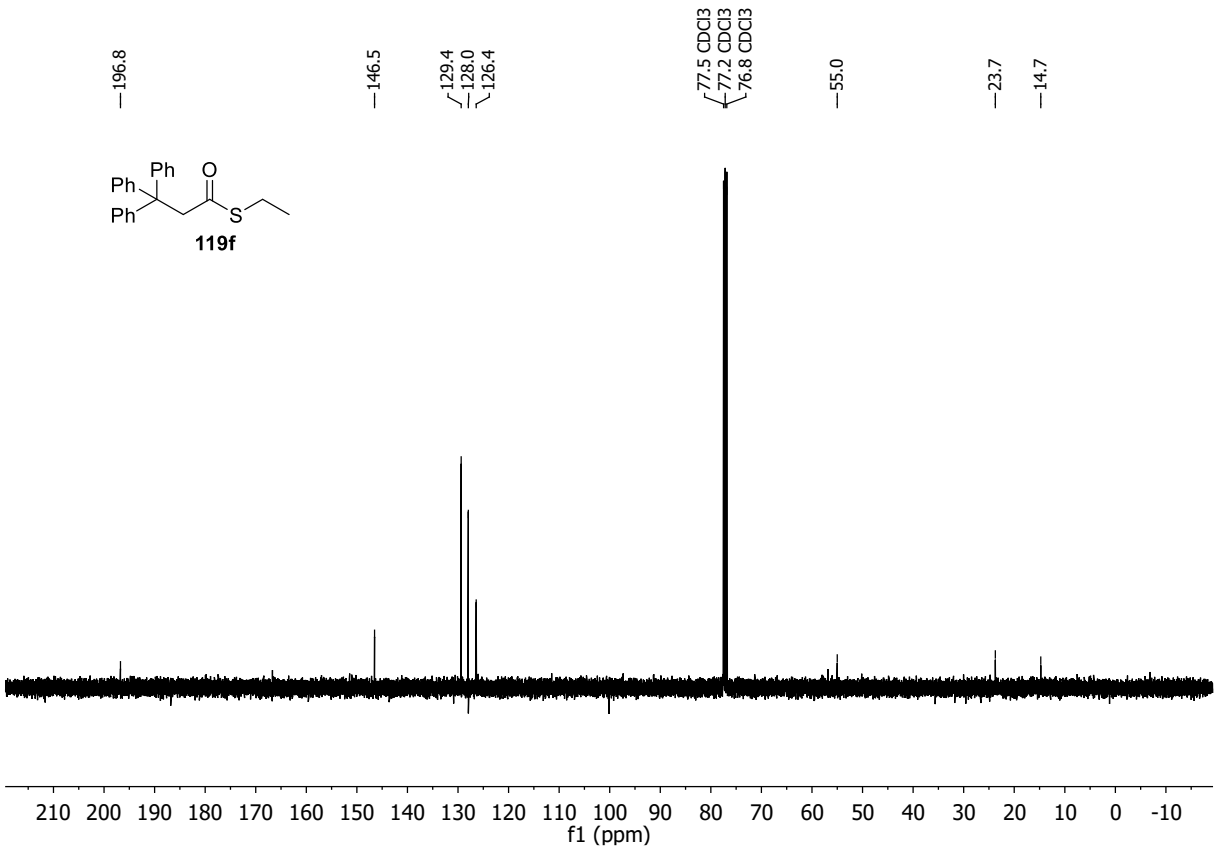
196.8
146.5
129.4
128.0
126.4
77.5 CDCl3
77.2 CDCl3
76.8 CDCl3
55.0
23.7
14.7
Ph
Ph
O
S
119f
210 200 190 180 170 160 150 140 130 120 110 100 90 80 70 60 50 40 30 20 10 0 -10
f1 (ppm)

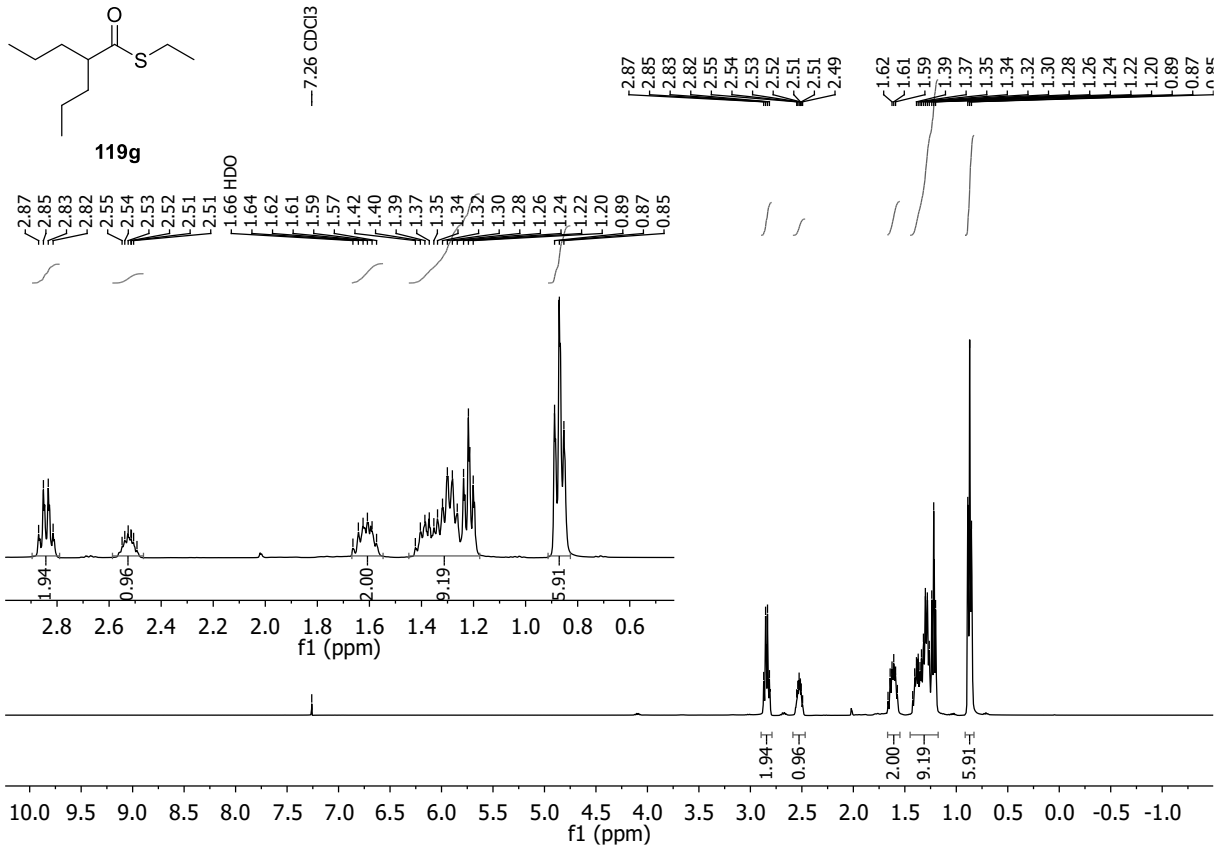
119g
7.26 CDCl3
HDO
1.94
0.96
2.00
9.19
5.91
f1 (ppm)

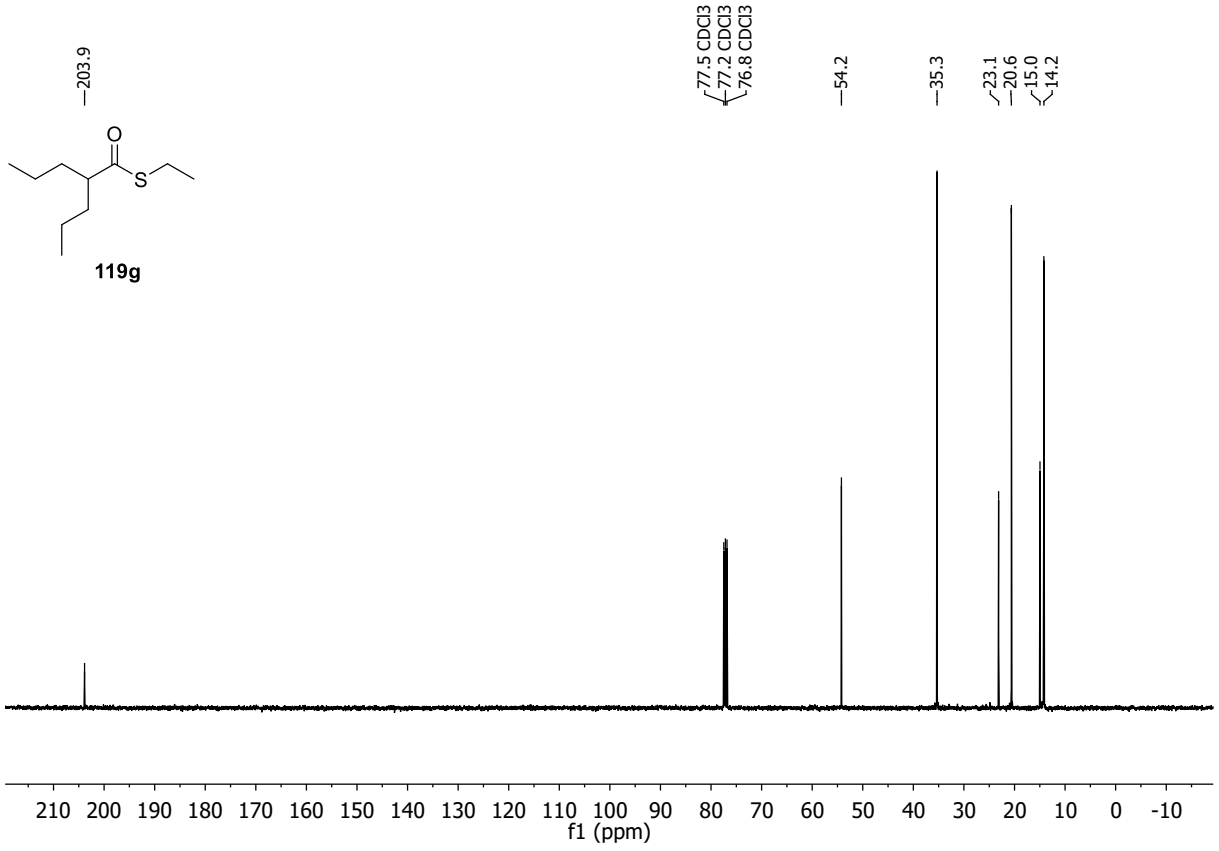
119g
203.9
77.5 CDCl3
77.2 CDCl3
76.8 CDCl3
54.2
35.3
23.1
20.6
15.0
14.2
f1 (ppm)

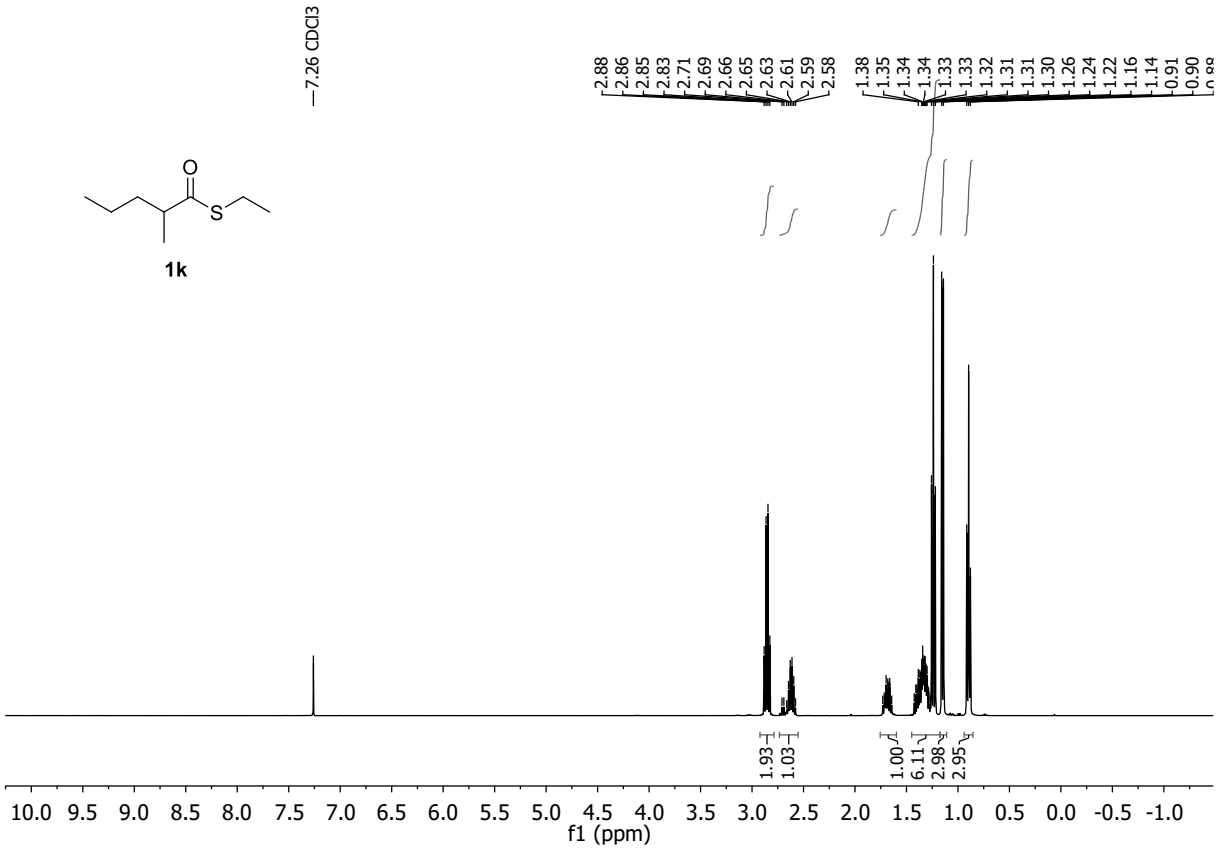
7.26 CDCl3
2.88
2.86
2.85
2.83
2.71
2.69
2.66
2.65
2.63
2.61
2.59
2.58
1.38
1.35
1.34
1.34
1.33
1.32
1.31
1.31
1.30
1.26
1.24
1.22
1.16
1.14
0.91
0.90
O
S
1k
1.93
1.03
1.00
6.11
2.98
2.95
10.0 9.5 9.0 8.5 8.0 7.5 7.0 6.5 6.0 5.5 5.0 4.5 4.0 3.5 3.0 2.5 2.0 1.5 1.0 0.5 0.0 -0.5 -1.0
f1 (ppm)

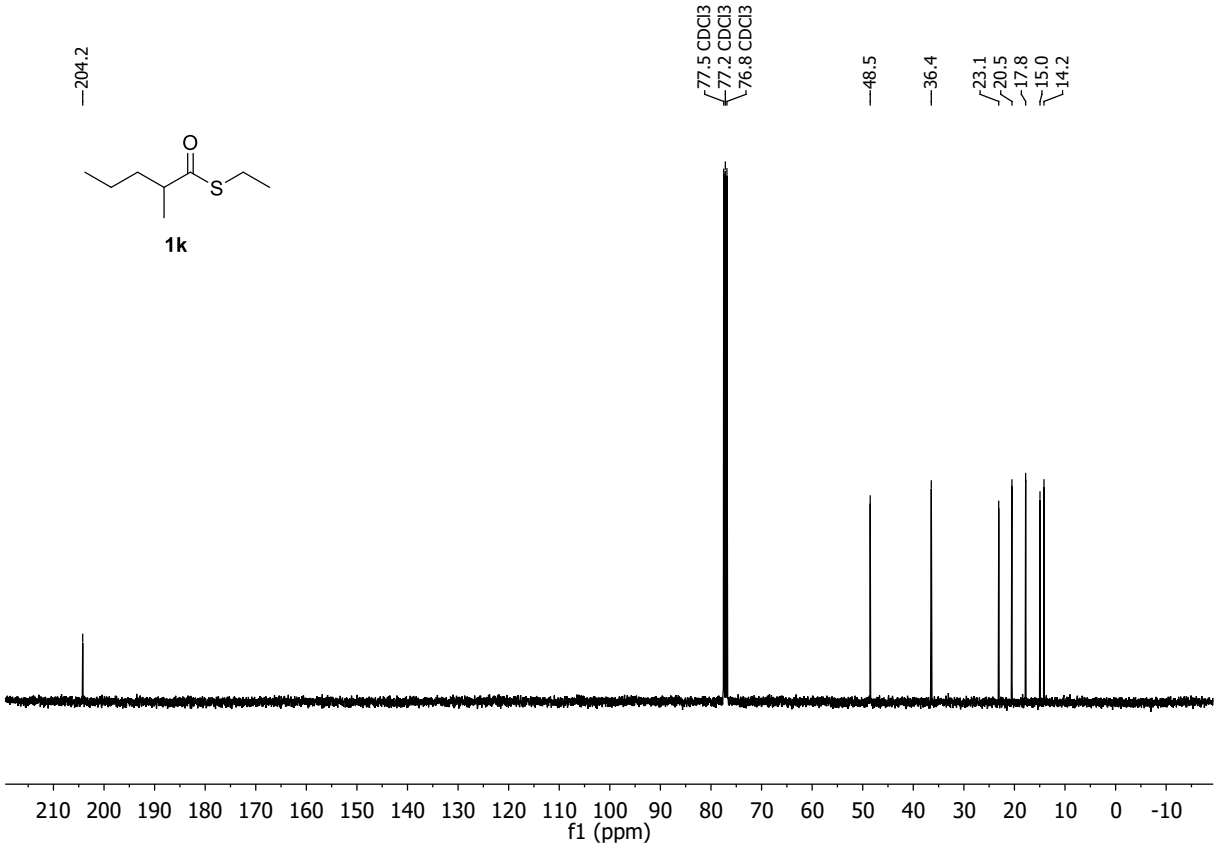
204.2
77.5 CDCl3
77.2 CDCl3
76.8 CDCl3
48.5
36.4
23.1
20.5
17.8
15.0
14.2
O
S
1k
210 200 190 180 170 160 150 140 130 120 110 100 90 80 70 60 50 40 30 20 10 0 -10
f1 (ppm)

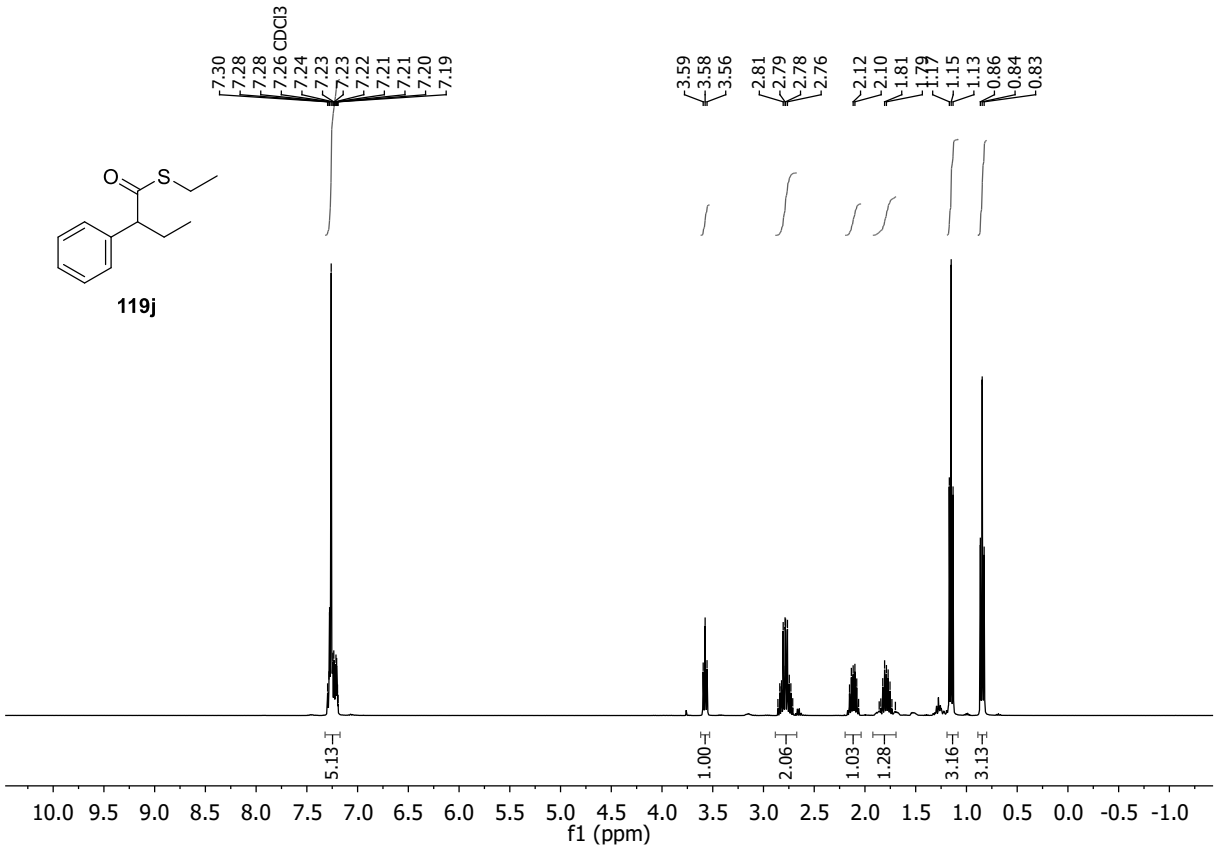
7.30
7.28
7.28
7.26 CDCl3
7.24
7.23
7.23
7.22
7.21
7.21
7.20
7.19
3.59
3.58
3.56
2.81
2.79
2.78
2.76
2.12
2.10
1.81
1.79
1.17
1.15
1.13
0.86
0.84
0.83
O
S
119j
5.13
1.00
2.06
1.03
1.28
3.16
3.13
10.0 9.5 9.0 8.5 8.0 7.5 7.0 6.5 6.0 5.5 5.0 4.5 4.0 3.5 3.0 2.5 2.0 1.5 1.0 0.5 0.0 -0.5 -1.0
f1 (ppm)

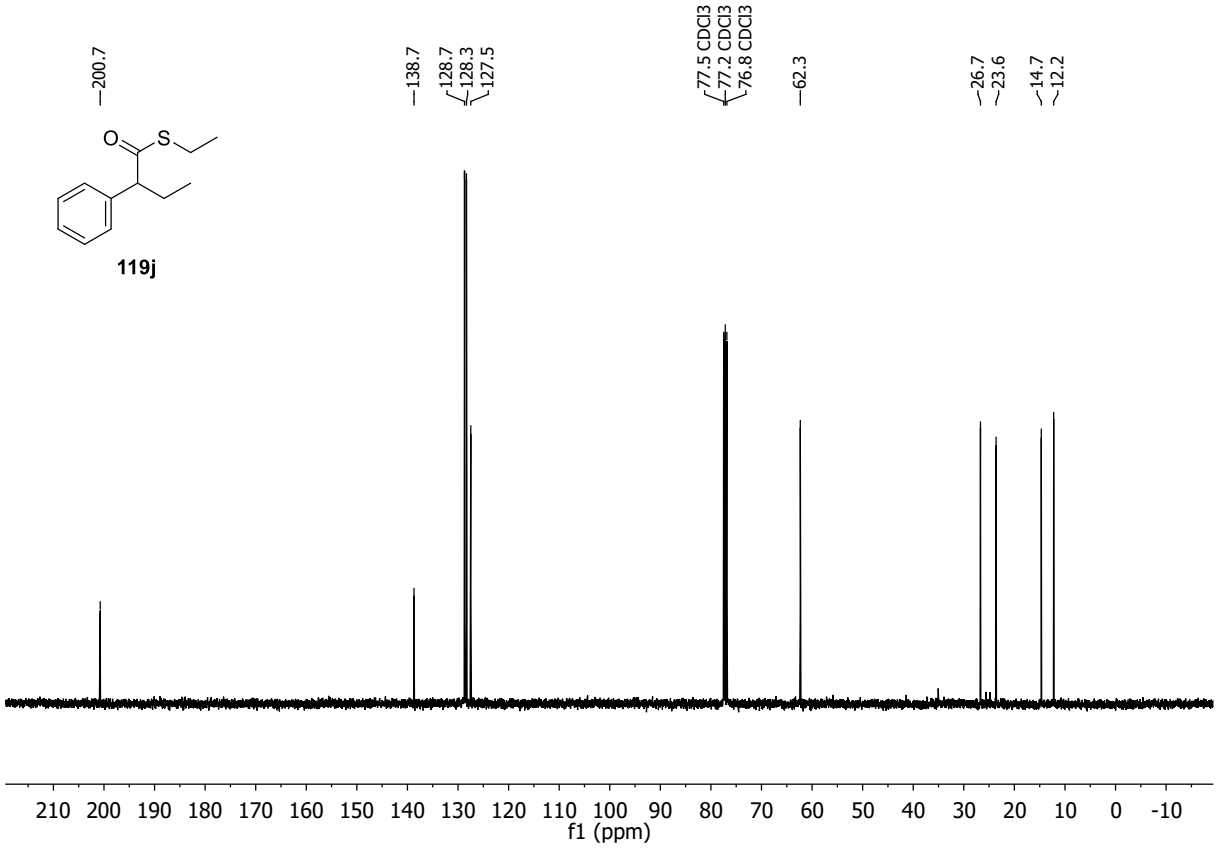
200.7
138.7
128.7
128.3
127.5
77.5 CDCl3
77.2 CDCl3
76.8 CDCl3
62.3
26.7
23.6
14.7
12.2
O
S
119j
210 200 190 180 170 160 150 140 130 120 110 100 90 80 70 60 50 40 30 20 10 0 -10
f1 (ppm)

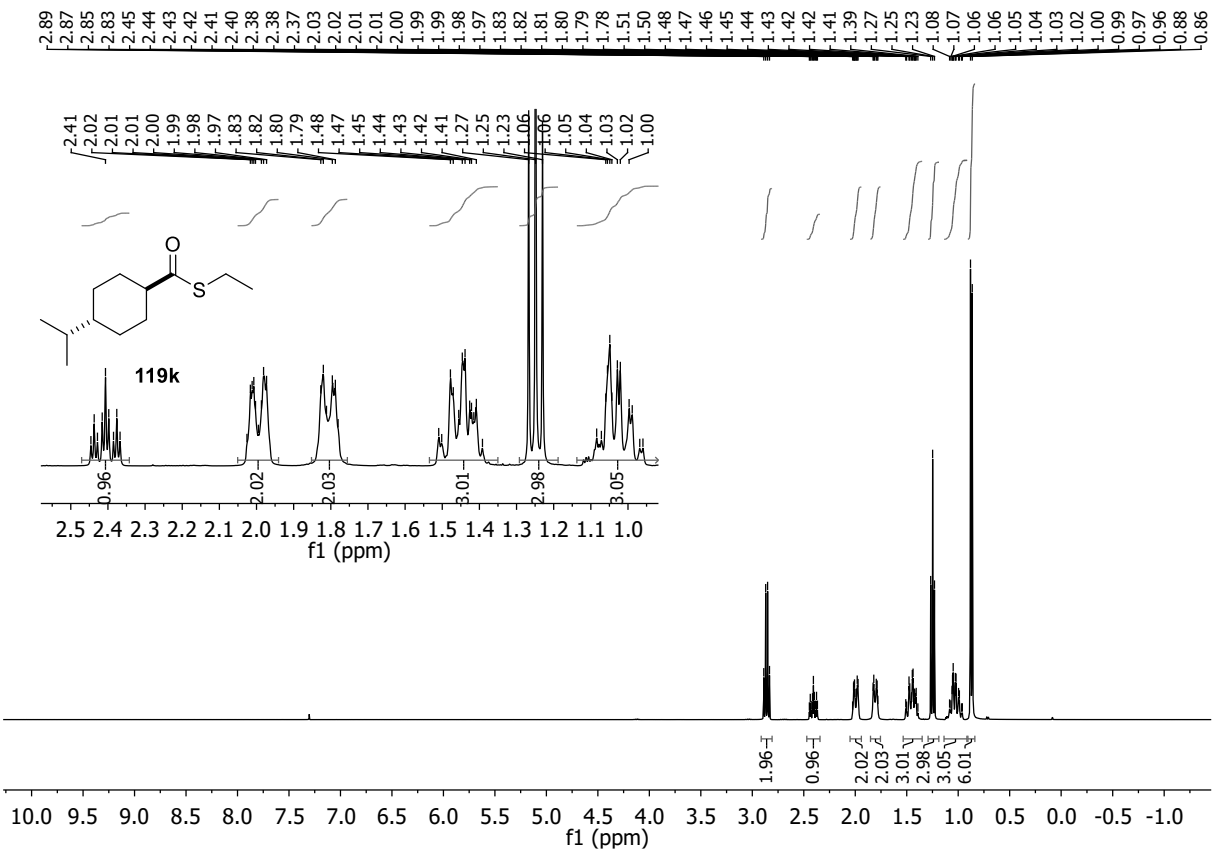
119k
f1 (ppm)

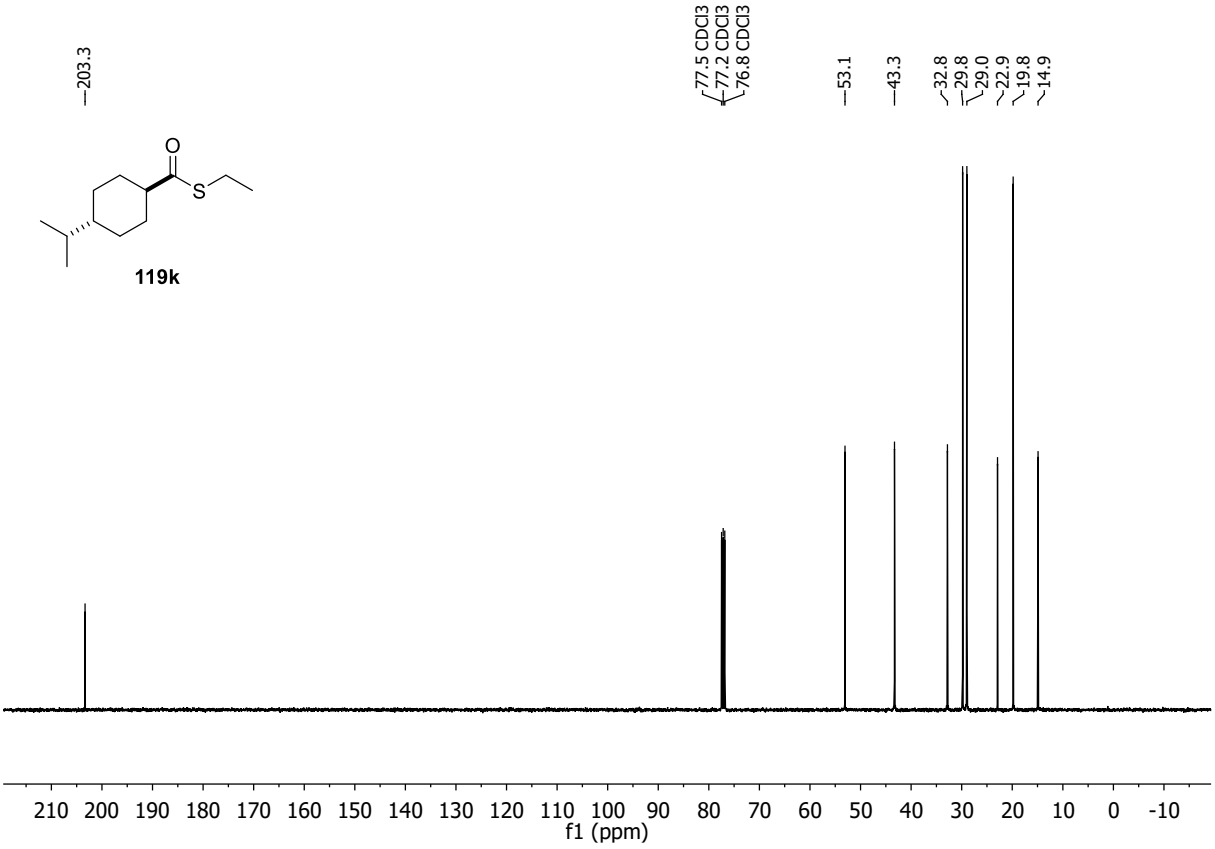
119k
f1 (ppm)

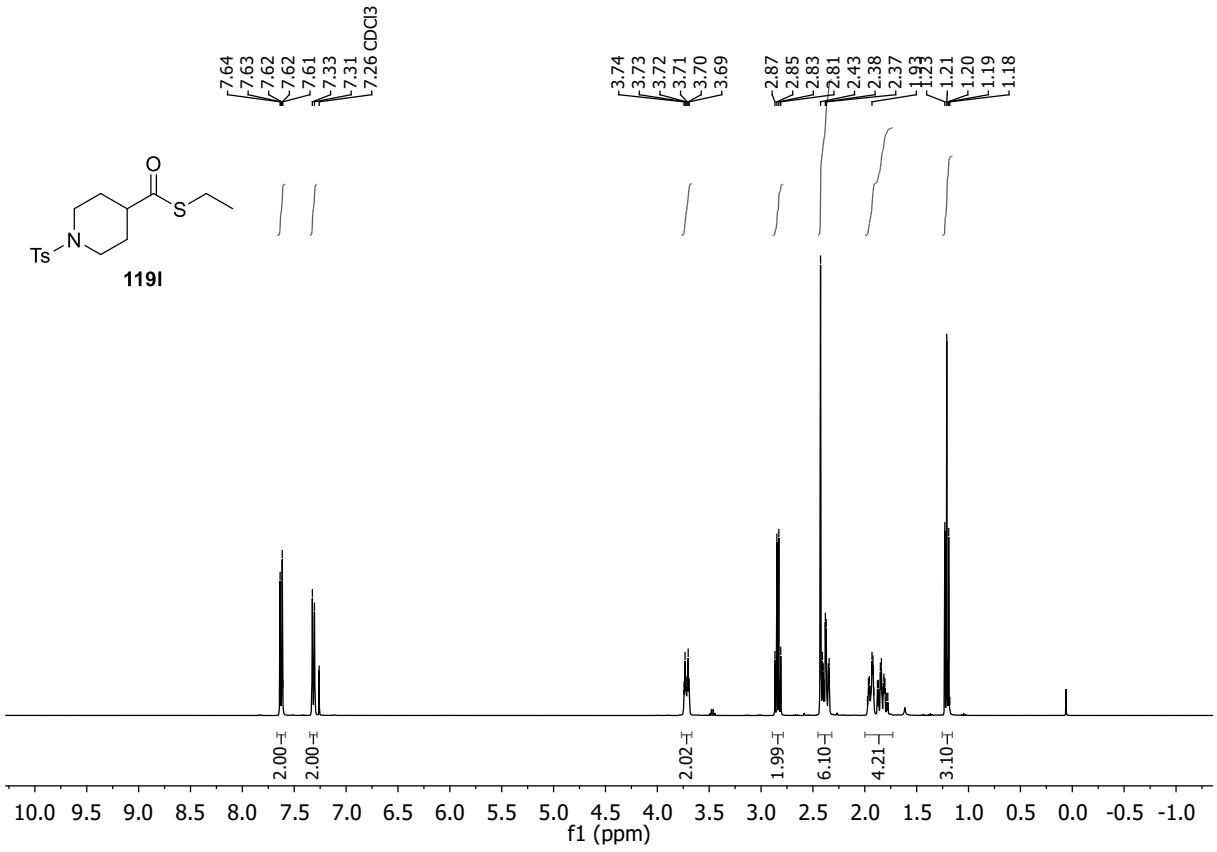
7.64
7.63
7.62
7.62
7.61
7.33
7.31
7.26 CDCl3
3.74
3.73
3.72
3.71
3.70
3.69
2.87
2.85
2.83
2.81
2.43
2.38
2.37
1.93
1.23
1.21
1.20
1.19
1.18
O
S
N
Ts
119l
2.00
2.00
2.02
1.99
6.10
4.21
3.10
10.0 9.5 9.0 8.5 8.0 7.5 7.0 6.5 6.0 5.5 5.0 4.5 4.0 3.5 3.0 2.5 2.0 1.5 1.0 0.5 0.0 -0.5 -1.0
f1 (ppm)

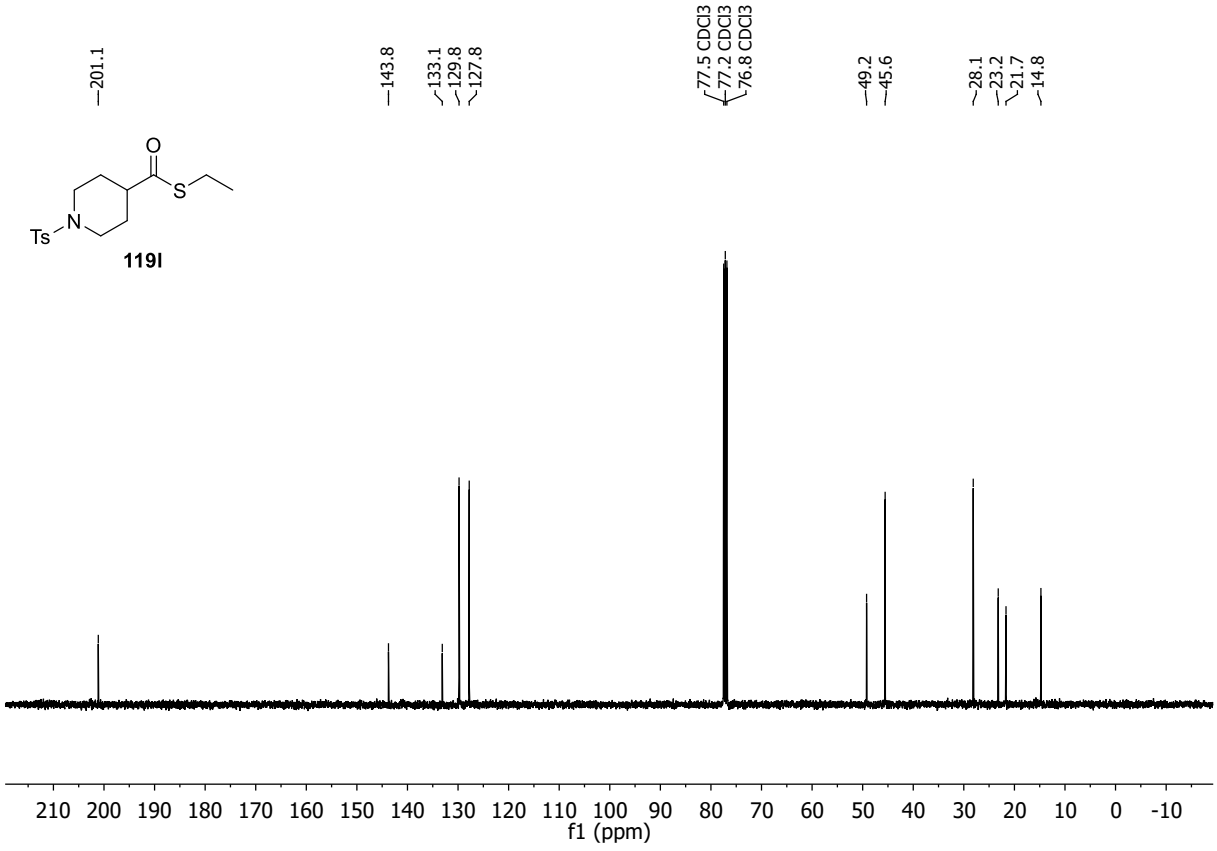
201.1
143.8
133.1
129.8
127.8
77.5 CDCl3
77.2 CDCl3
76.8 CDCl3
49.2
45.6
28.1
23.2
21.7
14.8
O
S
N
Ts
119l
210 200 190 180 170 160 150 140 130 120 110 100 90 80 70 60 50 40 30 20 10 0 -10
f1 (ppm)

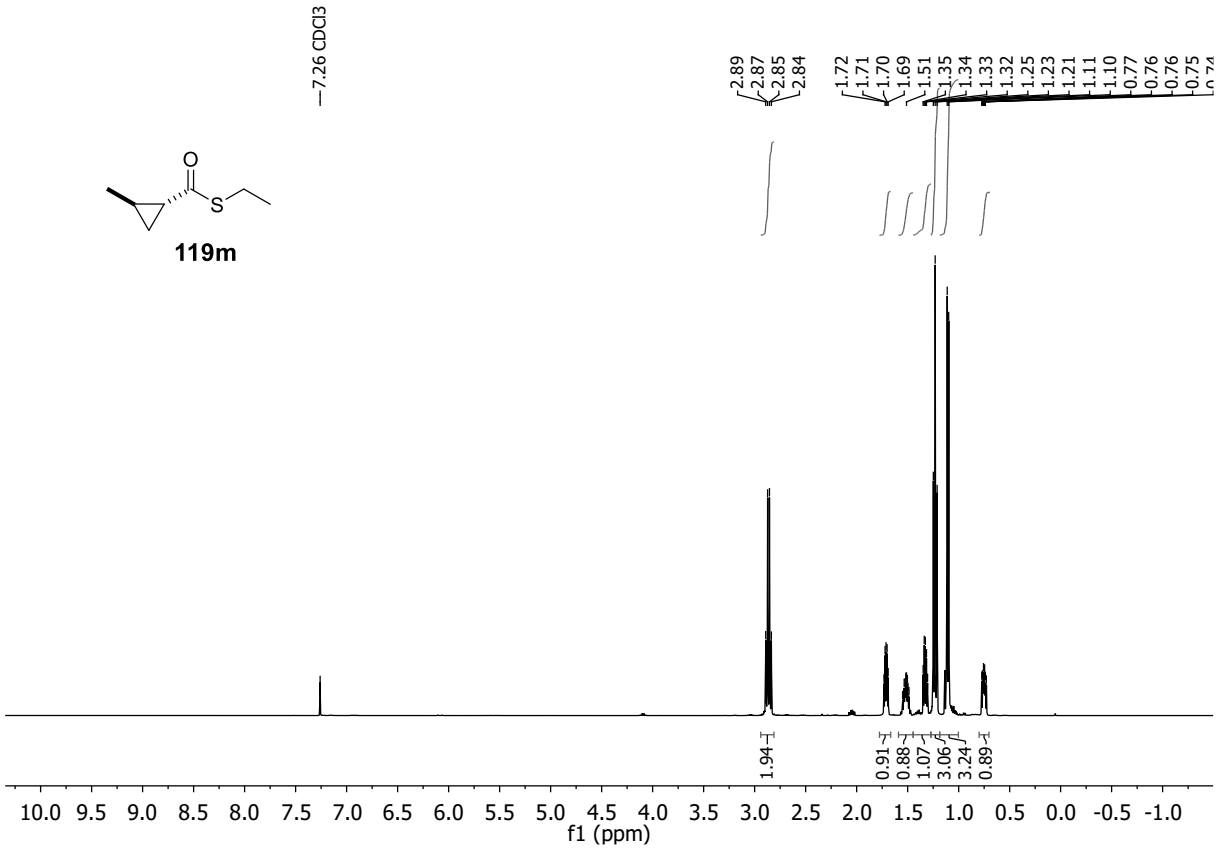
7.26 CDCl3
2.89
2.87
2.85
2.84
1.72
1.71
1.70
1.69
1.51
1.35
1.34
1.33
1.32
1.25
1.23
1.21
1.11
1.10
0.77
0.76
0.76
0.75
O
S
119m
1.94
0.91
0.88
1.07
3.06
3.24
0.89
10.0 9.5 9.0 8.5 8.0 7.5 7.0 6.5 6.0 5.5 5.0 4.5 4.0 3.5 3.0 2.5 2.0 1.5 1.0 0.5 0.0 -0.5 -1.0
f1 (ppm)

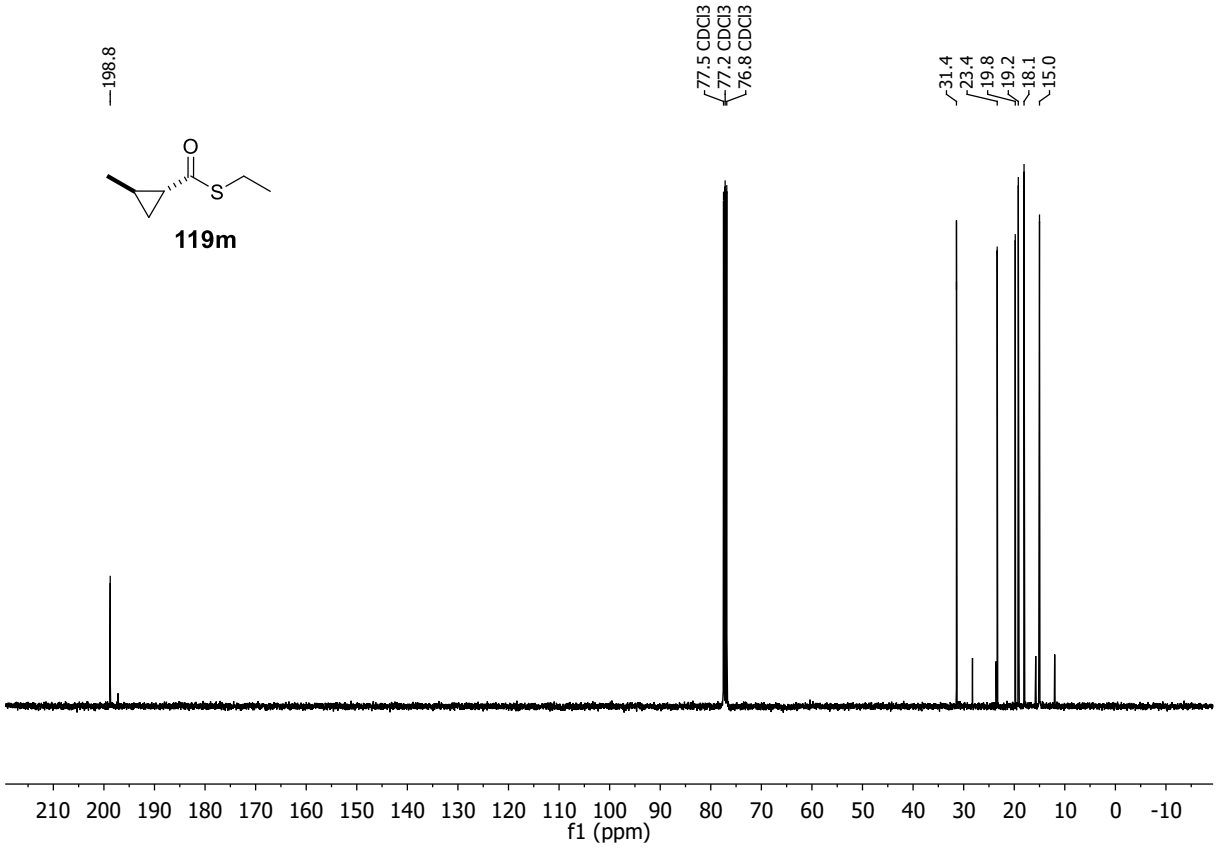
198.8
77.5 CDCl3
77.2 CDCl3
76.8 CDCl3
31.4
23.4
19.8
19.2
18.1
15.0
O
S
119m
210 200 190 180 170 160 150 140 130 120 110 100 90 80 70 60 50 40 30 20 10 0 -10
f1 (ppm)

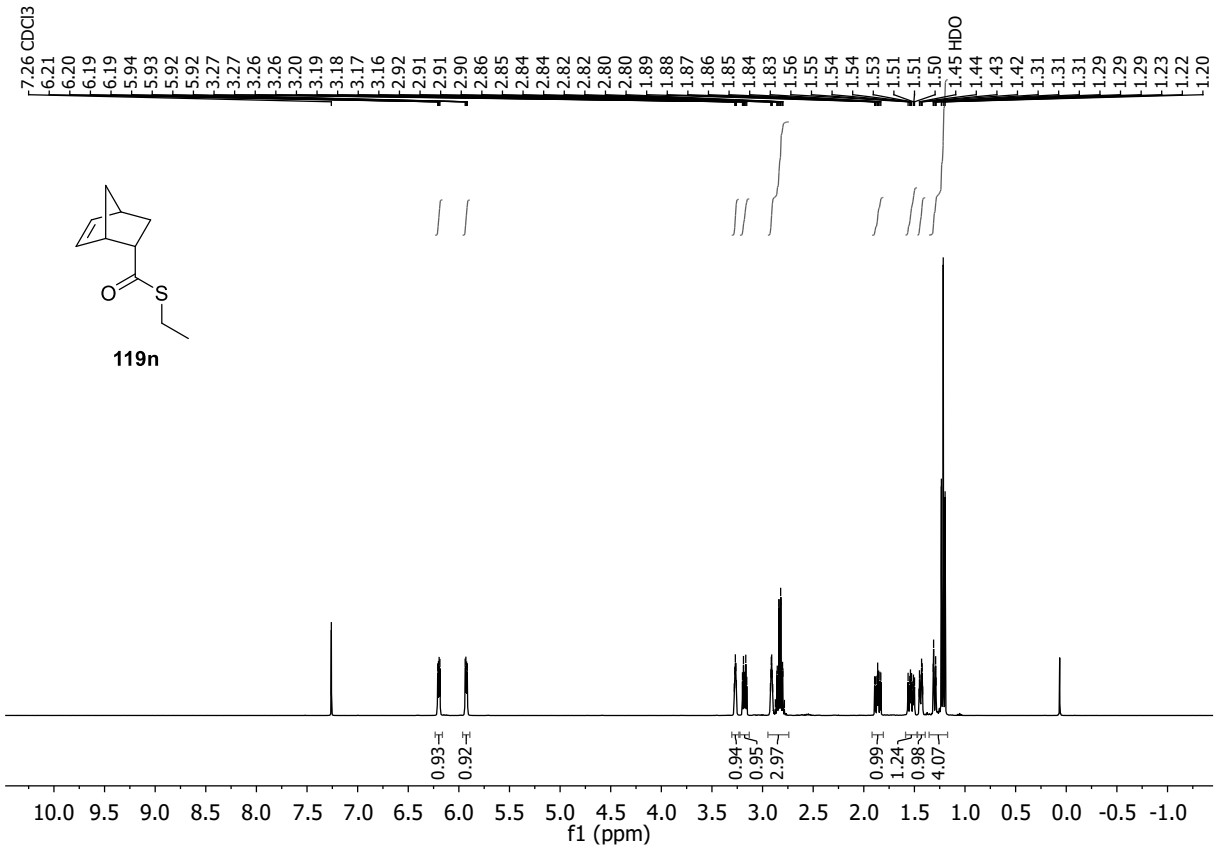
7.26 CDCl3
6.21
6.20
6.19
6.19
5.94
5.93
5.92
5.92
3.27
3.27
3.26
3.26
3.20
3.19
3.18
3.17
3.16
2.92
2.91
2.91
2.90
2.86
2.85
2.84
2.84
2.82
2.82
2.80
2.80
1.89
1.88
1.87
1.86
1.85
1.84
1.83
1.56
1.55
1.54
1.54
1.53
1.51
1.51
1.50
1.45 HDO
1.44
1.43
1.42
1.31
1.31
1.29
1.29
1.29
1.23
1.22
1.20
O
S
119n
0.93
0.92
0.94
0.95
2.97
0.99
1.24
0.98
4.07
10.0 9.5 9.0 8.5 8.0 7.5 7.0 6.5 6.0 5.5 5.0 4.5 4.0 3.5 3.0 2.5 2.0 1.5 1.0 0.5 0.0 -0.5 -1.0
f1 (ppm)

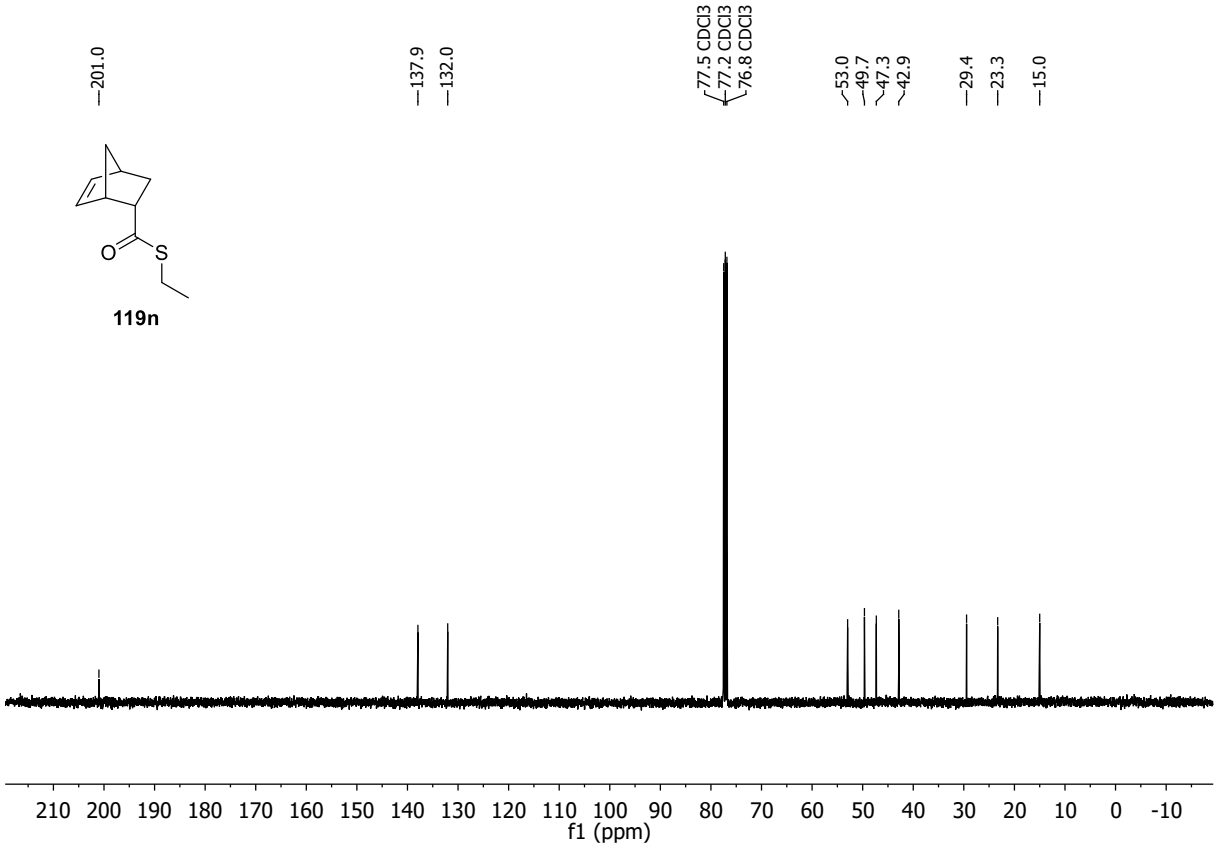
201.0
137.9
132.0
77.5 CDCl3
77.2 CDCl3
76.8 CDCl3
53.0
49.7
47.3
42.9
29.4
23.3
15.0
O
S
119n
210 200 190 180 170 160 150 140 130 120 110 100 90 80 70 60 50 40 30 20 10 0 -10
f1 (ppm)

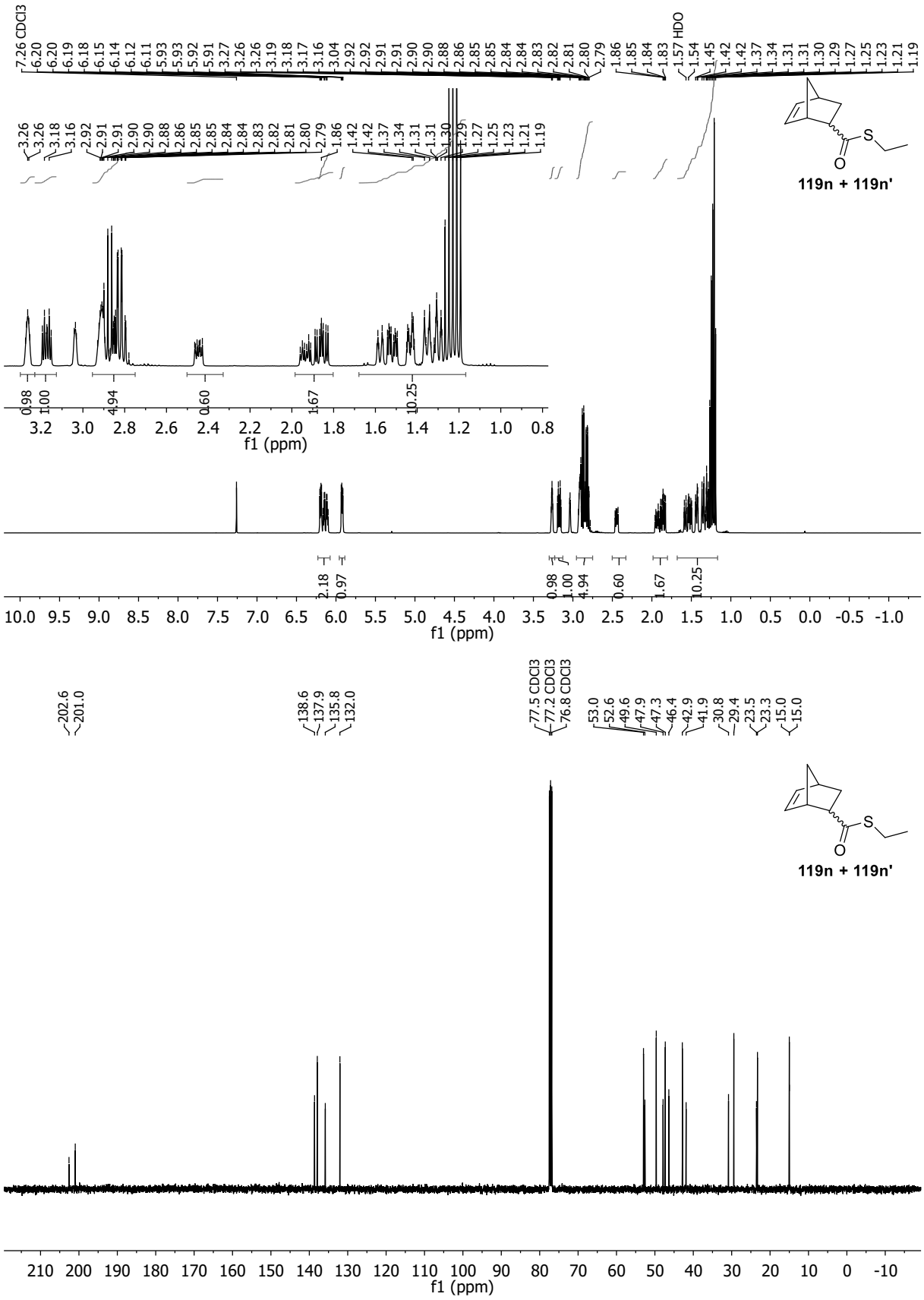
119n + 119n'
f1 (ppm)
119n + 119n'
f1 (ppm)

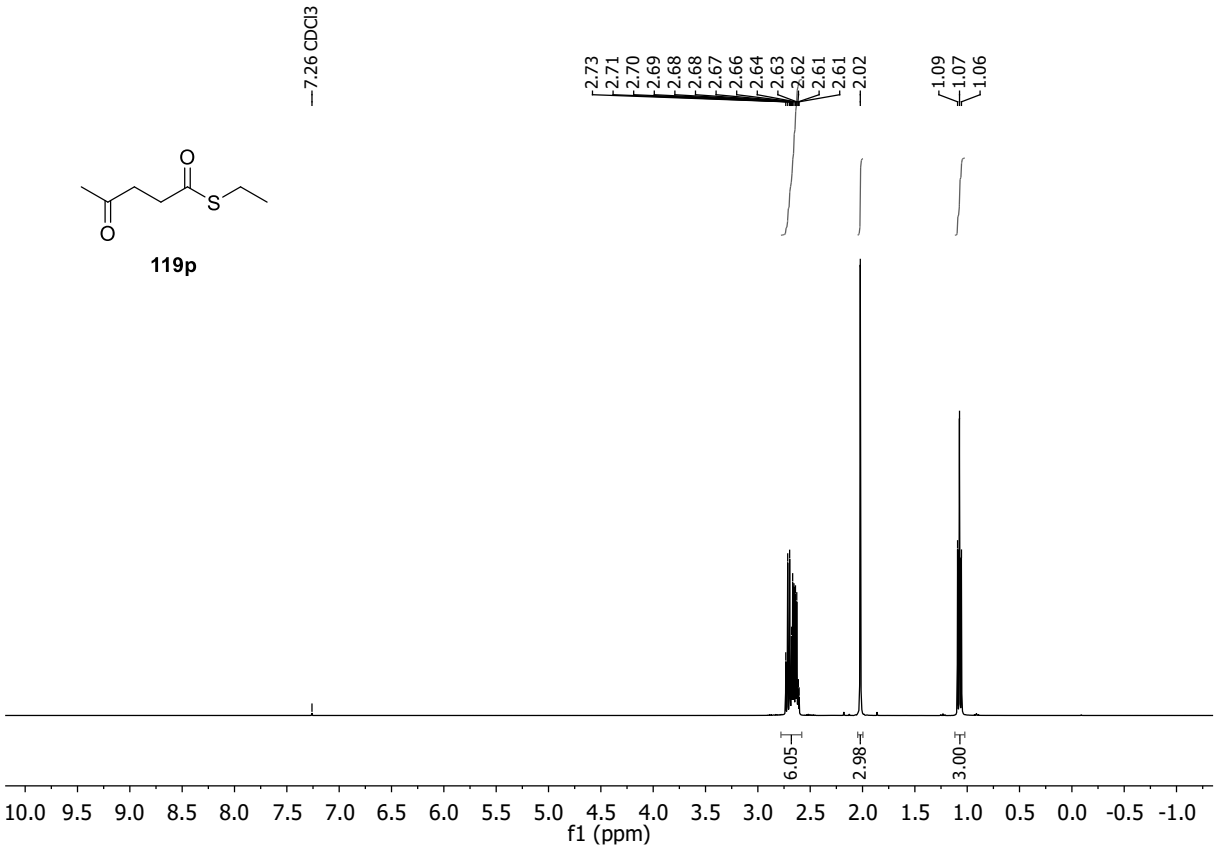
7.26 CDCl3
2.73
2.71
2.70
2.69
2.68
2.68
2.67
2.66
2.64
2.63
2.62
2.61
2.61
2.02
1.09
1.07
1.06
O
S
O
119p
6.05
2.98
3.00
10.0 9.5 9.0 8.5 8.0 7.5 7.0 6.5 6.0 5.5 5.0 4.5 4.0 3.5 3.0 2.5 2.0 1.5 1.0 0.5 0.0 -0.5 -1.0
f1 (ppm)

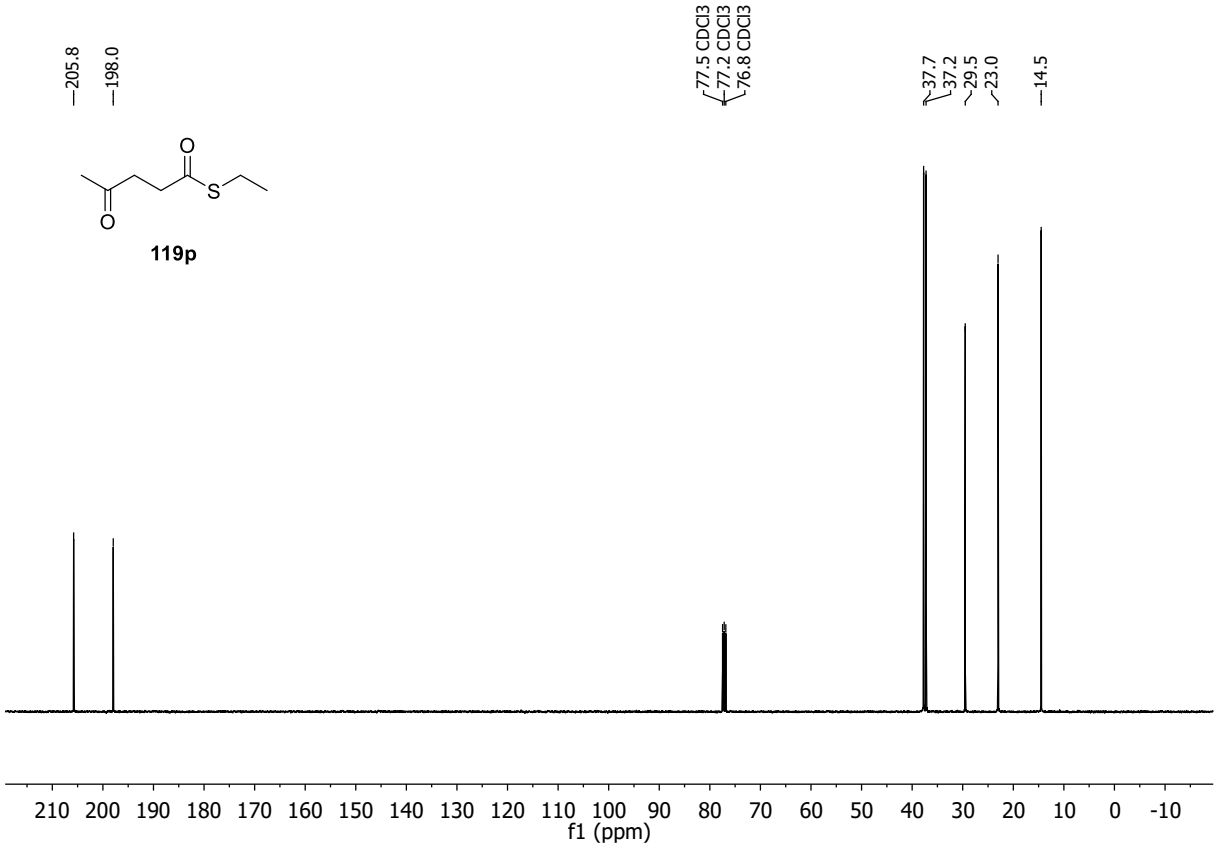
205.8
198.0
77.5 CDCl3
77.2 CDCl3
76.8 CDCl3
37.7
37.2
29.5
23.0
14.5
O
S
O
119p
210 200 190 180 170 160 150 140 130 120 110 100 90 80 70 60 50 40 30 20 10 0 -10
f1 (ppm)

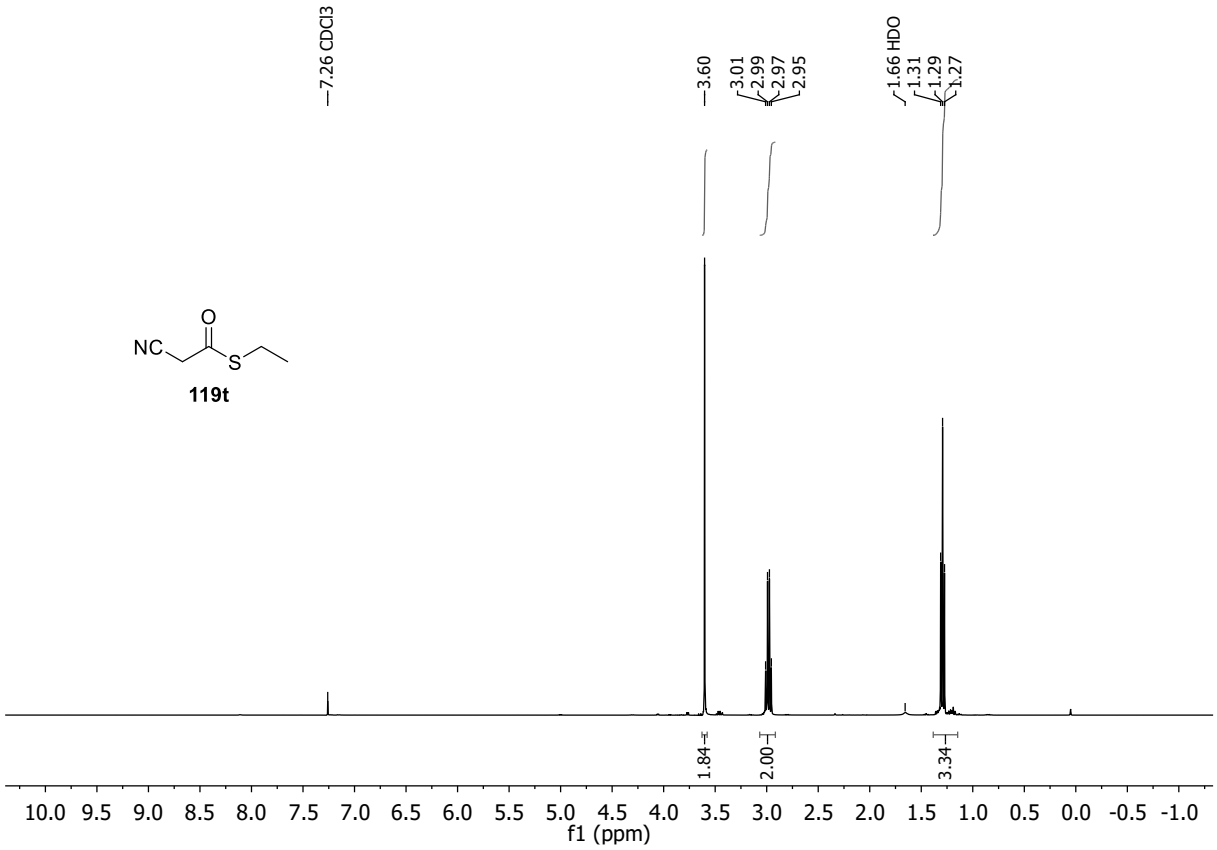
7.26 CDCl3
3.60
3.01
2.99
2.97
2.95
1.66 HDO
1.31
1.29
1.27
NC
O
S
119t
1.84
2.00
3.34
10.0 9.5 9.0 8.5 8.0 7.5 7.0 6.5 6.0 5.5 5.0 4.5 4.0 3.5 3.0 2.5 2.0 1.5 1.0 0.5 0.0 -0.5 -1.0
f1 (ppm)

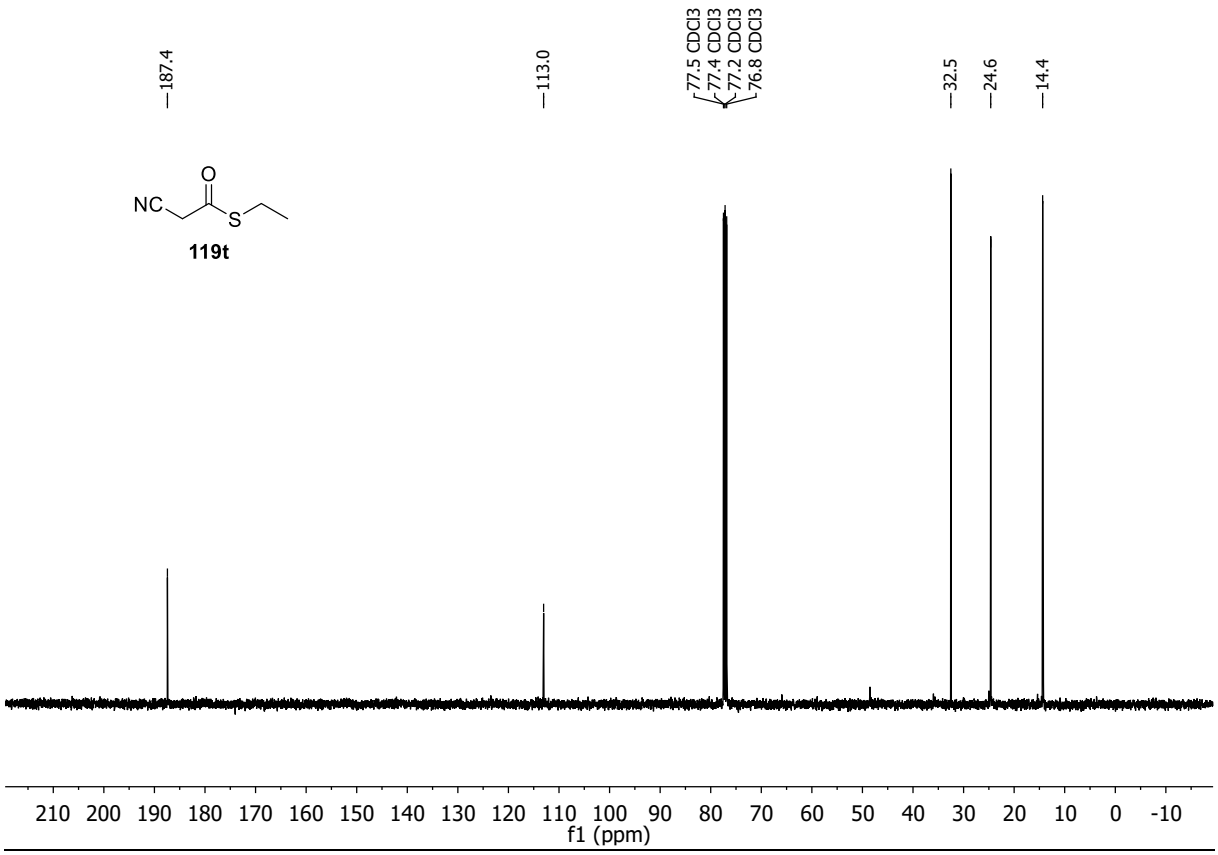
187.4
113.0
77.5 CDCl3
77.4 CDCl3
77.2 CDCl3
76.8 CDCl3
32.5
24.6
14.4
NC
O
S
119t
210 200 190 180 170 160 150 140 130 120 110 100 90 80 70 60 50 40 30 20 10 0 -10
f1 (ppm)

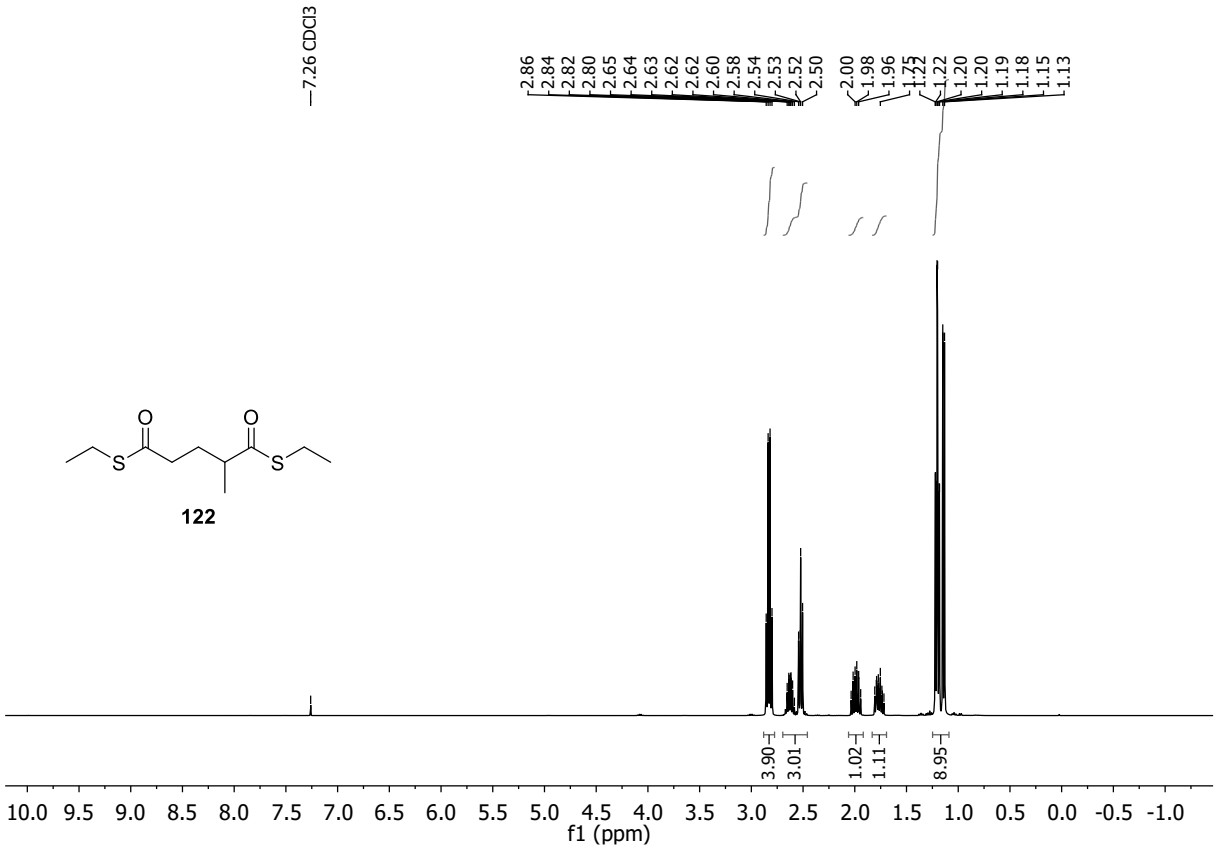
7.26 CDCl3
2.86
2.84
2.82
2.80
2.65
2.64
2.63
2.62
2.62
2.60
2.58
2.54
2.53
2.52
2.50
2.00
1.98
1.96
1.75
1.22
1.20
1.20
1.19
1.18
1.15
1.13
3.90
3.01
1.02
1.11
8.95
10.0 9.5 9.0 8.5 8.0 7.5 7.0 6.5 6.0 5.5 5.0 4.5 4.0 3.5 3.0 2.5 2.0 1.5 1.0 0.5 0.0 -0.5 -1.0
f1 (ppm)
O
O
S
S
122

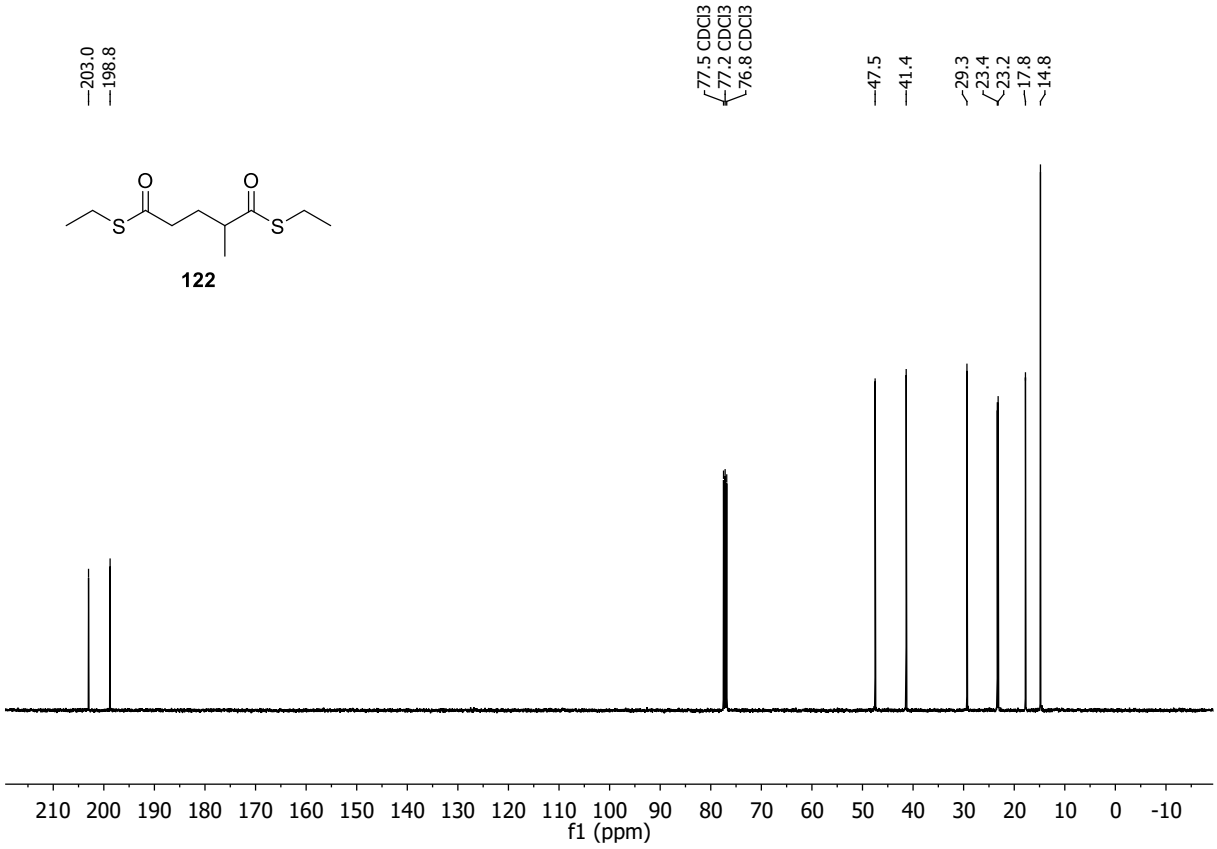
203.0
198.8
77.5 CDCl3
77.2 CDCl3
76.8 CDCl3
47.5
41.4
29.3
23.4
23.2
17.8
14.8
210 200 190 180 170 160 150 140 130 120 110 100 90 80 70 60 50 40 30 20 10 0 -10
f1 (ppm)
O
O
S
S
122

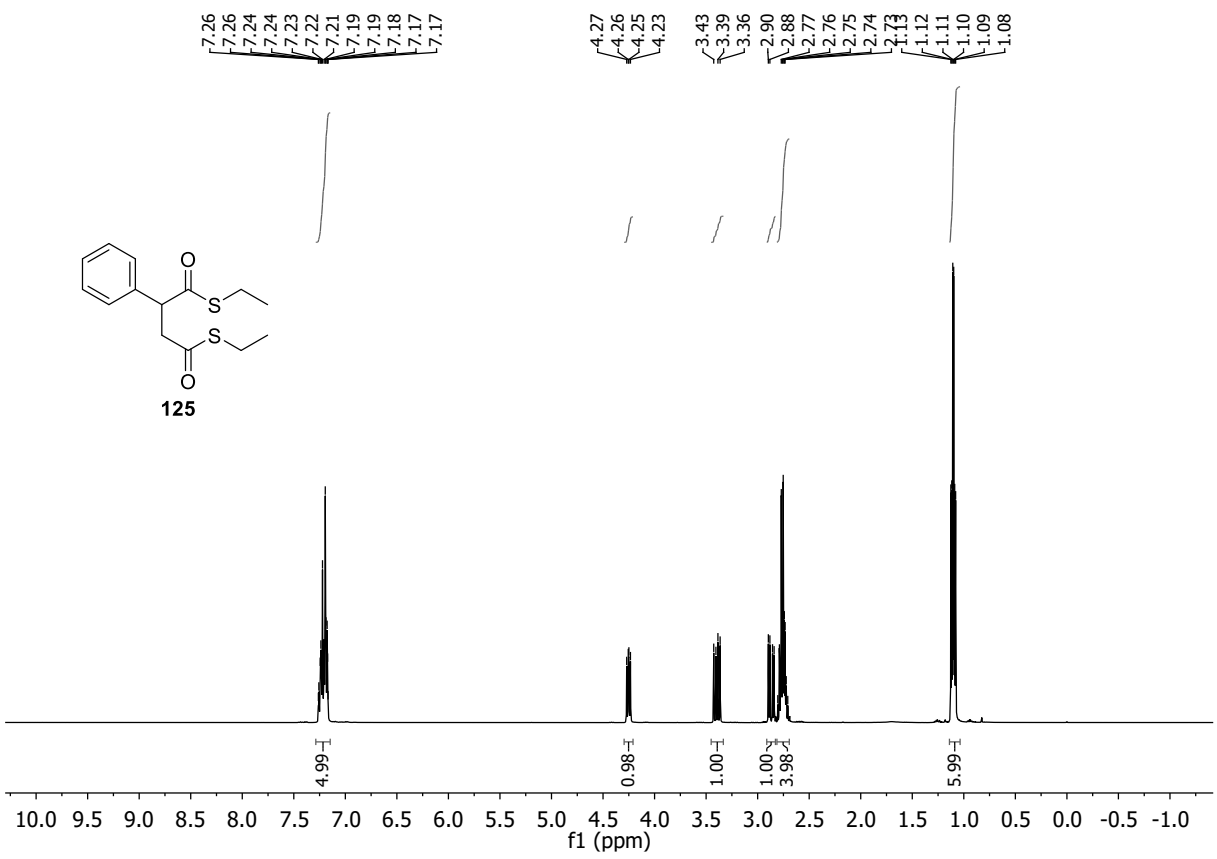
7.26
7.26
7.24
7.24
7.23
7.22
7.21
7.19
7.19
7.18
7.17
7.17
4.27
4.26
4.25
4.23
3.43
3.39
3.36
2.90
2.88
2.77
2.76
2.75
2.74
1.12
1.11
1.10
1.09
1.08
O
S
S
O
125
4.99
0.98
1.00
1.00
3.98
5.99
10.0 9.5 9.0 8.5 8.0 7.5 7.0 6.5 6.0 5.5 5.0 4.5 4.0 3.5 3.0 2.5 2.0 1.5 1.0 0.5 0.0 -0.5 -1.0
f1 (ppm)

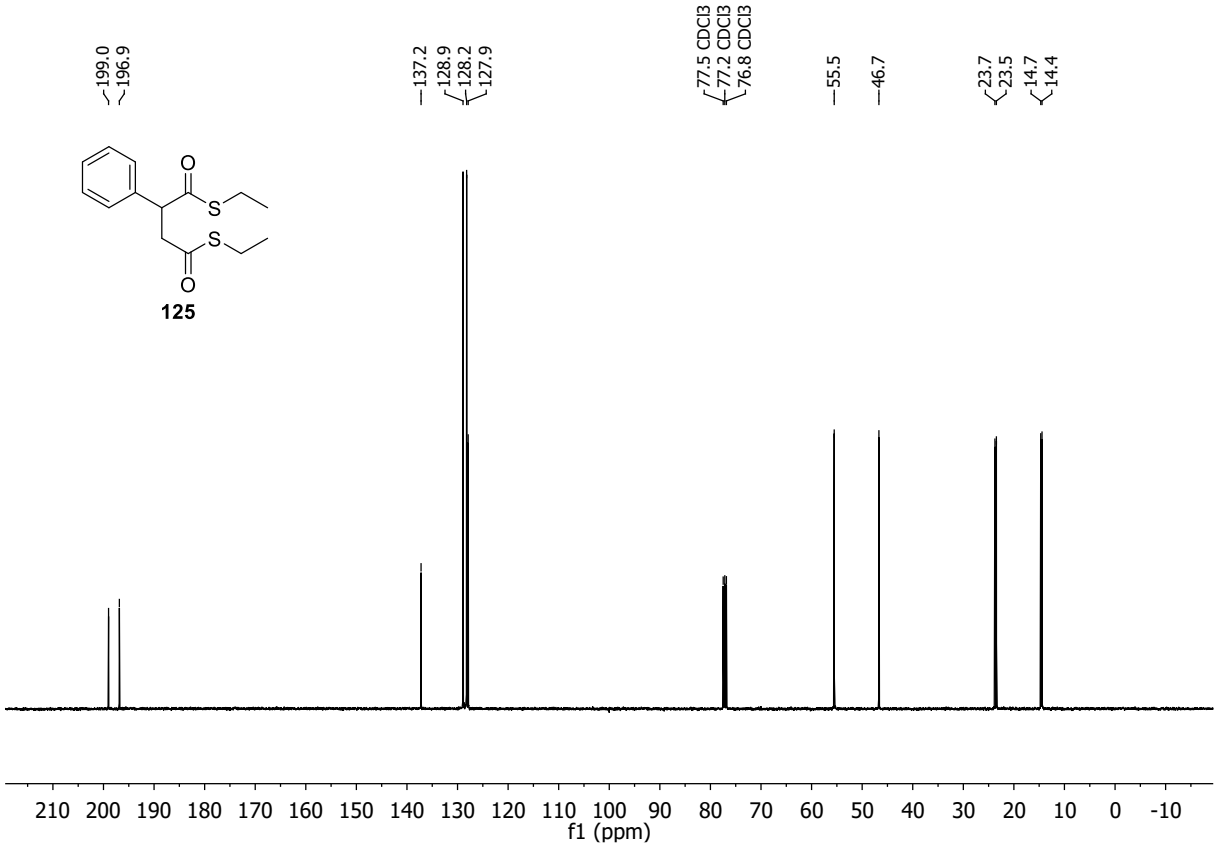
199.0
196.9
137.2
128.9
128.2
127.9
77.5 CDCl3
77.2 CDCl3
76.8 CDCl3
55.5
46.7
23.7
23.5
14.7
14.4
O
S
S
O
125
210 200 190 180 170 160 150 140 130 120 110 100 90 80 70 60 50 40 30 20 10 0 -10
f1 (ppm)

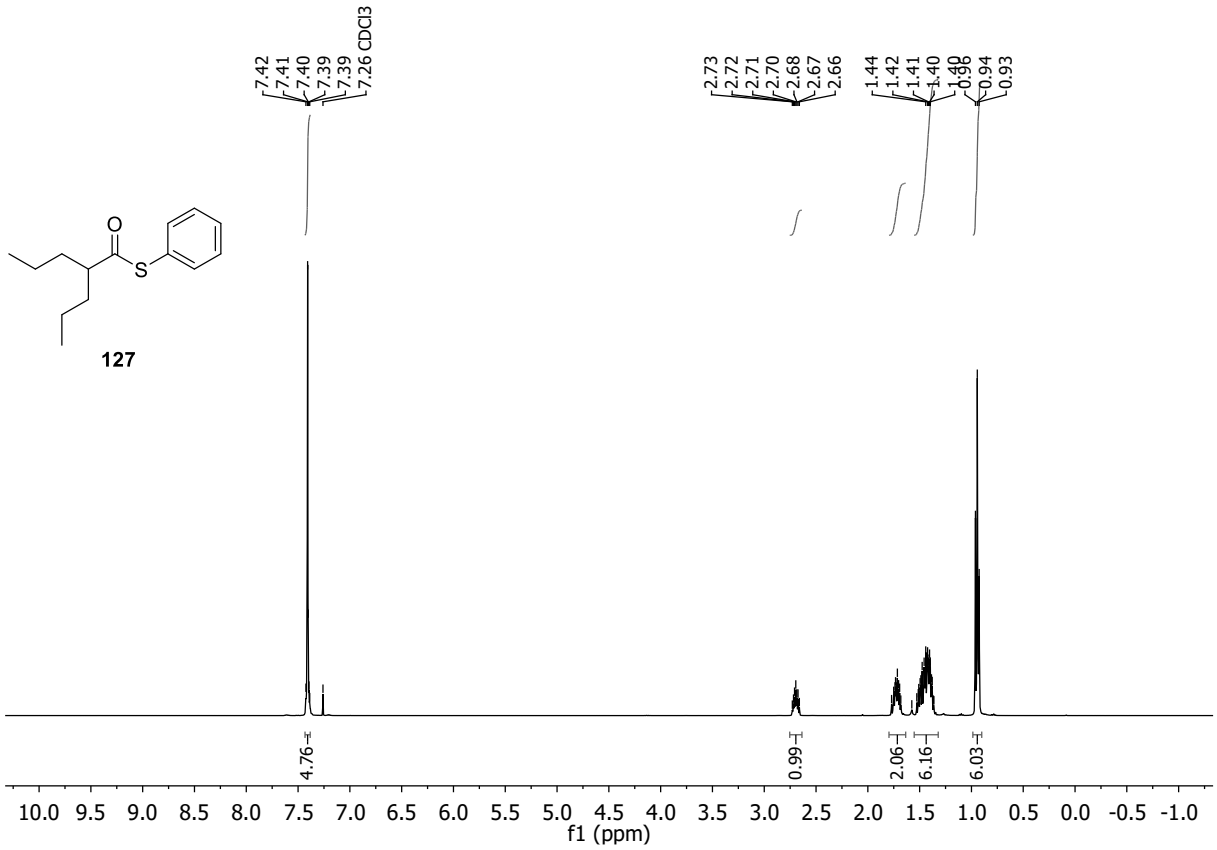
7.42
7.41
7.40
7.39
7.39
7.26 CDCl3
2.73
2.72
2.71
2.70
2.68
2.67
2.66
1.44
1.42
1.41
1.40
0.96
0.94
0.93
O
S
127
4.76
0.99
2.06
6.16
6.03
10.0 9.5 9.0 8.5 8.0 7.5 7.0 6.5 6.0 5.5 5.0 4.5 4.0 3.5 3.0 2.5 2.0 1.5 1.0 0.5 0.0 -0.5 -1.0
f1 (ppm)

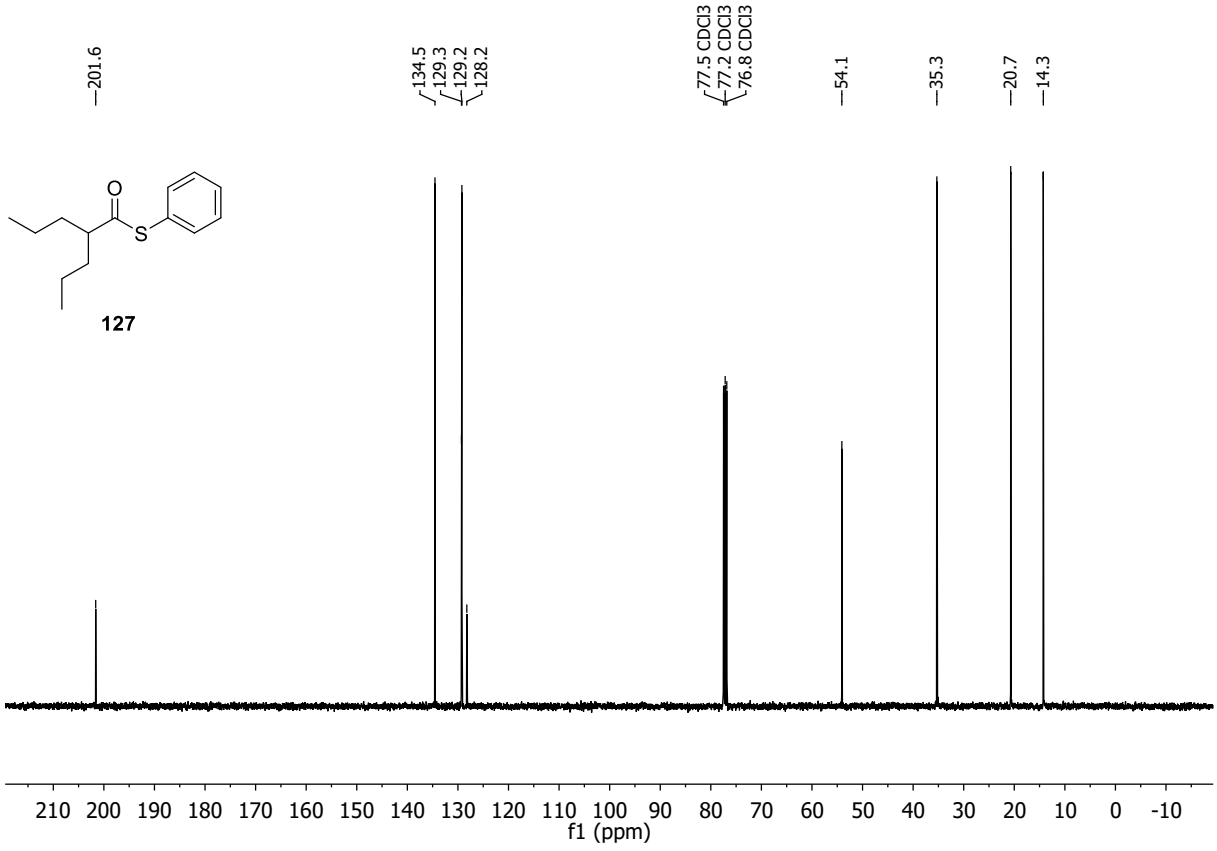
201.6
134.5
129.3
129.2
128.2
77.5 CDCl3
77.2 CDCl3
76.8 CDCl3
54.1
35.3
20.7
14.3
O
S
127
210 200 190 180 170 160 150 140 130 120 110 100 90 80 70 60 50 40 30 20 10 0 -10
f1 (ppm)

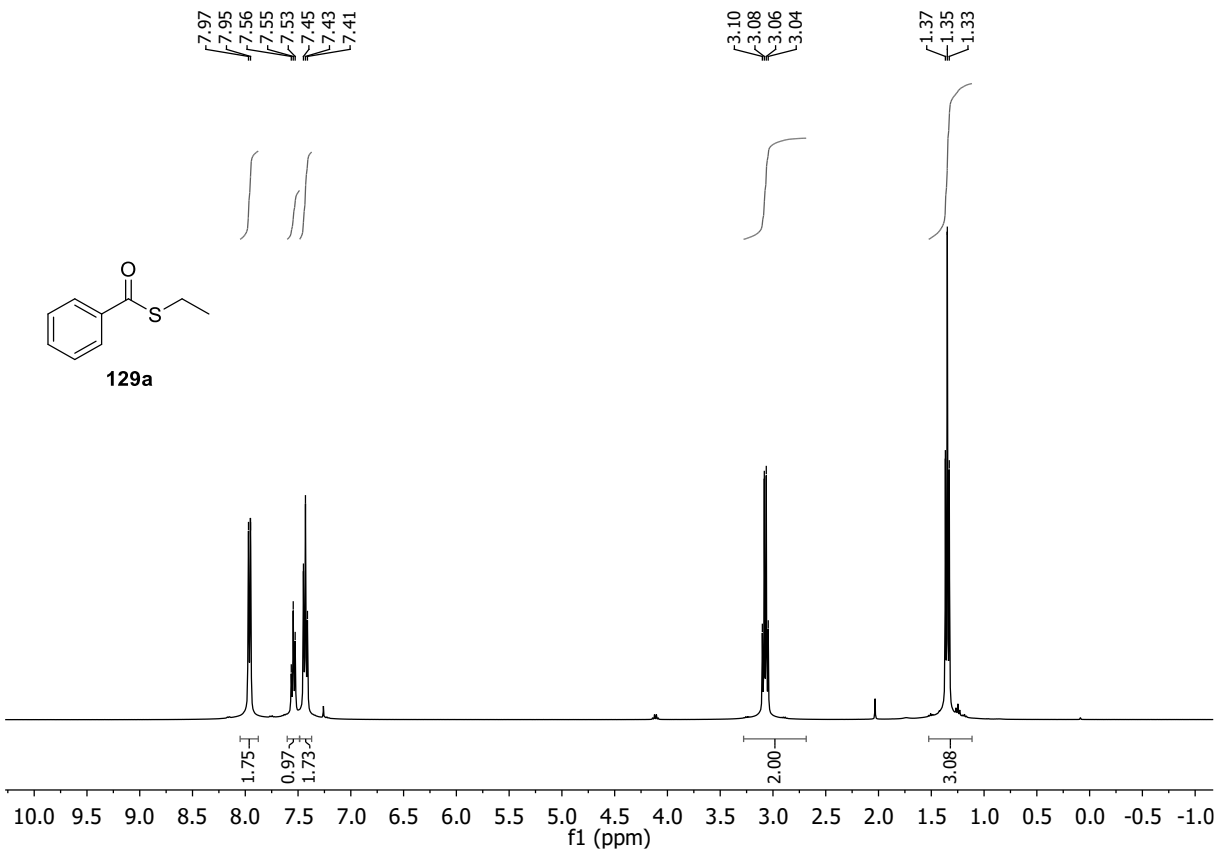
7.97
7.95
7.56
7.55
7.53
7.45
7.43
7.41
3.10
3.08
3.06
3.04
1.37
1.35
1.33
O
S
129a
1.75
0.97
1.73
2.00
3.08
10.0 9.5 9.0 8.5 8.0 7.5 7.0 6.5 6.0 5.5 5.0 4.5 4.0 3.5 3.0 2.5 2.0 1.5 1.0 0.5 0.0 -0.5 -1.0
f1 (ppm)

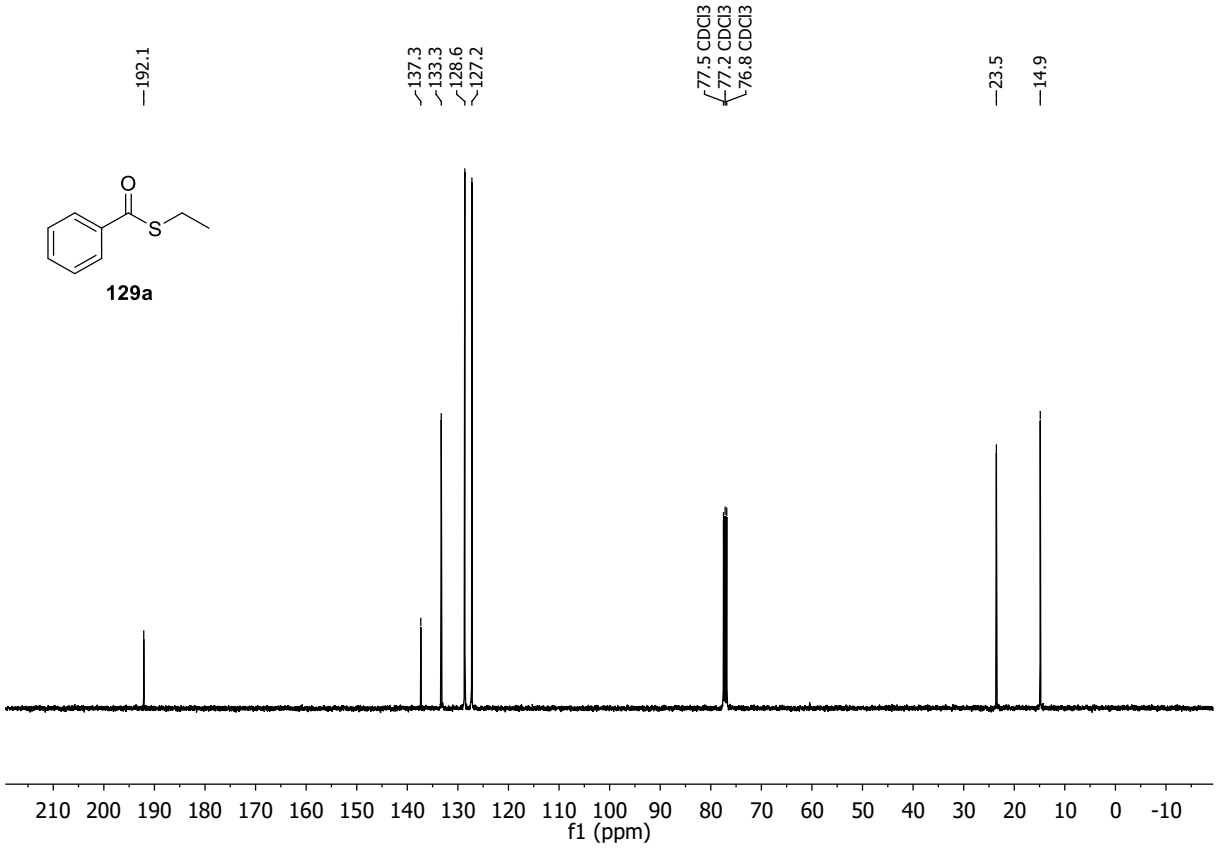
192.1
137.3
133.3
128.6
127.2
77.5 CDCl3
77.2 CDCl3
76.8 CDCl3
23.5
14.9
O
S
129a
210 200 190 180 170 160 150 140 130 120 110 100 90 80 70 60 50 40 30 20 10 0 -10
f1 (ppm)

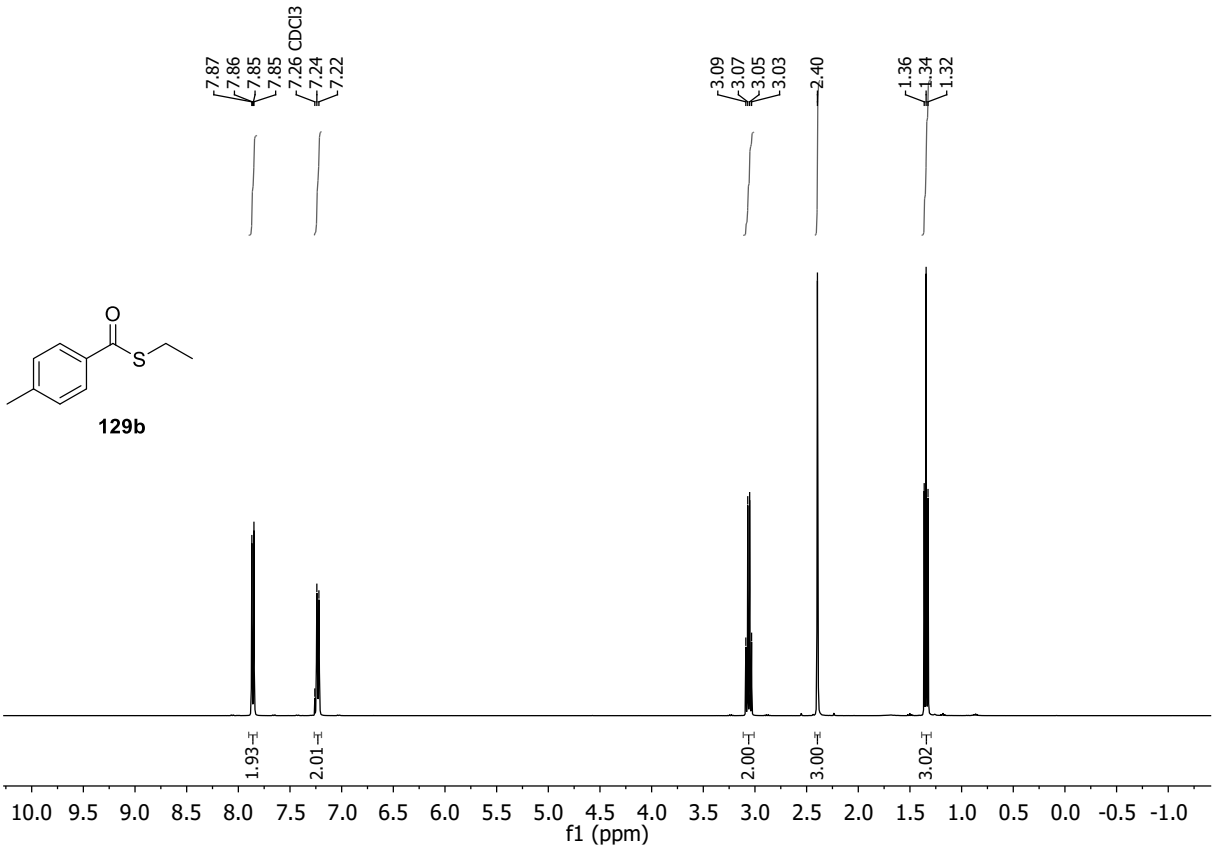
7.87
7.86
7.85
7.85
7.26 CDCl3
7.24
7.22
3.09
3.07
3.05
3.03
2.40
1.36
1.34
1.32
O
S
129b
1.93
2.01
2.00
3.00
3.02
10.0 9.5 9.0 8.5 8.0 7.5 7.0 6.5 6.0 5.5 5.0 4.5 4.0 3.5 3.0 2.5 2.0 1.5 1.0 0.5 0.0 -0.5 -1.0
f1 (ppm)

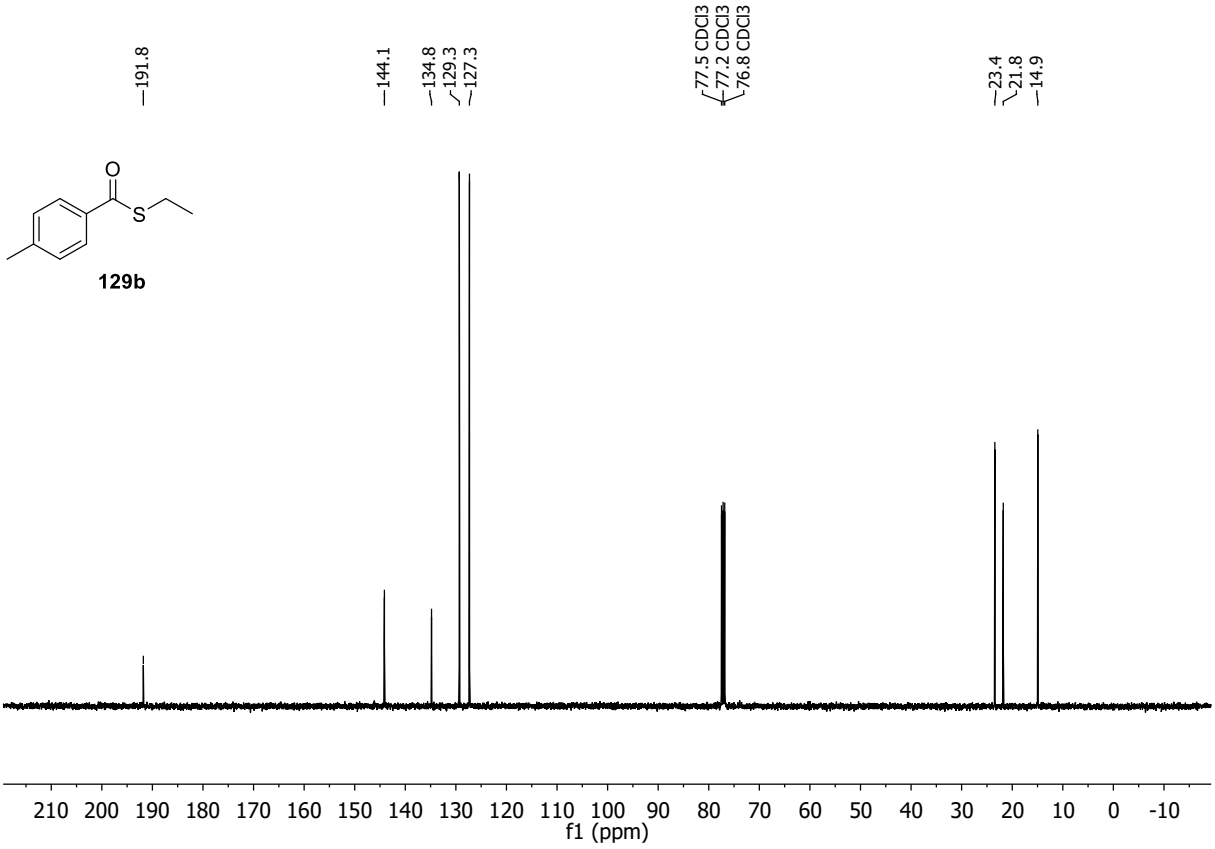
191.8
144.1
134.8
129.3
127.3
77.5 CDCl3
77.2 CDCl3
76.8 CDCl3
23.4
21.8
14.9
O
S
129b
210 200 190 180 170 160 150 140 130 120 110 100 90 80 70 60 50 40 30 20 10 0 -10
f1 (ppm)

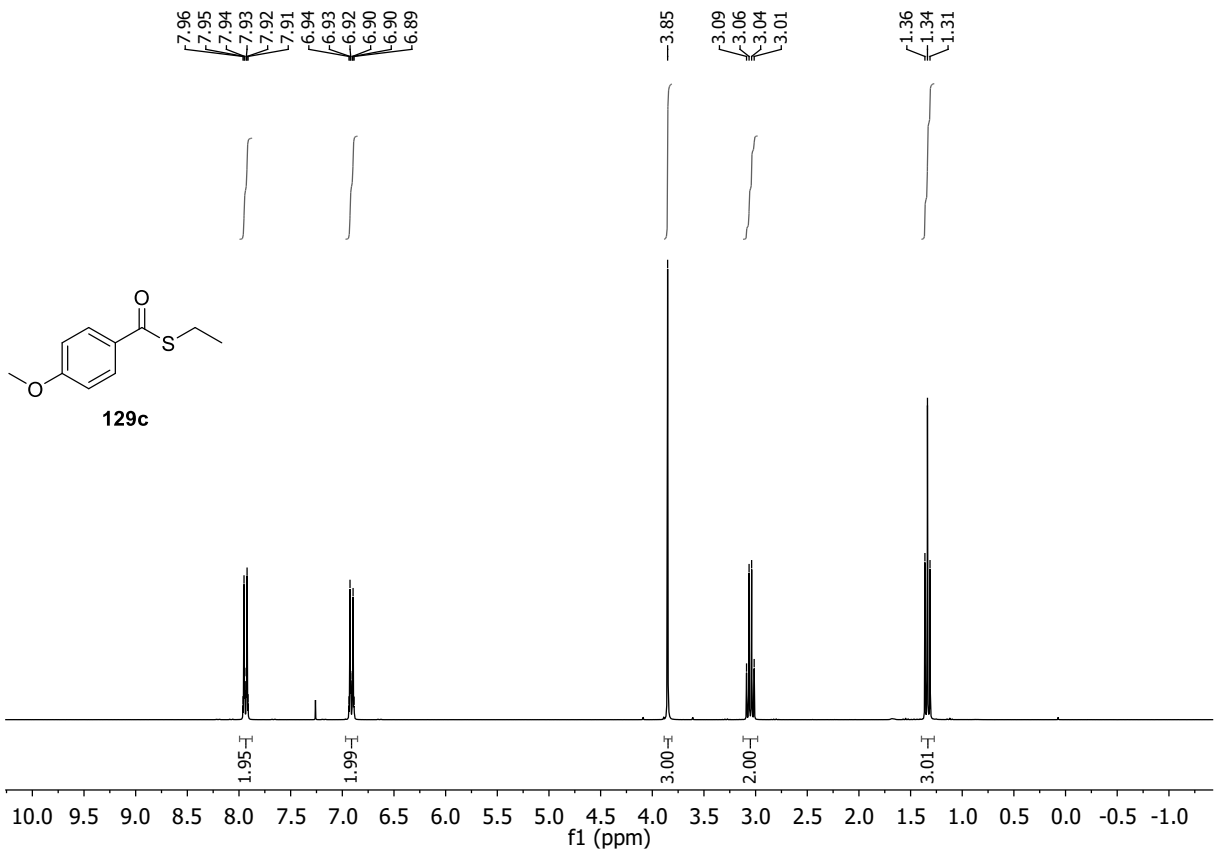
7.96
7.95
7.94
7.93
7.92
7.91
6.94
6.93
6.92
6.90
6.90
6.89
3.85
3.09
3.06
3.04
3.01
1.36
1.34
1.31
O
S
O
129c
1.95
1.99
3.00
2.00
3.01
10.0 9.5 9.0 8.5 8.0 7.5 7.0 6.5 6.0 5.5 5.0 4.5 4.0 3.5 3.0 2.5 2.0 1.5 1.0 0.5 0.0 -0.5 -1.0
f1 (ppm)

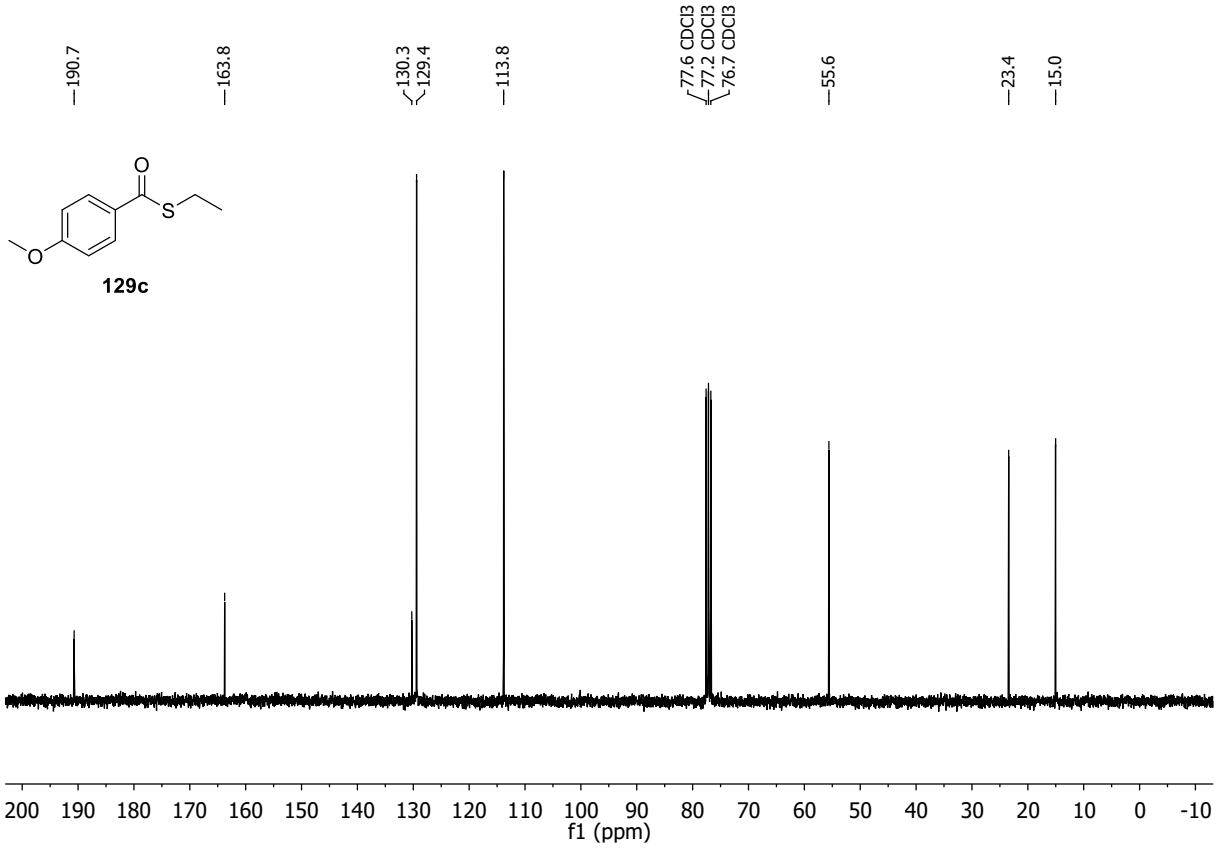
190.7
163.8
130.3
129.4
113.8
77.6 CDCl3
77.2 CDCl3
76.7 CDCl3
55.6
23.4
15.0
O
S
O
129c
200 190 180 170 160 150 140 130 120 110 100 90 80 70 60 50 40 30 20 10 0 -10
f1 (ppm)

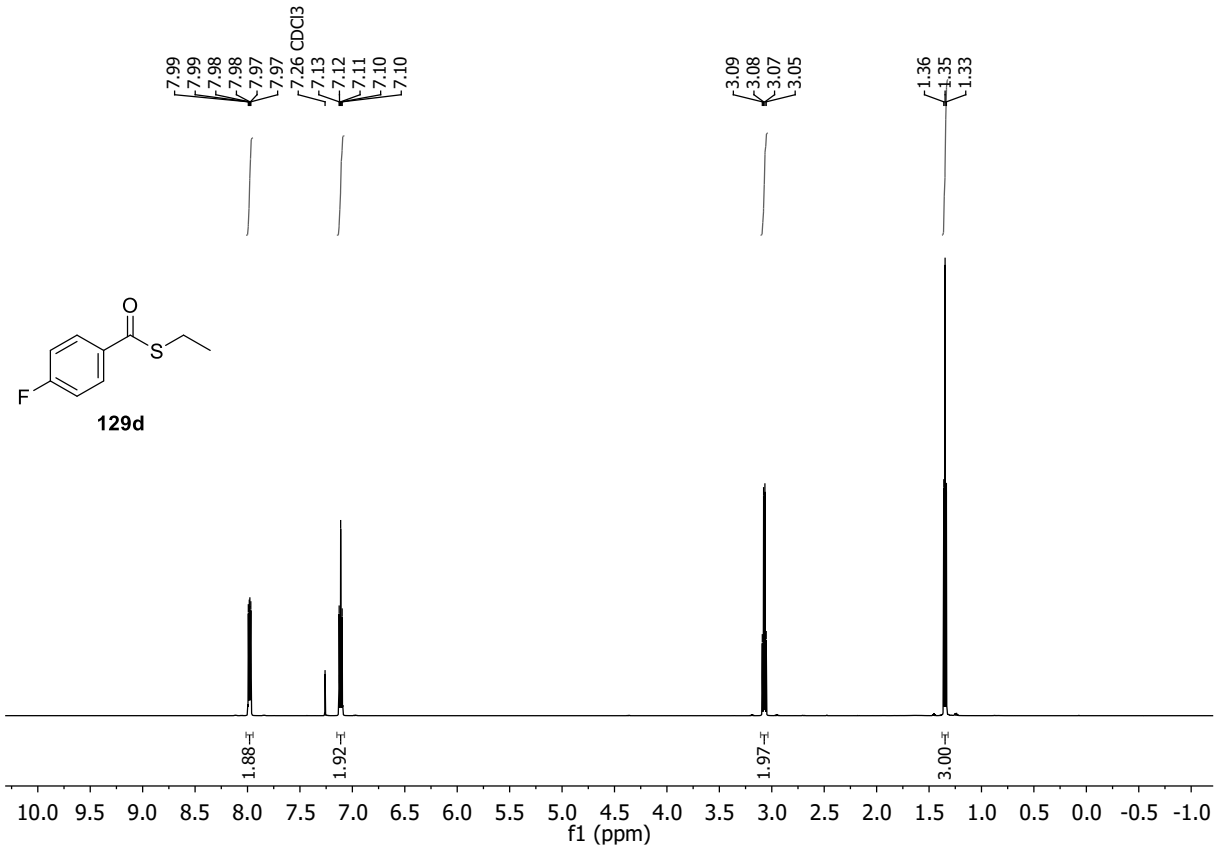
7.99
7.99
7.98
7.98
7.97
7.97
CDCl3
7.13
7.12
7.11
7.10
7.10
3.09
3.08
3.07
3.05
1.36
1.35
1.33
O
S
F
129d
1.88
1.92
1.97
3.00
10.0 9.5 9.0 8.5 8.0 7.5 7.0 6.5 6.0 5.5 5.0 4.5 4.0 3.5 3.0 2.5 2.0 1.5 1.0 0.5 0.0 -0.5 -1.0
f1 (ppm)

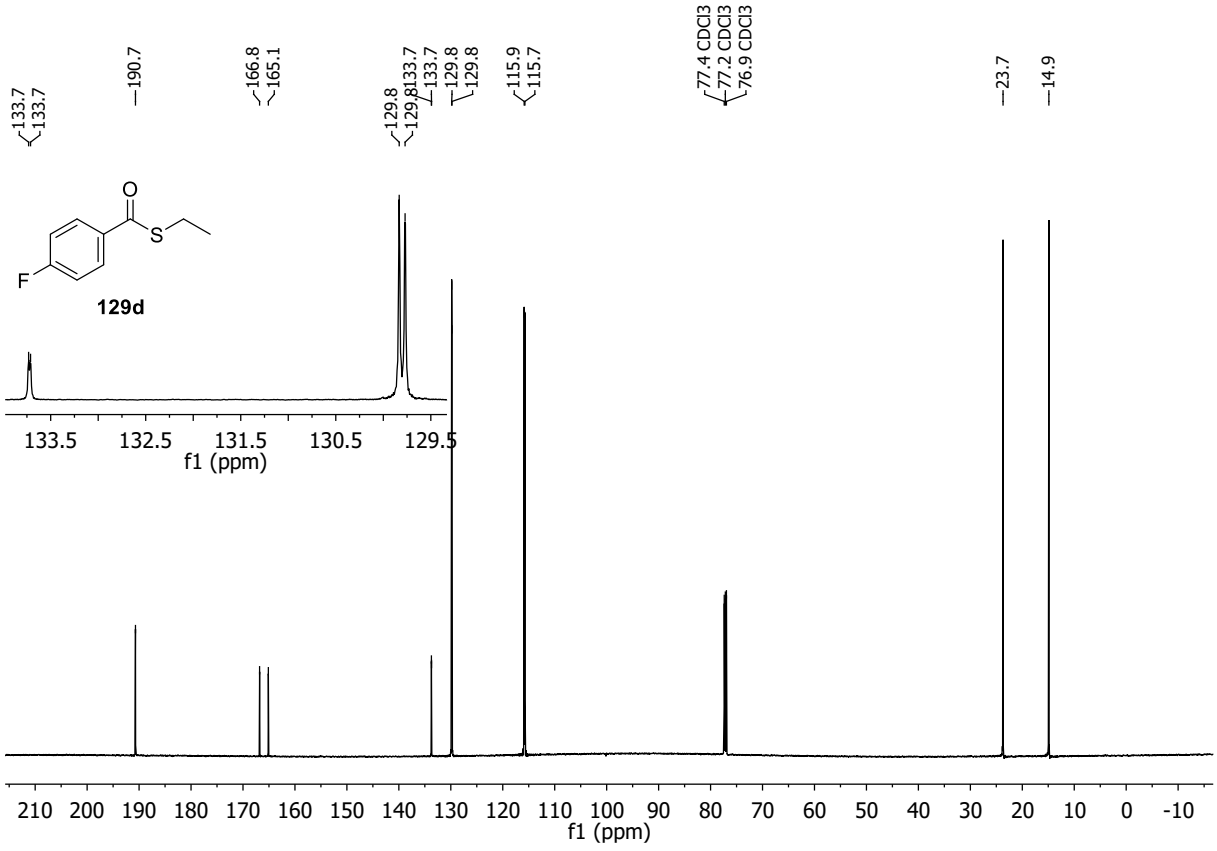
133.7
133.7
190.7
166.8
165.1
129.8
129.8
133.7
133.7
129.8
129.8
115.9
115.7
77.4 CDCl3
77.2 CDCl3
76.9 CDCl3
23.7
14.9
O
S
F
129d
133.5 132.5 131.5 130.5 129.5
f1 (ppm)
210 200 190 180 170 160 150 140 130 120 110 100 90 80 70 60 50 40 30 20 10 0 -10
f1 (ppm)

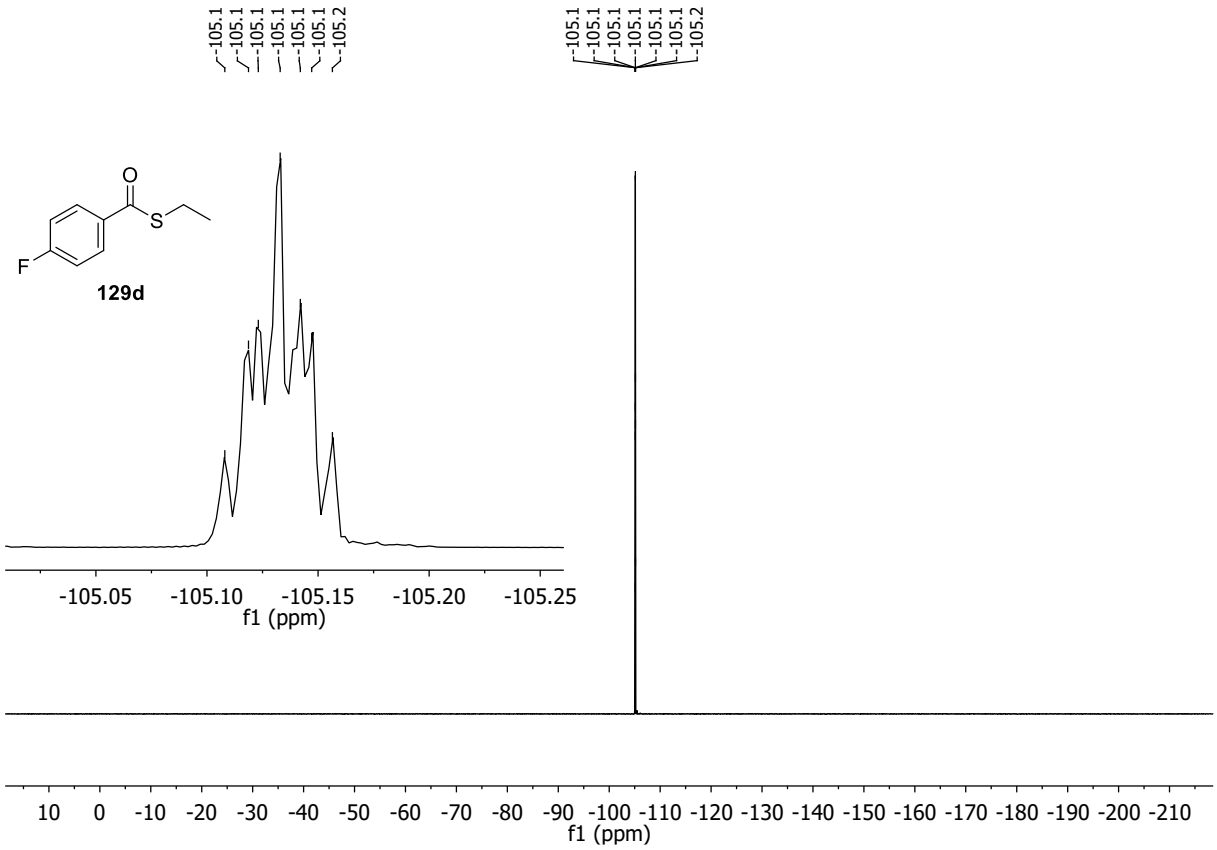
-105.1
-105.1
-105.1
-105.1
-105.1
-105.1
-105.2
-105.1
-105.1
-105.1
-105.1
-105.1
-105.1
-105.2
O
S
F
129d
-105.05
-105.10
-105.15
-105.20
-105.25
f1 (ppm)
10 0 -10 -20 -30 -40 -50 -60 -70 -80 -90 -100 -110 -120 -130 -140 -150 -160 -170 -180 -190 -200 -210
f1 (ppm)

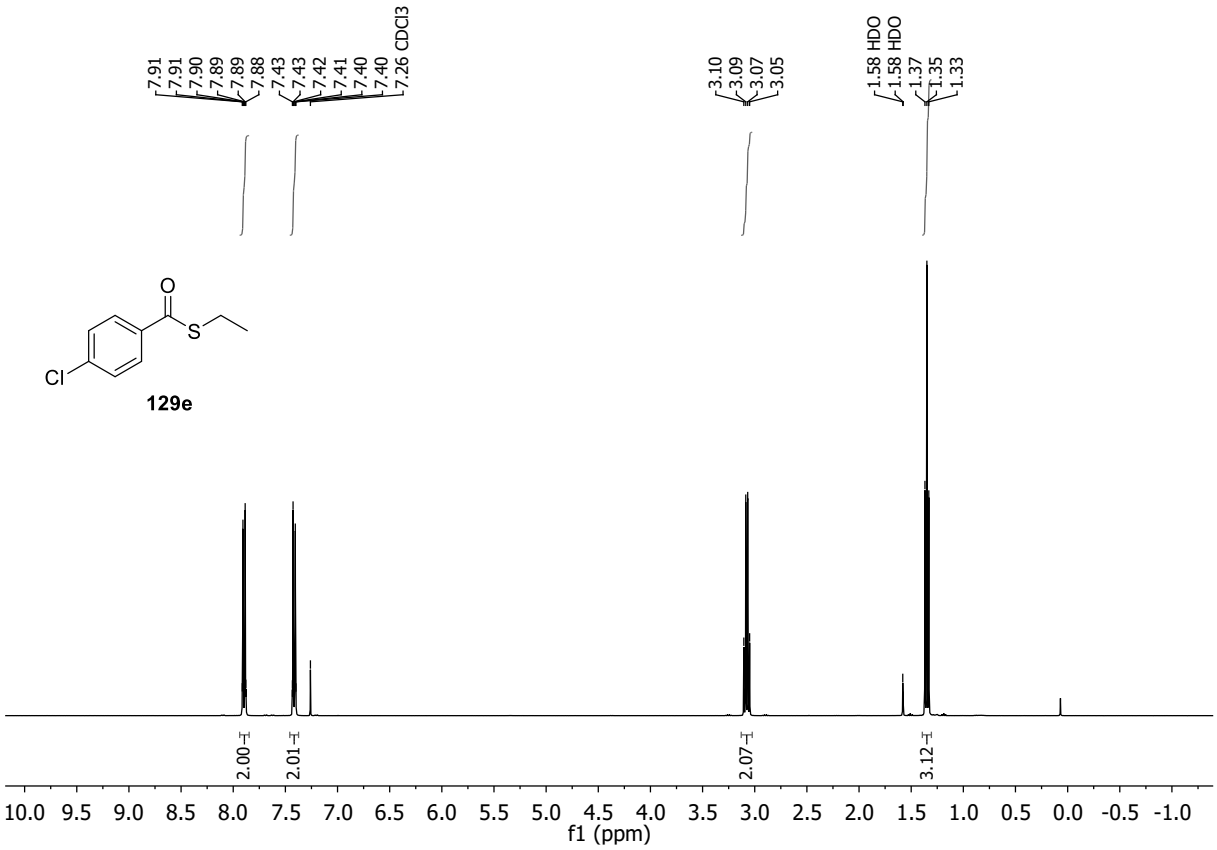
7.91
7.91
7.90
7.89
7.89
7.88
7.43
7.43
7.42
7.41
7.40
7.40
7.26 CDCl3
3.10
3.09
3.07
3.05
1.58 HDO
1.58 HDO
1.37
1.35
1.33
O
S
Cl
129e
2.00
2.01
2.07
3.12
10.0 9.5 9.0 8.5 8.0 7.5 7.0 6.5 6.0 5.5 5.0 4.5 4.0 3.5 3.0 2.5 2.0 1.5 1.0 0.5 0.0 -0.5 -1.0
f1 (ppm)

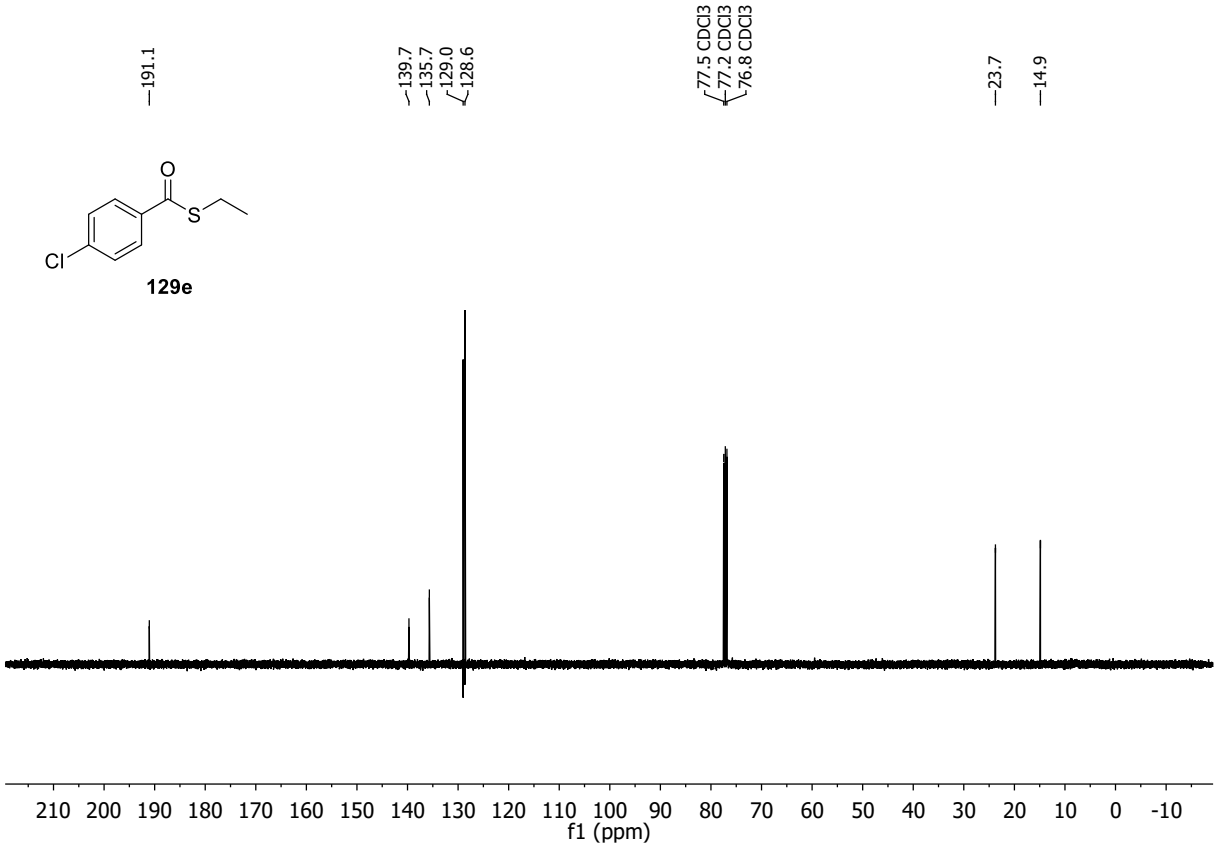
191.1
139.7
135.7
129.0
128.6
77.5 CDCl3
77.2 CDCl3
76.8 CDCl3
23.7
14.9
O
S
Cl
129e
210 200 190 180 170 160 150 140 130 120 110 100 90 80 70 60 50 40 30 20 10 0 -10
f1 (ppm)

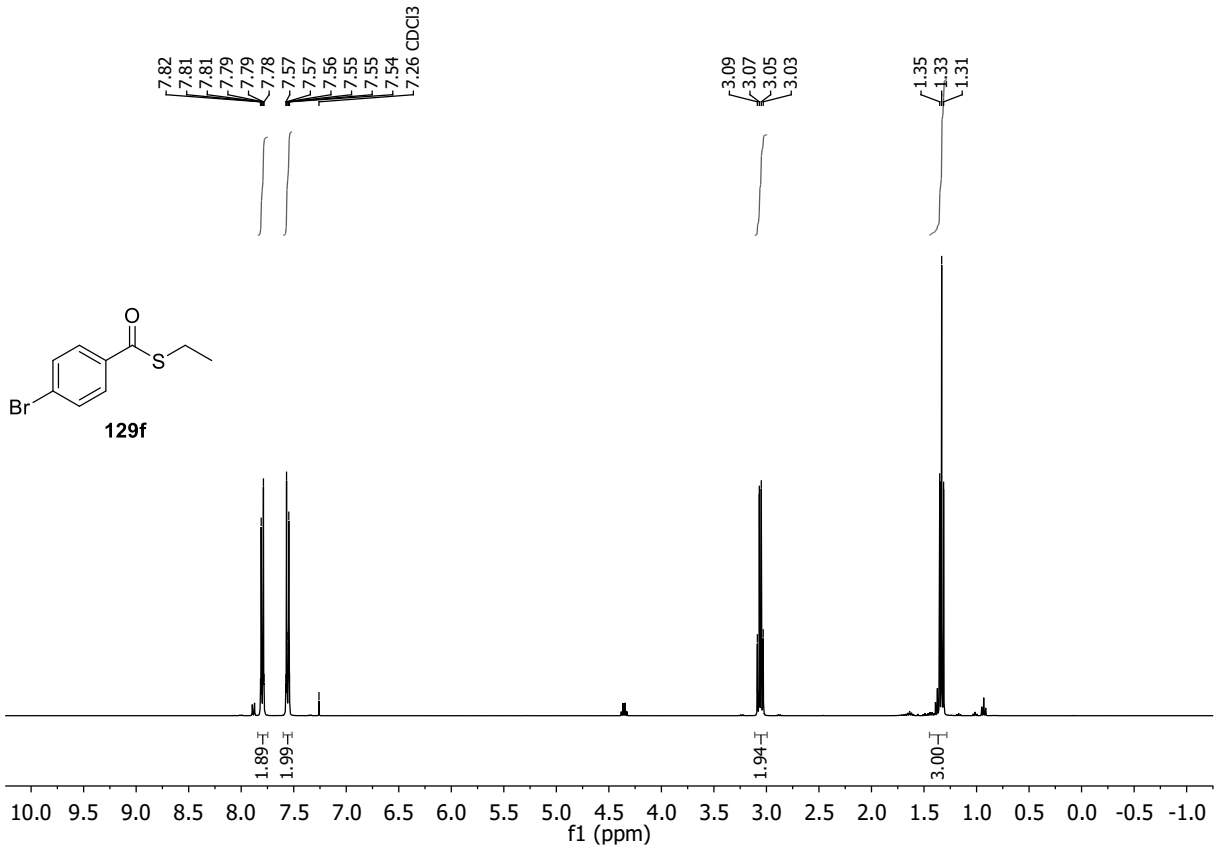
7.82
7.81
7.81
7.79
7.79
7.78
7.57
7.57
7.56
7.55
7.55
7.54
7.26 CDCl3
3.09
3.07
3.05
3.03
1.35
1.33
1.31
O
S
Br
129f
1.89
1.99
1.94
3.00
10.0 9.5 9.0 8.5 8.0 7.5 7.0 6.5 6.0 5.5 5.0 4.5 4.0 3.5 3.0 2.5 2.0 1.5 1.0 0.5 0.0 -0.5 -1.0
f1 (ppm)

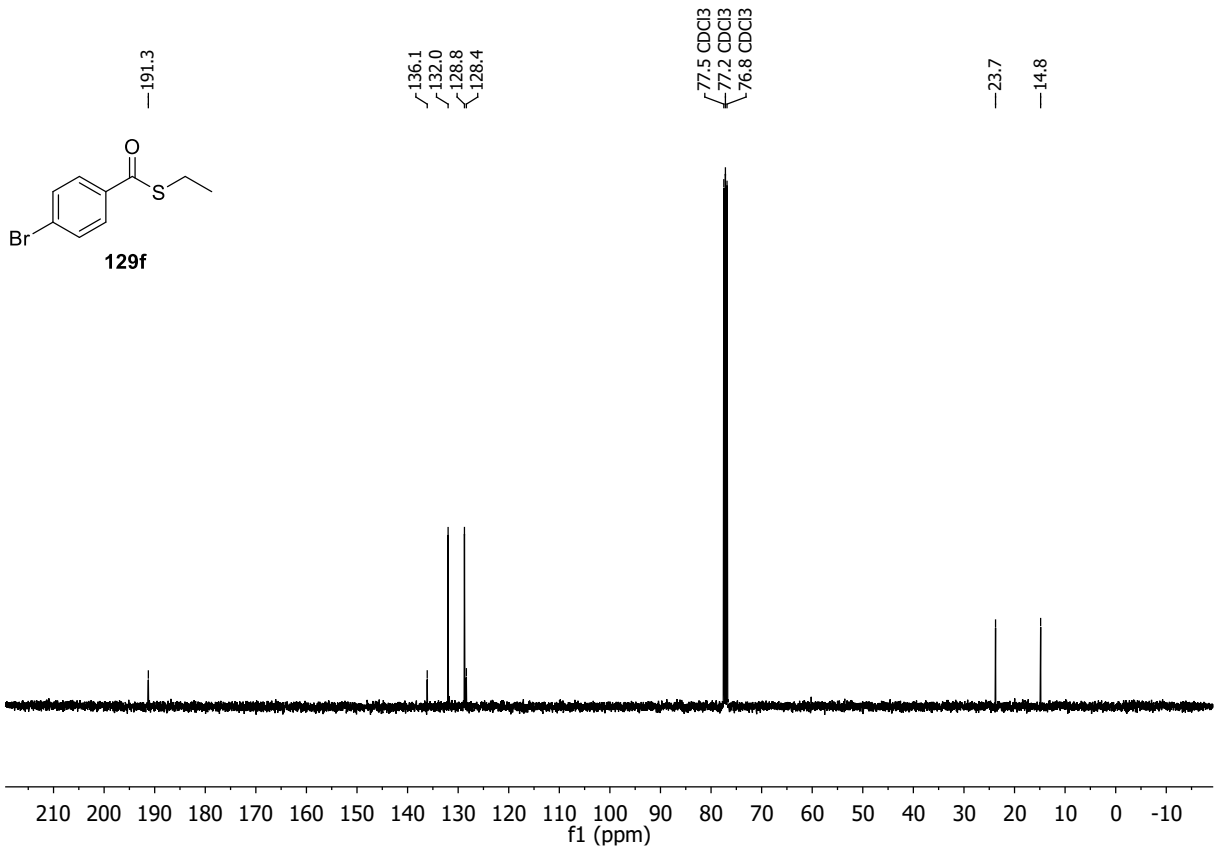
191.3
136.1
132.0
128.8
128.4
77.5 CDCl3
77.2 CDCl3
76.8 CDCl3
23.7
14.8
O
S
Br
129f
210 200 190 180 170 160 150 140 130 120 110 100 90 80 70 60 50 40 30 20 10 0 -10
f1 (ppm)

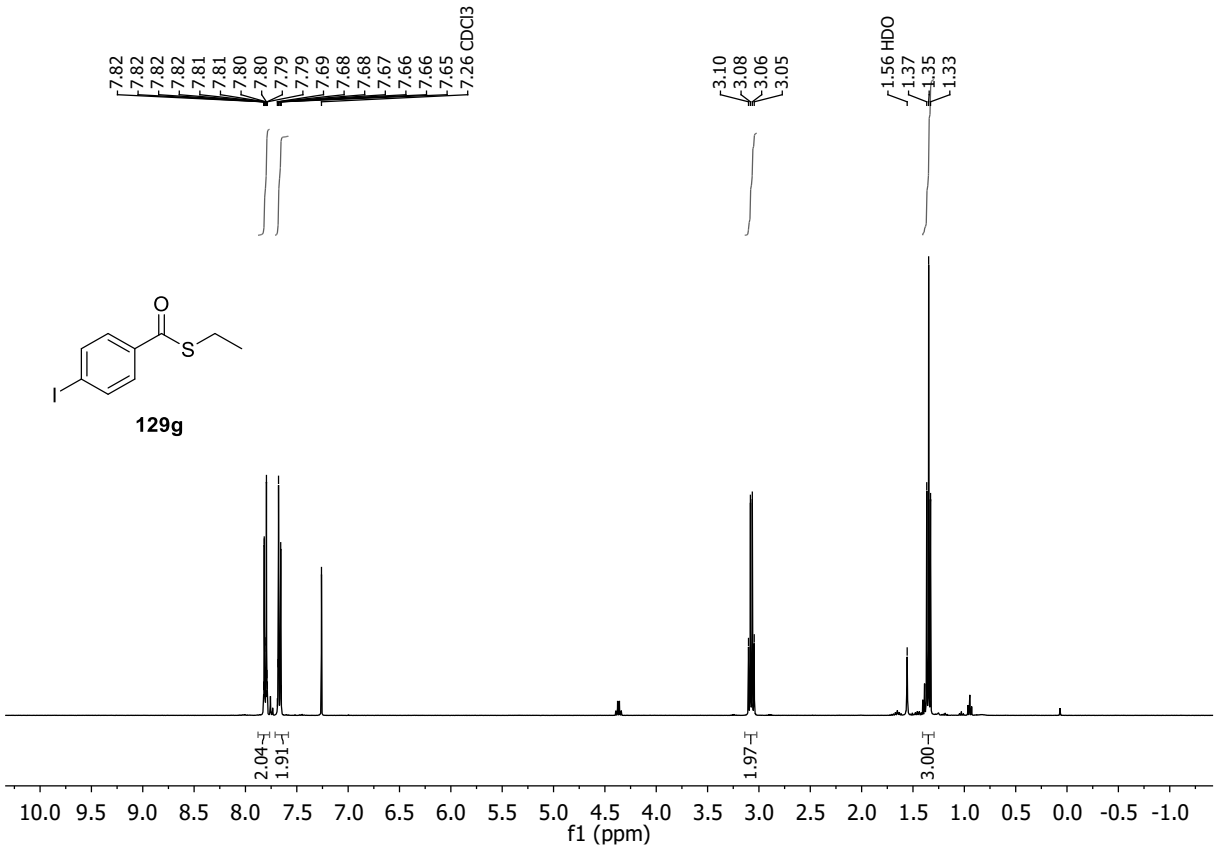
7.82
7.82
7.82
7.82
7.81
7.81
7.80
7.80
7.79
7.79
7.69
7.68
7.68
7.67
7.66
7.66
7.65
7.26 CDCl3
3.10
3.08
3.06
3.05
1.56 HDO
1.37
1.35
1.33
O
S
I
129g
2.04
1.91
1.97
3.00
10.0 9.5 9.0 8.5 8.0 7.5 7.0 6.5 6.0 5.5 5.0 4.5 4.0 3.5 3.0 2.5 2.0 1.5 1.0 0.5 0.0 -0.5 -1.0
f1 (ppm)

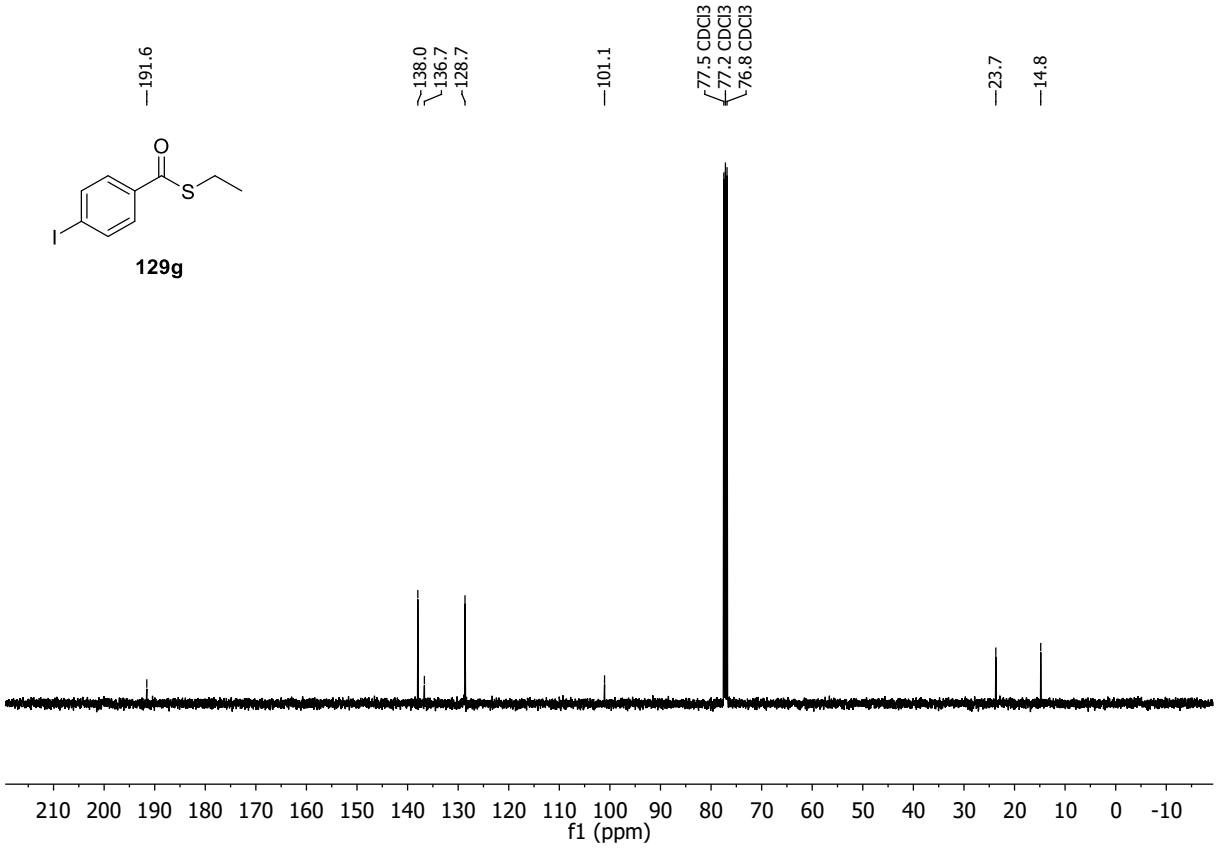
191.6
138.0
136.7
128.7
101.1
77.5 CDCl3
77.2 CDCl3
76.8 CDCl3
23.7
14.8
O
S
I
129g
210 200 190 180 170 160 150 140 130 120 110 100 90 80 70 60 50 40 30 20 10 0 -10
f1 (ppm)

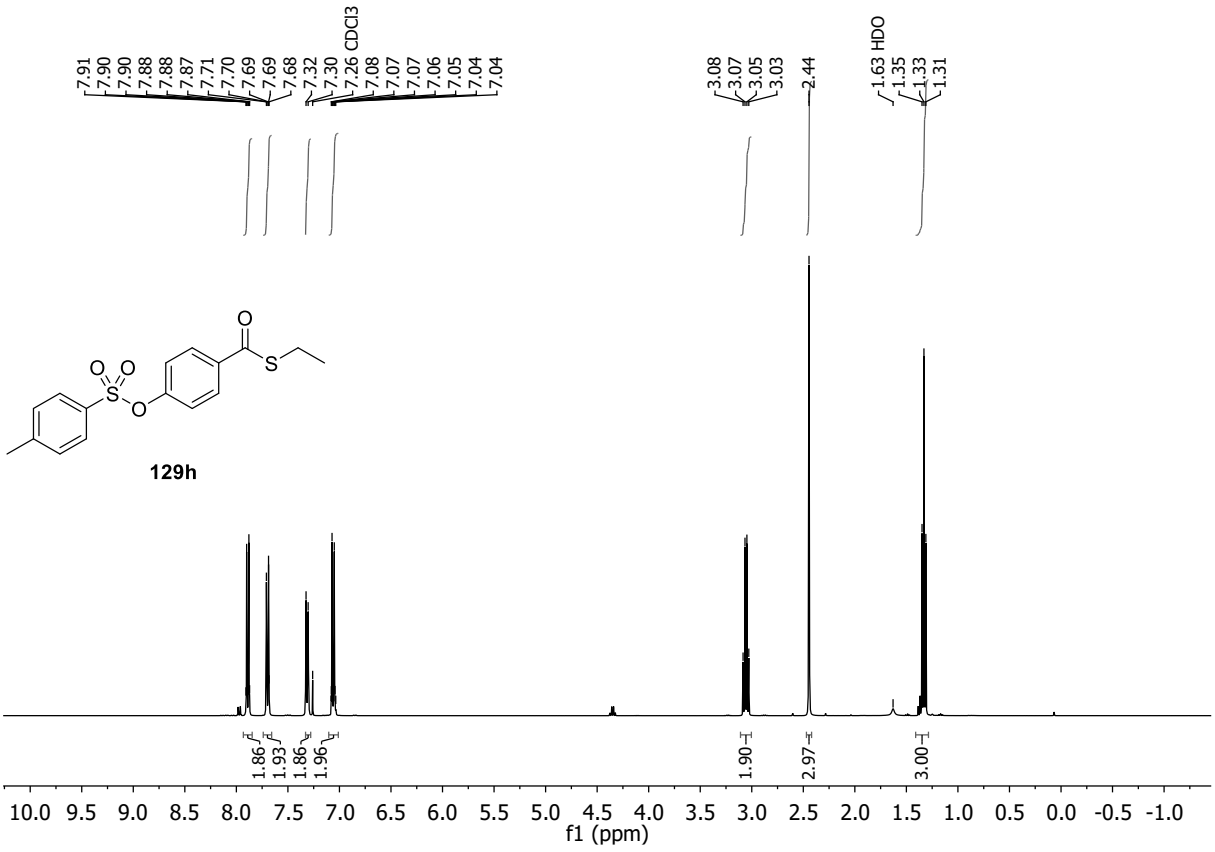
7.91
7.90
7.90
7.88
7.88
7.87
7.71
7.70
7.69
7.69
7.68
7.32
7.30
CDCl3
7.26
7.08
7.07
7.07
7.06
7.05
7.04
7.04
3.08
3.07
3.05
3.03
2.44
1.63
HDO
1.35
1.33
1.31
129h
1.86
1.93
1.86
1.96
1.90
2.97
3.00
10.0 9.5 9.0 8.5 8.0 7.5 7.0 6.5 6.0 5.5 5.0 4.5 4.0 3.5 3.0 2.5 2.0 1.5 1.0 0.5 0.0 -0.5 -1.0
f1 (ppm)

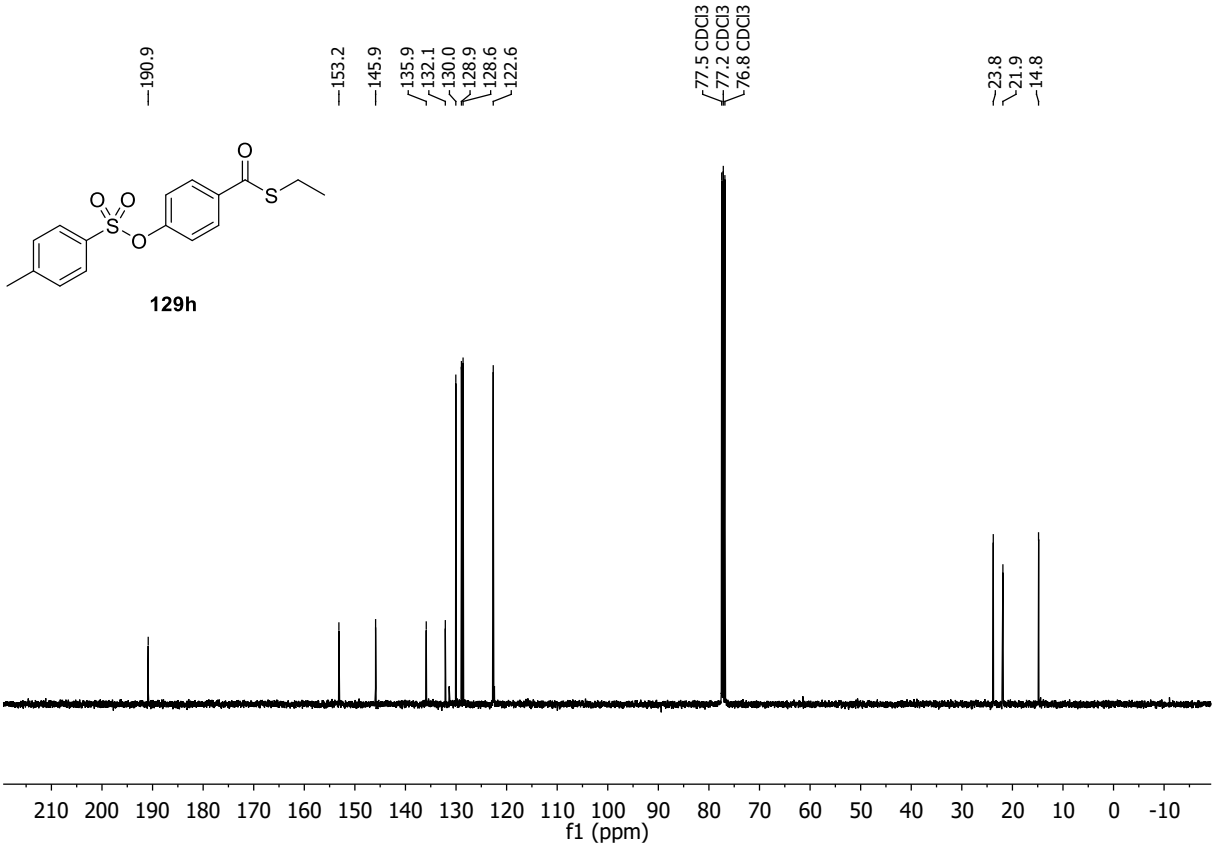
190.9
153.2
145.9
135.9
132.1
130.0
128.9
128.6
122.6
77.5 CDCl3
77.2 CDCl3
76.8 CDCl3
23.8
21.9
14.8
129h
210 200 190 180 170 160 150 140 130 120 110 100 90 80 70 60 50 40 30 20 10 0 -10
f1 (ppm)

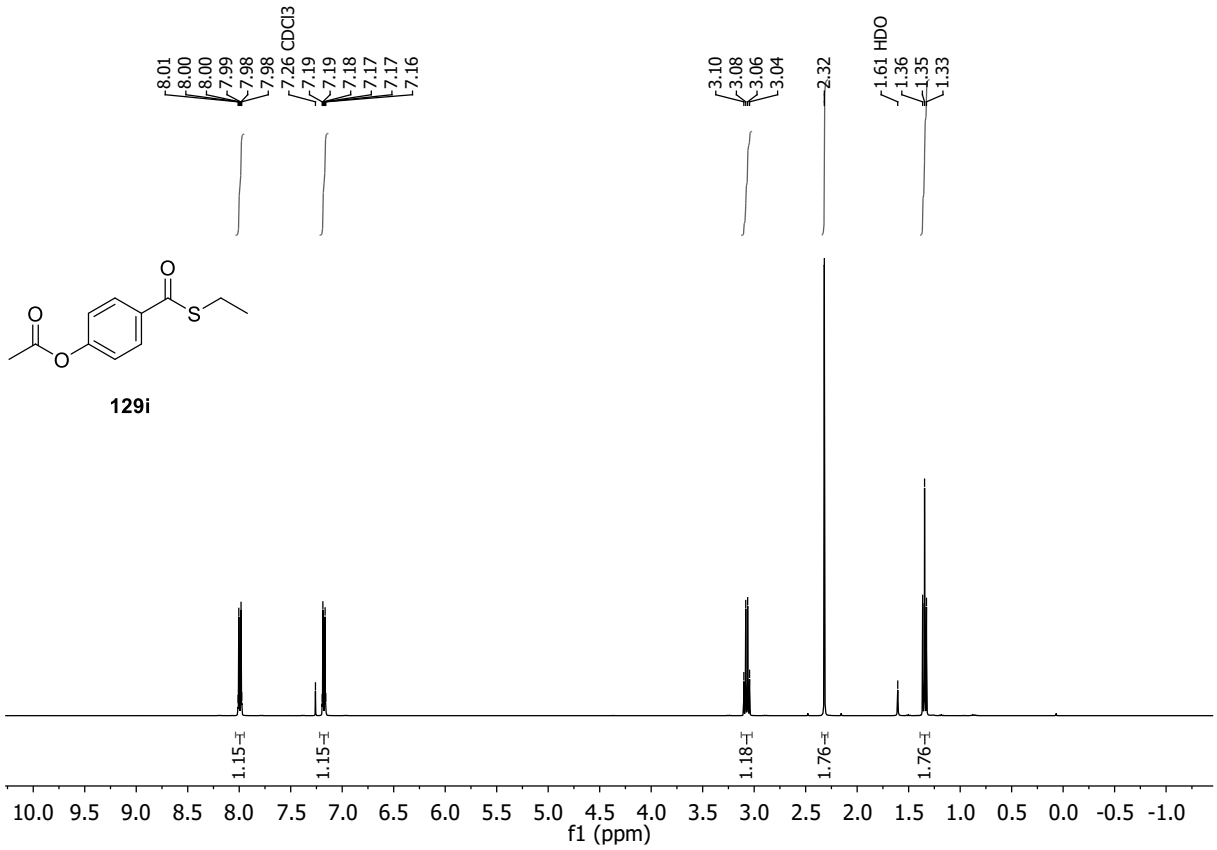
8.01
8.00
8.00
7.99
7.98
7.98
7.26 CDCl3
7.19
7.19
7.18
7.17
7.17
7.16
3.10
3.08
3.06
3.04
2.32
1.61 HDO
1.36
1.35
1.33
O
O
S
O
O
129i
1.15
1.15
1.18
1.76
1.76
10.0 9.5 9.0 8.5 8.0 7.5 7.0 6.5 6.0 5.5 5.0 4.5 4.0 3.5 3.0 2.5 2.0 1.5 1.0 0.5 0.0 -0.5 -1.0
f1 (ppm)

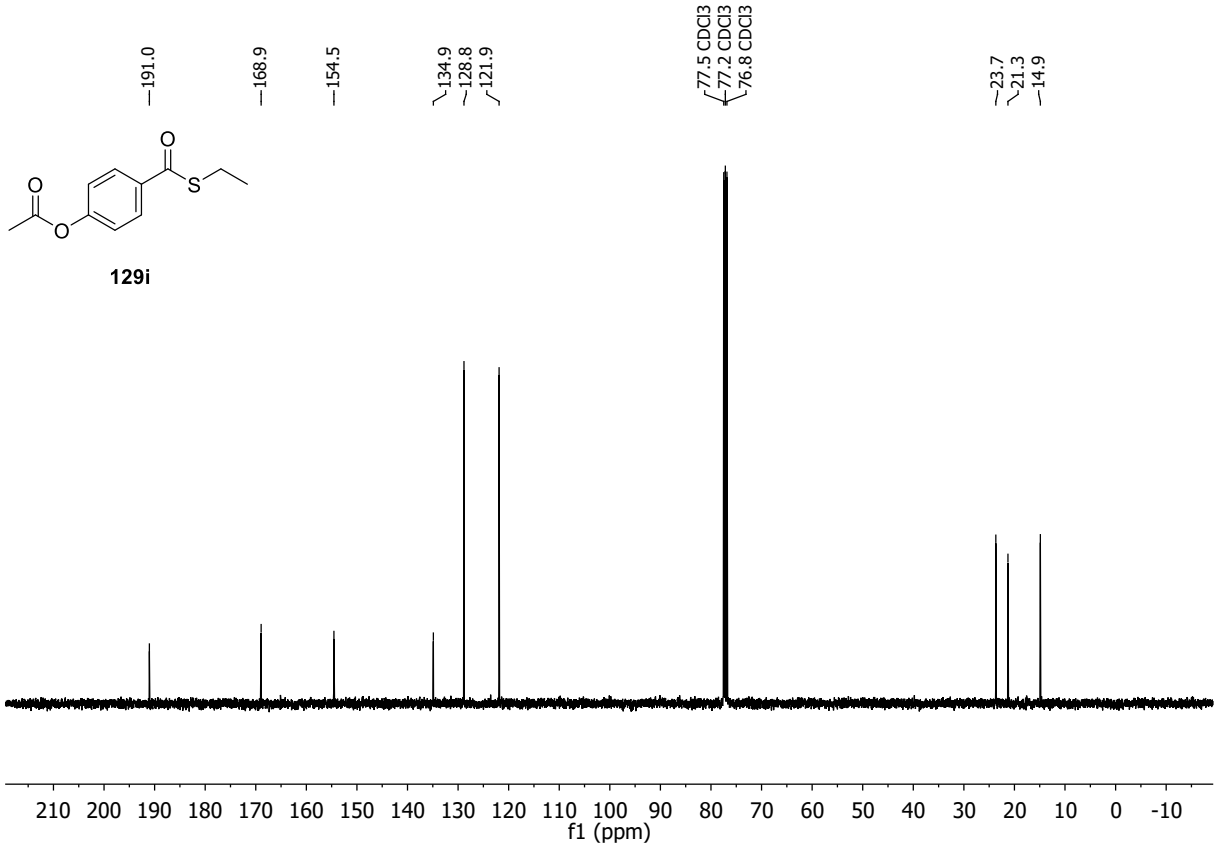
191.0
168.9
154.5
134.9
128.8
121.9
77.5 CDCl3
77.2 CDCl3
76.8 CDCl3
23.7
21.3
14.9
O
O
S
O
O
129i
210 200 190 180 170 160 150 140 130 120 110 100 90 80 70 60 50 40 30 20 10 0 -10
f1 (ppm)

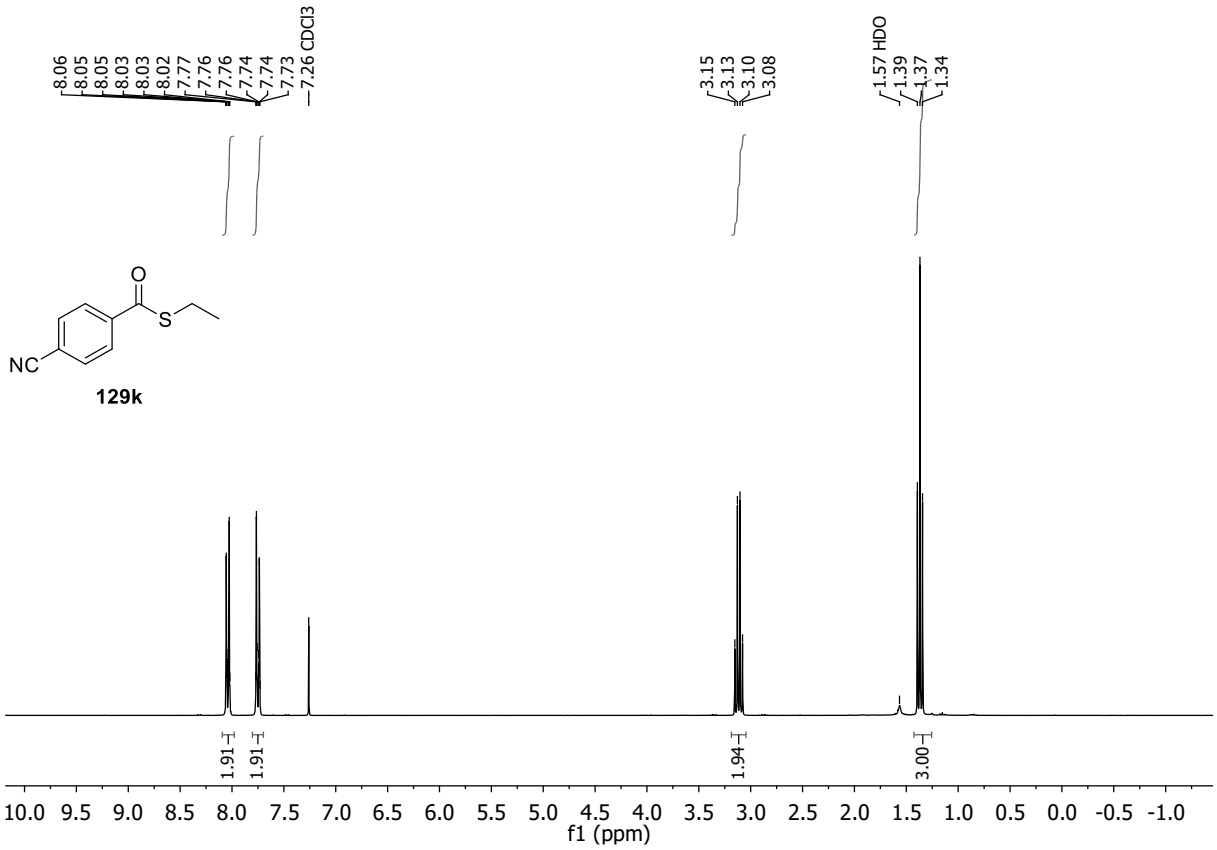
8.06
8.05
8.05
8.03
8.03
8.02
7.77
7.76
7.76
7.74
7.74
7.73
7.26 CDCl3
3.15
3.13
3.10
3.08
1.57 HDO
1.39
1.37
1.34
O
S
NC
129k
1.91
1.91
1.94
3.00
10.0 9.5 9.0 8.5 8.0 7.5 7.0 6.5 6.0 5.5 5.0 4.5 4.0 3.5 3.0 2.5 2.0 1.5 1.0 0.5 0.0 -0.5 -1.0
f1 (ppm)

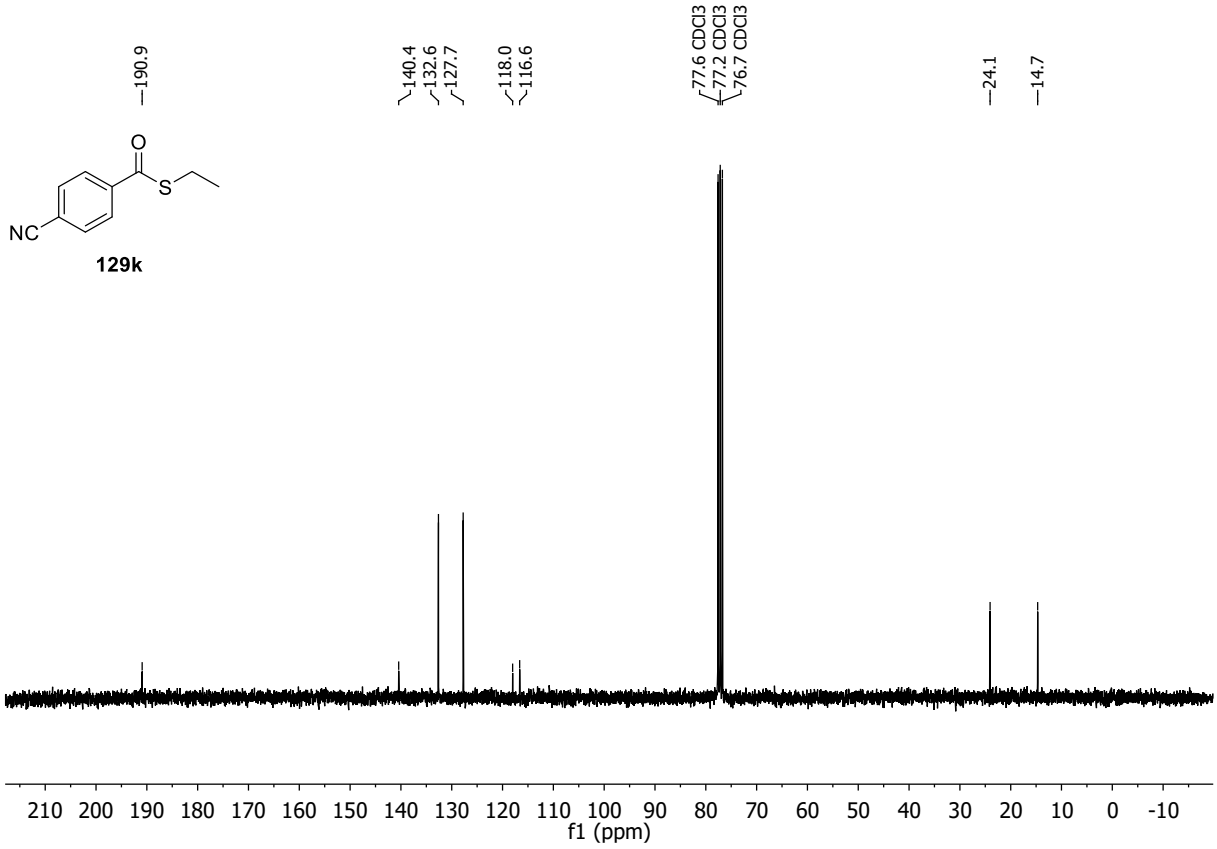
190.9
140.4
132.6
127.7
118.0
116.6
77.6 CDCl3
77.2 CDCl3
76.7 CDCl3
24.1
14.7
O
S
NC
129k
210 200 190 180 170 160 150 140 130 120 110 100 90 80 70 60 50 40 30 20 10 0 -10
f1 (ppm)

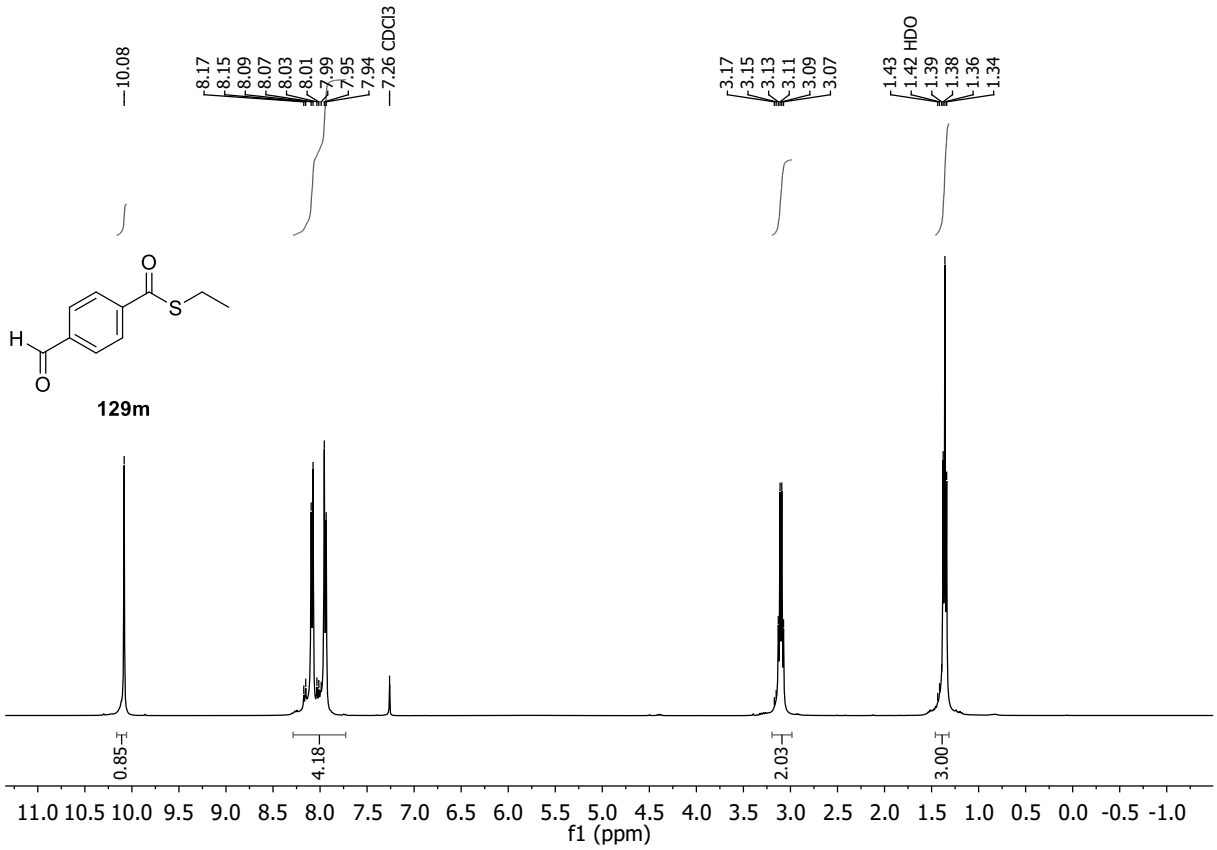
10.08
8.17
8.15
8.09
8.07
8.03
8.01
7.99
7.95
7.94
7.26 CDCl3
3.17
3.15
3.13
3.11
3.09
3.07
1.43
1.42 HDO
1.39
1.38
1.36
1.34
O
S
H
O
129m
0.85
4.18
2.03
3.00
11.0 10.5 10.0 9.5 9.0 8.5 8.0 7.5 7.0 6.5 6.0 5.5 5.0 4.5 4.0 3.5 3.0 2.5 2.0 1.5 1.0 0.5 0.0 -0.5 -1.0
f1 (ppm)

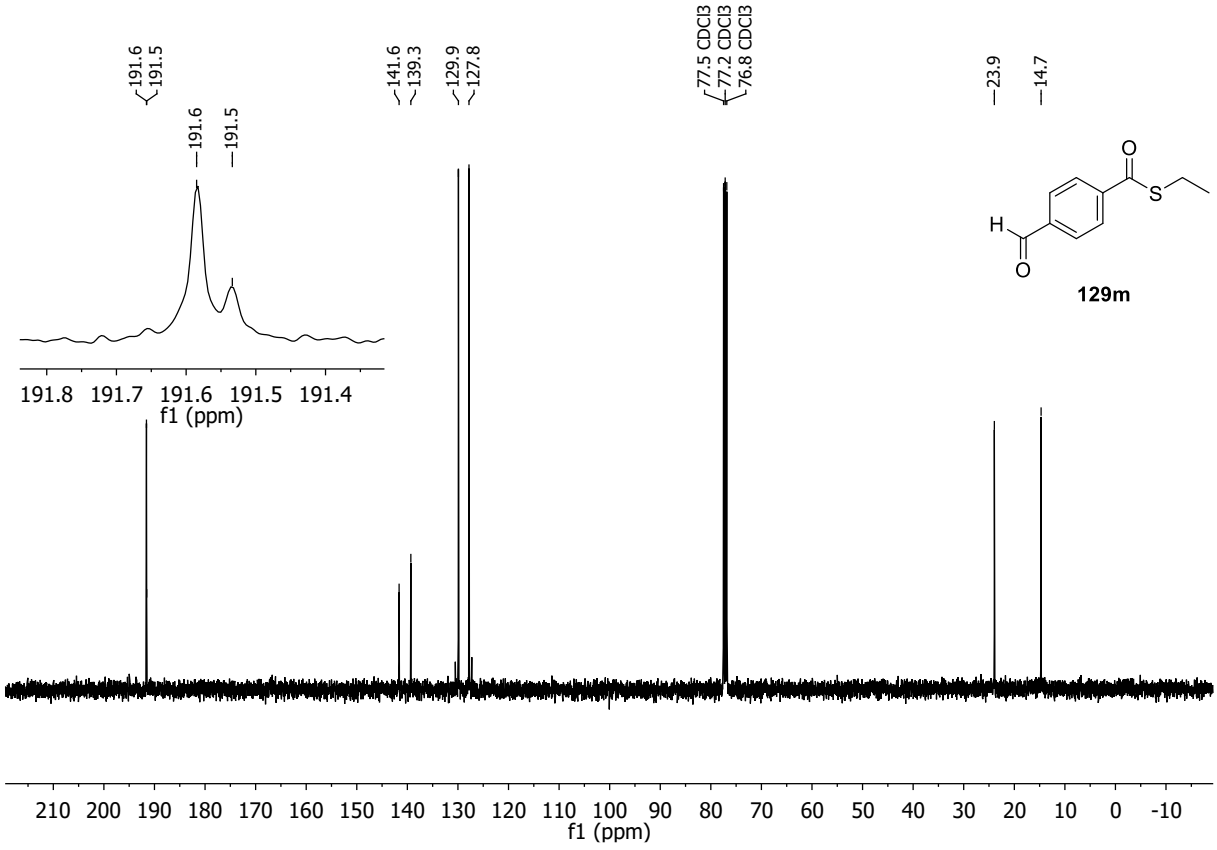
191.6
191.5
141.6
139.3
129.9
127.8
77.5 CDCl3
77.2 CDCl3
76.8 CDCl3
23.9
14.7
191.8 191.7 191.6 191.5 191.4
f1 (ppm)
O
S
H
O
129m
210 200 190 180 170 160 150 140 130 120 110 100 90 80 70 60 50 40 30 20 10 0 -10
f1 (ppm)

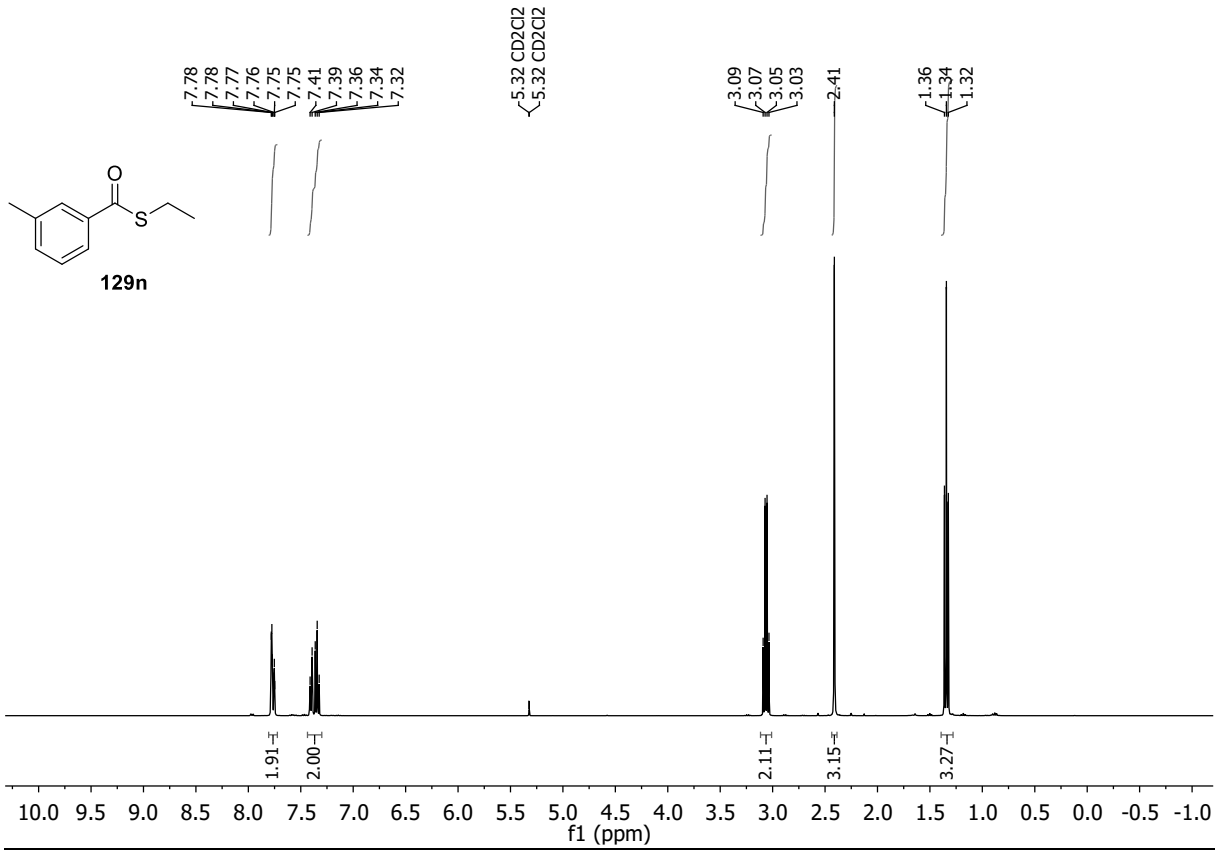
7.78
7.78
7.77
7.76
7.75
7.75
7.41
7.39
7.36
7.34
7.32
5.32 CD2Cl2
5.32 CD2Cl2
3.09
3.07
3.05
3.03
2.41
1.36
1.34
1.32
O
S
129n
1.91
2.00
2.11
3.15
3.27
10.0 9.5 9.0 8.5 8.0 7.5 7.0 6.5 6.0 5.5 5.0 4.5 4.0 3.5 3.0 2.5 2.0 1.5 1.0 0.5 0.0 -0.5 -1.0
f1 (ppm)

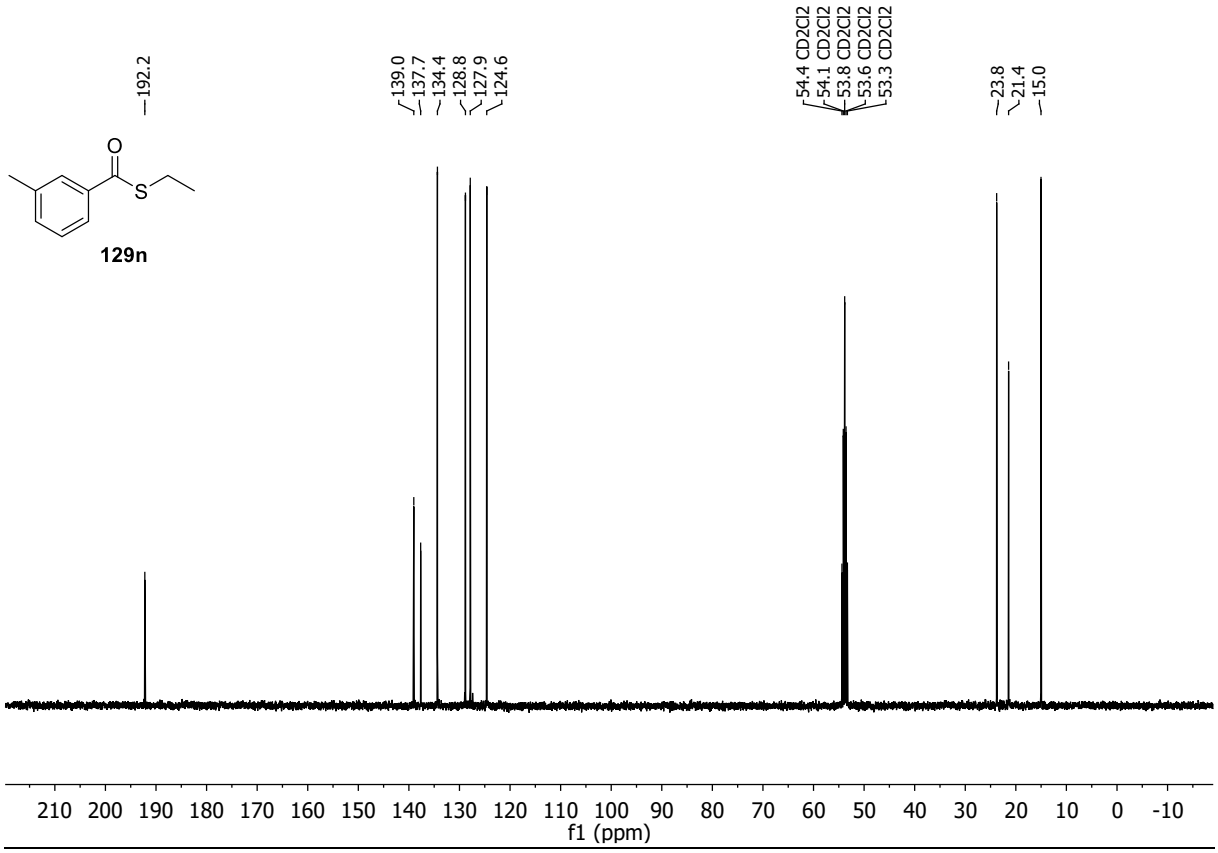
192.2
139.0
137.7
134.4
128.8
127.9
124.6
54.4 CD2Cl2
54.1 CD2Cl2
53.8 CD2Cl2
53.6 CD2Cl2
53.3 CD2Cl2
23.8
21.4
15.0
O
S
129n
210 200 190 180 170 160 150 140 130 120 110 100 90 80 70 60 50 40 30 20 10 0 -10
f1 (ppm)

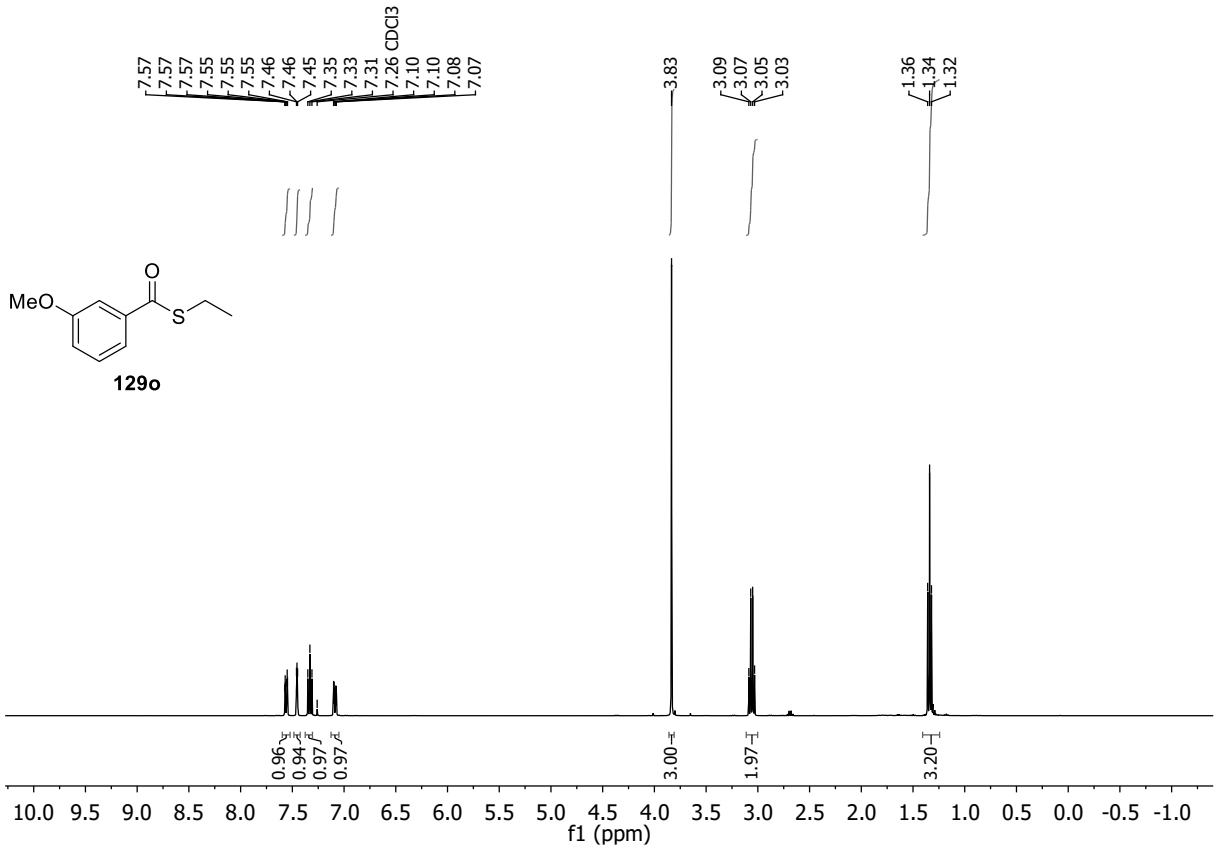
7.57
7.57
7.57
7.55
7.55
7.55
7.46
7.46
7.45
7.35
7.33
7.31
7.26 CDCl3
7.10
7.08
7.07
3.83
3.09
3.07
3.05
3.03
1.36
1.34
1.32
MeO
O
S
129o
0.96
0.94
0.97
0.97
3.00
1.97
3.20
10.0 9.5 9.0 8.5 8.0 7.5 7.0 6.5 6.0 5.5 5.0 4.5 4.0 3.5 3.0 2.5 2.0 1.5 1.0 0.5 0.0 -0.5 -1.0
f1 (ppm)

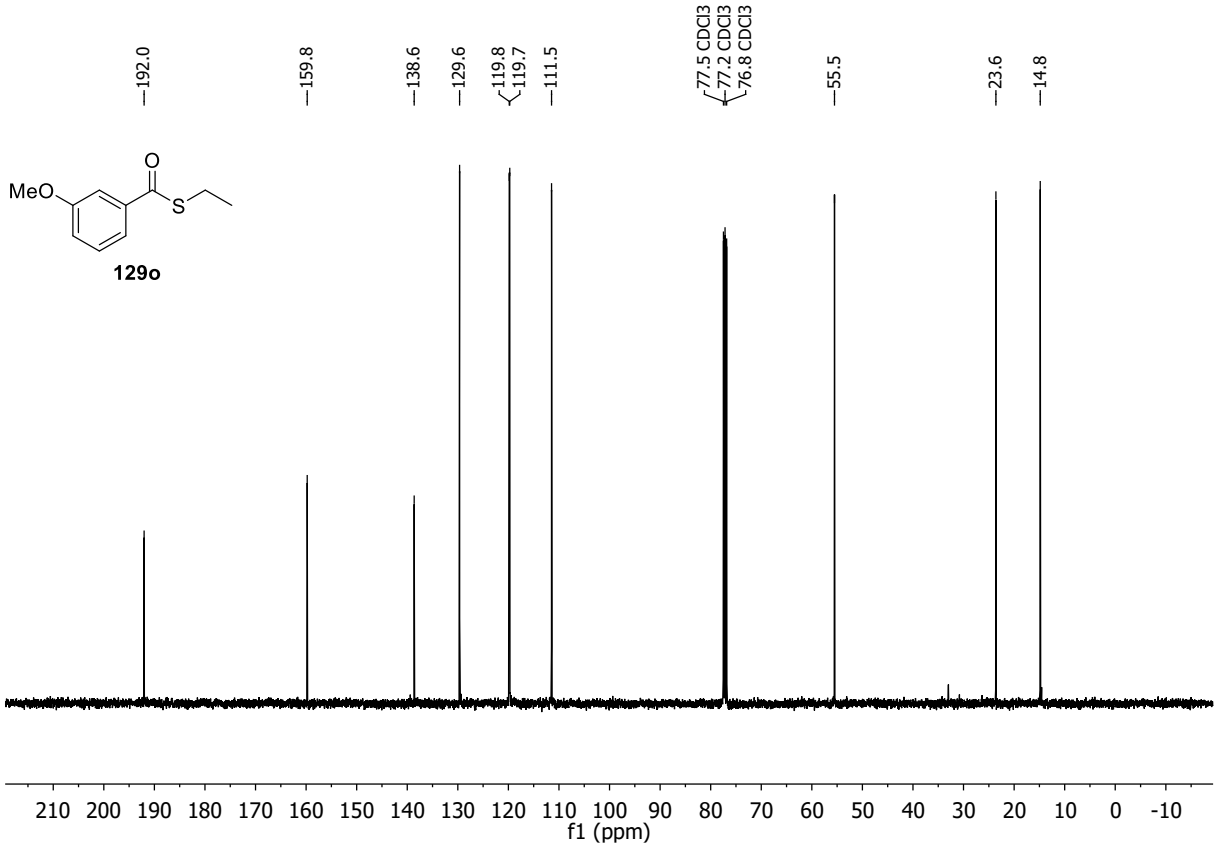
192.0
159.8
138.6
129.6
119.8
119.7
111.5
77.5 CDCl3
77.2 CDCl3
76.8 CDCl3
55.5
23.6
14.8
MeO
O
S
129o
210 200 190 180 170 160 150 140 130 120 110 100 90 80 70 60 50 40 30 20 10 0 -10
f1 (ppm)

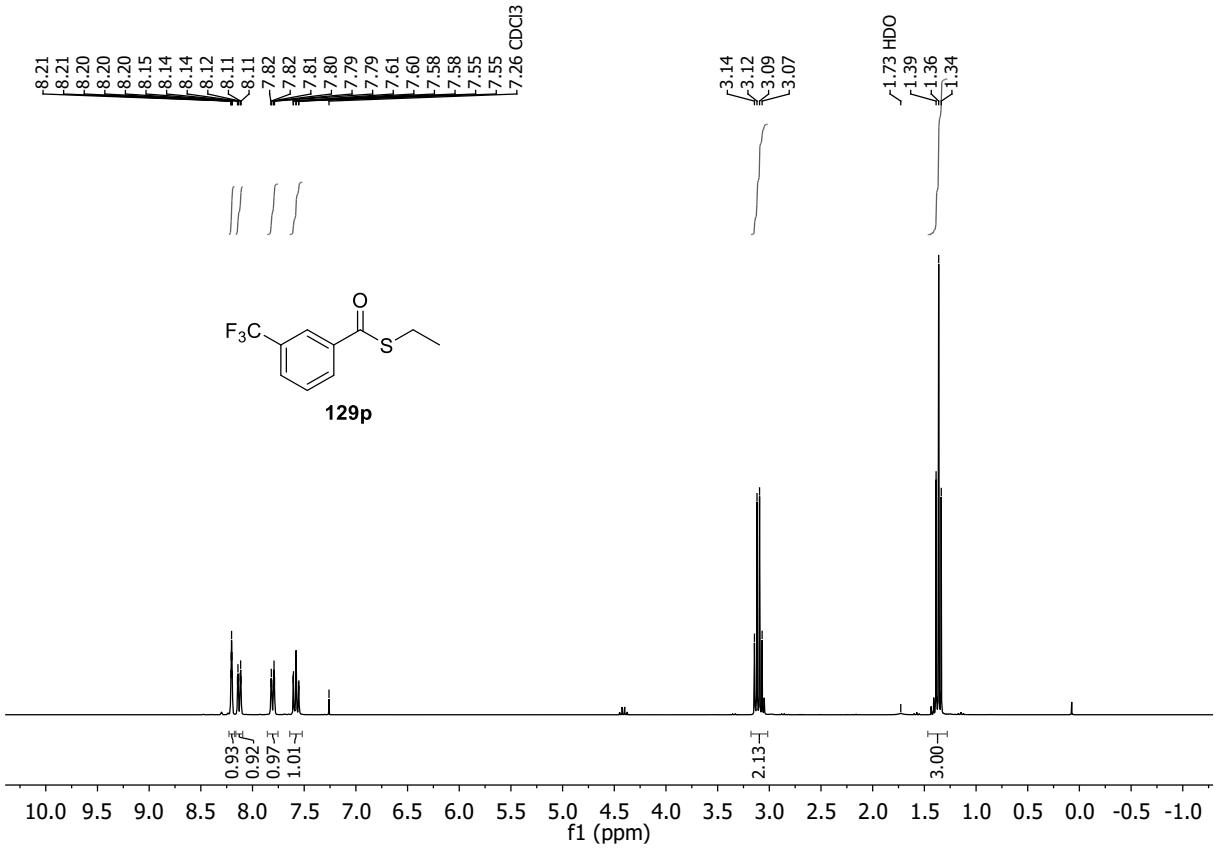
8.21
8.21
8.20
8.20
8.20
8.15
8.14
8.14
8.12
8.11
8.11
7.82
7.82
7.81
7.80
7.79
7.79
7.61
7.60
7.58
7.58
7.55
7.55
7.26 CDCl3
3.14
3.12
3.09
3.07
1.73 HDO
1.39
1.36
1.34
F3C
O
S
129p
0.93
0.92
0.97
1.01
2.13
3.00
10.0 9.5 9.0 8.5 8.0 7.5 7.0 6.5 6.0 5.5 5.0 4.5 4.0 3.5 3.0 2.5 2.0 1.5 1.0 0.5 0.0 -0.5 -1.0
f1 (ppm)

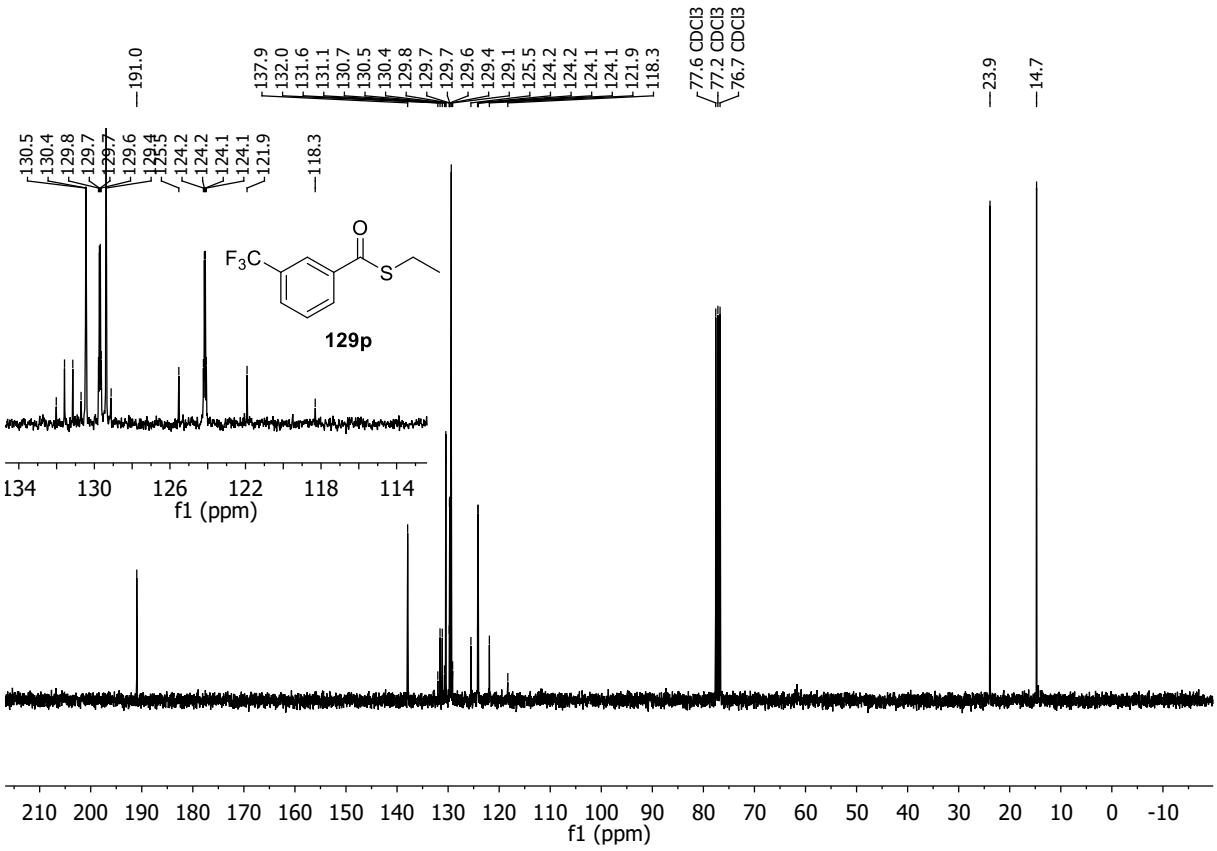
191.0
137.9
132.0
131.6
131.1
130.7
130.5
130.4
129.8
129.7
129.7
129.6
129.4
129.1
125.5
124.2
124.2
124.1
124.1
121.9
118.3
77.6 CDCl3
77.2 CDCl3
76.7 CDCl3
23.9
14.7
F3C
O
S
129p
134 130 126 122 118 114
f1 (ppm)
210 200 190 180 170 160 150 140 130 120 110 100 90 80 70 60 50 40 30 20 10 0 -10
f1 (ppm)


O
F3C
S
129p
-62.9
0 -5 -10 -15 -20 -25 -30 -35 -40 -45 -50 -55 -60 -65 -70 -75 -80 -85 -90 -95 -100
f1 (ppm)

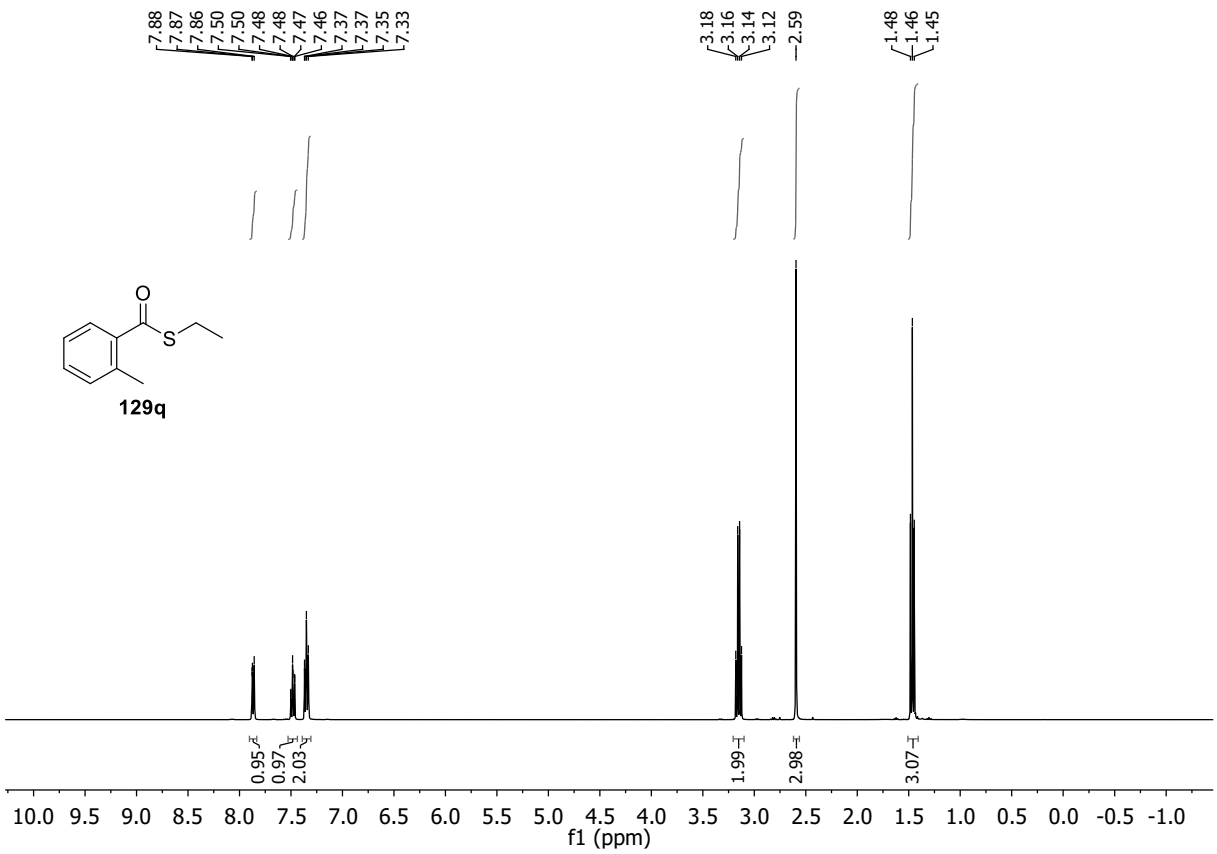
7.88
7.87
7.86
7.50
7.50
7.48
7.48
7.47
7.46
7.37
7.37
7.35
7.33
3.18
3.16
3.14
3.12
2.59
1.48
1.46
1.45
O
S
129q
0.95
0.97
2.03
1.99
2.98
3.07
10.0 9.5 9.0 8.5 8.0 7.5 7.0 6.5 6.0 5.5 5.0 4.5 4.0 3.5 3.0 2.5 2.0 1.5 1.0 0.5 0.0 -0.5 -1.0
f1 (ppm)

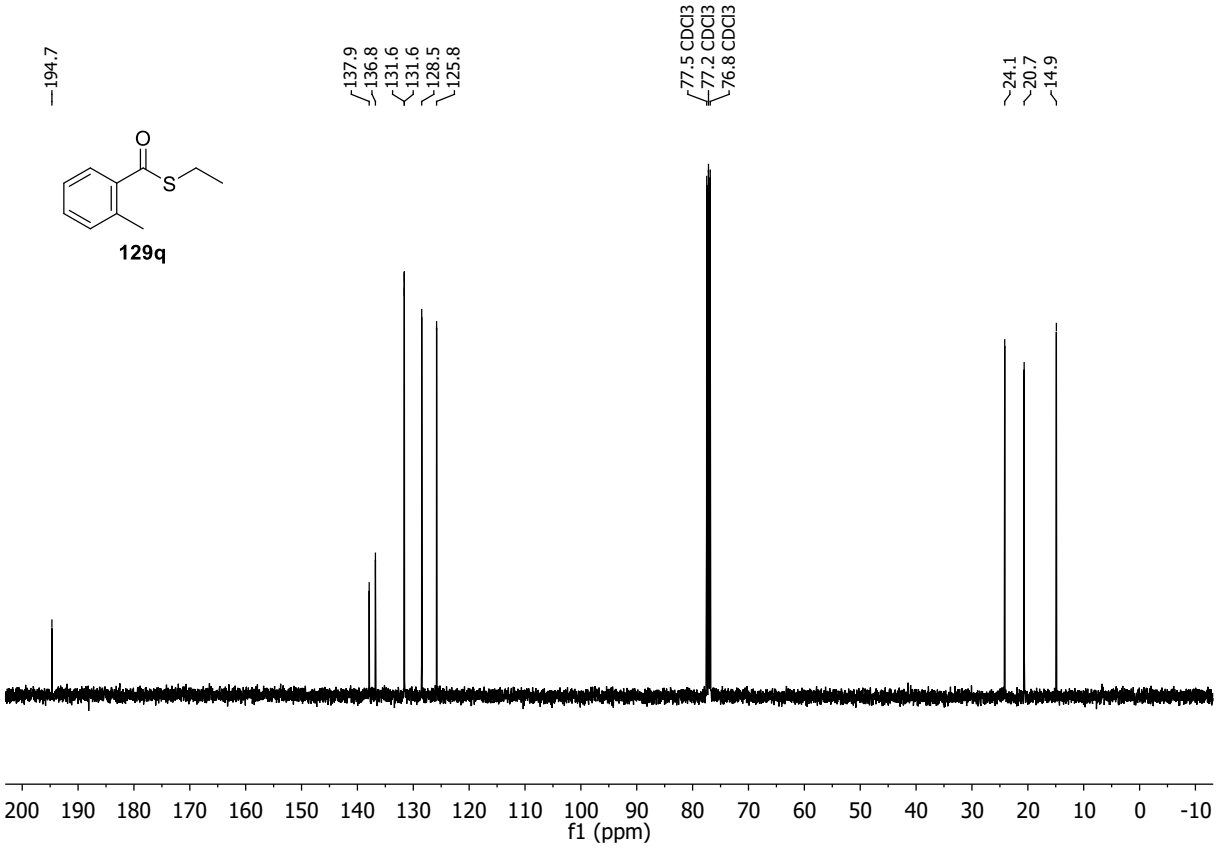
194.7
137.9
136.8
131.6
131.6
128.5
125.8
77.5 CDCl3
77.2 CDCl3
76.8 CDCl3
24.1
20.7
14.9
O
S
129q
200 190 180 170 160 150 140 130 120 110 100 90 80 70 60 50 40 30 20 10 0 -10
f1 (ppm)

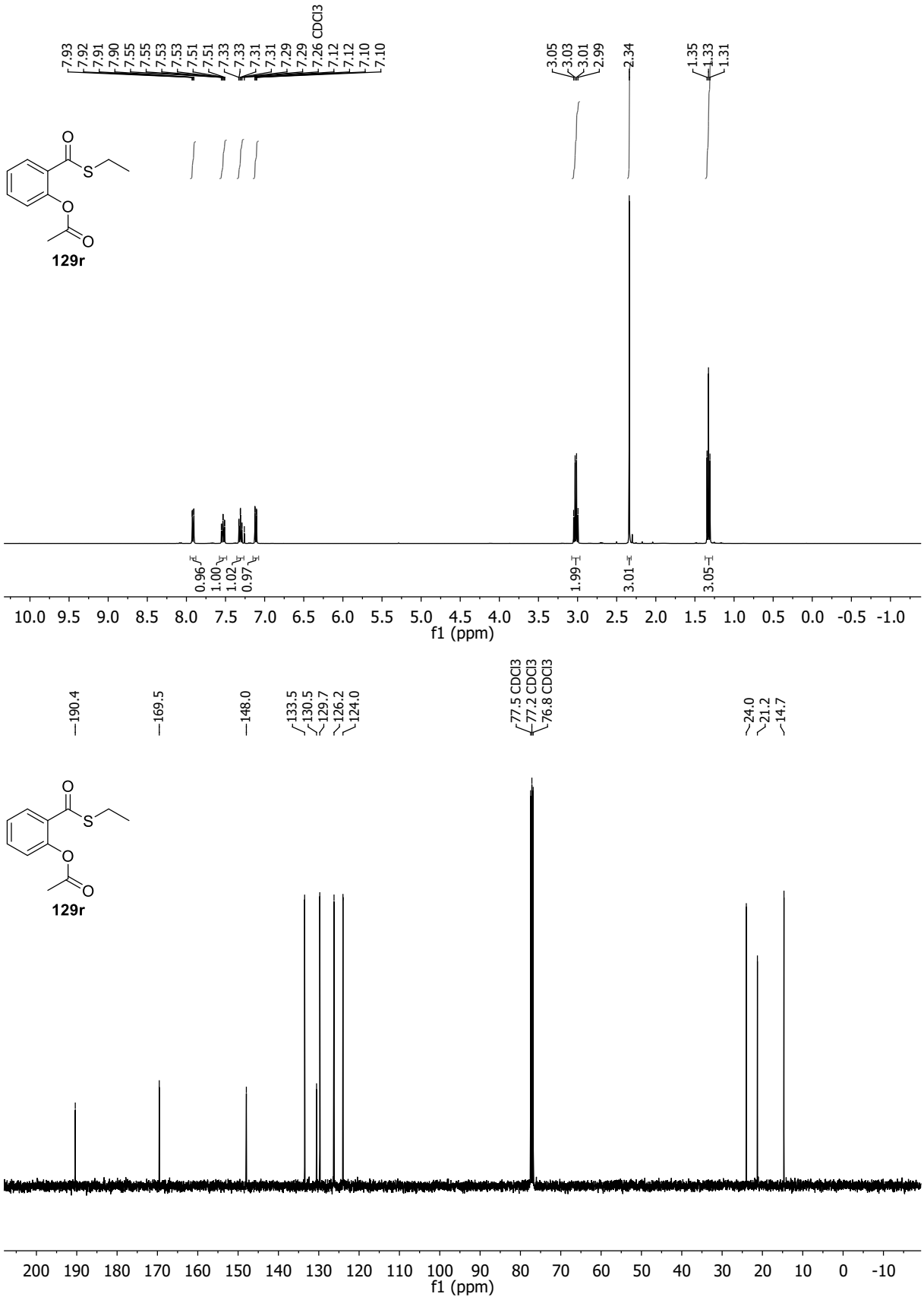
7.93
7.92
7.91
7.90
7.55
7.55
7.53
7.53
7.51
7.51
7.33
7.33
7.31
7.31
7.29
7.29
7.26 CDCl3
7.12
7.12
7.10
7.10
3.05
3.03
3.01
2.99
2.34
1.35
1.33
1.31
O
S
O
O
129r
0.96
1.00
1.02
0.97
1.99
3.01
3.05
10.0 9.5 9.0 8.5 8.0 7.5 7.0 6.5 6.0 5.5 5.0 4.5 4.0 3.5 3.0 2.5 2.0 1.5 1.0 0.5 0.0 -0.5 -1.0
f1 (ppm)
190.4
169.5
148.0
133.5
130.5
129.7
126.2
124.0
77.5 CDCl3
77.2 CDCl3
76.8 CDCl3
24.0
21.2
14.7
O
S
O
O
129r
200 190 180 170 160 150 140 130 120 110 100 90 80 70 60 50 40 30 20 10 0 -10
f1 (ppm)

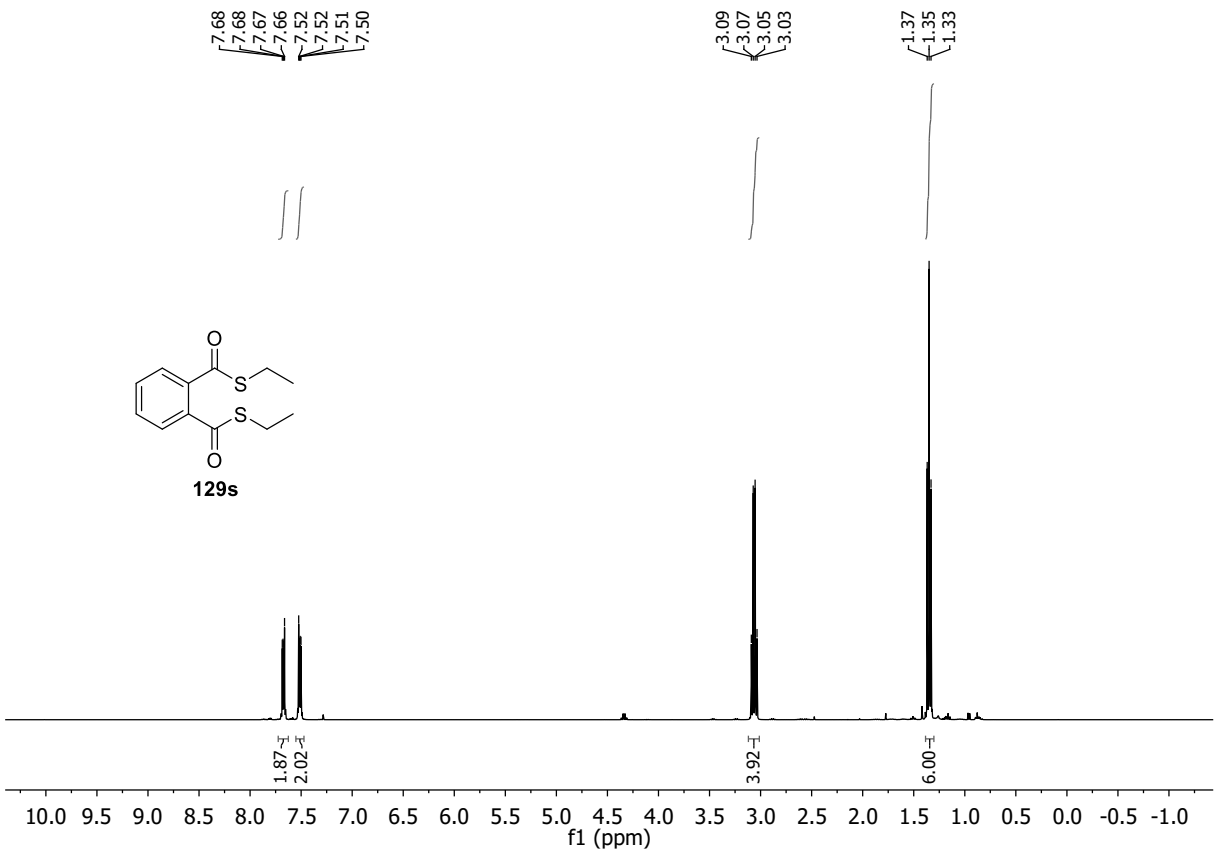
7.68
7.68
7.67
7.66
7.52
7.52
7.51
7.50
3.09
3.07
3.05
3.03
1.37
1.35
1.33
O
S
S
O
129s
1.87
2.02
3.92
6.00
10.0 9.5 9.0 8.5 8.0 7.5 7.0 6.5 6.0 5.5 5.0 4.5 4.0 3.5 3.0 2.5 2.0 1.5 1.0 0.5 0.0 -0.5 -1.0
f1 (ppm)

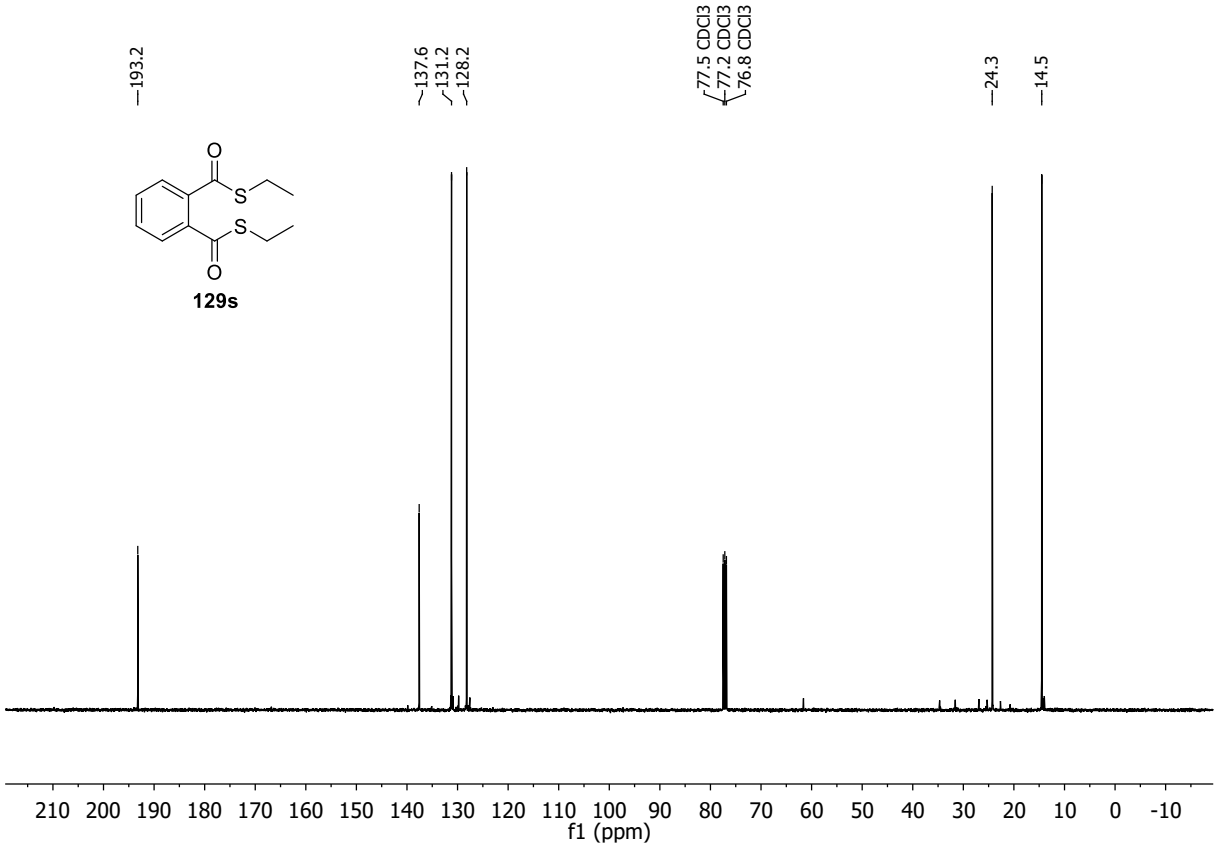
193.2
137.6
131.2
128.2
77.5 CDCl3
77.2 CDCl3
76.8 CDCl3
24.3
14.5
O
S
S
O
129s
210 200 190 180 170 160 150 140 130 120 110 100 90 80 70 60 50 40 30 20 10 0 -10
f1 (ppm)

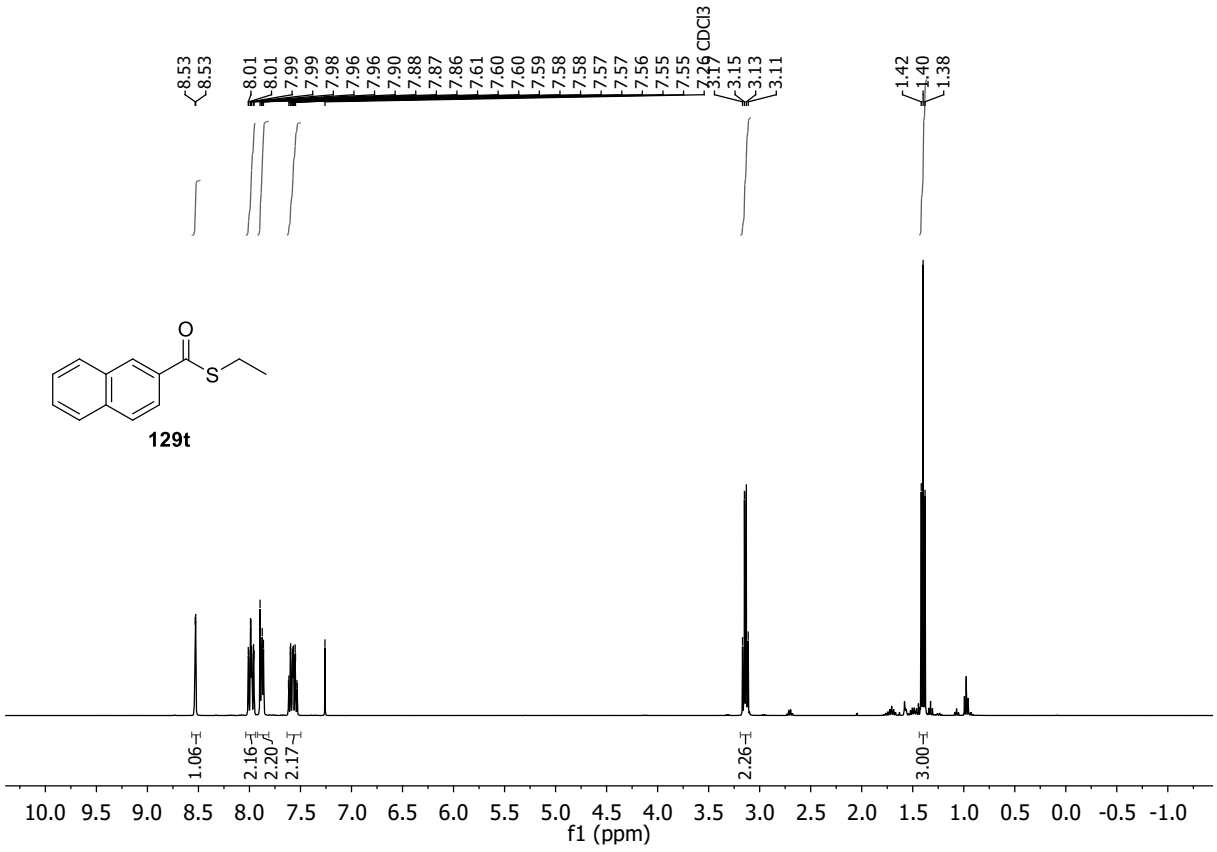
8.53
8.53
8.01
8.01
7.99
7.99
7.98
7.96
7.96
7.90
7.88
7.87
7.86
7.61
7.60
7.60
7.59
7.58
7.58
7.57
7.57
7.56
7.55
7.55
7.26 CDCl3
3.17
3.15
3.13
3.11
1.42
1.40
1.38
O
S
129t
1.06
2.16
2.20
2.17
2.26
3.00
10.0 9.5 9.0 8.5 8.0 7.5 7.0 6.5 6.0 5.5 5.0 4.5 4.0 3.5 3.0 2.5 2.0 1.5 1.0 0.5 0.0 -0.5 -1.0
f1 (ppm)

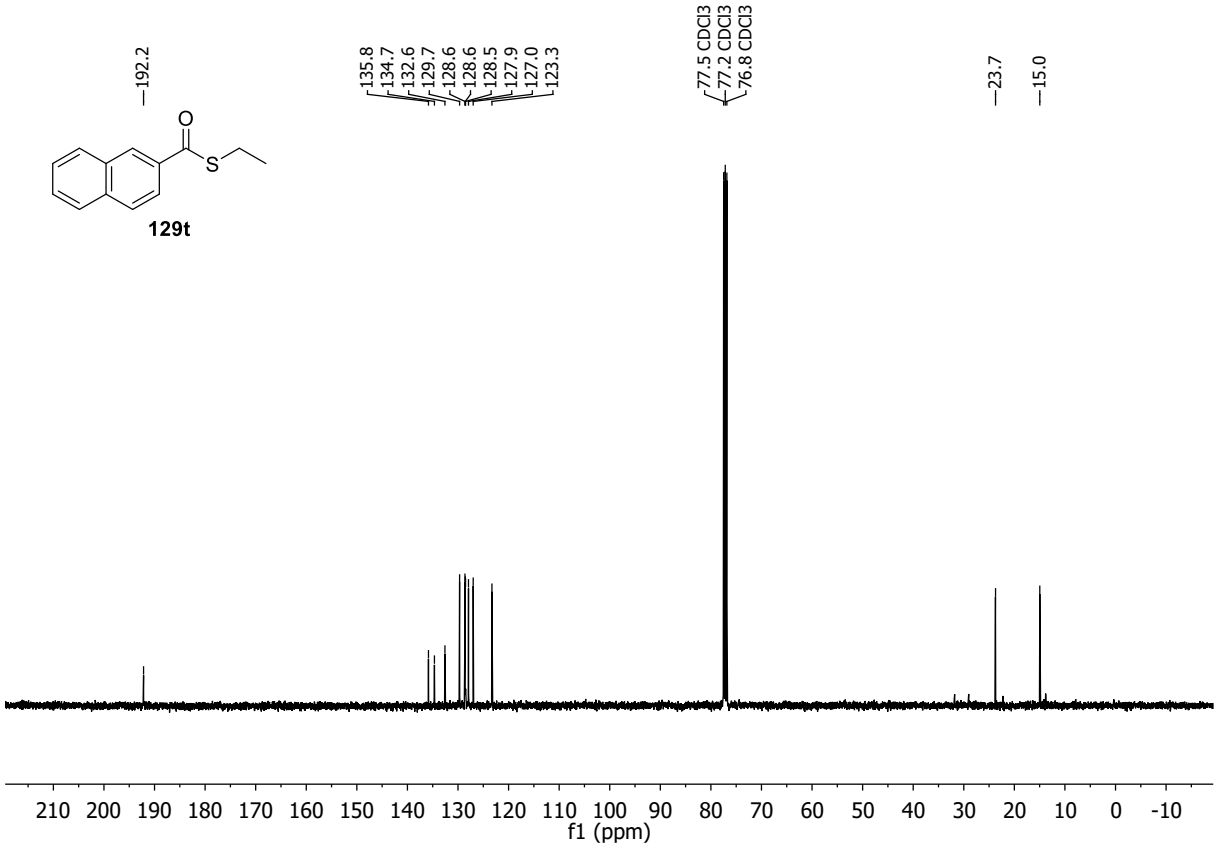
192.2
135.8
134.7
132.6
129.7
128.6
128.6
128.5
127.9
127.0
123.3
77.5 CDCl3
77.2 CDCl3
76.8 CDCl3
23.7
15.0
O
S
129t
210 200 190 180 170 160 150 140 130 120 110 100 90 80 70 60 50 40 30 20 10 0 -10
f1 (ppm)

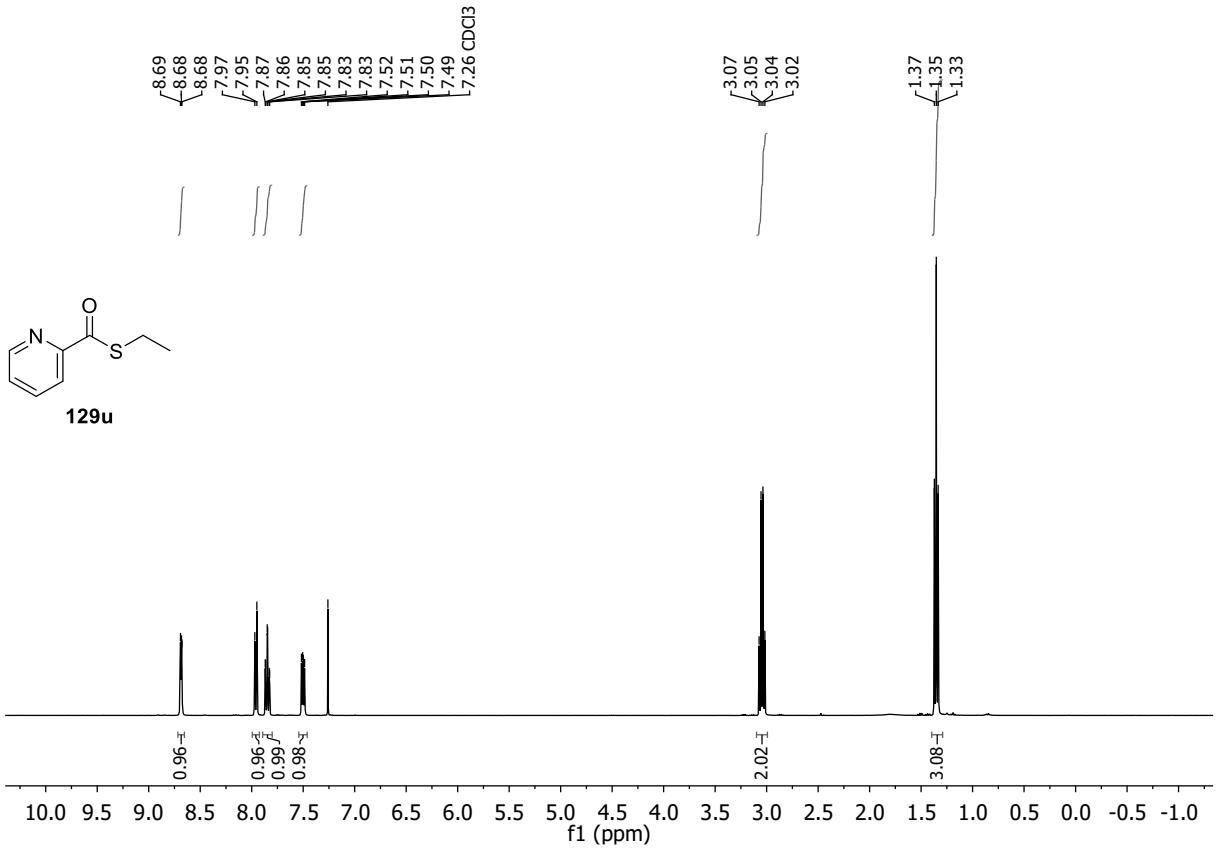
8.69
8.68
8.68
7.97
7.95
7.87
7.86
7.85
7.85
7.83
7.83
7.52
7.51
7.50
7.49
7.26 CDCl3
3.07
3.05
3.04
3.02
1.37
1.35
1.33
O
N
S
129u
0.96
0.96
0.99
0.98
2.02
3.08
10.0 9.5 9.0 8.5 8.0 7.5 7.0 6.5 6.0 5.5 5.0 4.5 4.0 3.5 3.0 2.5 2.0 1.5 1.0 0.5 0.0 -0.5 -1.0
f1 (ppm)

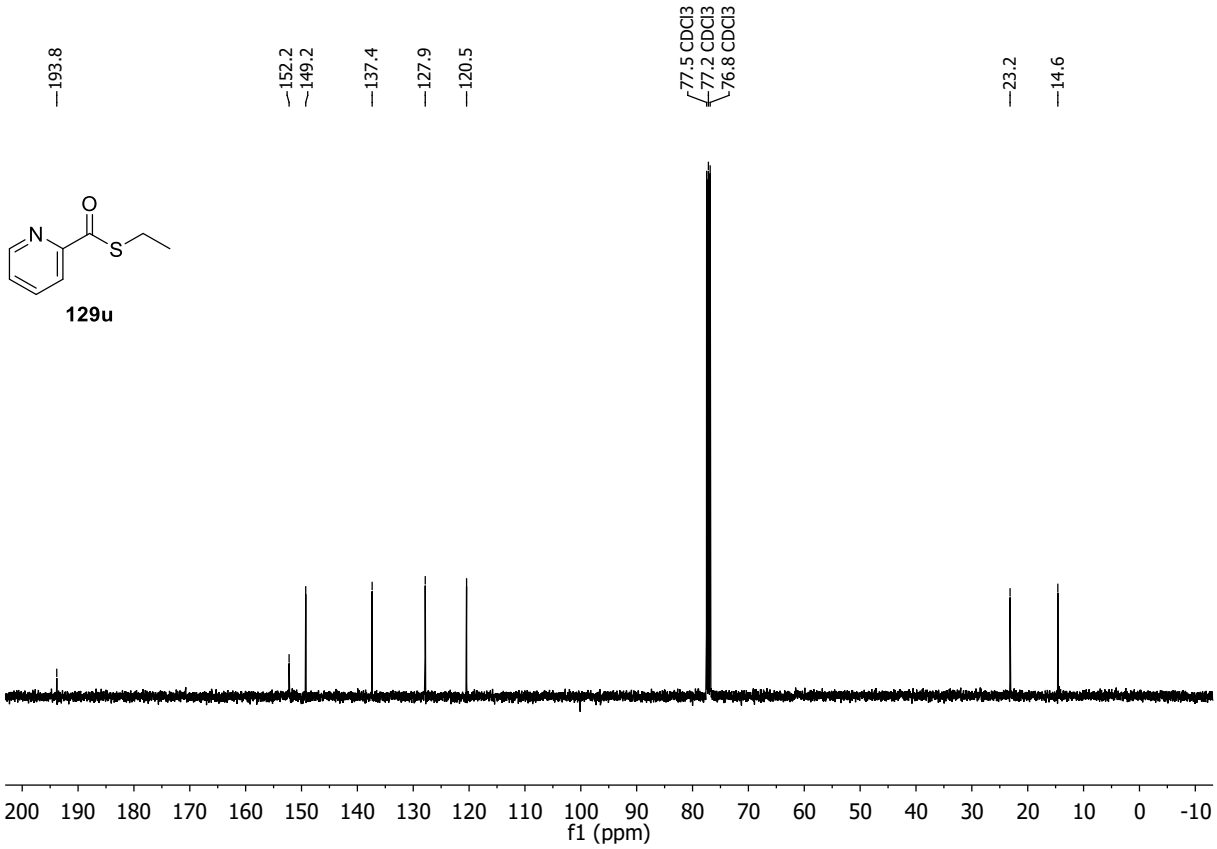
193.8
152.2
149.2
137.4
127.9
120.5
77.5 CDCl3
77.2 CDCl3
76.8 CDCl3
23.2
14.6
O
N
S
129u
200 190 180 170 160 150 140 130 120 110 100 90 80 70 60 50 40 30 20 10 0 -10
f1 (ppm)

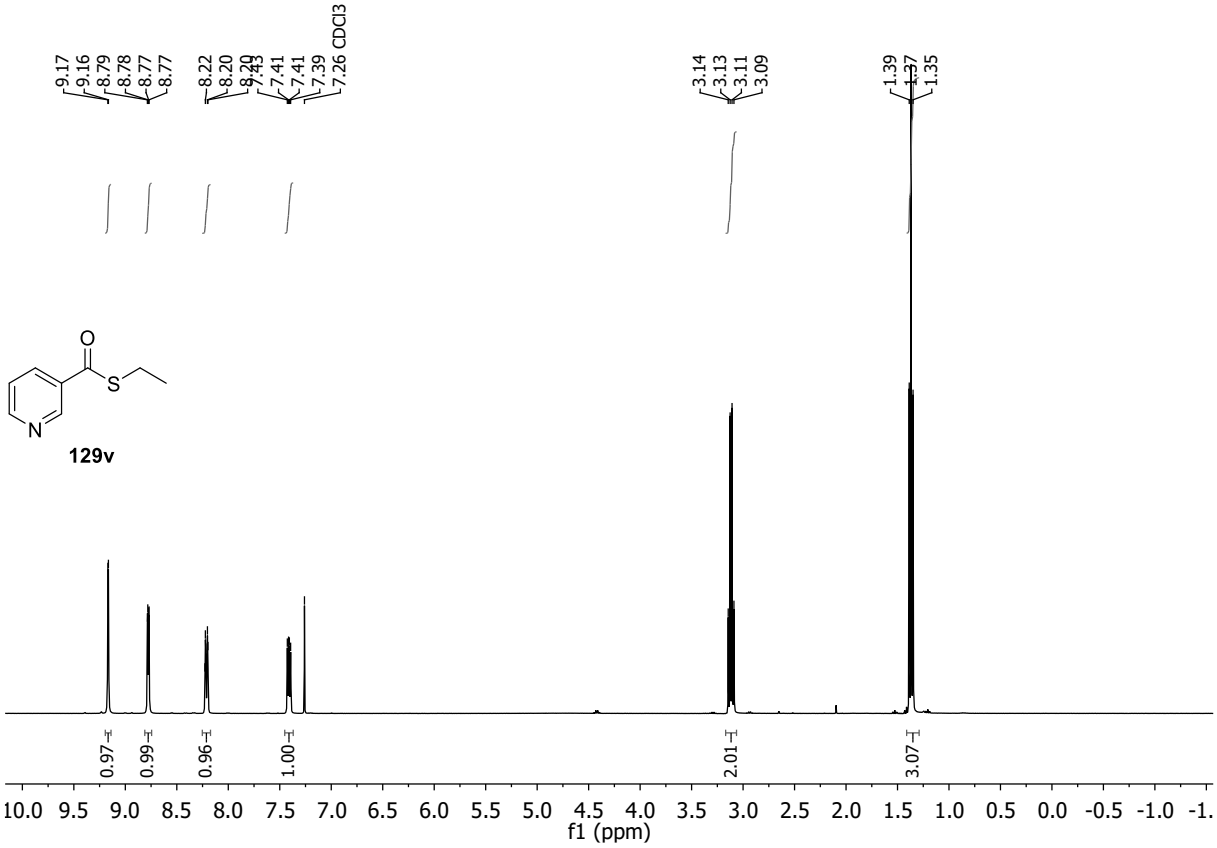
9.17
9.16
8.79
8.78
8.77
8.77
8.22
8.20
7.41
7.41
7.39
7.26 CDCl3
3.14
3.13
3.11
3.09
1.39
1.37
1.35
O
S
N
129v
0.97
0.99
0.96
1.00
2.01
3.07
10.0 9.5 9.0 8.5 8.0 7.5 7.0 6.5 6.0 5.5 5.0 4.5 4.0 3.5 3.0 2.5 2.0 1.5 1.0 0.5 0.0 -0.5 -1.0 -1.
f1 (ppm)

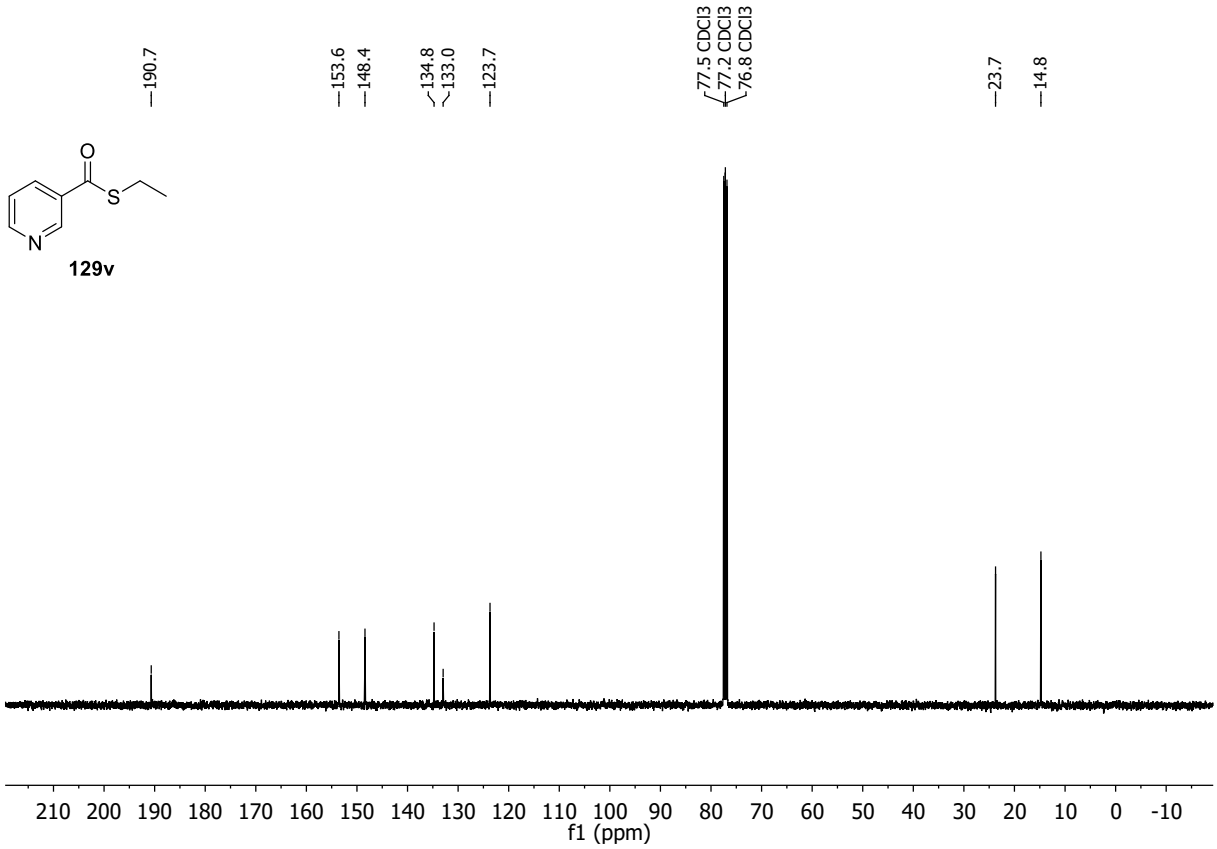
190.7
153.6
148.4
134.8
133.0
123.7
77.5 CDCl3
77.2 CDCl3
76.8 CDCl3
23.7
14.8
O
S
N
129v
210 200 190 180 170 160 150 140 130 120 110 100 90 80 70 60 50 40 30 20 10 0 -10
f1 (ppm)

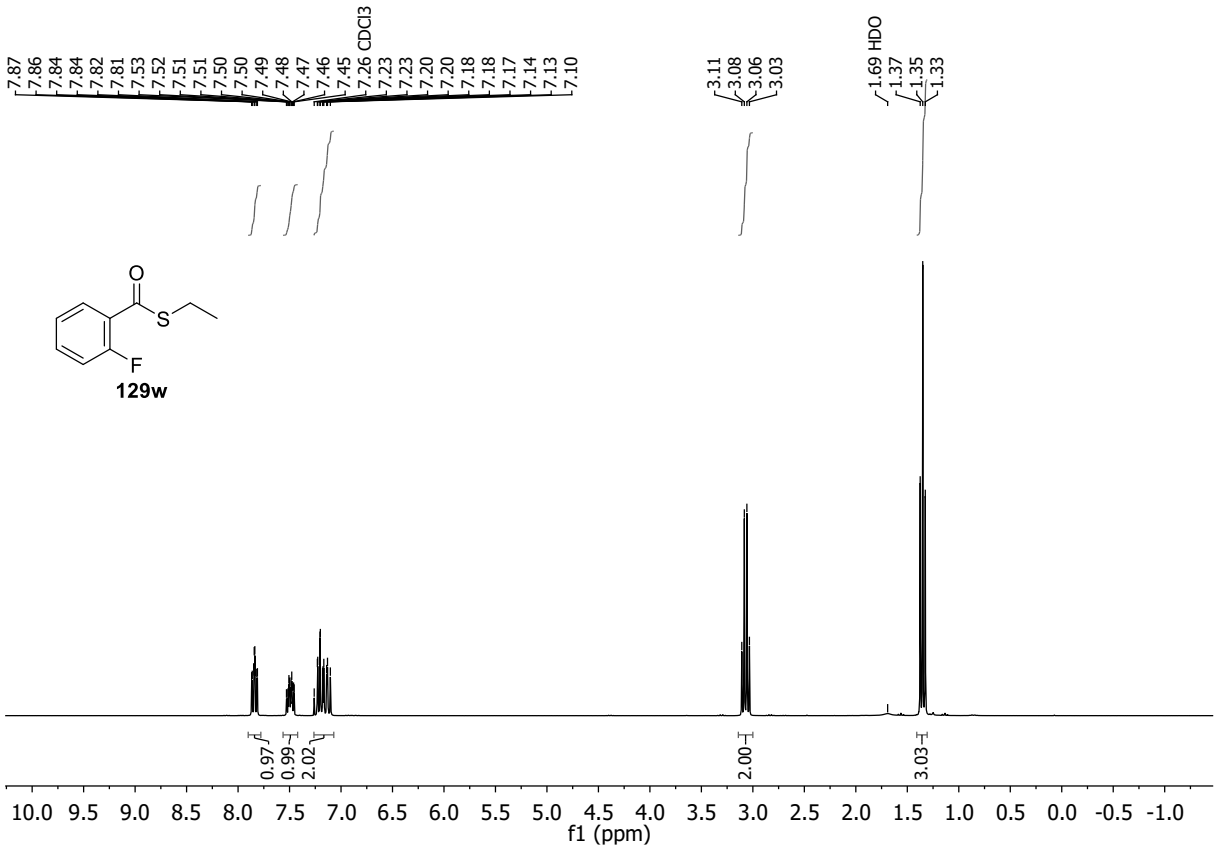
7.87
7.86
7.84
7.84
7.82
7.81
7.53
7.52
7.51
7.51
7.50
7.50
7.49
7.48
7.47
7.46
7.45
7.26 CDCl3
7.23
7.23
7.20
7.20
7.18
7.18
7.17
7.14
7.13
7.10
3.11
3.08
3.06
3.03
1.69 HDO
1.37
1.35
1.33
O
S
F
129w
0.97
0.99
2.02
2.00
3.03
10.0 9.5 9.0 8.5 8.0 7.5 7.0 6.5 6.0 5.5 5.0 4.5 4.0 3.5 3.0 2.5 2.0 1.5 1.0 0.5 0.0 -0.5 -1.0
f1 (ppm)

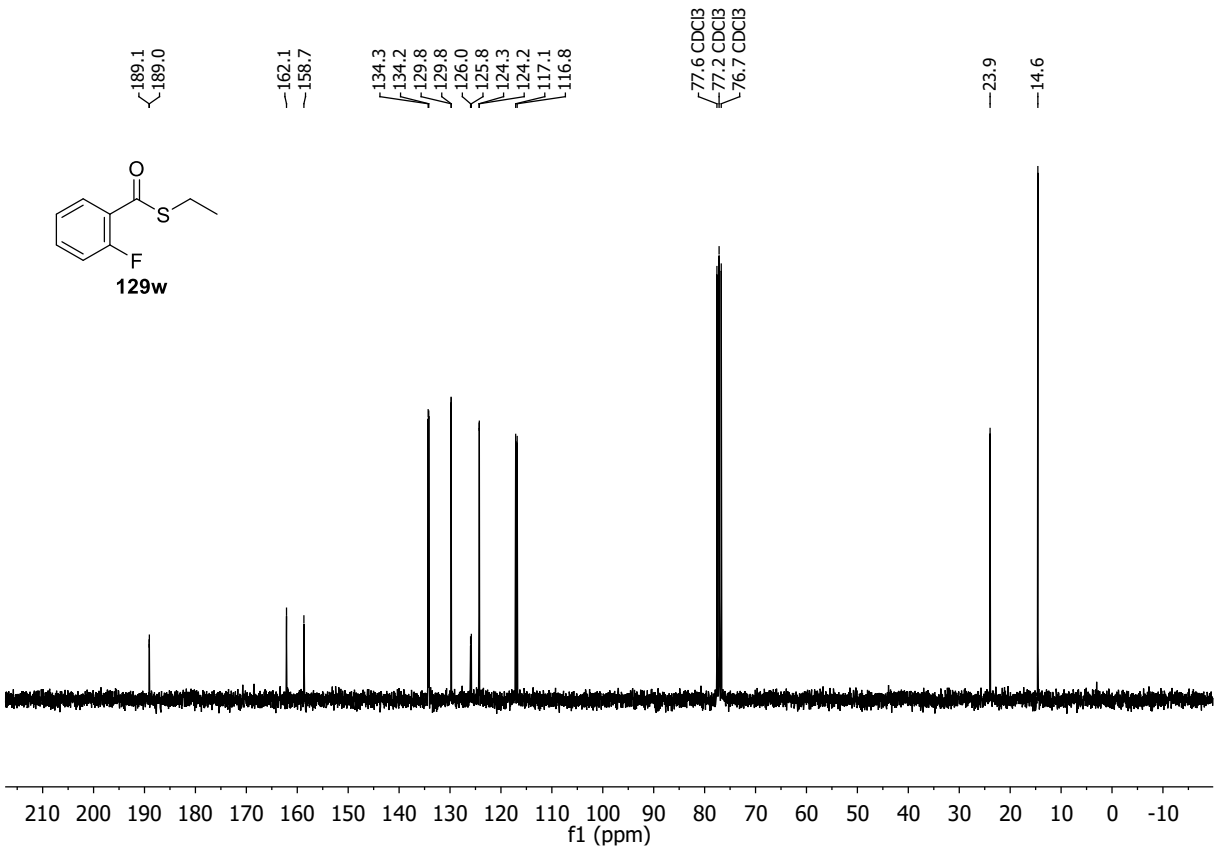
189.1
189.0
162.1
158.7
134.3
134.2
129.8
129.8
126.0
125.8
124.3
124.2
117.1
116.8
77.6 CDCl3
77.2 CDCl3
76.7 CDCl3
23.9
14.6
O
S
F
129w
210 200 190 180 170 160 150 140 130 120 110 100 90 80 70 60 50 40 30 20 10 0 -10
f1 (ppm)

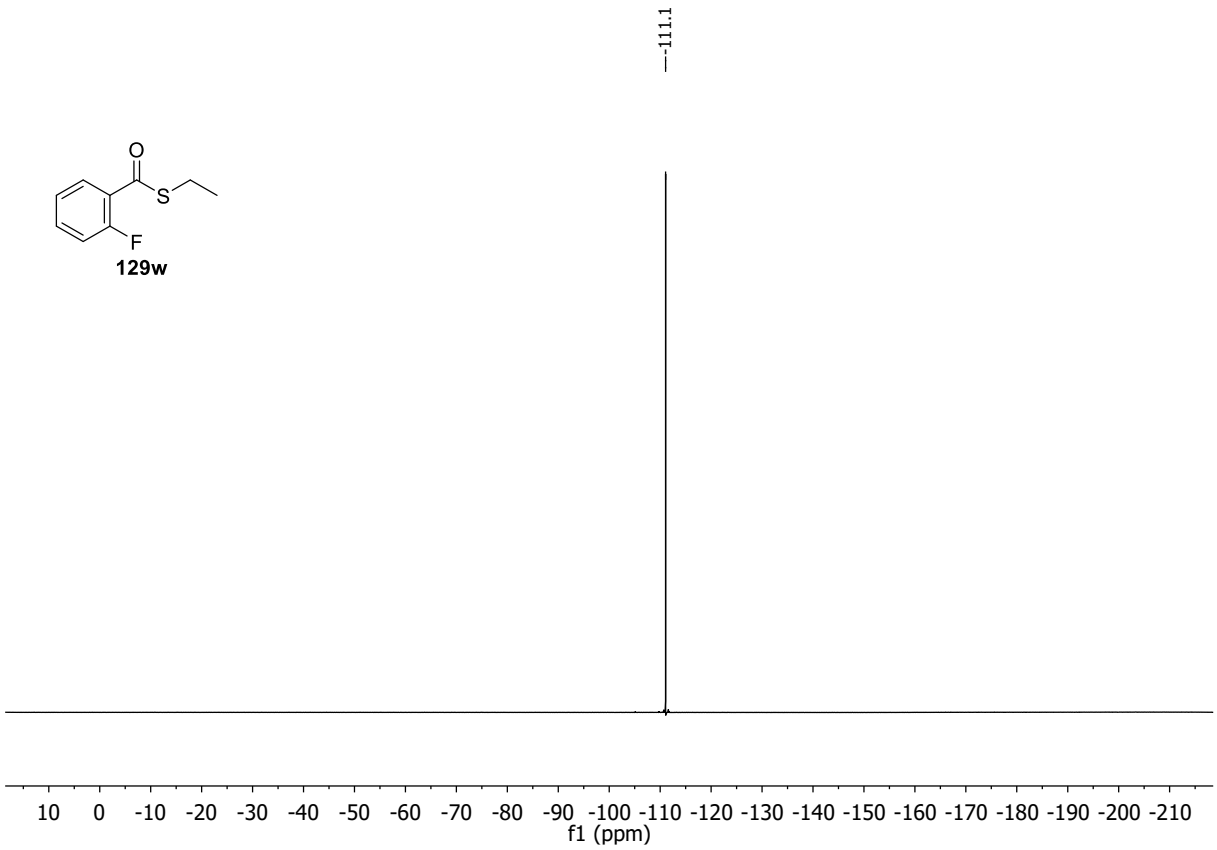
-111.1
O
S
F
129w
10 0 -10 -20 -30 -40 -50 -60 -70 -80 -90 -100 -110 -120 -130 -140 -150 -160 -170 -180 -190 -200 -210
f1 (ppm)

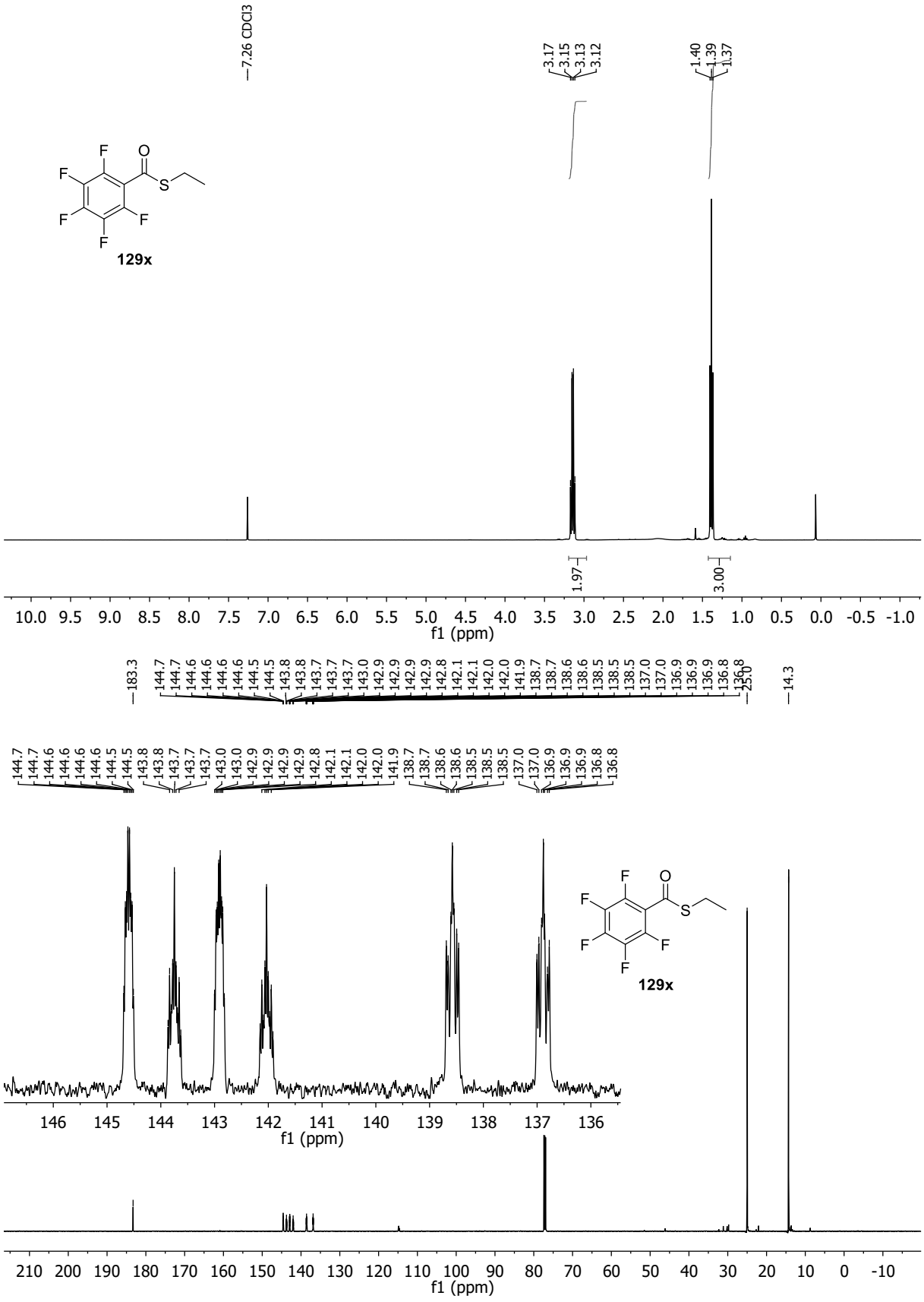
7.26 CDCl3
3.17
3.15
3.13
3.12
1.40
1.39
1.37
F
O
S
F
F
F
F
129x
1.97
3.00
f1 (ppm)
183.3
144.7
144.6
144.5
143.8
143.7
143.0
142.9
142.8
142.1
142.0
141.9
138.7
138.6
138.5
137.0
136.9
136.8
25.0
14.3
f1 (ppm)
f1 (ppm)

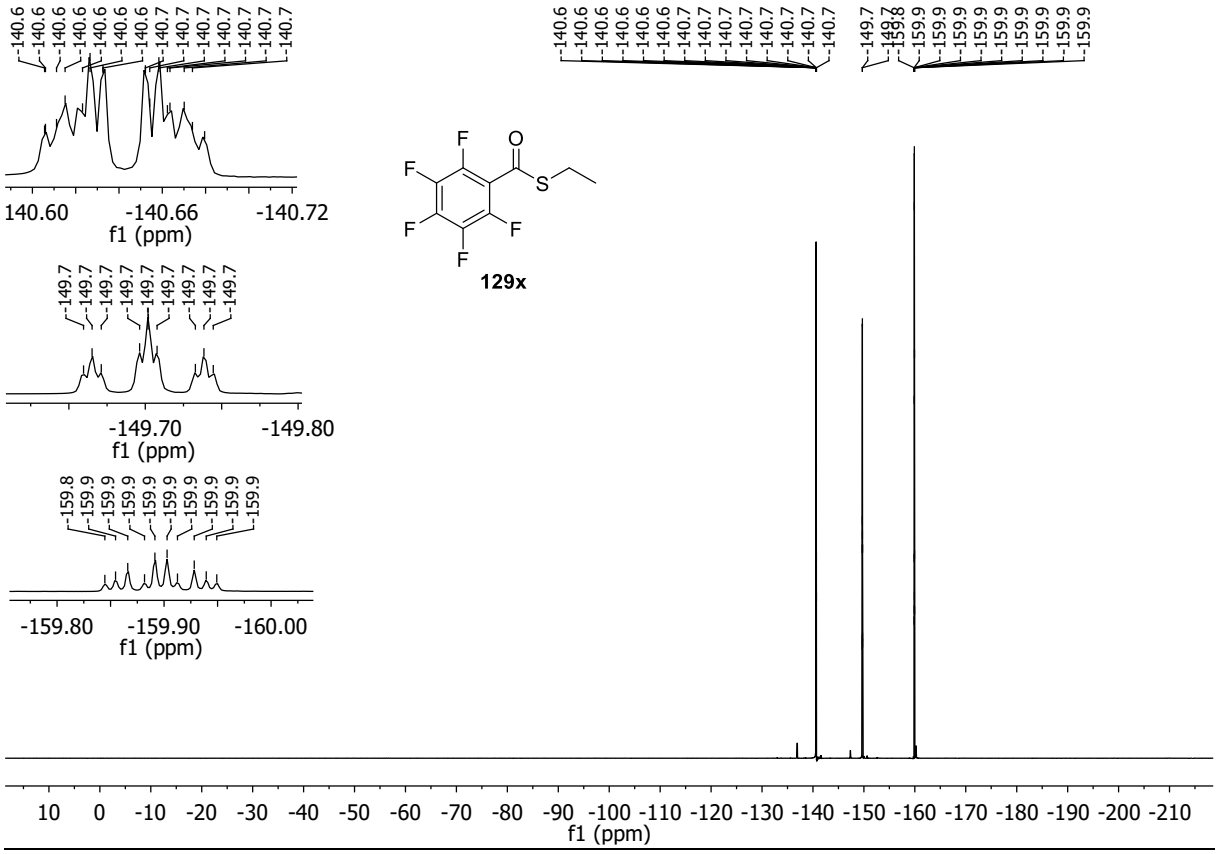
F
O
F
S
F
F
F
129x
140.60
-140.66
-140.72
f1 (ppm)
-149.70
-149.80
f1 (ppm)
-159.80
-159.90
-160.00
f1 (ppm)
10 0 -10 -20 -30 -40 -50 -60 -70 -80 -90 -100 -110 -120 -130 -140 -150 -160 -170 -180 -190 -200 -210
f1 (ppm)

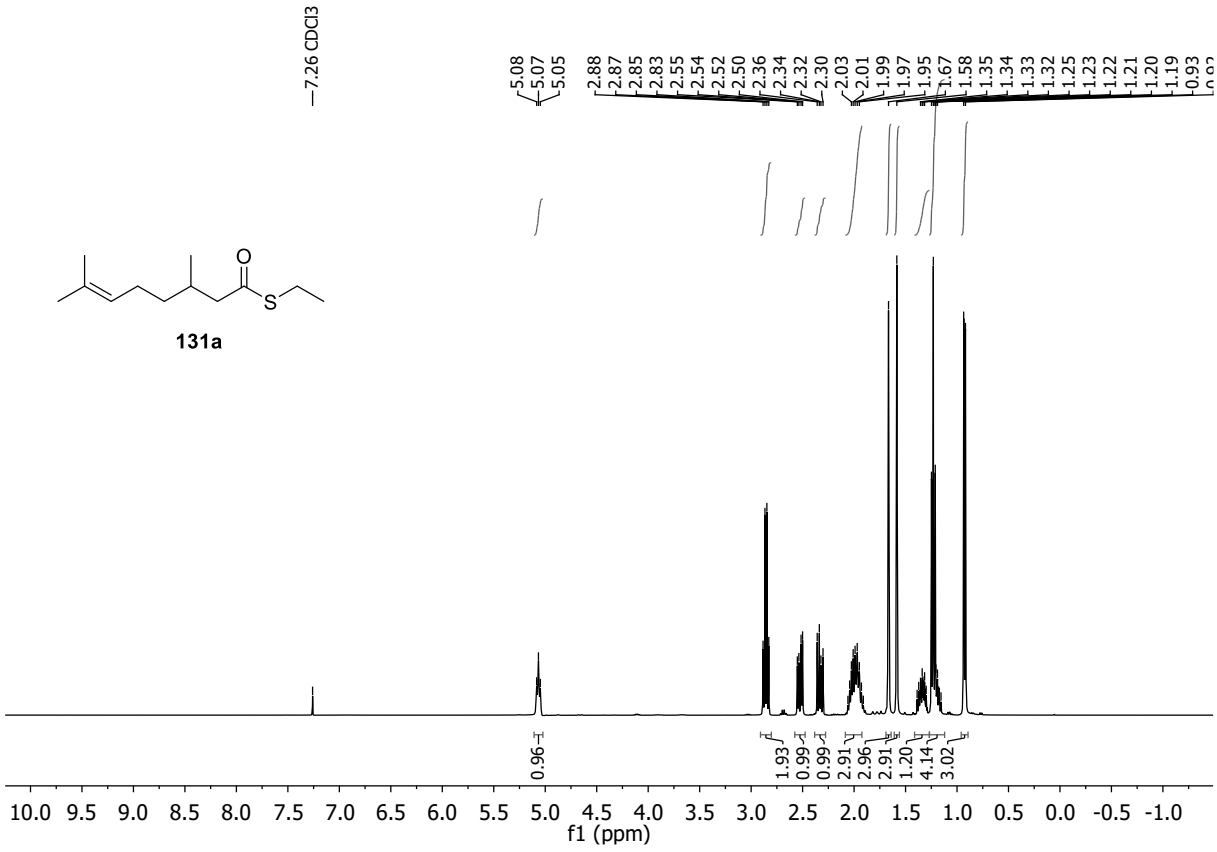
7.26 CDCl3
5.08
5.07
5.05
2.88
2.87
2.85
2.83
2.55
2.54
2.52
2.50
2.36
2.34
2.32
2.30
2.03
2.01
1.99
1.97
1.95
1.67
1.58
1.35
1.34
1.33
1.32
1.25
1.23
1.22
1.21
1.20
1.19
0.93
O
S
131a
0.96
1.93
0.99
0.99
2.91
2.96
2.91
1.20
4.14
3.02
10.0 9.5 9.0 8.5 8.0 7.5 7.0 6.5 6.0 5.5 5.0 4.5 4.0 3.5 3.0 2.5 2.0 1.5 1.0 0.5 0.0 -0.5 -1.0
f1 (ppm)

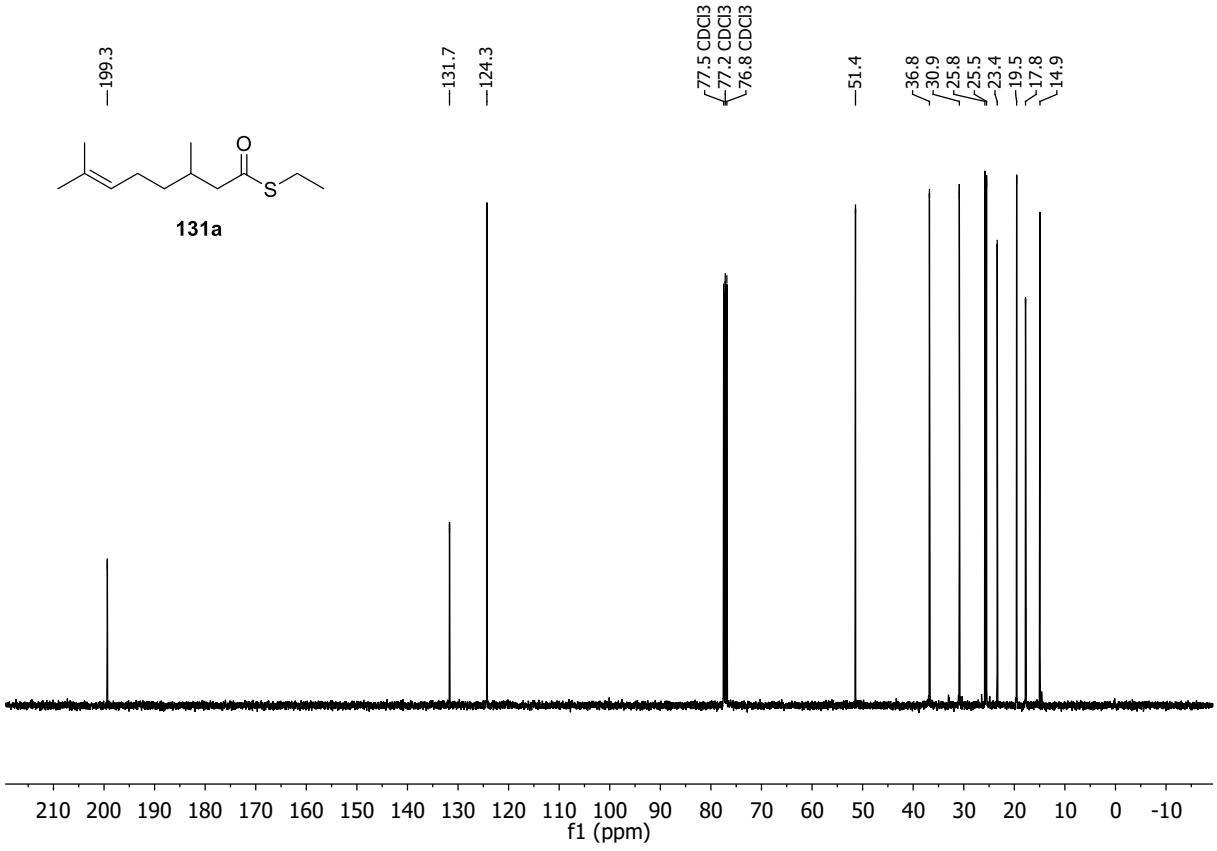
199.3
131.7
124.3
77.5 CDCl3
77.2 CDCl3
76.8 CDCl3
51.4
36.8
30.9
25.8
25.5
23.4
19.5
17.8
14.9
O
S
131a
210 200 190 180 170 160 150 140 130 120 110 100 90 80 70 60 50 40 30 20 10 0 -10
f1 (ppm)

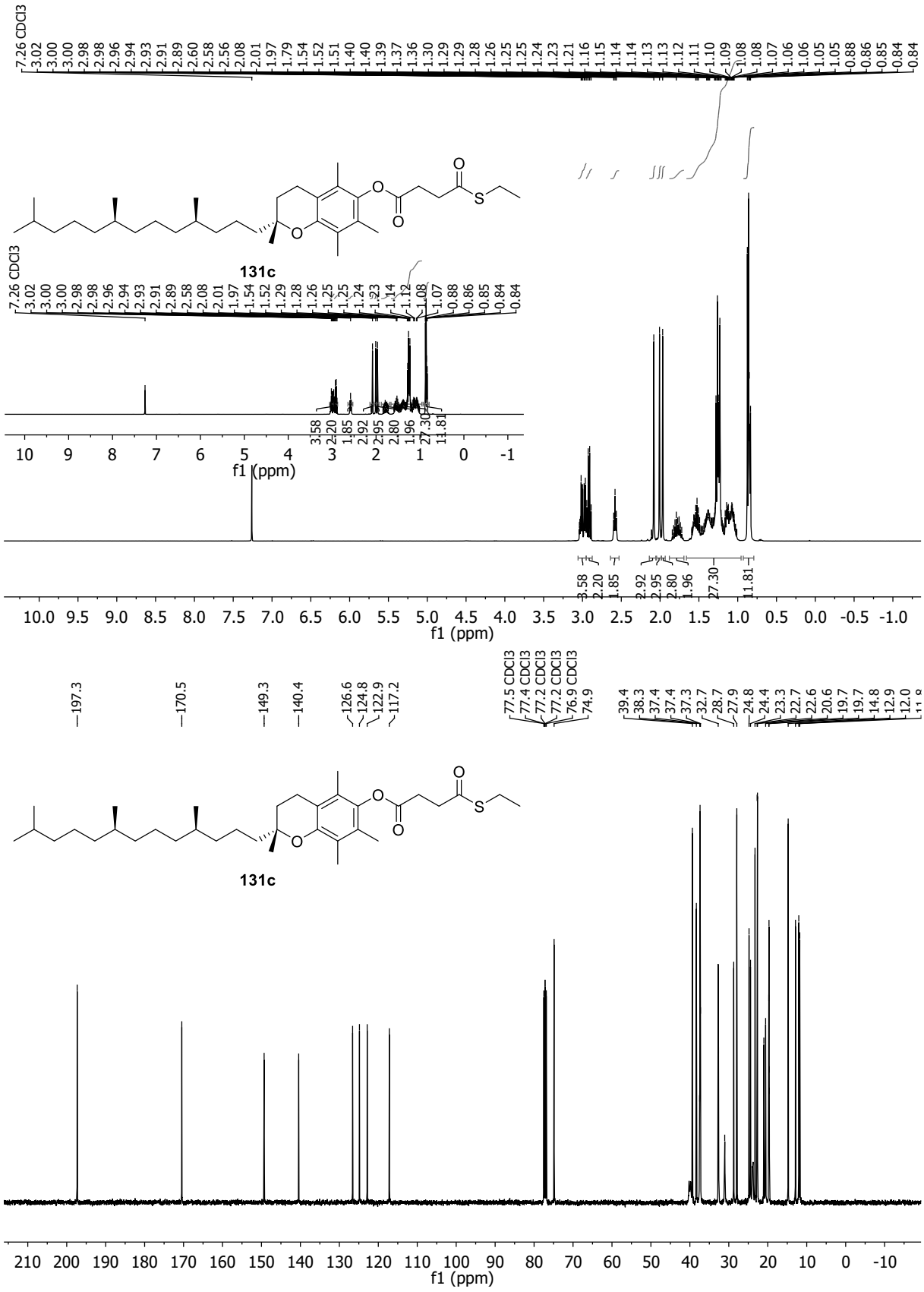
131c
f1 (ppm)
131c
f1 (ppm)

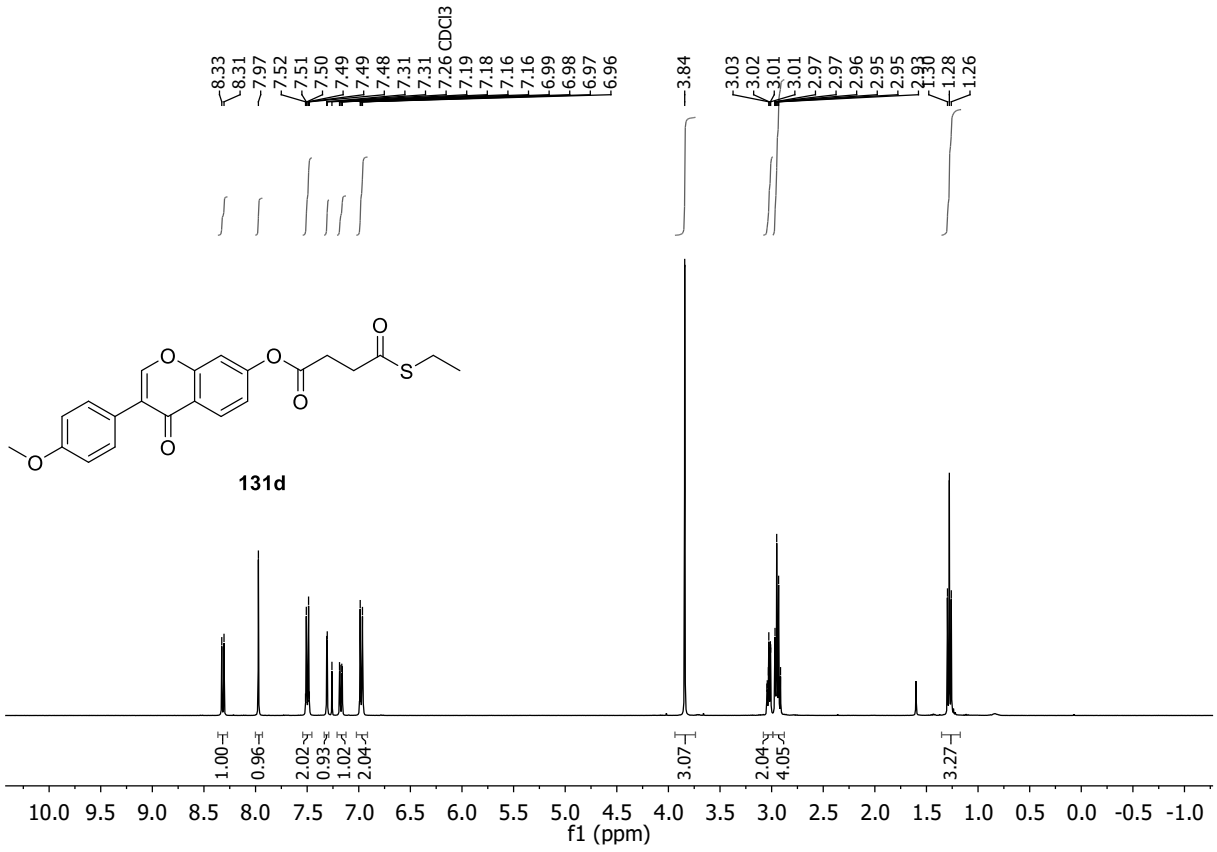
8.33
8.31
7.97
7.52
7.51
7.50
7.49
7.49
7.48
7.31
7.31
7.26 CDCl3
7.19
7.18
7.16
7.16
6.99
6.98
6.97
6.96
3.84
3.03
3.02
3.01
3.01
2.97
2.97
2.96
2.95
2.95
2.93
1.30
1.28
1.26
131d
1.00
0.96
2.02
0.93
1.02
2.04
3.07
2.04
4.05
3.27
10.0 9.5 9.0 8.5 8.0 7.5 7.0 6.5 6.0 5.5 5.0 4.5 4.0 3.5 3.0 2.5 2.0 1.5 1.0 0.5 0.0 -0.5 -1.0
f1 (ppm)

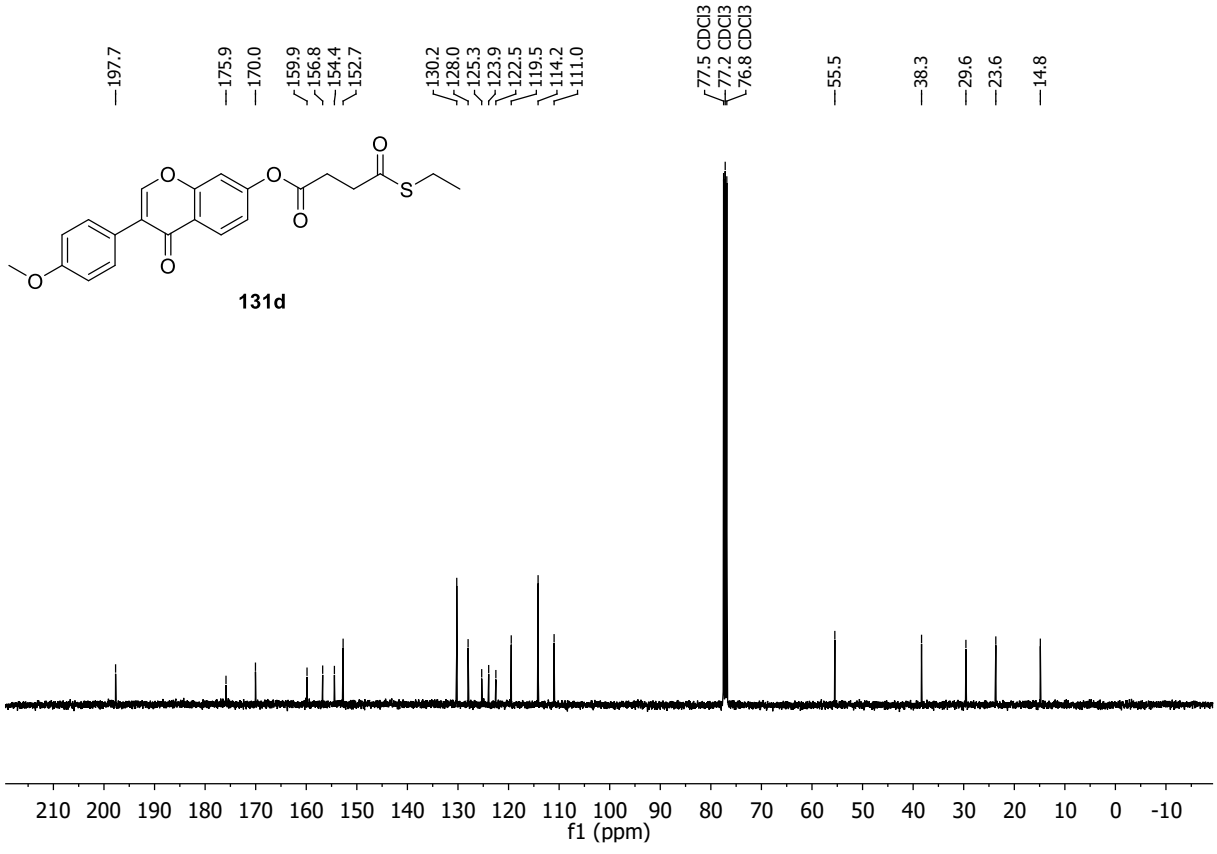
197.7
175.9
170.0
159.9
156.8
154.4
152.7
130.2
128.0
125.3
123.9
122.5
119.5
114.2
111.0
77.5 CDCl3
77.2 CDCl3
76.8 CDCl3
55.5
38.3
29.6
23.6
14.8
131d
210 200 190 180 170 160 150 140 130 120 110 100 90 80 70 60 50 40 30 20 10 0 -10
f1 (ppm)

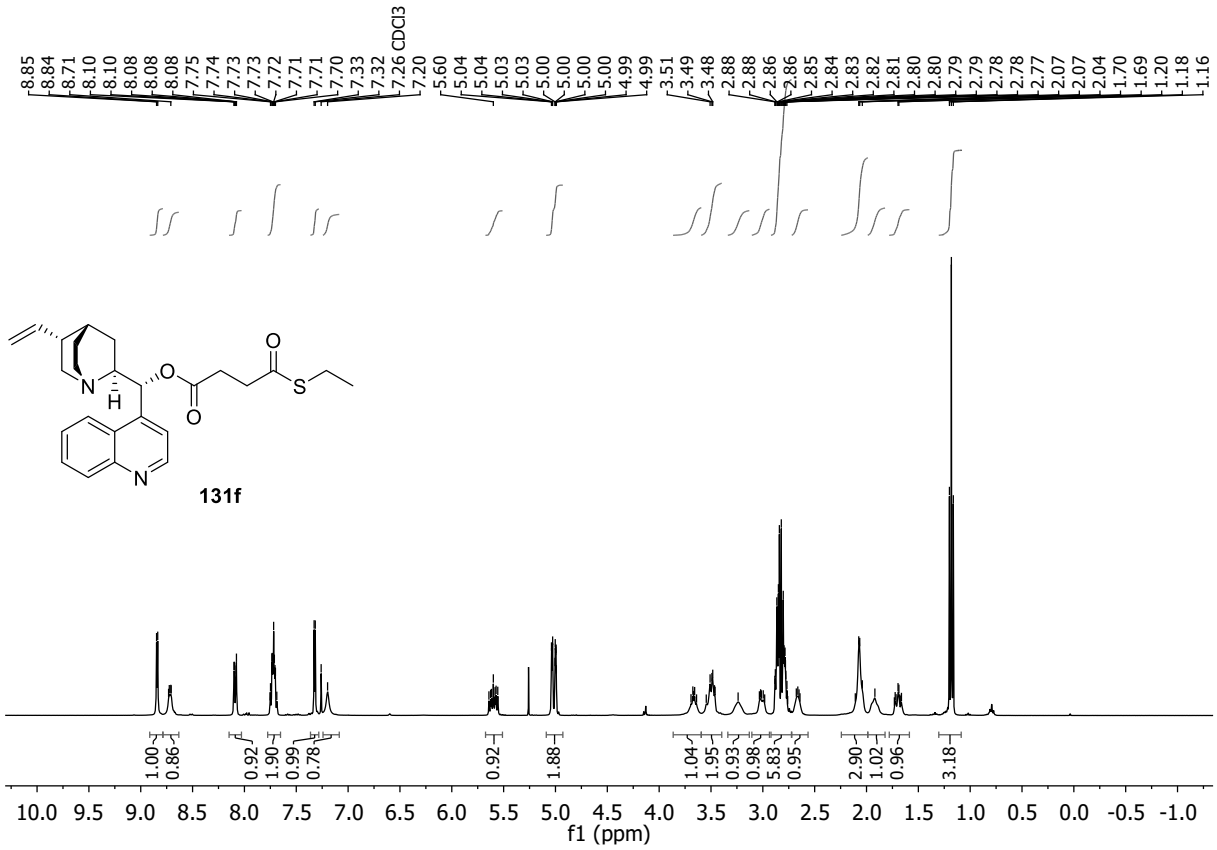
8.85 8.84 8.71 8.10 8.10 8.08 8.08 8.08 7.75 7.74 7.73 7.73 7.72 7.71 7.71 7.70 7.33 7.32 7.26 CDCl3 7.20 5.60 5.04 5.04 5.03 5.03 5.00 5.00 5.00 5.00 4.99 4.99 3.51 3.49 3.48 2.88 2.88 2.86 2.86 2.85 2.84 2.83 2.82 2.81 2.80 2.80 2.79 2.79 2.78 2.78 2.77 2.07 2.04 1.70 1.69 1.20 1.18 1.16
131f
1.00 0.86 0.92 1.90 0.99 0.78 0.92 1.88 1.04 1.95 0.93 0.98 5.83 0.95 2.90 1.02 0.96 3.18
10.0 9.5 9.0 8.5 8.0 7.5 7.0 6.5 6.0 5.5 5.0 4.5 4.0 3.5 3.0 2.5 2.0 1.5 1.0 0.5 0.0 -0.5 -1.0
f1 (ppm)

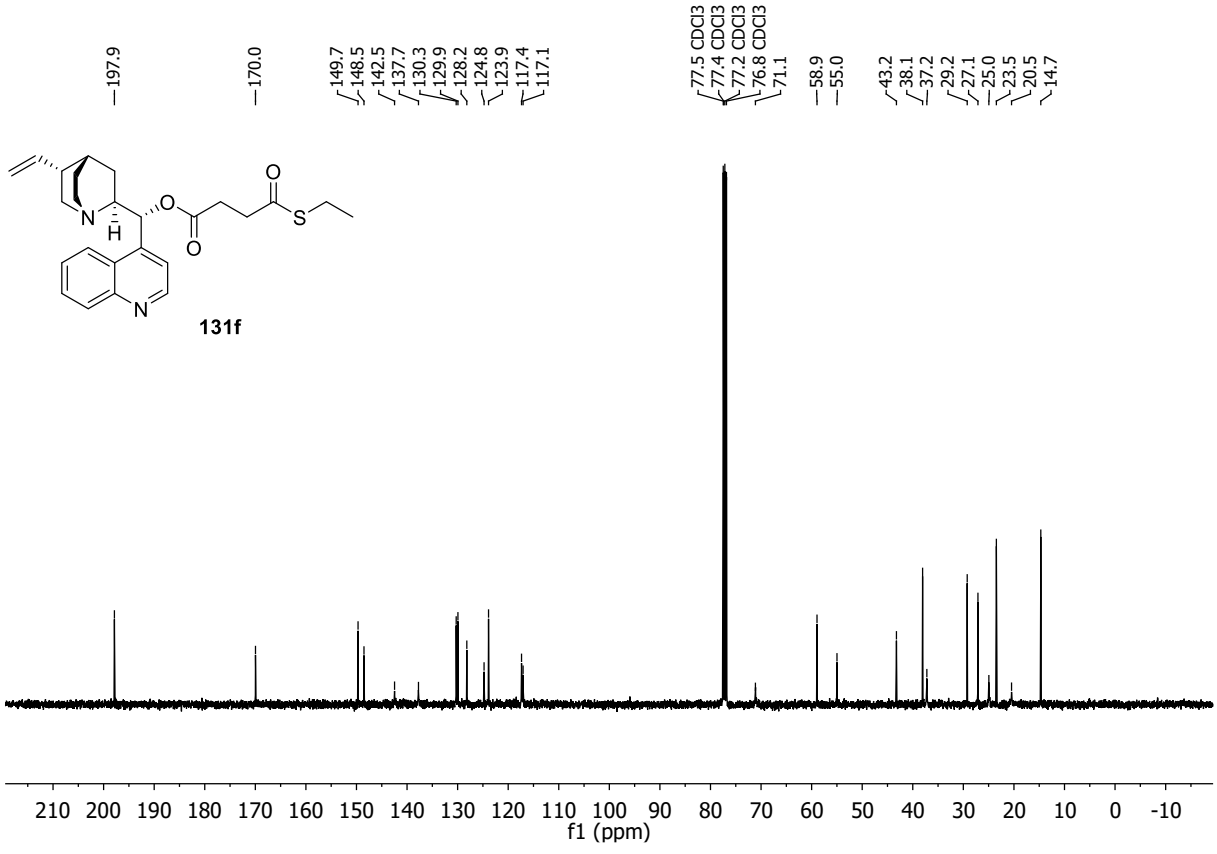
197.9 170.0 149.7 148.5 142.5 137.7 130.3 129.9 128.2 124.8 123.9 117.4 117.1 77.5 CDCl3 77.4 CDCl3 77.2 CDCl3 76.8 CDCl3 71.1 58.9 55.0 43.2 38.1 37.2 29.2 27.1 25.0 23.5 20.5 14.7
131f
210 200 190 180 170 160 150 140 130 120 110 100 90 80 70 60 50 40 30 20 10 0 -10
f1 (ppm)

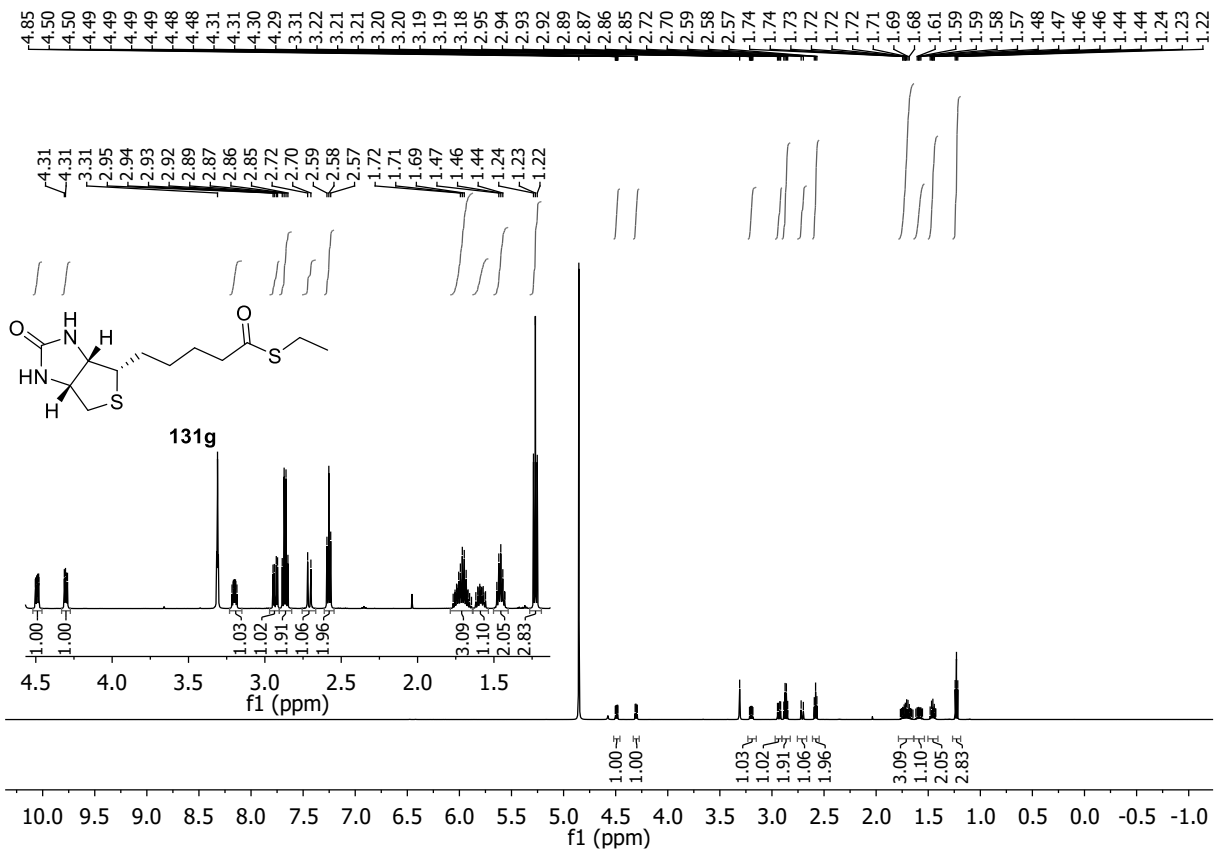
131g
f1 (ppm)

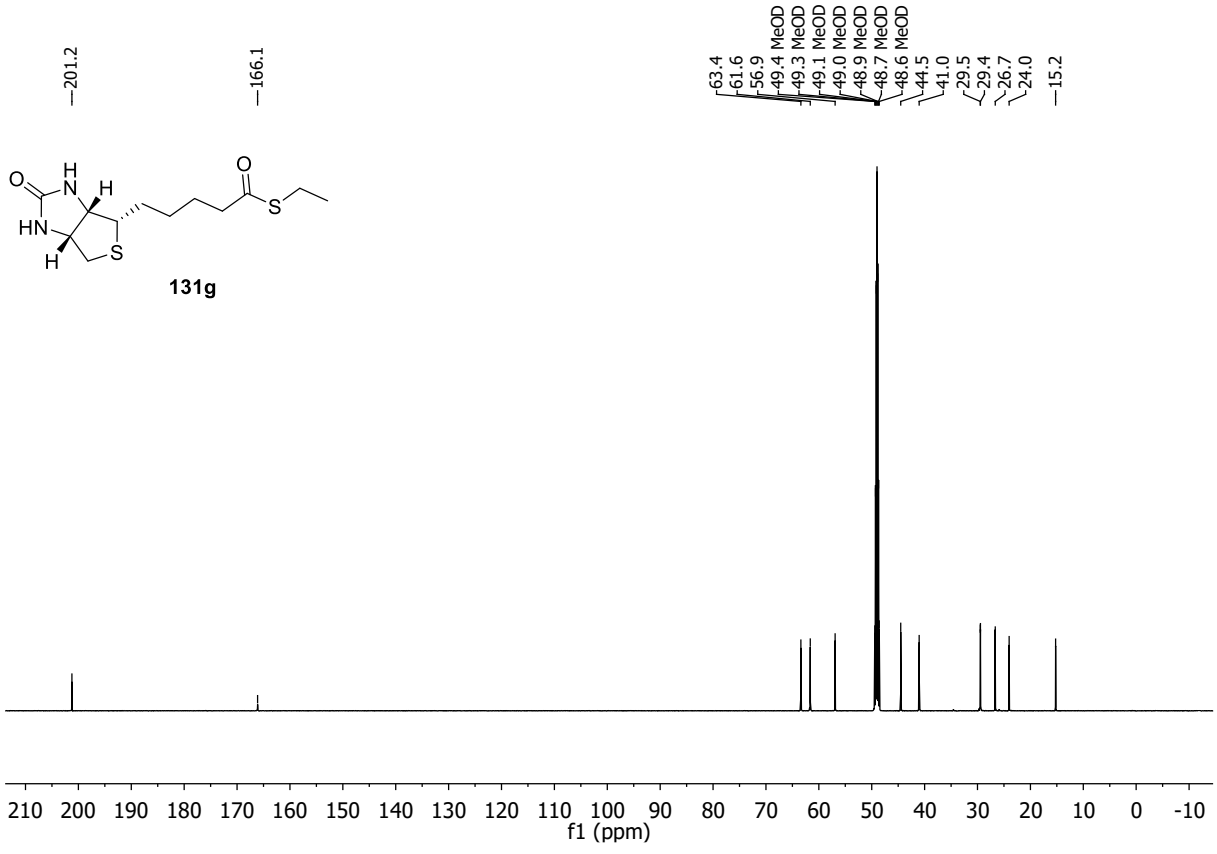
131g
f1 (ppm)

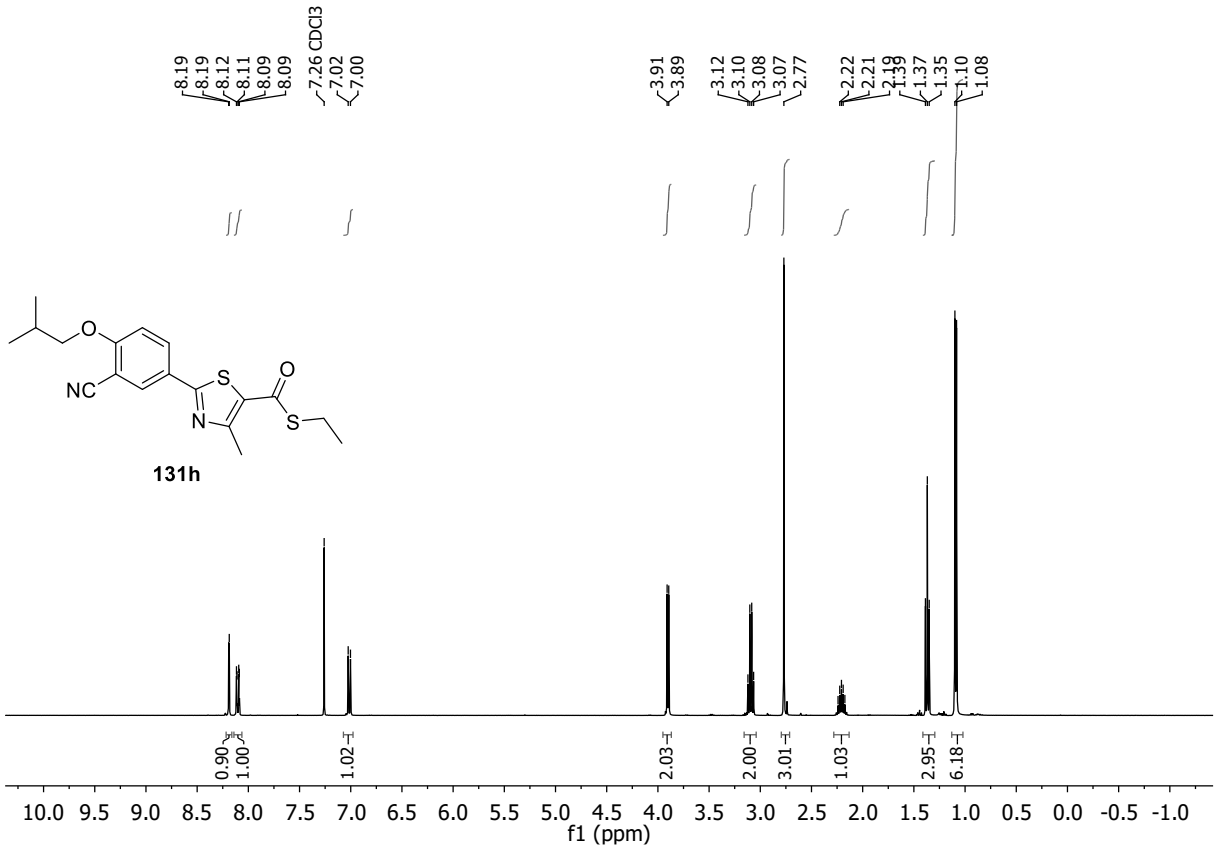
8.19
8.19
8.12
8.11
8.09
8.09
7.26 CDCl3
7.02
7.00
3.91
3.89
3.12
3.10
3.08
3.07
2.77
2.22
2.21
2.19
2.19
1.37
1.35
1.10
1.08
O
NC
S
N
O
S
131h
0.90
1.00
1.02
2.03
2.00
3.01
1.03
2.95
6.18
10.0 9.5 9.0 8.5 8.0 7.5 7.0 6.5 6.0 5.5 5.0 4.5 4.0 3.5 3.0 2.5 2.0 1.5 1.0 0.5 0.0 -0.5 -1.0
f1 (ppm)

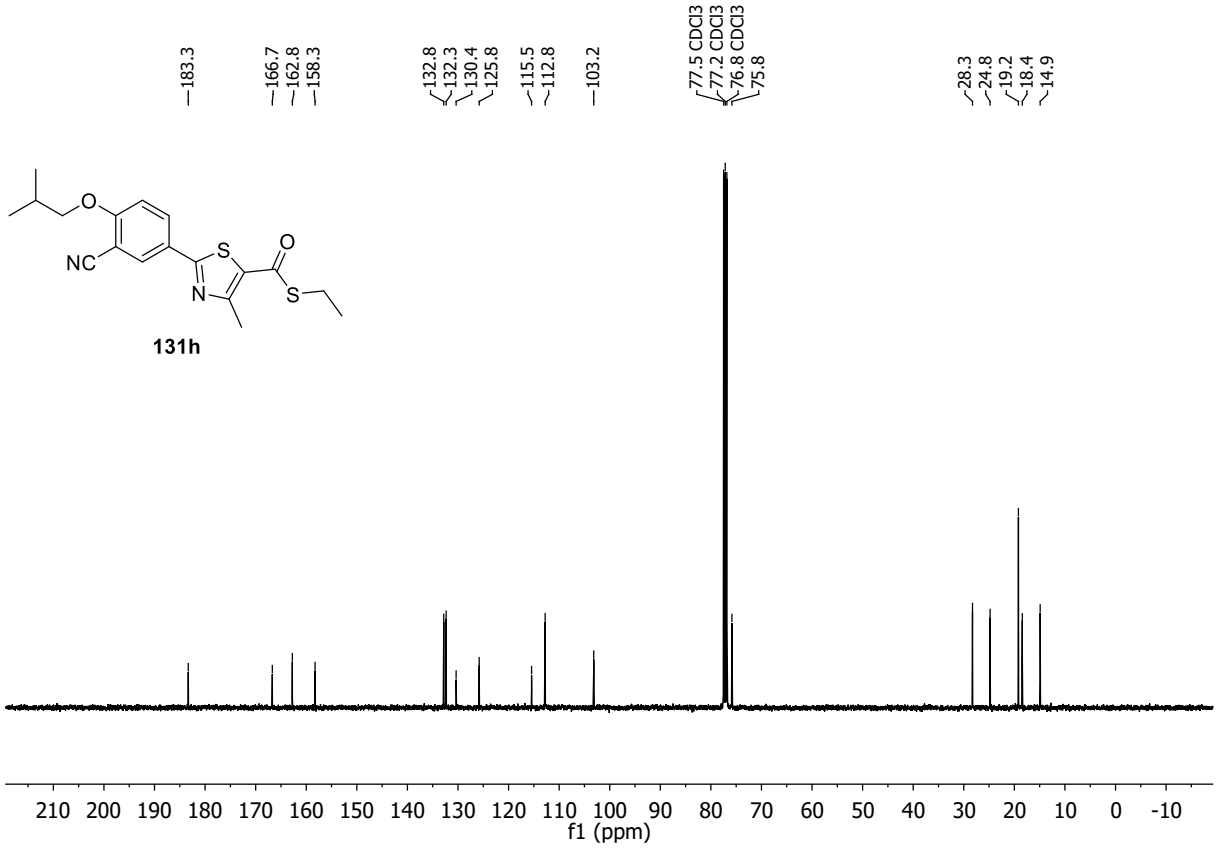
183.3
166.7
162.8
158.3
132.8
132.3
130.4
125.8
115.5
112.8
103.2
77.5 CDCl3
77.2 CDCl3
76.8 CDCl3
75.8
28.3
24.8
19.2
18.4
14.9
O
NC
S
N
O
S
131h
210 200 190 180 170 160 150 140 130 120 110 100 90 80 70 60 50 40 30 20 10 0 -10
f1 (ppm)

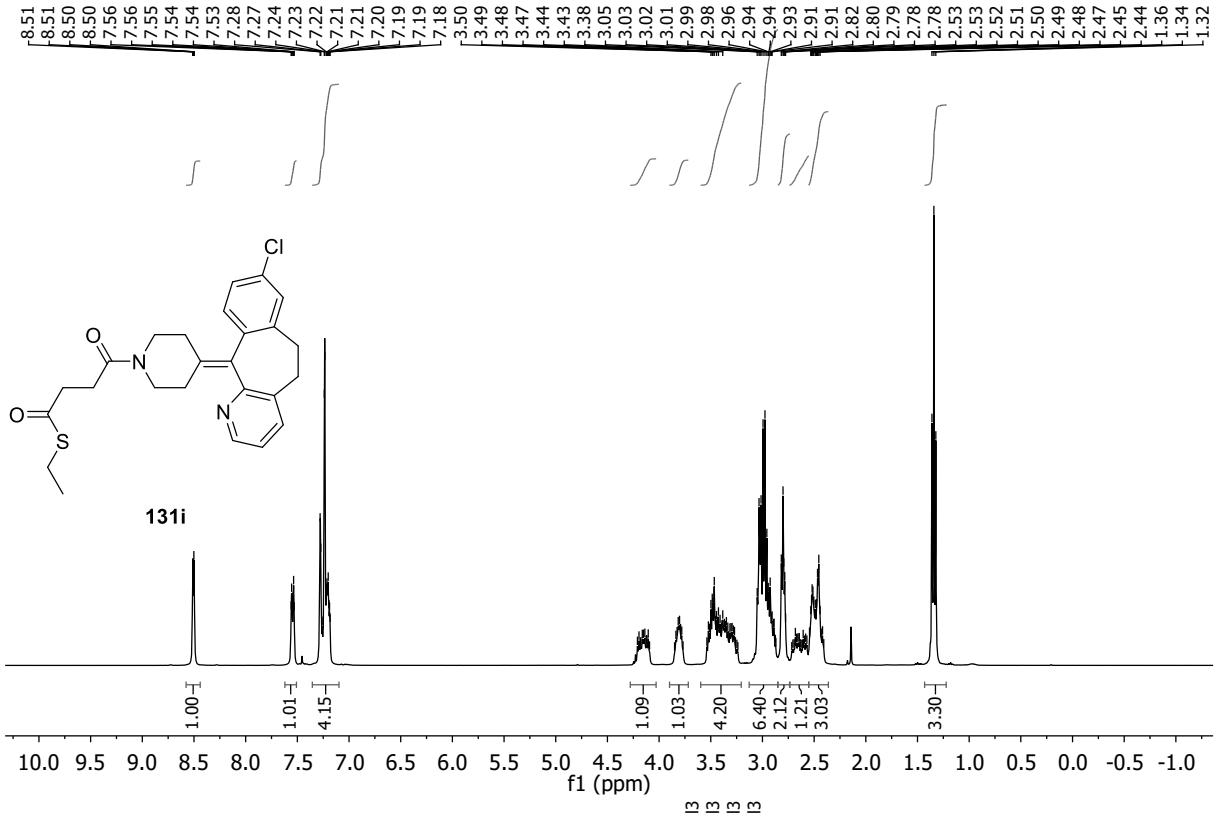
131i
f1 (ppm)

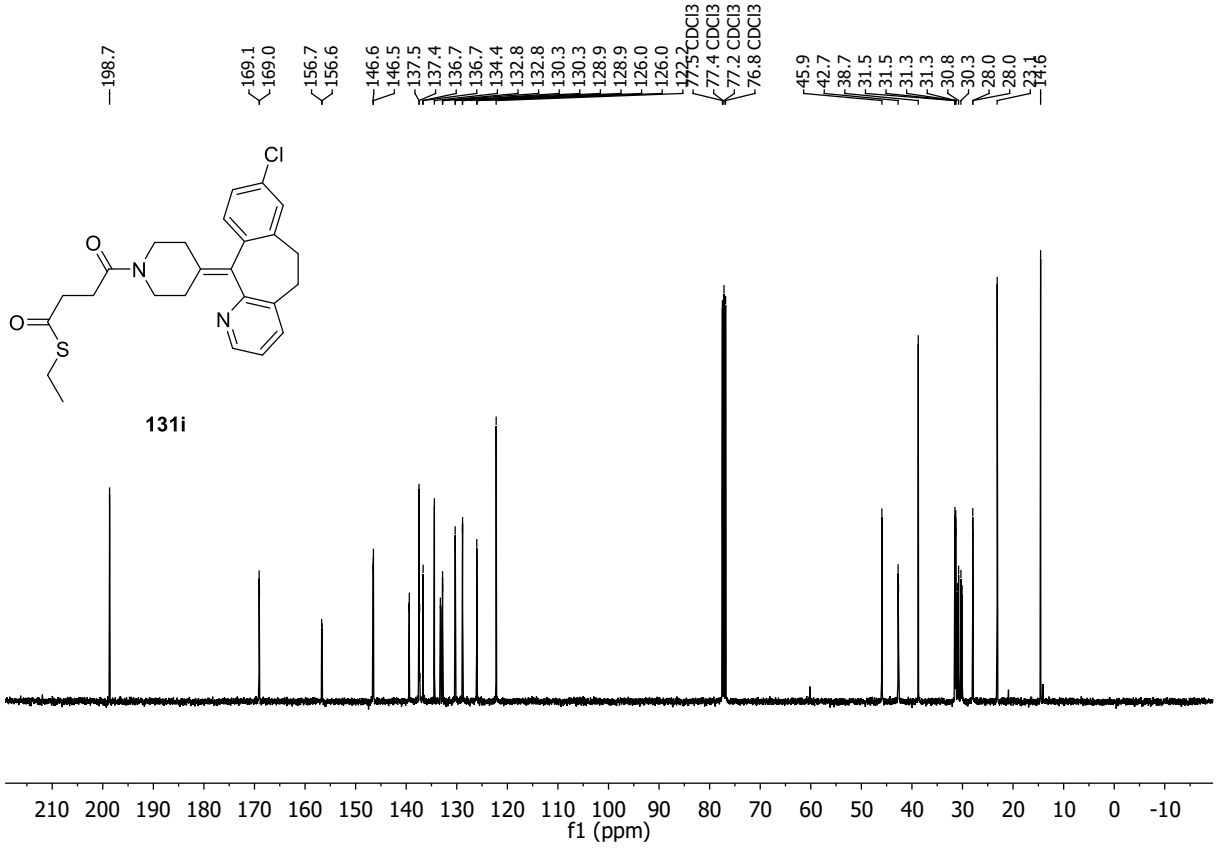
131i
f1 (ppm)

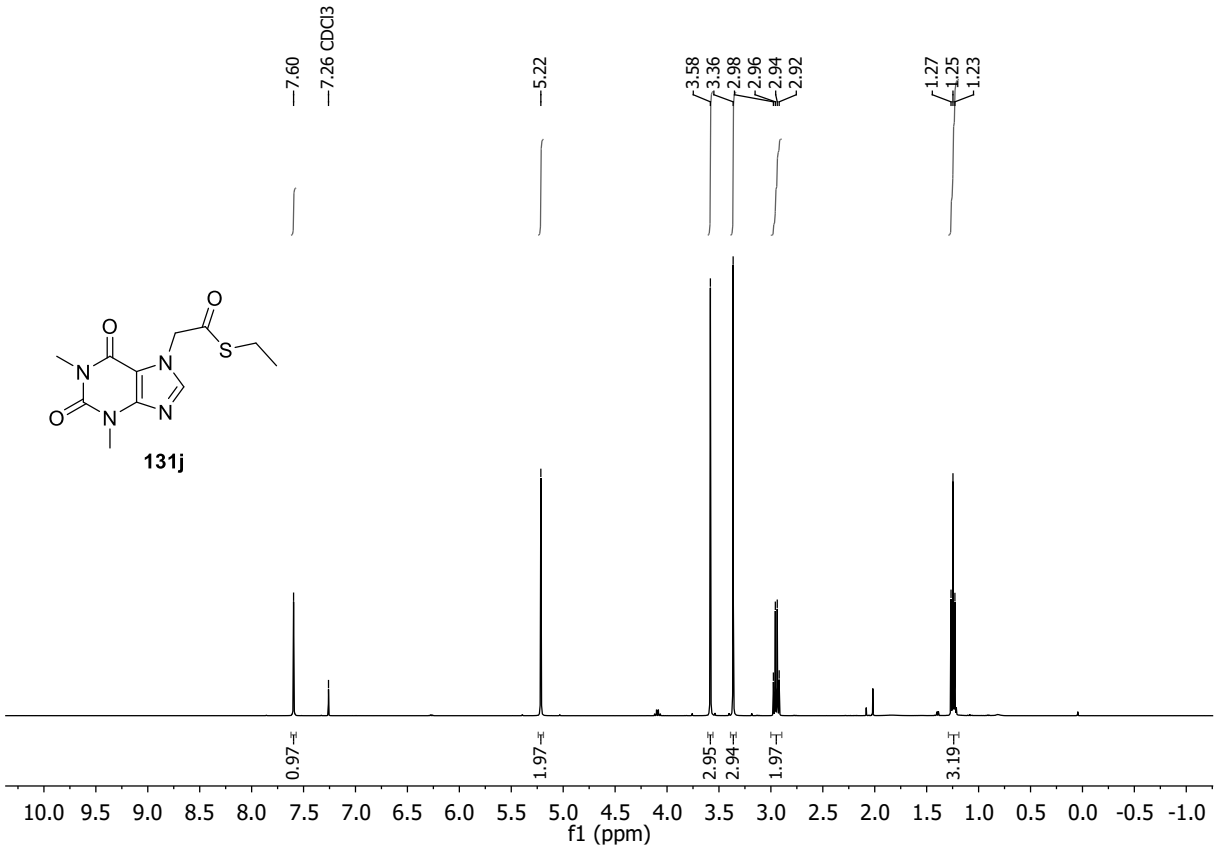
7.60
7.26 CDCl3
5.22
3.58
3.36
2.98
2.96
2.94
2.92
1.27
1.25
1.23
131j
0.97
1.97
2.95
2.94
1.97
3.19
f1 (ppm)

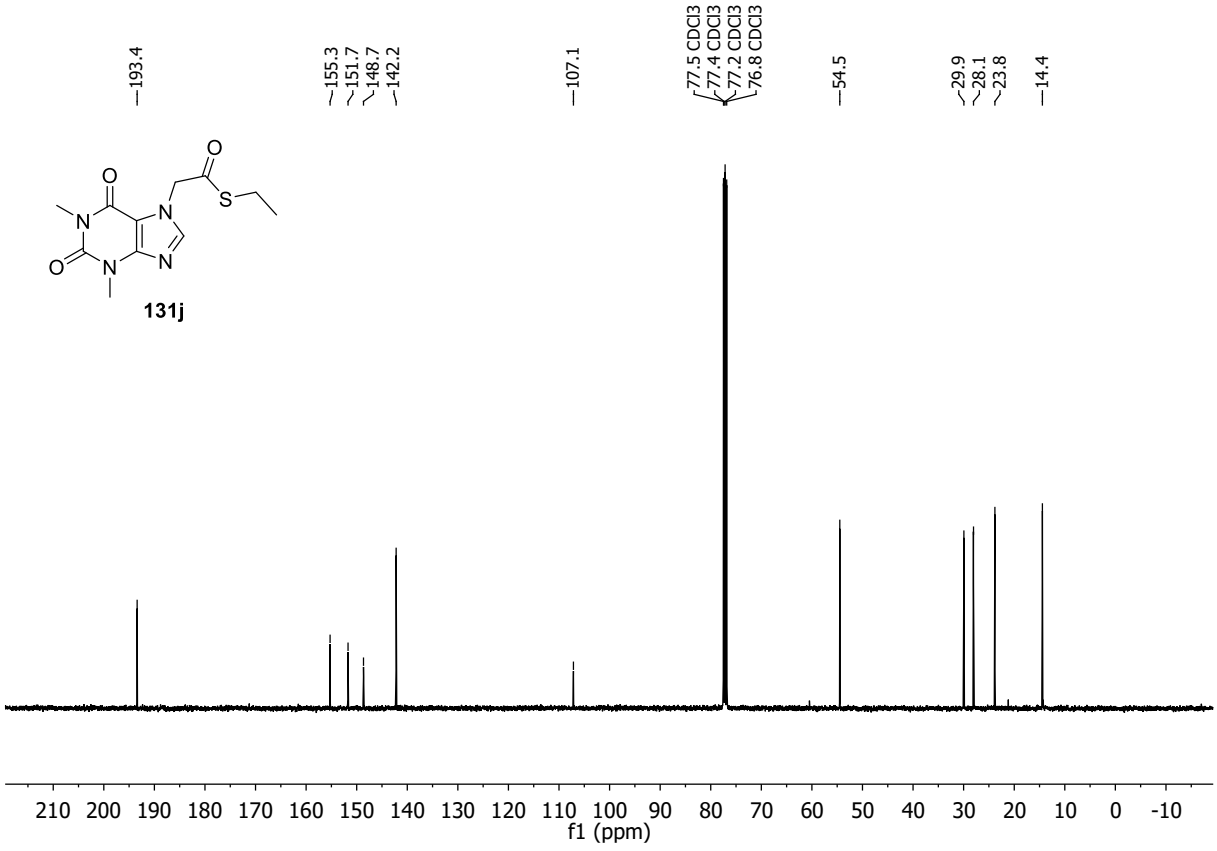
193.4
155.3
151.7
148.7
142.2
107.1
77.5 CDCl3
77.4 CDCl3
77.2 CDCl3
76.8 CDCl3
54.5
29.9
28.1
23.8
14.4
131j
f1 (ppm)

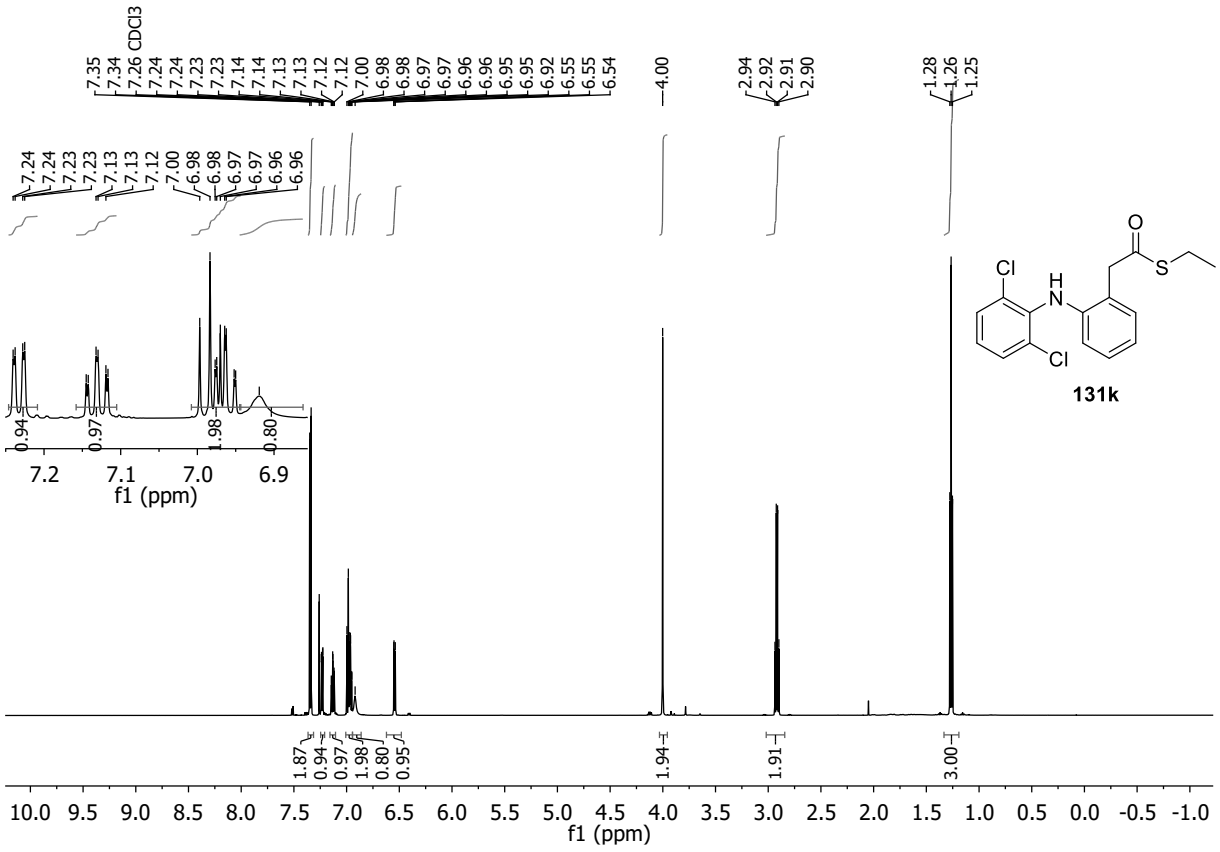
7.35
7.34
7.26 CDCl3
7.24
7.24
7.23
7.23
7.14
7.14
7.13
7.13
7.12
7.12
7.00
6.98
6.98
6.97
6.97
6.96
6.96
6.95
6.95
6.92
6.55
6.55
6.54
4.00
2.94
2.92
2.91
2.90
1.28
1.26
1.25
0.94
0.97
1.98
0.80
7.2
7.1
7.0
6.9
f1 (ppm)
1.87
0.94
0.97
1.98
0.80
0.95
1.94
1.91
3.00
10.0 9.5 9.0 8.5 8.0 7.5 7.0 6.5 6.0 5.5 5.0 4.5 4.0 3.5 3.0 2.5 2.0 1.5 1.0 0.5 0.0 -0.5 -1.0
f1 (ppm)
Cl
H
N
Cl
O
S
131k

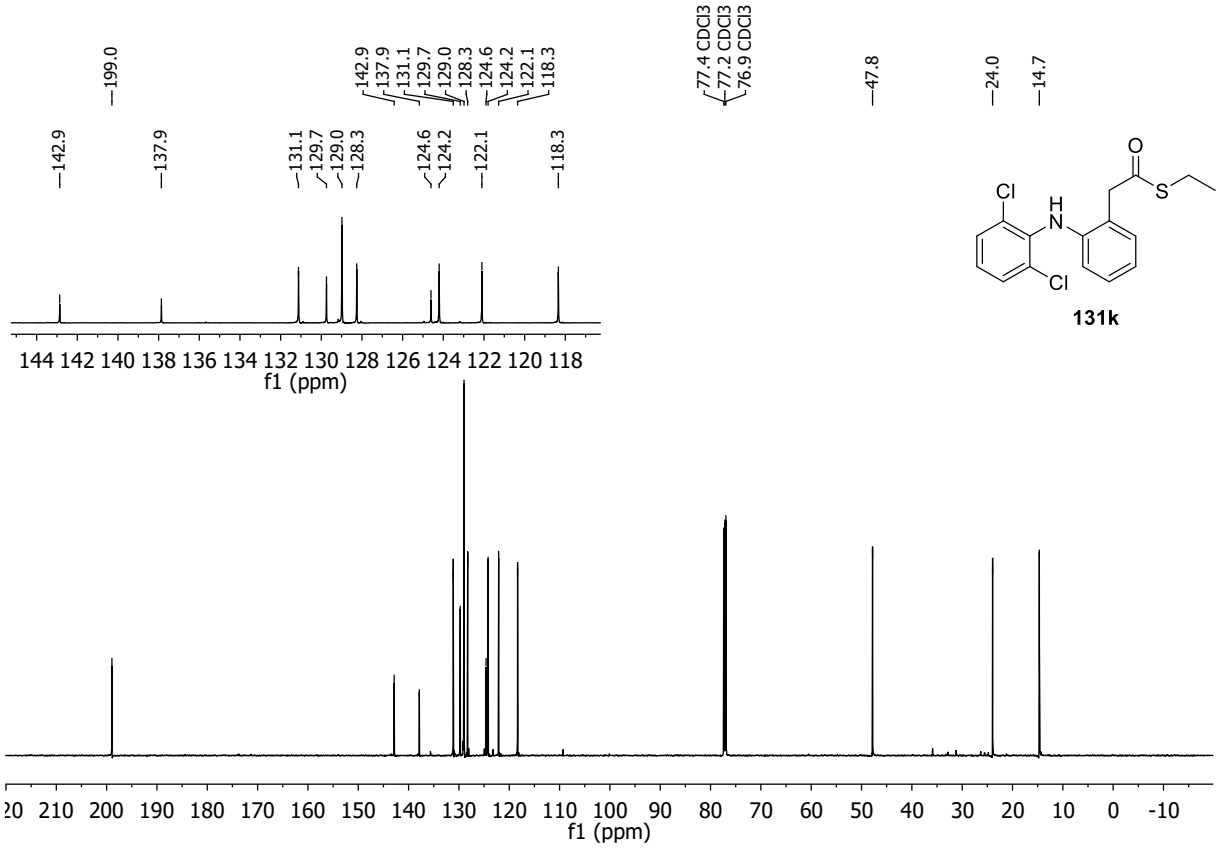
199.0
142.9
137.9
131.1
129.7
129.0
128.3
124.6
124.2
122.1
118.3
77.4 CDCl3
77.2 CDCl3
76.9 CDCl3
47.8
24.0
14.7
144 142 140 138 136 134 132 130 128 126 124 122 120 118
f1 (ppm)
220 210 200 190 180 170 160 150 140 130 120 110 100 90 80 70 60 50 40 30 20 10 0 -10
f1 (ppm)
Cl
H
N
Cl
O
S
131k

7.5 NMR Spectra of Ketones

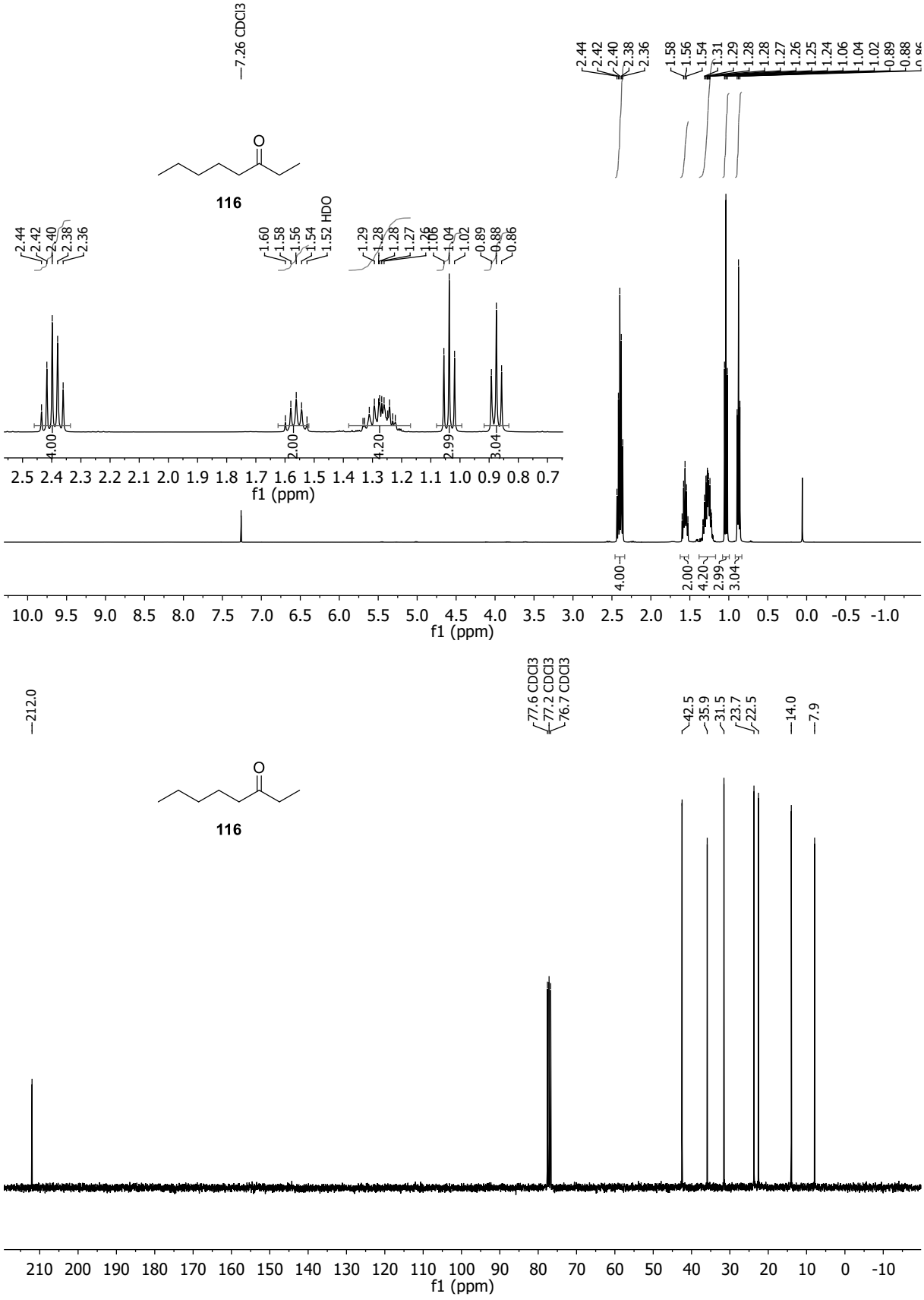

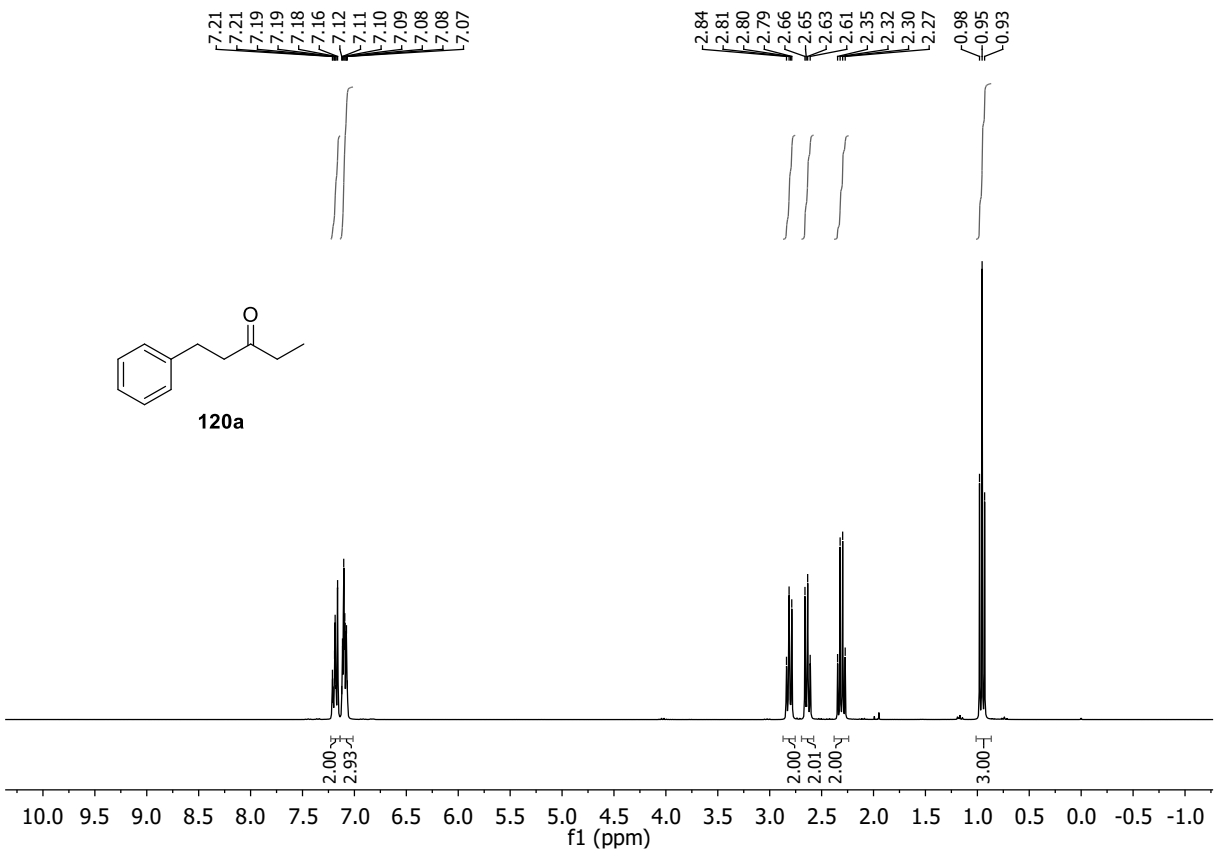
7.21
7.21
7.19
7.19
7.18
7.16
7.12
7.11
7.10
7.09
7.08
7.08
7.07
2.84
2.81
2.80
2.79
2.66
2.65
2.63
2.61
2.35
2.32
2.30
2.27
0.98
0.95
0.93
O
120a
2.00
2.93
2.00
2.01
2.00
3.00
10.0 9.5 9.0 8.5 8.0 7.5 7.0 6.5 6.0 5.5 5.0 4.5 4.0 3.5 3.0 2.5 2.0 1.5 1.0 0.5 0.0 -0.5 -1.0
f1 (ppm)

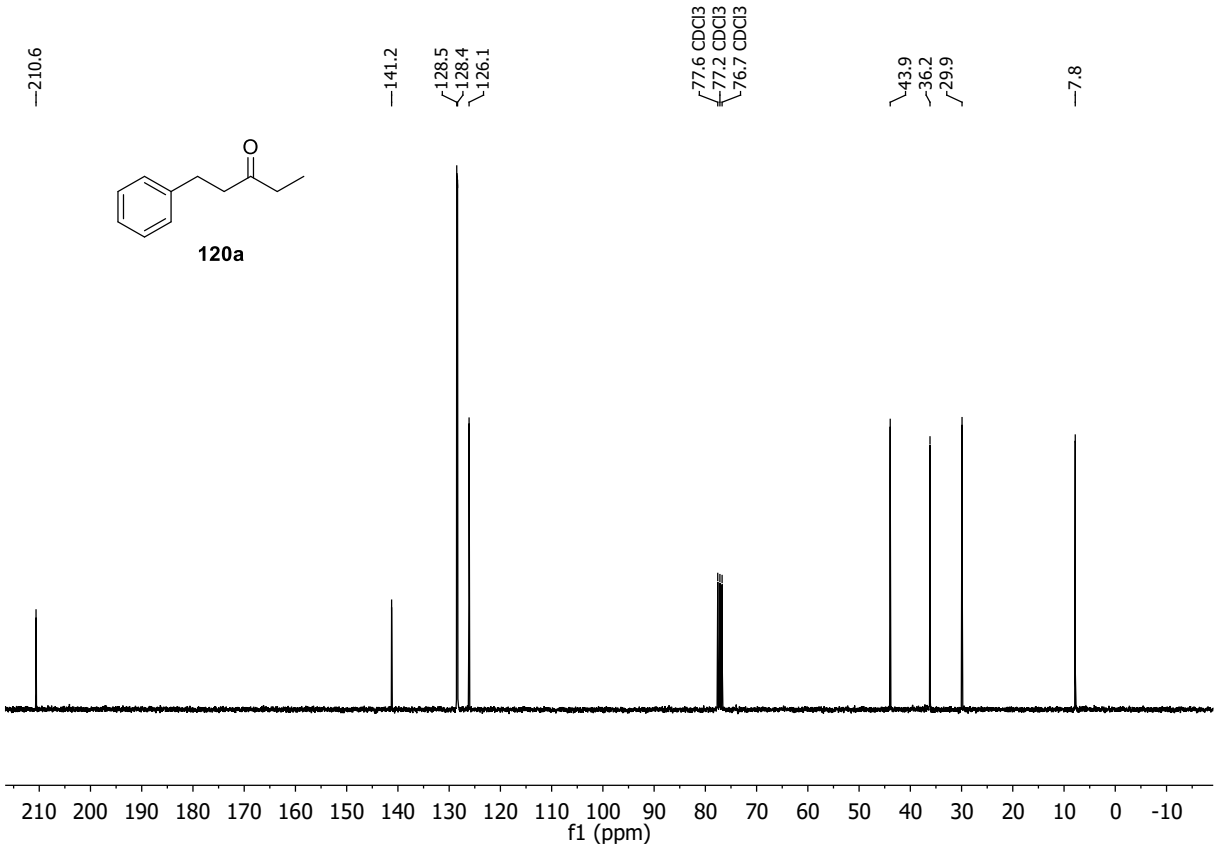
210.6
141.2
128.5
128.4
126.1
77.6 CDCl3
77.2 CDCl3
76.7 CDCl3
43.9
36.2
29.9
7.8
O
120a
210 200 190 180 170 160 150 140 130 120 110 100 90 80 70 60 50 40 30 20 10 0 -10
f1 (ppm)

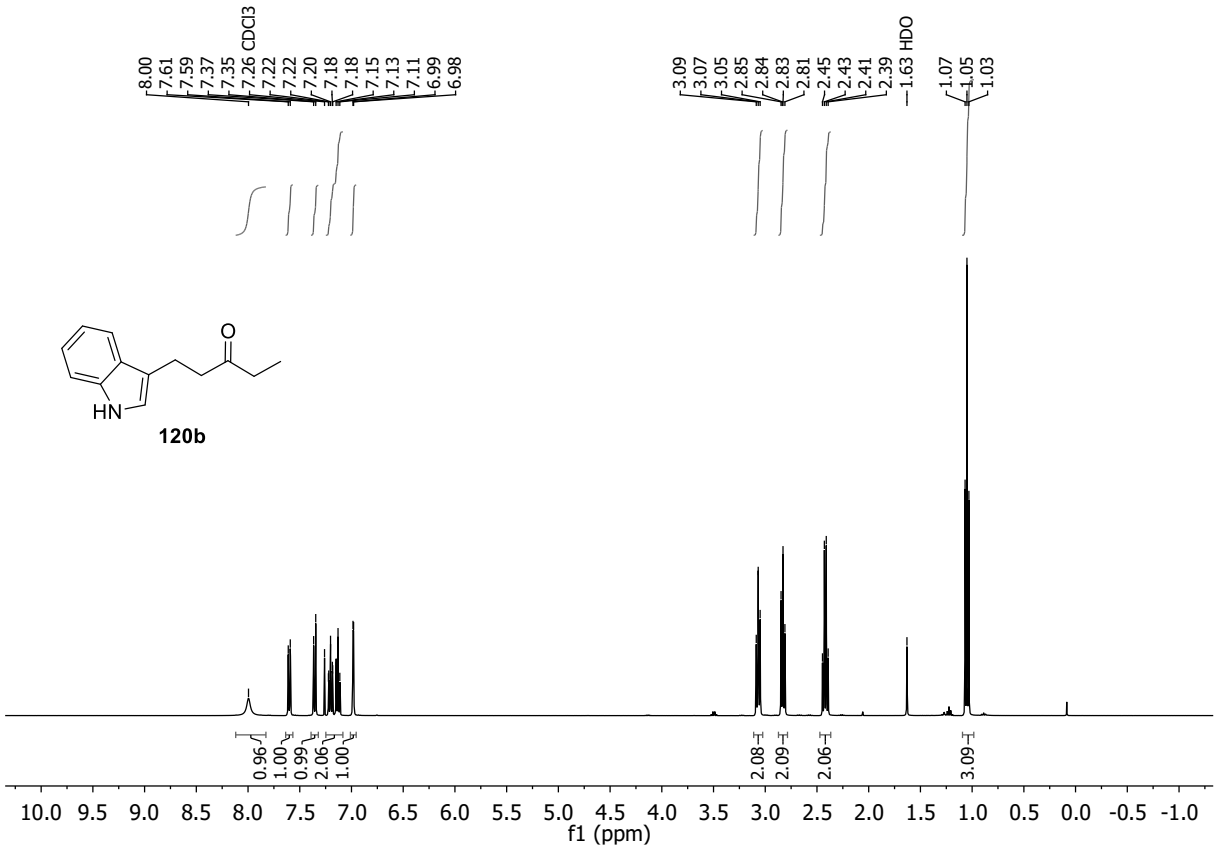
8.00
7.61
7.59
7.37
7.35
7.26 CDCl3
7.22
7.22
7.20
7.18
7.18
7.15
7.13
7.11
6.99
6.98
3.09
3.07
3.05
2.85
2.84
2.83
2.81
2.45
2.43
2.41
2.39
1.63 HDO
1.07
1.05
1.03
O
HN
120b
0.96
1.00
0.99
2.06
1.00
2.08
2.09
2.06
3.09
10.0 9.5 9.0 8.5 8.0 7.5 7.0 6.5 6.0 5.5 5.0 4.5 4.0 3.5 3.0 2.5 2.0 1.5 1.0 0.5 0.0 -0.5 -1.0
f1 (ppm)

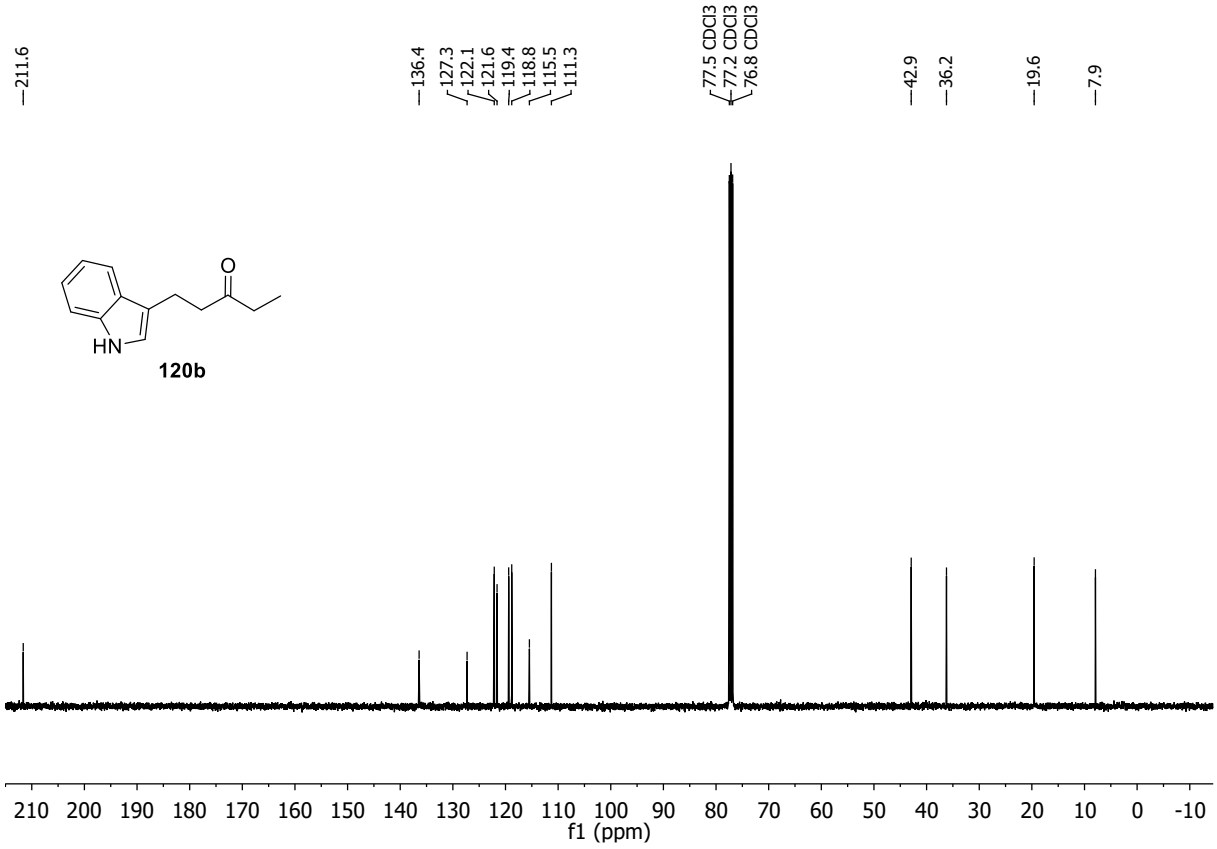
211.6
136.4
127.3
122.1
121.6
119.4
118.8
115.5
111.3
77.5 CDCl3
77.2 CDCl3
76.8 CDCl3
42.9
36.2
19.6
7.9
O
HN
120b
210 200 190 180 170 160 150 140 130 120 110 100 90 80 70 60 50 40 30 20 10 0 -10
f1 (ppm)

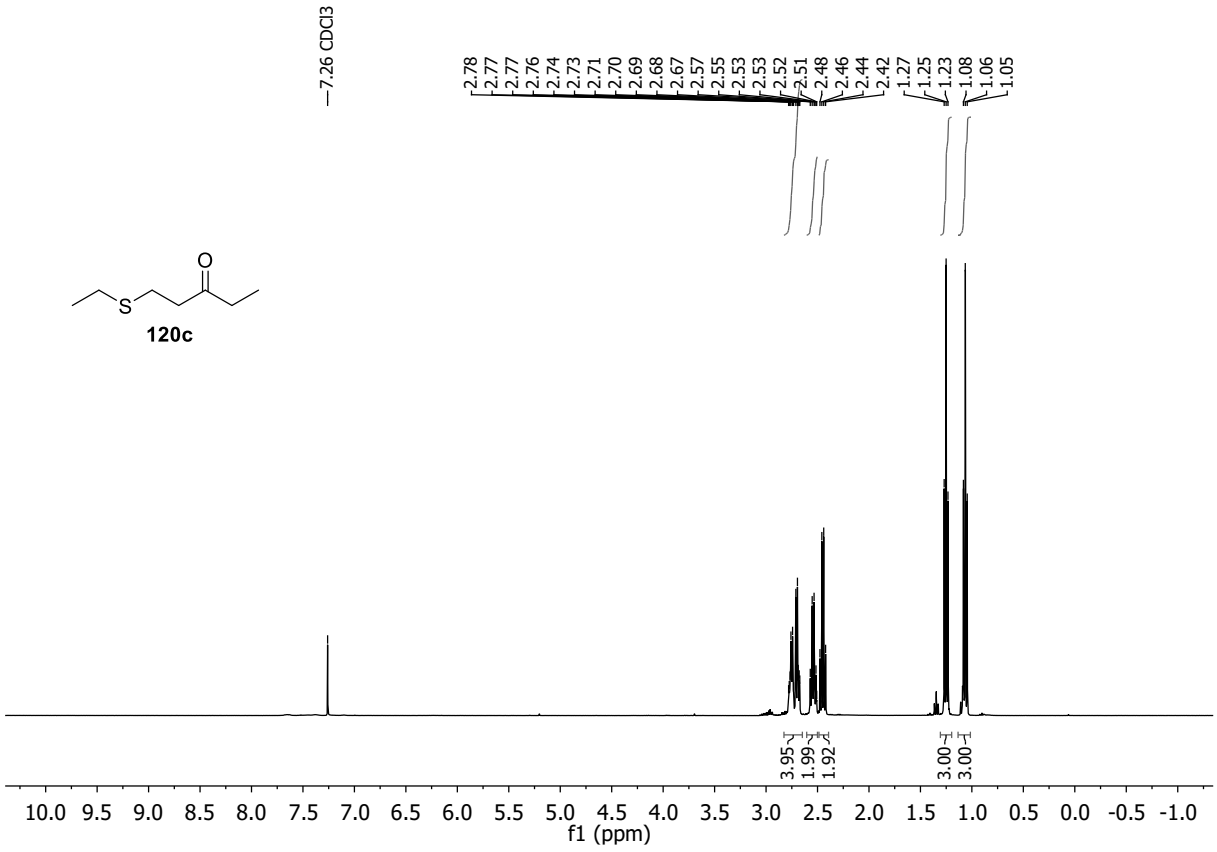
7.26 CDCl3
2.78
2.77
2.77
2.76
2.74
2.73
2.71
2.70
2.69
2.68
2.67
2.57
2.55
2.53
2.53
2.52
2.51
2.48
2.46
2.44
2.42
1.27
1.25
1.23
1.08
1.06
1.05
O
S
120c
3.95
1.99
1.92
3.00
3.00
10.0 9.5 9.0 8.5 8.0 7.5 7.0 6.5 6.0 5.5 5.0 4.5 4.0 3.5 3.0 2.5 2.0 1.5 1.0 0.5 0.0 -0.5 -1.0
f1 (ppm)

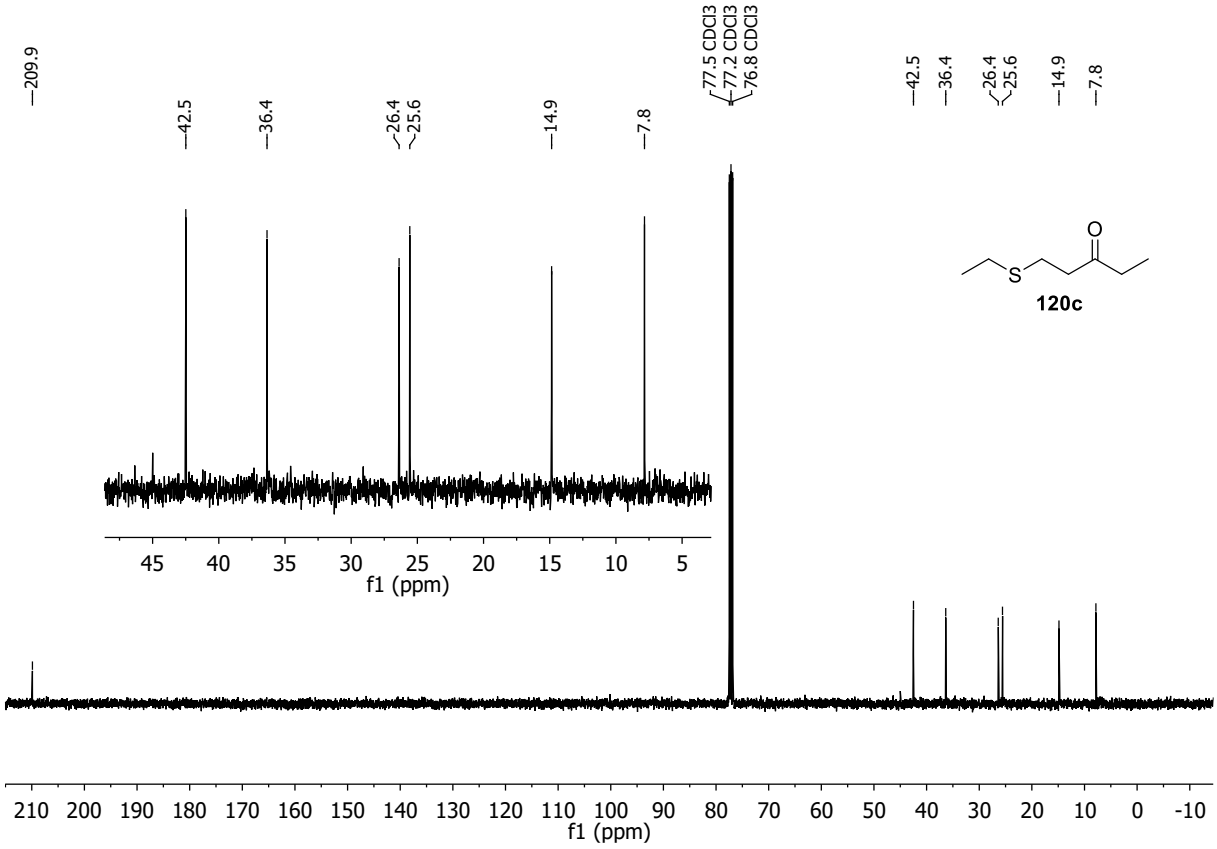
209.9
42.5
36.4
26.4
25.6
14.9
7.8
77.5 CDCl3
77.2 CDCl3
76.8 CDCl3
42.5
36.4
26.4
25.6
14.9
7.8
O
S
120c
45 40 35 30 25 20 15 10 5
f1 (ppm)
210 200 190 180 170 160 150 140 130 120 110 100 90 80 70 60 50 40 30 20 10 0 -10
f1 (ppm)

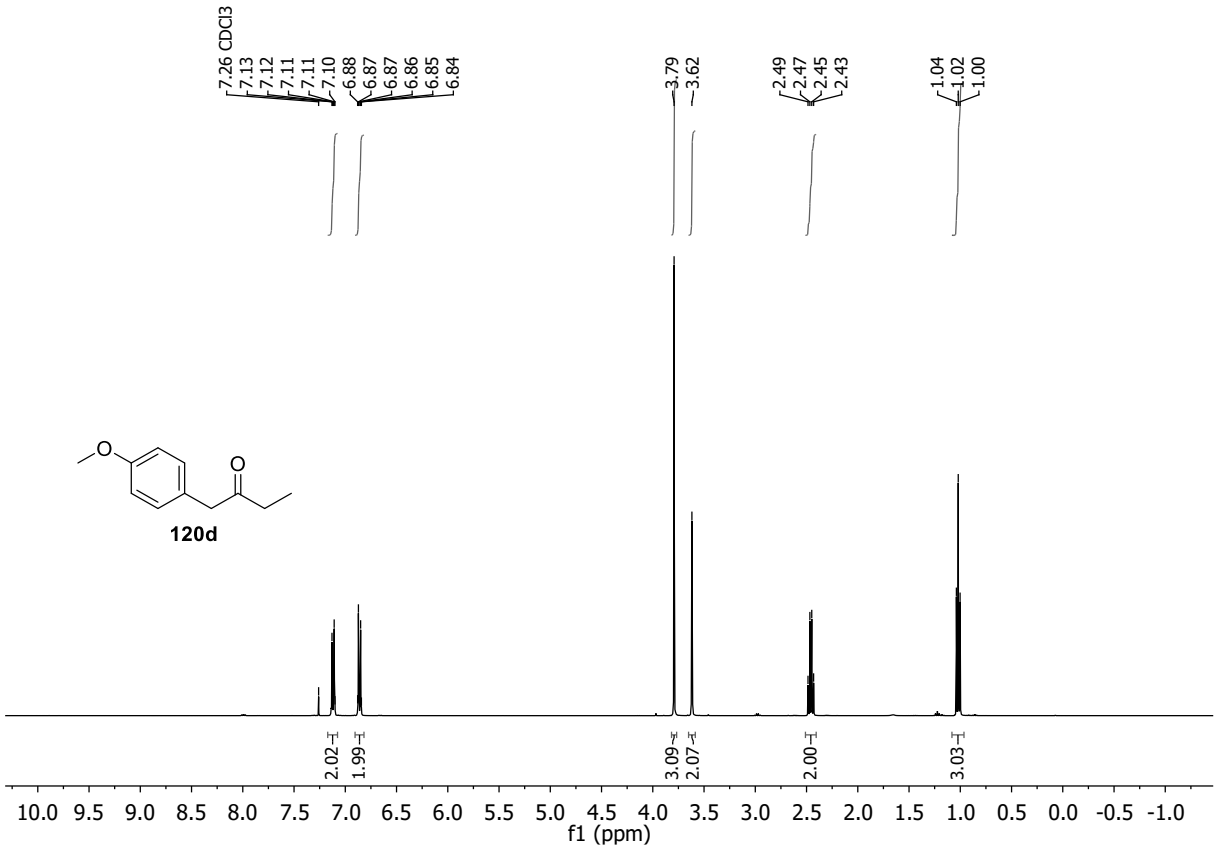
7.26 CDCl3
7.13
7.12
7.11
7.11
7.10
6.88
6.87
6.87
6.86
6.85
6.84
3.79
3.62
2.49
2.47
2.45
2.43
1.04
1.02
1.00
O
O
120d
2.02
1.99
3.09
2.07
2.00
3.03
10.0 9.5 9.0 8.5 8.0 7.5 7.0 6.5 6.0 5.5 5.0 4.5 4.0 3.5 3.0 2.5 2.0 1.5 1.0 0.5 0.0 -0.5 -1.0
f1 (ppm)

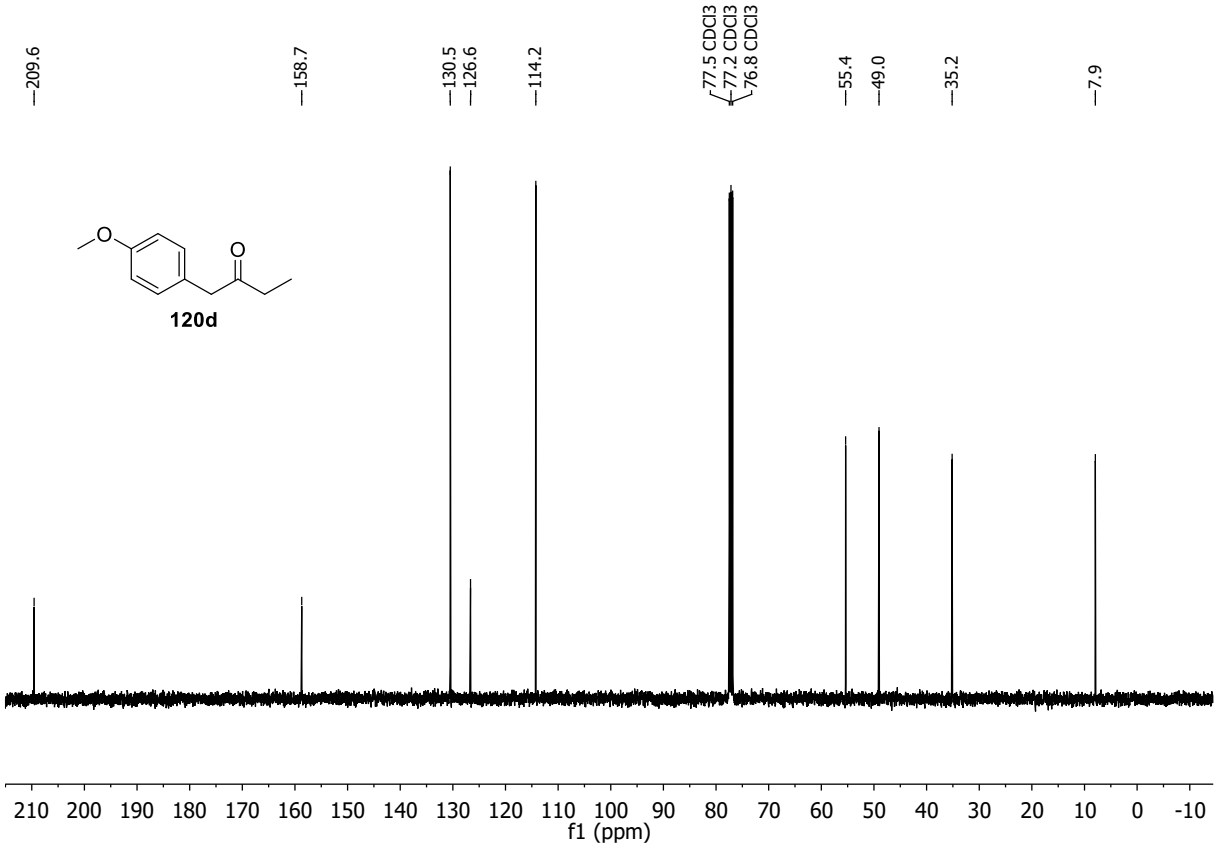
209.6
158.7
130.5
126.6
114.2
77.5 CDCl3
77.2 CDCl3
76.8 CDCl3
55.4
49.0
35.2
7.9
O
O
120d
210 200 190 180 170 160 150 140 130 120 110 100 90 80 70 60 50 40 30 20 10 0 -10
f1 (ppm)

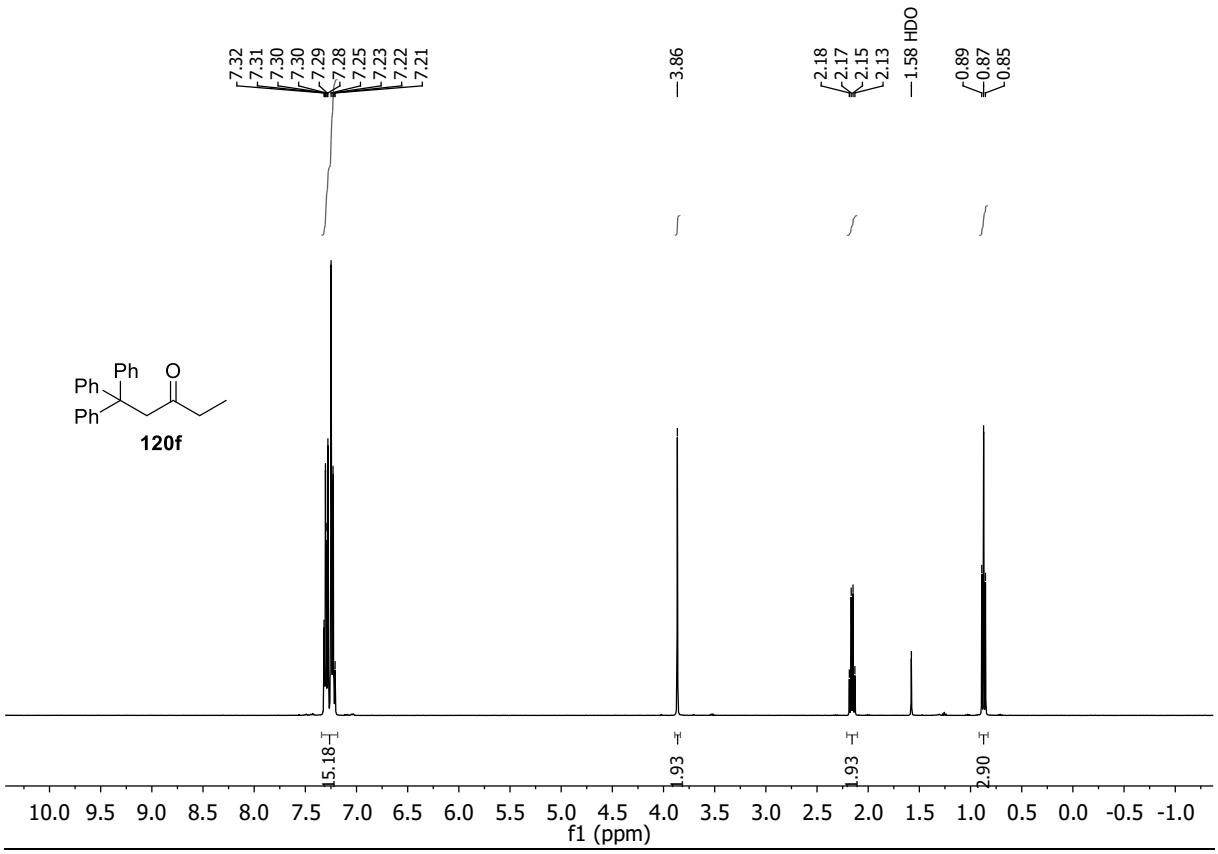
7.32
7.31
7.30
7.29
7.28
7.25
7.23
7.22
7.21
3.86
2.18
2.17
2.15
2.13
1.58 HDO
0.89
0.87
0.85
Ph
Ph
Ph
O
120f
15.18
1.93
1.93
2.90
10.0 9.5 9.0 8.5 8.0 7.5 7.0 6.5 6.0 5.5 5.0 4.5 4.0 3.5 3.0 2.5 2.0 1.5 1.0 0.5 0.0 -0.5 -1.0
f1 (ppm)

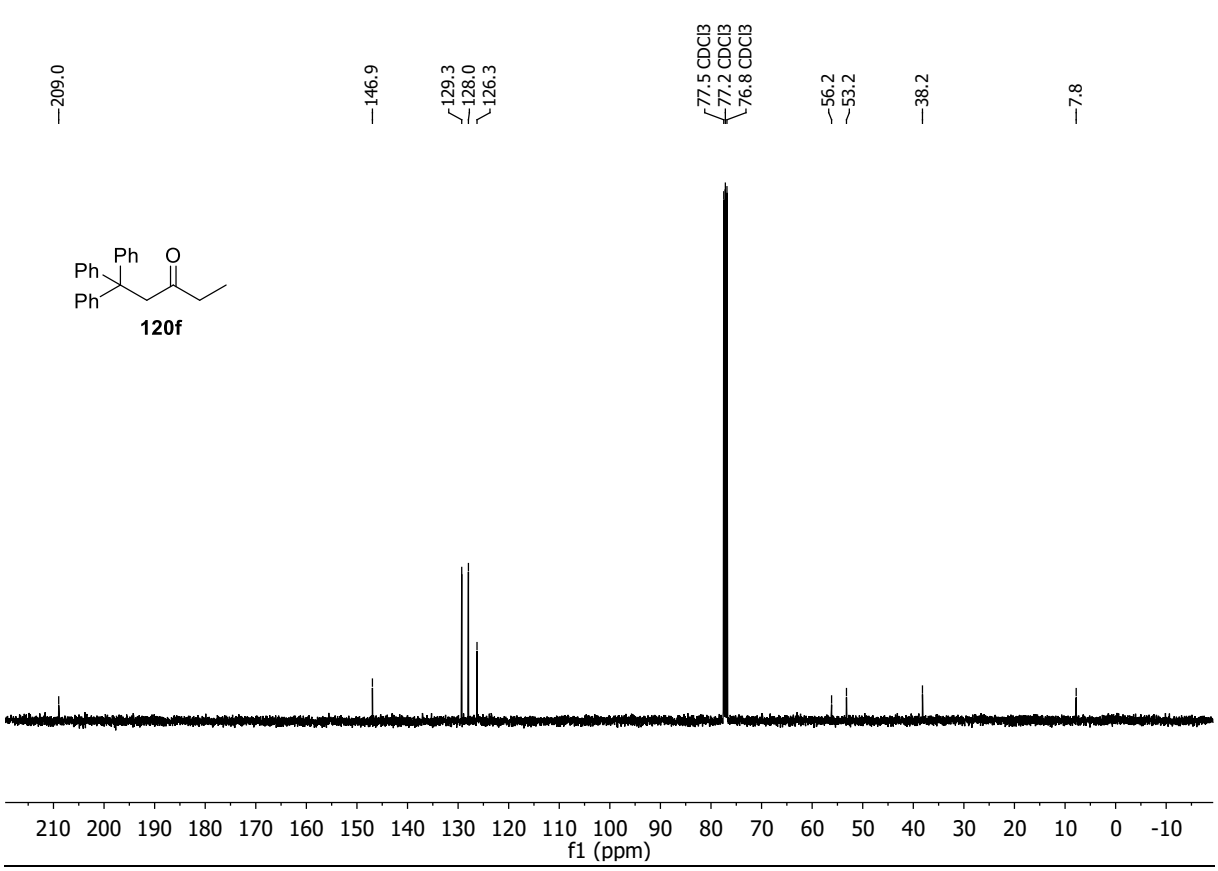
209.0
146.9
129.3
128.0
126.3
77.5 CDCl3
77.2 CDCl3
76.8 CDCl3
56.2
53.2
38.2
7.8
Ph
Ph
Ph
O
120f
210 200 190 180 170 160 150 140 130 120 110 100 90 80 70 60 50 40 30 20 10 0 -10
f1 (ppm)

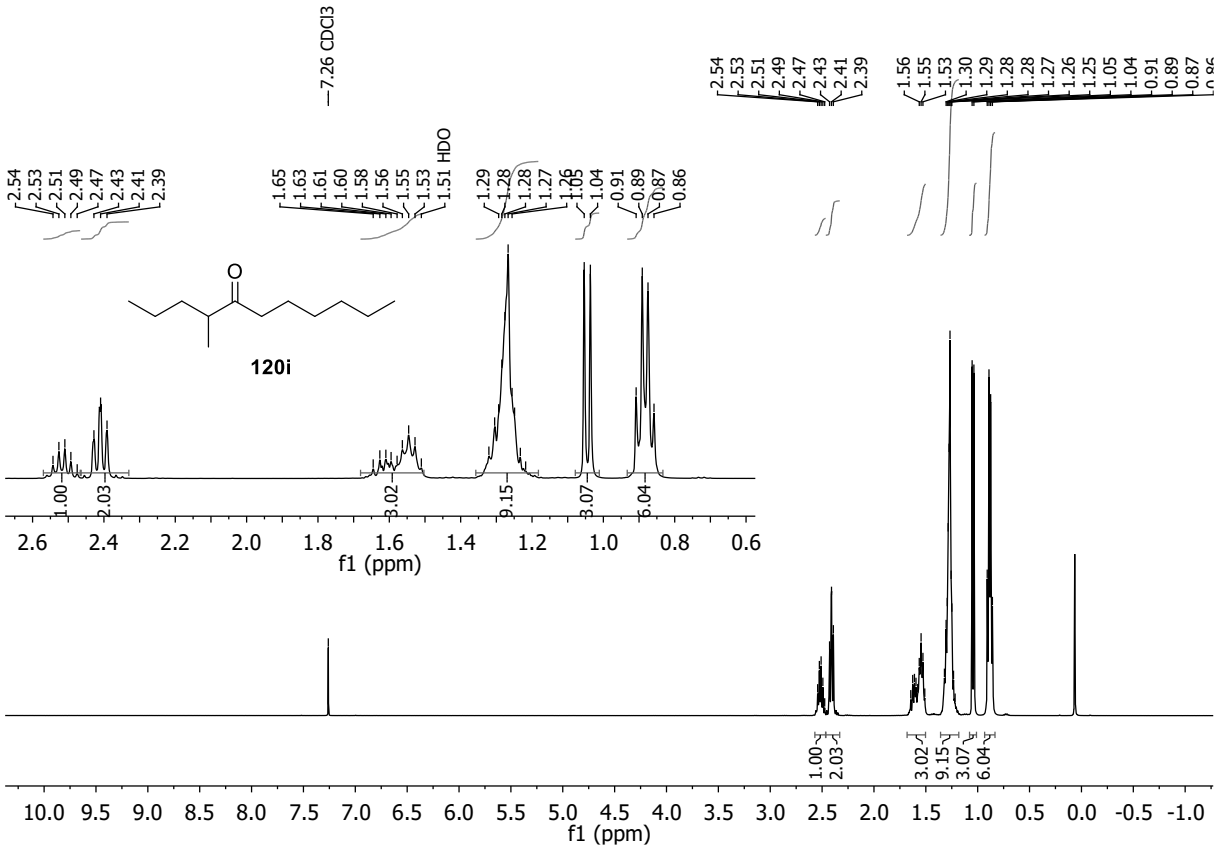
7.26 CDCl3
HDO
120i
f1 (ppm)

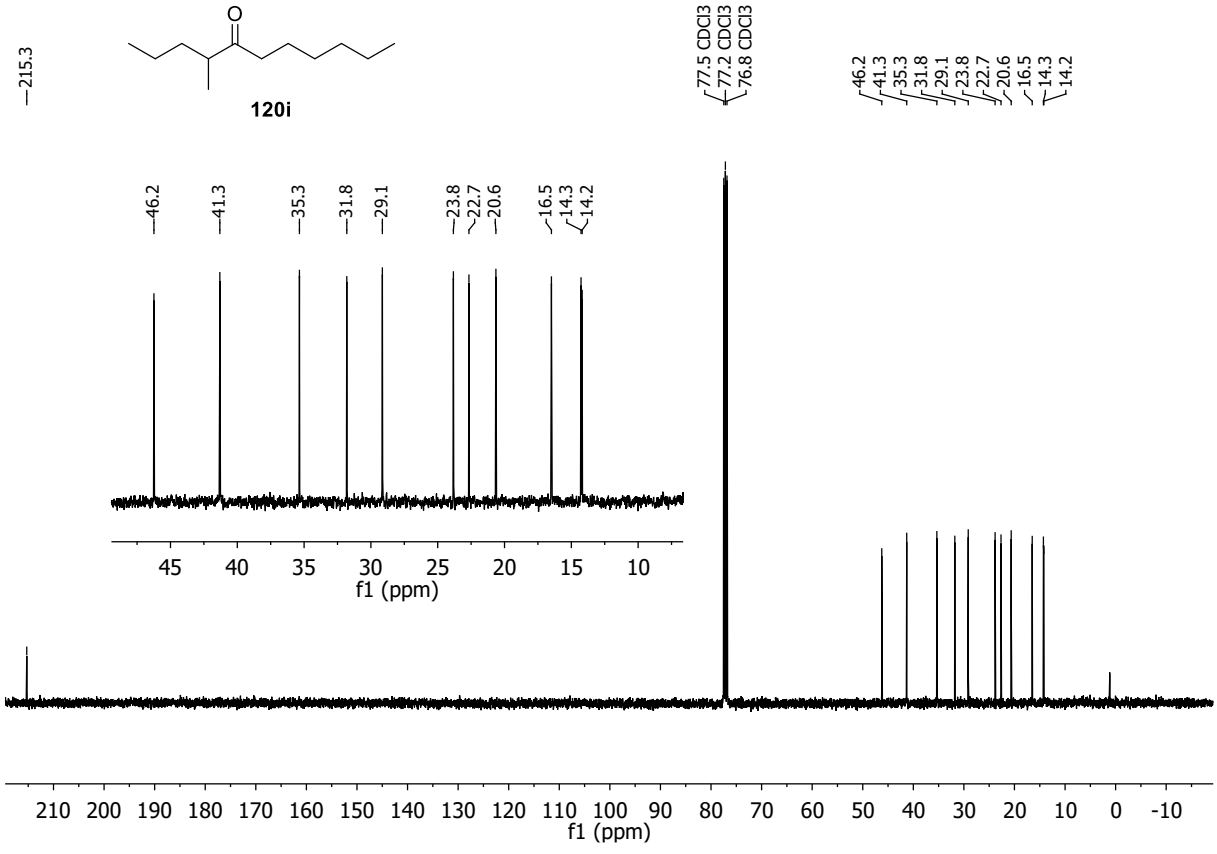
215.3
77.5 CDCl3
77.2 CDCl3
76.8 CDCl3
120i
f1 (ppm)

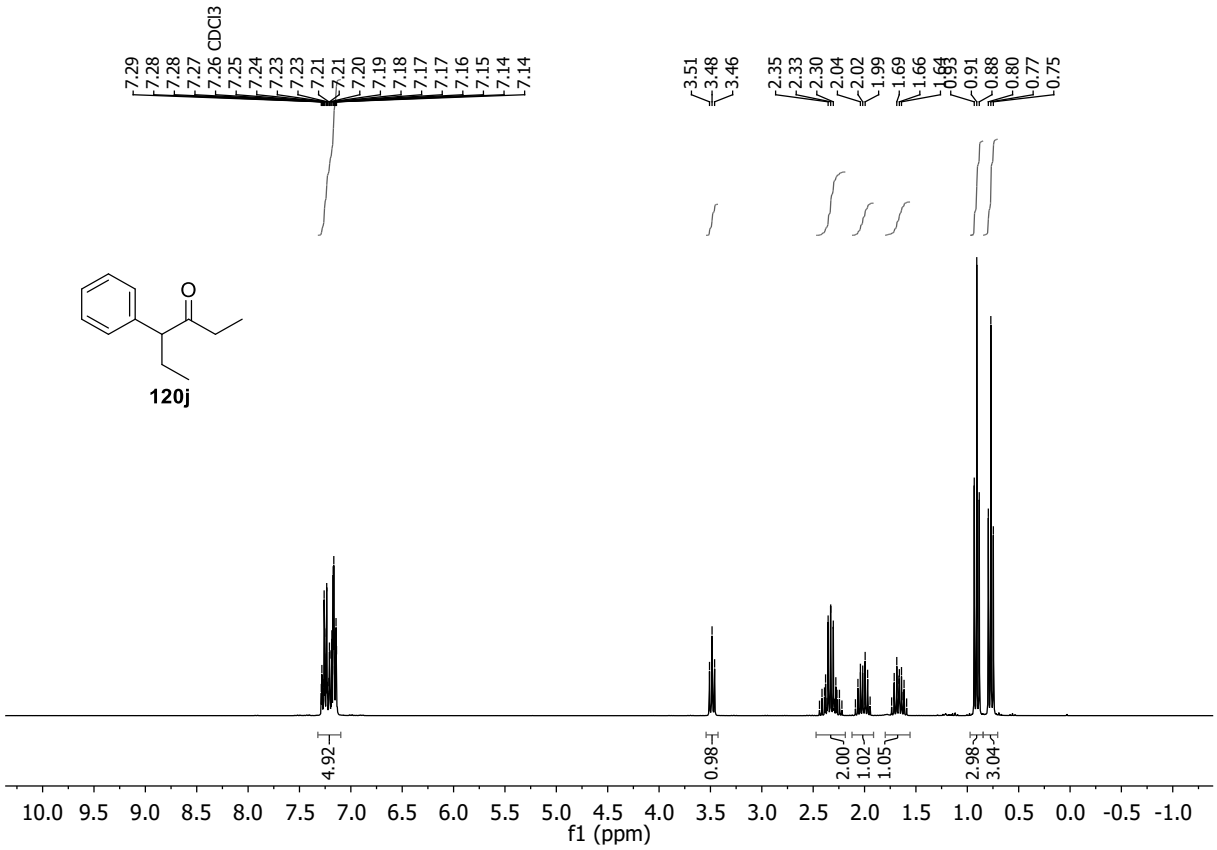
7.29
7.28
7.28
7.27
CDCl3
7.26
7.25
7.24
7.23
7.23
7.21
7.21
7.20
7.19
7.18
7.17
7.17
7.16
7.15
7.14
7.14
3.51
3.48
3.46
2.35
2.33
2.30
2.04
2.02
1.99
1.69
1.66
1.64
1.63
0.91
0.88
0.80
0.77
0.75
O
120j
4.92
0.98
2.00
1.02
1.05
2.98
3.04
10.0 9.5 9.0 8.5 8.0 7.5 7.0 6.5 6.0 5.5 5.0 4.5 4.0 3.5 3.0 2.5 2.0 1.5 1.0 0.5 0.0 -0.5 -1.0
f1 (ppm)

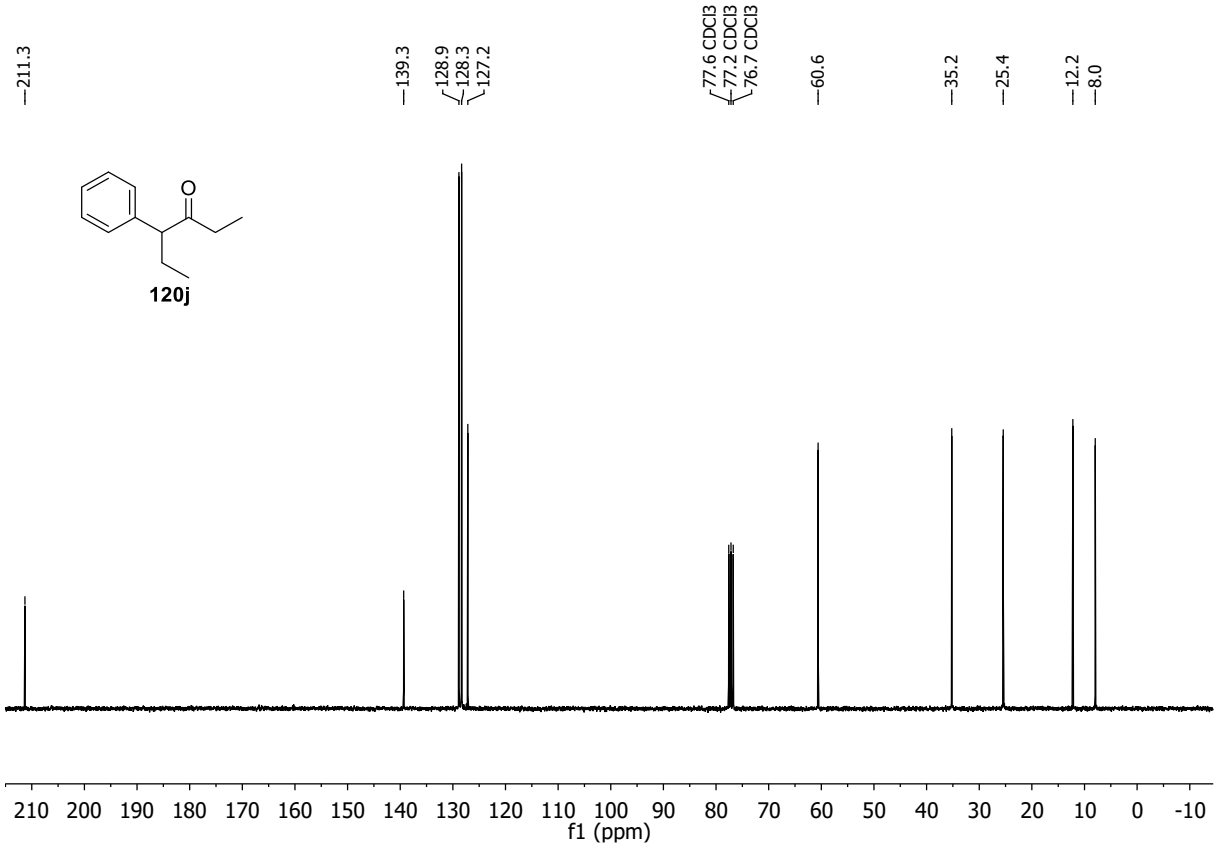
211.3
139.3
128.9
128.3
127.2
77.6 CDCl3
77.2 CDCl3
76.7 CDCl3
60.6
35.2
25.4
12.2
8.0
O
120j
210 200 190 180 170 160 150 140 130 120 110 100 90 80 70 60 50 40 30 20 10 0 -10
f1 (ppm)

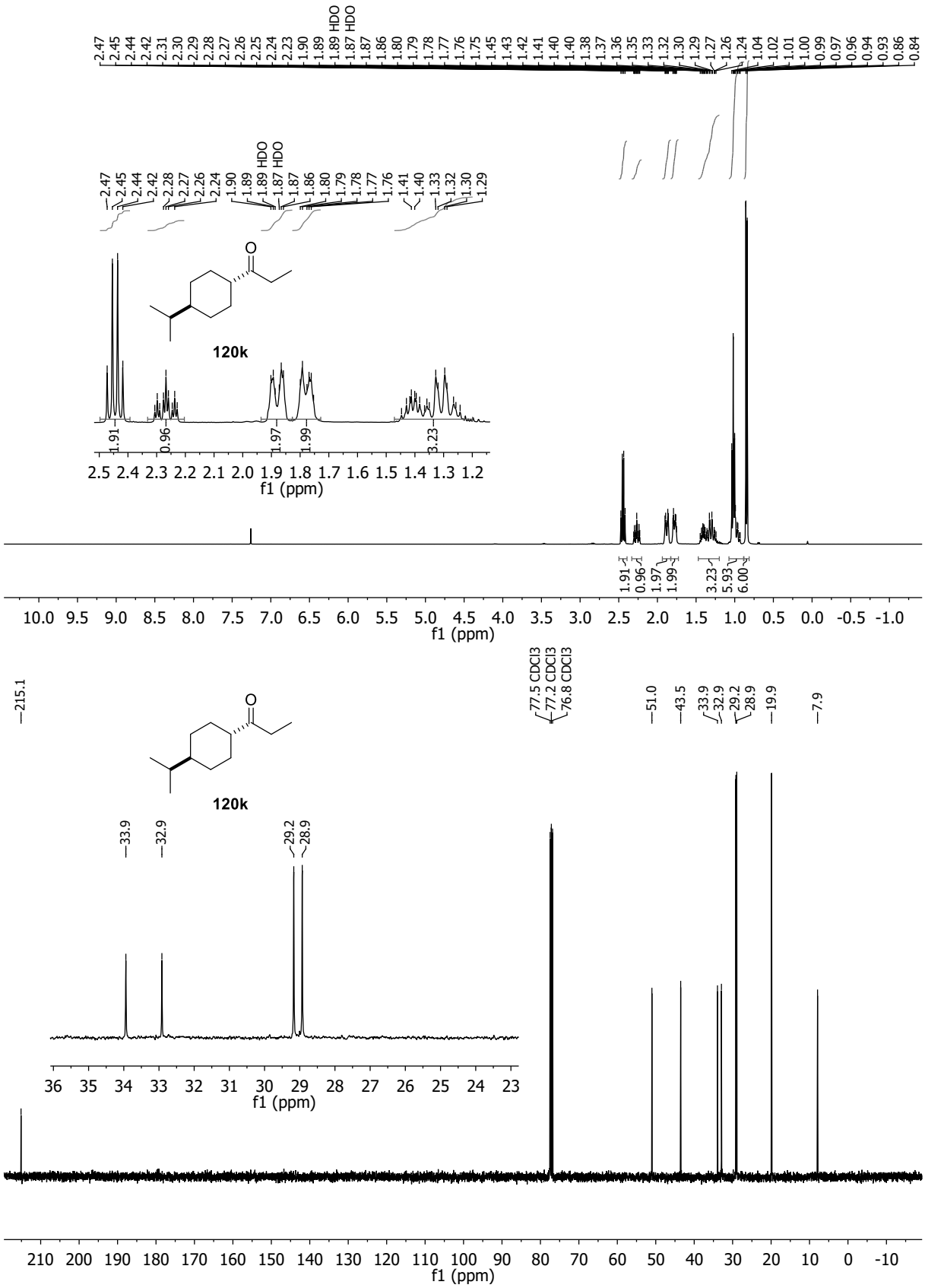
120k
f1 (ppm)
120k
f1 (ppm)
f1 (ppm)

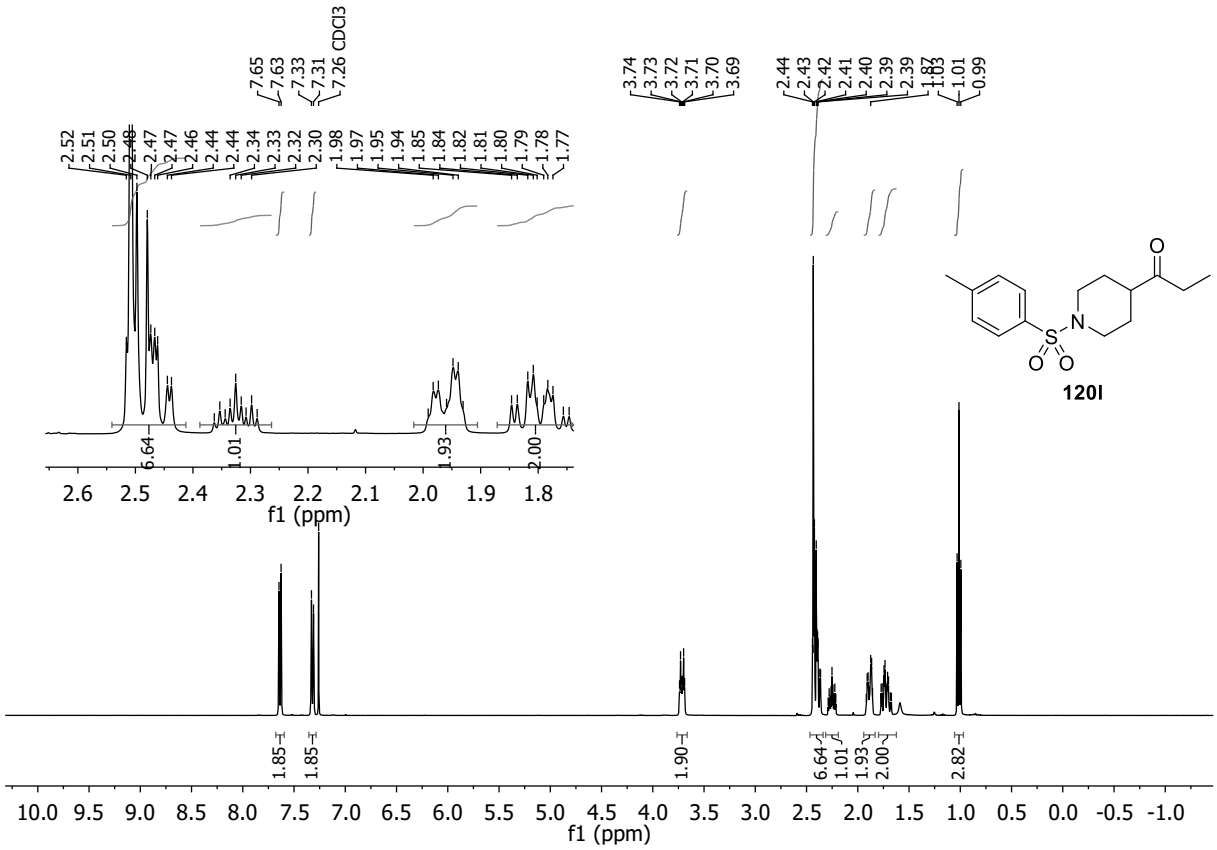
7.65
7.63
7.33
7.31
7.26 CDCl3
3.74
3.73
3.72
3.71
3.70
3.69
2.44
2.43
2.42
2.41
2.40
2.39
1.87
1.03
1.01
0.99
2.52
2.51
2.50
2.48
2.47
2.47
2.46
2.44
2.44
2.34
2.33
2.32
2.30
1.98
1.97
1.95
1.94
1.85
1.84
1.82
1.81
1.80
1.79
1.78
1.77
6.64
1.01
1.93
2.00
2.6 2.5 2.4 2.3 2.2 2.1 2.0 1.9 1.8
f1 (ppm)
O
N
S
O
O
120l
1.85
1.85
1.90
6.64
1.01
1.93
2.00
2.82
10.0 9.5 9.0 8.5 8.0 7.5 7.0 6.5 6.0 5.5 5.0 4.5 4.0 3.5 3.0 2.5 2.0 1.5 1.0 0.5 0.0 -0.5 -1.0
f1 (ppm)

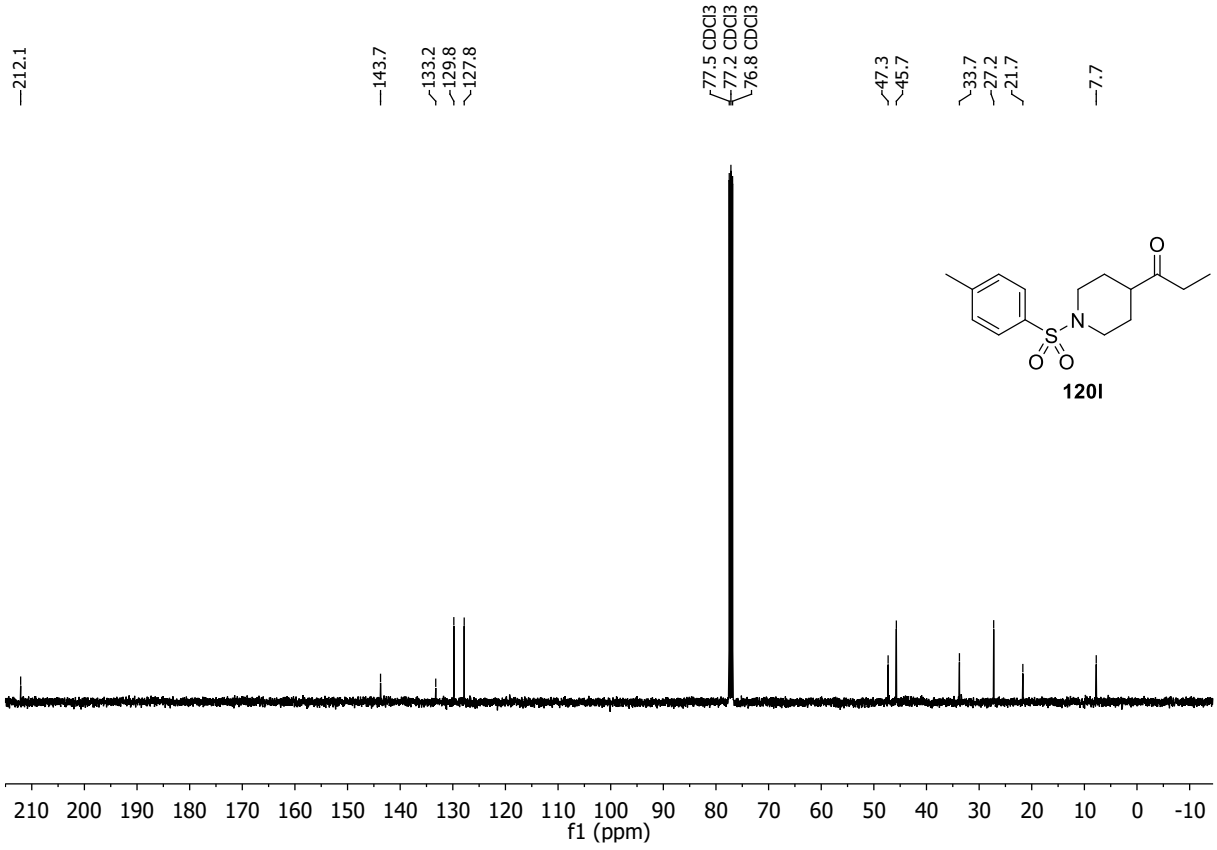
212.1
143.7
133.2
129.8
127.8
77.5 CDCl3
77.2 CDCl3
76.8 CDCl3
47.3
45.7
33.7
27.2
21.7
7.7
O
N
S
O
O
120l
210 200 190 180 170 160 150 140 130 120 110 100 90 80 70 60 50 40 30 20 10 0 -10
f1 (ppm)

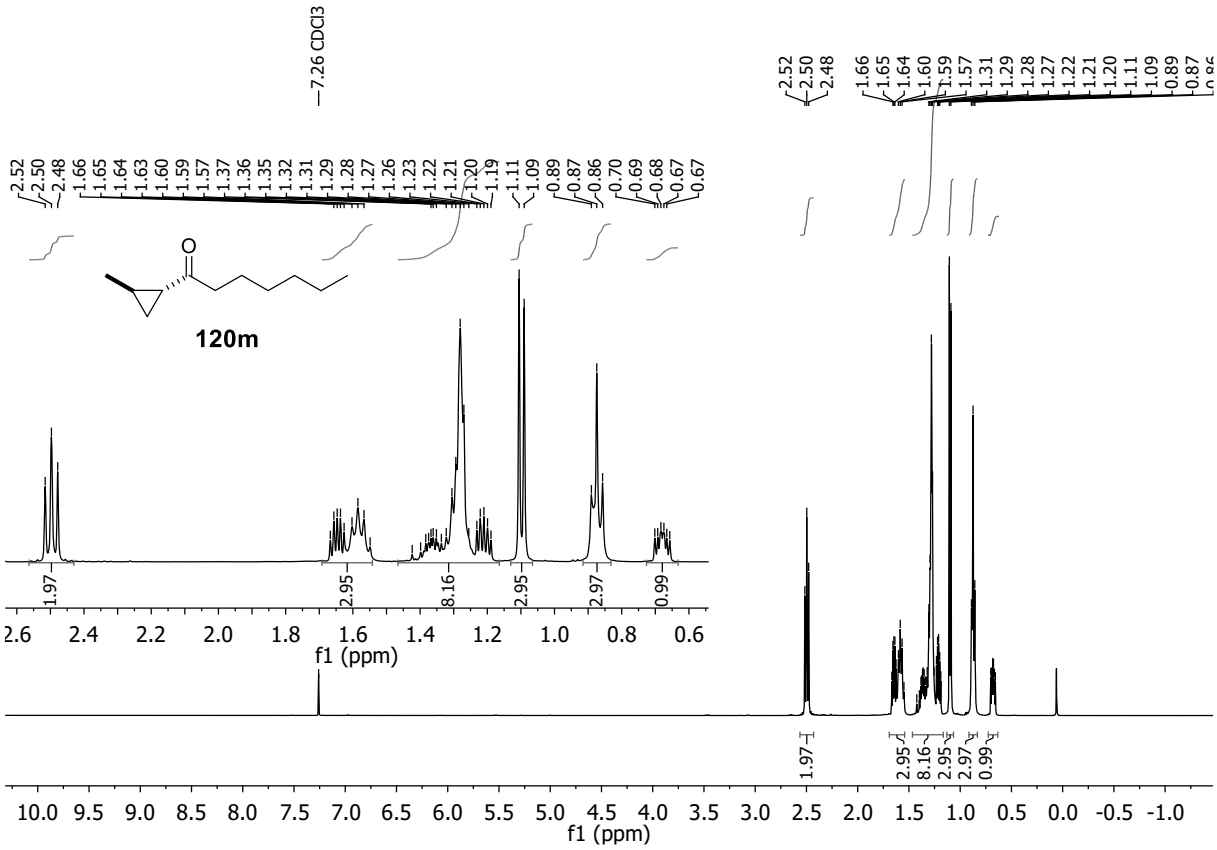
7.26 CDCl3
120m
f1 (ppm)

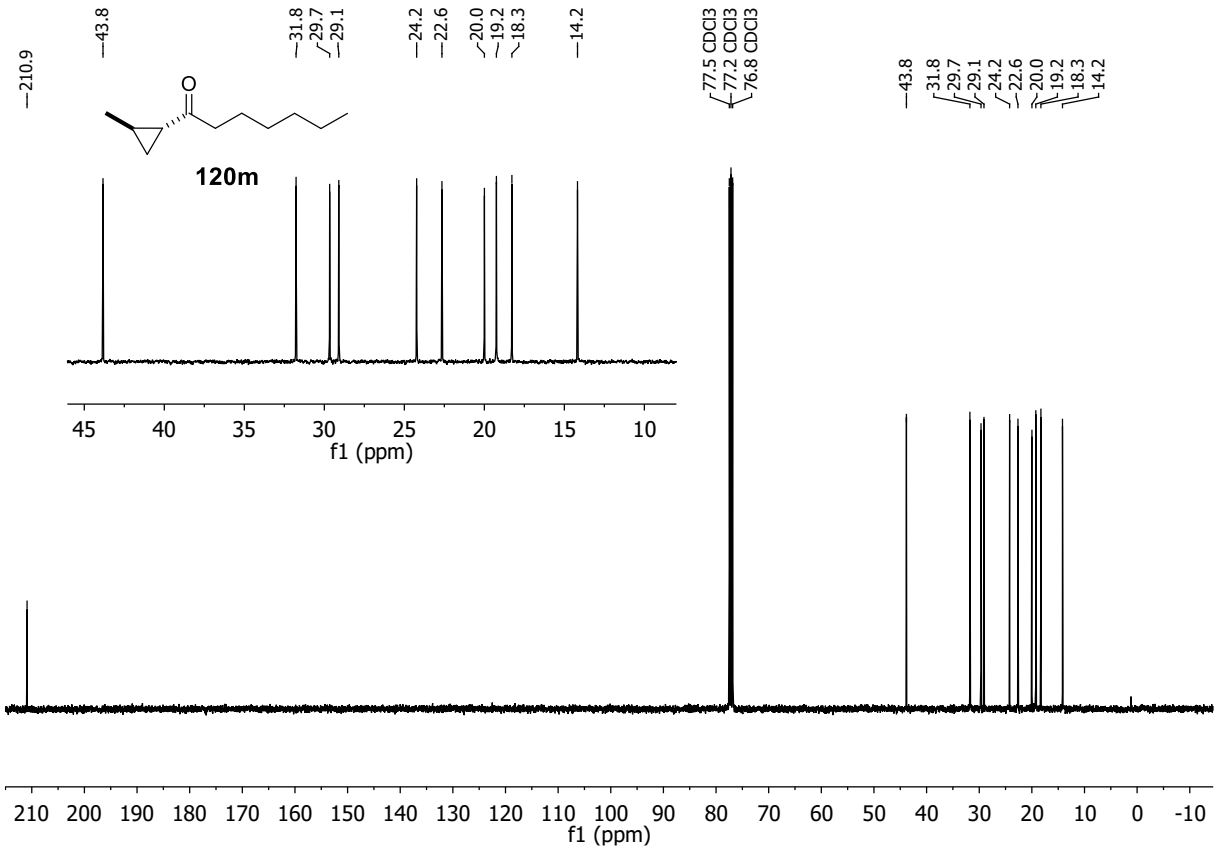
210.9
43.8
31.8
29.7
29.1
24.2
22.6
20.0
19.2
18.3
14.2
77.5 CDCl3
77.2 CDCl3
76.8 CDCl3
120m
f1 (ppm)

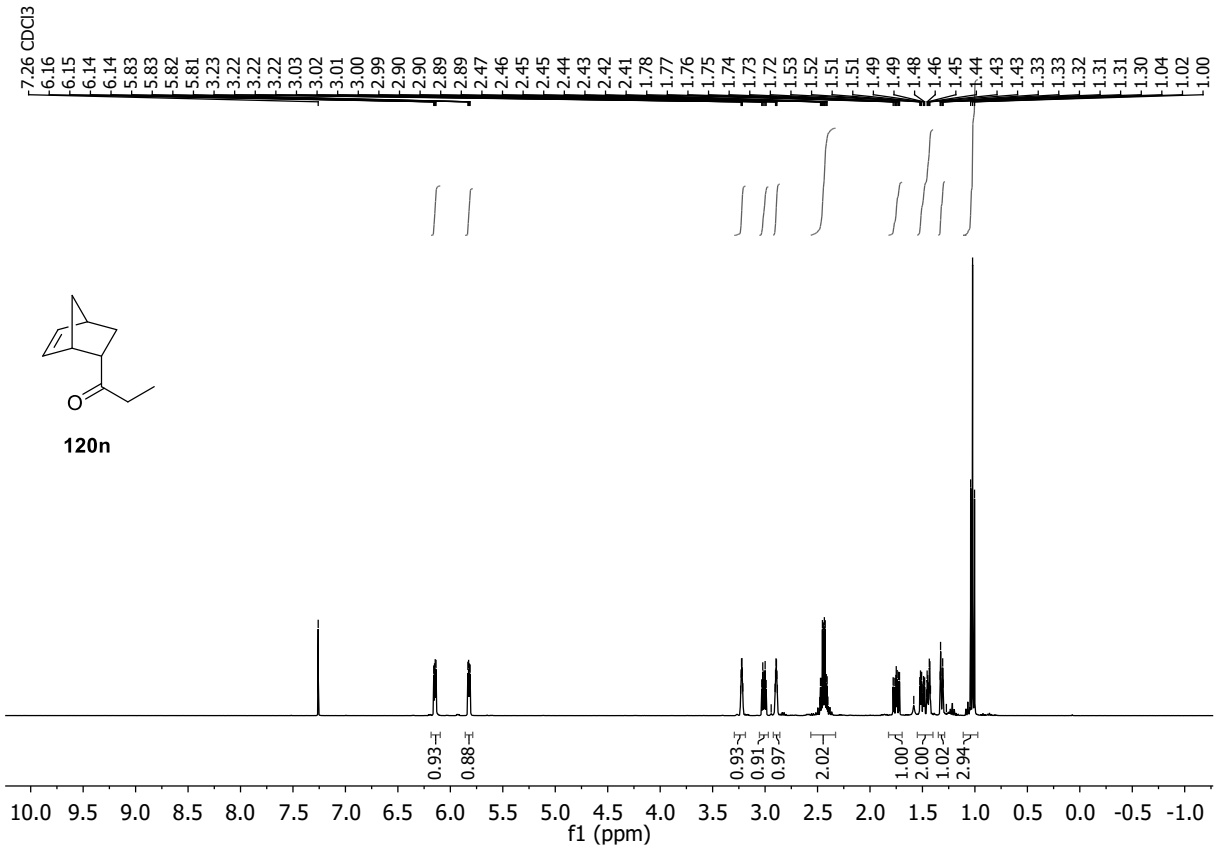
7.26 CDCl3
6.16 6.15 6.14 6.14 5.83 5.83 5.82 5.81 3.23 3.22 3.22 3.22 3.03 3.02 3.01 3.00 2.99 2.90 2.90 2.89 2.89 2.47 2.46 2.45 2.45 2.44 2.43 2.42 2.41 1.78 1.77 1.76 1.75 1.74 1.73 1.72 1.53 1.52 1.51 1.51 1.49 1.49 1.48 1.46 1.45 1.44 1.43 1.43 1.33 1.33 1.32 1.31 1.31 1.30 1.04 1.02 1.00
O
120n
0.93 0.88 0.93 0.91 0.97 2.02 1.00 2.00 1.02 2.94
10.0 9.5 9.0 8.5 8.0 7.5 7.0 6.5 6.0 5.5 5.0 4.5 4.0 3.5 3.0 2.5 2.0 1.5 1.0 0.5 0.0 -0.5 -1.0
f1 (ppm)

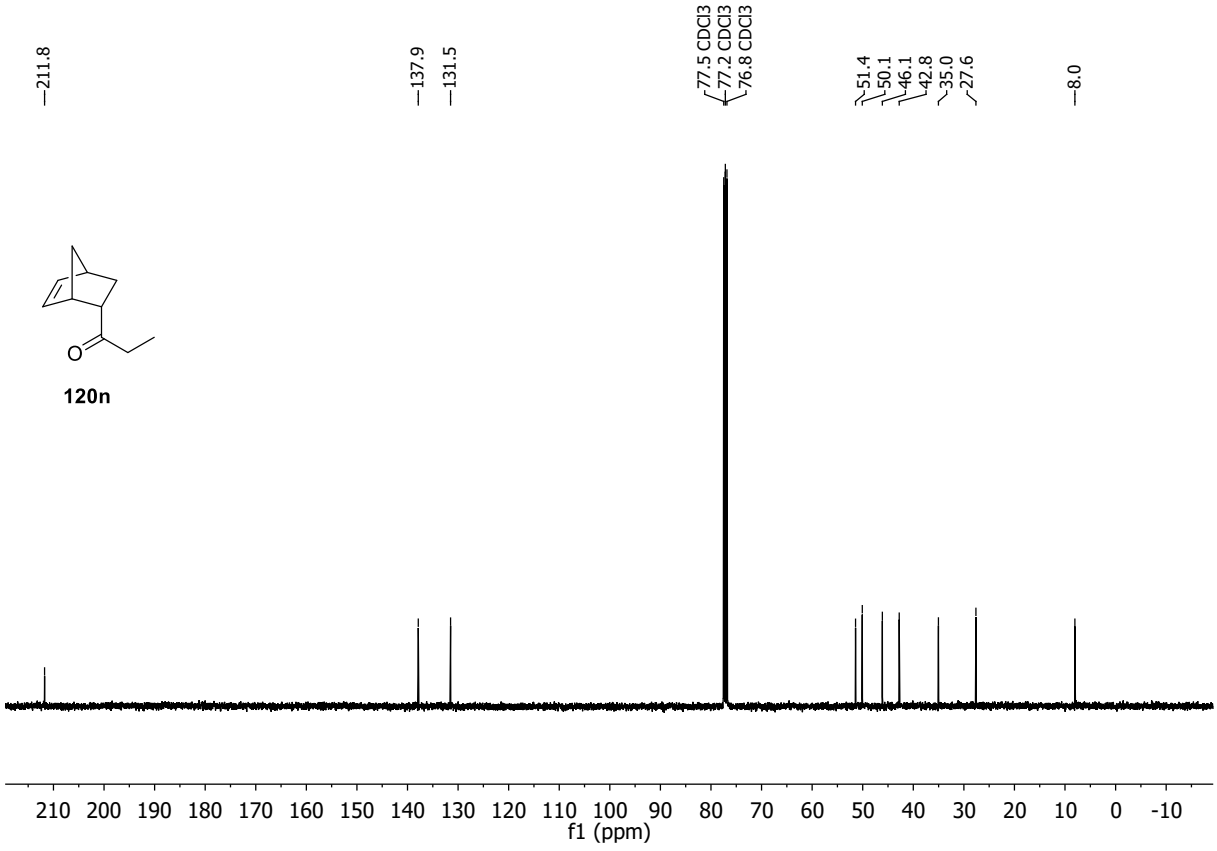
211.8
137.9
131.5
77.5 CDCl3
77.2 CDCl3
76.8 CDCl3
51.4
50.1
46.1
42.8
35.0
27.6
8.0
O
120n
210 200 190 180 170 160 150 140 130 120 110 100 90 80 70 60 50 40 30 20 10 0 -10
f1 (ppm)

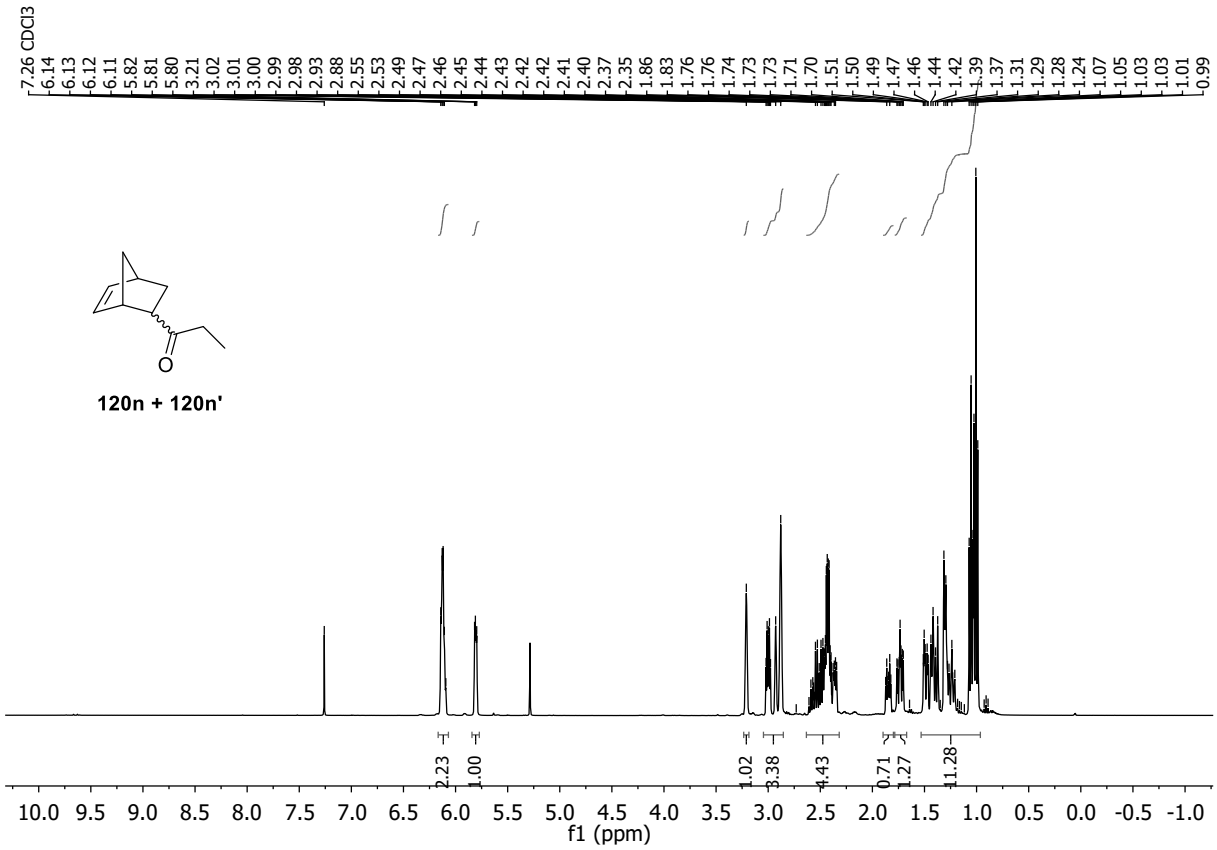
7.26 CDCl3
6.14
6.13
6.12
6.11
5.82
5.81
5.80
3.21
3.02
3.01
3.00
2.99
2.98
2.93
2.88
2.55
2.53
2.49
2.47
2.46
2.45
2.44
2.43
2.42
2.42
2.41
2.40
2.37
2.35
1.86
1.83
1.76
1.76
1.74
1.73
1.73
1.71
1.70
1.51
1.50
1.49
1.47
1.46
1.44
1.42
1.39
1.37
1.31
1.29
1.28
1.24
1.07
1.05
1.03
1.03
1.01
0.99
O
120n + 120n'
2.23
1.00
1.02
3.38
4.43
0.71
1.27
11.28
10.0 9.5 9.0 8.5 8.0 7.5 7.0 6.5 6.0 5.5 5.0 4.5 4.0 3.5 3.0 2.5 2.0 1.5 1.0 0.5 0.0 -0.5 -1.0
f1 (ppm)

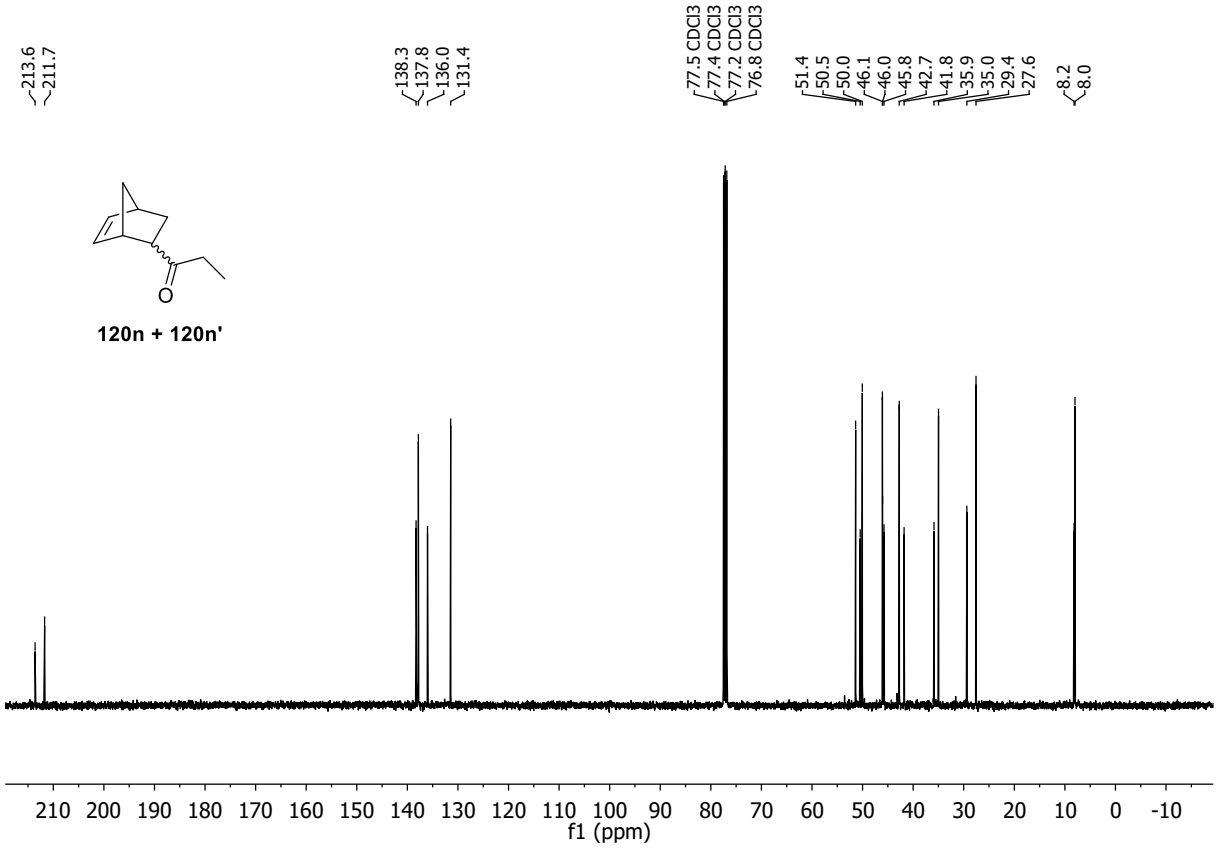
213.6
211.7
138.3
137.8
136.0
131.4
77.5 CDCl3
77.4 CDCl3
77.2 CDCl3
76.8 CDCl3
51.4
50.5
50.0
46.1
46.0
45.8
42.7
41.8
35.9
35.0
29.4
27.6
8.2
8.0
O
120n + 120n'
210 200 190 180 170 160 150 140 130 120 110 100 90 80 70 60 50 40 30 20 10 0 -10
f1 (ppm)

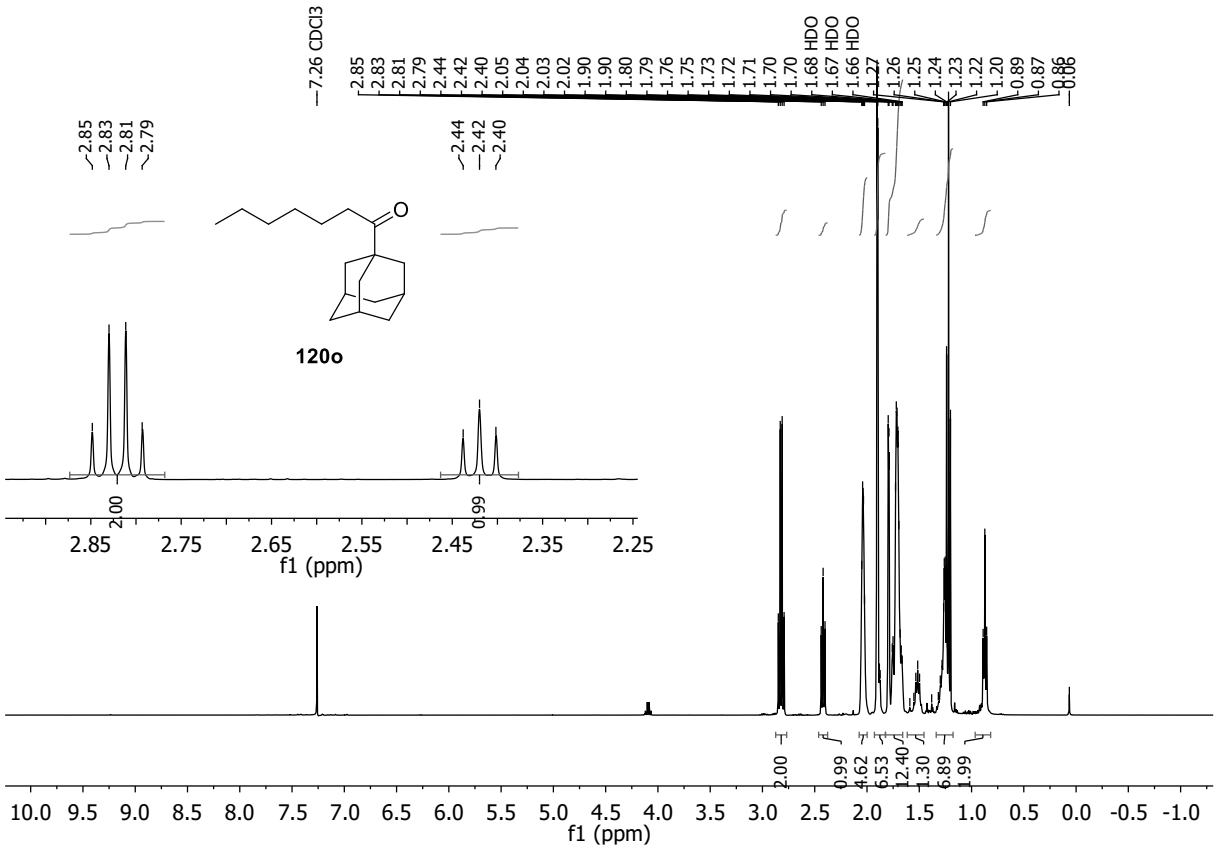
7.26 CDCl3
2.85
2.83
2.81
2.79
2.44
2.42
2.40
2.05
2.04
2.03
2.02
1.90
1.80
1.79
1.76
1.75
1.73
1.72
1.71
1.70
1.68 HDO
1.67 HDO
1.66 HDO
1.27
1.26
1.25
1.24
1.23
1.22
1.20
0.89
0.87
0.86
0.85
O
120o
2.00
0.99
2.85 2.75 2.65 2.55 2.45 2.35 2.25
f1 (ppm)
2.00
0.99
4.62
6.53
12.40
1.30
6.89
1.99
10.0 9.5 9.0 8.5 8.0 7.5 7.0 6.5 6.0 5.5 5.0 4.5 4.0 3.5 3.0 2.5 2.0 1.5 1.0 0.5 0.0 -0.5 -1.0
f1 (ppm)

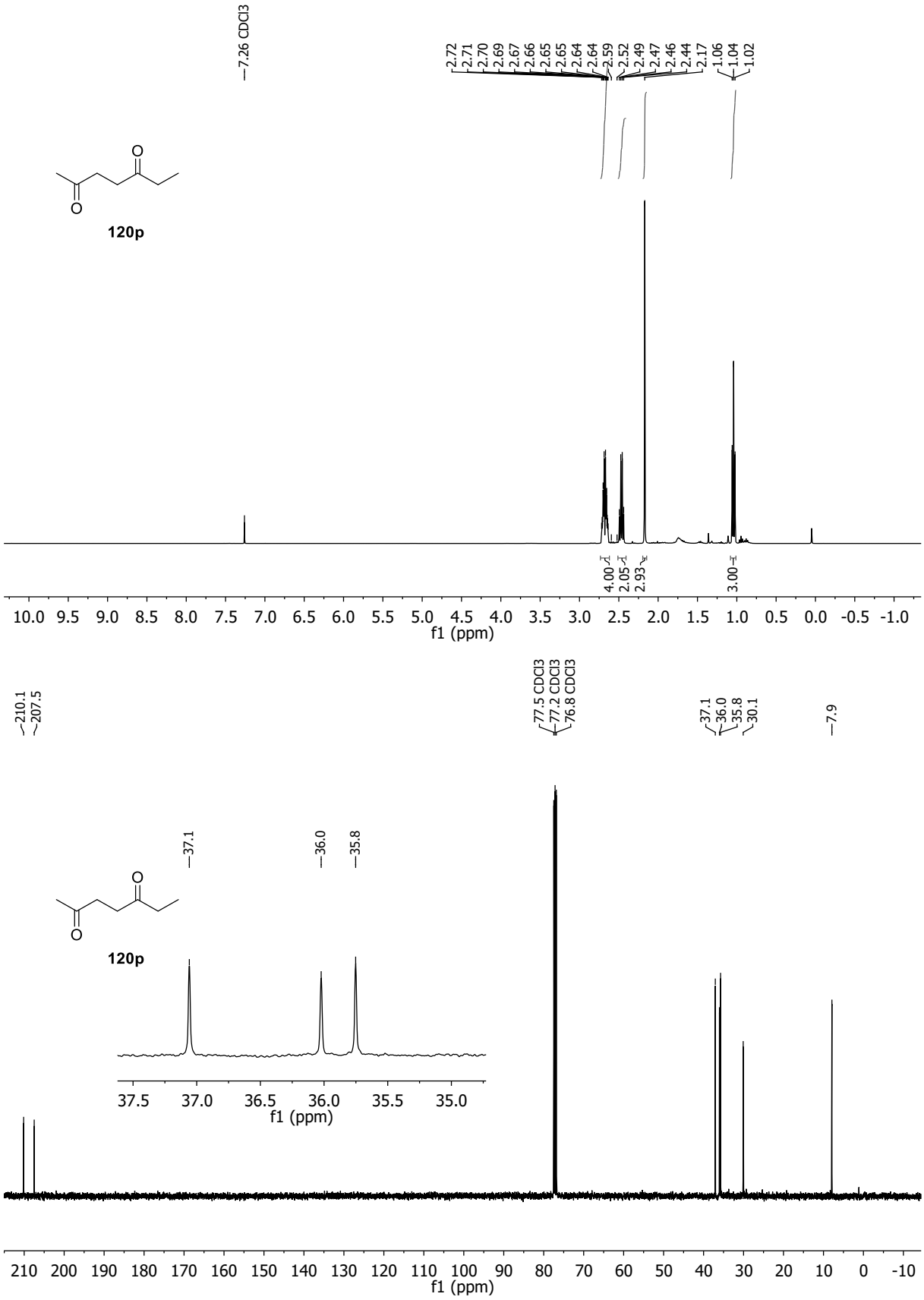
7.26 CDCl3
2.72
2.71
2.70
2.69
2.67
2.66
2.65
2.65
2.64
2.64
2.59
2.52
2.49
2.47
2.46
2.44
2.17
1.06
1.04
1.02
120p
4.00
2.05
2.93
3.00
f1 (ppm)
210.1
207.5
77.5 CDCl3
77.2 CDCl3
76.8 CDCl3
37.1
36.0
35.8
30.1
7.9
120p
f1 (ppm)
f1 (ppm)

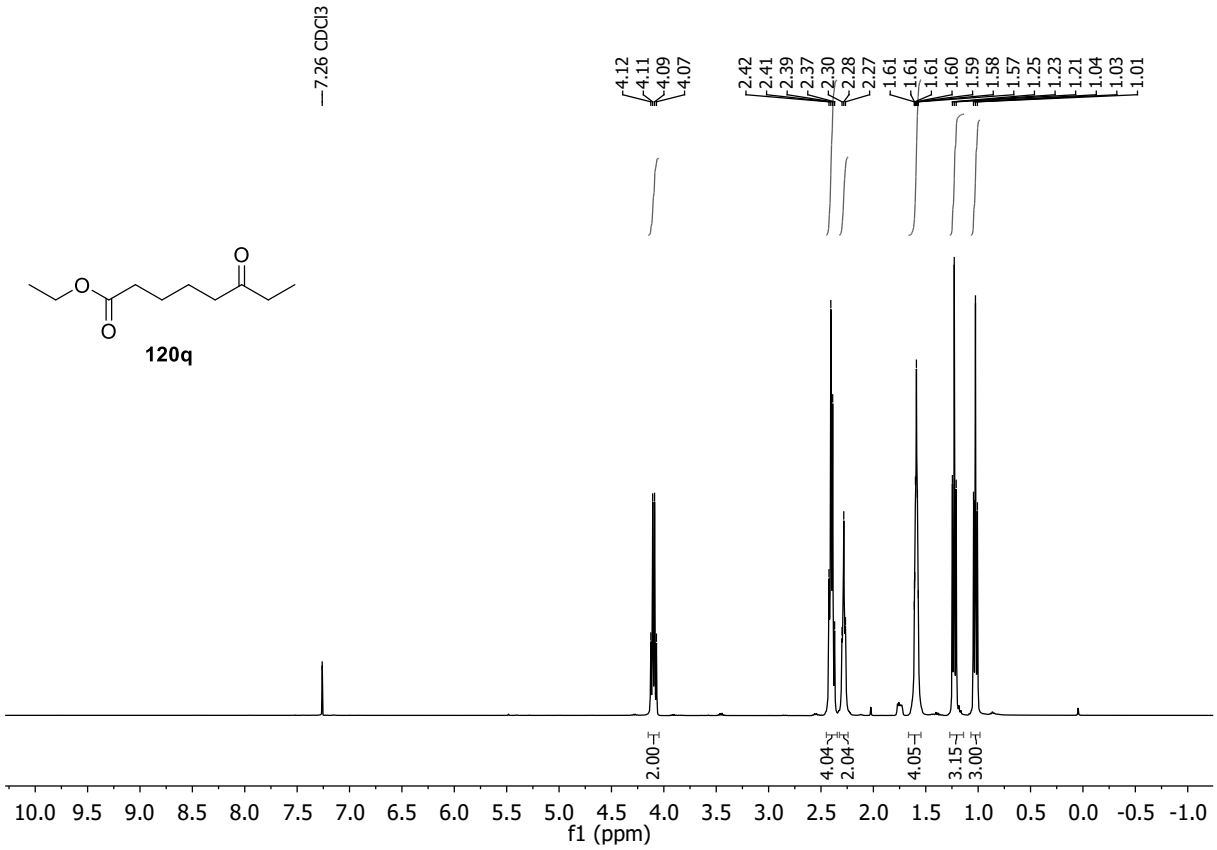
7.26 CDCl3
4.12
4.11
4.09
4.07
2.42
2.41
2.39
2.37
2.30
2.28
2.27
1.61
1.61
1.60
1.59
1.58
1.57
1.25
1.23
1.21
1.04
1.03
1.01
O
O
O
120q
2.00
4.04
2.04
4.05
3.15
3.00
10.0 9.5 9.0 8.5 8.0 7.5 7.0 6.5 6.0 5.5 5.0 4.5 4.0 3.5 3.0 2.5 2.0 1.5 1.0 0.5 0.0 -0.5 -1.0
f1 (ppm)

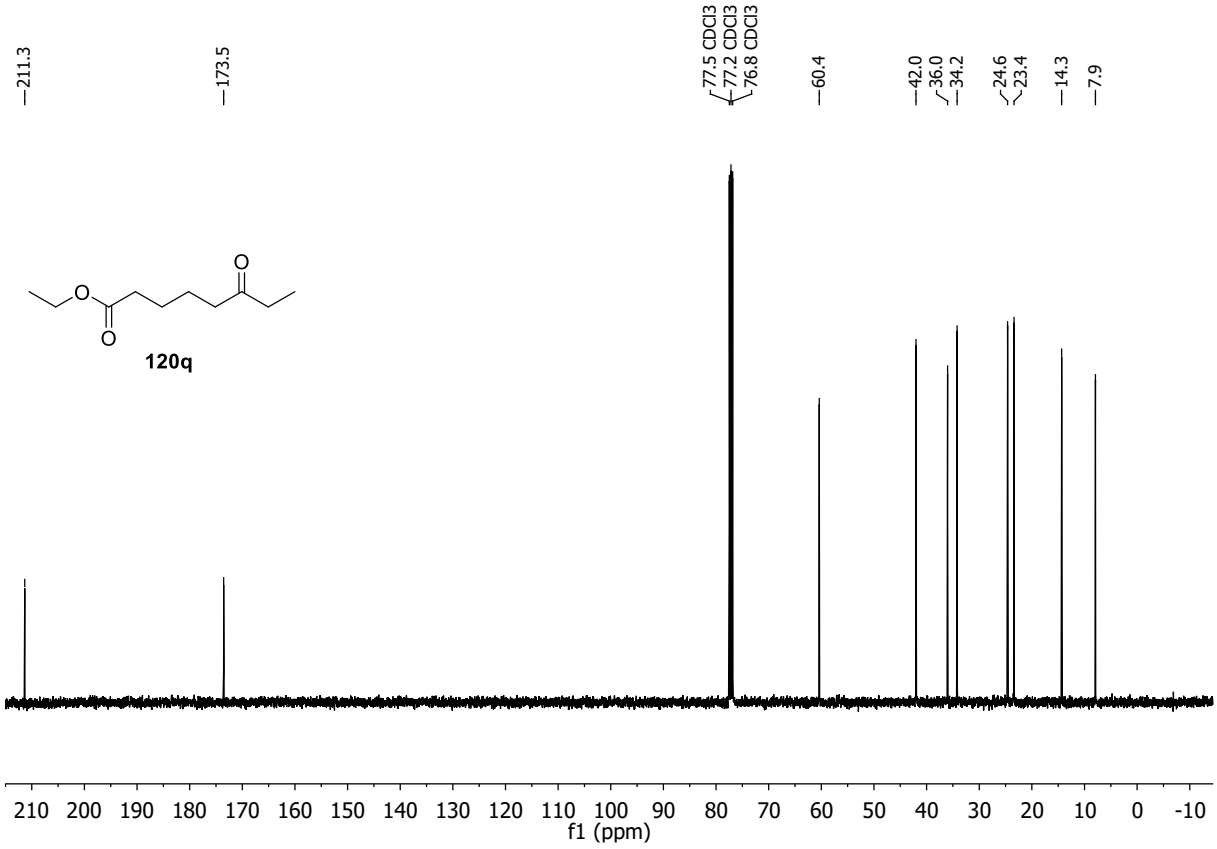
211.3
173.5
77.5 CDCl3
77.2 CDCl3
76.8 CDCl3
60.4
42.0
36.0
34.2
24.6
23.4
14.3
7.9
O
O
O
120q
210 200 190 180 170 160 150 140 130 120 110 100 90 80 70 60 50 40 30 20 10 0 -10
f1 (ppm)

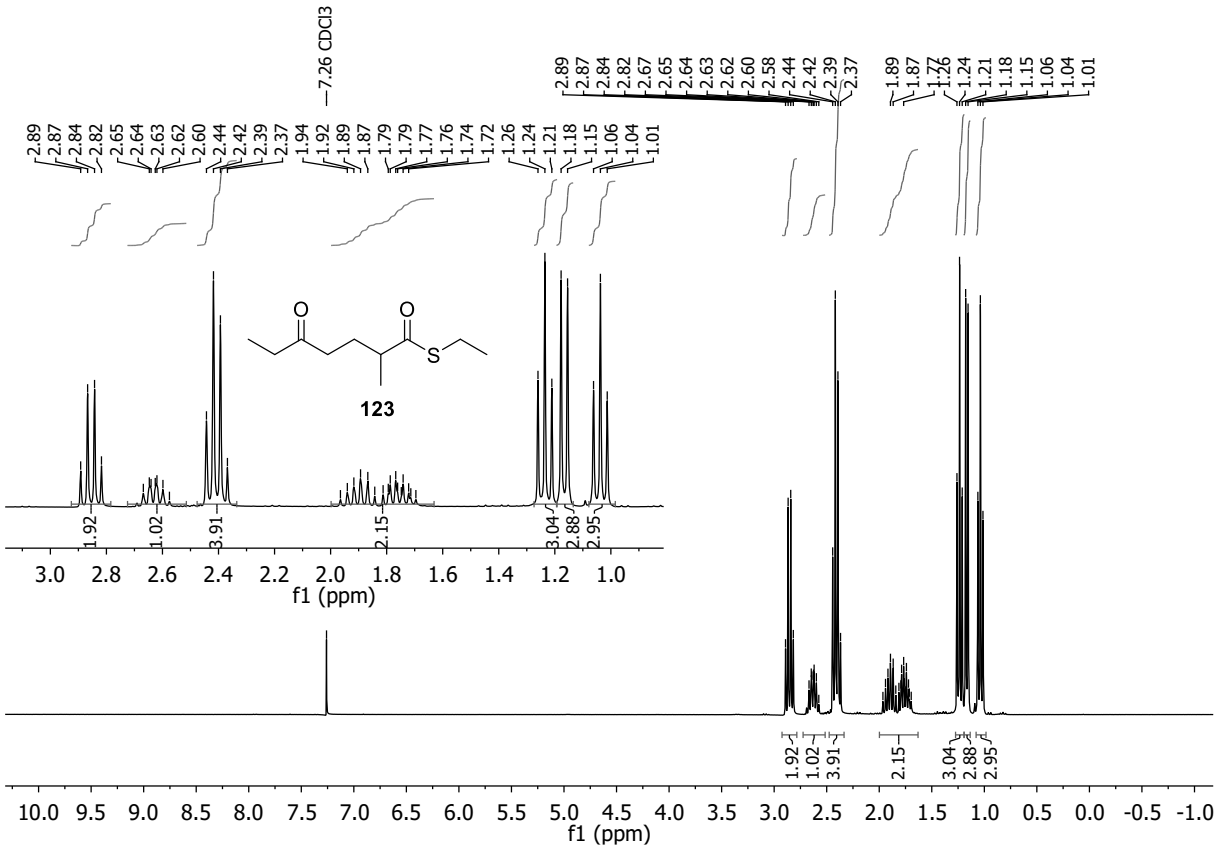
7.26 CDCl3
123
f1 (ppm)

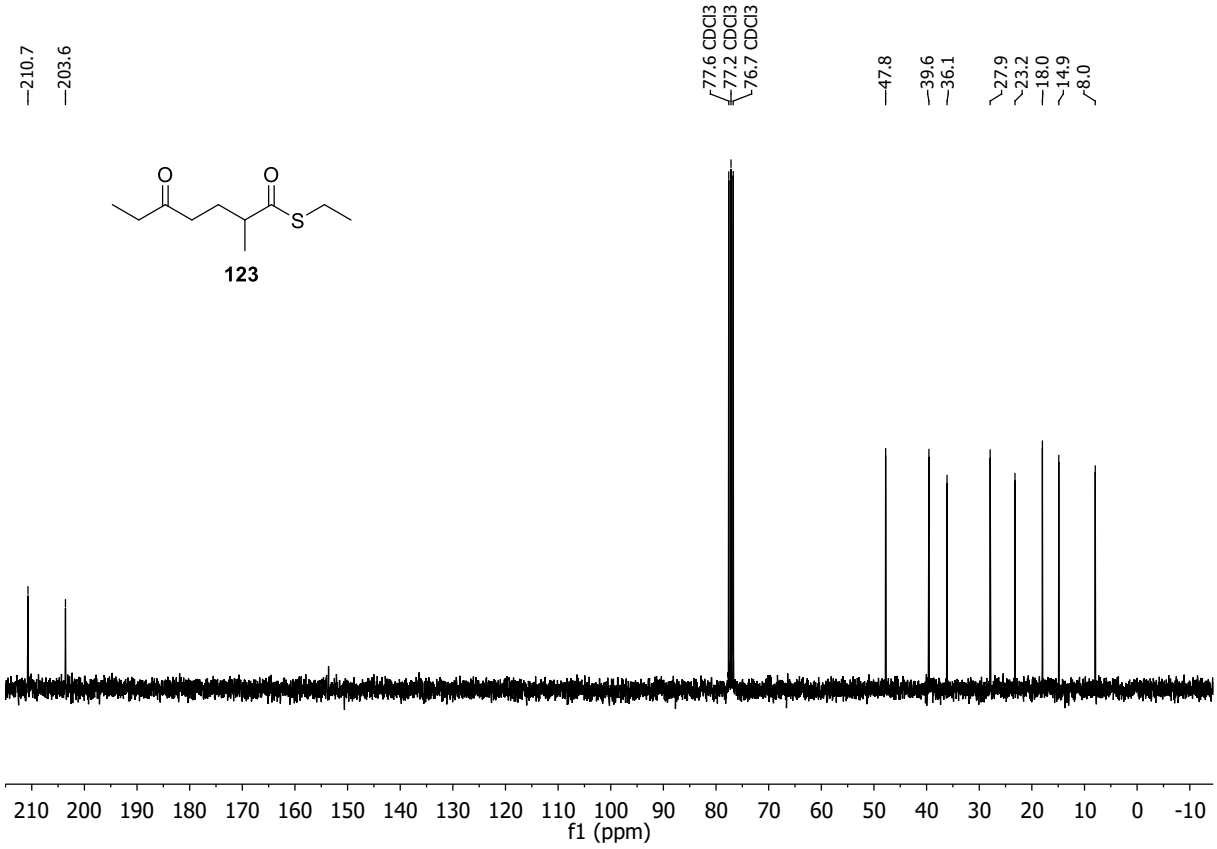
210.7
203.6
77.6 CDCl3
77.2 CDCl3
76.7 CDCl3
47.8
39.6
36.1
27.9
23.2
18.0
14.9
8.0
123
f1 (ppm)

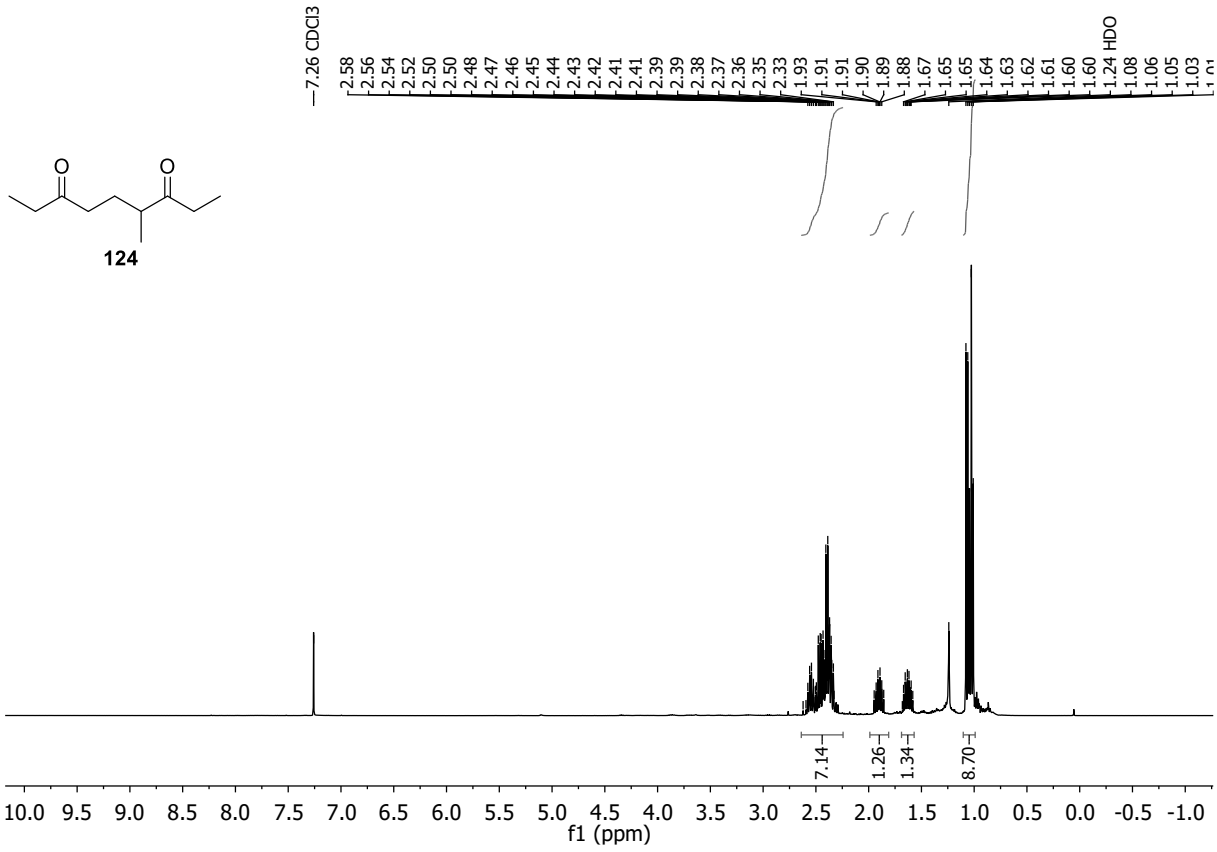
7.26 CDCl3
HDO
7.14
1.26
1.34
8.70
f1 (ppm)

124

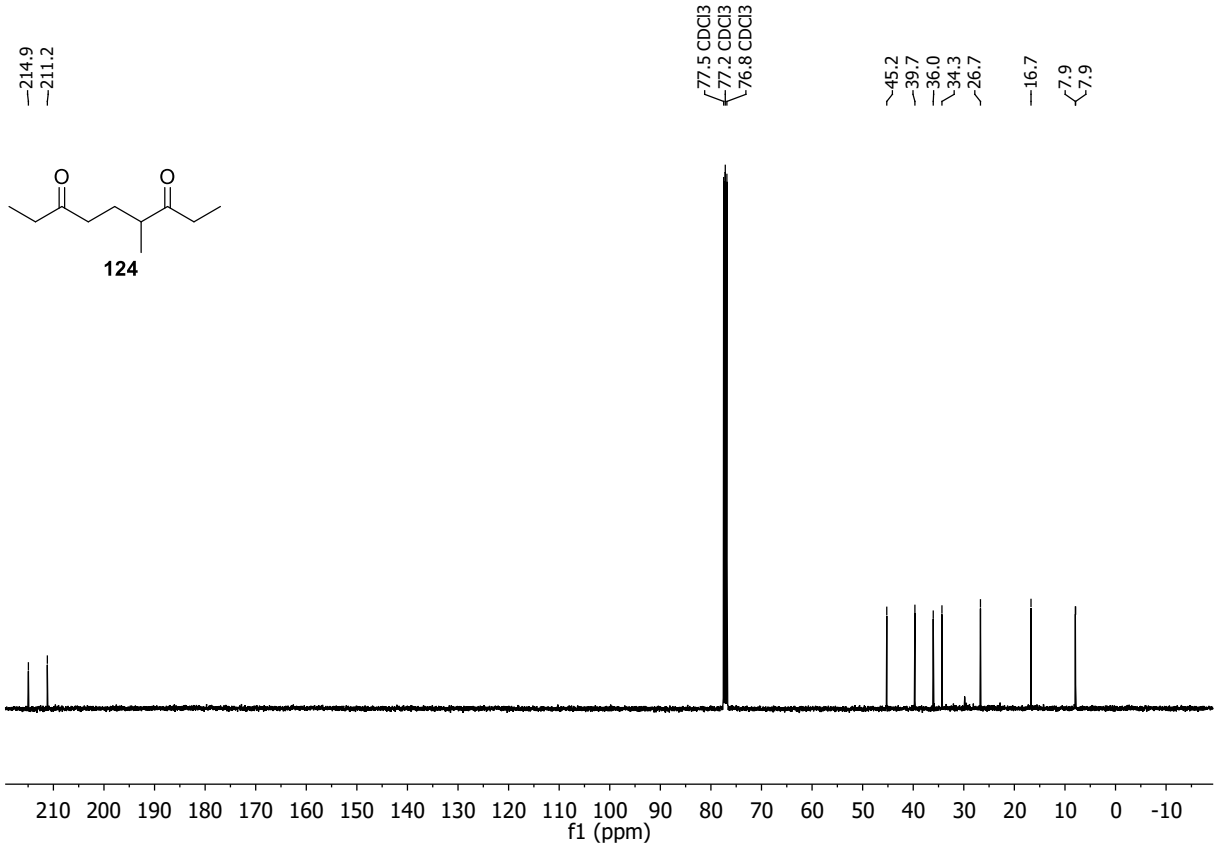
214.9
211.2
77.5 CDCl3
77.2 CDCl3
76.8 CDCl3
45.2
39.7
36.0
34.3
26.7
16.7
7.9
7.9
f1 (ppm)

124

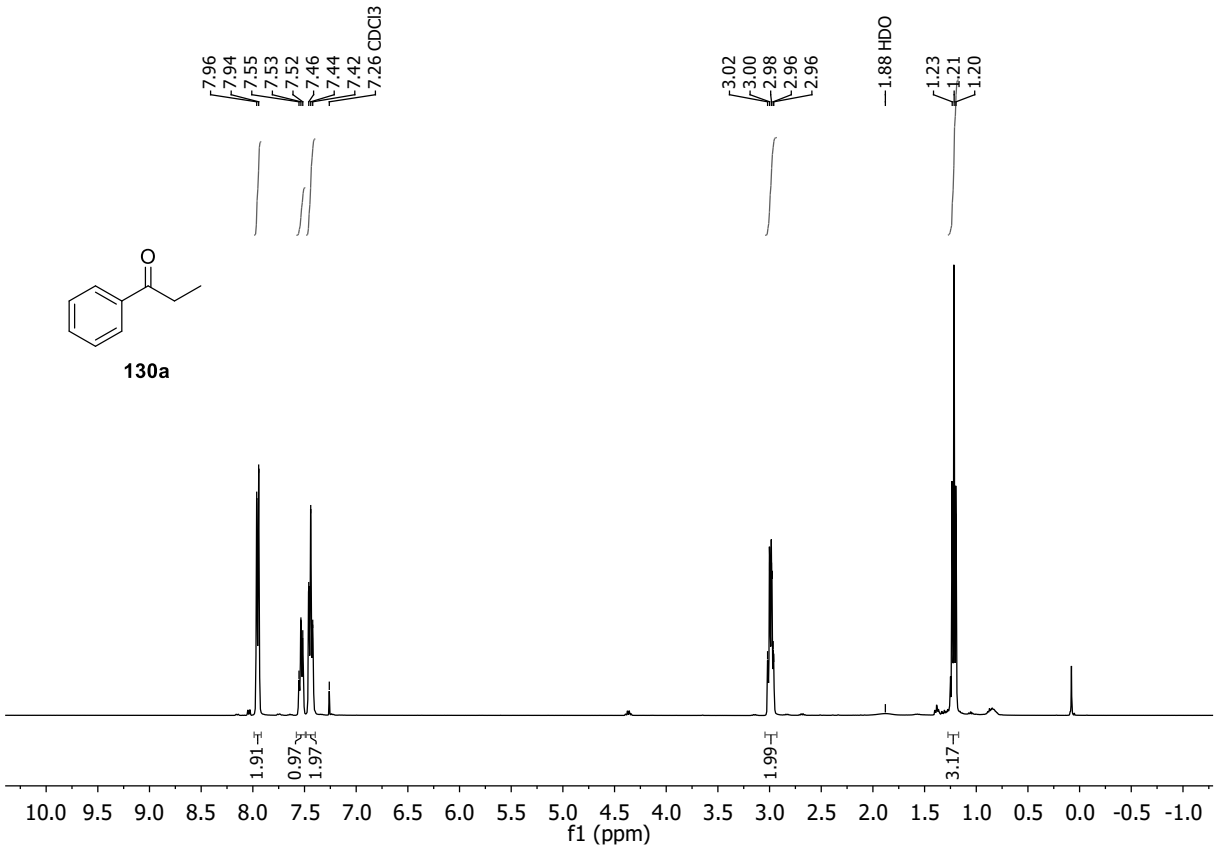
7.96
7.94
7.55
7.53
7.52
7.46
7.44
7.42
7.26 CDCl3
3.02
3.00
2.98
2.96
2.96
1.88 HDO
1.23
1.21
1.20
130a
1.91
0.97
1.97
1.99
3.17
f1 (ppm)

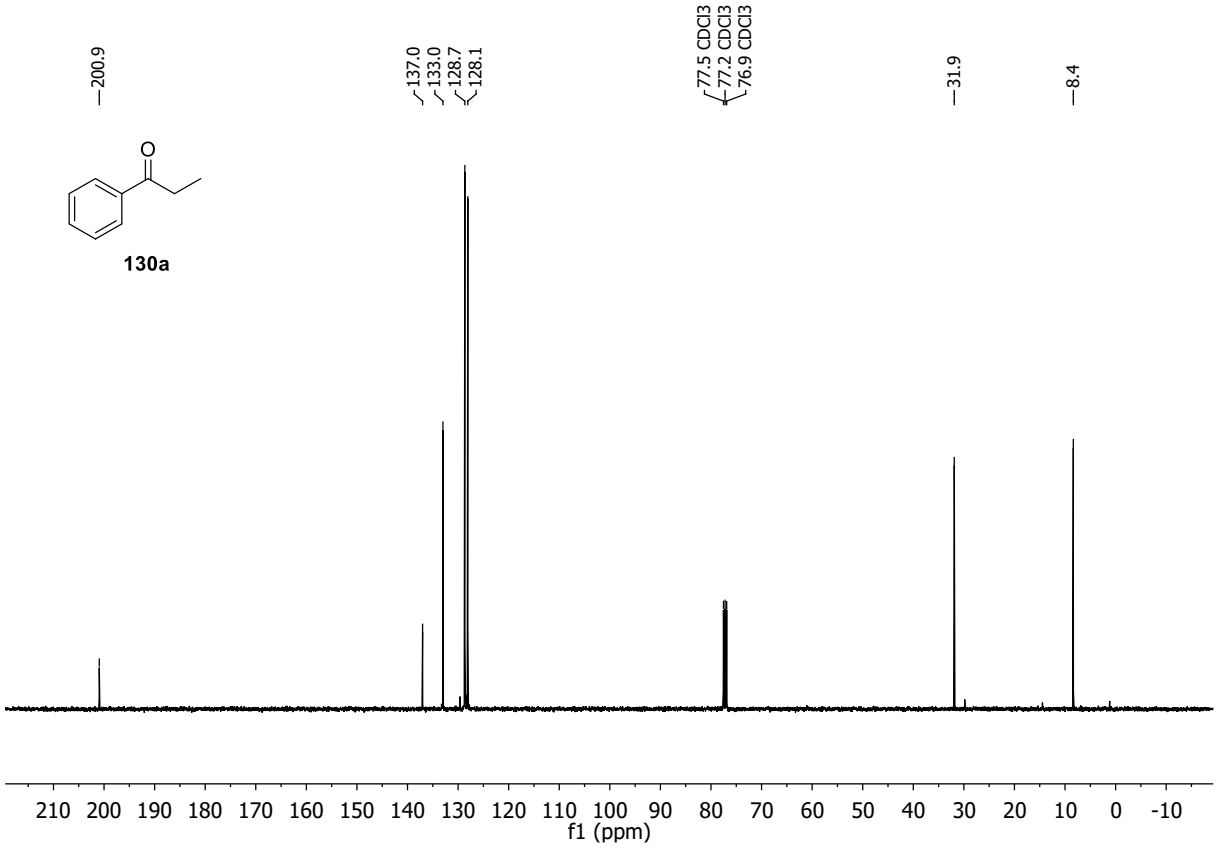
200.9
137.0
133.0
128.7
128.1
77.5 CDCl3
77.2 CDCl3
76.9 CDCl3
31.9
8.4
130a
f1 (ppm)

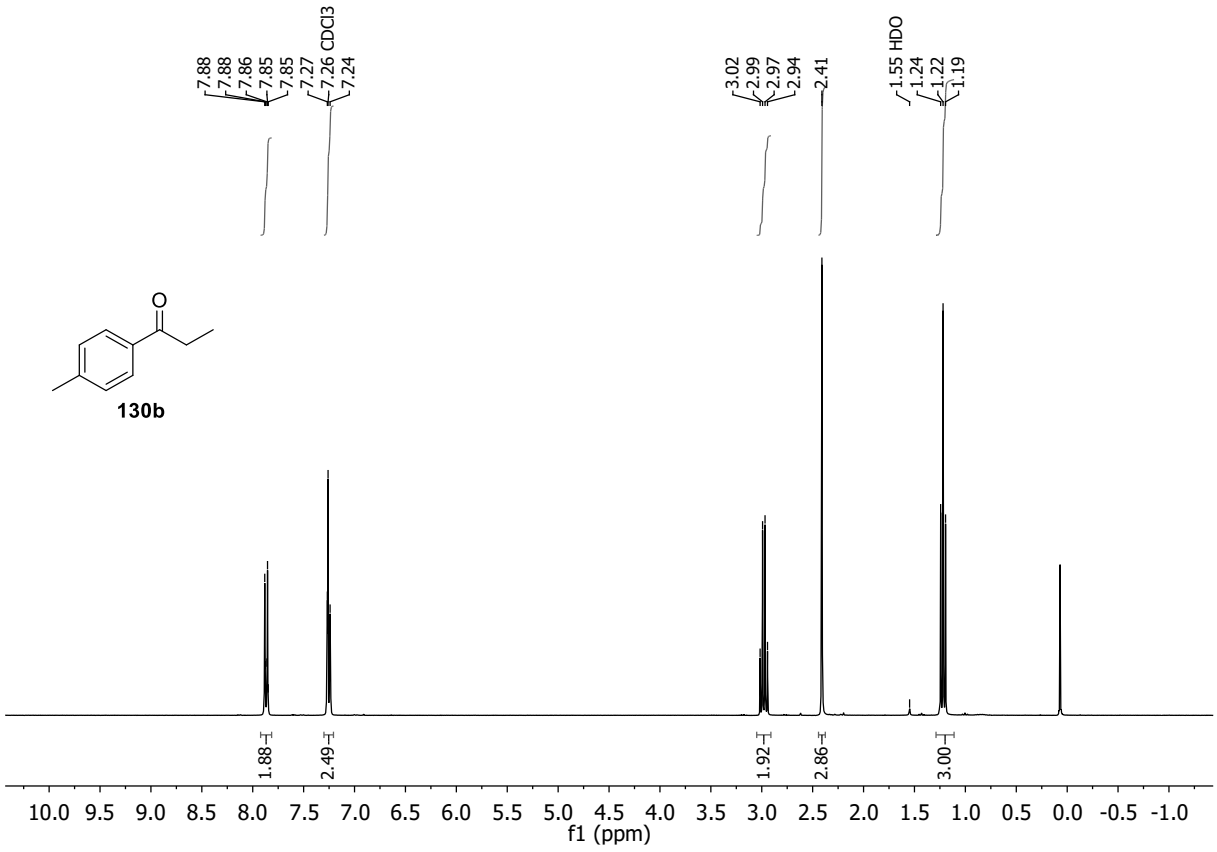
7.88
7.88
7.86
7.85
7.85
7.27
7.26 CDCl3
7.24
3.02
2.99
2.97
2.94
2.41
1.55 HDO
1.24
1.22
1.19
O
130b
1.88
2.49
1.92
2.86
3.00
10.0 9.5 9.0 8.5 8.0 7.5 7.0 6.5 6.0 5.5 5.0 4.5 4.0 3.5 3.0 2.5 2.0 1.5 1.0 0.5 0.0 -0.5 -1.0
f1 (ppm)

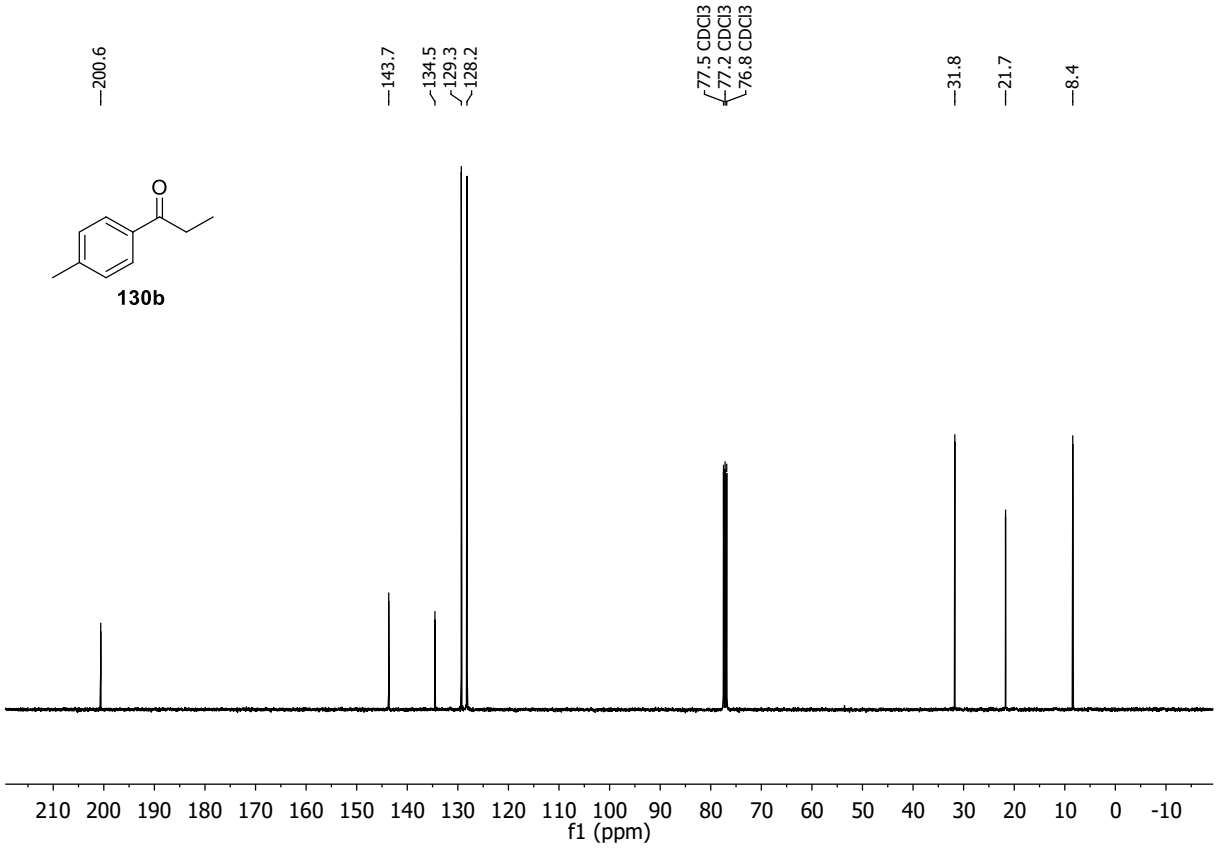
200.6
143.7
134.5
129.3
128.2
77.5 CDCl3
77.2 CDCl3
76.8 CDCl3
31.8
21.7
8.4
O
130b
210 200 190 180 170 160 150 140 130 120 110 100 90 80 70 60 50 40 30 20 10 0 -10
f1 (ppm)

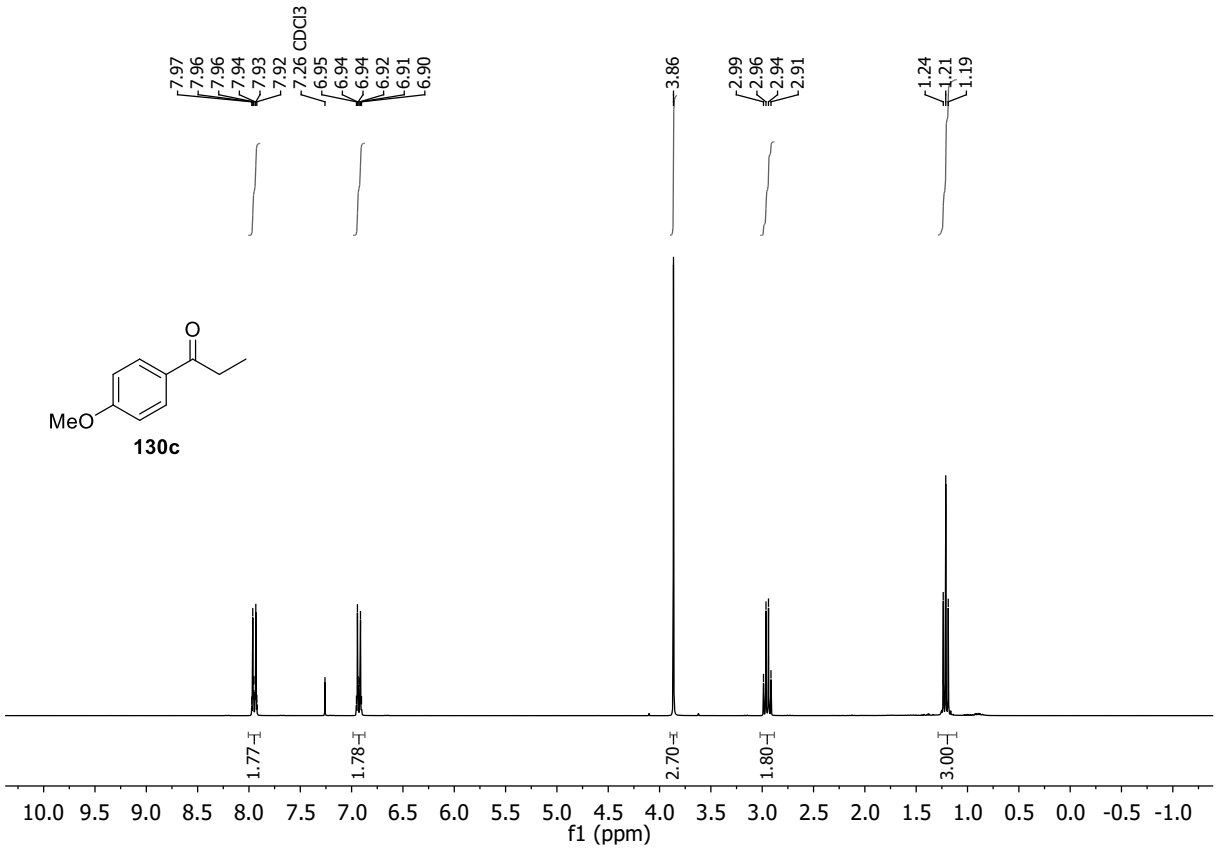
7.97
7.96
7.96
7.94
7.93
7.92
7.26 CDCl3
6.95
6.94
6.94
6.92
6.91
6.90
3.86
2.99
2.96
2.94
2.91
1.24
1.21
1.19
MeO
130c
1.77
1.78
2.70
1.80
3.00
10.0 9.5 9.0 8.5 8.0 7.5 7.0 6.5 6.0 5.5 5.0 4.5 4.0 3.5 3.0 2.5 2.0 1.5 1.0 0.5 0.0 -0.5 -1.0
f1 (ppm)

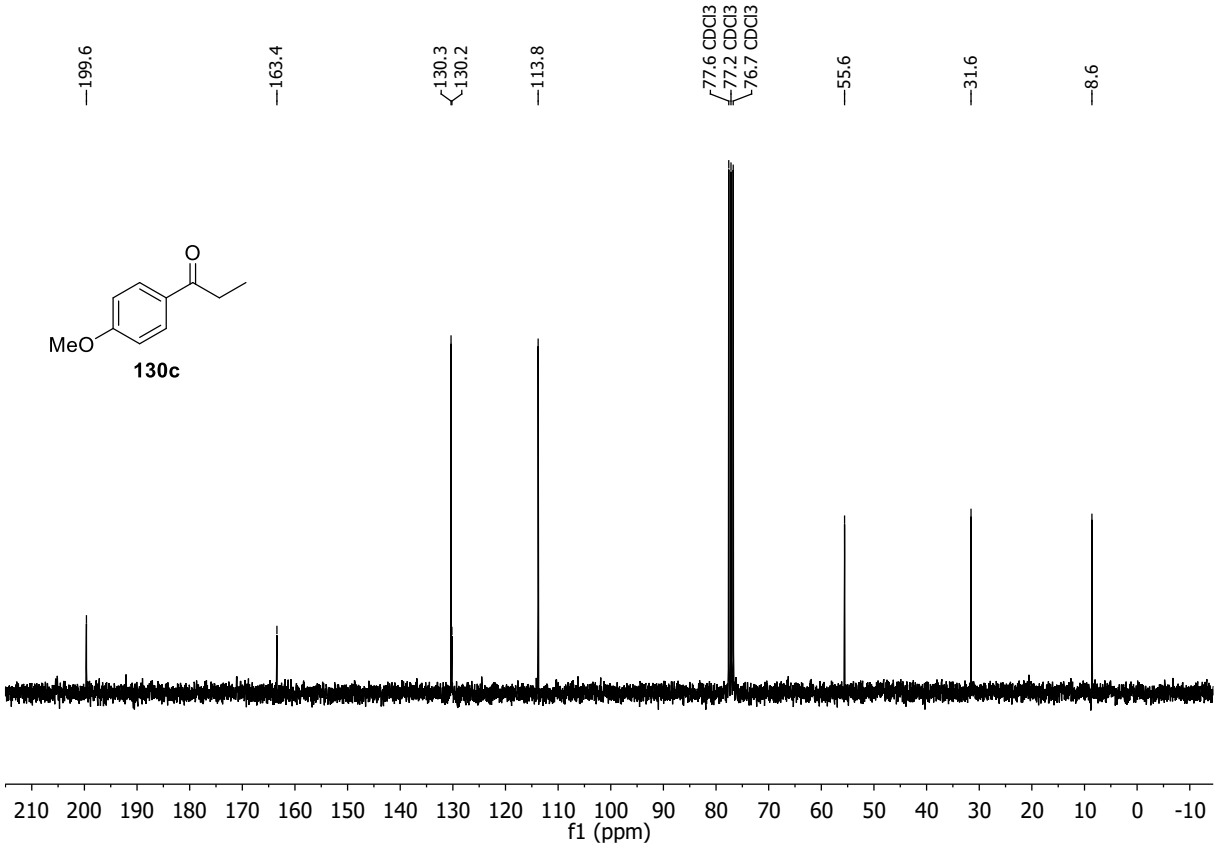
199.6
163.4
130.3
130.2
113.8
77.6 CDCl3
77.2 CDCl3
76.7 CDCl3
55.6
31.6
8.6
MeO
130c
210 200 190 180 170 160 150 140 130 120 110 100 90 80 70 60 50 40 30 20 10 0 -10
f1 (ppm)

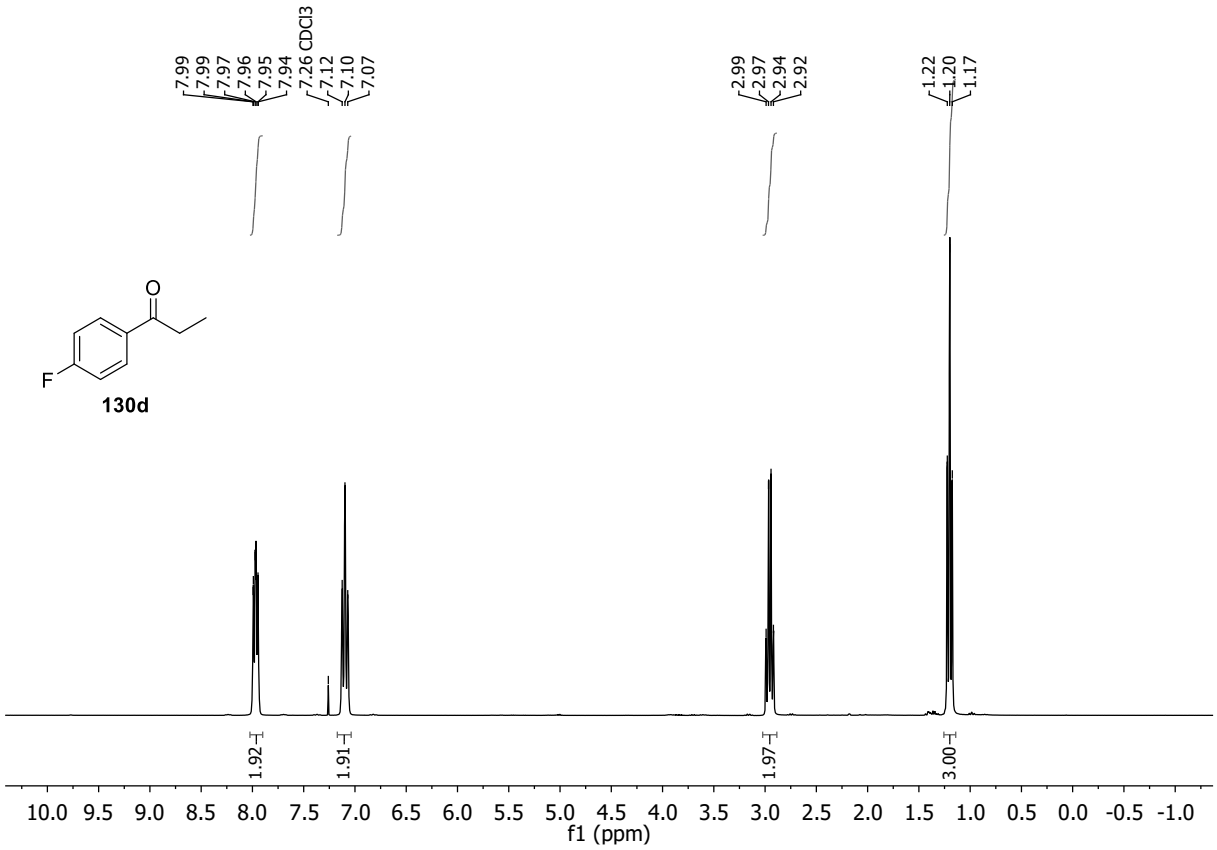
7.99
7.99
7.97
7.96
7.95
7.94
7.26 CDCl3
7.12
7.10
7.07
2.99
2.97
2.94
2.92
1.22
1.20
1.17
O
F
130d
1.92
1.91
1.97
3.00
10.0 9.5 9.0 8.5 8.0 7.5 7.0 6.5 6.0 5.5 5.0 4.5 4.0 3.5 3.0 2.5 2.0 1.5 1.0 0.5 0.0 -0.5 -1.0
f1 (ppm)

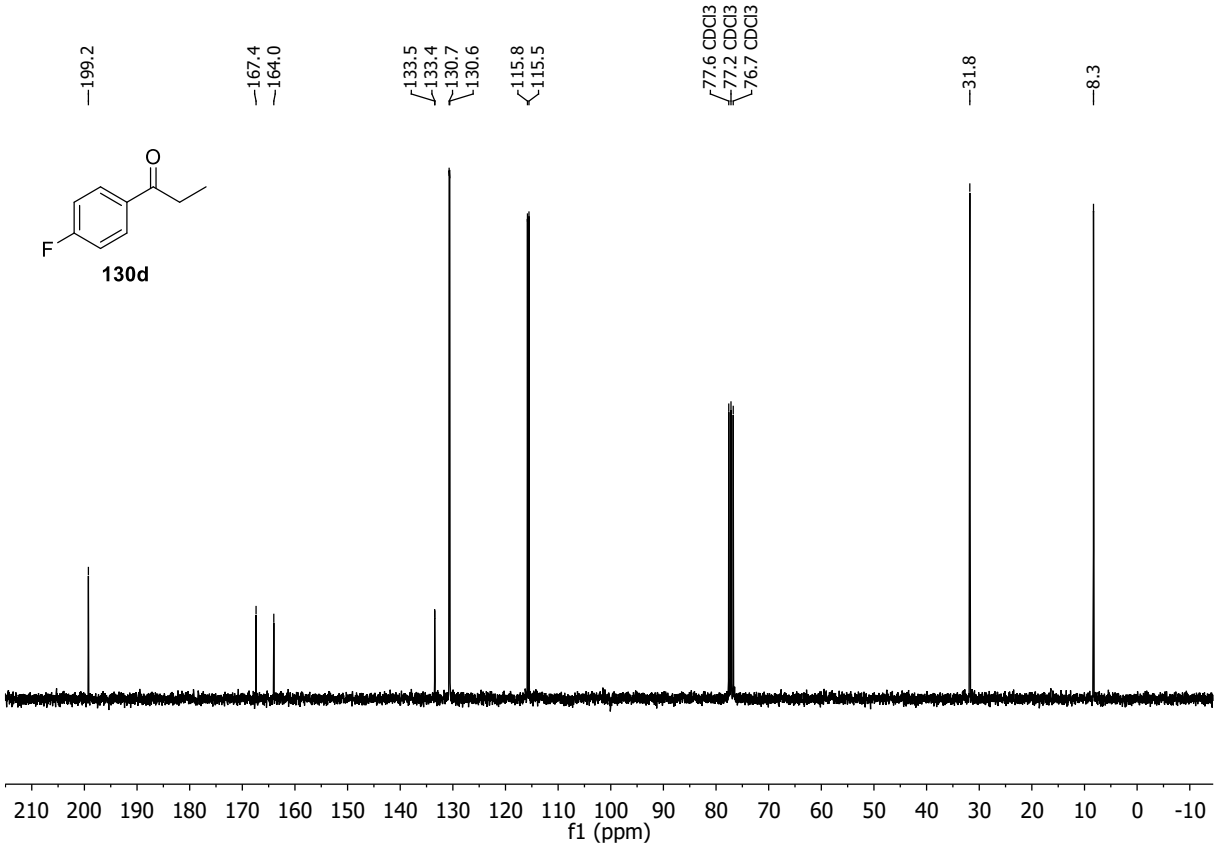
199.2
167.4
164.0
133.5
133.4
130.7
130.6
115.8
115.5
77.6 CDCl3
77.2 CDCl3
76.7 CDCl3
31.8
8.3
O
F
130d
210 200 190 180 170 160 150 140 130 120 110 100 90 80 70 60 50 40 30 20 10 0 -10
f1 (ppm)

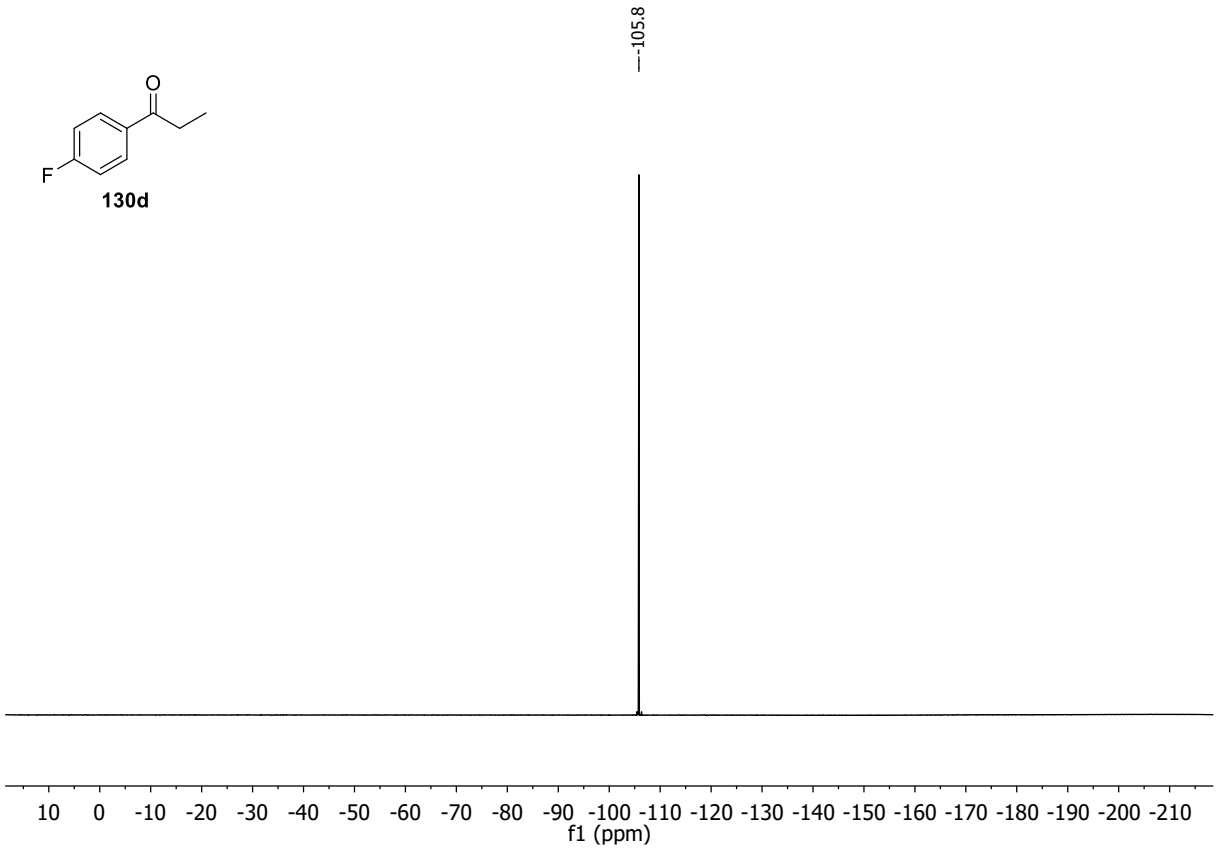
-105.8
O
F
130d
10 0 -10 -20 -30 -40 -50 -60 -70 -80 -90 -100 -110 -120 -130 -140 -150 -160 -170 -180 -190 -200 -210
f1 (ppm)

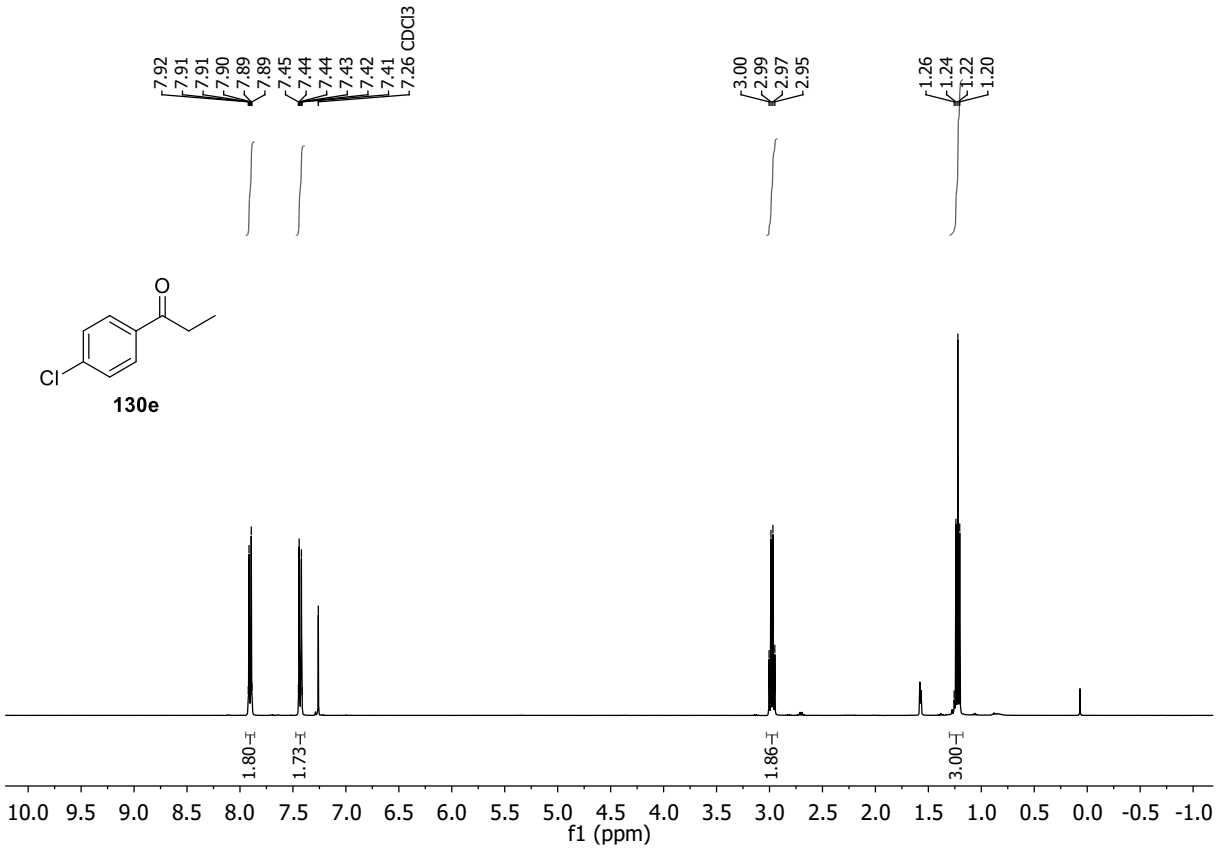
7.92
7.91
7.91
7.90
7.89
7.89
7.45
7.44
7.44
7.43
7.42
7.41
7.26 CDCl3
3.00
2.99
2.97
2.95
1.26
1.24
1.22
1.20
O
Cl
130e
1.80
1.73
1.86
3.00
10.0 9.5 9.0 8.5 8.0 7.5 7.0 6.5 6.0 5.5 5.0 4.5 4.0 3.5 3.0 2.5 2.0 1.5 1.0 0.5 0.0 -0.5 -1.0
f1 (ppm)

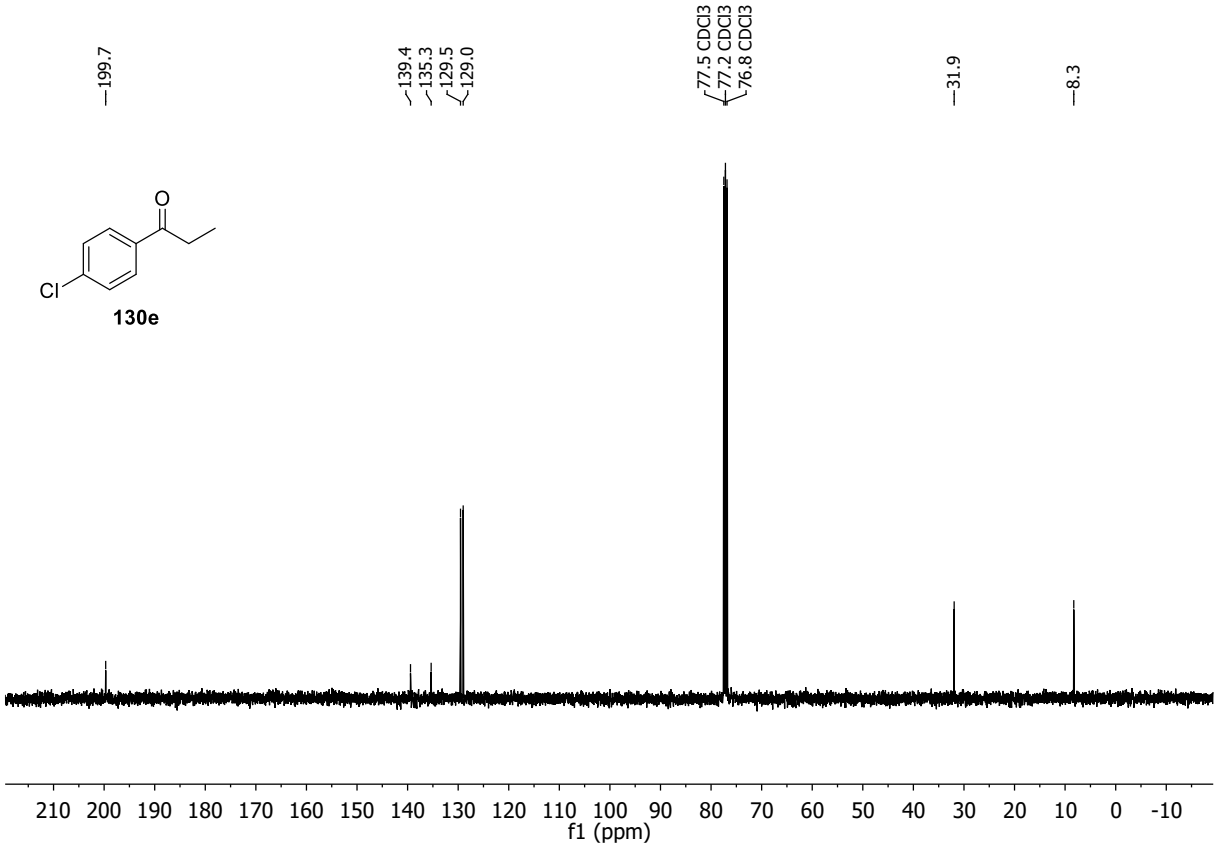
199.7
139.4
135.3
129.5
129.0
77.5 CDCl3
77.2 CDCl3
76.8 CDCl3
31.9
8.3
O
Cl
130e
210 200 190 180 170 160 150 140 130 120 110 100 90 80 70 60 50 40 30 20 10 0 -10
f1 (ppm)

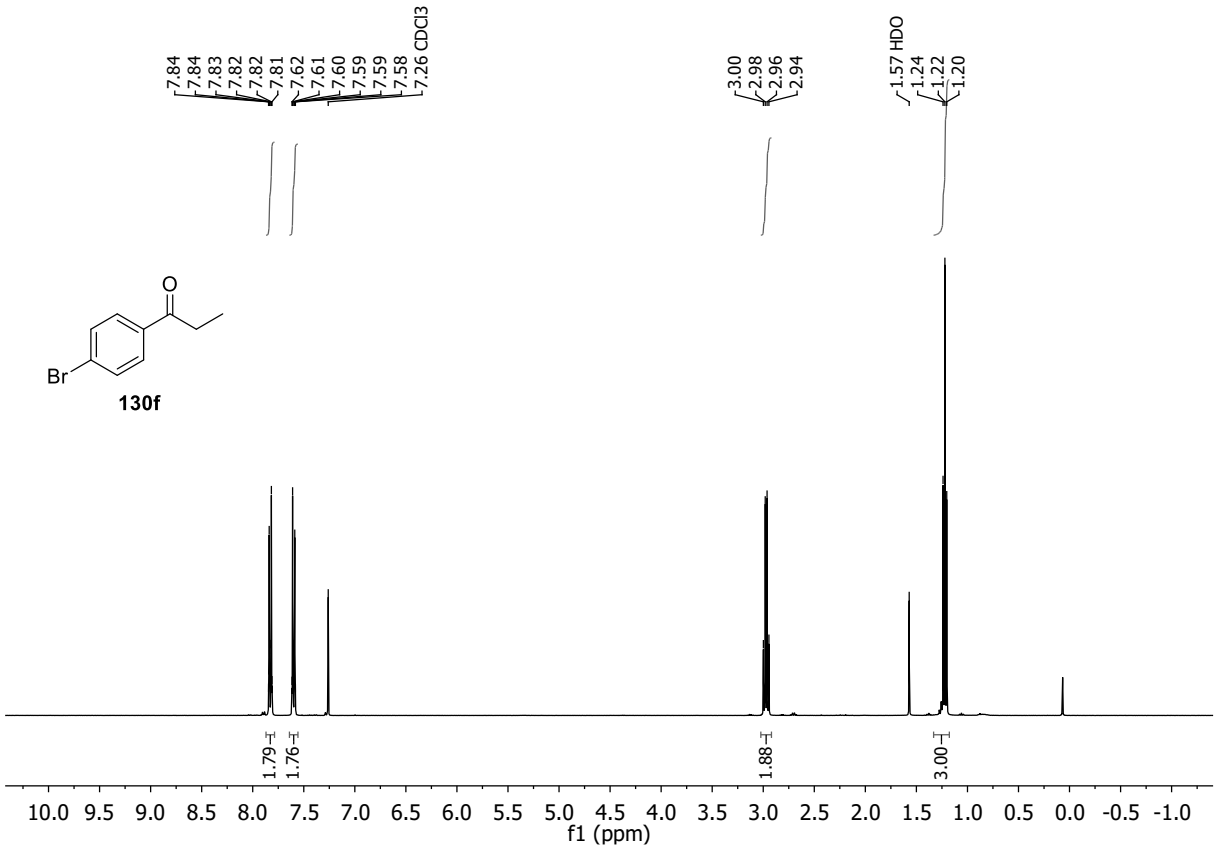
7.84
7.84
7.83
7.82
7.82
7.81
7.62
7.61
7.60
7.59
7.59
7.58
7.26 CDCl3
3.00
2.98
2.96
2.94
1.57 HDO
1.24
1.22
1.20
O
Br
130f
1.79
1.76
1.88
3.00
10.0 9.5 9.0 8.5 8.0 7.5 7.0 6.5 6.0 5.5 5.0 4.5 4.0 3.5 3.0 2.5 2.0 1.5 1.0 0.5 0.0 -0.5 -1.0
f1 (ppm)

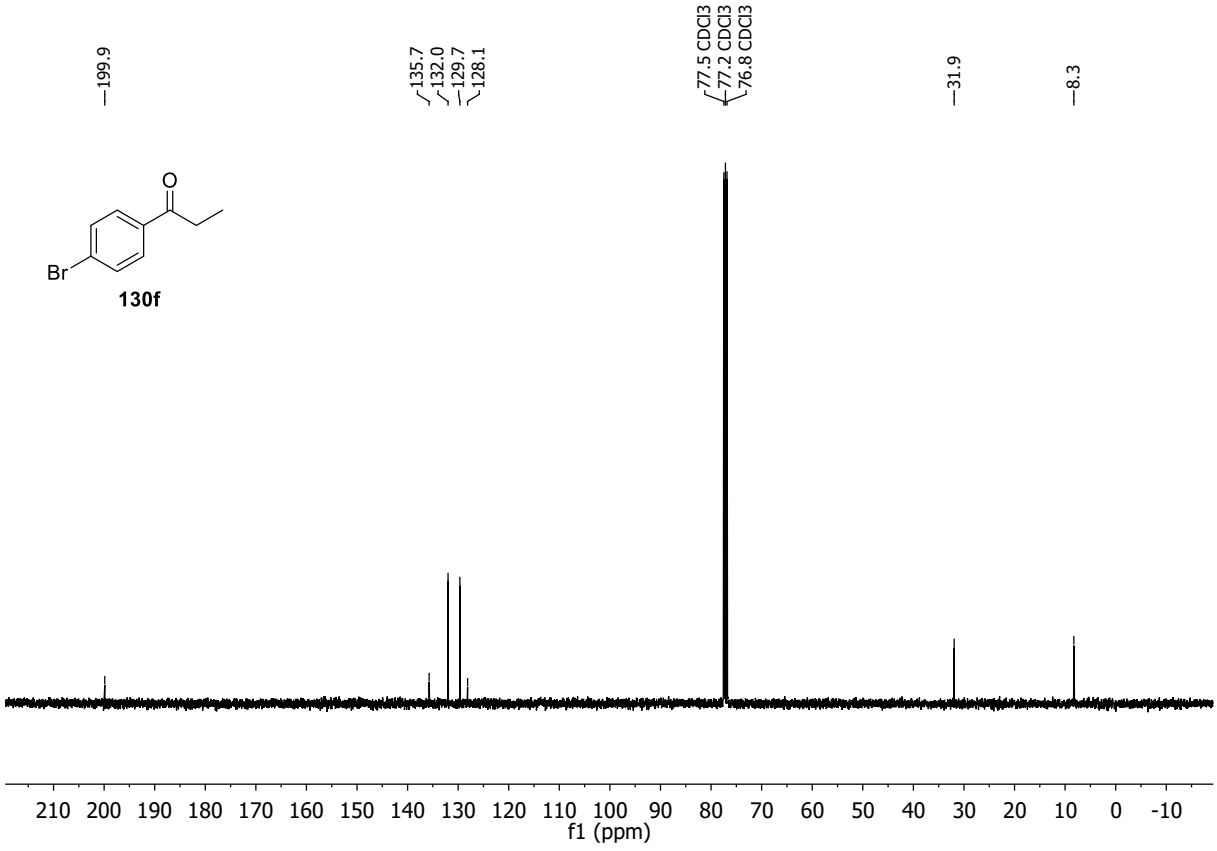
199.9
135.7
132.0
129.7
128.1
77.5 CDCl3
77.2 CDCl3
76.8 CDCl3
31.9
8.3
O
Br
130f
210 200 190 180 170 160 150 140 130 120 110 100 90 80 70 60 50 40 30 20 10 0 -10
f1 (ppm)

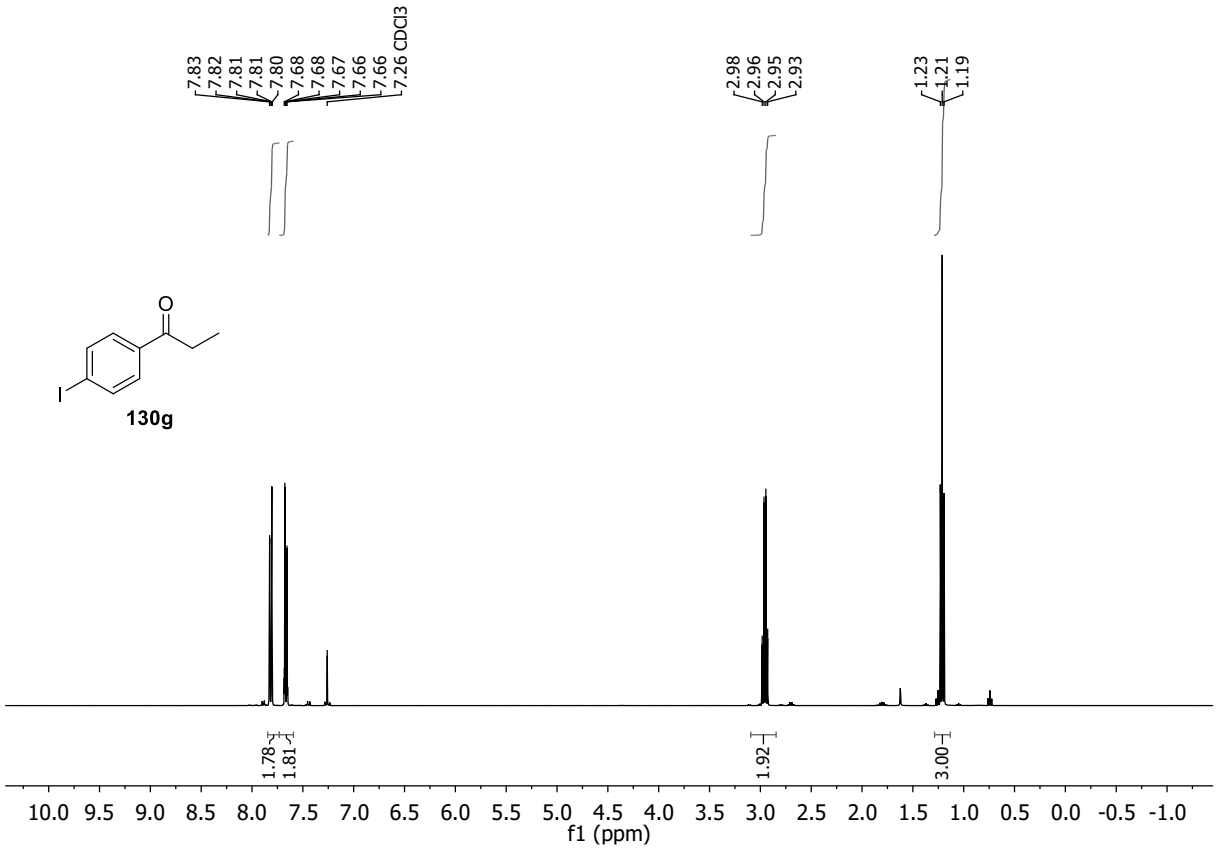
7.83
7.82
7.81
7.81
7.80
7.68
7.68
7.67
7.66
7.66
7.26 CDCl3
2.98
2.96
2.95
2.93
1.23
1.21
1.19
O
I
130g
1.78
1.81
1.92
3.00
10.0 9.5 9.0 8.5 8.0 7.5 7.0 6.5 6.0 5.5 5.0 4.5 4.0 3.5 3.0 2.5 2.0 1.5 1.0 0.5 0.0 -0.5 -1.0
f1 (ppm)

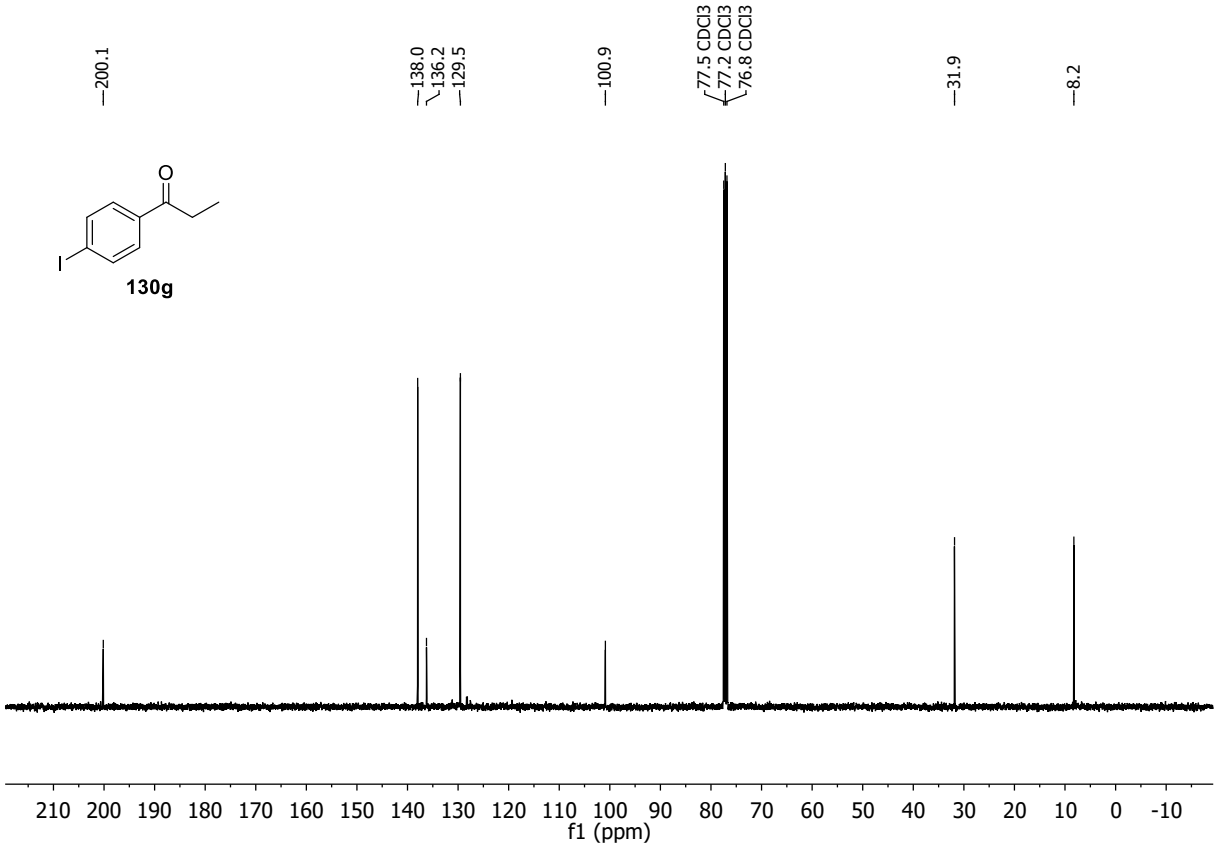
200.1
138.0
136.2
129.5
100.9
77.5 CDCl3
77.2 CDCl3
76.8 CDCl3
31.9
8.2
O
I
130g
210 200 190 180 170 160 150 140 130 120 110 100 90 80 70 60 50 40 30 20 10 0 -10
f1 (ppm)

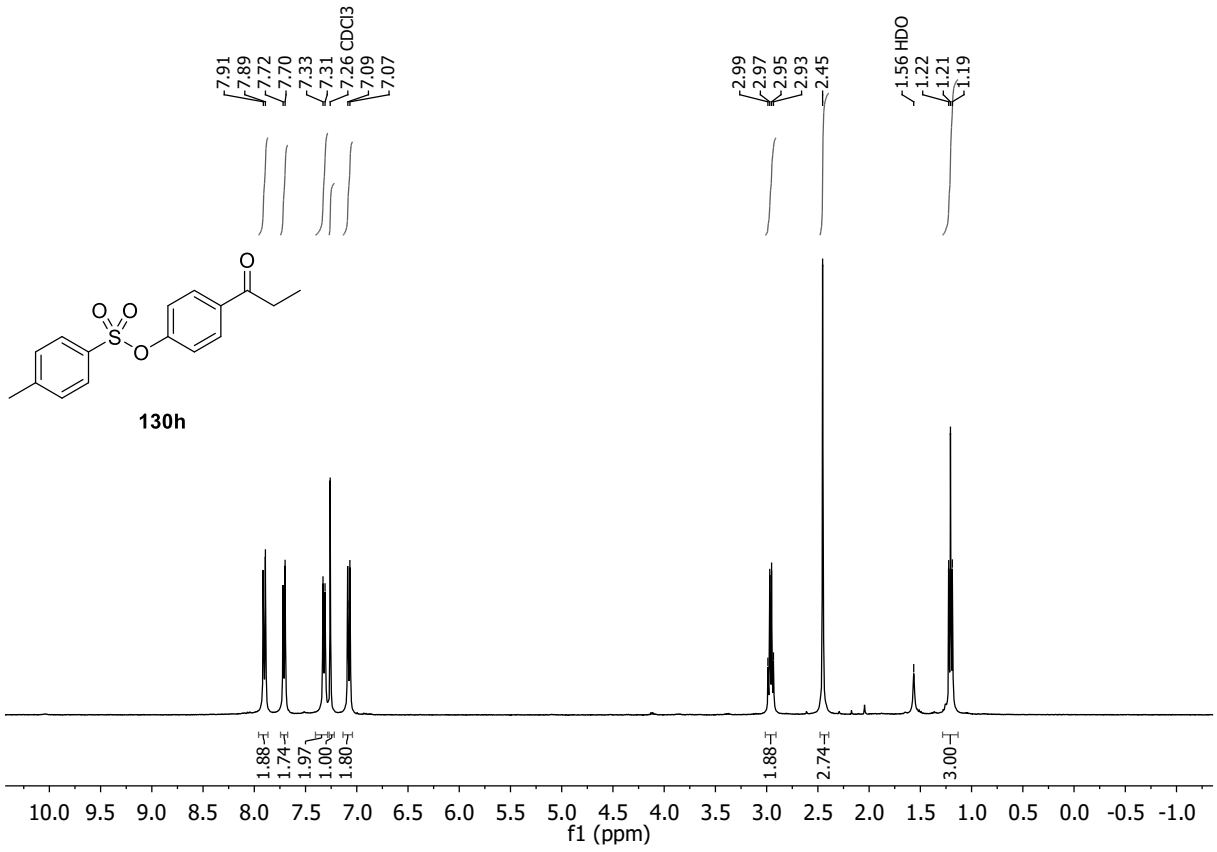
7.91
7.89
7.72
7.70
7.33
7.31
7.26 CDCl3
7.09
7.07
2.99
2.97
2.95
2.93
2.45
1.56 HDO
1.22
1.21
1.19
130h
1.88
1.74
1.97
1.00
1.80
1.88
2.74
3.00
f1 (ppm)

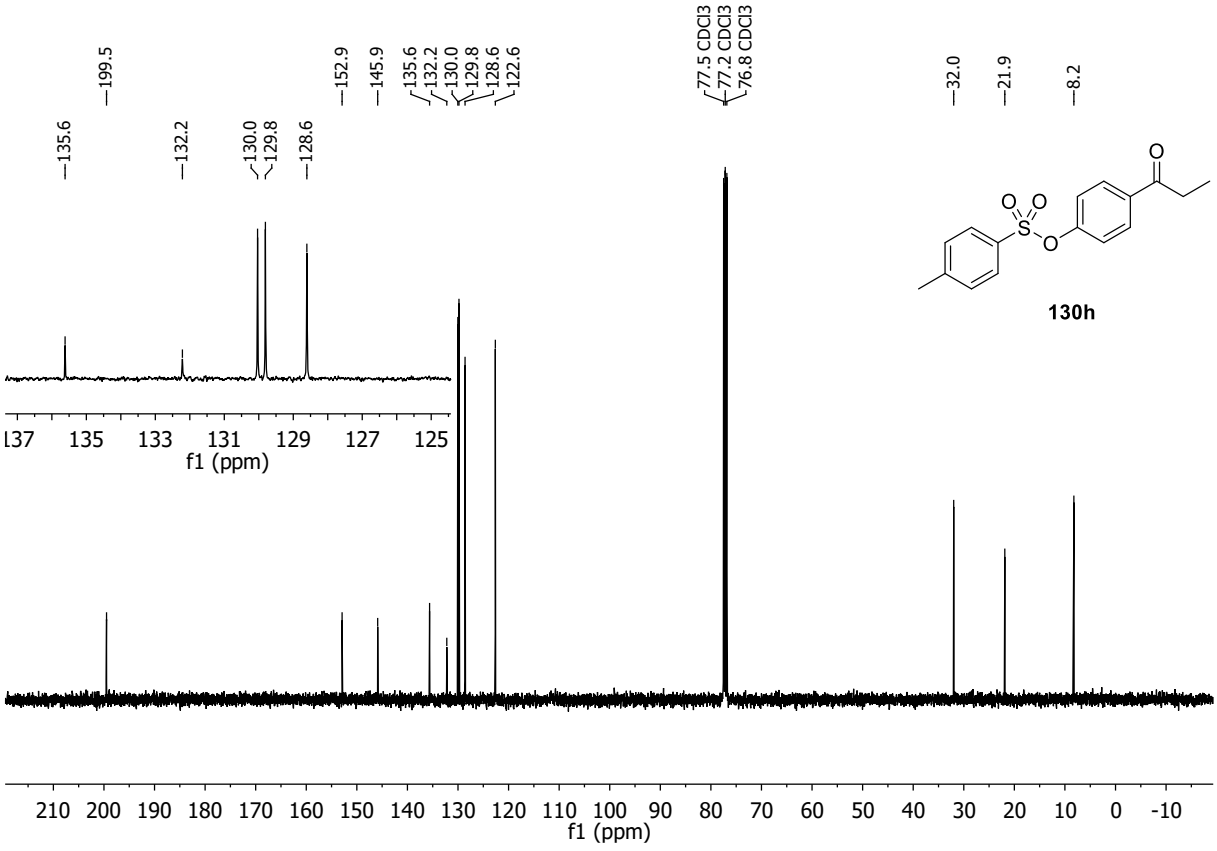
199.5
152.9
145.9
135.6
132.2
130.0
129.8
128.6
122.6
77.5 CDCl3
77.2 CDCl3
76.8 CDCl3
32.0
21.9
8.2
135.6
132.2
130.0
129.8
128.6
130h
f1 (ppm)

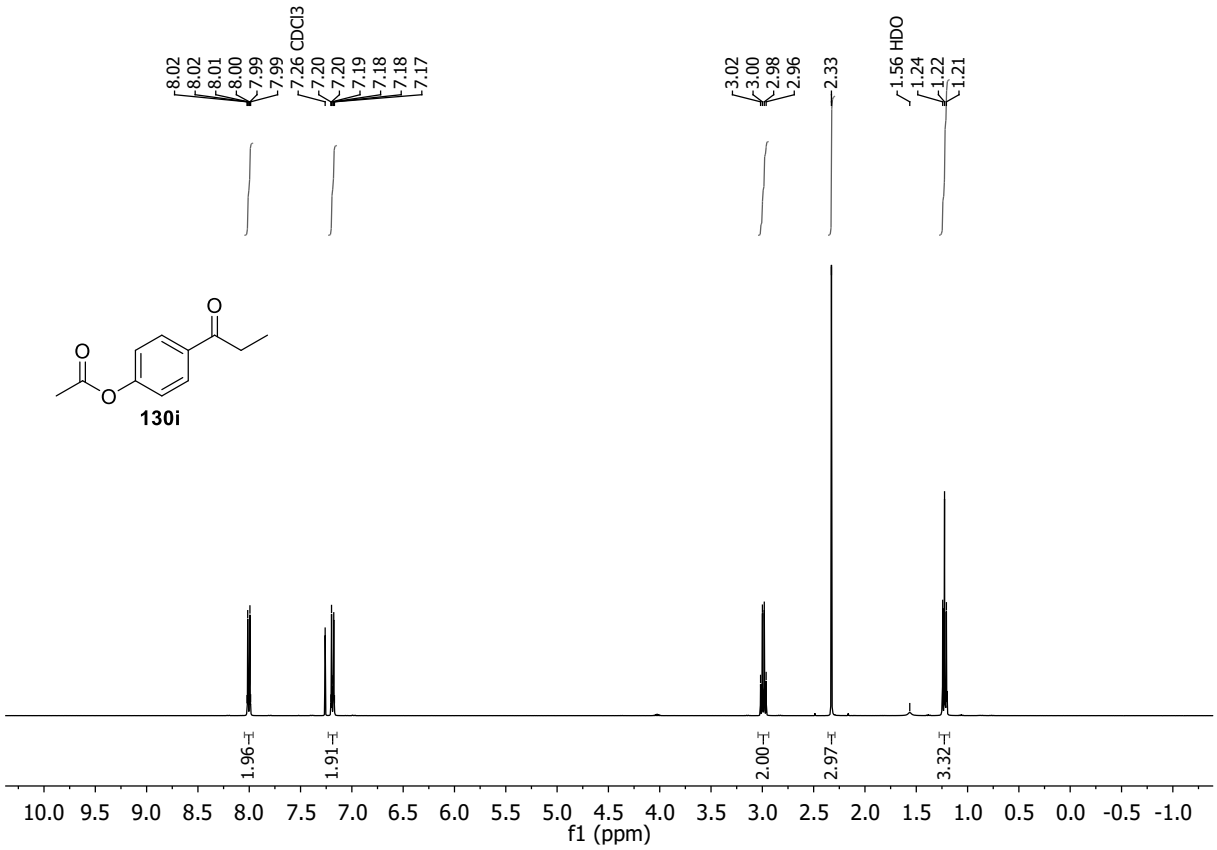
8.02
8.02
8.01
8.00
7.99
7.99
7.26 CDCl3
7.20
7.20
7.19
7.18
7.18
7.17
3.02
3.00
2.98
2.96
2.33
1.56 HDO
1.24
1.22
1.21
130i
1.96
1.91
2.00
2.97
3.32
f1 (ppm)

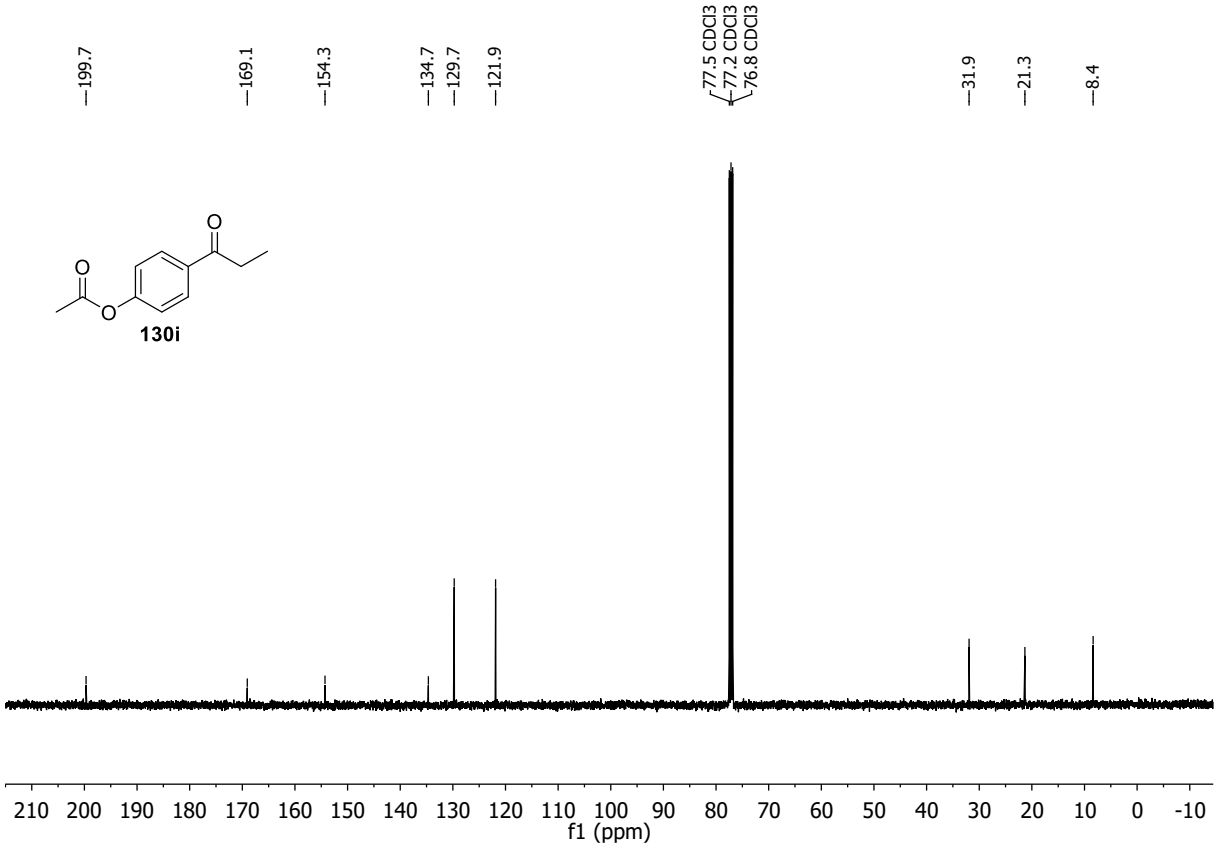
199.7
169.1
154.3
134.7
129.7
121.9
77.5 CDCl3
77.2 CDCl3
76.8 CDCl3
31.9
21.3
8.4
130i
f1 (ppm)

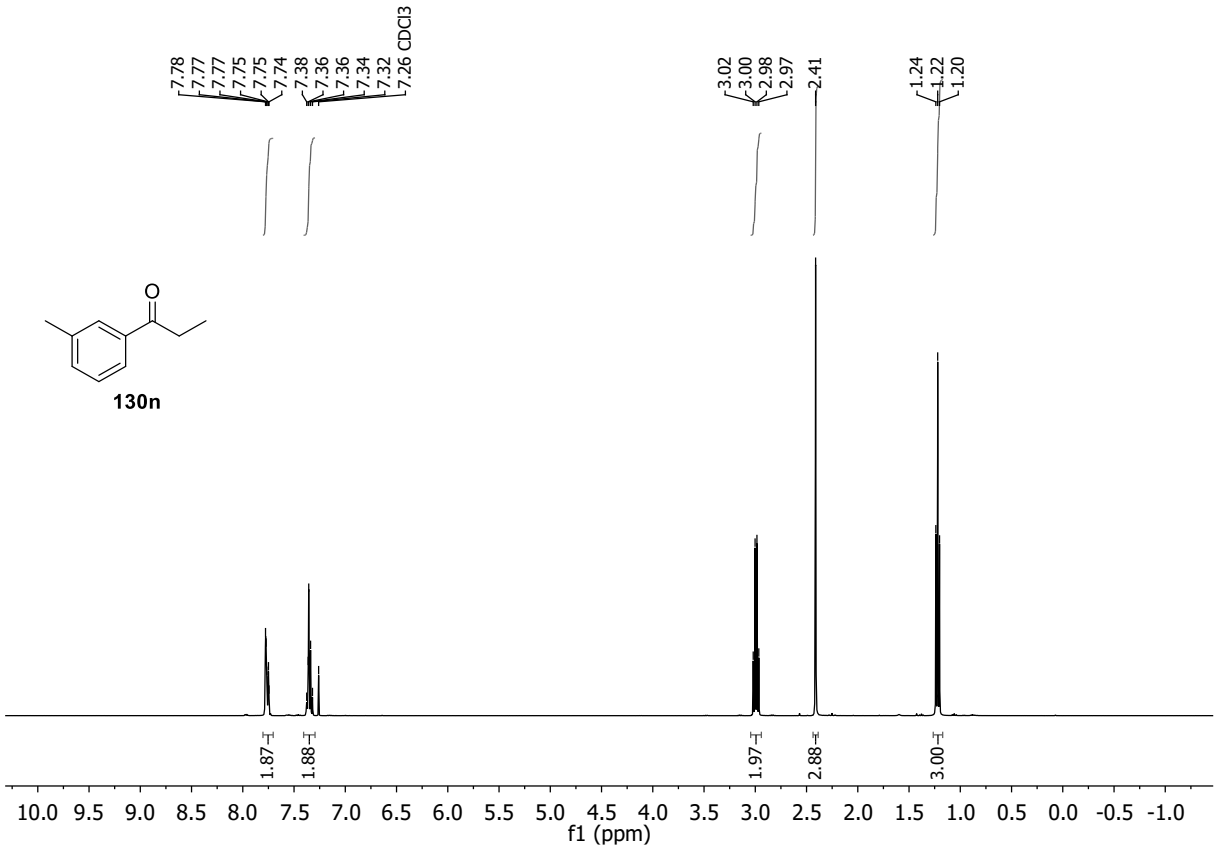
7.78
7.77
7.77
7.75
7.75
7.74
7.38
7.36
7.36
7.34
7.32
7.26 CDCl3
3.02
3.00
2.98
2.97
2.41
1.24
1.22
1.20
130n
1.87
1.88
1.97
2.88
3.00
f1 (ppm)

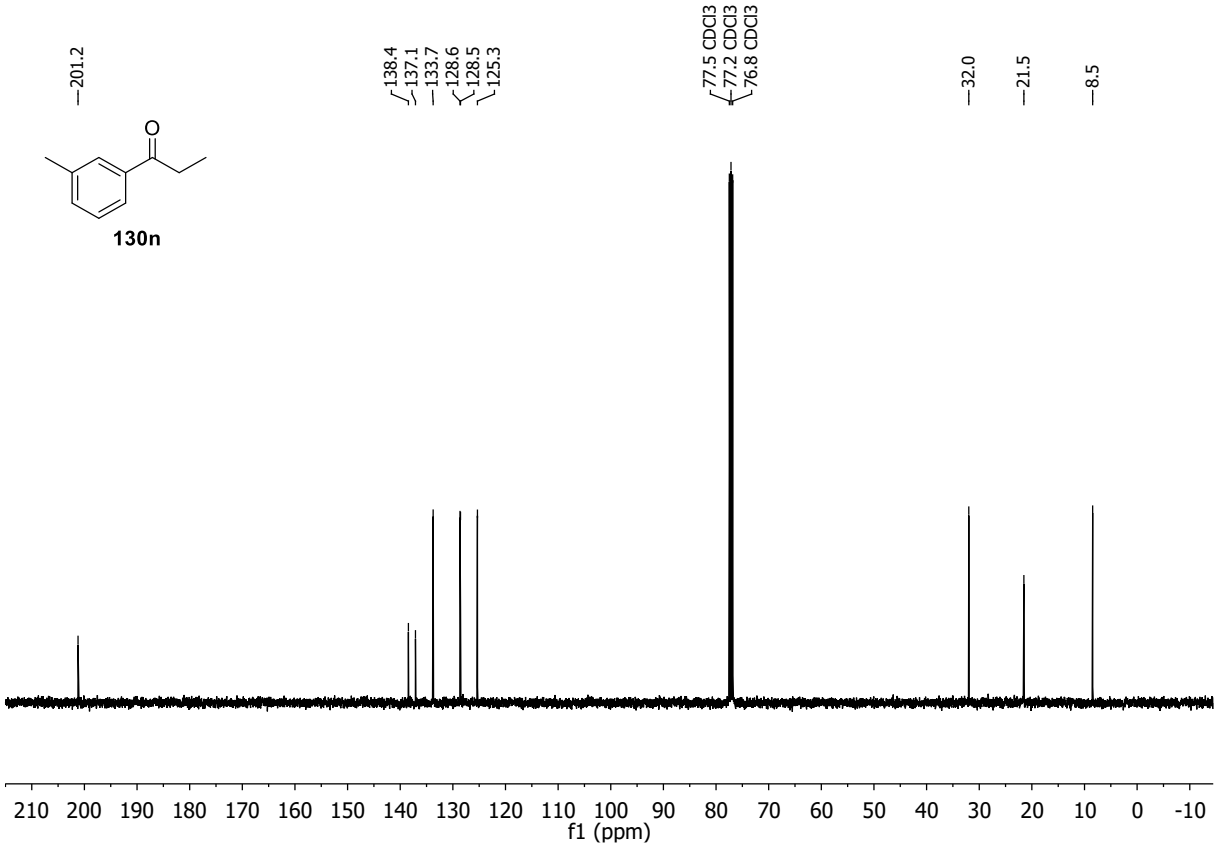
201.2
138.4
137.1
133.7
128.6
128.5
125.3
77.5 CDCl3
77.2 CDCl3
76.8 CDCl3
32.0
21.5
8.5
130n
f1 (ppm)

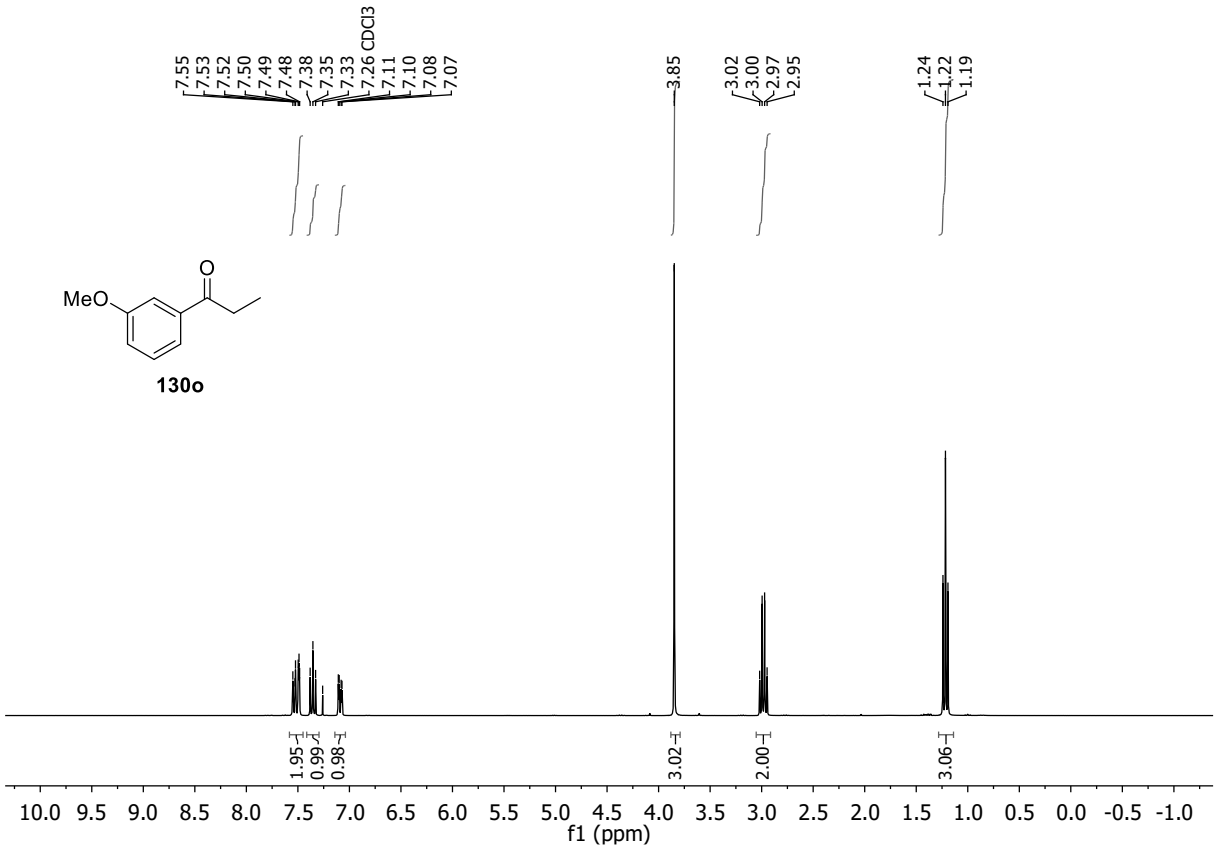
7.55
7.53
7.52
7.50
7.49
7.48
7.38
7.35
7.33
7.26 CDCl3
7.11
7.10
7.08
7.07
3.85
3.02
3.00
2.97
2.95
1.24
1.22
1.19
MeO
O
130o
1.95
0.99
0.98
3.02
2.00
3.06
10.0 9.5 9.0 8.5 8.0 7.5 7.0 6.5 6.0 5.5 5.0 4.5 4.0 3.5 3.0 2.5 2.0 1.5 1.0 0.5 0.0 -0.5 -1.0
f1 (ppm)

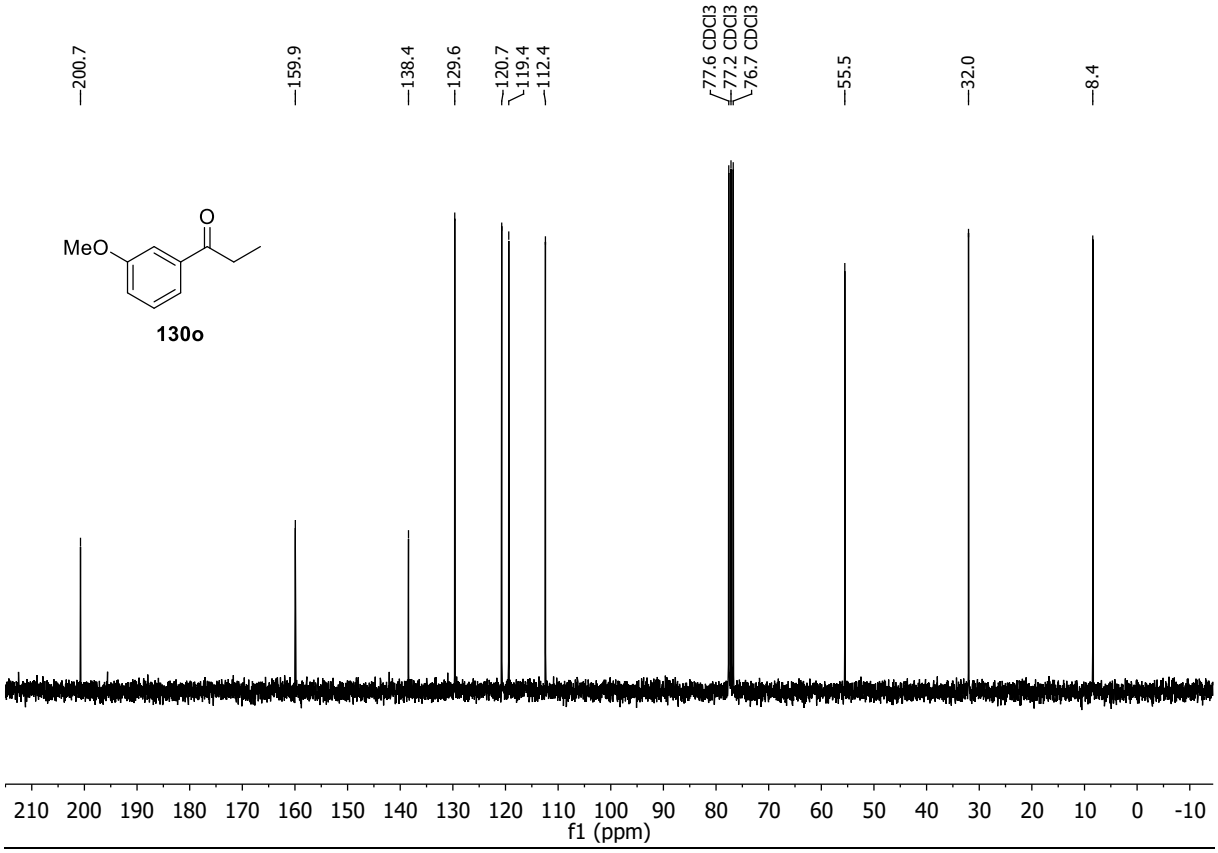
200.7
159.9
138.4
129.6
120.7
119.4
112.4
77.6 CDCl3
77.2 CDCl3
76.7 CDCl3
55.5
32.0
8.4
MeO
O
130o
210 200 190 180 170 160 150 140 130 120 110 100 90 80 70 60 50 40 30 20 10 0 -10
f1 (ppm)

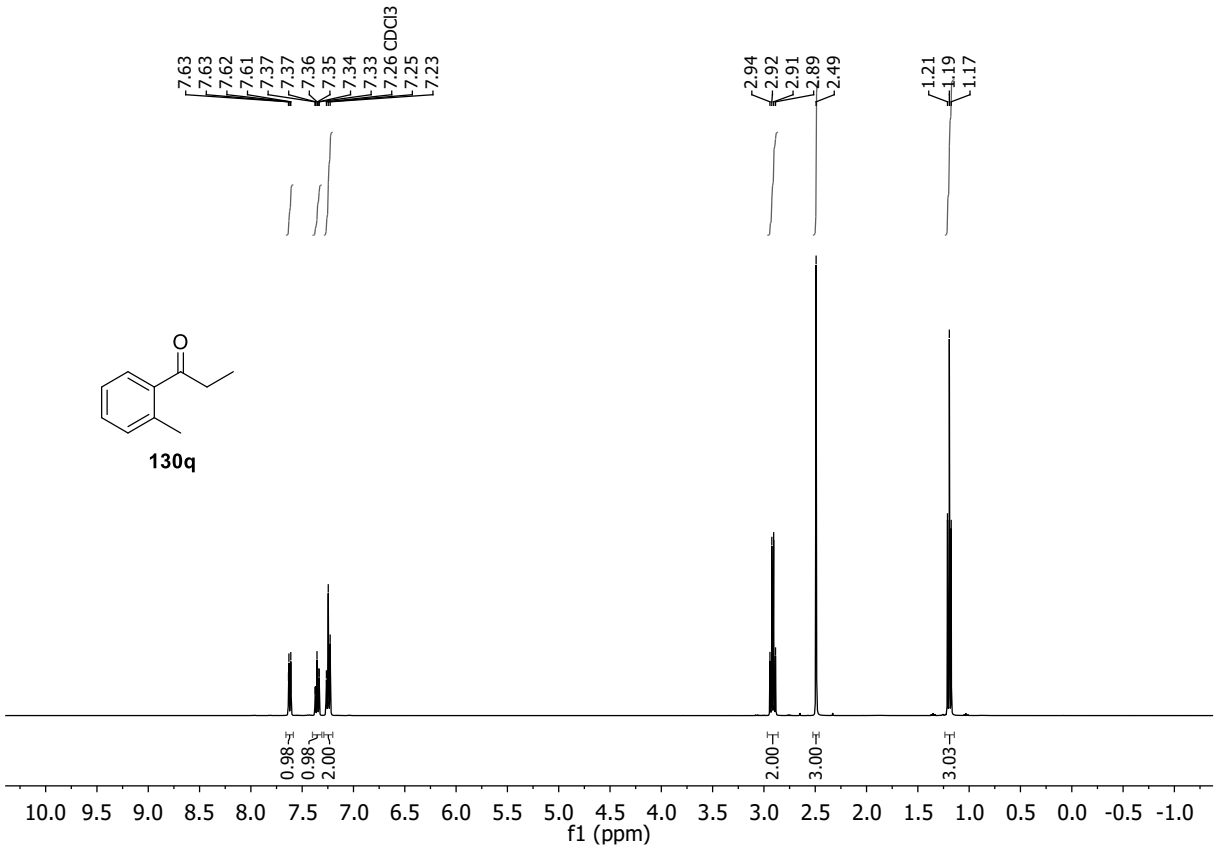
7.63
7.63
7.62
7.61
7.37
7.37
7.36
7.35
7.34
7.33
7.26 CDCl3
7.25
7.23
2.94
2.92
2.91
2.89
2.49
1.21
1.19
1.17
O
130q
0.98
0.98
2.00
2.00
3.00
3.03
10.0 9.5 9.0 8.5 8.0 7.5 7.0 6.5 6.0 5.5 5.0 4.5 4.0 3.5 3.0 2.5 2.0 1.5 1.0 0.5 0.0 -0.5 -1.0
f1 (ppm)

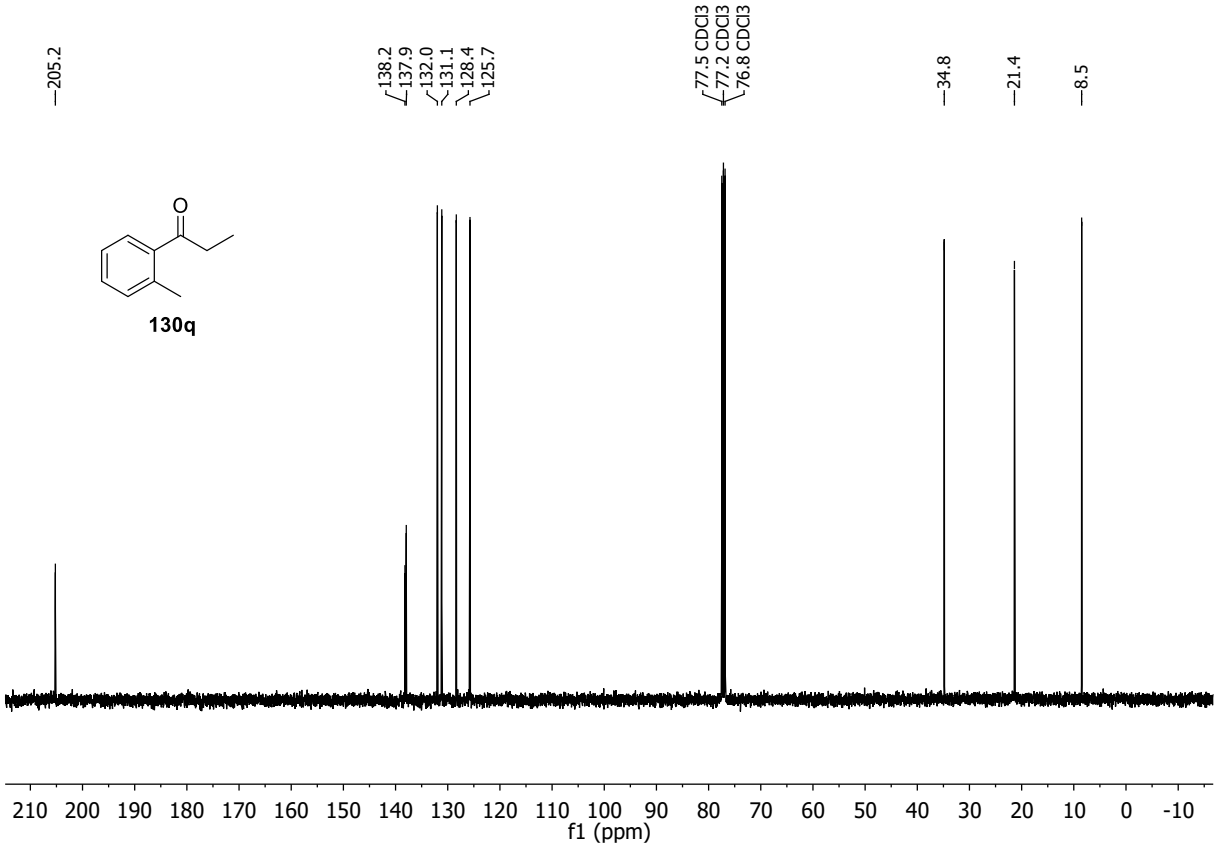
205.2
138.2
137.9
132.0
131.1
128.4
125.7
77.5 CDCl3
77.2 CDCl3
76.8 CDCl3
34.8
21.4
8.5
O
130q
210 200 190 180 170 160 150 140 130 120 110 100 90 80 70 60 50 40 30 20 10 0 -10
f1 (ppm)

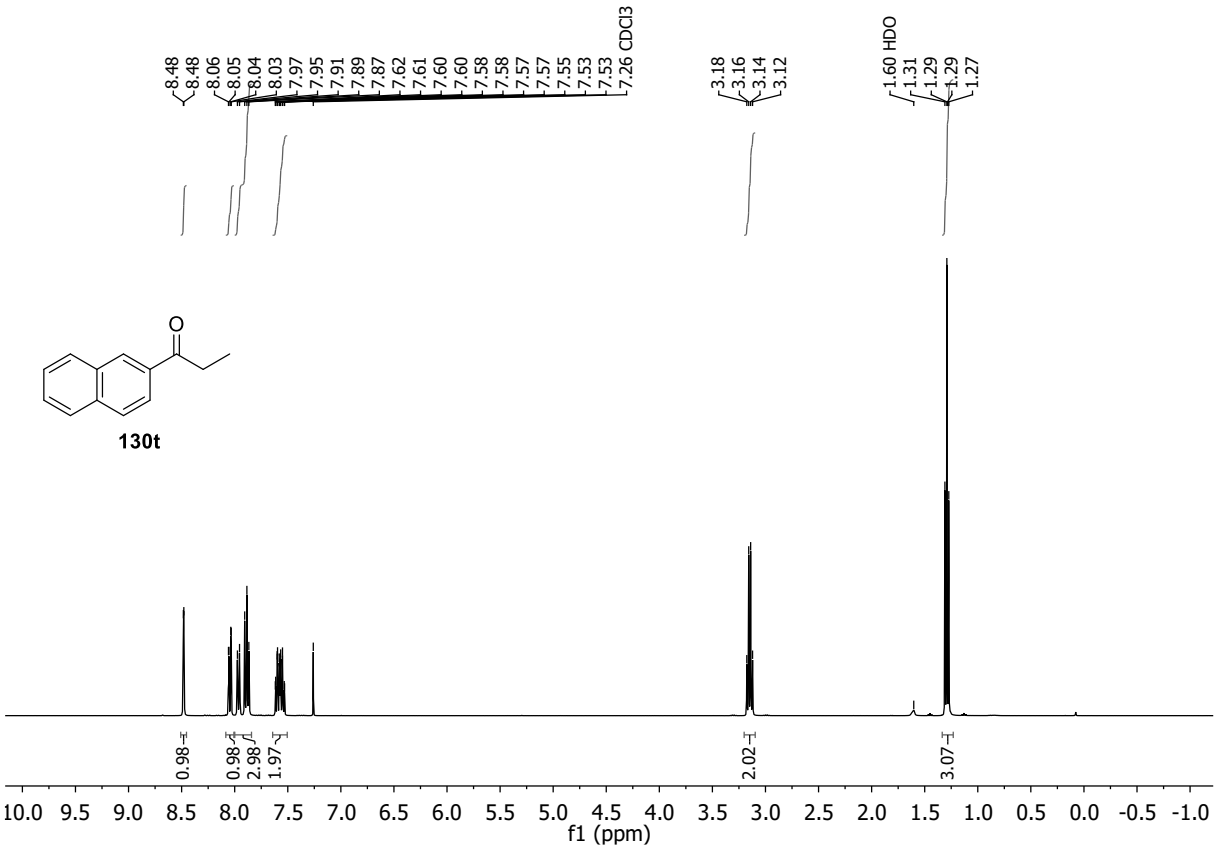
8.48
8.48
8.06
8.05
8.04
8.03
7.97
7.95
7.91
7.89
7.87
7.62
7.61
7.60
7.60
7.58
7.58
7.57
7.57
7.55
7.53
7.53
7.26 CDCl3
3.18
3.16
3.14
3.12
1.60 HDO
1.31
1.29
1.29
1.27
O
130t
0.98
0.98
2.98
1.97
2.02
3.07
10.0 9.5 9.0 8.5 8.0 7.5 7.0 6.5 6.0 5.5 5.0 4.5 4.0 3.5 3.0 2.5 2.0 1.5 1.0 0.5 0.0 -0.5 -1.0
f1 (ppm)

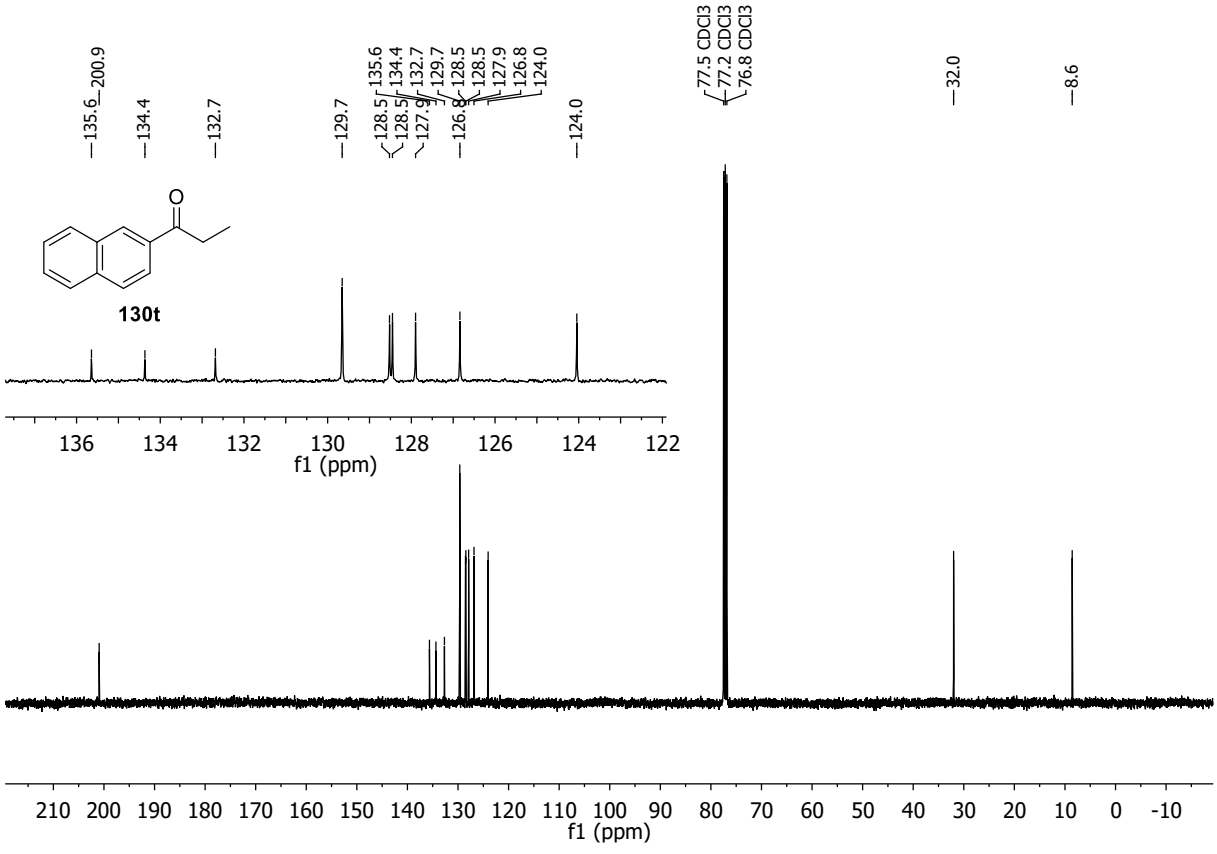
200.9
135.6
134.4
132.7
129.7
128.5
128.5
127.9
129.7
128.5
128.5
127.9
126.8
124.0
124.0
77.5 CDCl3
77.2 CDCl3
76.8 CDCl3
32.0
8.6
O
130t
136 134 132 130 128 126 124 122
f1 (ppm)
210 200 190 180 170 160 150 140 130 120 110 100 90 80 70 60 50 40 30 20 10 0 -10
f1 (ppm)

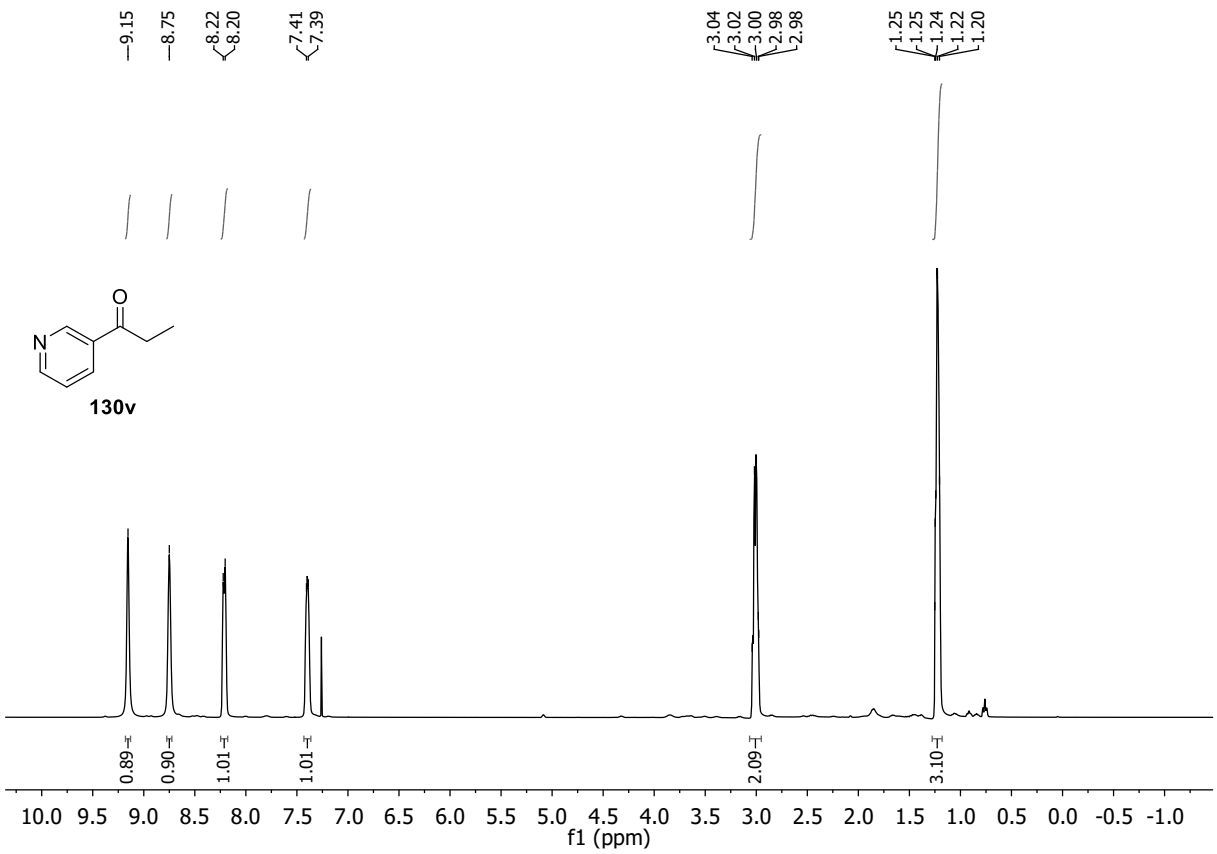
9.15
8.75
8.22
8.20
7.41
7.39
3.04
3.02
3.00
2.98
2.98
1.25
1.25
1.24
1.22
1.20
O
N
130v
0.89
0.90
1.01
1.01
2.09
3.10
10.0 9.5 9.0 8.5 8.0 7.5 7.0 6.5 6.0 5.5 5.0 4.5 4.0 3.5 3.0 2.5 2.0 1.5 1.0 0.5 0.0 -0.5 -1.0
f1 (ppm)

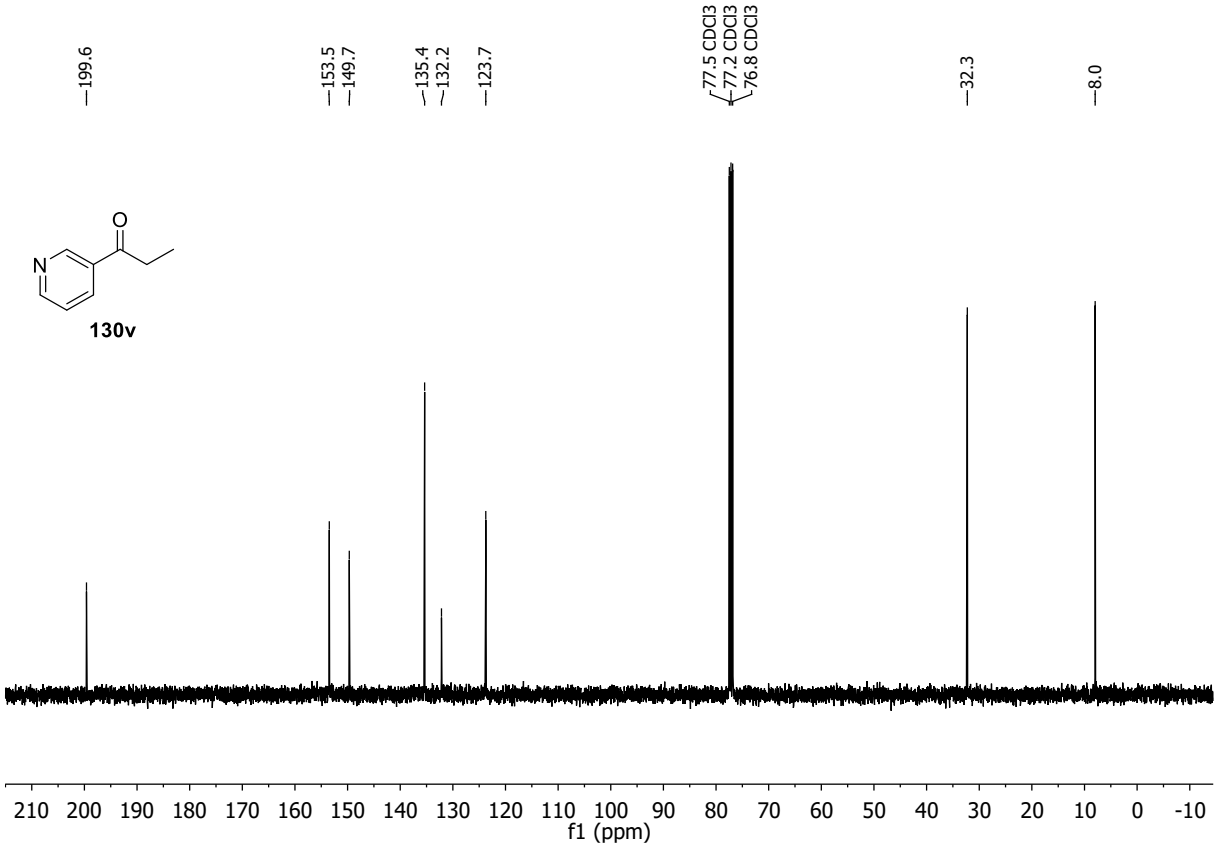
199.6
153.5
149.7
135.4
132.2
123.7
77.5 CDCl3
77.2 CDCl3
76.8 CDCl3
32.3
8.0
O
N
130v
210 200 190 180 170 160 150 140 130 120 110 100 90 80 70 60 50 40 30 20 10 0 -10
f1 (ppm)

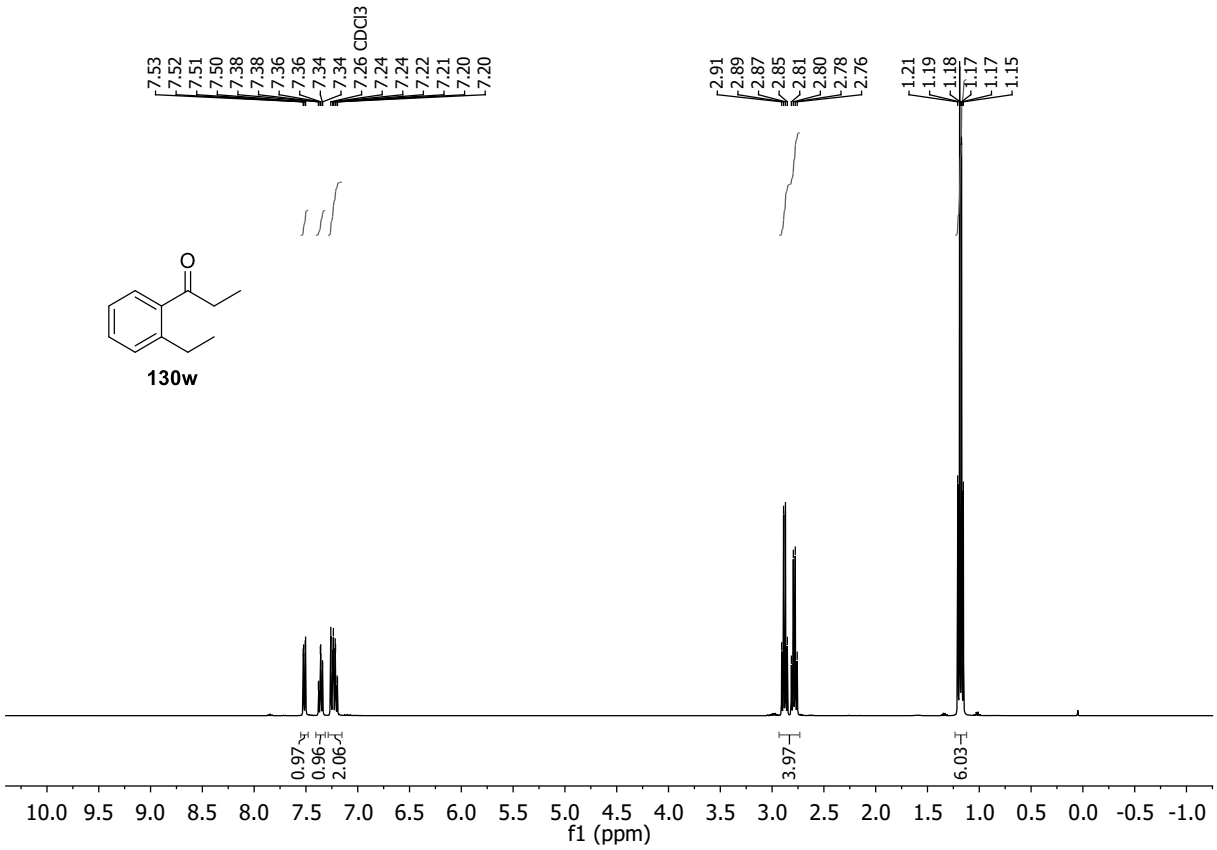
7.53
7.52
7.51
7.50
7.38
7.38
7.36
7.36
7.34
7.34
7.26 CDCl3
7.24
7.24
7.22
7.21
7.20
7.20
2.91
2.89
2.87
2.85
2.81
2.80
2.78
2.76
1.21
1.19
1.18
1.17
1.17
1.15
O
130w
0.97
0.96
2.06
3.97
6.03
10.0 9.5 9.0 8.5 8.0 7.5 7.0 6.5 6.0 5.5 5.0 4.5 4.0 3.5 3.0 2.5 2.0 1.5 1.0 0.5 0.0 -0.5 -1.0
f1 (ppm)

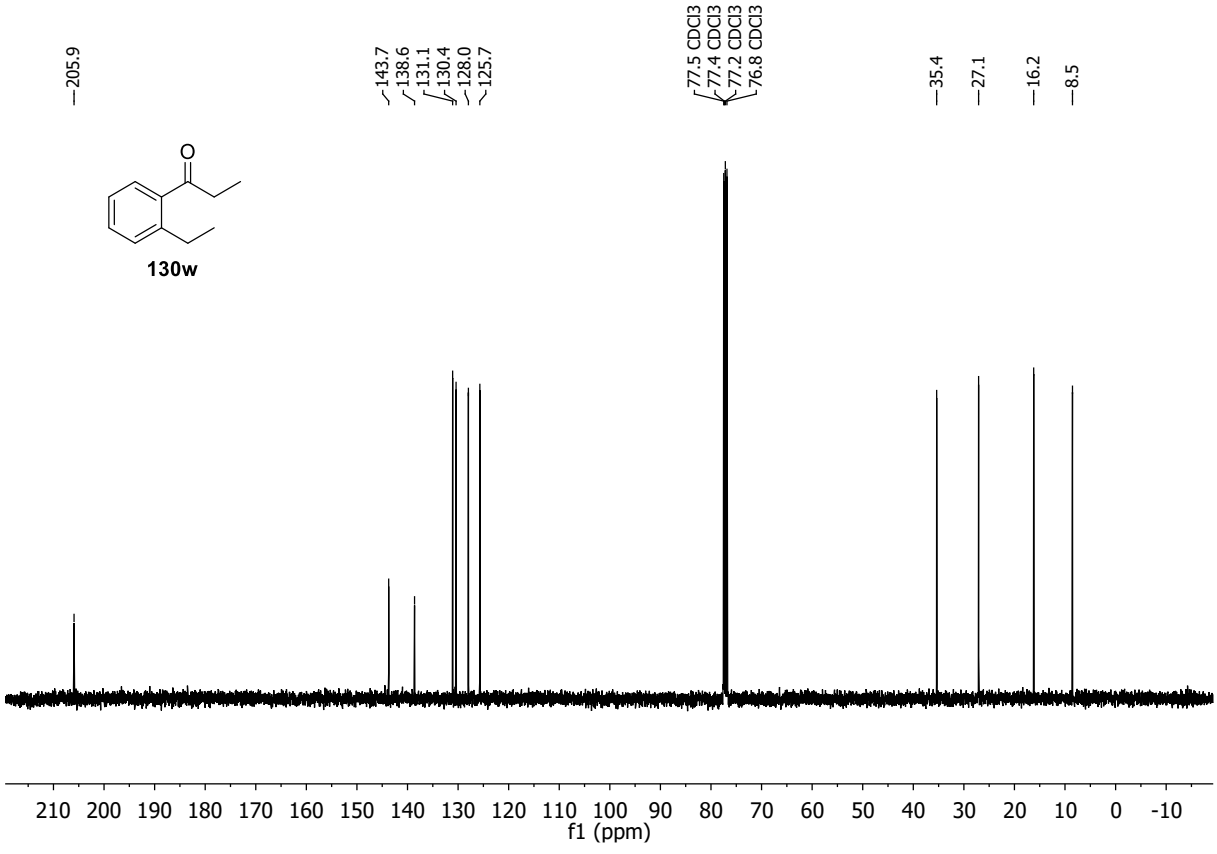
205.9
143.7
138.6
131.1
130.4
128.0
125.7
77.5 CDCl3
77.4 CDCl3
77.2 CDCl3
76.8 CDCl3
35.4
27.1
16.2
8.5
O
130w
210 200 190 180 170 160 150 140 130 120 110 100 90 80 70 60 50 40 30 20 10 0 -10
f1 (ppm)

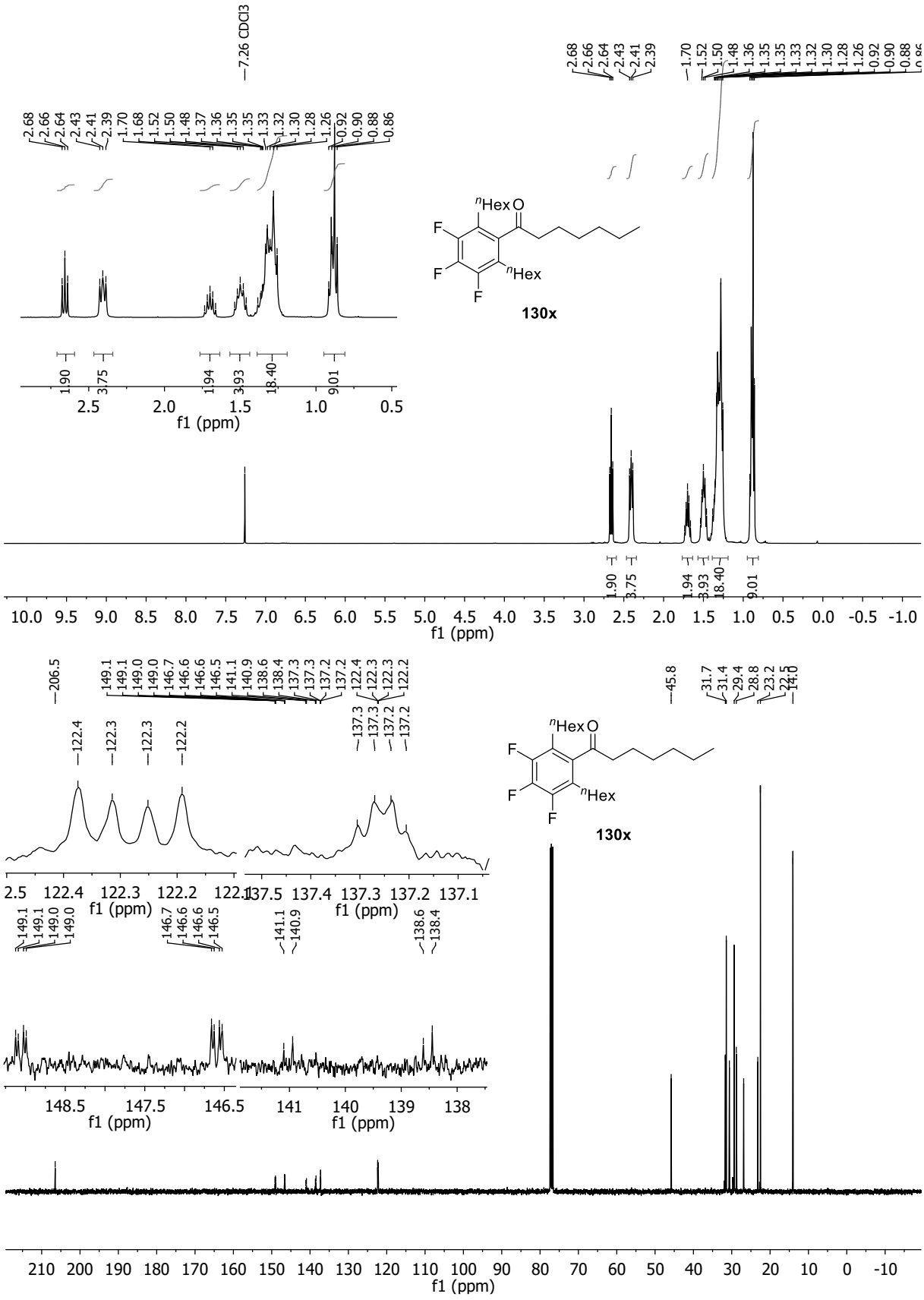
7.26 CDCl3
2.68 2.66 2.64 2.43 2.41 2.39 1.70 1.68 1.52 1.50 1.48 1.37 1.36 1.35 1.33 1.32 1.30 1.28 1.26 0.92 0.90 0.88 0.86
1.90 3.75 1.94 3.93 18.40 9.01
2.5 2.0 1.5 1.0 0.5
f1 (ppm)
nHex O
F
F
F
nHex
130x
10.0 9.5 9.0 8.5 8.0 7.5 7.0 6.5 6.0 5.5 5.0 4.5 4.0 3.5 3.0 2.5 2.0 1.5 1.0 0.5 0.0 -0.5 -1.0
f1 (ppm)
206.5
149.1 149.1 149.0 149.0 146.7 146.6 146.6 146.5 141.1 140.9 138.6 138.4 137.3 137.3 137.2 137.2 122.4 122.3 122.3 122.2 137.3 137.3 137.2 137.2
122.4 122.3 122.3 122.2
2.5 122.4 122.3 122.2 122.1
f1 (ppm)
137.5 137.4 137.3 137.2 137.1
f1 (ppm)
149.1 149.1 149.0 149.0 146.7 146.6 146.6 146.5 141.1 140.9 138.6 138.4
148.5 147.5 146.5
f1 (ppm)
141 140 139 138
f1 (ppm)
45.8 31.7 31.4 29.4 28.8 23.2 22.5 14.0
210 200 190 180 170 160 150 140 130 120 110 100 90 80 70 60 50 40 30 20 10 0 -10
f1 (ppm)

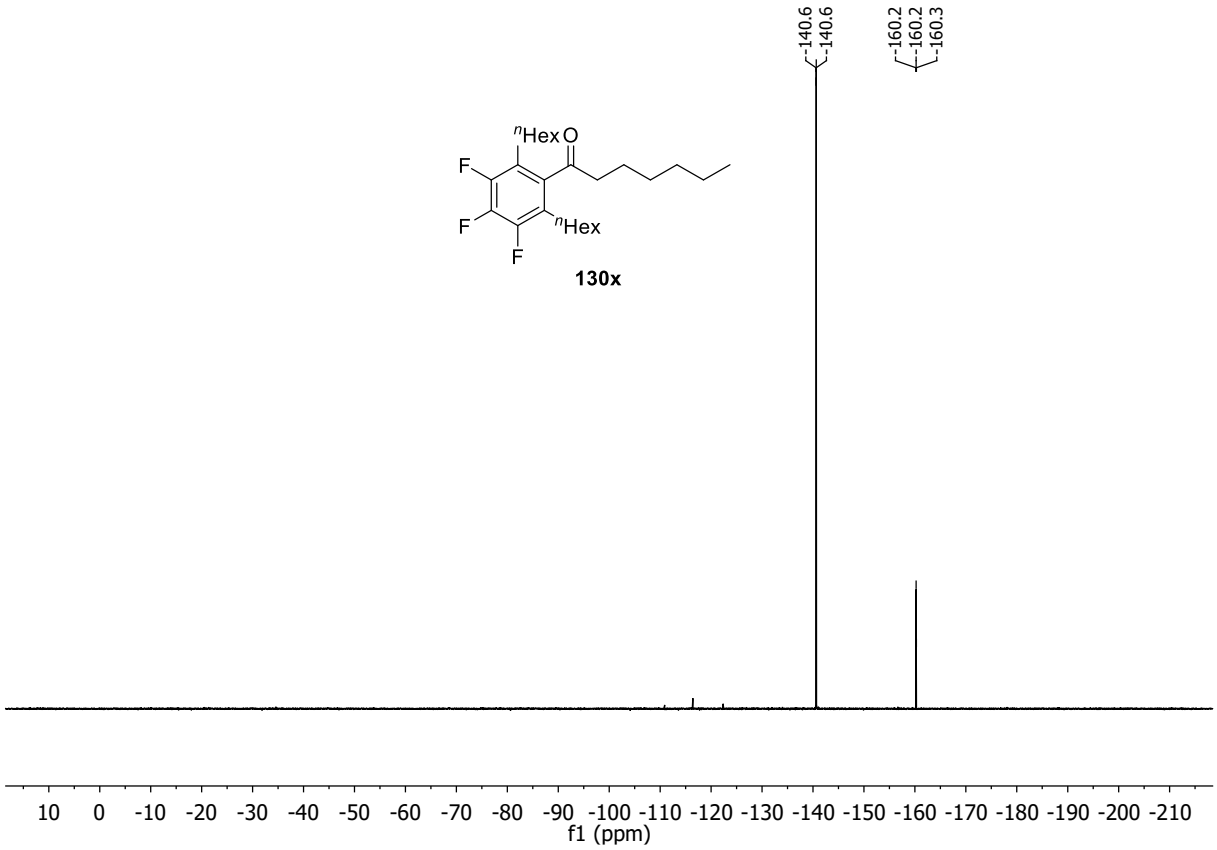
-140.6
-140.6
-160.2
-160.2
-160.3
nHex
O
F
F
F
nHex
130x
10 0 -10 -20 -30 -40 -50 -60 -70 -80 -90 -100 -110 -120 -130 -140 -150 -160 -170 -180 -190 -200 -210
f1 (ppm)

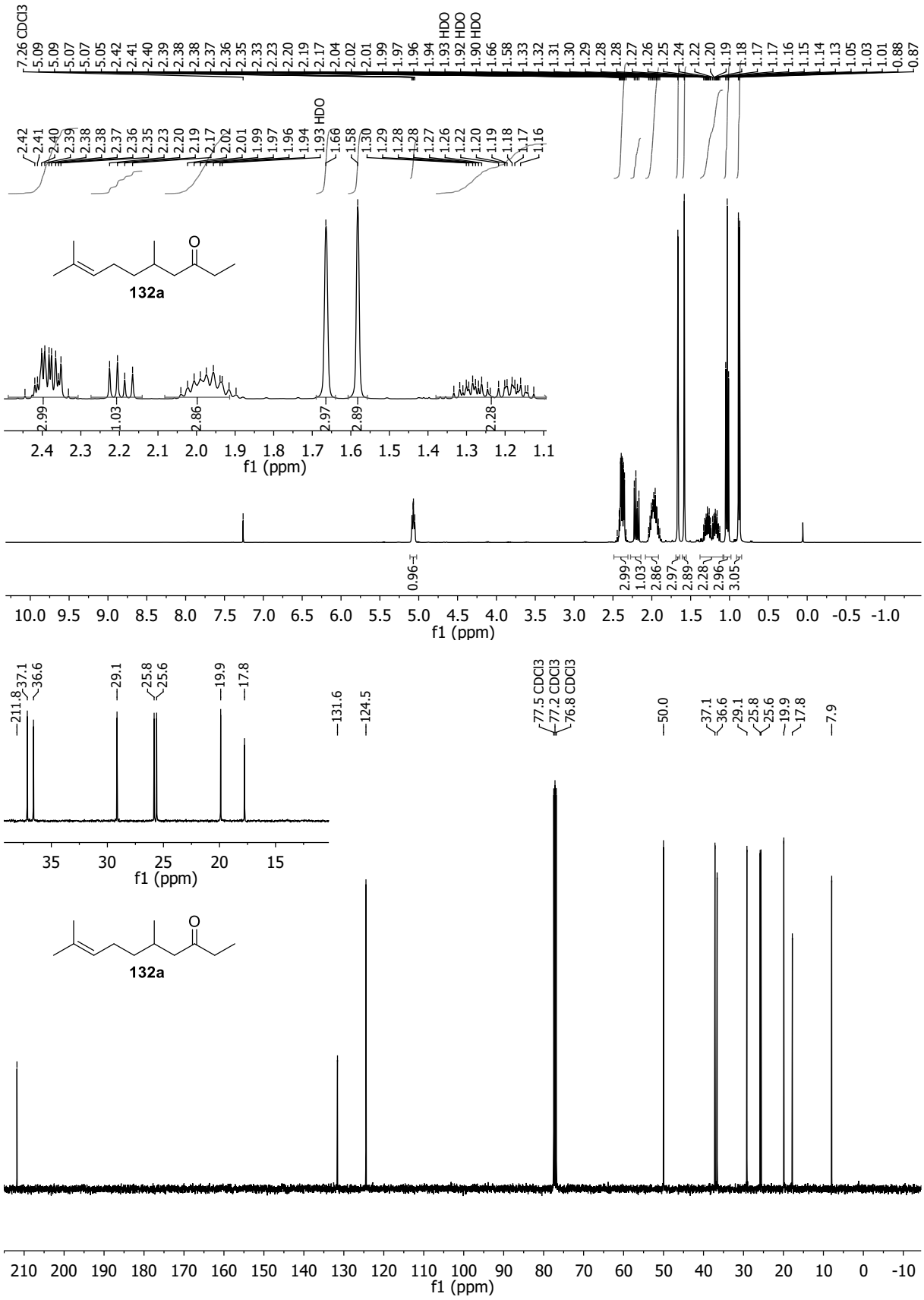
7.26 CDCl3
HDO
132a
f1 (ppm)
77.5 CDCl3
77.2 CDCl3
76.8 CDCl3
132a
f1 (ppm)

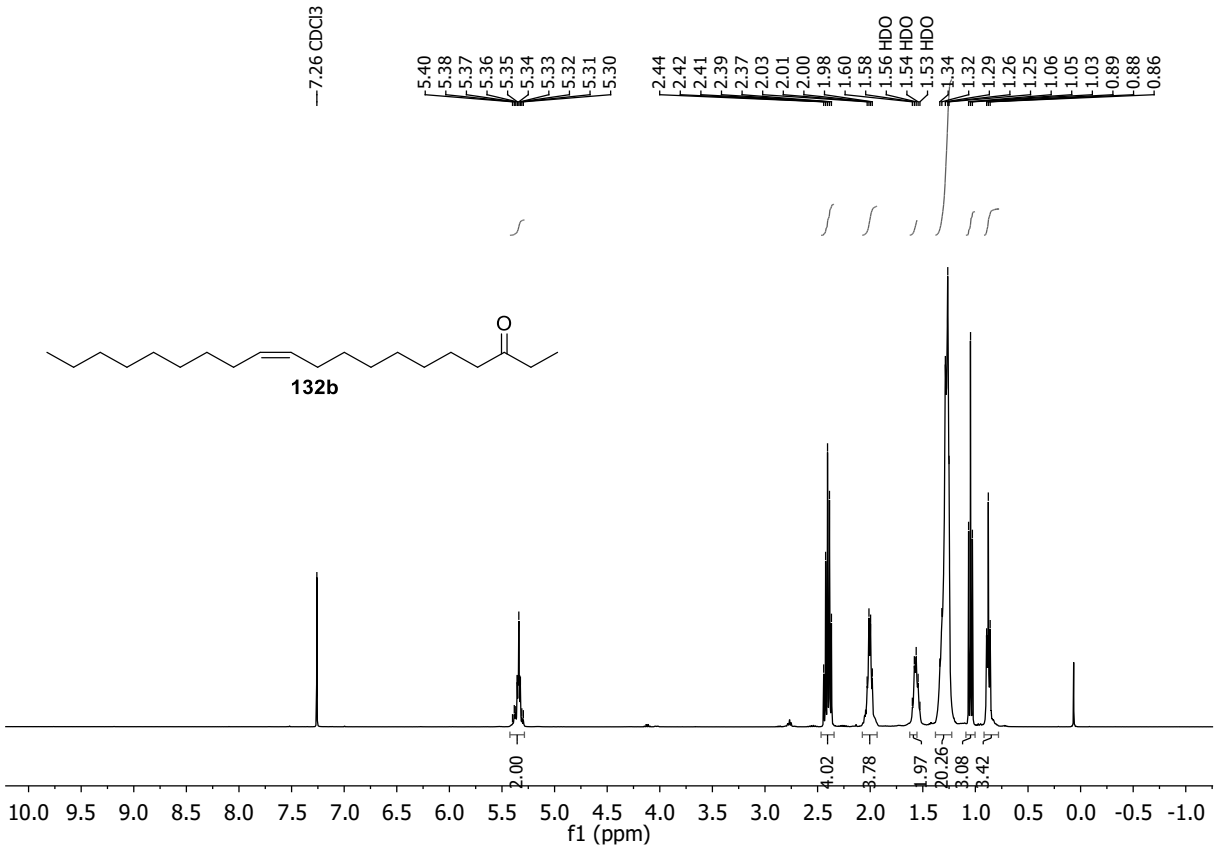
7.26 CDCl3
5.40
5.38
5.37
5.36
5.35
5.34
5.33
5.32
5.31
5.30
2.44
2.42
2.41
2.39
2.37
2.03
2.01
2.00
1.98
1.60
1.58
1.56 HDO
1.54 HDO
1.53 HDO
1.34
1.32
1.29
1.26
1.25
1.06
1.05
1.03
0.89
0.88
0.86
O
132b
2.00
4.02
3.78
1.97
20.26
3.08
3.42
10.0 9.5 9.0 8.5 8.0 7.5 7.0 6.5 6.0 5.5 5.0 4.5 4.0 3.5 3.0 2.5 2.0 1.5 1.0 0.5 0.0 -0.5 -1.0
f1 (ppm)

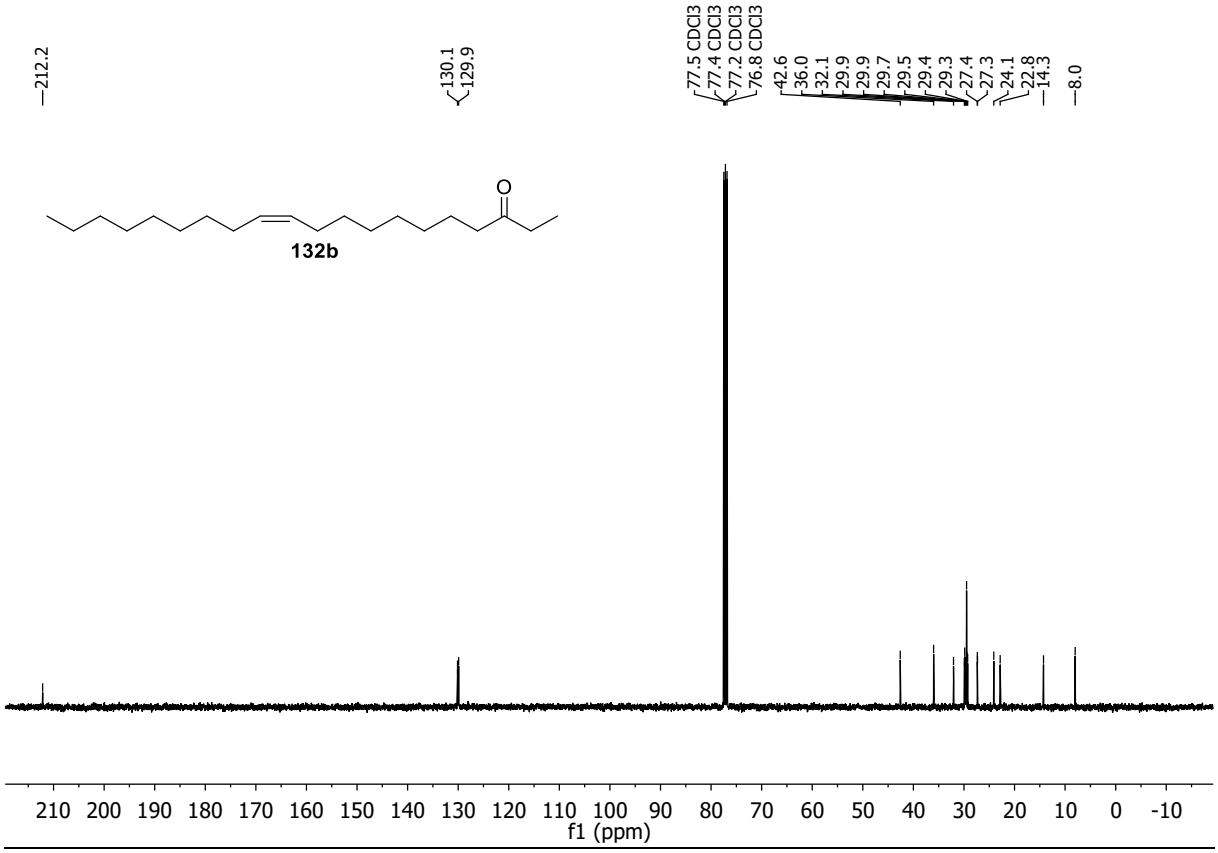
212.2
130.1
129.9
77.5 CDCl3
77.4 CDCl3
77.2 CDCl3
76.8 CDCl3
42.6
36.0
32.1
29.9
29.9
29.7
29.5
29.4
29.3
27.4
27.3
24.1
22.8
14.3
8.0
O
132b
210 200 190 180 170 160 150 140 130 120 110 100 90 80 70 60 50 40 30 20 10 0 -10
f1 (ppm)

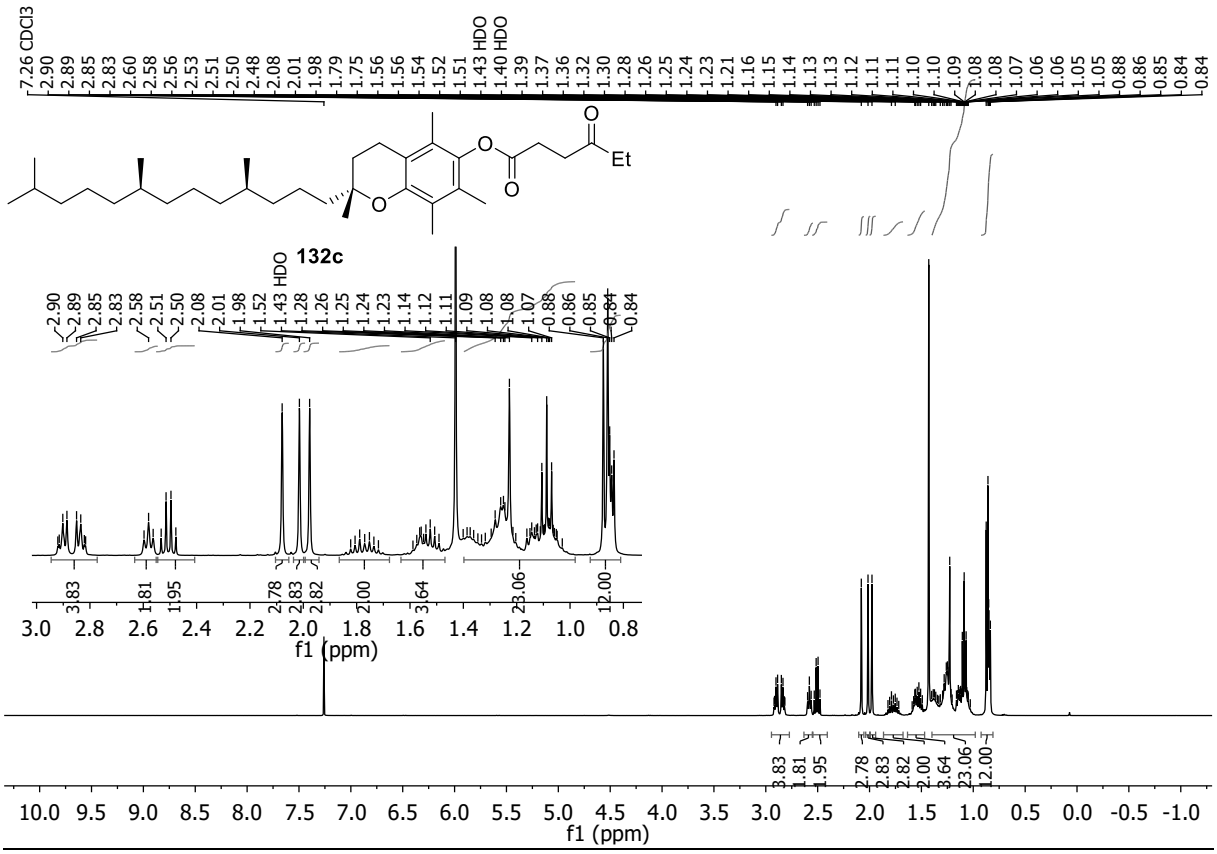
7.26 CDCl3
HDO
Et
O
132c
f1 (ppm)

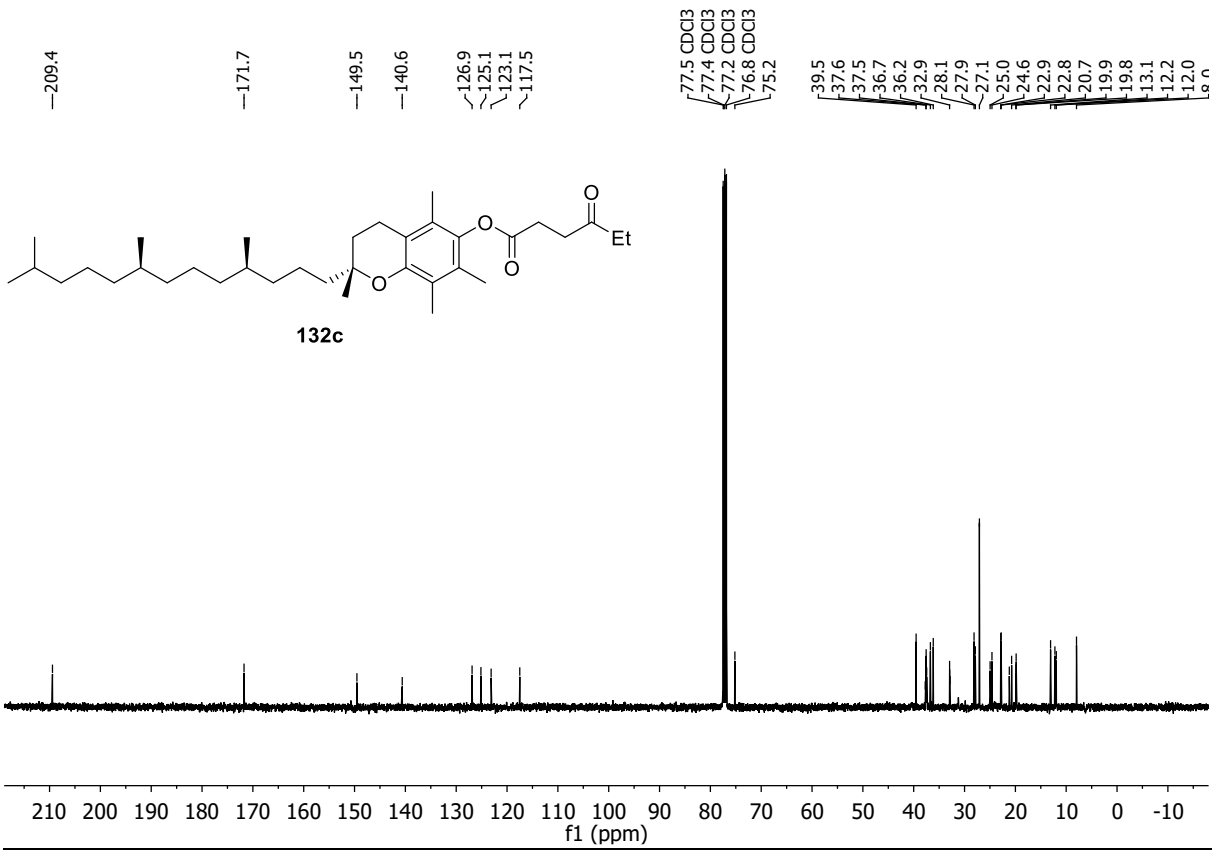
209.4
171.7
149.5
140.6
126.9
125.1
123.1
117.5
77.5 CDCl3
77.4 CDCl3
77.2 CDCl3
76.8 CDCl3
75.2
Et
O
132c
f1 (ppm)

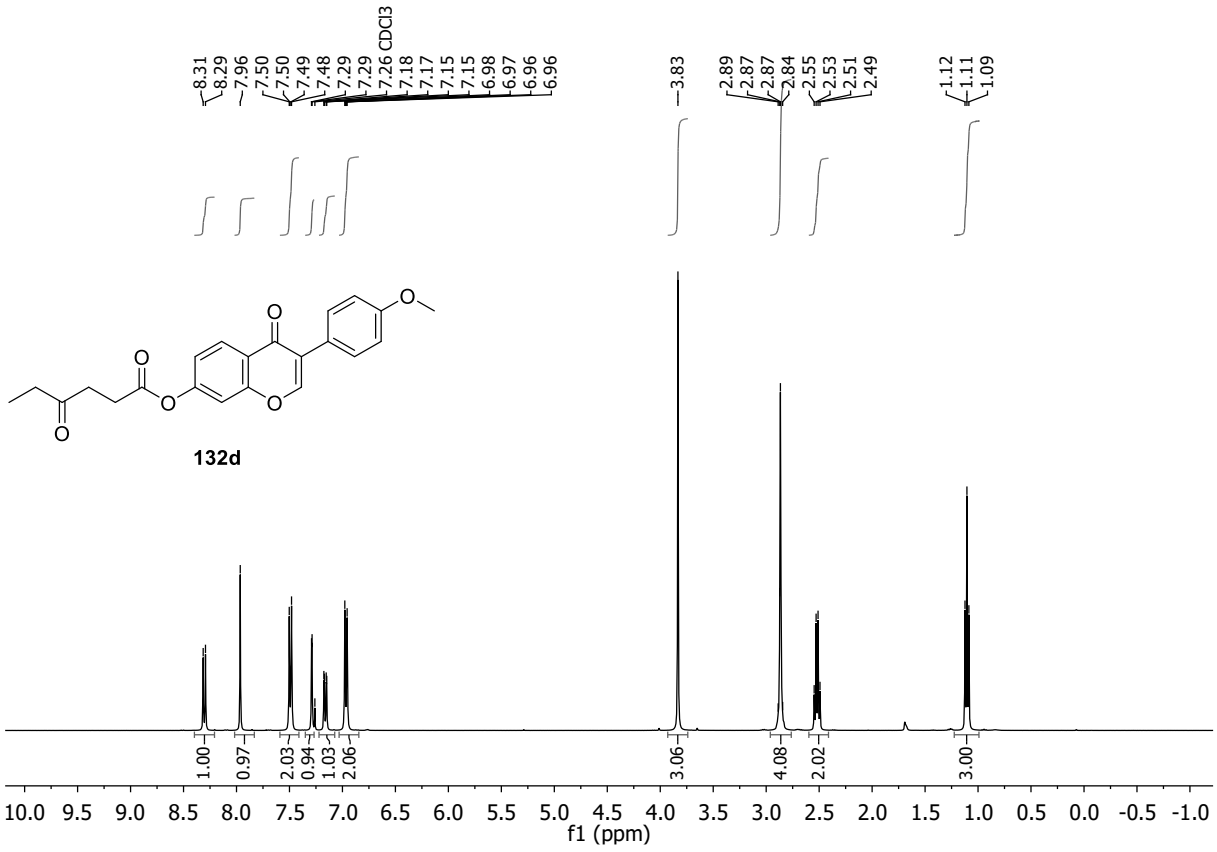
8.31
8.29
7.96
7.50
7.50
7.49
7.48
7.29
7.29
7.26 CDCl3
7.18
7.17
7.15
7.15
6.98
6.97
6.96
6.96
3.83
2.89
2.87
2.87
2.84
2.55
2.53
2.51
2.49
1.12
1.11
1.09
132d
1.00
0.97
2.03
0.94
1.03
2.06
3.06
4.08
2.02
3.00
f1 (ppm)

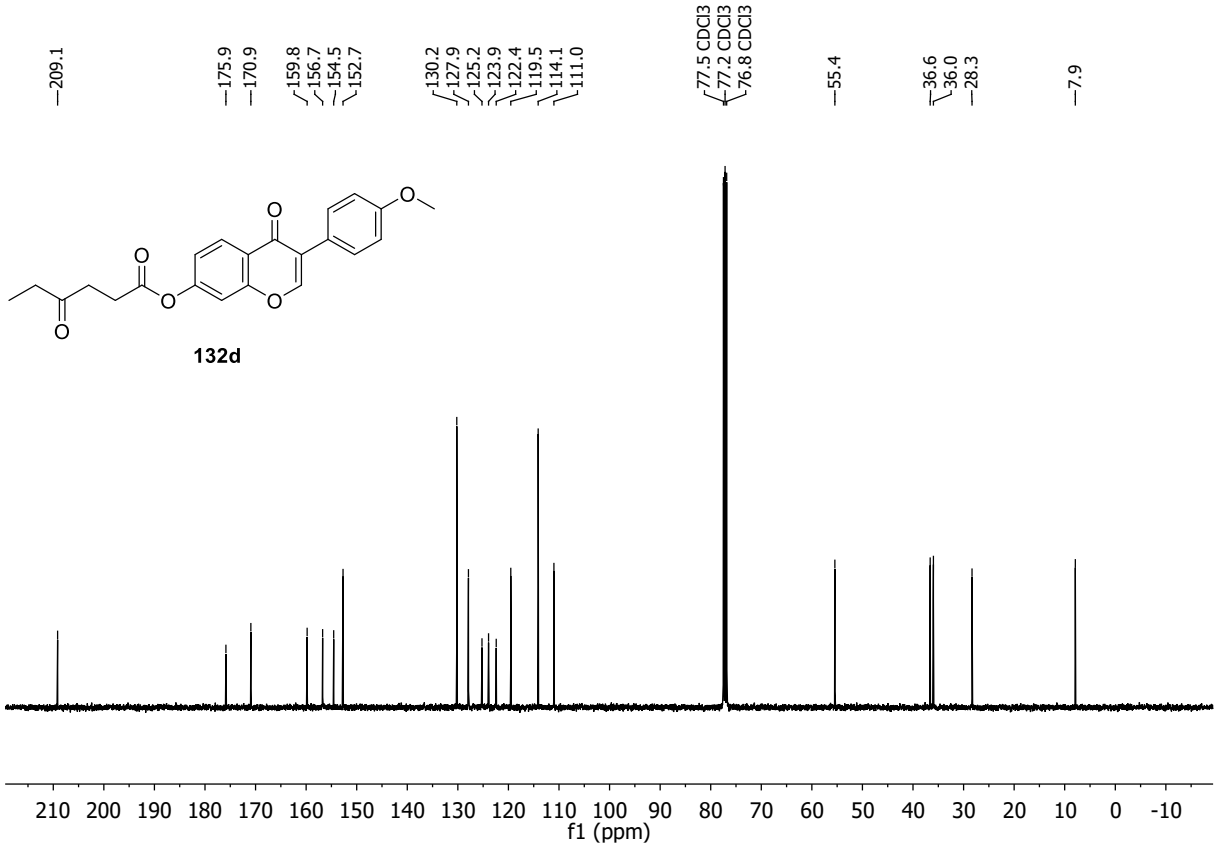
209.1
175.9
170.9
159.8
156.7
154.5
152.7
130.2
127.9
125.2
123.9
122.4
119.5
114.1
111.0
77.5 CDCl3
77.2 CDCl3
76.8 CDCl3
55.4
36.6
36.0
28.3
7.9
132d
f1 (ppm)

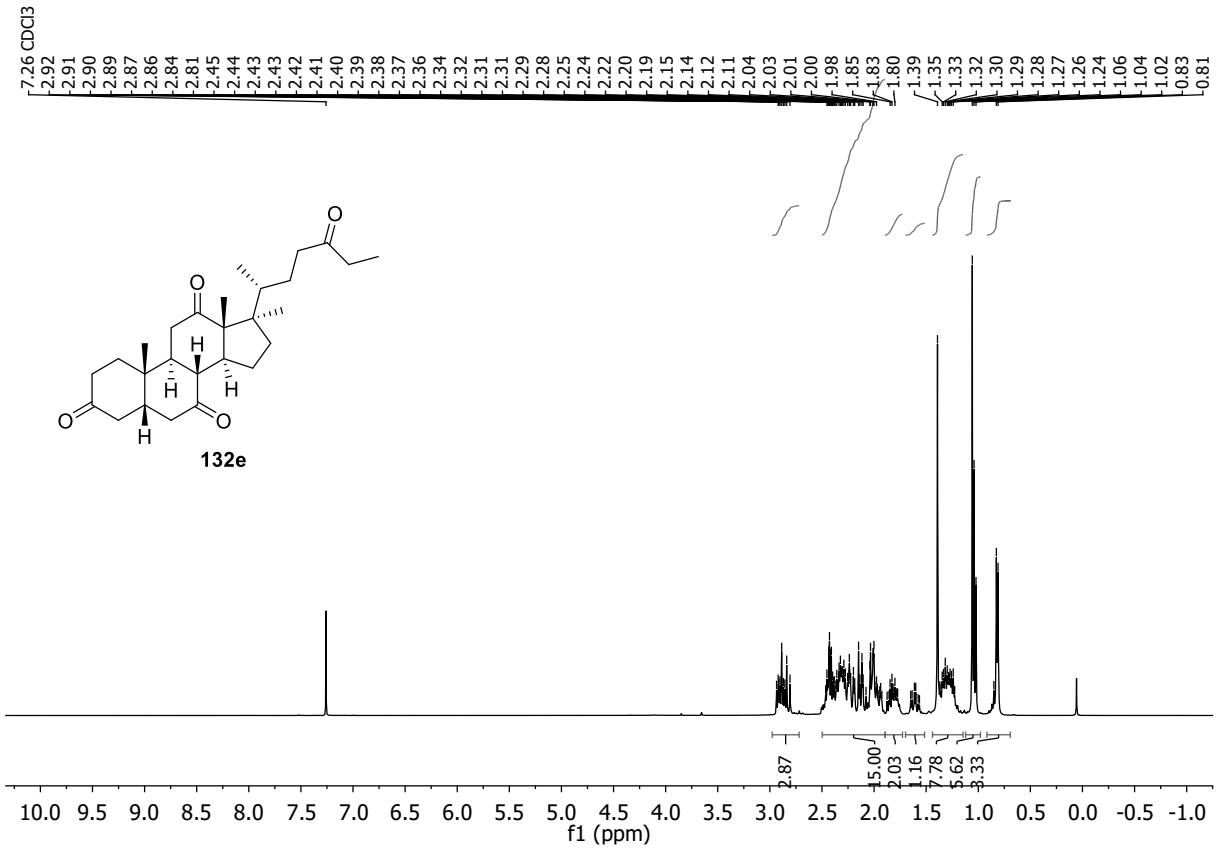
7.26 CDCl3
2.92
2.91
2.90
2.89
2.87
2.86
2.84
2.81
2.45
2.44
2.43
2.43
2.42
2.41
2.40
2.39
2.38
2.37
2.36
2.34
2.32
2.31
2.31
2.29
2.28
2.25
2.24
2.22
2.20
2.19
2.15
2.14
2.12
2.11
2.04
2.03
2.01
2.00
1.98
1.85
1.83
1.80
1.39
1.35
1.33
1.32
1.30
1.29
1.28
1.27
1.26
1.24
1.06
1.04
1.02
0.83
0.81
O
O
H
H
H
O
O
H
132e
2.87
15.00
2.03
1.16
7.78
5.62
3.33
10.0 9.5 9.0 8.5 8.0 7.5 7.0 6.5 6.0 5.5 5.0 4.5 4.0 3.5 3.0 2.5 2.0 1.5 1.0 0.5 0.0 -0.5 -1.0
f1 (ppm)

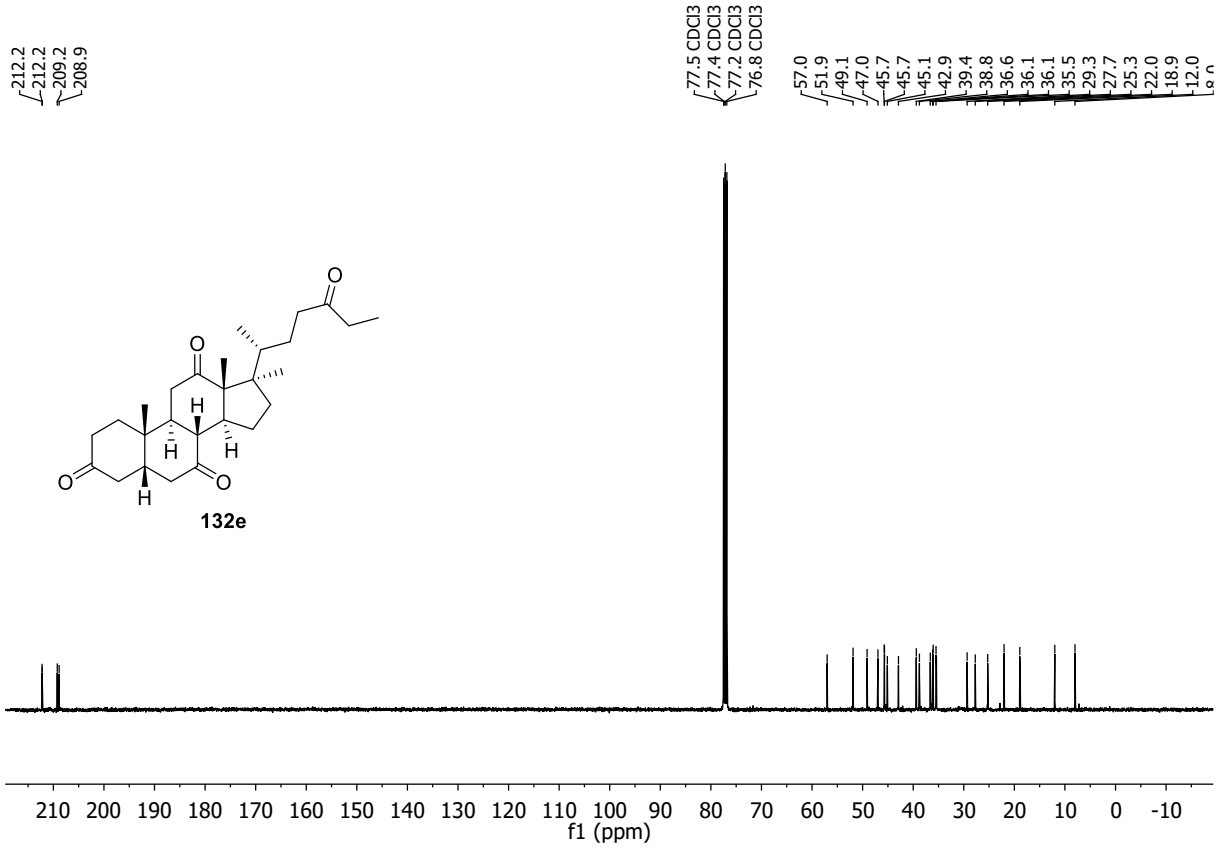
212.2
212.2
209.2
208.9
77.5 CDCl3
77.4 CDCl3
77.2 CDCl3
76.8 CDCl3
57.0
51.9
49.1
47.0
45.7
45.7
45.1
42.9
39.4
38.8
36.6
36.1
36.1
35.5
29.3
27.7
25.3
22.0
18.9
12.0
O
O
H
H
H
O
O
H
132e
210 200 190 180 170 160 150 140 130 120 110 100 90 80 70 60 50 40 30 20 10 0 -10
f1 (ppm)

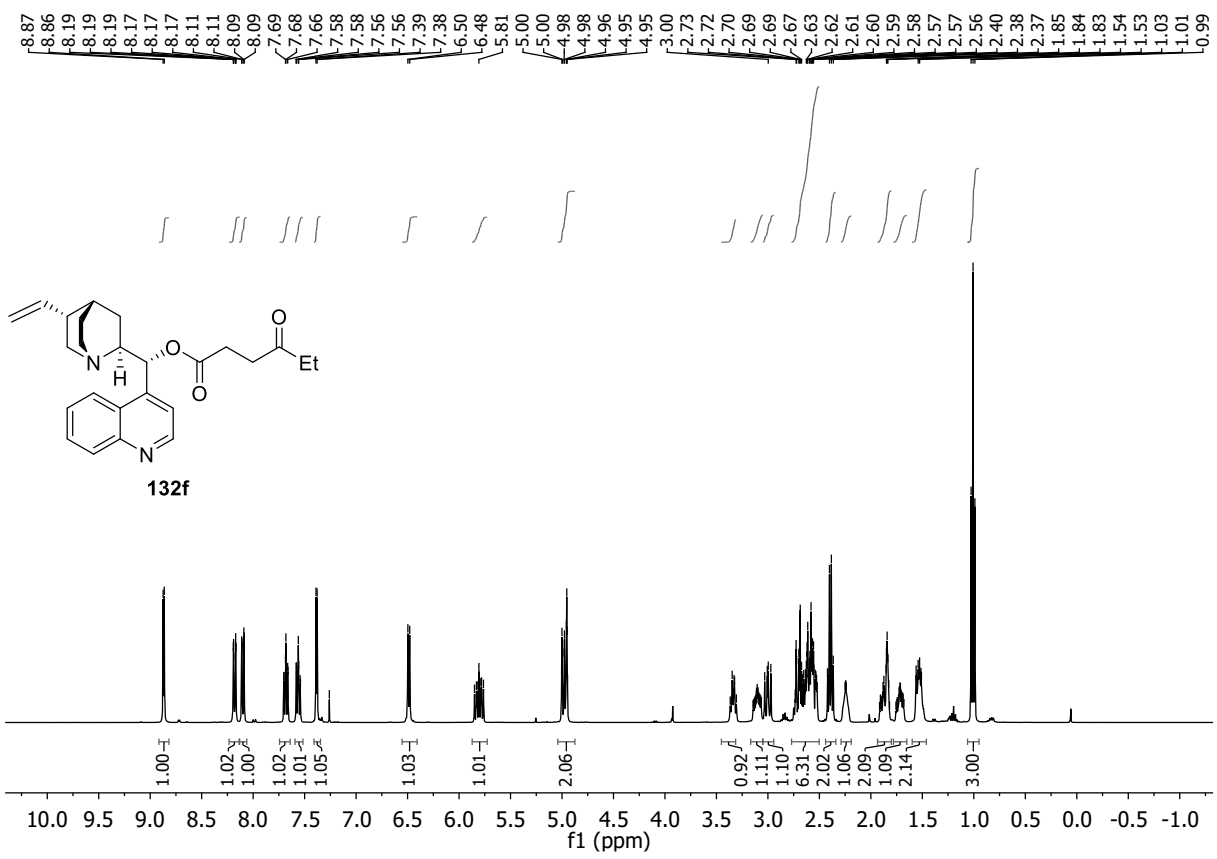
8.87 8.86 8.19 8.19 8.19 8.17 8.17 8.17 8.11 8.11 8.09 8.09
7.69 7.68 7.66 7.58 7.58 7.56 7.56 7.39 7.38 6.50 6.48 5.81
5.00 5.00 4.98 4.98 4.96 4.95 4.95
3.00 2.73 2.72 2.70 2.69 2.69 2.67 2.63 2.62 2.61 2.60 2.59 2.58 2.57 2.57 2.56 2.40 2.38 2.37 1.85 1.84 1.83 1.54 1.53 1.03 1.01 0.99
O
Et
O
O
N
H
N
132f
1.00 1.02 1.00 1.02 1.01 1.05 1.03 1.01 2.06 0.92 1.11 1.10 6.31 2.02 1.06 2.09 1.09 2.14 3.00
10.0 9.5 9.0 8.5 8.0 7.5 7.0 6.5 6.0 5.5 5.0 4.5 4.0 3.5 3.0 2.5 2.0 1.5 1.0 0.5 0.0 -0.5 -1.0
f1 (ppm)

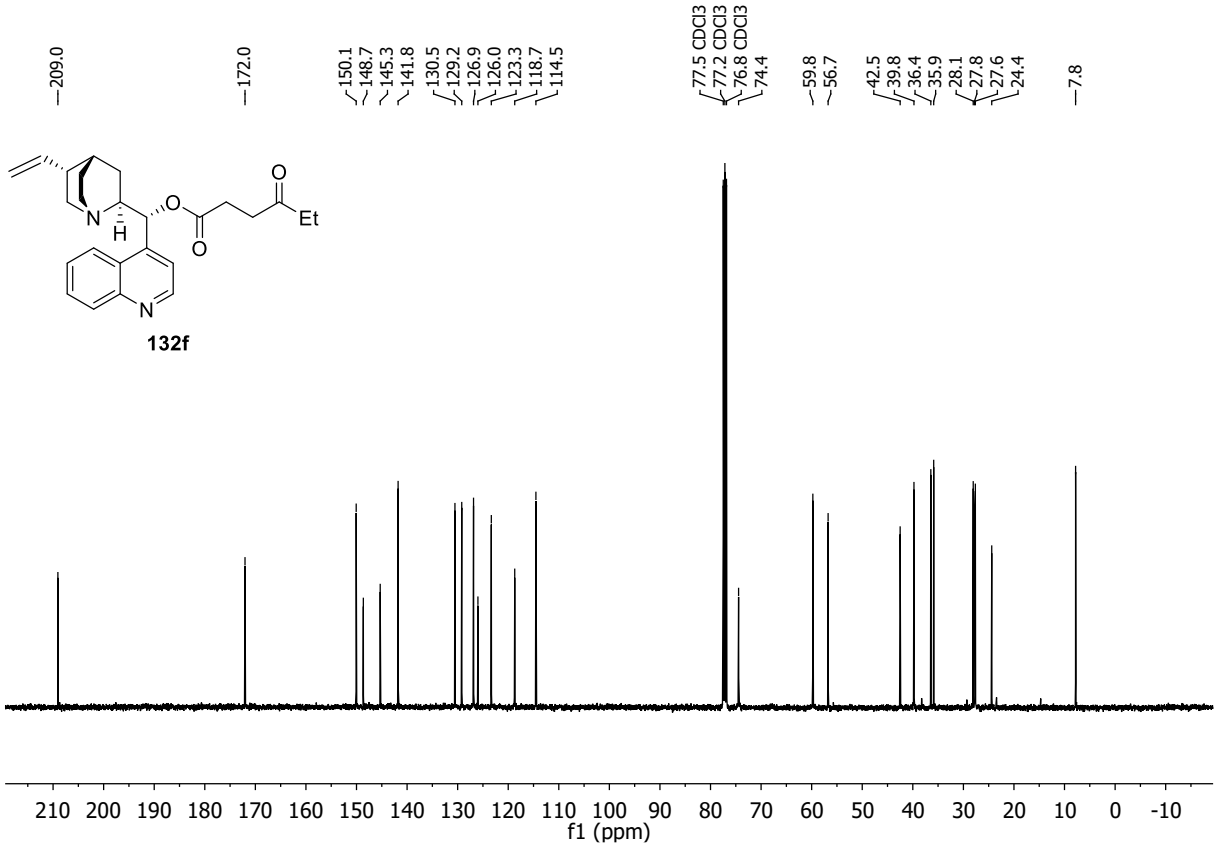
209.0
172.0
150.1 148.7 145.3 141.8 130.5 129.2 126.9 126.0 123.3 118.7 114.5
77.5 CDCl3 77.2 CDCl3 76.8 CDCl3 74.4
59.8 56.7
42.5 39.8 36.4 35.9 28.1 27.8 27.6 24.4
7.8
O
Et
O
O
N
H
N
132f
210 200 190 180 170 160 150 140 130 120 110 100 90 80 70 60 50 40 30 20 10 0 -10
f1 (ppm)

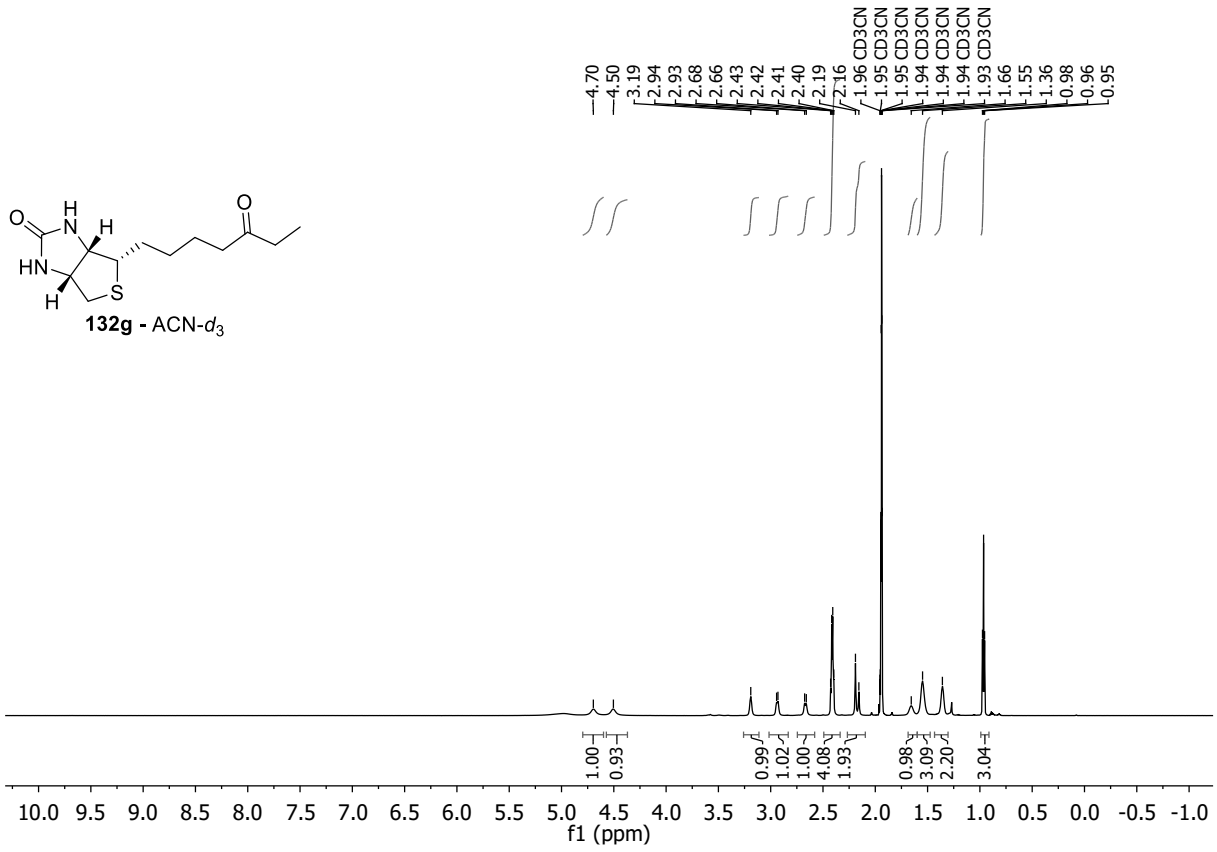
4.70
4.50
3.19
2.94
2.93
2.68
2.66
2.43
2.42
2.41
2.40
2.19
2.16
1.96 CD3CN
1.95 CD3CN
1.95 CD3CN
1.94 CD3CN
1.94 CD3CN
1.94 CD3CN
1.93 CD3CN
1.66
1.55
1.36
0.98
0.96
0.95
1.00
0.93
0.99
1.02
1.00
4.08
1.93
0.98
3.09
2.20
3.04
10.0 9.5 9.0 8.5 8.0 7.5 7.0 6.5 6.0 5.5 5.0 4.5 4.0 3.5 3.0 2.5 2.0 1.5 1.0 0.5 0.0 -0.5 -1.0
f1 (ppm)
132g - ACN-d3

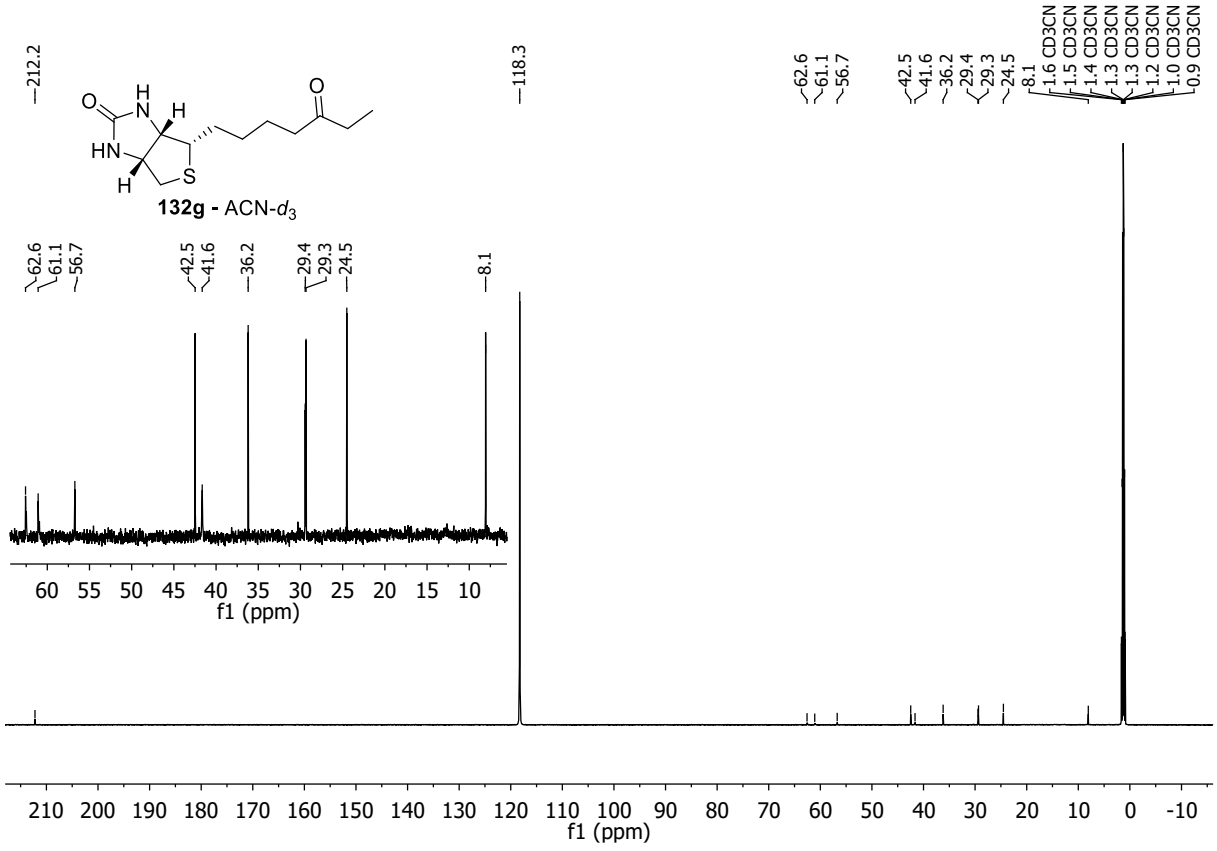
212.2
118.3
62.6
61.1
56.7
42.5
41.6
36.2
29.4
29.3
24.5
8.1
1.6 CD3CN
1.5 CD3CN
1.4 CD3CN
1.3 CD3CN
1.3 CD3CN
1.2 CD3CN
1.0 CD3CN
0.9 CD3CN
60 55 50 45 40 35 30 25 20 15 10
f1 (ppm)
210 200 190 180 170 160 150 140 130 120 110 100 90 80 70 60 50 40 30 20 10 0 -10
f1 (ppm)
132g - ACN-d3

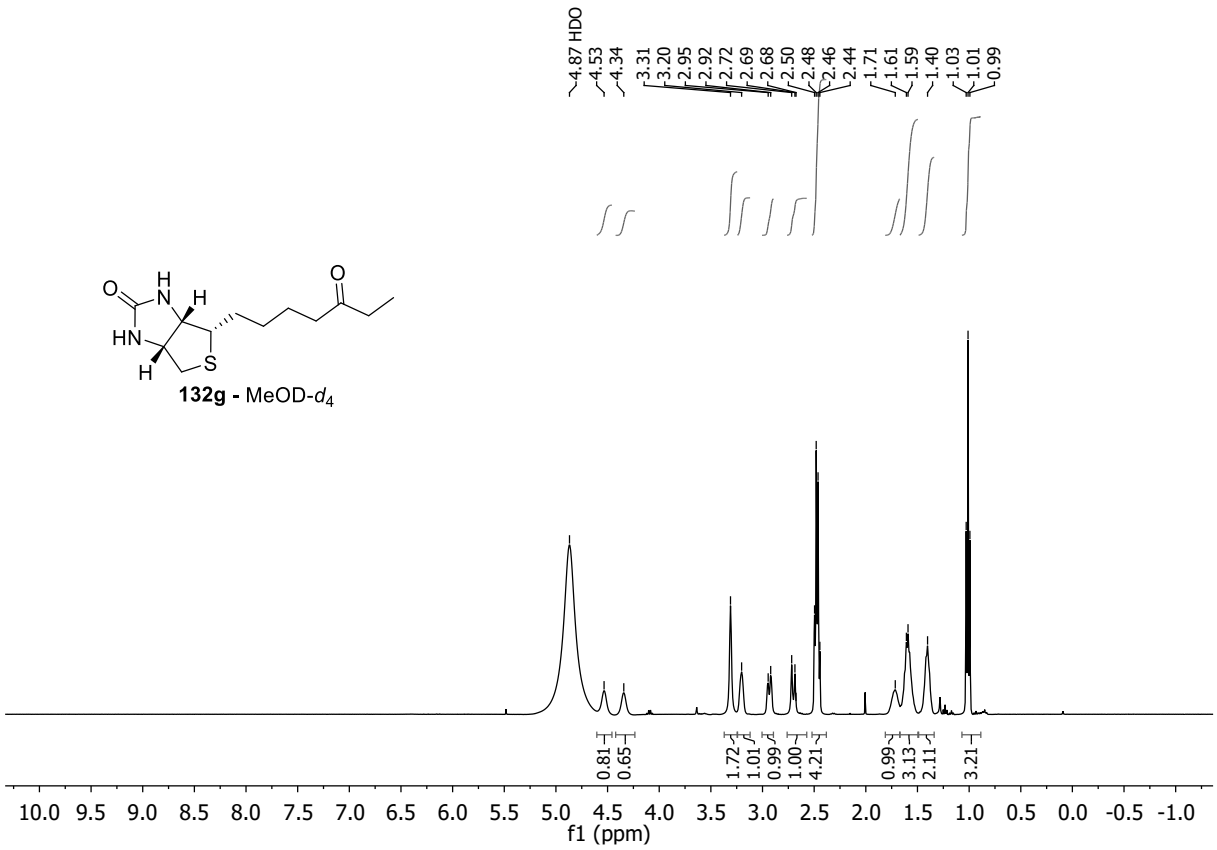
4.87 HDO
4.53
4.34
3.31
3.20
2.95
2.92
2.72
2.69
2.68
2.50
2.48
2.46
2.44
1.71
1.61
1.59
1.40
1.03
1.01
0.99
132g - MeOD-d4
0.81
0.65
1.72
1.01
0.99
1.00
4.21
0.99
3.13
2.11
3.21
f1 (ppm)

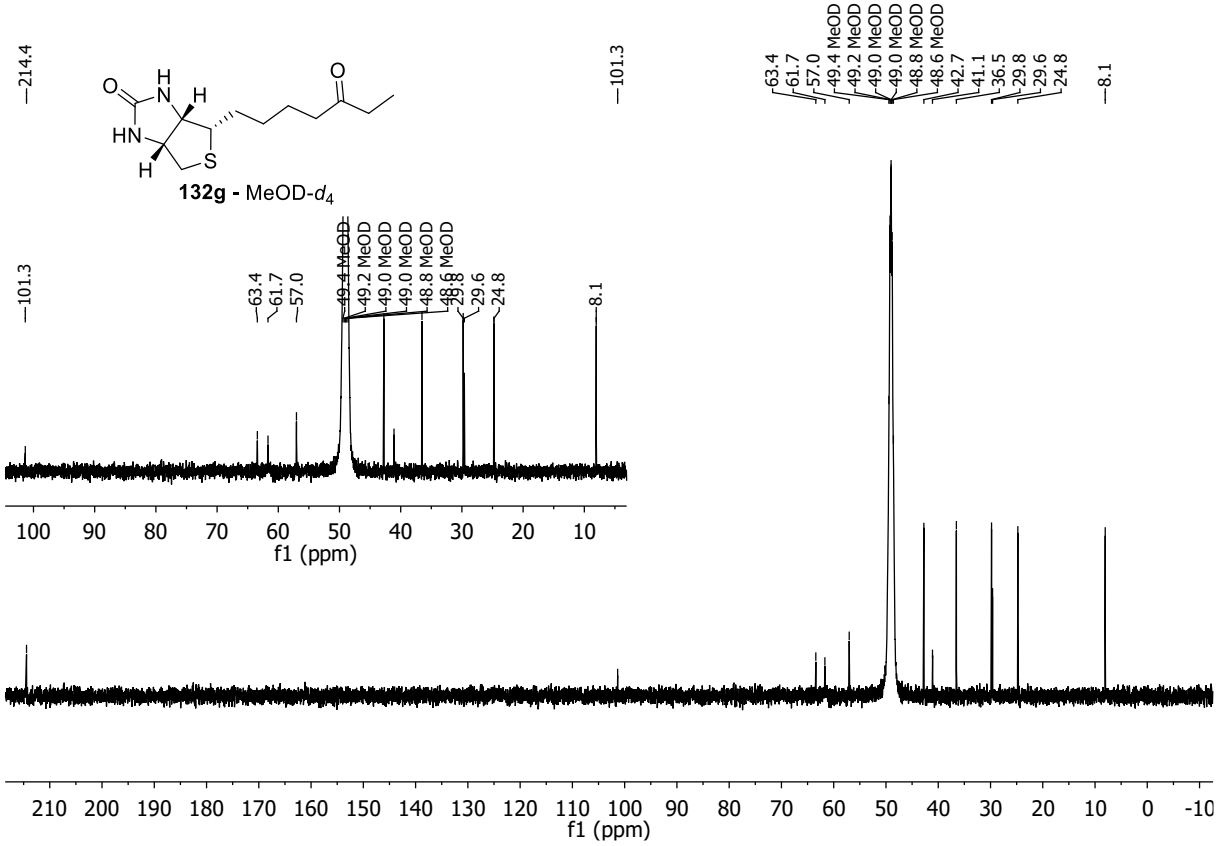
214.4
101.3
63.4
61.7
57.0
49.4 MeOD
49.2 MeOD
49.0 MeOD
49.0 MeOD
48.8 MeOD
48.6 MeOD
42.7
41.1
36.5
29.8
29.6
24.8
8.1
132g - MeOD-d4
f1 (ppm)

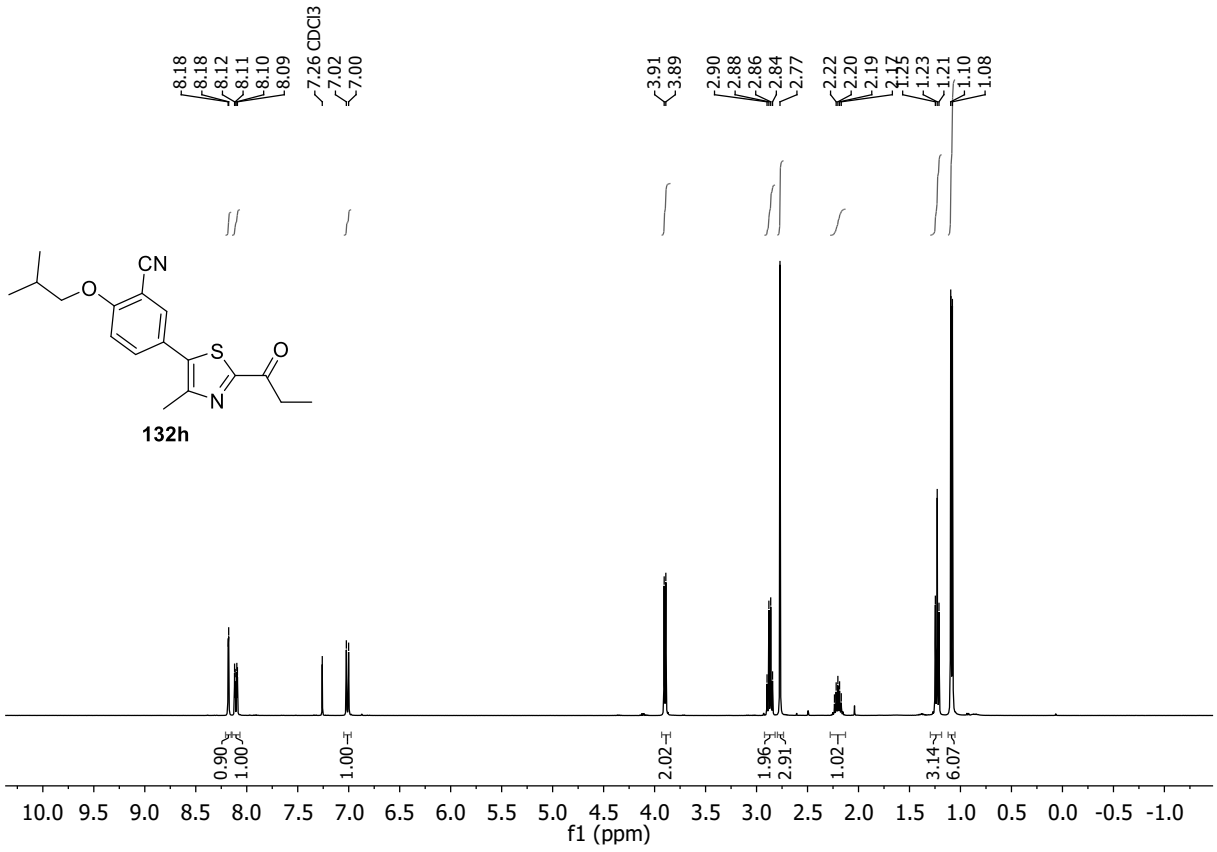
8.18
8.18
8.12
8.11
8.10
8.09
7.26 CDCl3
7.02
7.00
3.91
3.89
2.90
2.88
2.86
2.84
2.77
2.22
2.20
2.19
1.23
1.21
1.10
1.08
CN
O
S
N
O
132h
0.90
1.00
1.00
2.02
1.96
2.91
1.02
3.14
6.07
10.0 9.5 9.0 8.5 8.0 7.5 7.0 6.5 6.0 5.5 5.0 4.5 4.0 3.5 3.0 2.5 2.0 1.5 1.0 0.5 0.0 -0.5 -1.0
f1 (ppm)

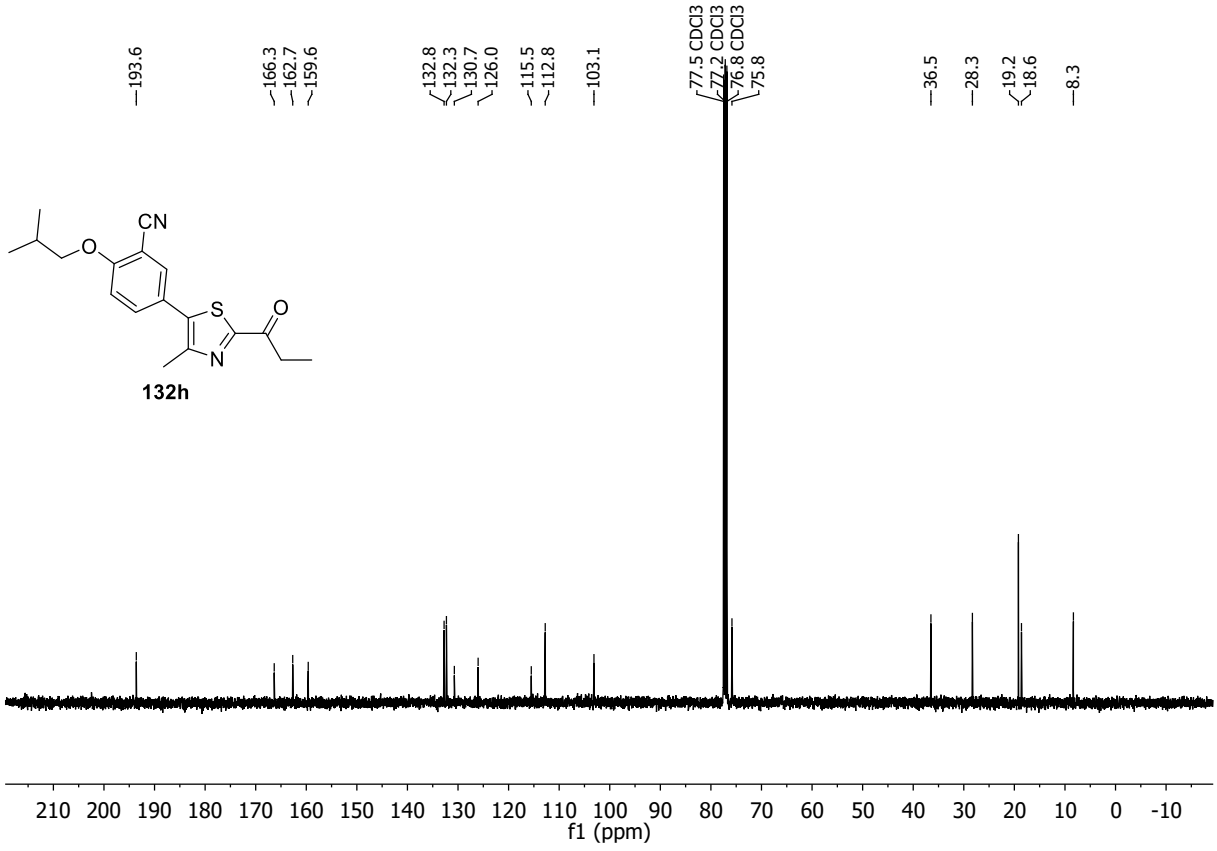
193.6
166.3
162.7
159.6
132.8
132.3
130.7
126.0
115.5
112.8
103.1
77.5 CDCl3
77.2 CDCl3
76.8 CDCl3
75.8
36.5
28.3
19.2
18.6
8.3
CN
O
S
N
O
132h
210 200 190 180 170 160 150 140 130 120 110 100 90 80 70 60 50 40 30 20 10 0 -10
f1 (ppm)

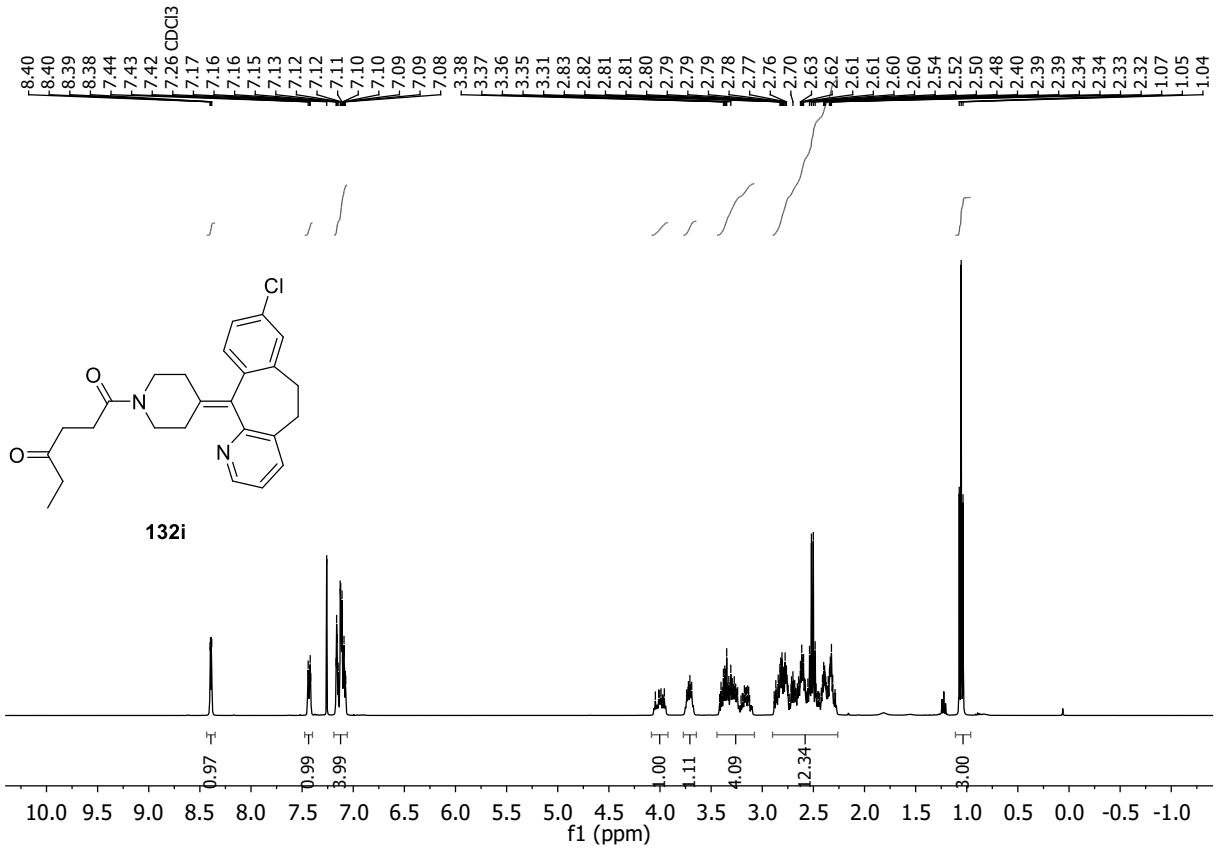
8.40 8.40 8.39 8.38 7.44 7.43 7.42 7.26 CDCl3 7.17 7.16 7.16 7.15 7.13 7.12 7.12 7.11 7.10 7.09 7.09 7.08 3.38 3.37 3.36 3.35 3.31 2.83 2.82 2.81 2.81 2.80 2.79 2.79 2.79 2.78 2.77 2.76 2.70 2.63 2.62 2.61 2.61 2.60 2.60 2.54 2.52 2.50 2.48 2.40 2.39 2.39 2.34 2.34 2.33 2.32 1.07 1.05 1.04
Cl
O
N
O
N
132i
0.97
0.99
3.99
1.00
1.11
4.09
12.34
3.00
10.0 9.5 9.0 8.5 8.0 7.5 7.0 6.5 6.0 5.5 5.0 4.5 4.0 3.5 3.0 2.5 2.0 1.5 1.0 0.5 0.0 -0.5 -1.0
f1 (ppm)

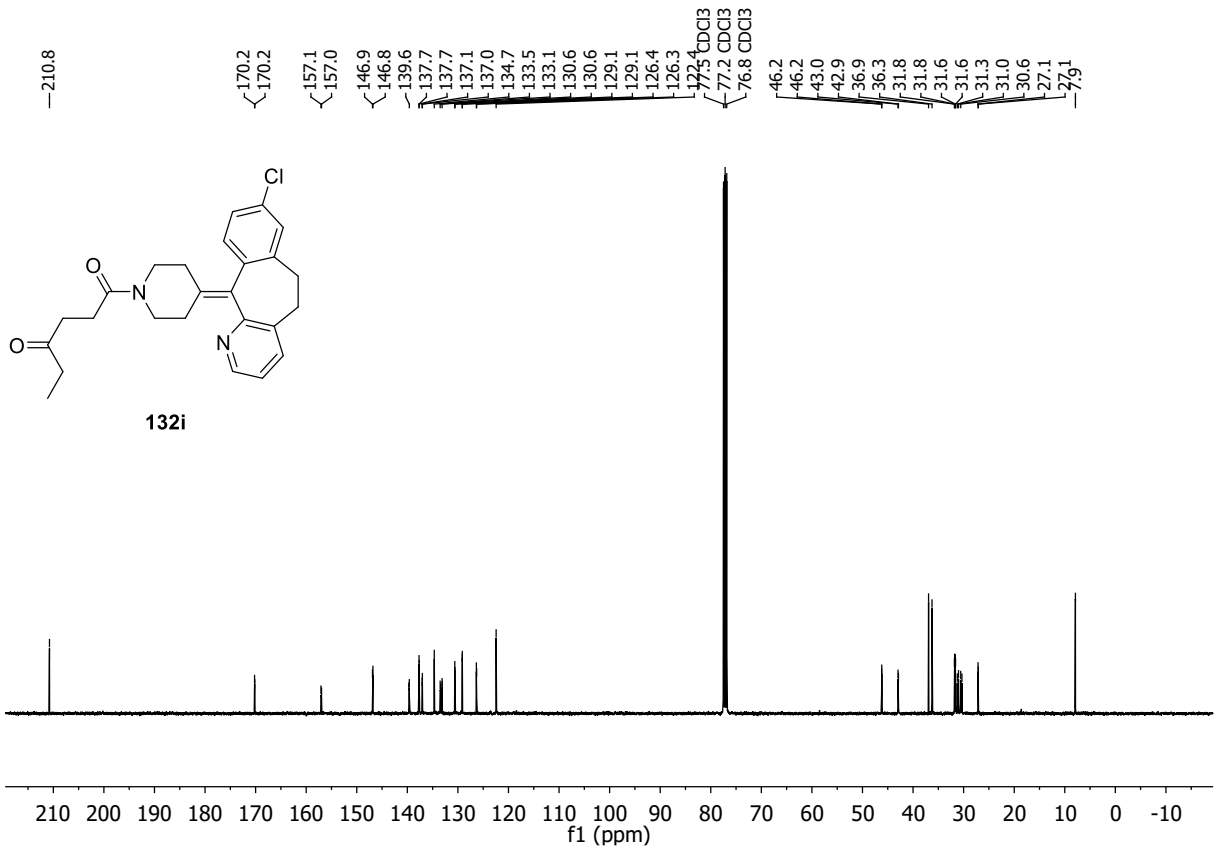
210.8
170.2
170.2
157.1
157.0
146.9
146.8
139.6
137.7
137.7
137.1
137.0
134.7
133.5
133.1
130.6
130.6
129.1
129.1
126.4
126.3
122.4
77.5 CDCl3
77.2 CDCl3
76.8 CDCl3
46.2
46.2
43.0
42.9
36.9
36.3
31.8
31.8
31.6
31.6
31.3
31.0
30.6
27.1
27.1
Cl
O
N
O
N
132i
210 200 190 180 170 160 150 140 130 120 110 100 90 80 70 60 50 40 30 20 10 0 -10
f1 (ppm)

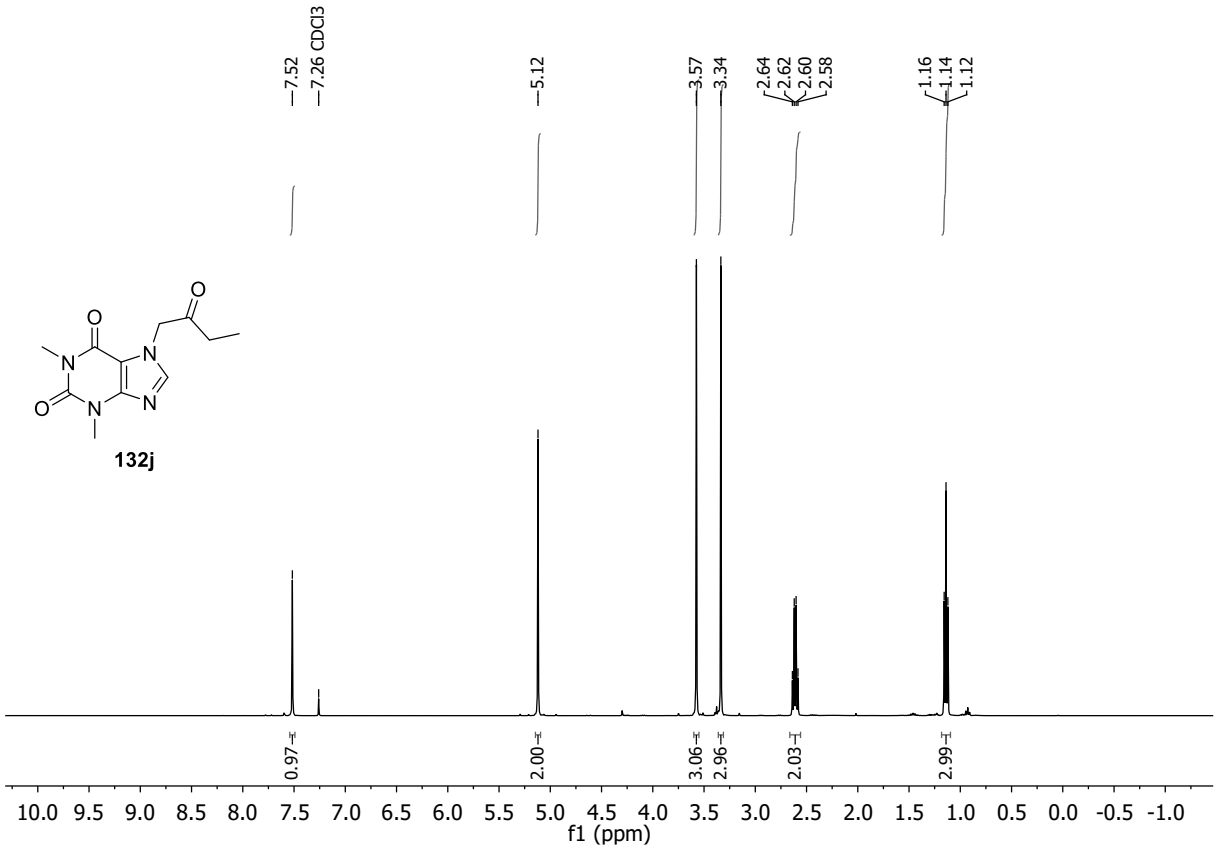
7.52
7.26 CDCl3
5.12
3.57
3.34
2.64
2.62
2.60
2.58
1.16
1.14
1.12
0.97
2.00
3.06
2.96
2.03
2.99
f1 (ppm)

132j

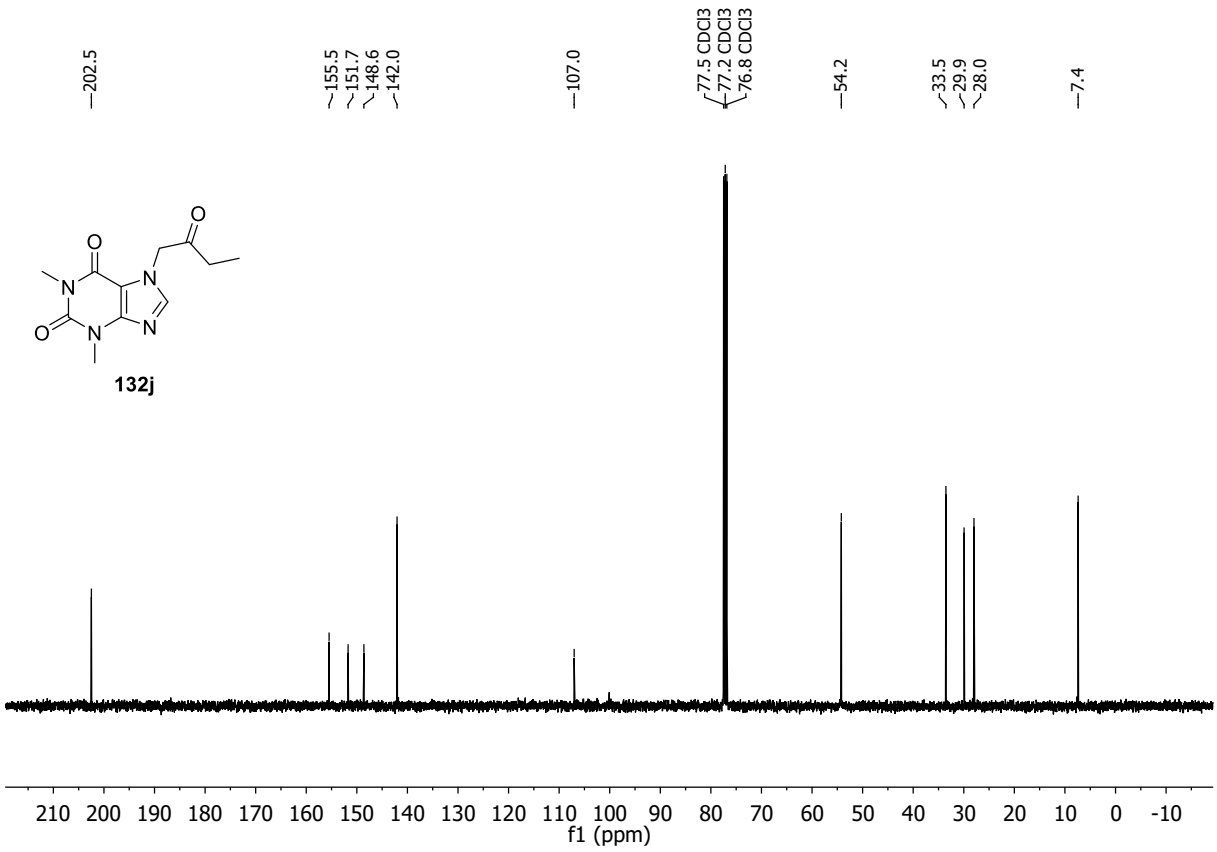
202.5
155.5
151.7
148.6
142.0
107.0
77.5 CDCl3
77.2 CDCl3
76.8 CDCl3
54.2
33.5
29.9
28.0
7.4
f1 (ppm)

132j

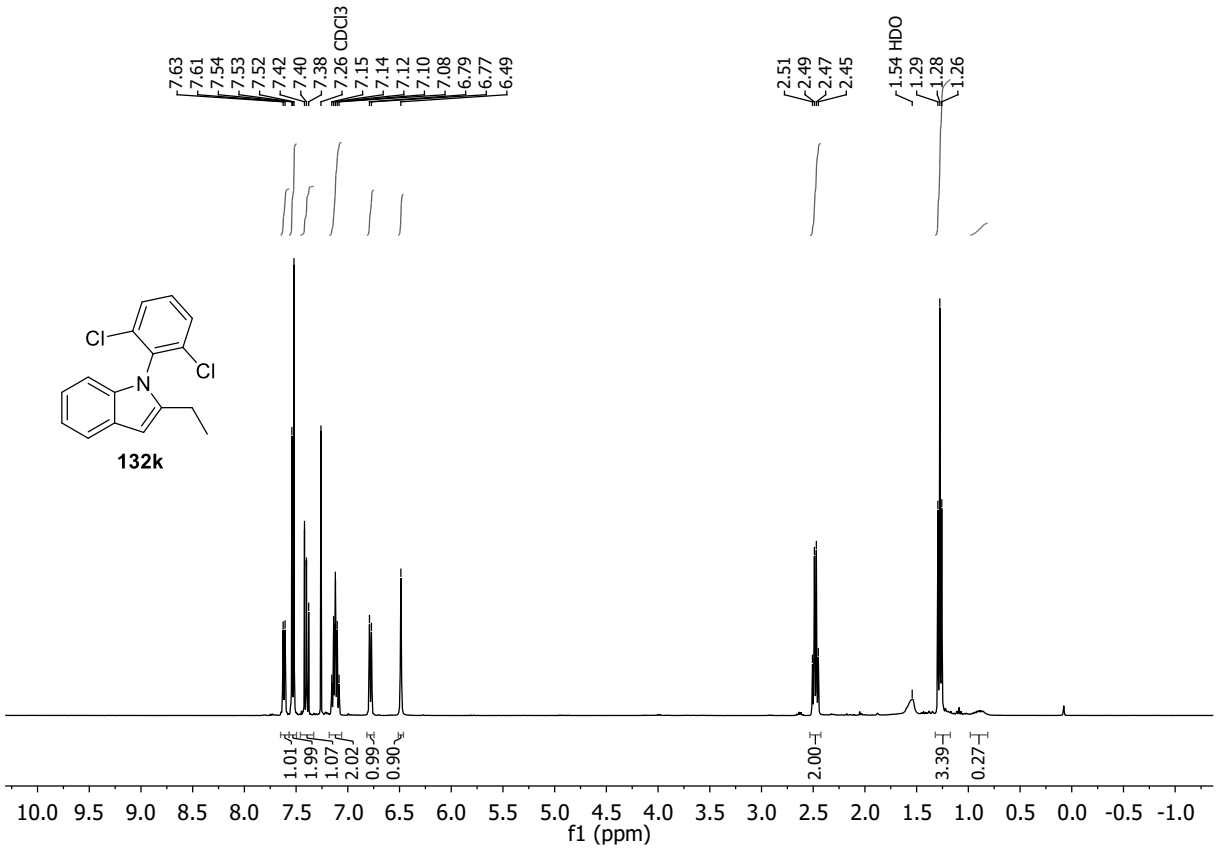
7.63
7.61
7.54
7.53
7.52
7.42
7.40
7.38
CDCl3
7.26
7.15
7.14
7.12
7.10
7.08
6.79
6.77
6.49
2.51
2.49
2.47
2.45
HDO
1.54
1.29
1.28
1.26
Cl
Cl
N
132k
1.01
1.99
1.07
2.02
0.99
0.90
2.00
3.39
0.27
10.0 9.5 9.0 8.5 8.0 7.5 7.0 6.5 6.0 5.5 5.0 4.5 4.0 3.5 3.0 2.5 2.0 1.5 1.0 0.5 0.0 -0.5 -1.0
f1 (ppm)

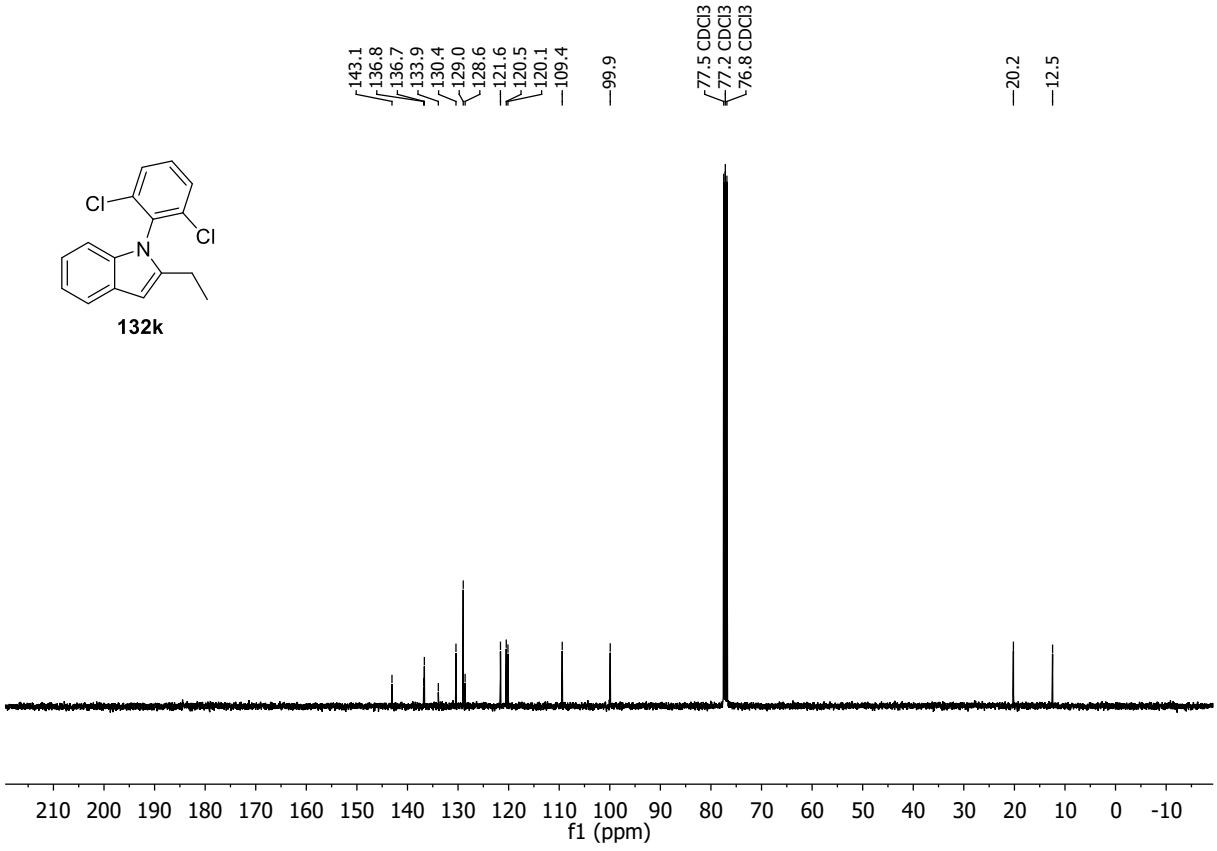
143.1
136.8
136.7
133.9
130.4
129.0
128.6
121.6
120.5
120.1
109.4
99.9
77.5 CDCl3
77.2 CDCl3
76.8 CDCl3
20.2
12.5
Cl
Cl
N
132k
210 200 190 180 170 160 150 140 130 120 110 100 90 80 70 60 50 40 30 20 10 0 -10
f1 (ppm)

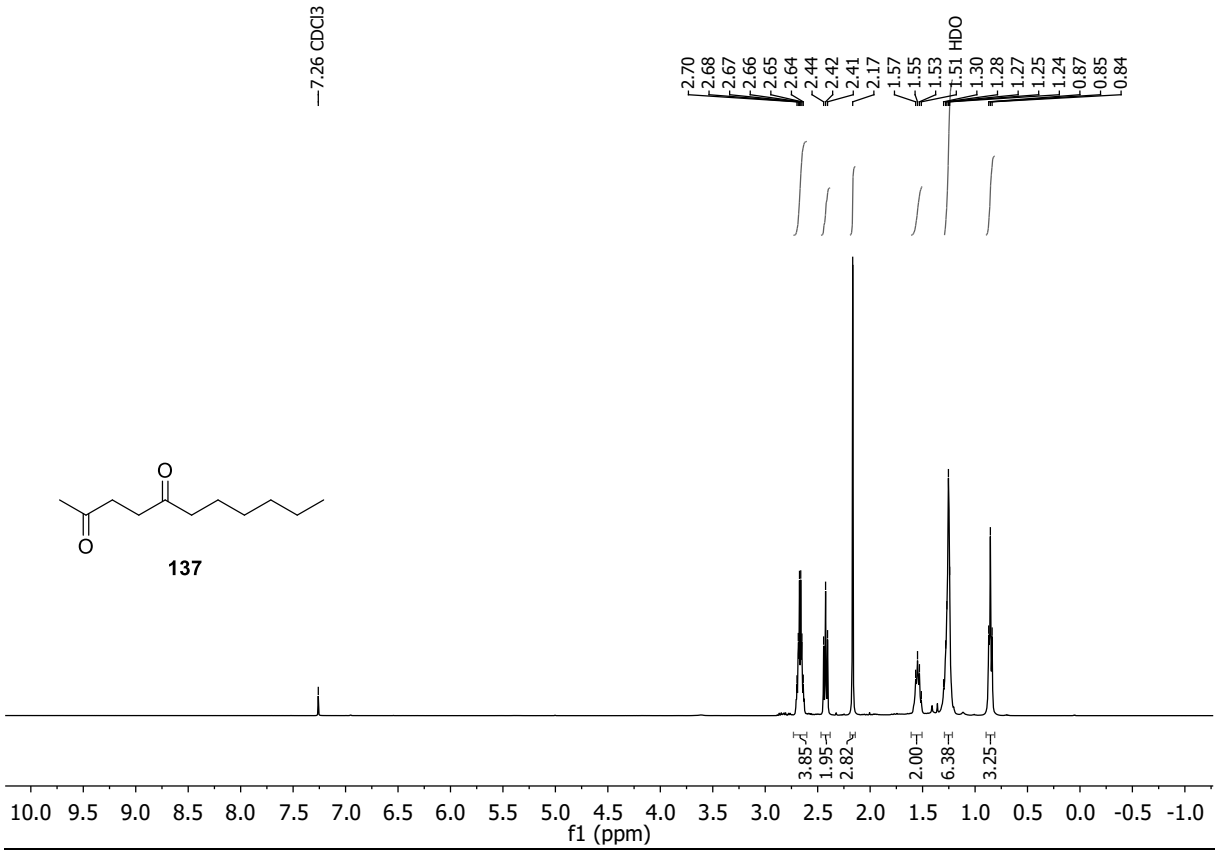
7.26 CDCl3
2.70
2.68
2.67
2.66
2.65
2.64
2.44
2.42
2.41
2.17
1.57
1.55
1.53
1.51 HDO
1.30
1.28
1.27
1.25
1.24
0.87
0.85
0.84
O
O
137
3.85
1.95
2.82
2.00
6.38
3.25
10.0 9.5 9.0 8.5 8.0 7.5 7.0 6.5 6.0 5.5 5.0 4.5 4.0 3.5 3.0 2.5 2.0 1.5 1.0 0.5 0.0 -0.5 -1.0
f1 (ppm)

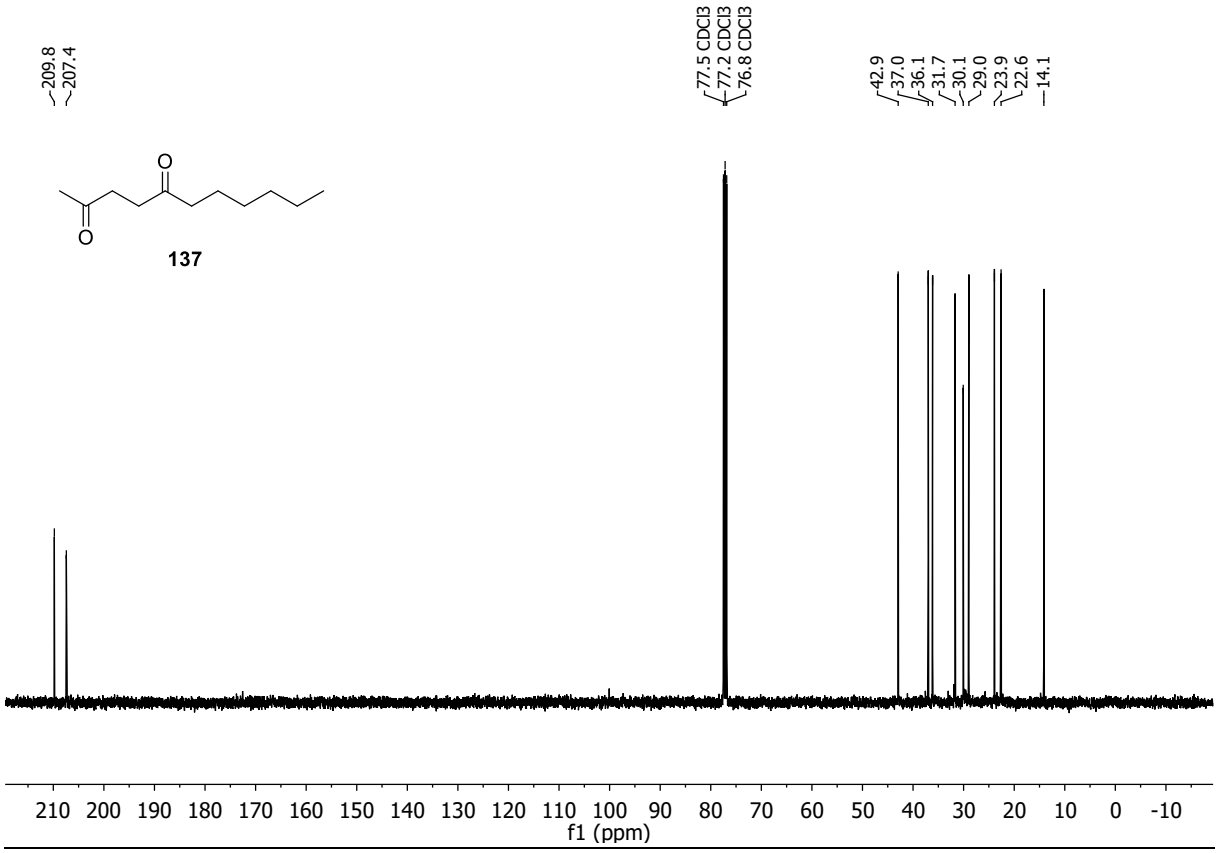
209.8
207.4
77.5 CDCl3
77.2 CDCl3
76.8 CDCl3
42.9
37.0
36.1
31.7
30.1
29.0
23.9
22.6
14.1
O
O
137
210 200 190 180 170 160 150 140 130 120 110 100 90 80 70 60 50 40 30 20 10 0 -10
f1 (ppm)

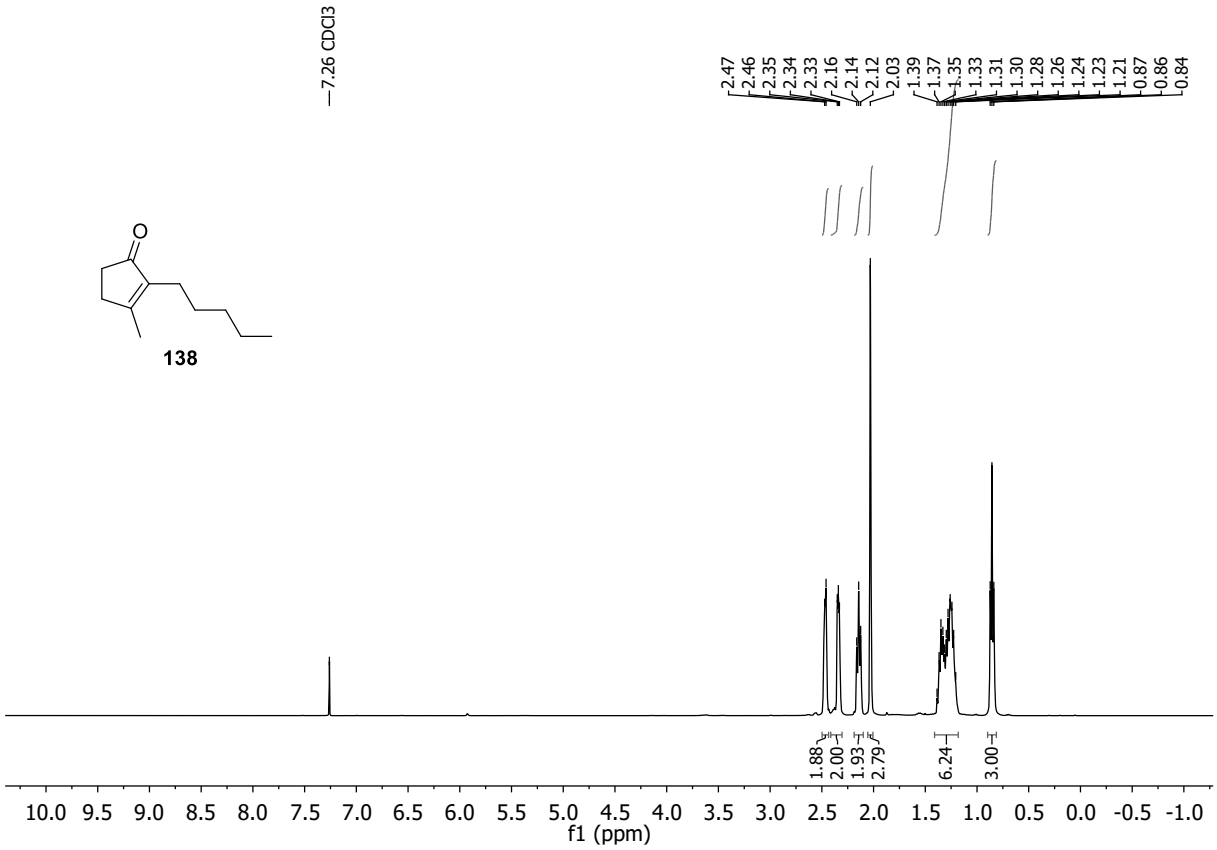
7.26 CDCl3
2.47
2.46
2.35
2.34
2.33
2.16
2.14
2.12
2.03
1.39
1.37
1.35
1.33
1.31
1.30
1.28
1.26
1.24
1.23
1.21
0.87
0.86
0.84
O
138
1.88
2.00
1.93
2.79
6.24
3.00
10.0 9.5 9.0 8.5 8.0 7.5 7.0 6.5 6.0 5.5 5.0 4.5 4.0 3.5 3.0 2.5 2.0 1.5 1.0 0.5 0.0 -0.5 -1.0
f1 (ppm)

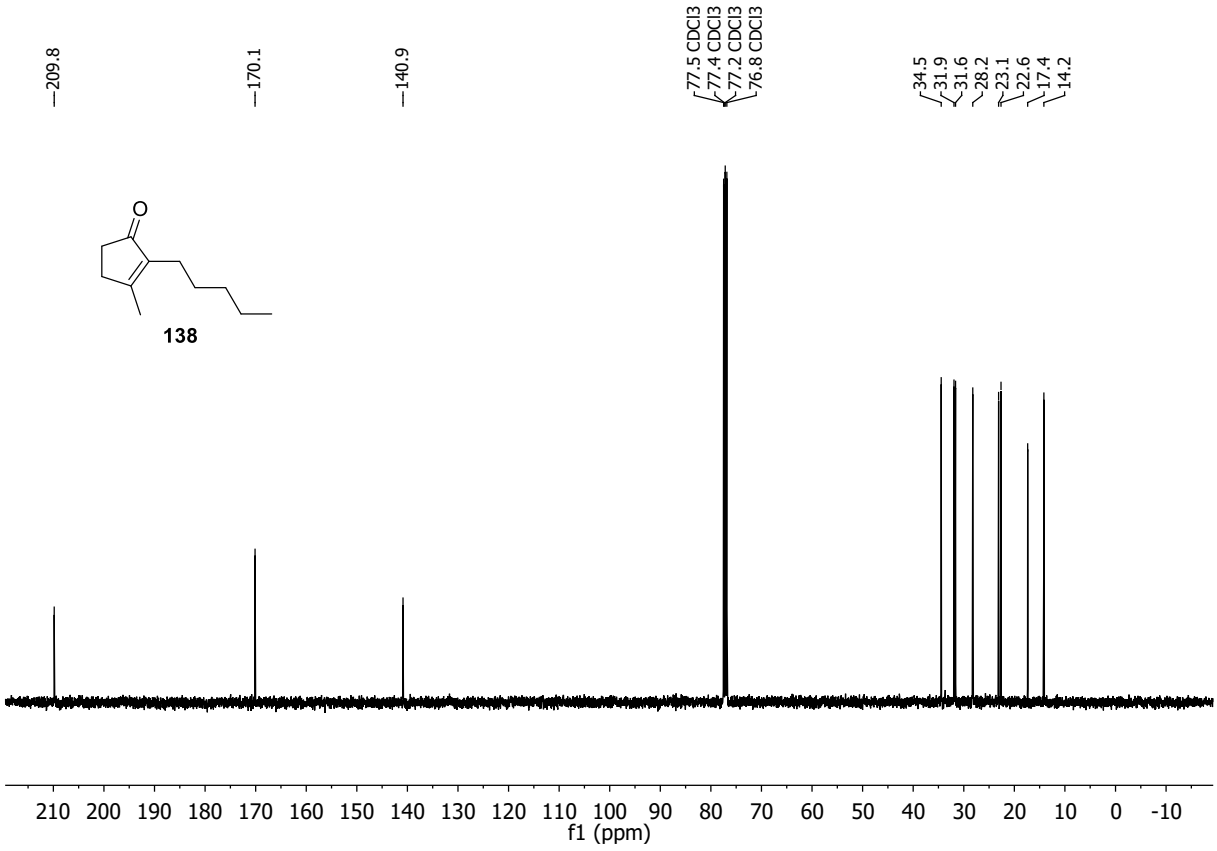
209.8
170.1
140.9
77.5 CDCl3
77.4 CDCl3
77.2 CDCl3
76.8 CDCl3
34.5
31.9
31.6
28.2
23.1
22.6
17.4
14.2
O
138
210 200 190 180 170 160 150 140 130 120 110 100 90 80 70 60 50 40 30 20 10 0 -10
f1 (ppm)

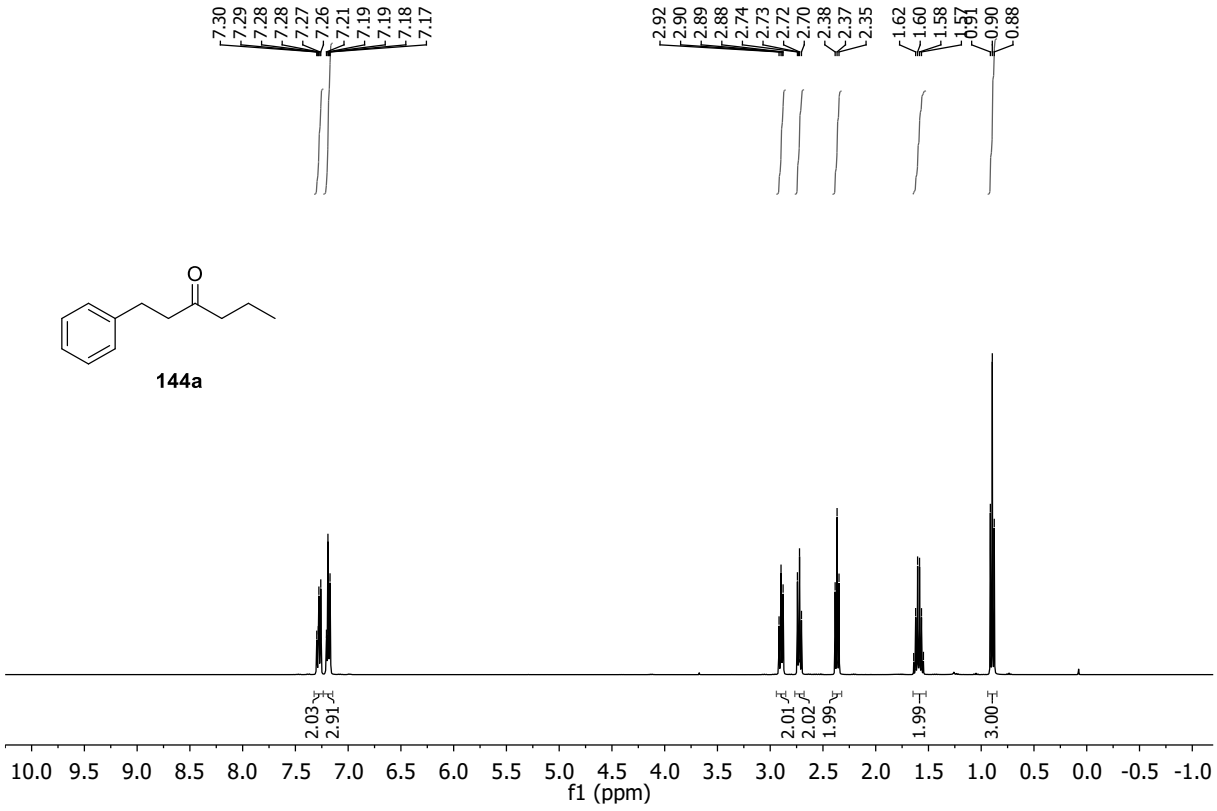
7.30
7.29
7.28
7.28
7.27
7.26
7.21
7.19
7.19
7.18
7.17
2.92
2.90
2.89
2.88
2.74
2.73
2.72
2.70
2.38
2.37
2.35
1.62
1.60
1.58
1.57
1.91
0.90
0.88
O
144a
2.03
2.91
2.01
2.02
1.99
1.99
3.00
10.0 9.5 9.0 8.5 8.0 7.5 7.0 6.5 6.0 5.5 5.0 4.5 4.0 3.5 3.0 2.5 2.0 1.5 1.0 0.5 0.0 -0.5 -1.0
f1 (ppm)

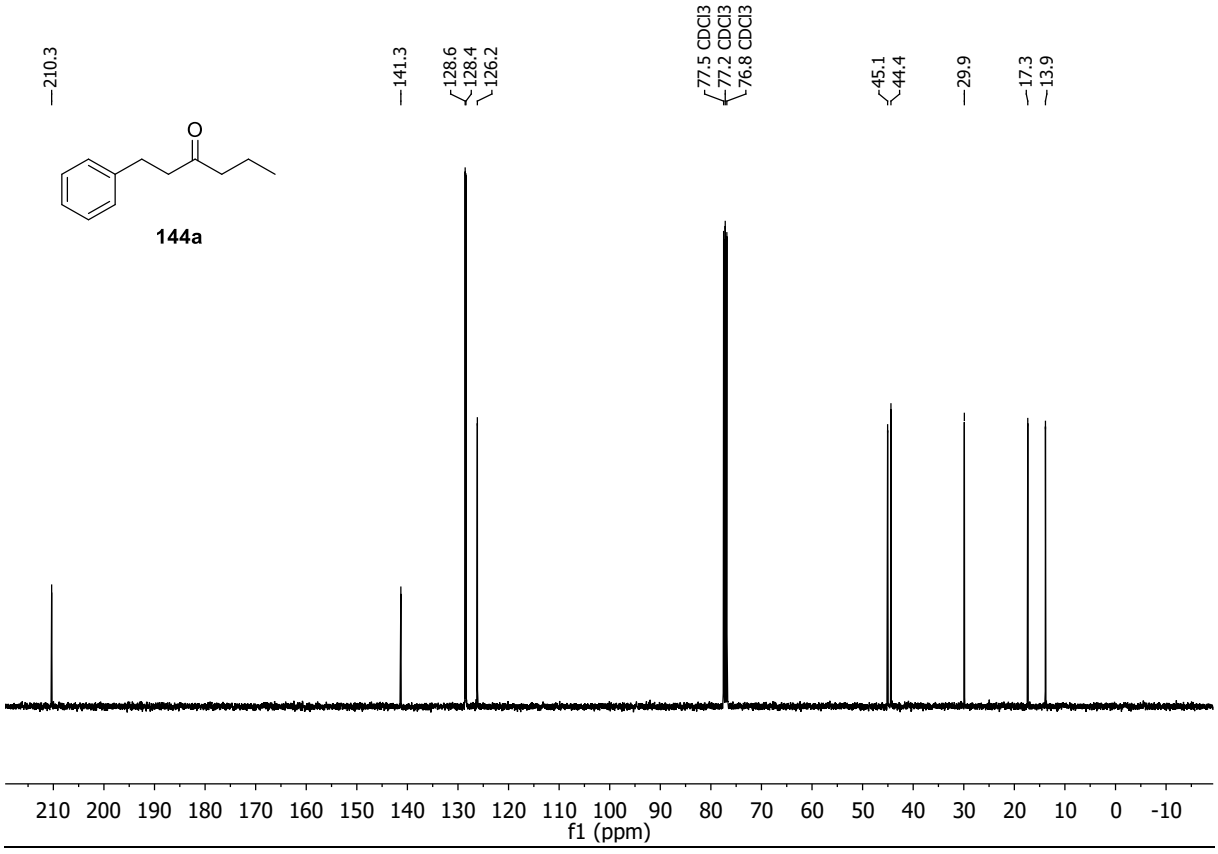
210.3
141.3
128.6
128.4
126.2
77.5 CDCl3
77.2 CDCl3
76.8 CDCl3
45.1
44.4
29.9
17.3
13.9
O
144a
210 200 190 180 170 160 150 140 130 120 110 100 90 80 70 60 50 40 30 20 10 0 -10
f1 (ppm)

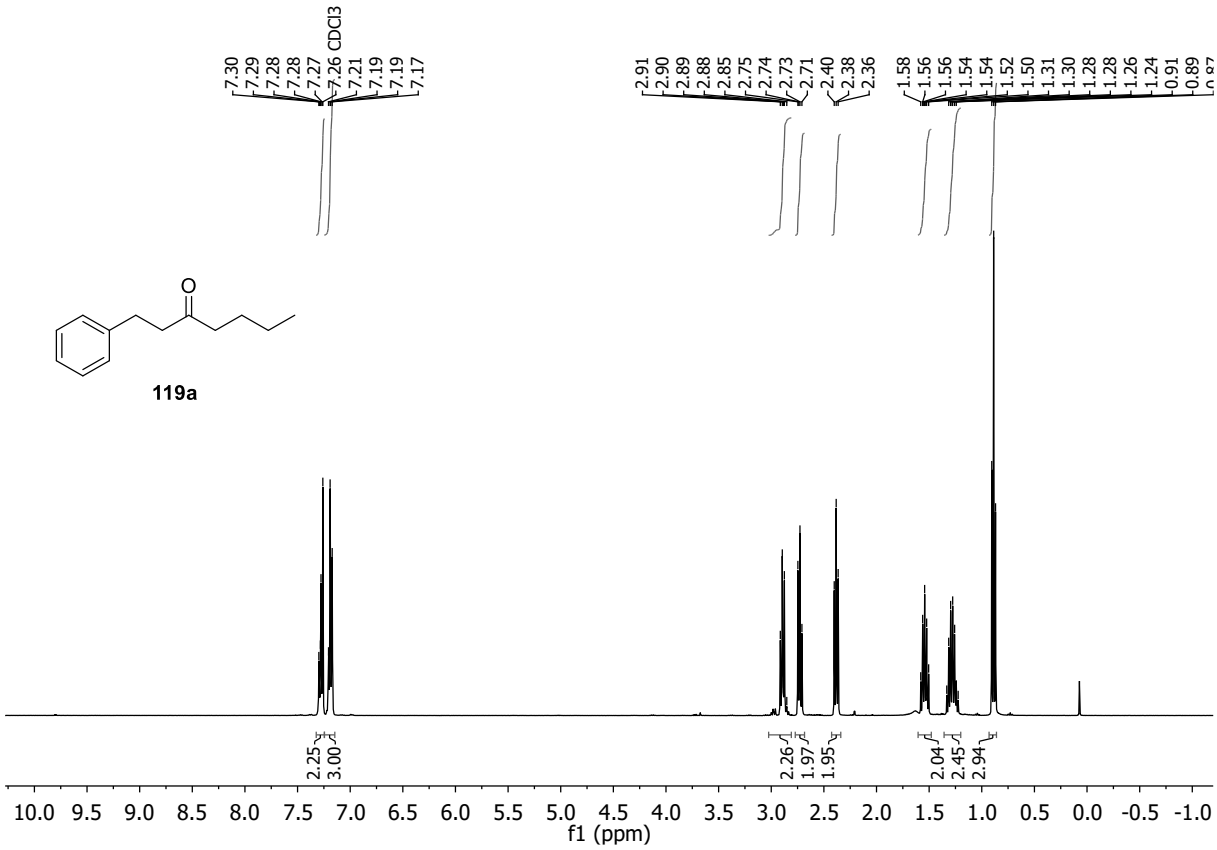
7.30
7.29
7.28
7.28
7.27
7.26 CDCl3
7.21
7.19
7.19
7.17
2.91
2.90
2.89
2.88
2.85
2.75
2.74
2.73
2.71
2.40
2.38
2.36
1.58
1.56
1.56
1.54
1.54
1.52
1.50
1.31
1.30
1.28
1.28
1.26
1.24
0.91
0.89
O
119a
2.25
3.00
2.26
1.97
1.95
2.04
2.45
2.94
10.0 9.5 9.0 8.5 8.0 7.5 7.0 6.5 6.0 5.5 5.0 4.5 4.0 3.5 3.0 2.5 2.0 1.5 1.0 0.5 0.0 -0.5 -1.0
f1 (ppm)

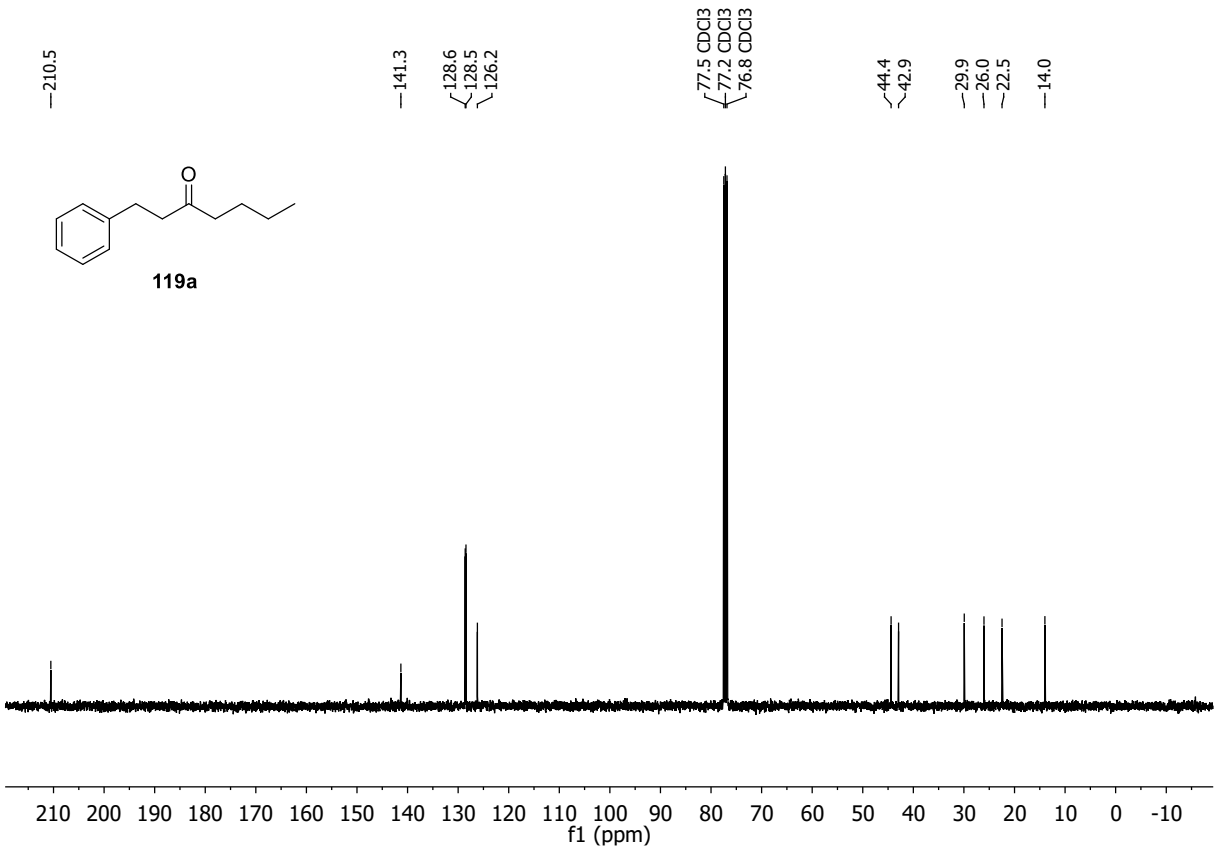
210.5
141.3
128.6
128.5
126.2
77.5 CDCl3
77.2 CDCl3
76.8 CDCl3
44.4
42.9
29.9
26.0
22.5
14.0
O
119a
210 200 190 180 170 160 150 140 130 120 110 100 90 80 70 60 50 40 30 20 10 0 -10
f1 (ppm)

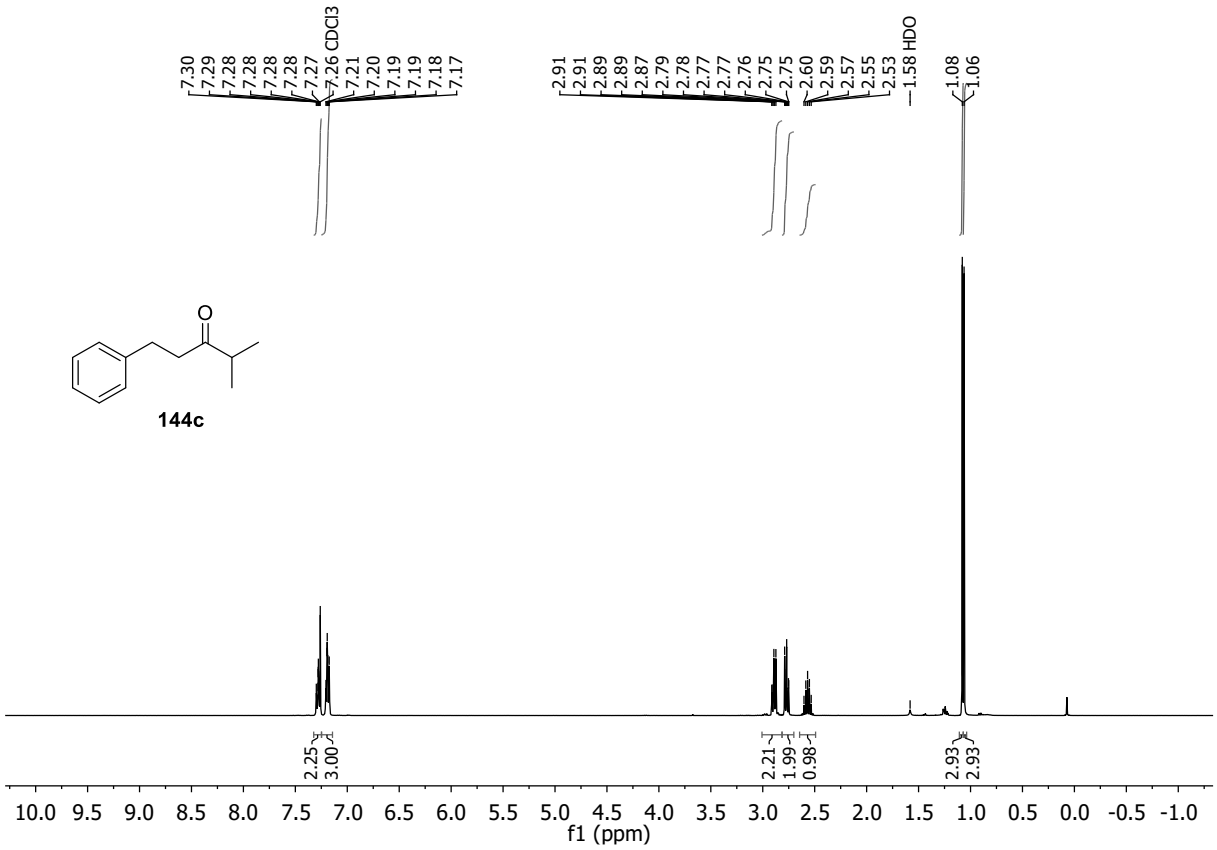
7.30
7.29
7.28
7.28
7.28
7.28
7.27
7.26 CDCl3
7.21
7.20
7.19
7.19
7.18
7.17
2.91
2.91
2.89
2.89
2.87
2.79
2.78
2.77
2.77
2.76
2.75
2.75
2.60
2.59
2.57
2.55
2.53
1.58 HDO
1.08
1.06
O
144c
2.25
3.00
2.21
1.99
0.98
2.93
2.93
10.0 9.5 9.0 8.5 8.0 7.5 7.0 6.5 6.0 5.5 5.0 4.5 4.0 3.5 3.0 2.5 2.0 1.5 1.0 0.5 0.0 -0.5 -1.0
f1 (ppm)

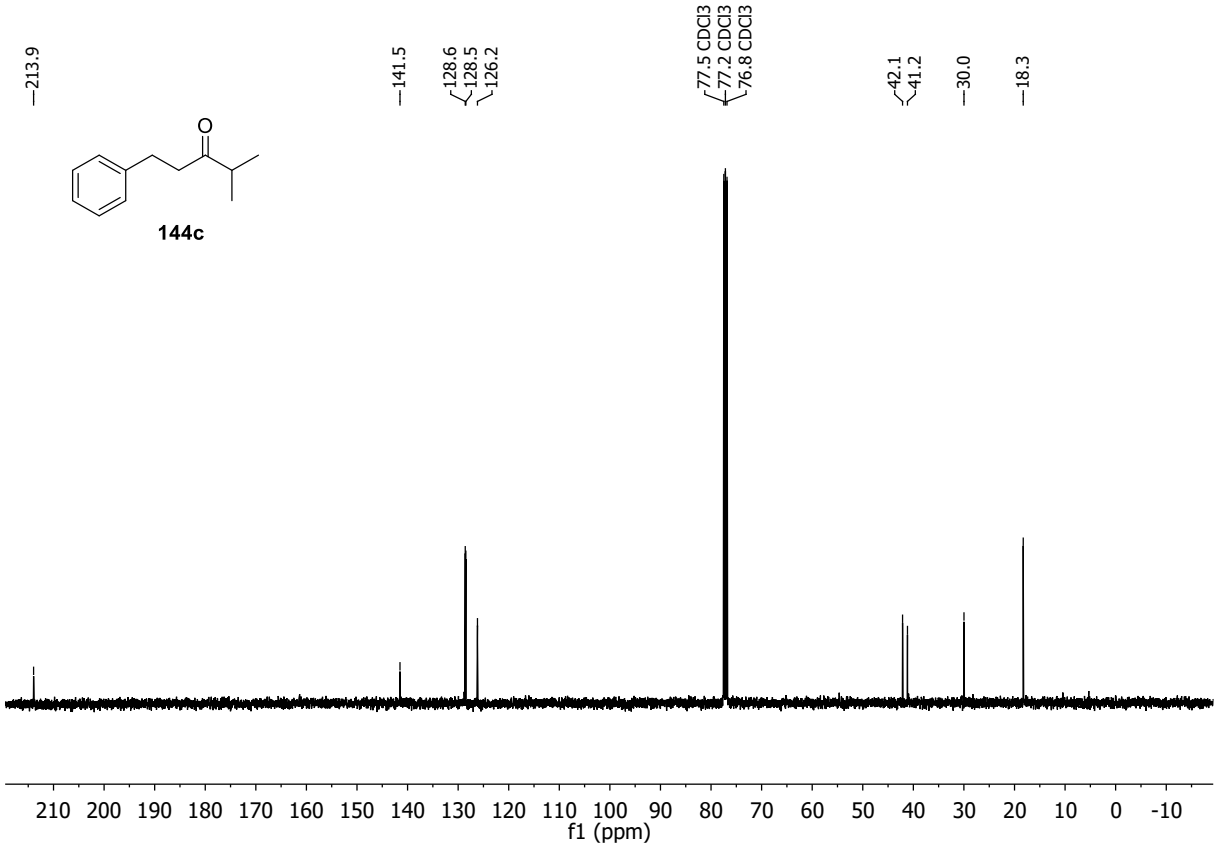
213.9
141.5
128.6
128.5
126.2
77.5 CDCl3
77.2 CDCl3
76.8 CDCl3
42.1
41.2
30.0
18.3
O
144c
210 200 190 180 170 160 150 140 130 120 110 100 90 80 70 60 50 40 30 20 10 0 -10
f1 (ppm)

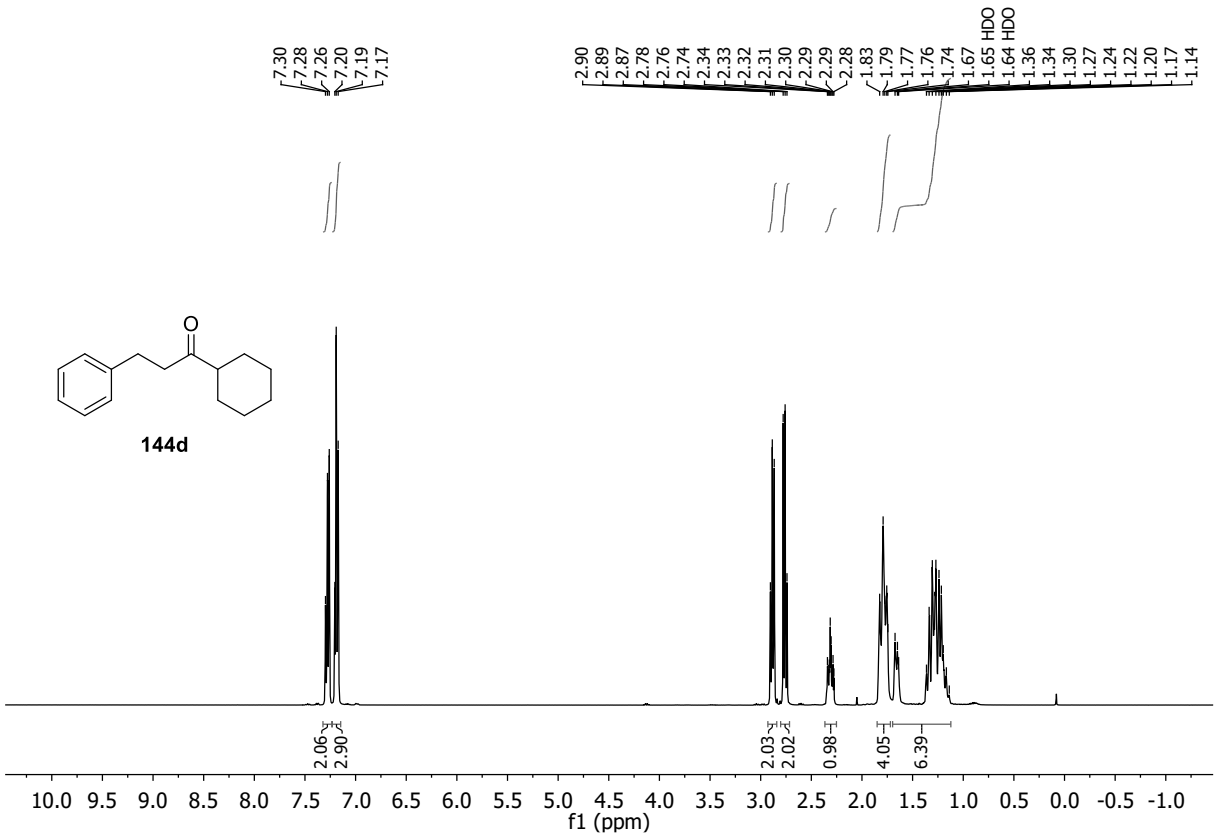
7.30
7.28
7.26
7.20
7.19
7.17
2.90
2.89
2.87
2.78
2.76
2.74
2.34
2.33
2.32
2.31
2.30
2.29
2.29
2.28
1.83
1.79
1.77
1.76
1.74
1.67
1.65 HDO
1.64 HDO
1.36
1.34
1.30
1.27
1.24
1.22
1.20
1.17
1.14
O
144d
2.06
2.90
2.03
2.02
0.98
4.05
6.39
10.0 9.5 9.0 8.5 8.0 7.5 7.0 6.5 6.0 5.5 5.0 4.5 4.0 3.5 3.0 2.5 2.0 1.5 1.0 0.5 0.0 -0.5 -1.0
f1 (ppm)

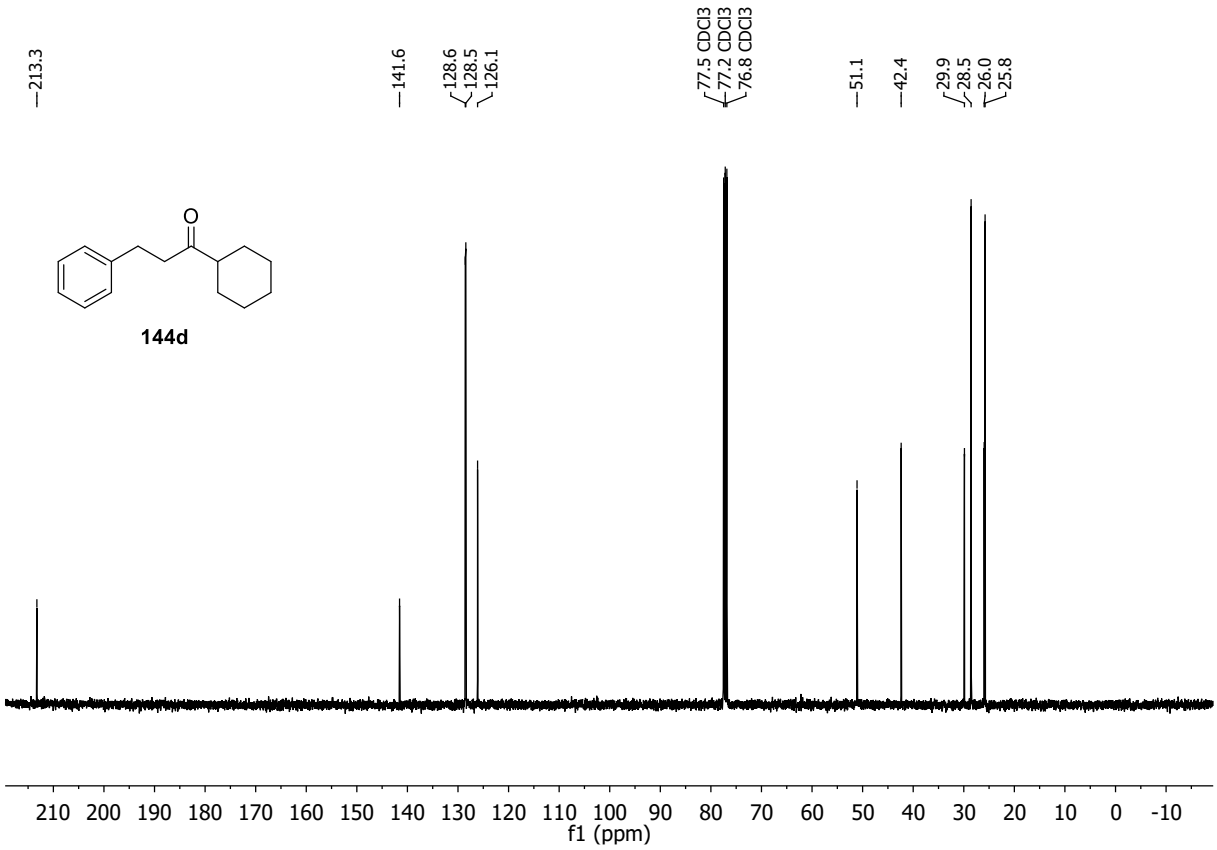
213.3
141.6
128.6
128.5
126.1
77.5 CDCl3
77.2 CDCl3
76.8 CDCl3
51.1
42.4
29.9
28.5
26.0
25.8
O
144d
210 200 190 180 170 160 150 140 130 120 110 100 90 80 70 60 50 40 30 20 10 0 -10
f1 (ppm)

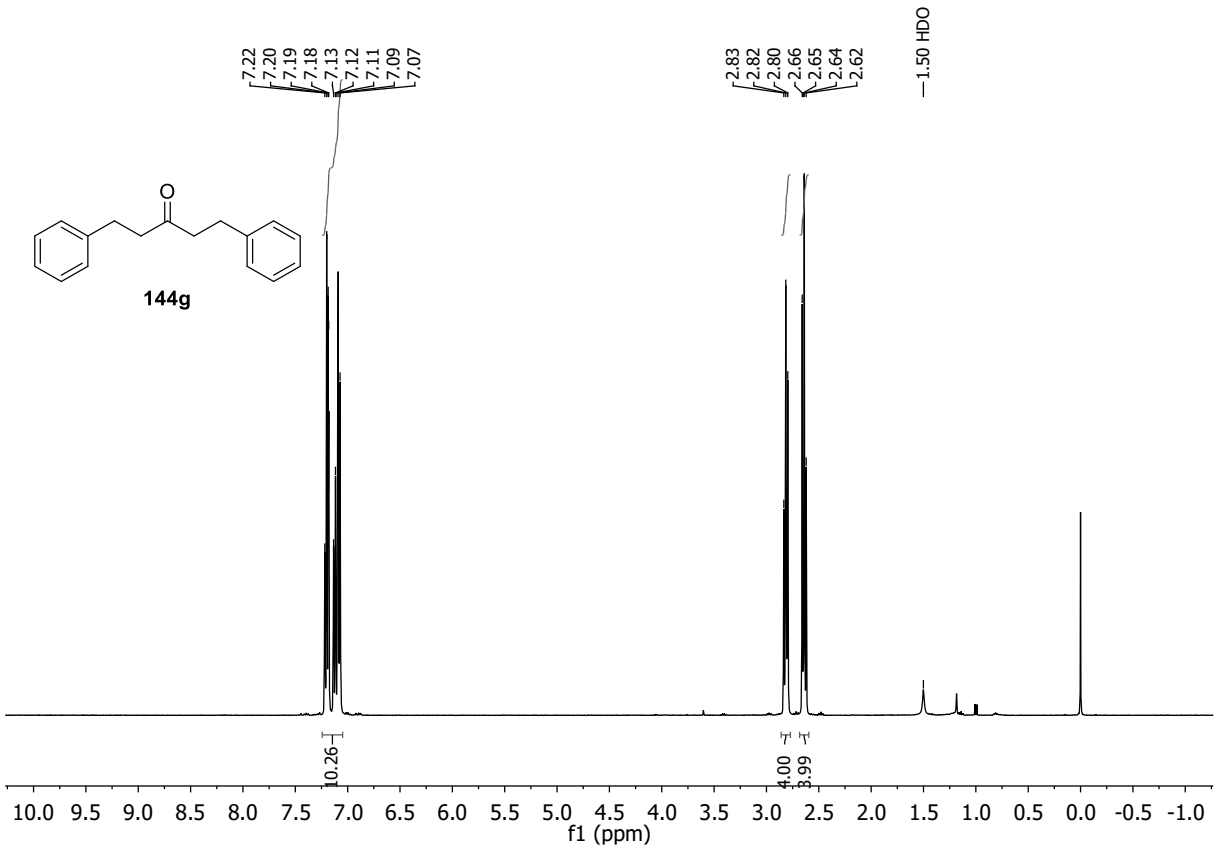
7.22
7.20
7.19
7.18
7.13
7.12
7.11
7.09
7.07
2.83
2.82
2.80
2.66
2.65
2.64
2.62
1.50 HDO
O
144g
10.26
4.00
3.99
10.0 9.5 9.0 8.5 8.0 7.5 7.0 6.5 6.0 5.5 5.0 4.5 4.0 3.5 3.0 2.5 2.0 1.5 1.0 0.5 0.0 -0.5 -1.0
f1 (ppm)

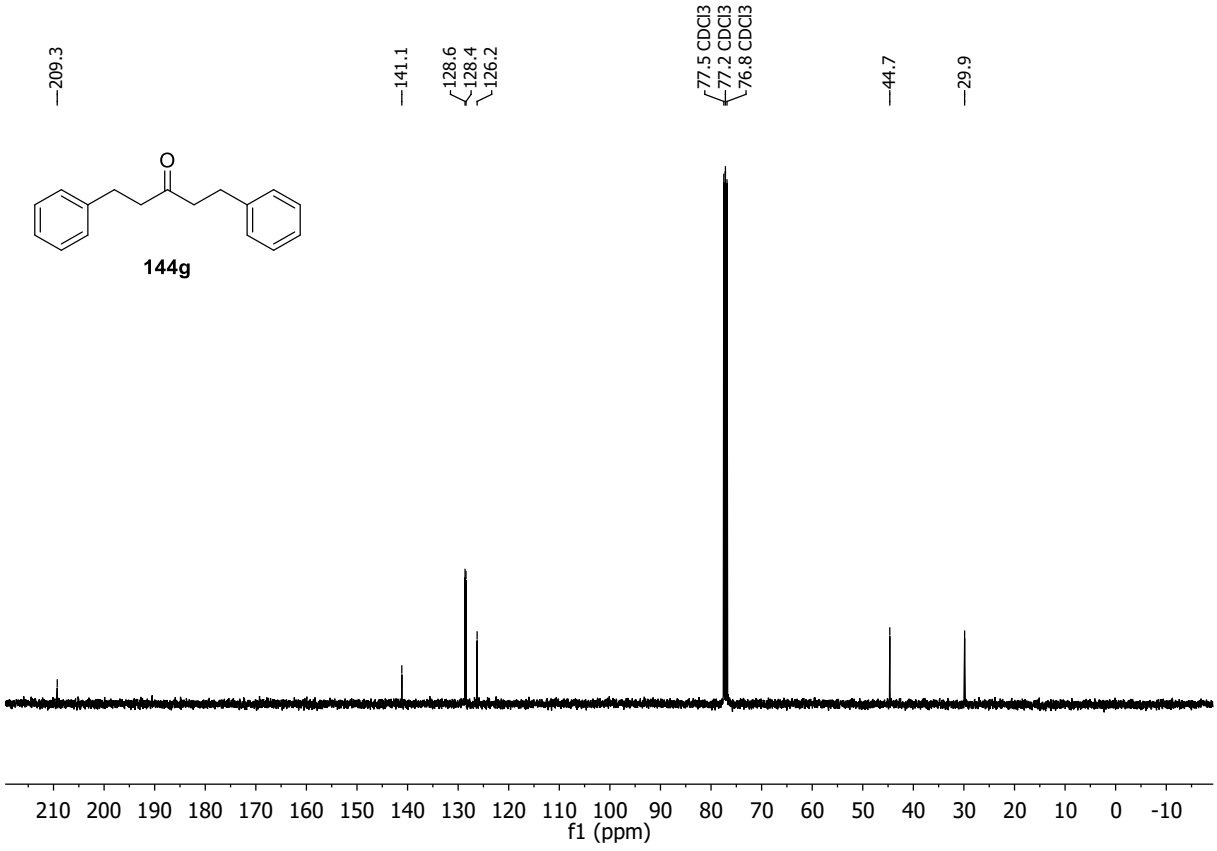
209.3
141.1
128.6
128.4
126.2
77.5 CDCl3
77.2 CDCl3
76.8 CDCl3
44.7
29.9
O
144g
210 200 190 180 170 160 150 140 130 120 110 100 90 80 70 60 50 40 30 20 10 0 -10
f1 (ppm)

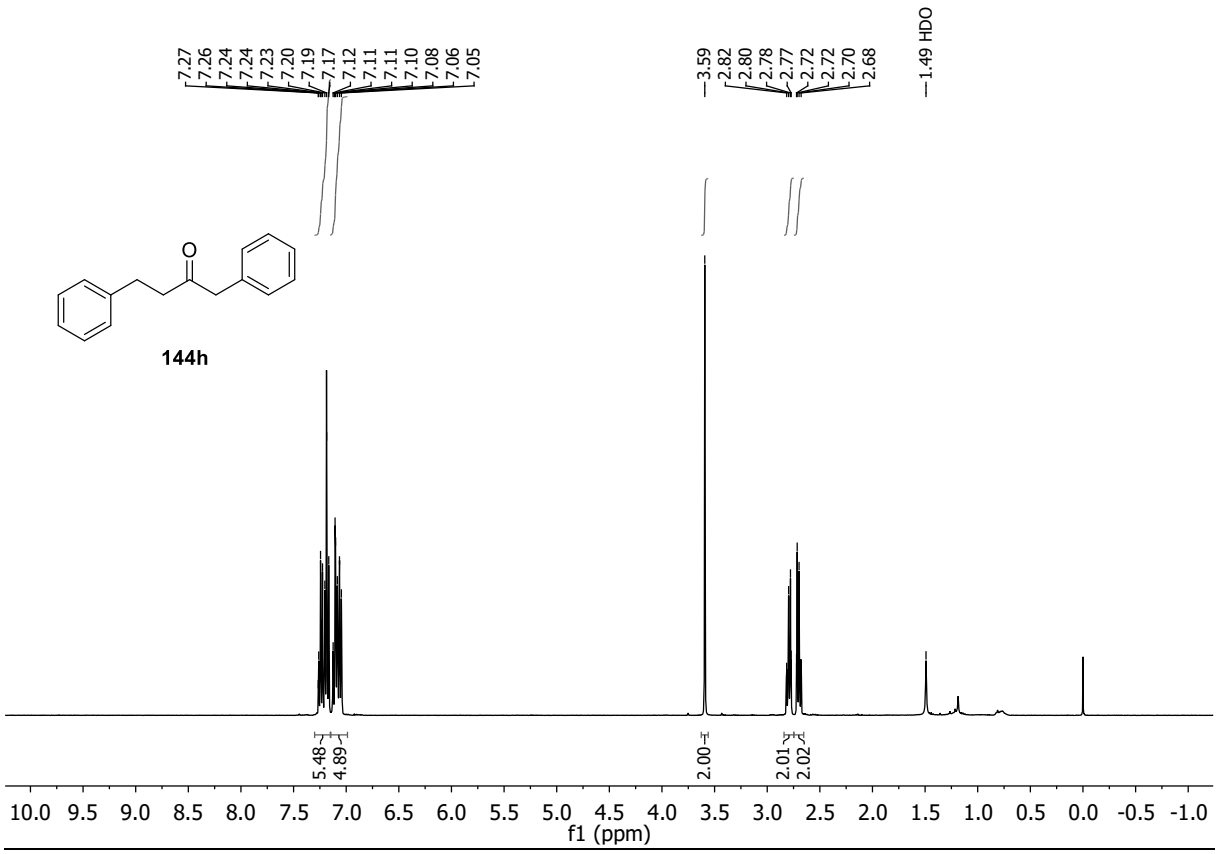
7.27
7.26
7.24
7.24
7.23
7.20
7.19
7.17
7.12
7.11
7.11
7.10
7.08
7.06
7.05
3.59
2.82
2.80
2.78
2.77
2.72
2.72
2.70
2.68
1.49 HDO
O
144h
5.48
4.89
2.00
2.01
2.02
10.0 9.5 9.0 8.5 8.0 7.5 7.0 6.5 6.0 5.5 5.0 4.5 4.0 3.5 3.0 2.5 2.0 1.5 1.0 0.5 0.0 -0.5 -1.0
f1 (ppm)

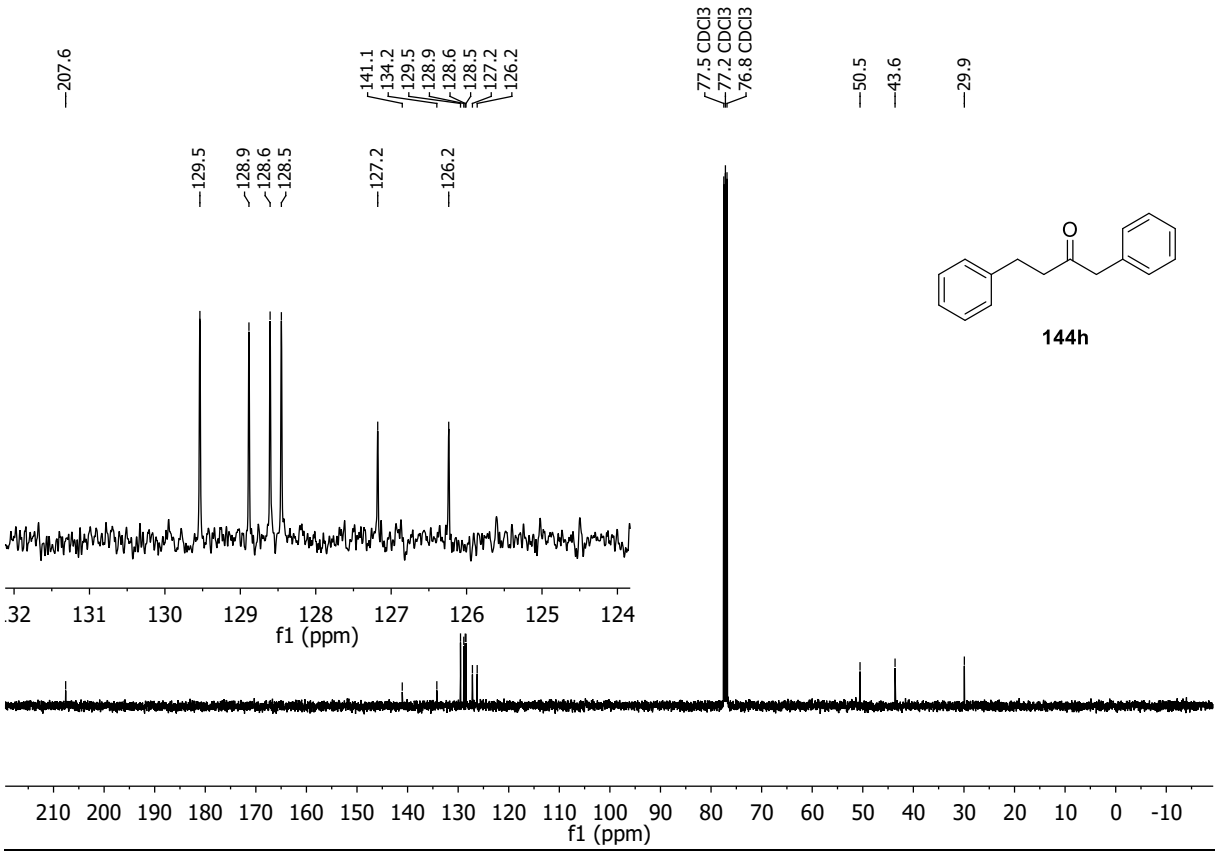
207.6
141.1
134.2
129.5
128.9
128.6
128.5
127.2
126.2
77.5 CDCl3
77.2 CDCl3
76.8 CDCl3
50.5
43.6
29.9
129.5
128.9
128.6
128.5
127.2
126.2
O
144h
32 131 130 129 128 127 126 125 124
f1 (ppm)
210 200 190 180 170 160 150 140 130 120 110 100 90 80 70 60 50 40 30 20 10 0 -10
f1 (ppm)

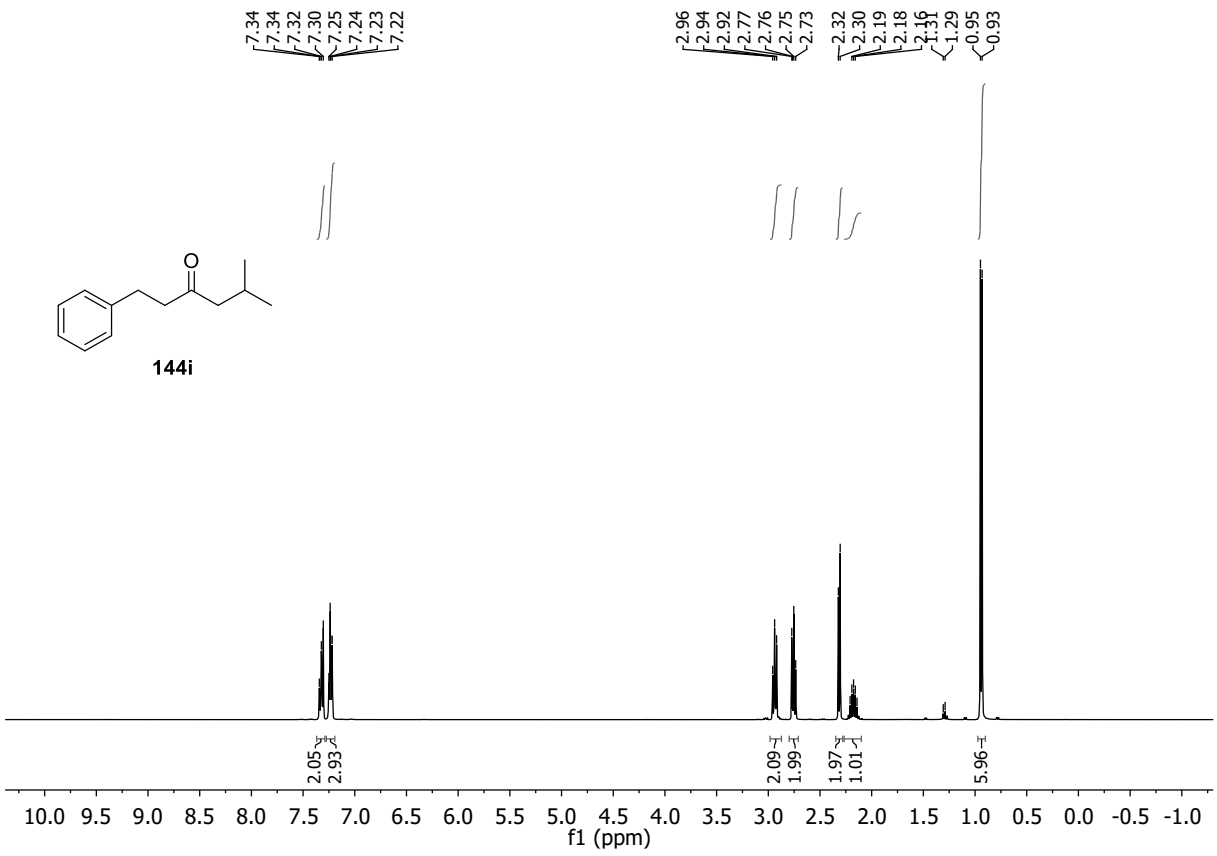
7.34
7.34
7.32
7.30
7.25
7.24
7.23
7.22
2.96
2.94
2.92
2.77
2.76
2.75
2.73
2.32
2.30
2.19
2.18
2.16
1.31
1.29
0.95
0.93
O
144i
2.05
2.93
2.09
1.99
1.97
1.01
5.96
10.0 9.5 9.0 8.5 8.0 7.5 7.0 6.5 6.0 5.5 5.0 4.5 4.0 3.5 3.0 2.5 2.0 1.5 1.0 0.5 0.0 -0.5 -1.0
f1 (ppm)

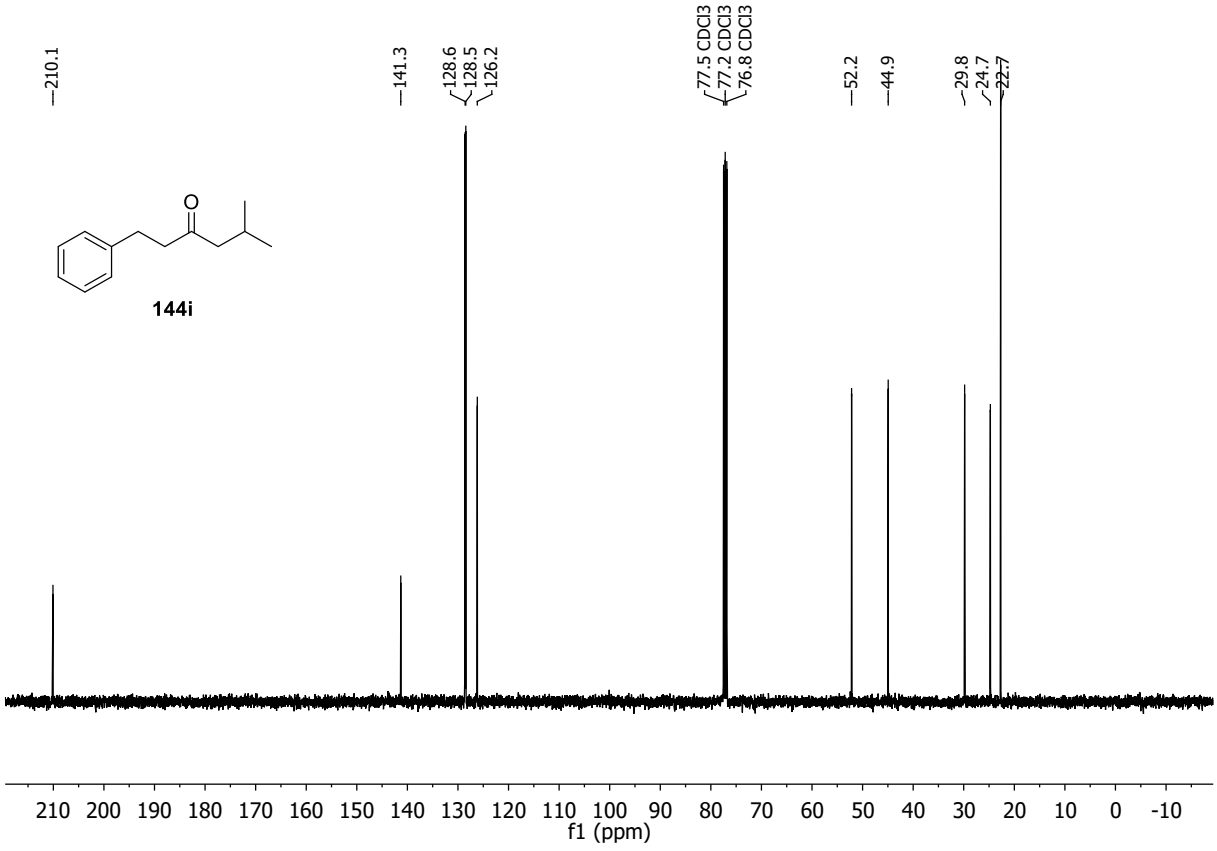
210.1
141.3
128.6
128.5
126.2
77.5 CDCl3
77.2 CDCl3
76.8 CDCl3
52.2
44.9
29.8
24.7
22.7
O
144i
210 200 190 180 170 160 150 140 130 120 110 100 90 80 70 60 50 40 30 20 10 0 -10
f1 (ppm)

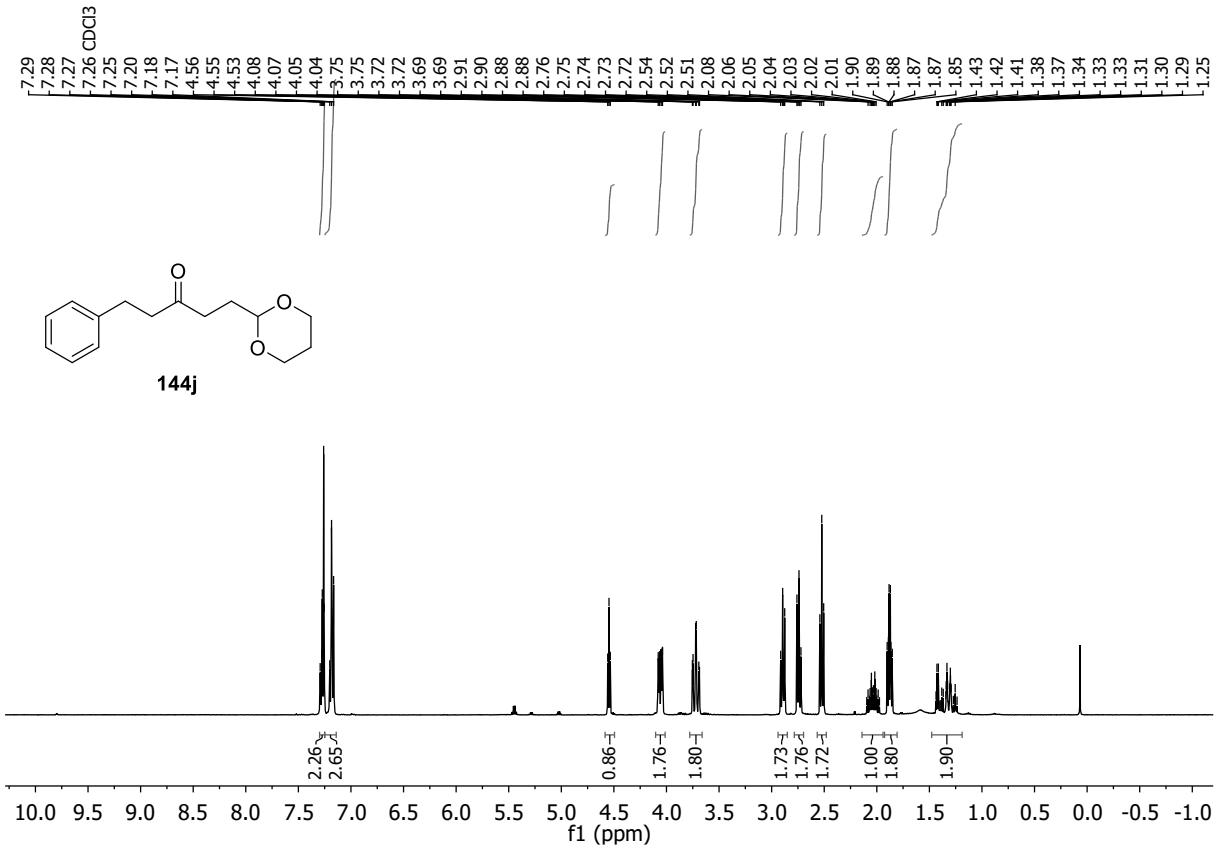
7.29
7.28
7.27
CDCl3
7.26
7.25
7.20
7.18
7.17
4.56
4.55
4.53
4.08
4.07
4.05
4.04
3.75
3.75
3.72
3.72
3.69
3.69
2.91
2.90
2.88
2.88
2.76
2.75
2.74
2.73
2.72
2.54
2.52
2.51
2.08
2.06
2.05
2.04
2.03
2.02
2.01
1.90
1.89
1.88
1.87
1.87
1.85
1.43
1.42
1.41
1.38
1.37
1.34
1.33
1.33
1.31
1.30
1.29
1.25
O
O
O
144j
2.26
2.65
0.86
1.76
1.80
1.73
1.76
1.72
1.00
1.80
1.90
10.0 9.5 9.0 8.5 8.0 7.5 7.0 6.5 6.0 5.5 5.0 4.5 4.0 3.5 3.0 2.5 2.0 1.5 1.0 0.5 0.0 -0.5 -1.0
f1 (ppm)

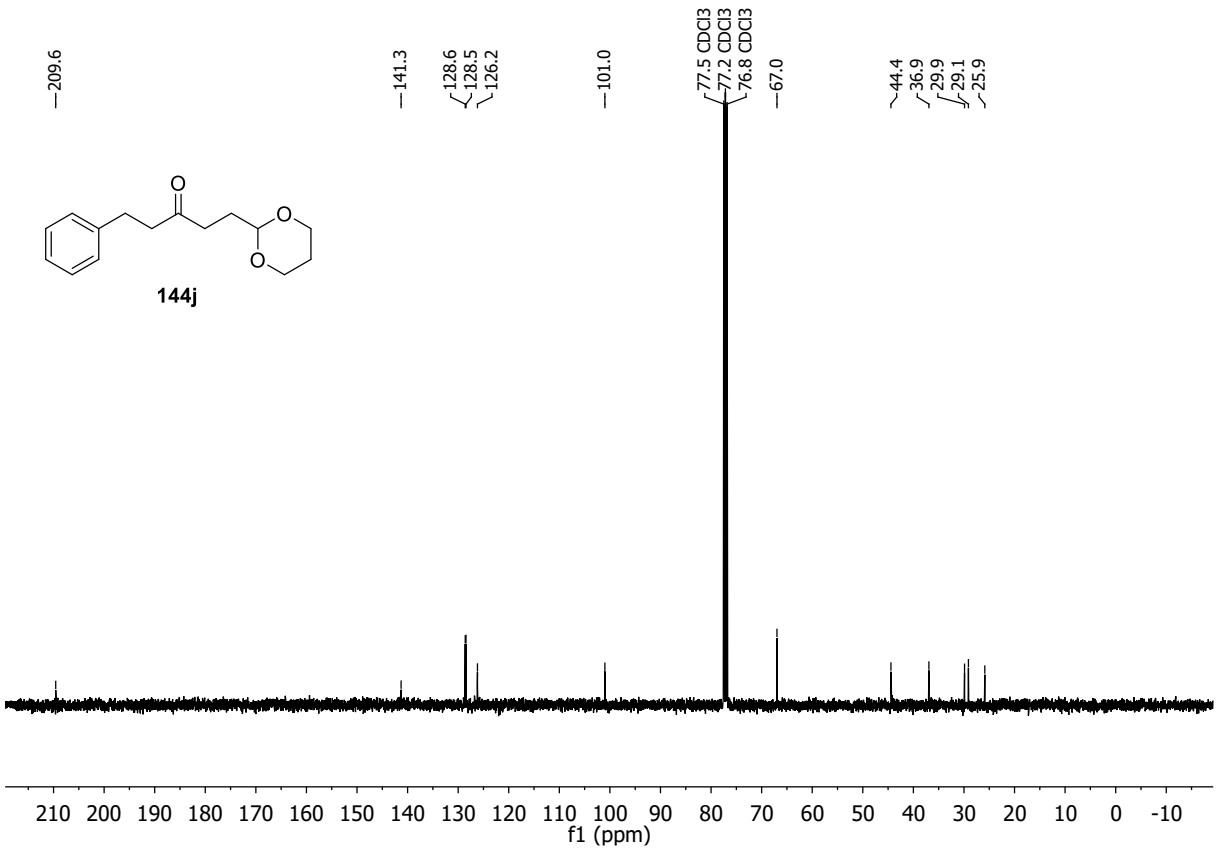
209.6
141.3
128.6
128.5
126.2
101.0
77.5 CDCl3
77.2 CDCl3
76.8 CDCl3
67.0
44.4
36.9
29.9
29.1
25.9
O
O
O
144j
210 200 190 180 170 160 150 140 130 120 110 100 90 80 70 60 50 40 30 20 10 0 -10
f1 (ppm)

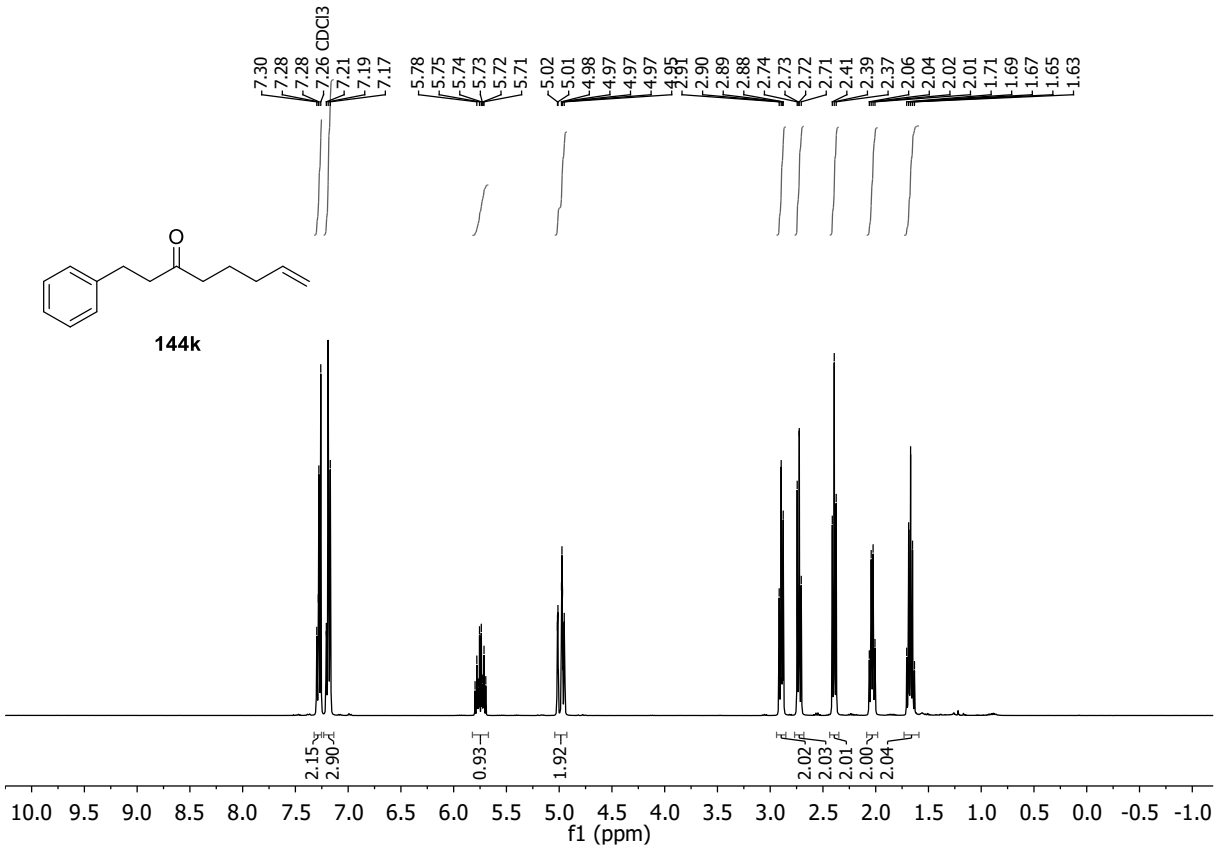
7.30
7.28
7.28
7.26 CDCl3
7.21
7.19
7.17
5.78
5.75
5.74
5.73
5.72
5.71
5.02
5.01
4.98
4.97
4.97
4.95
4.91
2.90
2.89
2.88
2.74
2.73
2.72
2.71
2.41
2.39
2.37
2.06
2.04
2.02
2.01
1.71
1.69
1.67
1.65
1.63
O
144k
2.15
2.90
0.93
1.92
2.02
2.03
2.01
2.00
2.04
10.0 9.5 9.0 8.5 8.0 7.5 7.0 6.5 6.0 5.5 5.0 4.5 4.0 3.5 3.0 2.5 2.0 1.5 1.0 0.5 0.0 -0.5 -1.0
f1 (ppm)

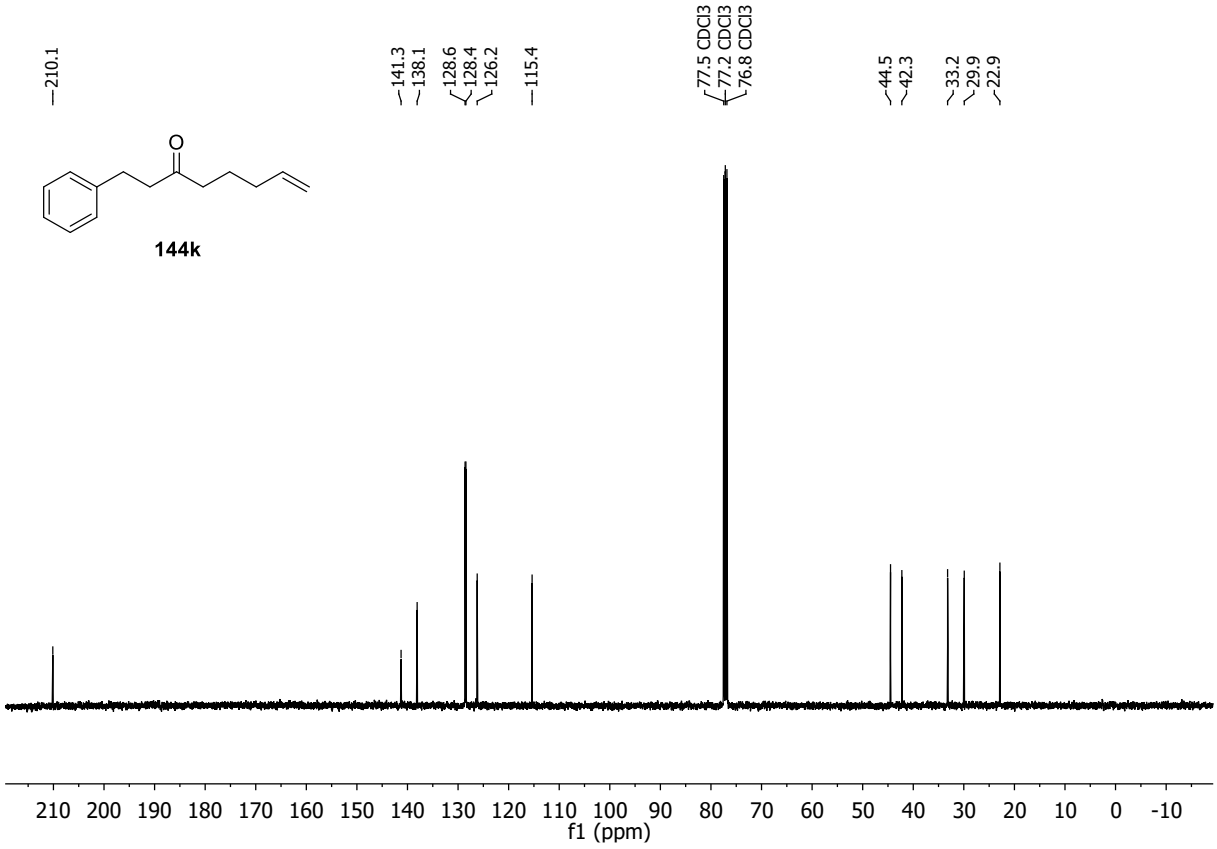
210.1
141.3
138.1
128.6
128.4
126.2
115.4
77.5 CDCl3
77.2 CDCl3
76.8 CDCl3
44.5
42.3
33.2
29.9
22.9
O
144k
210 200 190 180 170 160 150 140 130 120 110 100 90 80 70 60 50 40 30 20 10 0 -10
f1 (ppm)

7.6 NMR Spectra of Miscellaneous Compounds

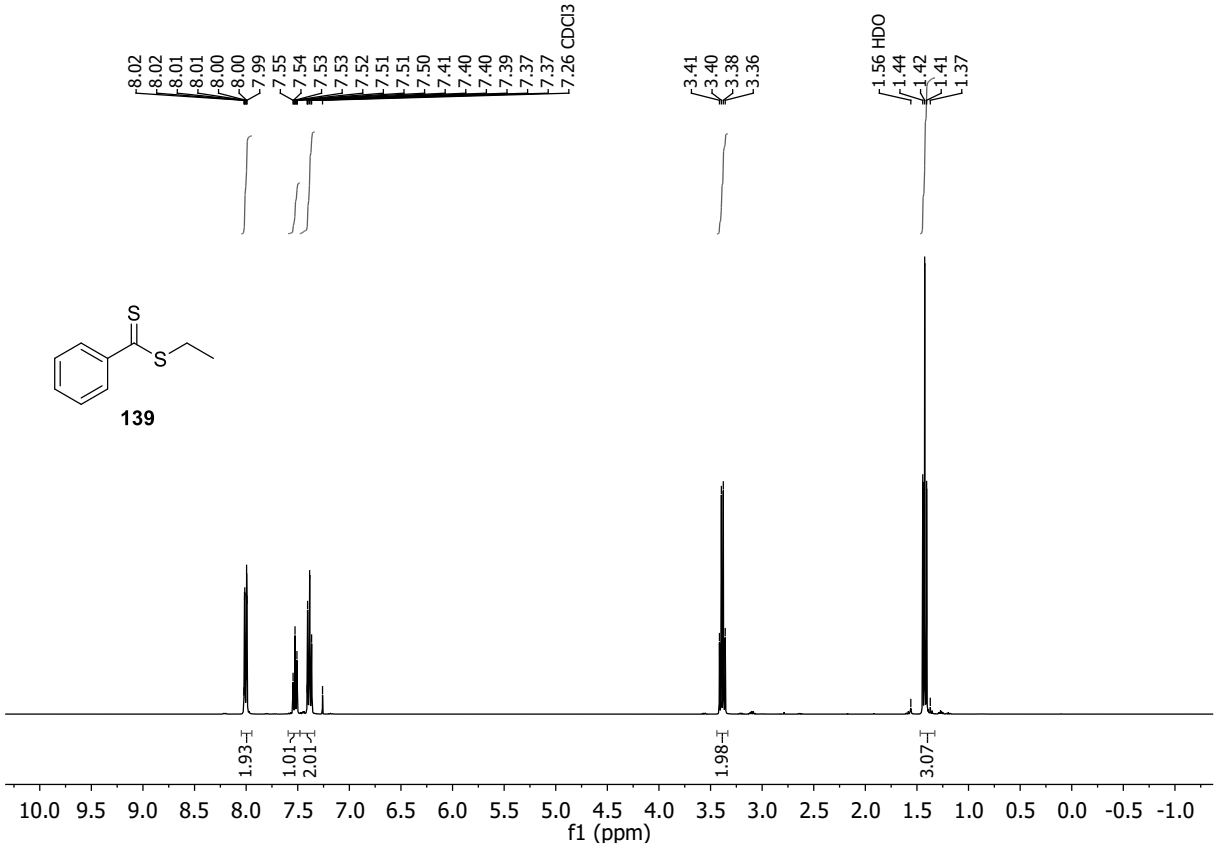

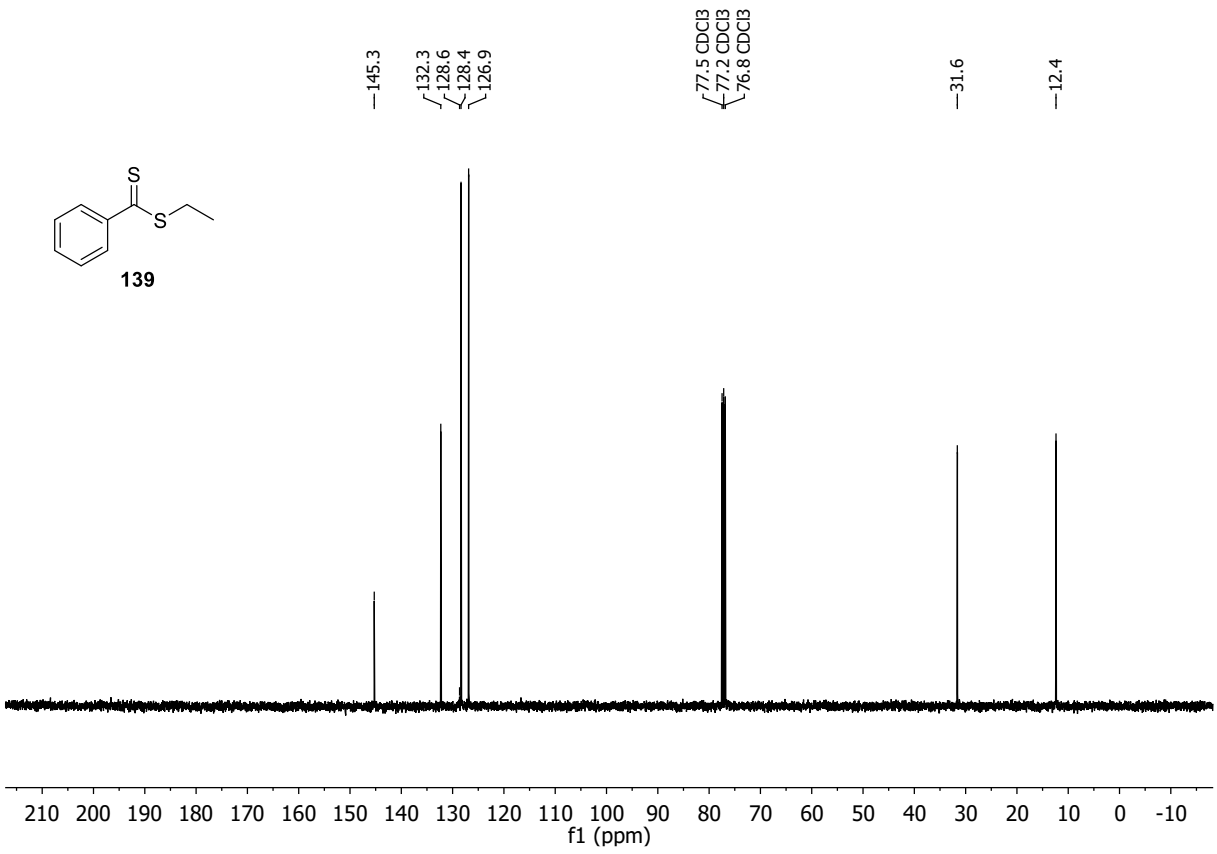

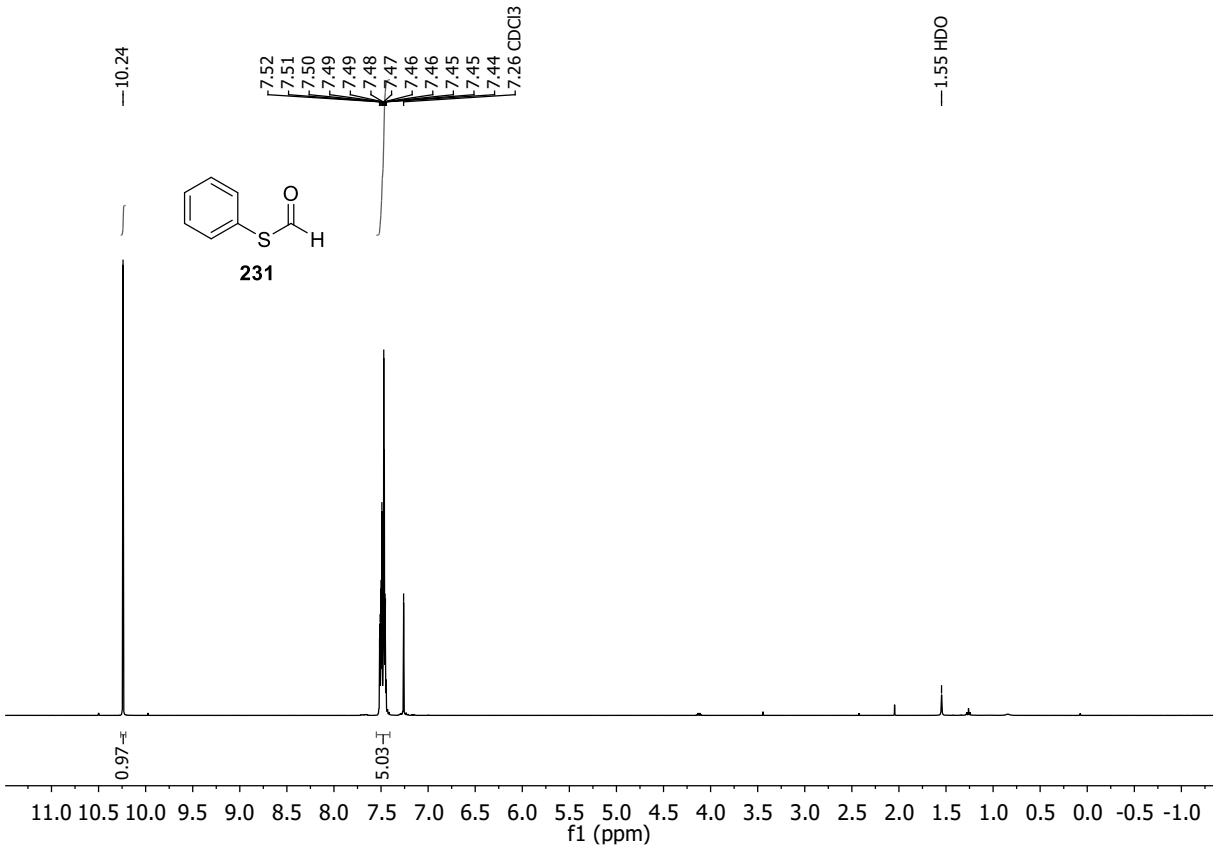
10.24
7.52
7.51
7.50
7.49
7.49
7.48
7.47
7.46
7.46
7.45
7.45
7.44
7.26 CDCl3
1.55 HDO
O
S
H
231
0.97
5.03
11.0 10.5 10.0 9.5 9.0 8.5 8.0 7.5 7.0 6.5 6.0 5.5 5.0 4.5 4.0 3.5 3.0 2.5 2.0 1.5 1.0 0.5 0.0 -0.5 -1.0
f1 (ppm)

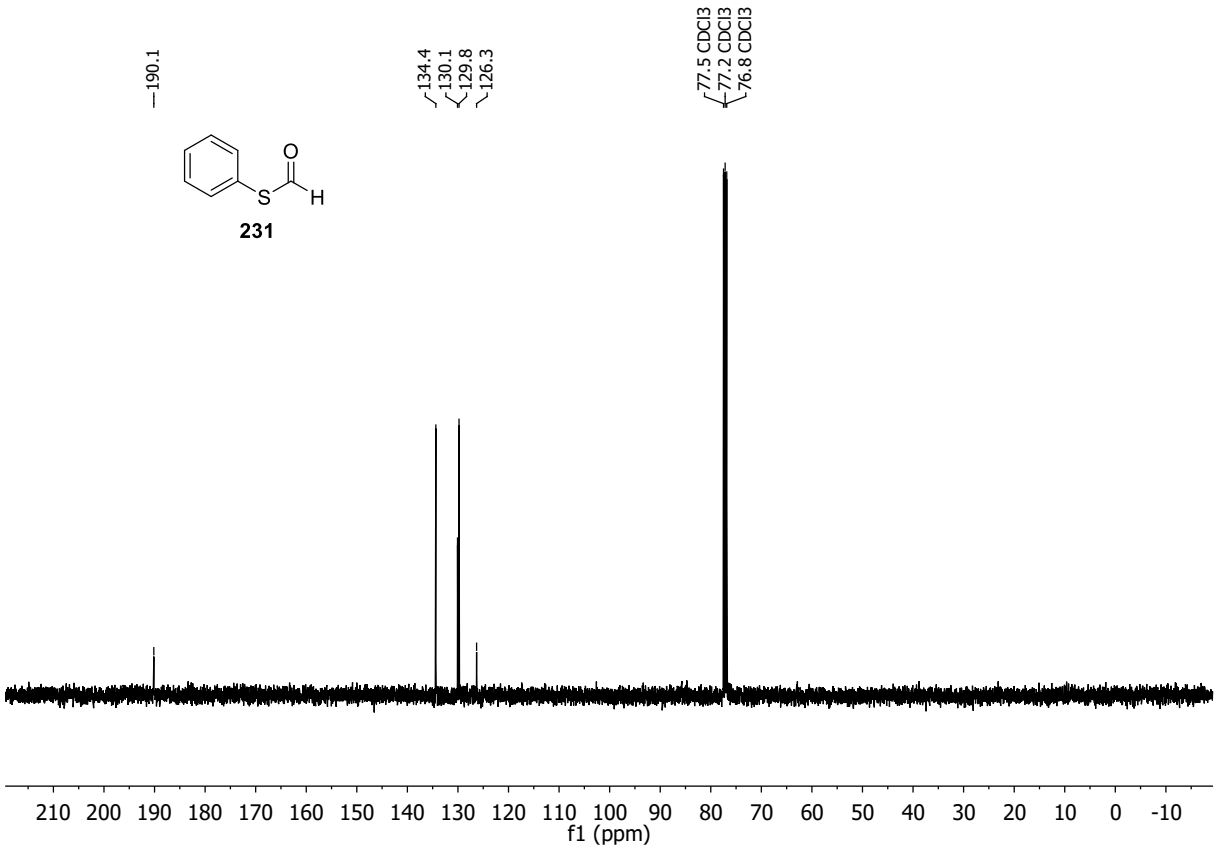
190.1
134.4
130.1
129.8
126.3
77.5 CDCl3
77.2 CDCl3
76.8 CDCl3
O
S
H
231
210 200 190 180 170 160 150 140 130 120 110 100 90 80 70 60 50 40 30 20 10 0 -10
f1 (ppm)

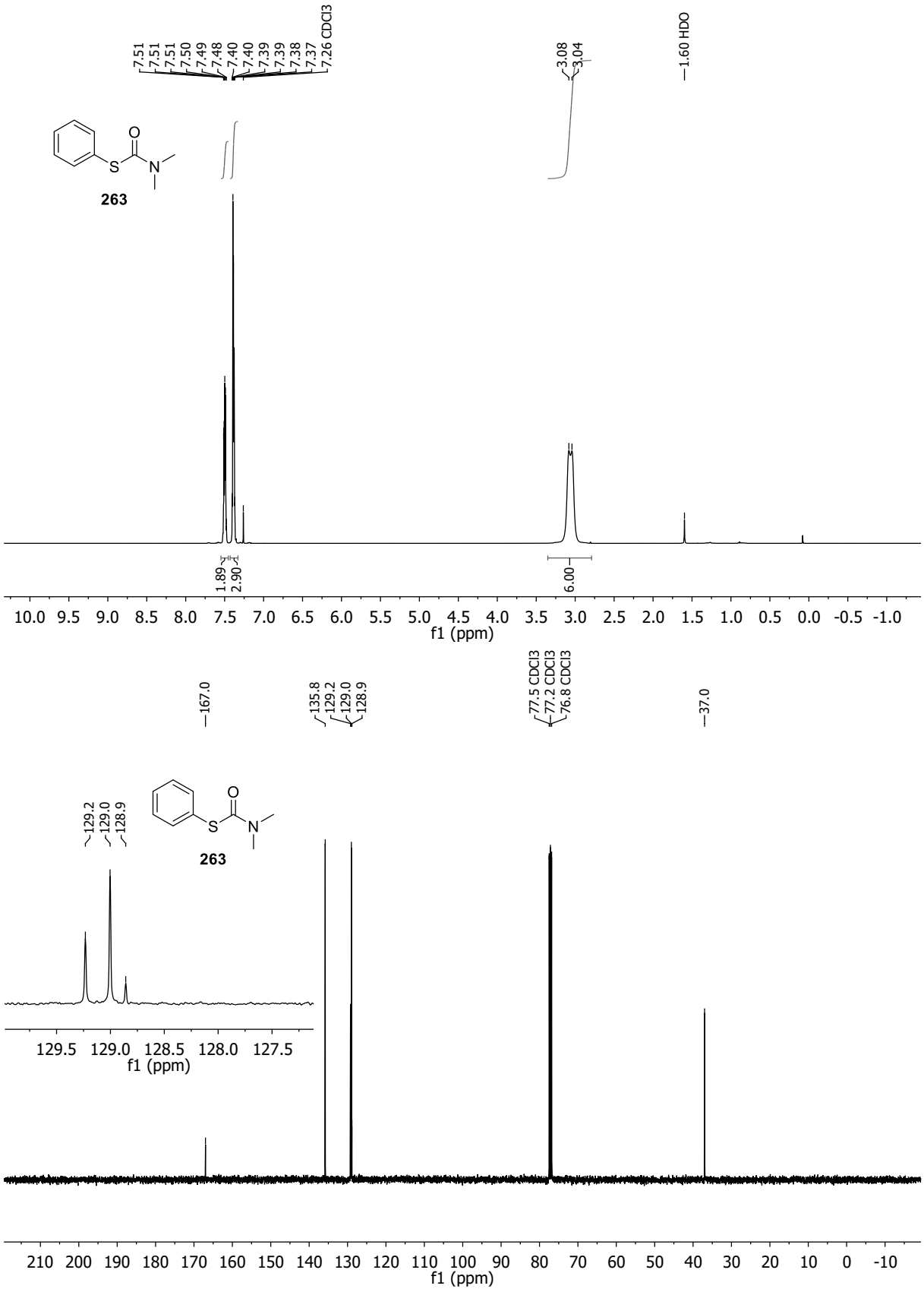
7.51
7.51
7.51
7.50
7.49
7.48
7.40
7.40
7.39
7.39
7.38
7.37
7.26 CDCl3
3.08
3.04
1.60 HDO
263
1.89
2.90
6.00
f1 (ppm)
167.0
135.8
129.2
129.0
128.9
77.5 CDCl3
77.2 CDCl3
76.8 CDCl3
37.0
263
f1 (ppm)

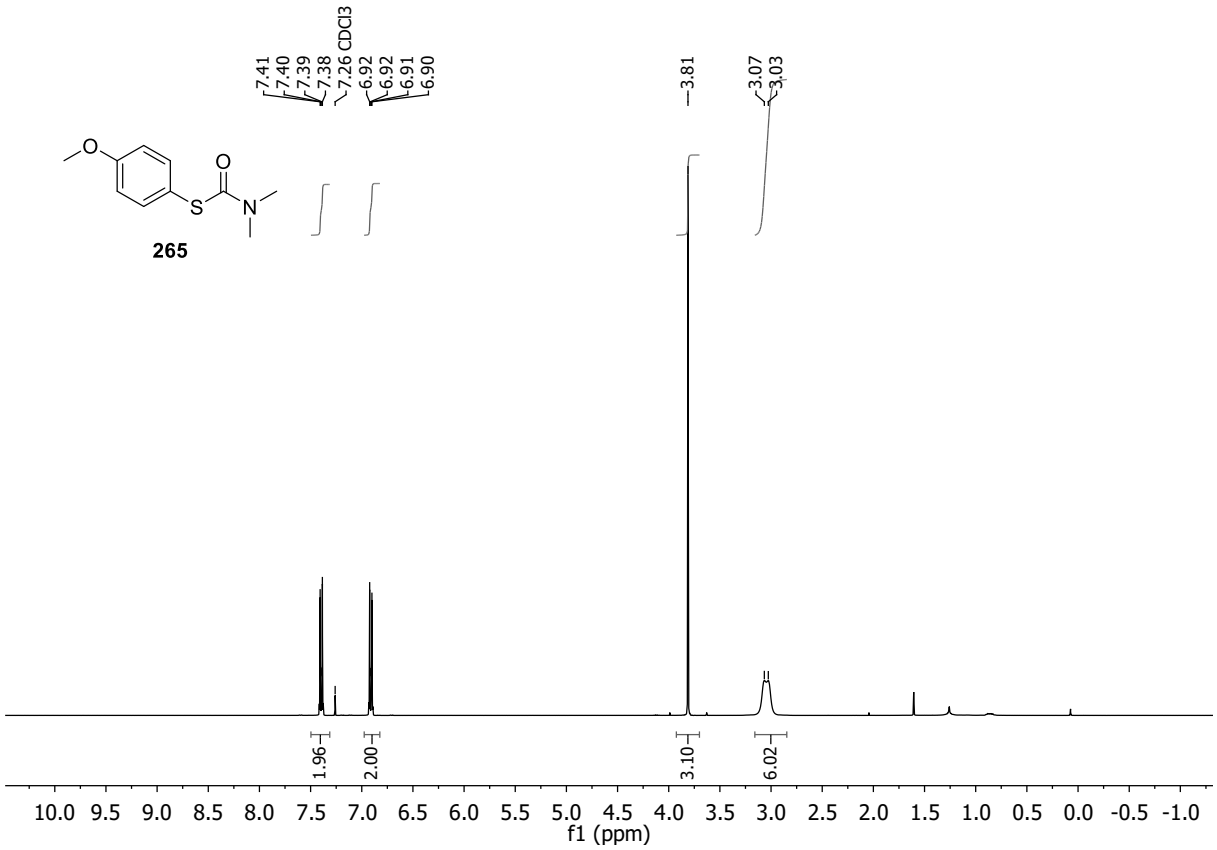
7.41
7.40
7.39
7.38
7.26 CDCl3
6.92
6.92
6.91
6.90
3.81
3.07
3.03
O
S
N
O
265
1.96
2.00
3.10
6.02
10.0 9.5 9.0 8.5 8.0 7.5 7.0 6.5 6.0 5.5 5.0 4.5 4.0 3.5 3.0 2.5 2.0 1.5 1.0 0.5 0.0 -0.5 -1.0
f1 (ppm)

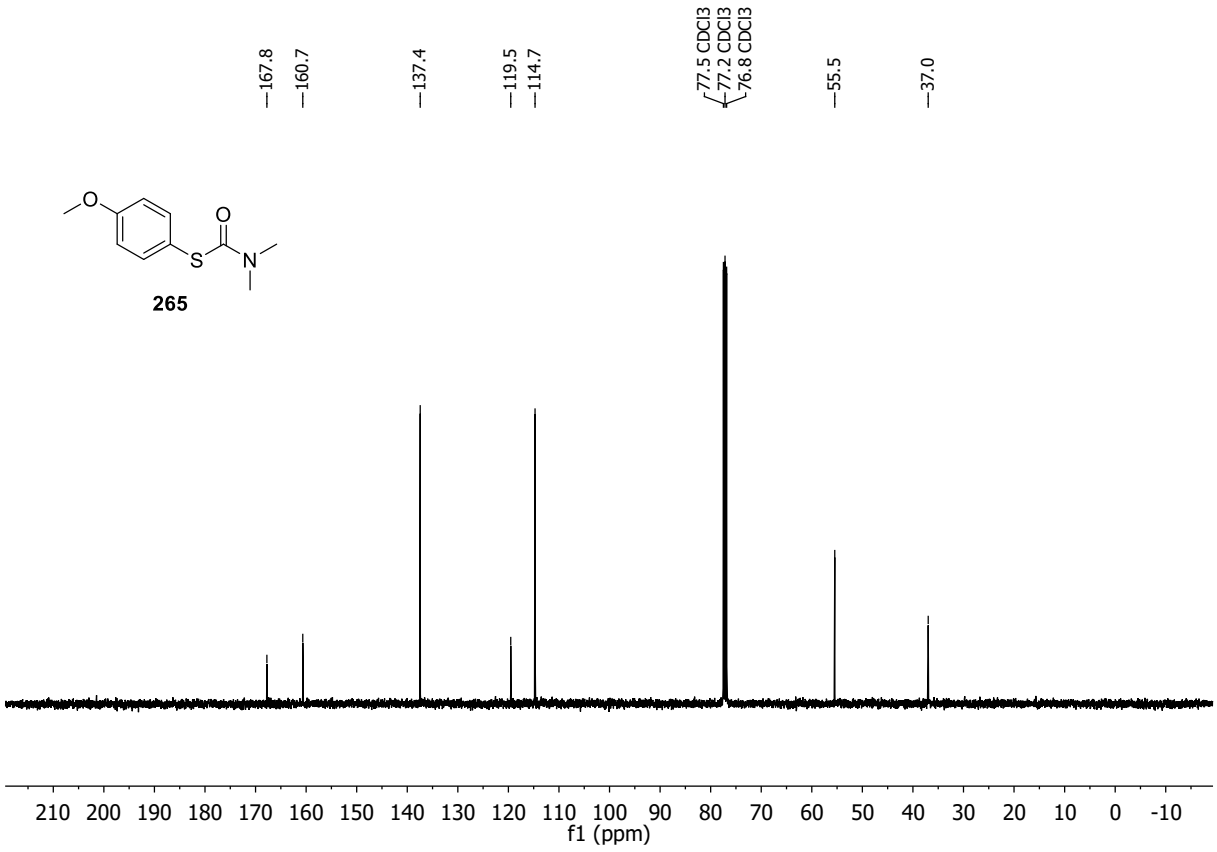
167.8
160.7
137.4
119.5
114.7
77.5 CDCl3
77.2 CDCl3
76.8 CDCl3
55.5
37.0
O
S
N
O
265
210 200 190 180 170 160 150 140 130 120 110 100 90 80 70 60 50 40 30 20 10 0 -10
f1 (ppm)

7.7 GC-calibrations

The quantification of GC-yields was achieved by adding a standard compound (*n*-pentadecane) to reaction mixtures before quenching (usually 100 µL) and applying the general formula:

$$\frac{A(compound)}{A(standard)} = R \cdot \frac{m(compound)}{m(standard)}$$

R: Response factor of compound
A: Peak area determined by GC-FID
m: mass of compound

The R values were determined by GC calibrations of respective compounds with pentadecane in ethyl acetate and measuring different mass ratios.

S-ethyl hexanethioate (**115a**)

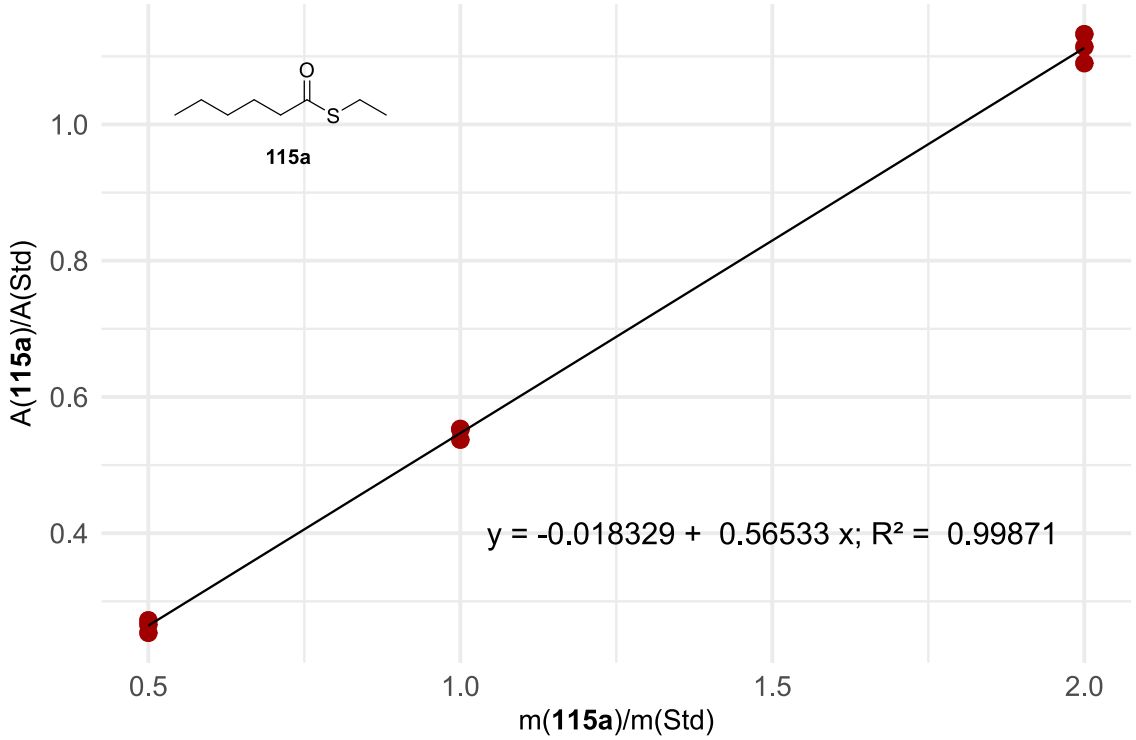

Mass ratio $\left[\frac{\text{mg (Thioester)}}{\text{mg (Std)}}\right]$	A (Thioester)	A (Std)	Area ratio $\left[\frac{\text{A(Thioester)}}{\text{A (Std)}}\right]$
2	1280.46	1174.91	1.08983
2	1179.71	1041.56	1.13263
2	1326.13	1190.43	1.11399
1	1354.55	2452.88	0.55222
1	1267.9	2360.24	0.53719
1	1396.66	2524.61	0.55322
0.5	742.16	2725.46	0.27231
0.5	572.54	2256.31	0.25375
0.5	646.49	2431.59	0.26587

Octan-3-one (**116**)

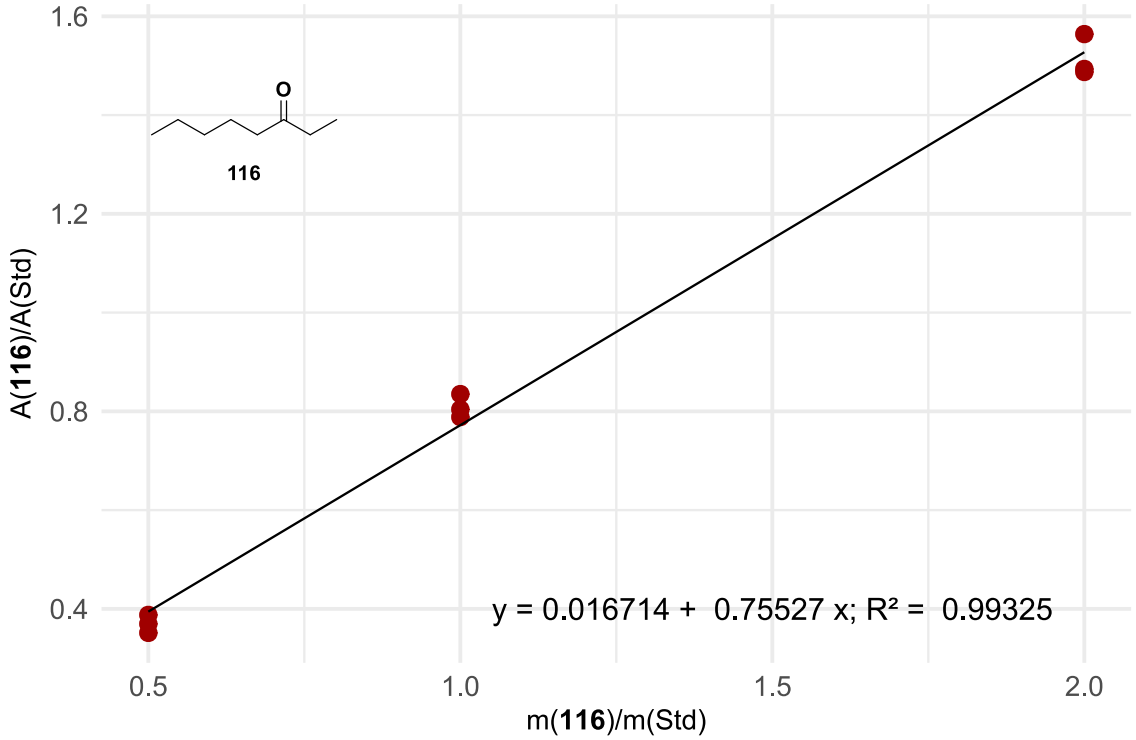

Mass ratio $\left[\frac{\text{mg (Ketone)}}{\text{mg (Std)}}\right]$	A (Ketone)	A (Std)	Area ratio $\left[\frac{\text{A(Ketone)}}{\text{A (Std)}}\right]$
2	2106.35	1416.28	1.48724
2	2083.63	1332.24	1.56401
2	2094.51	1402.53	1.4933
1	2114.74	2532.78	0.83495
1	2135.04	2707.7	0.78851
1	2203.07	2740.25	0.80397
0.5	1033.79	2942.11	0.35138
0.5	1007.78	2726.59	0.36961
0.5	1044.16	2692.83	0.38776

S-ethyl 2-propylpentanethioate (**119g**)

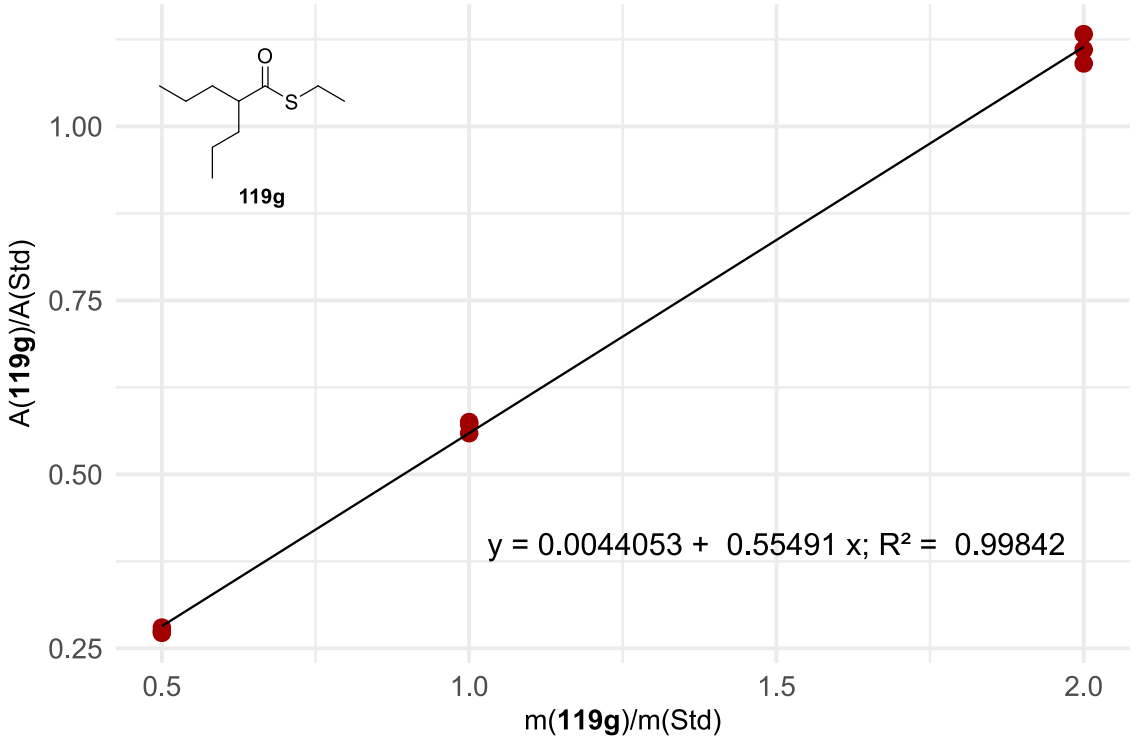

Mass ratio $\left[\frac{mg\ (Thioester)}{mg\ (Std)}\right]$	**A (Thioester)**	**A (Std)**	**Area ratio** $\left[\frac{A(Thioester)}{A\ (Std)}\right]$
2	1179.71	1041.56	1.13263
2	1434.49	1292.1	1.11019
2	1419.66	1301.99	1.09037
1	1503.81	2614.12	0.57526
1	1499.16	2681.25	0.55913
1	1524.91	2666.18	0.57194
0.5	733.15	2618.6	0.27998
0.5	757.29	2760.1	0.27437
0.5	742.16	2725.46	0.27231

S-ethyl adamantane-1-carbothioate (**119o**)

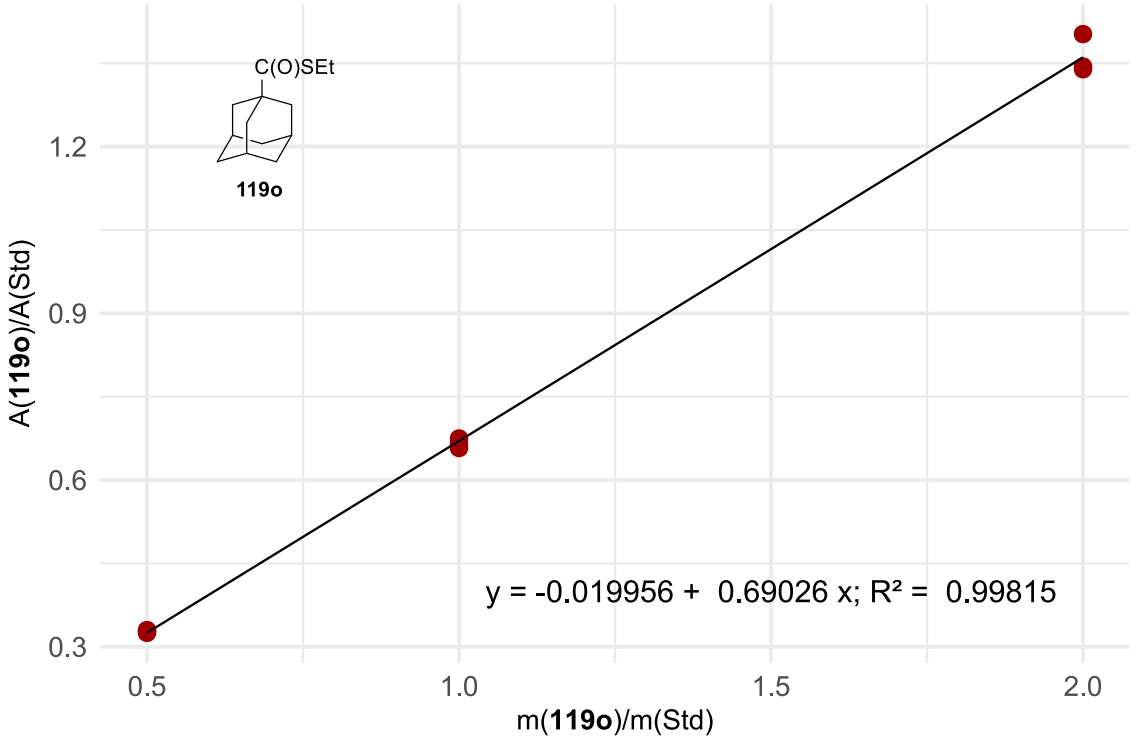

Mass ratio $\left[\frac{\text{mg (Thioester)}}{\text{mg (Std)}}\right]$	A (Thioester)	A (Std)	Area ratio $\left[\frac{\text{A(Thioester)}}{\text{A (Std)}}\right]$
2	1559.7	1112.16	1.40242
2	1630.03	1217.2	1.33916
2	1647.46	1225.74	1.34405
1	1581.74	2405.4	0.65758
1	1425.64	2112.69	0.67480
1	1560.57	2340.45	0.66678
0.5	809.28	2489.78	0.32504
0.5	652.96	1989.37	0.32822
0.5	736.88	2232.3	0.33010

S-ethyl pentanethioate (**151**)

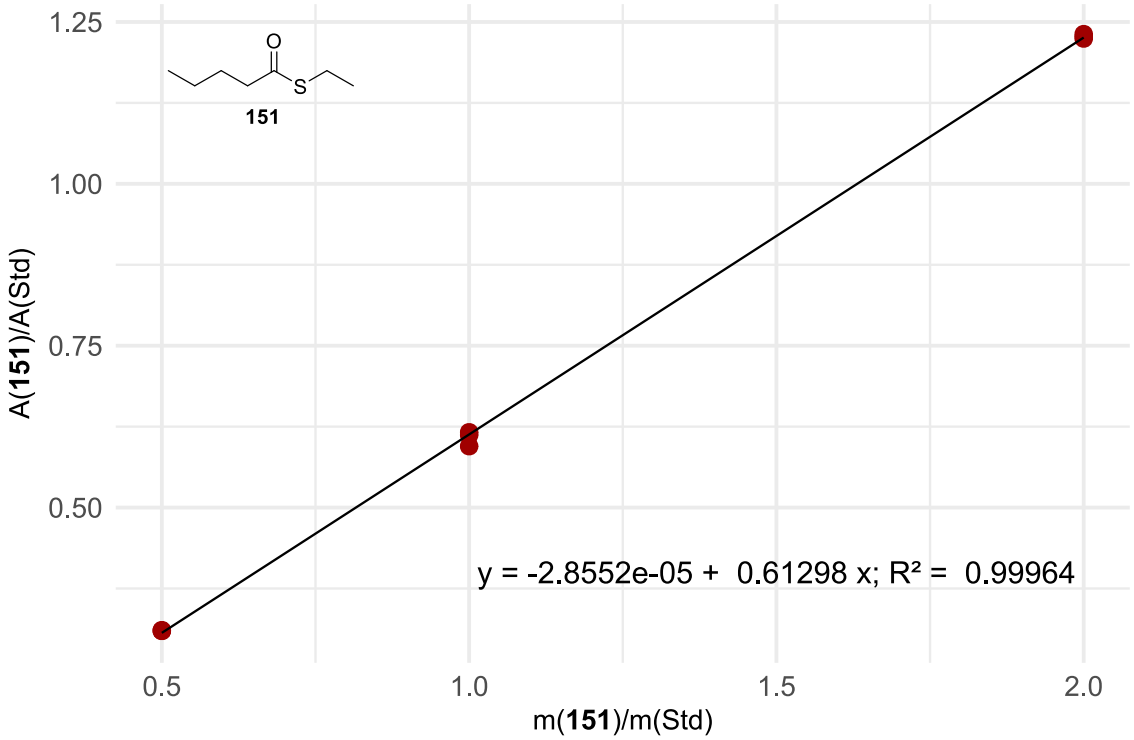

Mass ratio $\left[\frac{\text{mg (Thioester)}}{\text{mg (Std)}}\right]$	A (Thioester)	A (Std)	Area ratio $\left[\frac{\text{A(Thioester)}}{\text{A (Std)}}\right]$
2	13612.00	11117.60	1.22437
2	13290.00	10793.40	1.23131
2	14546.00	11851.80	1.22732
1	6656.74	10800.30	0.61635
1	5979.20	9769.17	0.61205
1	7202.48	12110.10	0.59475
0.5	6949.03	22365.00	0.31071
0.5	7014.00	22665.80	0.30945
0.5	6851.78	22125.60	0.30968

Heptan-3-one (**152**)

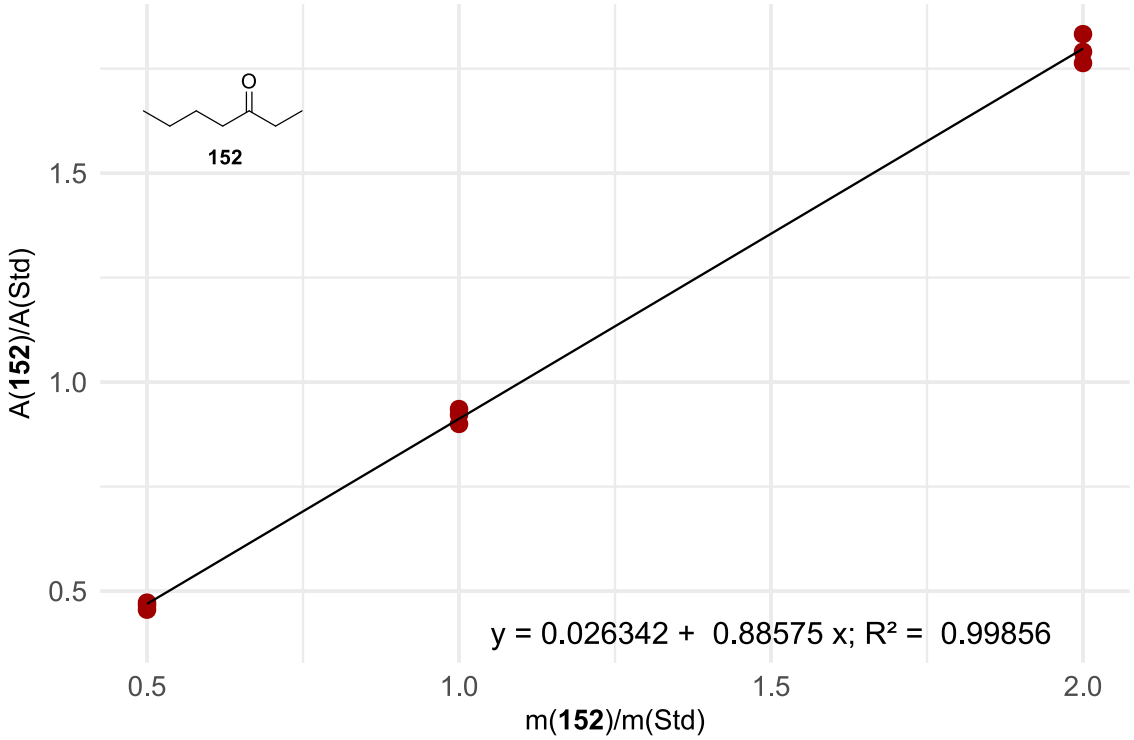

Mass ratio $\left[\frac{\text{mg (Ketone)}}{\text{mg (Std)}}\right]$	**A (Ketone)**	**A (Std)**	**Area ratio** $\left[\frac{\text{A(Ketone)}}{\text{A (Std)}}\right]$
2	17452.80	9522.99	1.83270
2	20510.50	11455.80	1.79040
2	18600.60	10548.40	1.76336
1	9738.69	10562.70	0.92199
1	8797.39	9403.20	0.93557
1	8432.41	9370.75	0.89986
0.5	8329.92	18291.40	0.45540
0.5	9568.78	20255.60	0.47240
0.5	8228.96	17668.50	0.46574

Hexanophenone (**149**)

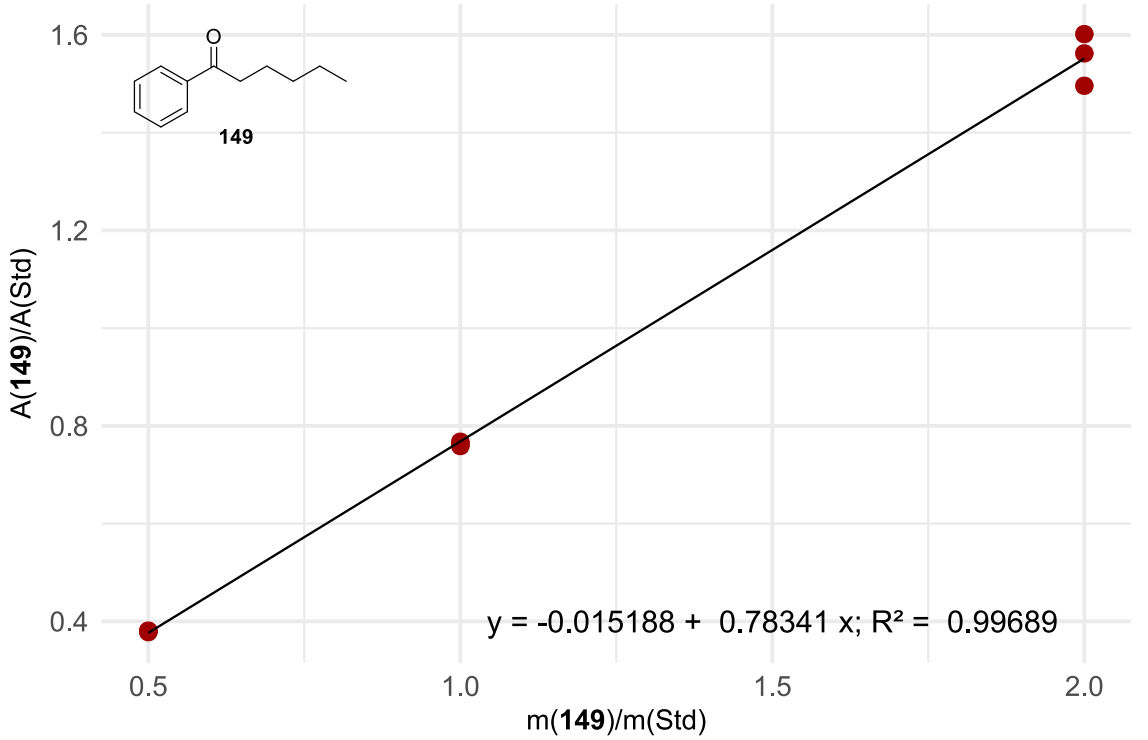

Mass ratio $\left[\frac{\text{mg (Ketone)}}{\text{mg (Std)}}\right]$	A (Ketone)	A (Std)	Area ratio $\left[\frac{\text{A(Ketone)}}{\text{A (Std)}}\right]$
2	2499.18	1670.68	1.49590
2	2323.85	1450.91	1.60163
2	2445.26	1565.30	1.56219
1	1148.79	1496.61	0.76761
1	1273.93	1679.00	0.75873
1	1178.39	1542.91	0.76376
0.5	1187.37	3141.57	0.37796
0.5	1199.90	3155.43	0.38027
0.5	1472.22	3863.74	0.38103

Propiophenone (**130a**)

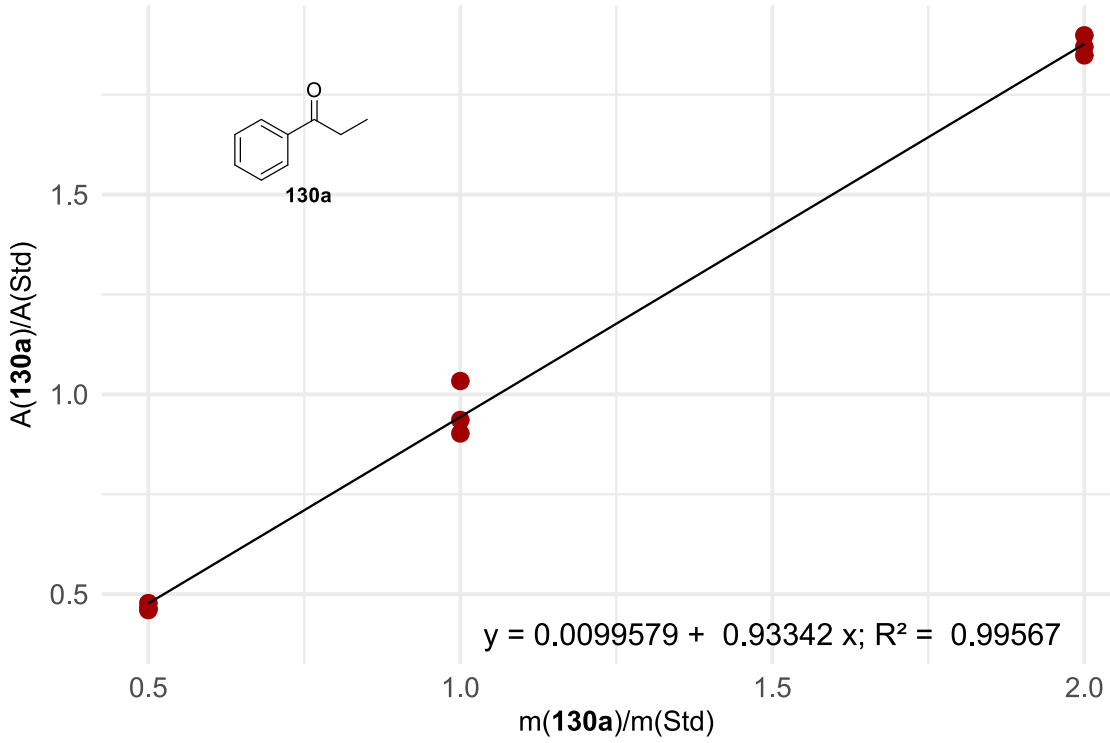

Mass ratio $\left[\frac{\text{mg (Ketone)}}{\text{mg (Std)}}\right]$	A (Ketone)	A (Std)	Area ratio $\left[\frac{\text{A(Ketone)}}{\text{A (Std)}}\right]$
2	26240.2	13793.0	1.90243
2	27312.8	14641.4	1.86545
2	26812.1	14493.7	1.84991
1	14558.9	15636.9	0.93106
1	15507.0	15004.4	1.03350
1	12874.4	14303.7	0.90008
0.5	13793.2	28936.1	0.47668
0.5	13793.2	28936.1	0.47668
0.5	13757.9	30026.9	0.45819

S-phenyl thioformate (**231**)

This substrate was observed to decompose with H_2 as carrier gas. While the loss was determined to be considerably smaller with N_2 as carrier gas, errors due to decomposition have to be taken into account.

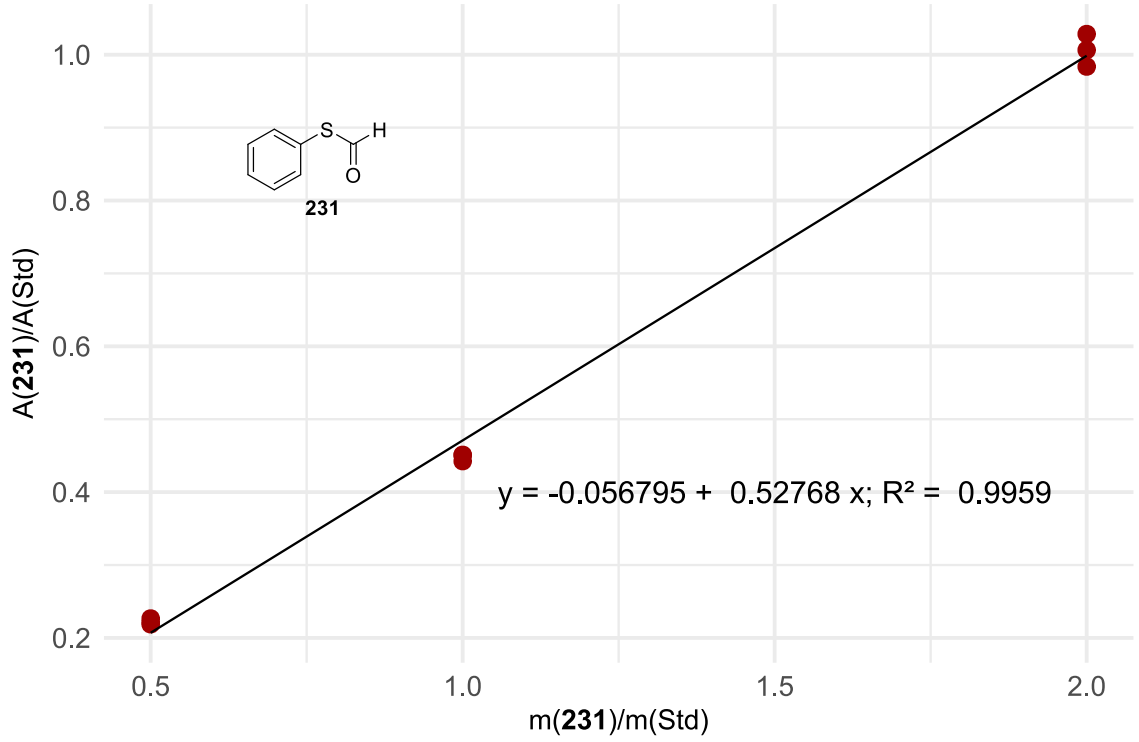

Mass ratio $\left[\frac{\text{mg (Thioformate)}}{\text{mg (Std)}}\right]$	A (Thioformate)	A (Std)	Area ratio $\left[\frac{\text{A(Thioformate)}}{\text{A (Std)}}\right]$
2	871.19	847.14	1.02839
2	925.01	940.36	0.98368
2	969.88	963.67	1.00644
1	397.76	881.66	0.45115
1	403.16	894.81	0.45056
1	393.02	888.29	0.44245
0.5	426.82	1883.03	0.22667
0.5	418.97	1892.07	0.22144
0.5	407.17	1861.88	0.21869

Anisaldehyde (**247**)

This substrate was observed to decompose with H_2 as carrier gas. While the loss was determined to be considerably smaller with N_2 as carrier gas, errors due to decomposition have to be taken into account.

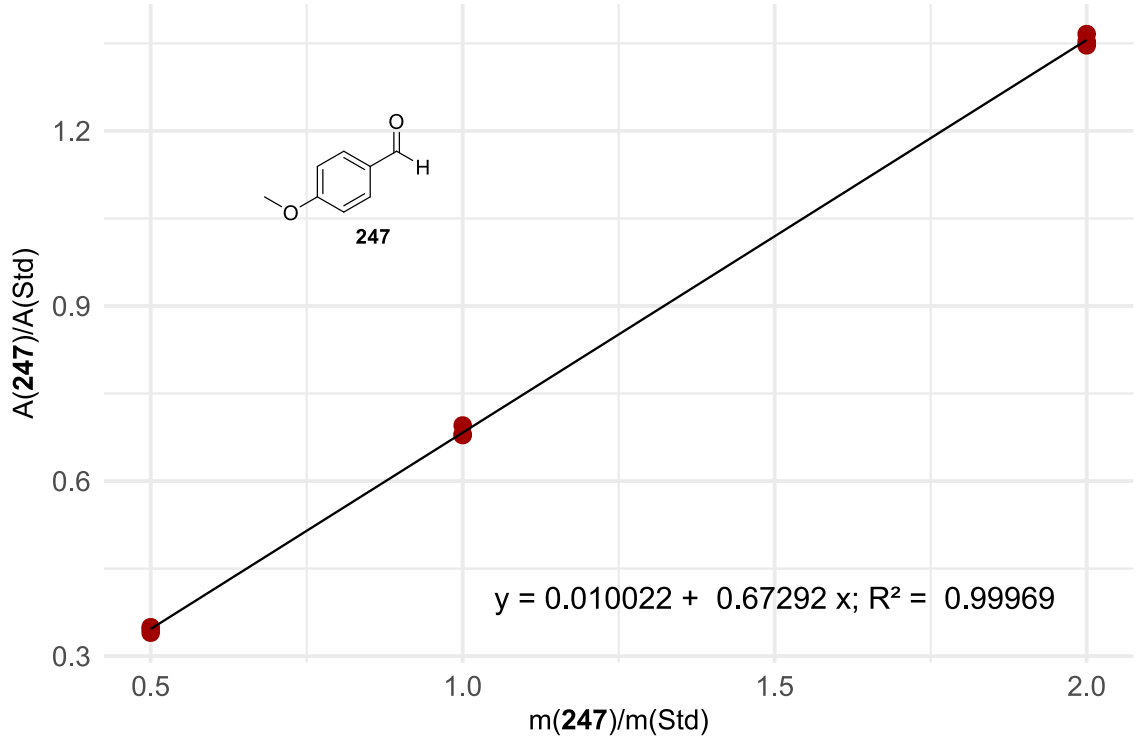

Mass ratio $\left[\frac{\text{mg (Aldehyde)}}{\text{mg (Std)}}\right]$	A (Aldehyde)	A (Std)	Area ratio $\left[\frac{\text{A(Aldehyde)}}{\text{A (Std)}}\right]$
2	13025.5	9624.59	1.353356
2	12935.1	9469.16	1.366024
2	13504.7	10029.6	1.346484
1	7067.35	10413.5	0.678672
1	6578.23	9460.37	0.695346
1	6627.74	9746.72	0.679997
0.5	6650.26	19203.7	0.346301
0.5	6832.52	20094.8	0.340014
0.5	7191.28	20565.5	0.349677

7.8 Acknowledgement/Danksagung

Zuallererst möchte ich mich bei meiner Betreuerin Prof. Dr. Ivana Fleischer bedanken, die (letzt-)endlich ihr "Jun.-" bald abgeben darf. Danke für die herzliche Aufnahme in deine Arbeitsgruppe und dass du mich auf wilde Thiochemie losgelassen hast, auch wenn meine Themenwahl retrospektiv nicht ganz einfach war. Ich hoffe, dass viele weitere Veröffentlichungen über 3d-Metalle - und damit meine ich nicht nur Nickel – dieser Arbeit folgen werden. Vielen Dank für die netten Seminardiskussionen, die Ratschläge im Laufe der Jahre und das offene Ohr für jeden (Miss-)Erfolg im Rahmen der Chemie.

Ich bedanke mich bei Prof. Dr. Thomas Ziegler für die Übernahme des Zweitgutachtens ganz herzlich.

Now, it is just right to thank my colleagues who likely suffered from my smelly endeavors! Especially, Regina Oechsner with whom I had the joy to work with for (has it already been) 4 years and our countless discussions that were only hissed about – “you fight like an old couple”. Admittedly, the working group would not have been the same without you. Alex Caciuleanu whose Rumanian charm and the countless talks we shared, taught me a lot – ah yeah and setting fire in the lab once… that as well. Anne and Savva, who also shared the joys of sulfur chemistry. Lastly, Robert and Ivo whom I wish success and all necessary creativity in their research to come – I’m so happy that sulfur persists!

The “old school” of the working group deserves a thankful mention as they paved the way when I was starting out: Paul Henry Gehrtz who started this whole project to begin with, but who inspired an everlasting interest in synthesis and simple pragmatism when it came to lab work; Benni Ciszek and Prasad Kathe, aka “the boys”, which granted me all special wisdoms in the beginning of my PhD and steel pantherous hours in the lab; as well as Vera Hirschbeck and Marlene Böldl. I consider myself lucky enough to be one of the last ones to have worked alongside the people with whom it all started. Thank you again for taking me up so nicely and some of the substrates you left for me. Tanno Schmidt also deserves a small thank you as he was always present in the lab with a fierce motivation when the main body of the manganese project was in the making. And not to forget: Jakob Pablo Lebon (!), with whom I could discuss a lot of the results presented in this thesis, leading to some of the presented results. Thank you for over 8 years of talks, ideas and not to forget: gossip.

I want to thank my practicum/bachelor students (chronologically): Jonas Riedmeier, Christian Wilhelm, Ralf Kern, Sabrina Jeltsch, Niklas Kehl, Linda Biehler, Robert Richter and last, but not least, Timo Neumann, with whom I could share my joy of odorous work, but equally teach and learn from each and every one of them. Thank you for your dedicated work.

I also want to thank Dr. Guillaume Lefevre, who initiated the collaboration on Twitter (of all places) and gave this work a more solid foundation to stand on. Thank you for your work and the discussions we had. I hope that you will remember sulfur chemistry fondly.

Natürlich wäre all diese Arbeit nicht möglich gewesen ohne die Arbeit ein paar sehr wichtiger Menschen an der Universität: die MS-Abteilung, die NMR-Abteilung, die Glasbläser, das Werkstattpersonal und die Mitarbeiter des zentralen chemischen Instituts. Vielen Dank für Ihre Arbeit und Ihre Hilfe, wann immer etwas dringende Aufmerksamkeit brauchte.

Ein besonderes Dankeschön geht an meine Korrekturleser: Regina, Alex, Robert, Julian und Judith. Vielen Dank an euch! Ohne euch wären diese Seiten wahrscheinlich ein absolutes Chaos - vielleicht mit schönerem englischem Vokabular - aber trotzdem ein Chaos.

Nicht unerwähnt bleiben soll auch die ganze Familia der berüchtigten, fantastischen, viel Schönheit-verströmenden Knochenmühle Tübingen: Gschwendo, Kevin, Arne, Patrick, Vivek, Katha, Björn, Jenny, Judy, Kittl, Fbier, Jorge, Elvis(<3) und all die anderen, mit denen ich seit 6 Jahren trainieren durfte. Eine Zeit die sich vielleicht treffend mit *Klaus-Rausnehmen-Kreis* zusammenfassen lässt. Danke für jedes einzelne toughe Training. Viele liebevolle Kittens.

Ich möchte mich bei meiner Familie bedanken, die mich die ganze Zeit über unterstützt hat, was gegeben der Pandemie und allem drumherum sehr sehr wichtig war. Danke für die unzähligen Wochenends-skypes und sonstige Telefonate und v.a. Hilfe bei jedem Problem (sofern es nicht mit Chemie zu tun hatte).

Nun bleibt nur noch Judith Tettenborn zu danken, der ich nicht nur meinen Dank, sondern auch meine herzlichste Liebe schenken darf. Wenn ich es mir recht überlege: Es ist irgendwie ironisch, jemandem zu danken, der mich eher aus dem Labor herausholte, statt mich dort zu lassen. Trotzdem danke ich dir, dass du für mich da warst: Bei Erfolgen, Misserfolgen und den Verrücktheiten des "How please?!", nämlich dem Schreiben der Dissertation. Du hast es so viel schöner gemacht und ohne dich wäre es nicht in diesem Ausmaß möglich gewesen.